Novel Biomimetic Polymeric Nanoconjugates as Drug Delivery Carriers for Poorly Soluble Drugs

Adeola Tawakalitu Kola-Mustapha

October 2013

Novel Biomimetic Polymeric Nanoconjugates as Drug Delivery Carriers for Poorly Soluble Drugs.

Adeola Tawakalitu Kola-Mustapha

PhD thesis submitted in partial fulfillment of its requirement; awarded by

De Montfort University Leicester UK

October 2013

i. Statement

The work presented in this thesis was carried out by the author in the Leicester School of Pharmacy within the Faculty of Health and Life Sciences (De Montfort University) from January 2010 to October 2013. Unless otherwise accredited, the work was carried out by the author and has not been submitted in any other form for any other degree or qualification.

ii. Acknowledgements

I do appreciate the encouragement, motivation; support and understanding of my first Supervisor Dr Amos Olusegun Abioye throughout my research. I learnt a lot from him, right from my undergraduate studies at the Faculty of Pharmacy, University of Lagos, Nigeria up to the PhD level at the De Montfort University, Leicester UK. His guidance and patience have inspired me in to continuing my research in the Pharmaceutical Sciences. I thank him for having enough faith in me to accept me as his research student, mentoring me and ensuring the successful completion of this work against all odds. I am incredibly fortunate to have worked with such a knowledgable scientist.

I acknowledge Dr Walkiria Schlindwein for co-supervising my work up till my transfer from MPhil to PhD. The kind gesture of Prof Joan Taylor in continuing the supervision and offering me a bench space in her laboratory is also appreciated. This gave me an opportunity to interact with her research group members - Dr Tarsem Sahota, Ahmed Alsabih, Mohammed Albihed, Dolly Jacobs and Christine E-Ching Luo. Indeed I appreciate Dr Tarsem Sahota's invaluable time spent advising, encouraging and training me on the use of the rheometer.

I thank Ms Angela Ferguson for training me initially at the start of my research and still continued to provide technical assistance whenever asked; always ensuring my seamless use of the relevant equipments and laboratories. I appreciate her selflessness in assisting and training me when needed. I thank Dr Richard Webster and the entire technical staff of Pharmaceutics, Ian, Jo, Anona and Peter for their technical assistance and immense support.

I thank the combined team of Ian Fletcher, Paul Taylor, Rachel Armitage, Matt Rosser and Liz O'Brien for assisting with Scanning Electron Micrographs. I thank Nasmin and Umesh for their help while using the Pharmaceutical Chemistry Laboratory. I thank Dr David Armitage for his assistance with the Atomic Force Microscopy images. I thank Dr Ketan Ruparelia for assisting with the Nuclear Magnetic Resonance experiments.

I thank Prof Yvonne Perrie for permitting me to use the Particle size and Zeta potential Analyzer in her laboratory at the Aston University, Birmingham. I thank Alex Wilkinson, for training me on the use of the equipment.

My heartfelt gratitude to my colleague Joseph Darkwah, for his support; kind words and patience displayed in bailing me out of difficult situations. I also thank my wonderful research colleagues, Sohail, Ken and Alex for their support.

I thank Prof N. D. Ifudu of the University of Lagos for supervising my undergraduate, Masters' degree thesis and the early stages of my PhD work. I am entirely grateful to him for ensuring a seamless transfer of my PhD at the Univeristy of Lagos to De Montfort University. I also thank Prof H. A. B. Coker for his immeasurable support through the years. I appreciate Prof A. F. B. Mabadeje's words of encouragement and support. I acknowledge all my teachers from my primary school days through to my undergraduate studies in the Department of Pharmacology and the Faculty of Pharmacy, University of Lagos.

I thank my friend Lola Akintoye for all the years of sisterhood, friendship and constant support. I am grateful to the CMF family; the Bioshoguns, Kadaras, Afinowis, Sis Fatimah, Aunty Yemi, Bukky, Latifah, Fatimah; Mr and Mrs Ali for making my stay in the UK a memorable one. Special thanks to Toyin and her daughters for encouraging me to pick up swimming as part of my fitness programme. I can't forget the home baked delicacies and meals she sent to me as a routine. I am truly blessed to have them as great friends.

I thank my friend Ronke Olaleye and her family for her love, support and endless phone calls to ensure that I am doing fine. To Biola, Lola, Jemilah, Isla, Taiwo and old girls of FGGC Owerri, you are truly appreciated. I thank Sis Bisola, Sis Jummai, Sis Bola, Hajia Bilkis and the entire MICA family for their generousity, thoughtfulness, encouragement and advice. I appreciate Alhaja Olatunji's prayers and encouragement. It is indeed impossible to acknowledge all the people who helped me to make it through.

I appreciate the support of my extended family, the Lasisis, Adekus, Gbadamosis, Zubairs, Adenekans and Ogunsholas, its one love all the way. I thank my mum and dad for their invaluable support and sacrifice. I thank my mum for taking care of my children while I was away. Her dedication and selflessness in making sure we are all fine is unparalleled. Mum, you are my 'jewel of inestimable value'. Dad, you are invaluable too. I thank my siblings whom I had the fortune of growing up with; and their spouses, Bolaji, Fola and Adeola, Ismail, Peju and Tajudeen. I appreciate Adepeju for always giving me a shoulder to cry on and going through the different phases of the PhD with me. I thank my children Hikmah, Mukhtar, Iman and Al-Amin for their incredible show of patience and understanding while I was away. Thanks to my niece and nephews; Fareedah, Fahiz and Adam. My maternal Grandma's words of encouragement and prayers are appreciated. I thank Abdul-Razaq for his love, patience and total support throughout my studies. May Allaah reward his noble intention and ease the implementation. The unconditional love and support of my entire family is indeed invaluable.

Yes, I wouldn't have proceeded to do my PhD without the advice and encouragement of my late husband, Ayodele Abdulhakim. He believed so much in me and was always there to cheer me on. I remember the ease with which he switched roles with me to facilitate my successful attendance of my undergraduate and Master's classes; how he helped with my write ups and listened to my presentations to boost my confidence. He always advised me to do research work 'in tune with the world development'. I miss you and I am indeed humbled by your selflessness.

All Praises and thanks are due to Allaah, the Lord of mankind and all that exists.

iii. Abstract

Active Pharmaceutical Ingredients with poor solubility have presented significant difficulties in drug product design and development including slow and ineffective absorption leading to inadequate and variable bioavailability. Therefore it has become increasingly desirable to overcome the low aqueous solubility of drug candidates and develop more novel and innovative formulation approaches to increase the dissolution rate of the poorly soluble drugs. This work focuses on the formulation of novel amorphous ibuprofen-polymer nanoconjugates based on the polymer-drug complexation in order to improve its physical and dissolution characteristics without the use of toxic organic solvents. Plain and ibuprofen-loaded binary and ternary nanoconjugates were prepared using four modified co-precipitation techniques including melt solubilization; alkaline solubilization; surfactant solubilization and hydrotropic complexation techniques. A remarkably high loading capacity was achieved ranging from 89.05 to 99.49% across the four techniques and polymer-polymer ratio of 50:50 was found to be most efficient. All the four techniques reduced the size of ibuprofen (2.87 μm) significantly in the presence of 2.0 $x10^{-3}$ mM of Diethylaminoethyl Dextran (DEAE-Dextran) in the order melt solubilization (203.25 nm) > alkaline solubilization (185.68 nm) > surfactant (Tween 80) solubilization (122.17 nm) > hydrotropic complexation (77.92 nm). 5.0 x 10^{-4} mM of chitosan also reduced the size of ibuprofen from 2872.12 to 10.70 nm (268-fold reduction). The FTIR spectroscopic analysis revealed electrostatic, hydrophobic and hydrogen bonding interaction between solubilized ibuprofen and the cationic polymers (DEAE-Dextran and chitosan) to form a new product (an amide). Polymer-polymer complexation also occurred between DEAE-Dextran and gellan as well as chitosan and gellan to a different extent depending on the mixing ratios. ^{1}H and ^{13}C NMR analysis confirmed the conjugation between ibuprofen and each of the cationic polymers as well as the formation of a new amide product. DSC thermal analysis showed that the nanoconjugates exhibited new broad and diffuse peaks confirming that they did exist in amorphous state as multiple complexes. The TGA thermograms of the binary

nanoconjugates exhibited one step degradation profile compared with the physical mixture which exhibited two steps. However the ternary nanoconjugates exhibited two steps degradation profile confirming the formation of multiple complexes. Marked enhancement of drug release was achieved by the four techniques compared with the ibuprofen control. All the DG (DEAE-Dextran - Gellan) complexes exhibited a higher release profile than ibuprofen control. Fickian and non-Fickian anomalous mechanisms were deduced for the drug release of ibuprofen from the binary conjugates. The ternary nanoconjugates exhibited non-Fickian (anomalous) diffusion, Fickian diffusion and Super Case II transport release mechanisms. The ternary nanoconjugate hydrogels exhibited complete release (100%) within 48 h. The lowest concentration of DEAE-Dextran, Gellan – Ibuprofen – DEAE-Dextran (GIbDD) 2:0.125, increased the release of ibuprofen by 13.4% however higher concentrations of DEAE-Dextran decreased the release profile steadily. It was concluded that DEAE-Dextran has potentials in the formulation of modified (extended) release of ibuprofen. The most prominent mechanism of release of ibuprofen from the nanoconjugate hydrogel was Super Case II transport. SEM and AFM micrographs of the drug loaded composite pharmaceutical films exhibited concentric spheres with two and three layers for the binary and ternary films respectively. This supports the evidence of internalization of ibuprofen by the polyelectrolyte complex. The FTIR and DSC results confirmed electrostatic and hydrophobic interactions between ibuprofen and DEAE-Dextran as well as between gellan and DEAE-Dextran. Thermal analysis revealed that plain bilayer films were thermally more stable than composite films. The addition of ibuprofen significantly increased ($p < 0.05$, $n = 4$) the swelling ratio of the films compared with films without the drug. The drug loaded bilayer films exhibited Fickian diffusion mechanism while the dominating mechanism for composite films was anomalous (Non-Fickian) transport. From the foregoing, it was evident that ibuprofen-polymer nanoconjugate present a novel tool for the delivery of ibuprofen with potential application for transdermal delivery.

iv. Table of contents

v. List of figures

vi. List of tables

CHAPTER ONE

1.0. Introduction

1.1. Background of studies

The delivery of poorly soluble drugs has been a major research concern in the recent past. More than 40% of newly discovered drugs and 90% of approved drugs have poor solubility, poor permeability or both and approximately 16% have less than optimal performance specifically because of poor solubility and low bioavailability [1]. Aqueous solubility of active pharmaceutical ingredients is a key parameter in drug design and formulation development because a drug molecule has to be water soluble to be readily delivered to the cellular membrane, at the same time they need to be hydrophobic to cross the membrane. A balance of both properties can be utilized to develop various solubilization systems that can deliver water-insoluble drug to therapeutic target sites.

Poor water solubility of bioactive agents (solubility < 100 µg/mL) has presented significant difficulties in drug product development including slow and ineffective absorption leading to inadequate and variable bioavailability as well as therapeutic failure. Application of genomics, high – throughput screening, combinatorial chemistry, informatics and miniaturization has generated a lot of drug candidates however it has been difficult to maximize their biopharmaceutical properties [2]. It has therefore become increasingly desirable to overcome the low aqueous solubility of drug candidates and develop more robust novel and innovative smart formulation approaches to increase the dissolution rates of the poorly soluble drugs.

Previous formulation research efforts to improve oral and topical bioavailability of poorly soluble drugs include addition of release accelerating excipients; invasive sustained release implants which can only be used for very low doses; osmotic pump system; solubilization in surfactant systems; micronization; formation of water-soluble complexes; pro-drug design; spray drying *etc.* [3-4].

However for many drugs, these approaches do not lead to a sufficiently high increase in solubility, dissolution velocity and subsequent bioavailability. Of significant research interest is the development of Indomethacin (Osmosin) tablet with limited gastro intestinal adverse effects. It was hailed as formulation breakthrough for non steroidal anti-inflammatory drugs (NSAIDs). The unique feature of Osmosin is the release of the active drug via a continuous osmotic pump system over a period of 10 to 11 h along the gastro intestinal tract rather than by tablet disintegration. Over 400,000 prescriptions were written between December 1982 and June 1983 when it was first approved. However, bleeding, perforation and death in extreme cases have been reported [5]. This could be due to burst release profile which may have exposed certain parts of the gastro intestinal tract to high concentrations of indomethacin. The adverse effects of oral non steroidal anti-inflammatory drugs in general have been recognized as a considerable cost burden.

Current formulation research approaches are focused on macromolecular assembly of amphiphiles; self emulsifying systems; nanonization; nanocrystallization based on top-down and bottom-up techniques; co-precipitation; short acting patches as transdermal delivery systems; liposome dermal delivery matrix etc. [6-10].

Model poorly soluble drug in this study is Ibuprofen. Ibuprofen [(±)-2-4-[2-methylpropyl] phenyl propanoic acid] is a derivative of propionic acid which is a naturally occurring carboxylic acid with a molecular weight of 206.28 g/mol and molecular formula $C_{13}H_{18}O_2$ shown in Figure 1. Ibuprofen is a white crystalline powder highly insoluble in water but readily soluble in organic solvents such as ethanol with a melting point between 75 and 78 °C [11]. It has two enantiomers in a racemic mixture (R) and (S) – Ibuprofen of which S- is the active form in the human body but R- form can be enzymatically converted to the active or *vice versa*. Ibuprofen has a pK_a value of 4.5 to 4.6 [12] and it is dissolved at higher pH value because of the ionization of its carboxylic acid group. It is a potent non steroidal anti-inflammatory drug (NSAID) widely used in the treatment of rheumatoid arthritis, osteoarthritis, ankylosing spondylitis and mild to moderate pains associated with migraine, fever and dysmenorrhea. It is considered the safest of the NSAIDs in the treatment of pain due to

inflammatory responses and feverish conditions. It is one of the most frequently prescribed and best tolerated NSAID, especially in children, because of its high benefit-to-risk profile [13-14].The inflammatory activity of ibuprofen is due to the inhibition of cyclooxygenase-2 (COX-2) an enzyme responsible for the production of inflammatory mediators such as prostaglandins [15].

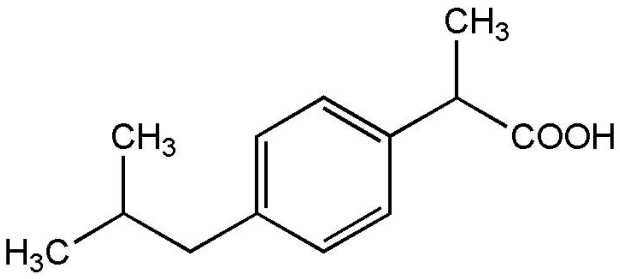

Figure 1: The chemical structure of ibuprofen.

When administered orally, conventional dosage forms of ibuprofen are rapidly and almost completely absorbed from the gastro intestinal tract with peak plasma concentrations between 15 and 25 µg/mL occurring within 1 to 2 h [16]. The excretion is usually complete after 24 h of administering the last dose. However ibuprofen has hydrophobic characteristics, practically insoluble in water with saturation solubility of 49 µg/mL at room temperature [17]. Therefore it is difficult to formulate as aqueous solution and the dosage release from aqueous based hydrogels could be variable and unpredictable. Ibuprofen also has a short biological half-life (approximately 2 h) and its solubility and permeability are pH dependent [18]. It is poorly soluble at acidic pH of the stomach but solubilizes at alkaline pH of the small intestine. Its poor solubility (log P value 3.6) in the stomach limits its absorption before gastric emptying (30 min to 2 h) occurs. Although ibuprofen solubilizes in the small intestine, its ionized species cannot permeate through the intestinal membrane [19]. It follows that when administered orally, ibuprofen tends to be eliminated from the gastro-intestinal tract before having the opportunity to dissolve fully and be absorbed into the circulation, resulting in incomplete absorption as well as low and erratic bioavailability with a consequent poor dosing proportionality [1]. This phenomenon translates to low systemic bioavailability requiring the use of high and multiple daily dosing to maintain the required plasma concentration for effective

therapeutic activity. The usual consequence includes wasted dosing as well as potentially serious gastro intestinal side effects such as bleeding and ulceration. Ibuprofen belongs to the Biopharmaceutics Classification System (BCS) class II which exhibits poor water solubility and high membrane permeability [20]. The rate limiting step for BCS class II drugs is dissolution. BCS which was proposed by Amidon *et al.* is a system that classifies orally administered drugs into four classes based on their solubility and intestinal permeability [21]. Attempts to enhance drug solubility of BCS class II drugs have been shown to correlate well with increased bioavailability [22]. It has also been reported that rapid absorption rate of oral formulations of ibuprofen enhanced its analgesic properties [23].

The high dose requirement and poor solubility of ibuprofen have limited its application in transdermal drug delivery and all efforts in this regard have not been successful. Although ibuprofen is available as bulk topical gels, the drug loading efficiency has been limited by its poor solubility and the dosage is highly variable. Presently, it is difficult to quantify the effective dose for pain relief in the existing ibuprofen topical gels and other drug patches due to inadequate skin penetration profiles. Formulation strategies are still required to design fixed dose topical ibuprofen gel with enhanced dissolution profile adaptable for transdermal delivery in the management of pain.

Pain is the most common symptom for which patients seek help. Over 10 million adults (6 million women and 4 million men) in the UK consult their GP each year with arthritis and related conditions. The prevalence increases with age with 1 in 10 people aged between 15 and 24 years consulting their GP each year with a musculoskeletal problem increasing to 1 in 3 people over the age of 75 years [24]. Between 2006 and 2007 in England and Wales, a total of 58,952 hip replacements and 62,150 knee replacements were carried out with between 94 and 97% due to osteoathritis [25]. Pain relief is a significant part of arthritis treatment and varieties of commercial topical formulations containing ibuprofen are available to manage arthritic conditions.

In most developed economies, adults are living longer and they continue to make frantic efforts to lead an active lifestyle. This tends to expose them to continuous incidence of pain as a result of muscle and joint injury or underlining disease condition. It has been projected that half of the adult UK population will be aged over 50 years within the next 20 years [26]. It follows that the demand for pain management will continue to increase hence further research into optimization of ibuprofen delivery is inevitably a continuous process.

The delivery of NSAIDs through the skin for soft tissue and joint pain has been shown to be as equally effective as and preferred over the oral route in randomized clinical studies because they offer fast onset of actions as they are applied directly to the target site with fewer side effects. Local irritation of the skin such as pruritus and dermatitis which resolved on withdrawal of the therapy was also reported [27]. Literature is replete of randomized clinical studies that demonstrate the superiority of topical NSAIDs over placebo however comparison with oral NSAIDs has not been conclusive. It was reported that topical NSAIDs are highly effective in relieving pain functions and stiffness during the first few weeks of treatment of osteoarthritis compared with placebo but were less effective than oral NSAIDs at any given week [28]. However it was evident that topically applied NSAIDs presented far less 'common side effects' than the oral route [29]. The group on oral route had more severe respiratory adverse effects. The authors opined that topical NSAIDs diffuse directly into the target joints and tissues [30]. This may imply high concentration of the drug at the site of action but low plasma concentration which is the reverse of oral administration. Furthermore over 80% of orally administered drug is removed by the digestive system with a consequent reduced therapeutic effect and severe localized side effects due to increased dose [28].

Transdermal route of drug delivery has gained significant attention recently because it avoids the pre-systemic metabolism and instability in acidic environment of the stomach when administered orally. It also provides consistent levels of drug at the site of action for prolonged period of time. Transdermal formulations are designed to facilitate diffusion through the layers of the skin into the systemic circulation [31], while for topical drug formulations, the site of action is the tissue directly

underlying the application site, including the soft tissue and peripheral nerves [29]. The skin offers diverse advantages as a site of drug administration however due to its natural properties as a protection barrier and the intrinsically poor permeability of the drug, permeation of poorly soluble drug through the skin is difficult. It is therefore necessary to search for new strategies to enhance the penetration of drugs [32]. Drug carrier systems have been proposed in order to favour the transport of drugs through the skin, enabling drug retention and in some cases allowing a controlled release [33-36]. Polymeric nanoparticles have also been reported to form a depot in the hair follicles, giving a targeted drug controlled drug delivery [37].

New research efforts are being focused on lipid coated microgels [38] and short acting patches as transdermal delivery systems but both have been limited by poor transcutaneous absorption with inaccurate and unpredictable dosages.

Hydrogels have been of great value in topical administration of many drugs based on their high water content (95%) [39], reduced surface tension with water, soft and rubbery consistency characteristics. Their water holding capacity is based on the presence of hydrophilic groups such as amino, carboxyl and hydroxyl groups in the polymer chains. Their three dimensional polymer networks are capable of absorbing and retaining large amount of water and swelling; this could modulate their biocompatibility, permeability and hydrodynamic, surface and mechanical properties. These properties could be modified to control the movement of drug molecules of different sizes to diffuse into the polymer network (drug loading) and design intelligent controlled release systems for site specific drug delivery. Hydrogels have been used to develop oral, nasal, ocular, rectal, transdermal and implantable drug delivery systems (DDS) [40]. The concept of 'intelligent', 'smart' or 'stimuli'-responsive DDS is based on the swelling and permeability characteristics of hydrogels and their ability to undergo structural changes in response to physical, chemical and biological stimuli (*bio mimetic)*.

Hydrogels liquefy on contact with the skin without visible stain compared with cream, ointment or pastes. Their high proportion of water allows free movement of drug molecules as in pure water. Generally the mobility of aqueous solutions predisposes them to absorption problems and erratic bioavailability because they only allow a short contact time with the skin or mucosa. Research efforts to solving this problem include distribution of the drug in micelles and liposomes, electrostatic interaction of the drug with the gel polymer and suspending the drug in the gel matrix [41]. However the rheological properties of gel formulations could increase contact time via mucoadhesion (mucosa) resulting to increased absorption if there is sufficient amount of active drug in the hydrogel throughout the contact period. Research efforts to date have not been able to establish the desired improvement in drug loading efficiency, absorption and bioavailability profiles of hydrogels therefore research interest in this area is continuous.

1.2. Previous research efforts in delivering poorly soluble drugs

Formulation approaches used in delivering poorly soluble drugs include traditional methods of solubility enhancement through particle size reduction via comminution, solvent recrystallization and spray drying; addition of surfactants such as tweens and poloxamer; polymer inclusion complexation (e.g. cyclodextrin); inorganic complexation; coordination and chelation *etc*. Other novel techniques include self-emulsifying systems; nanoparticularization by solvent evaporation, co-precipitation, emulsion polymerization and co-crystallization as well as nanoconjugation or nano-complexation [42-53].

Particle size reduction by micronization generally increases the surface area of drug powder leading to increase in total surface area and improved dissolution properties of the drug [42]. However various disadvantages of these technique have been reported including formation of coarse drug powder with broad particle size distribution due to particle re-aggregation and scaling in the spiral jet mills; contamination of particles with toxic solvents; degradation of products due to thermal or mechanical stress and its unsuitability for drugs with high dose since it does not alter the saturation

solubility of drug [42]. Liversidge and Conzentino prepared a nanoparticulate dispersion of naproxen using pearl milling technique. They used Zirconium Oxide beads in the roller mill to produce naproxen nanocrystals with reduced particle size from 20 µm to 270 nm and improved stability against agglomeration in gastric fluid as well as reduced gastric irritation and improved absorption rates in rats [43].

Peters *et al.* produced clofazimine nanosuspension with particle size suitable for intravenuous injection and passive targeting of the reticuloendothelial system using high pressure homogenization technique [44]. Velaga *et al.* also used solutions enhanced dispersion by supercritical fluids (SEDS) to prepare hydrocortisone particles from acetone and methanol solvents. The authors were able to control the crystallinity of the particles and characterize the morphology and aerodynamic properties of the particles which maybe adaptable for the preparation of inhalation powders for pulmonary delivery [45-46]; Rapid expansion from supercritical to aqueous solution (RESAS) technique was adapted by Young *et al*. to prepare stable suspensions of submicron particles of cyclosporine with particle sizes between 400 and 700 nm. The particle growth and agglomeration was impeded by surfactant (tween 80)-mediated steric stabilization [47]. Spray freezing to liquid (SFL) technique was used by Hu *et al.* to produce micronized carbamazepine powders with significantly enhanced dissolution rates when compared with the bulk carbamazepine [48].

Ibuprofen nanoparticles were formed by rapid expansion of supercritical fluid in a liquid solvent (RESOLV) [49] however, the ibuprofen nanoparticles formed were quick to agglomerate into large aggregates leading to broad particle size distribution. A post production stabilization scheme which involved the use of polymeric or oligomeric stabilization agent - poly (N-vinyl-2-pyrrolidone) was required to reduce the aggregation of the ibuprofen nanoparticles. The authors reported that the carrier-free solid drug nanoparticles obtained from RESOLV exhibited high drug loading capacity with increased efficacy at reduced excipient concentration. The strength of this technique is that RESOLV does not utilize any surfactant or organic solvent.

Surfactants have been used to improve the dissolution of poorly soluble drugs by lowering the surface tension and increasing the solubility of the drug within the solvent. They are also used to stabilize drugs dissolved in microemulsions and suspensions. Kayser *et al.* used tween 80 as surfactant to develop amphothericin nanosuspension using high pressure homogenization technique. The resulting nanosuspension exhibited significant reduction in liver parasite (*Leishmania amastigotes*) load by 28.6% indicating an improved oral absorption and systemic efficacy when compared with commercial formulations available [50].

Drug inclusion complexation with cyclodextrin has been reported to solubilize high dose drug products and drugs with high melting points. Cyclodextrins (CDs) are cyclic oligosaccharides with its natural derivatives possessing limited aqueous solubility however the synthetic CDs have improved solubility but limited drug inclusion capacity. The solubilizing effects of CDs have been improved by their addition to hydrophilic polymers. Maestrelli *et al.* prepared two hydrophobic drugs, triclosan and furosemide, complexed with cyclodextrin and further entrapped in the chitosan nanocarrier. The authors found that the drug-cyclodextrin complex was efficiently entrapped in the nanoparticle system [34] and the drug release profile of the drugs was biphasic with an initial fast release followed by a delayed release phase. This nanosystem offered a potential in transmucosal delivery of hydrophobic drugs.

Nanoconjugation or nano-complexation has also been used in the delivery of poorly soluble drugs. Nanoparticles as drug carriers can be formed from biocompatible and biodegradable materials such as polymers. In recent years, biodegradable polymeric nanoparticles have attracted considerable attention as potential drug delivery devices in view of their applications in the controlled release of drugs; targeting particular organs/tissues; as carriers of DNA (Deoxyribonucleic acid) in gene therapy, and in their ability to deliver proteins, peptides and genes through the per oral route**.** Nanosizing of poorly soluble drugs is a rapidly developing technique in the field of medicine to achieve safe and effective drug delivery [51]. Their potential applications include enhanced molar solubility, increased dissolution velocity, controlled release, tissue targeting in cancer therapy,

carrier action for the delivery of peptides, enhanced cell penetration, improved efficacy and reduced side effects *etc.*[52-53].

Nanoscale drug delivery systems enhance solubility and dissolution rates due to massive increase in specific surface area; they can also cross the capillary barriers and flow freely in blood circulation enhancing the bioavailability of the drug. Polymeric nanoparticles have high structural integrity due to the rigidity of the polymer matrix.

Nanoparticles for the purpose of drug delivery are amorphous or crystalline submicron (< 1 μm) solid, colloidal particles including nanospheres and nanocapsules of sizes between 10 and 1000 nm [54]. Nanocapsules are vesicular systems in which the drug is confined to a cavity (aqueous or oily core) surrounded by a unique polymer membrane or shell like wall, while nanospheres are matrix systems in which the drug is physically and uniformly dispersed [55]. Polymer nanoparticle is a collective term used for any type of polymer nanoparticle, particularly for both nanocapsules and nanospheres.

First polymer nanoparticles for pharmaceuticals were prepared in the late 1960's and early 1970's [56]. Different techniques have been employed in the production of polymeric nanosized drug particles based on preformed polymers or by direct polymerization of monomers. Polymerization of monomers involves techniques such as micro-emulsion, mini-emulsion, surfactant-free emulsion and interfacial polymerization. Preformed polymers utilize techniques such as solvent evaporation, salting out, dialysis and supercritical fluid technology.

Solvent evaporation was the first method and the most widely used in the preparation of polymeric nanoparticles. The method of preparation involves the dispersion of the polymer in volatile solvents by high speed homogenizers or ultrasonication to form emulsions on addition of the aqueous phase containing stabilizers, which gives a nanosuspension on evaporation of the solvent, diffusing through the continuous phase, by continuous stirring, heat or vacuum [57]. The emulsions are either prepared as single emulsions (oil-in-water emulsion) or double emulsions (water-in-oil-in-water

emulsion). The nanosuspension formed is then ultra-centrifuged and washed with distilled water to remove additives and lyophilized. The organic solvent should be able to dissolve both the oil and polymer, be partially water soluble to aid the diffusion step and be safely removed under reduced pressure [58]. Ethyl acetate has been used to replace dichloromethane and chloroform based on its better toxicological profile [59]. Lemoine and Preat prepared poly (D, L-lactide-coglycolide) (PLGA) nanoparticles loaded with hemagglutinin (HA) by the single and double emulsion methods to achieve 200 nm particle size [60]. Poly vinylalcohol PVA (emulsion) or Span 40 (double emulsion) was used as surfactants. Increased concentration of PVA resulted in marked decrease of particle size. PVA decreased the particle size compared to Span 40. The particle size was influenced by the surfactant type and concentration; homogenizer speed and evaporation. The PLGA nanoparticles were easily resuspended after freeze drying without variation in size. HA was well encapsulated, however, it was difficult to quantify the amount of HA encapsulated within the nanoparticles.

The simplicity of the solvent evaporation method has been overwhelmed by the possibility of the nano droplets coalescing during evaporation thereby affecting the final particle size and morphology and the method being time consuming [61].

Salting-out method involves the separation of water miscible solvent from aqueous solvent. It could also be described as a modified emulsification/solvent diffusion method. Alleman *et al.* prepared polymeric nanoparticles by adding a high concentration of electrolyte (sodium chloride, calcium chloride, and magnesium chloride or magnesium acetate) containing water soluble stabilizing polymer (polyvinylpyrrolidone or hydroxyethlcellulose) to acetone polymer solution under continuous stirring. The acetone was prevented from mixing with water by the saturated aqueous solution via salting out. Addition of excess water facilitated the complete diffusion of acetone into the aqueous phase resulting in the production of nanospheres [62]. The authors avoided the use of surfactants and chlorinated solvents in the preparation.

Salting-out is non-dependent on temperature, which makes it useful in the preparation of heat sensitive substances [63]. It also minimizes stress to protein encapsulants [64]. However, it is applied exclusively to lypophilic drugs and its cumbersome extensive washing up steps has limited its use [65].

Nanoprecipitation method developed by Fessi *et al.* [66] is also referred to as solvent displacement method. It is based on the interfacial deposition of a polymer after displacement of a semi-polar solvent, miscible with water from a lipophilic solution. Solvent diffusing rapidly into non-solvent phase causes a decrease in the interfacial tension between the two phases, increasing the surface area and ultimately forming small droplets of organic solvent [66]. The slow addition of the organic phase to the aqueous phase under moderate stirring results in polymeric nanoparticles. Yordanov and Dushkin prepared poly (butylcyanocrylate) nanoparticles loaded with chlorambucil coated with three stabilizers (Polysorbate-80, Pluronic-F68 and Dextran 40) [67]. The solvent used was acetone with nanoparticle sizes in the range of 210 to 269 nm. The authors suggested that the polysorbate-80 coated nanoparticles could overcome blood-brain barrier and multi drug resistance in cancer therapy. Nehilla *et al*. prepared surfactant free ubiquinone (CoQ10) loaded PLGA nanoparticles with acetone as solvent [68]. Particle sizes of about 165 nm were achieved with sustained release for two weeks. It has great potential in antioxidant therapy.

There are three stages in the process of particle formation in nanoprecipitation method : nucleation, growth and aggregation as described by Lince *et al.* [69]. Nucleation is the creation of a new solid phase from a super-saturated solution where small clusters are initiated; molecular growth is the attachment of the single molecules into the particle matrix after diffusion from the bulk of the supersaturated solution to the particle surface and it is the continuous rate of change of particle size; while aggregation occurs when individual nuclei coalesce into larger clusters and is based on the frequency of collisions and their stability. The particle size distribution is determined by the rate of each stage and this principle is based on super-saturation which is the ratio of polymer concentration and the solubility of the polymer in the solvent mixture [69]. Barichello *et al.* assessed

the drawback and advantages of this method and found that hydrophilic drugs such as vancomycin and phenobarbital were poorly encapsulated by PLGA nanoparticles with encapsulation efficiency of 12.1% and 9.1% respectively while lipophilic drugs such as cyclosporin A and indomethacin had good encapsulation efficiency of 83.7% and 93.9% respectively [70]. Encapsulation had been increased from 2.6 to 9.3% , by modifying the solubility of cloricromene (anti-ischemic drug) in poly (D,L-lactide)–PLA nanoparticles by changes in pH to 11; increasing the aqueous pH from 5.8 to 9.3 increased the encapsulation efficiency from 11 to 58% for procaine hydrochloride PLGA nanoparticles [71-72].

Ibuprofen nanoparticles were prepared based on dextran-drug conjugates applying *in situ* activation of N,N(')-carbonyldiimidazole (CDI) by nanoprecipitation method via dialysis and dropping technique [73]. The molecules self assembled into nanoparticles in the absence of surfactants. However, improved stability of the nanoparticles can be obtained by the addition of non-ionic polymeric surfactant. A remarkably high loading capacity was achieved with the drug content obtained varying from 37 to 71%. The authors assumed that the hydrophobic ibuprofen moieties are located in the interior of the particles because it is established that nanoparticles based on dextran esters possess a hydrophobic core [74]. Nanoprecipitation is a simple and reproducible method, but the low polymer concentration in the organic phase has posed a formulation challenge which is a drawback.

Dialysis involves dissolving the polymer in organic solvent and placing it inside a dialysis tube with proper molecular weight cut off performed against a non-solvent miscible with the former miscible solvent. Lee *et al.* prepared carboxylic acid poly (ethylene oxide)-poly (lactide) (PEO-PLA) block nanoparticles with particle size range of 30 to 40 nm suitable for injectable drug carrier and drug loading efficiency increased when carboxylic acid content was increased in the block copolymer [75].

Co-precipitation method is a modification of complex coarcervation method. Complex coarcervation is formed in a system with two dispersed hydrophilic colloids of oppositely charged electrolytes when mixed in an aqueous solution. The colloid-rich phase is called the coarcervate phase while the

phase with the little colloid is called the equilibrium fluid [76]. Micrometric or nanometric particles are formed based on process variables which include temperature, pH, ionic strength, molecular weight and polyelectrolyte concentration.

Co-precipitation is used in the preparation of nano-scale core-shell particles and it enhances the dispersion stability of poorly soluble drugs during storage. It is a technique used in microencapsulation. Co-precipitation can be induced in systems which contain anionic and cationic hydrophilic colloids. Ibuprofen sodium salt nanoparticles stabilized by diethylaminoethyl dextran, DEAE-Dextran (Ddex) were prepared via the co-precipitation method [8]. DEAE-Dextran was deposited unto precipitated ibuprofen (Ib) particles from a supersaturated solution through electrostatic interaction. The authors found the particles had a core-shell structure formed at pH 6 for Ddex/Ib weight ratio of 5:1 containing 32% of ibuprofen. Ibuprofen was further identified as the core and DEAE-Dextran as the shell. Electrostatic complexation was found to dominate the Ddex/Ib particles instead of the co-precipitation mechanism.

Emulsion polymerization involves the polymerization of monomers. Water can be used as the dispersing medium. Based on surfactant, it can be grouped as conventional emulsion polymerization or surfactant-free emulsion polymerization [77]. Conventional emulsion polymerization utilizes water, a monomer of low water solubility, water soluble initiator and a surfactant in its formulation reaction to produce polymeric nanoparticles containing many polymer chains. Four differentially charged surfactants (sodium dodecyl sulphate-(SDS); cetyltrimethylammonium bromide-(CTAB); 3-(N,N-dimethylmyristylammonio)propanosulfonate-(DMMA-PS) and dodecanoic acid 2(2-hydroxyethoxy)ethyl ester-(DDA-HEEE)) were used to prepare poly (butyl acrylate-styrene) nanoparticle emulsions loaded with antibacterial agent penicillin with particle size range of 42 to 332 nm [78]. Removal of surfactants is time consuming with additional cost burden a drawback. Therefore, surfactant-free emulsion polymerization has been used as alternative. Surfactant-free polymerization utilizes deionized water, a water soluble initiator (potassium persulfate) and monomers (vinyl or acryl monomers), where stabilization of polymeric nanoparticles occurs through

the use of ionizable initiators [61]. Bao and Zhang prepared poly (methyl metacrylate) – PMMA nanoparticles by polymerization of methyl metacrylate (MMA) using microwave irradiation [79]. The particle size obtained was controlled by the concentration of MMA (monomer). The particle size increased linearly from 103 to 215 nm as MMA increased from 0 to 0.3 mol/L. Monodisperse and superfine PMMA microspheres were achieved by the polymerization reaction.

The use of most synthetic surfactants has been limited by their toxicity. Therefore this research focuses on using novel, natural, safe and biodegradable polymers to prepare polymeric nano-complex carrier systems to enhance the solubility, dissolution, permeability, release profiles as well as predictable bioavailability of poorly soluble drugs.

1.3. Polymers used in the preparation of nano-conjugates

Natural polymers have attracted attention as potential vehicles for the sustained/controlled release of bioactive materials in recent years. Natural polymers are used more when compared with various synthetic and semi synthetic polymers due to safety issues associated with synthetic polymers although they can be tailored to give a wider range of properties.

Gellan gum is a water soluble, linear anionic polysaccharide gelling agent produced by *Sphingomonas elodea*. It consists of tetrasaccharide repeating units of glucose, glucuronic acid and rhamnose in the 2:1:1 ratio [80] shown in Figure 2.

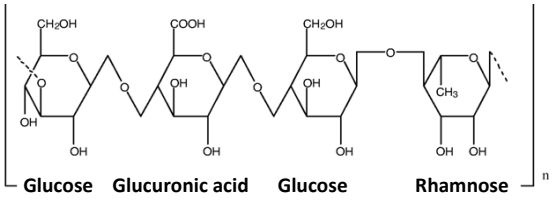

Figure 2 The chemical structure of gellan gum [81].

The gelation of gellan gum is either temperature dependent or cation (monovalent or divalent) induced [82]. The gelation process starts with the formation of double helical junctions from random coil chains, then the aggregation of the double helical segments forming a three dimensional

network by complexation with cations and hydrogen bonding with water [83]. Gellan gum is stable over a wide pH range of 2 to 10 [84]. The pK_a value of gellan gum is 3.06 [85]. Its molecular weight is greater than 70 000 Daltons with 95% above 500 000 Daltons. Gellan gum is mainly used as stabilizer or thickening agent. Gellan gum has been reported to be completely safe for use in food. The European Union has permitted its use as an additive (E418) with generally recognized as safe (GRAS) status in the United States [86] . Miyazaki *et al.* exploited the *in situ* gelling characteristics of gellan in the stomach of animal models (rats and rabbits) in the oral delivery of theophylline [87]. The sustained release of theophylline was achieved for over a period of at least 6 h. Recently, Yang *et al.* prepared chitosan-calcium-gellan beads for controlled release of bovine serum albumin (BSA) protein by combining of ionic gelation and polyelectrolyte complexation methods [88]. Its encapsulation efficiency was in the range of 62 to 85%. The authors found the release of BSA was mainly triggered by Fickian diffusion mechanism with a potential of being a new carrier for the controlled release of protein.

Diethylaminoethyl-Dextran (DEAE-Dextran) is a water soluble polycationic derivative of Dextran produced by reacting diethylaminoethyl chloride with Dextran shown in Figure 3. It is supplied in hydrochloride form. It is freely soluble in water and salt solutions and biodegradable [89]. It has mean molecular weight > 500 000. The solubility is unaffected by pH within the range of 4 to 10. The high amount of hydroxyl groups facilitates the introduction of drugs into its structure [73].

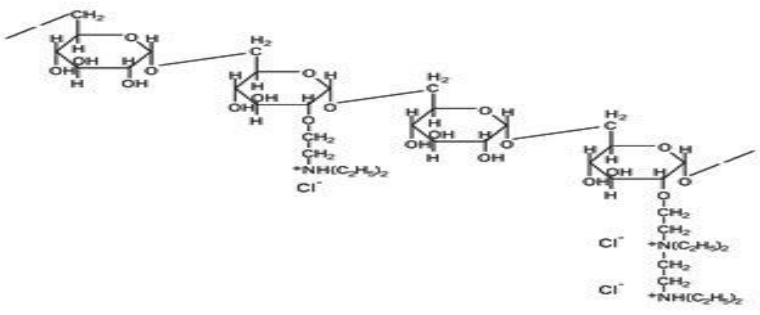

Figure 3 The chemical structure of DEAE-Dextran.

Chitosan is an amino-polysaccharide derived from alkaline deacetylation of chitin, present in the fungal cell walls and exoskeleton of arthropods [90]. Chitosan consists of linear copolymers of (1→4)-2-amino-2-deoxy-β-D-glucan (GlcN) shown in Figure 4. Chitosan is insoluble in water, but soluble in acidic aqueous media due to the protonation of the chitosan amino groups. Chitosan has been used in the preparation of nanoparticles and microparticles due to its characteristics which include its cationic nature, biodegradability, biocompatibility, non toxicity and mucoadhesive character. Low molecular weight chitosan used in this study has a molecular weight in the range of 50 000 to 190 000 Daltons. Chitosan is a positively charged polymer at low pH values (below its pK_a) value. The reported pK_a value of chitosan is 6.5 [91]. Addition of a strong base beyond pH 6.2 leads to the formation of a gel-like precipitate which is due to the neutralization of chitosan amino groups, and the removal of repulsive inter-chain electrostatic forces. This therefore allows for extensive hydrogen bonding and hydrophobic interactions between chains [92]. It spontaneously associates with negatively charged polyions in solution to form polyelectrolyte complexes. The positively charged amino groups of chitosan interact electrostatically with the negatively charged carboxylic acid group of the glucuronic acid unit in gellan gum to form a chitosan-gellan polyelectrolyte complex by self-assembly of their counter ions [93].

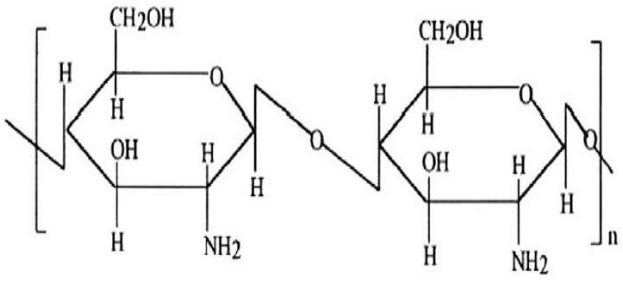

Figure 4 The chemical structure of chitosan.

Various methods for producing chitosan nanoparticles are described in the literature [94-95]. Mao *et al.* prepared chitosan-DNA nanoparticles by complex coarcervation method [91]. The optimized particle size was in the range of 100 to 250 nm with a narrow distribution. The encapsulated plasmid DNA was partially protected from nuclease degradation by the chitosan-DNA nanoparticles. The

nanoparticles were further loaded with chloroquine (CQ) and the drug loading of CQ was found to be 5.2%. The authors reported that *in vitro* drug release could not be accurately determined due to small sample size obtained. Fernadez-Urrusuno *et al.* prepared insulin-loaded chitosan nanoparticles by ionic gelation via mixing insulin with tripolyphosphate (TPP) solution and chitosan solution. Particle size range of 300 to 400 nm with positive surface change in the range of +54 to +25 mV was obtained. The drug loading obtained was up to 55%. The authors found that insulin association was mediated by an ionic interaction mechanism. The nasal absorption of insulin was enhanced by the chitosan nanoparticles.

1.4. Polymer Therapeutics

Polymer Therapeutics entities was first defined as nanomedicines by Prof Ruth Duncan [96]. Polymer therapeutics is made up of complex systems with rationally designed covalent chemical bond between a water soluble carrier and the bioactive molecule(s) [97]. These include polymeric drugs, polymer-drug conjugates, polymer-protein conjugates, polymeric micelles covalently bound to drugs and polyplexes for gene and protein delivery. Drug-polymer conjugates enhance aqueous solubility and also changes the pharmacokinetics of the whole organism and at sub-cellular level thereby possibly enhancing drug therapeutic value [98-99]. The physical properties of polymers have been found to have unique properties useful in the treatment of human diseases, improved drug targeting and circulation, leading to polymer drugs currently being used in routine clinical use [98].

It has been demonstrated that polymer-drug conjugation engenders nano-sized multi-component constructs (nanomedicine) [100]; enhances drug's aqueous solubility, permeability and retention [97, 101]; promotes accumulation and preferential uptake by targeted cells [102]; decreased toxicity; improved pharmacokinetics and programmed drug release profile [103]. These polymer-drug conjugates are considered as New Chemical Entities (NCEs) not conventional pharmaceutical dosage formulation or drug delivery systems that simply physically entrap the drug [97].

In 1990, Maeda *et al*. developed the first polymer-protein conjugate. It consisted of two polymer chains of styrene-co-maleic anhydride (SMA) covalently bound to the antitumor protein neocarzinostatin (NCS) [104]. This conjugate was known as Zinostatin stimalmer (SMANCS). Oily SMANCs was shown to inhibit tumour growth by a range of 63 to 82% in mice bearing various solid tumours [105]. A large number of hepatoma patients treated with SMANCS in the first clinical evaluation showed that 95% had tumour shrinkage and 86% had a decreased concentration of α-fetoprotein level [104]. Polyethylene Glycol conjugated with protein (PEGylated proteins) in the case of PEG-catalase has been reported to retain 93% of its enzyme activity, resisted digestion by enzymes from *Streptomyces griseus,* and enhanced circulating lives in the blood of acatalasemic mice during repetitive intravenous injection [106]. There has also been an increase in the use of responsive polymer-protein bioconjugates (RPPB) for biotechnological applications. These types of polymers respond to different environmental stimuli such as a change in temperature, pH, ionic strength or presence or absence of a specific metabolite in solution *etc*. They undergo rapid yet reversible macroscopic physical and/or chemical changes. The conjugation between responsive polymers and proteins is said to improve functional stability of the protein in different reaction microenvironments, effectively allowing diversification of drug functions. Research has stressed the importance of site-directed bioconjugation, as random conjugation of polymer to protein was shown to lead to heterogeneity which causes denaturation of the protein. However the attachment of polymer to a specific site on the protein may lead to functional stability with better conjugation efficiency. The improvement in functional stability is underpinned by the polymer's ability to protect the protein from its local microenvironment until it reaches its target, at which point the polymer releases the protein and enhances the desolvation properties involved in the protein's binding to its target.

The conjugation between polymer and enzyme has been researched in depth over the past couple of decades. The first polymer-enzyme (PEGylated enzyme) to be approved for clinical use was the conjugation between PEG and L-asparaginase, also known as Oncaspar® [107]. In 1994, Oncaspar®,

an anti-tumour PEGylated protein, was approved for the treatment of acute lymphoblastic leukaemia. This conjugate involved the formation of multiple PEG chains linked to the enzyme with advantages of reduced hypersensitivity, longer plasma half life and slower total clearance. The conjugation between PEG and recombinant arginine deaminase (PEG-rhArg) has been developed to treat hepatocellular carcinoma as a single agent or combined with 5-fluorouracil (5-FU) [108]. It was noted that the activity and stability of orderly-arranged enzyme bioconjugates is typically higher than for the randomly-conjugated enzyme because specific conformations of the bioconjugate may optimize availability of substrate without, on the other hand, modifying the active site. PEG-granulocyte stimulating factor (PEG-GCSF), neulasta has also been used to prevent cancer chemotherapy induced neutropenia with benefit of less frequent administration [109]. It was noted that polymer-cytokine conjugates, like polymer-protein conjugates generally, display enhanced activity as a result of enhanced bioavailability without loss of function. Polymer-proteins are now used routinely anti-cancer therapeutics as an adjunct to chemotherapy [96].

Due to the clinical success of polymer-protein conjugates and polymer-peptide conjugates, research has focused on developing strategies to form equally effective polymer-drug conjugates. Polymer-drug conjugates are defined as nano-sized hybrid constructs that bind with the biomolecule covalently to ensure efficient delivery and adequate availability at the site of action [110]. The combination of drug and polymer has been shown to be effective in cancer therapy, and is becoming accepted as a new class of antitumour agents [99]. In contrast with the bioavailability-enhancing effects of polymers on proteins, the enhancement of drugs by polymers appears to be due to increased stability, which leads to enhanced permeability and retention [111]. This type of conjugation has the ability to improve the therapy of common drug-resistant solid tumours by decreasing toxicity and improving activity in chemotherapy-refractory patients. The modification is often mediated by the formation of stable bonds such as ester, amide, and disulphide. These bond linkages must be stable enough to prevent the early release of the drug, i.e. during transport before cellular localization of the drug. Covalent bonds (e.g. ester or amide) are stable and could deliver the

drug at the targeted site, but such bonds may only easily release the targeting agent (peptides) under the influence of acceptable environmental change [112]. N-(2-Hydroxypropyl) methacrylamide (HPMA) copolymers were used as carriers for most of the anticancer drug conjugates. Two HPMA copolymer-doxorubicin conjugates were produced in the early 1980s by Duncan *et al.* which progressed into phase I/II evaluation [113]. In terms of physical stability, Williams *et al.* investigated the use of polymer-drug conjugates to modify the physical properties (improving aqueous stability) of the cytotoxic drug, 7-ethyl-10-hydroxycamptothecin (SN-38) using reversible addition fragmentation chain transfer [114]. The research emphasized the importance of growing a water soluble polymer of defined size, composition and shape from hydrophobic antitumour agents. This offers a means of improving the physical properties of the drug while simultaneously introducing specific targeting elements. This work also stressed the importance of the site at which the polymer is attached to the drug to the success of the conjugate formed, as has been found for polymer-protein conjugates.

Polyethylene glycol (PEG) and N-(2-hydroxypropyl) methacrylamide (HPMA) copolymers used as the polymer components in polymer-protein and polymer-drug conjugates respectively are non-biodegradable. A number of polymer-protein conjugates have been in the market since the 90's however none of the polymer-drug conjugates under intensive research efforts have yet reached the market [97]. The slow progression of transforming polymer-drug conjugates into clinically useful medicines for clinical evaluation for regulatory approval has been due to clinical failure owing to 'wrong conjugate rational design' that yielded unspecific drug release [115-116].

Polymer–protein conjugates are in the market or in the clinical development phase [117]. Issues of great consideration regarding the suitability of polymers or their conjugates for development include; safety following acute or chronic use, primary metabolites that could be formed and their fate, reproducibility, possibility of achieving validated characterization of all components, acceptable stability and suitability for patients, reproducible efficacy, cost effectiveness and variability based on the physical attributes of the polymers and terminologies used [117].

1.5. Polyelectrolyte Complexation (PEC)

Polyelectrolytes are macromolecular species with repeating units bearing charged groups. Positively or negatively charged entities are formed when the charged group dissociate in aqueous solution. Polyelectrolyte complexes (PECs) are association complexes formed due to electrostatic attraction between oppositely charged polyions (polymer-polymer, polymer-drug and polymer-drug-polymer [118]. PECs circumvents the use of chemical crosslinking agents, thereby reducing the toxicity and other side effects associated with the cross-linkers.

Polyelectrolytes are classified based on electrochemistry as cationic (DEAE-Dextran and chitosan), anionic (gellan) and zwitterionic (proteins). They are also classified based on origin as natural, synthetic and chemically modified biopolymers.

Polymeric self-assembly or polyelectrolyte complex is formed by the spontaneous association of oppositely charged polyelectrolytes in solution. The complex formed is insoluble in aqueous solution. The use of chemical cross-linking is avoided, which reduces the possible toxicity and unwanted side effects that may be caused by the potential cross-linkers.

PEC could be formed by using a possible mechanism of electrostatic forces and Flory-Huggins mixing free energies of the polyelectrolytes [119-121]. PECs formed are applied in different dosage forms for the formulation of stable aggregated macromolecules.

The formation of polyelectrolyte complexes involves 3 steps as shown in Figure 5 [118]. A primary complex is formed in the first step based on Coulomb forces. This undergoes intracomplex formation in the second step based on new bonds formation and correction of the polymer chains distorted. And finally undergoes intercomplex aggregation process in the third step based on aggregation of secondary complexes via hydrophobic interactions.

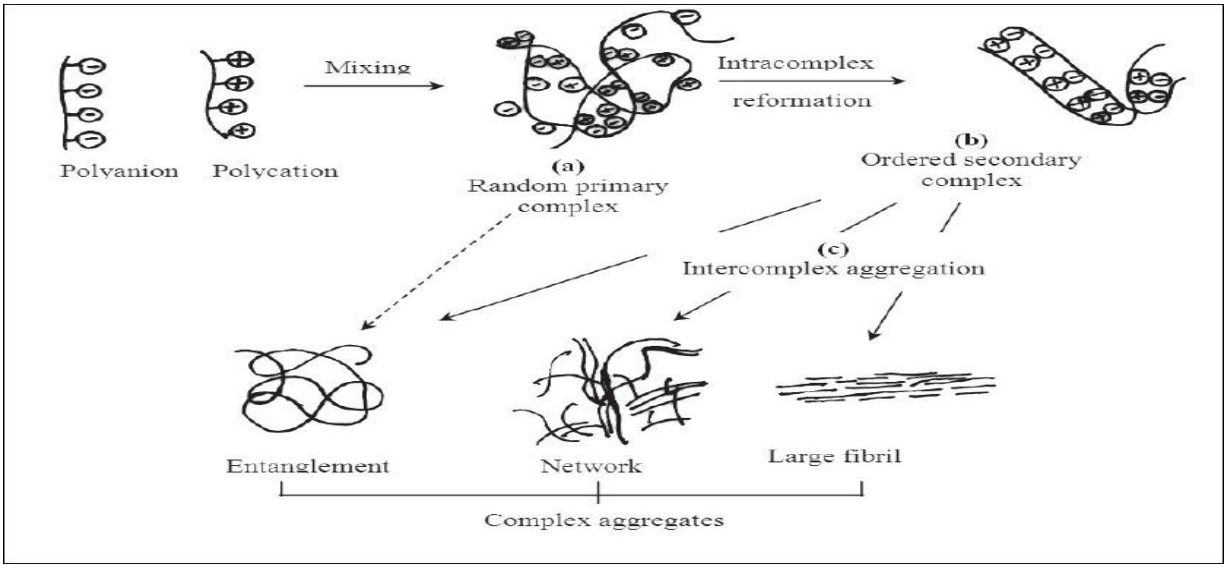

Figure 5 Schematic representation of the formation and aggregation of PECs (a) Primary complex formation (b) Formation process within intracomplexes (c) Inter complex aggregation process [118].

Factors affecting the formation and stability of polyelectrolyte complexes include: the density of the charges on the polyelectrolytes, the charge distribution over the polymeric chains, the degree of ionization of each of the oppositely charged polyelectrolytes, the concentration of the polyelectrolytes, the molecular weight of the polyelectrolytes, the order of mixing, the ratio of mix, time taken for interaction to be completed, the nature of the ionic groups, the charge distribution over the polymeric chains, the position of the ionic groups on the polymeric chains, the polymer chain flexibility, the temperature; ionic strength and pH of the reaction medium [122-124].

The occurrence of charge to charge interaction of polymer-drug and polymer-polymer has been investigated for controlled release of drugs [125-126]. Genta *et al.* prepared oxychitin-chitosan microcapsules with encapsulation efficiency of 49 to 67% [125]. The microcapsules exhibited external layer of polyelectrolyte complex and a core of oxychitin with miconazole crystals and it delayed the release of miconazole. Macleod *et al.* also investigated the polyelectrolyte complex between pectin and chitosan loaded with paracetamol in the film preparation [126]. The results suggested that a bimodal drug release of paracetamol can be achieved when applied as a film coat to tablets for an increased rate of release in the colon.

Four possible mechanisms of complexation of the active drug with the PEC include: entrapment of the active drug during complex formation; incorporation of the drug into the complex after it has formed; binding of the drug to one polyelectrolyte before complexation; and the drug forming a PEC itself by acting as a poly-ion [127]. Drug release can be by solution equilibrium, ion exchange, charge interactions, de-complexation or degradation of the complex [118]. Soluble non-stoichiometric complexes are formed when PECs are made with excess of one charge while insoluble stoichiometric complexes or precipitate are formed when the PECs has equal amounts of both charges [128].

These PECs have been characterized using different techniques including measurements of turbidity, ionic strength, pH [129] viscosity [130], weight polymer ratio in the solution [131], light scattering [132], infrared spectroscopy, thermal analysis, NMR, pK_a and powder X-ray diffraction [133].

Swellable drug-polyelectrolyte matrices (SDPM) were investigated by Jimenez-Kairuz *et al.* by loading different basic drugs-atenolol, lidocaine and metoclopramide onto carbomer. The basic drugs were slowly released from the matrix with release rates observed in water remaining almost constant over time approaching zero order kinetics. When water was replaced with sodium chloride (NaCl) solution, the release rate was not modified in NaCl solution with the kinetics exhibiting a departure from zero order kinetics but was raised in acidic media (0.1 N HCl) with a moderate burst effect. They found that lidocaine and atenolol matrices showed delivery properties based on the proportion of drug loading [134]. Interfacial polyelectrolyte complexation method was used by Liao *et al.* to prepare drug loaded chitosan-alginate fibers [135]. This method showed great potentials for producing drug loaded fibers with high encapsulation efficiency of 72 to 92% and sustained release kinetics exhibited by avidin and platelet-derived growth factor-bb (PDGF-bb) with sustained release of up to 3 weeks. The prolonged release of diltiazem clorhydrate from two polymer matrices system chitosan-alginate and chitosan-carrageenan PECs or mixtures were compared by Tapia *et al.* [136]. They found that chitosan-alginate systems exhibited a better prolonged release profile of diltiazem clorhydrate than chitosan-carrageenan systems because the drug release is controlled at low percentage of the polymers in the formulation. For the chitosan-alginate systems, the swelling

behaviours of the polymer controlled the drug release from the matrix while for the chitosan-carrageenan the release mechanism was disintegration instead of the swelling of matrix. The effect of polymer-polymer and polymer-drug interaction; and the release profile of amoxicillin trihydrate and amoxicillin sodium from different copolymer concentration of chitosan and polyacrylic acid were studied by de la Torre *et al.* [137]. The swelling degree of amoxicillin sodium was found to be higher than the amoxicillin trihydrate hydrogels. The degree of ionization highly controlled the water uptake properties of the hydrogels. Amoxicillin sodium exhibited a slightly faster release profile than the amoxicillin trihydrate formulations. Non-Fickian or anomalous release mechanism was exhibited by both amoxicillin sodium and amoxicillin trihydrate formulations.

Ionotropic gelation method was used by Win *et al.* to prepare ibuprofen loaded phosphorylated chitosan (PCS)-tripolyphosphate (TPP) PEC gel beads [138]. The release rate of ibuprofen from PCS gel beads in different dissolution medium was found to be higher at pH 7.4 than at pH 1.4 due to the electrostatic repulsion between negatively ionized carboxyl group of ibuprofen and phosphate group in PCS in pH 7.4 media; and higher solubility of ibuprofen at pH 7.4 (alkaline medium). Solid interpolymer complex as controlled release matrix for oral delivery was prepared by Rolfes *et al.* [139]. The method was based on either encapsulating the drug in the interpolymer complex before spay drying or adding it at a later stage of the formulation process.

PEC nanoscale hydrogels have also been studied for the purpose of poorly soluble drug delivery. Dispersed nanogel particles are of particular interest because they exhibit intrinsic properties of gels combined with the properties of colloids, such as micro heterogeneous structure, small size and high surface to volume ratio. Drug delivery from colloidal systems dispersed in a hydrogel appears to be unique when compared with the delivery from traditional topical and dermatological formulations.

Solid lipid nanoparticle (SLN) and nanostructured lipid carrier (NLC) enriched hydrogels were developed for transdermal delivery of nitrendipine [140]. The developed gels increased the efficacy of nitrendipine for the therapy of hypertension in comparison with oral nitrendipine. Carbopol SLN

and carbopol NLC gels significantly controlled hypertension from the first hour. Both the Solid Lipid Nanoparticle (SLN) and the Nanostructured Lipid Carrier (NLC) dispersions and the gels enriched with SLN and NLC possessed a sustained drug release over a period of 24 h.

Patel *et al.* developed cationic hydrogels with specific delivery for antibiotics in the treatment of *H. pylori* infection in peptic ulcer disease [141]. Drug release from the freeze-dried chitosan-poly (ethylene oxide) (PEO) semi-inter penetrating network (IPN) hydrogels after 2 h in simulated gastric fluid (SGF) for amoxicillin and metronidazole were 65% and 59% respectively. The results suggested that the freeze dried chitosan-PEO semi-IPN could be used for local delivery of antibiotics in the acidic environment of the gastric fluid.

PEC multi-layer is an example of PECs on the surface scale. One polycation/polyanion layer is called double layer or bilayer. On immersion of polyanion layer of film into polycation solution, there is a diffusion of the polycation chain towards the film which strongly interacts with the outer negative layer to form polyelectrolyte complexes. PEC nanoparticles are examples of PEC in the field of dispersions.

The interaction between oppositely charged polymers, copolymers and surfactants in aqueous media could give rise to the formation of association nano-structures or complexes which exhibit a core-shell in form of dense coarcervate of micelles surrounded by the polymer. Drugs can be covalently bound or physically entrapped in the core of the polymeric nano-complexes. In the present study, advantage is being taken of the electrostatic interaction between oppositely charged polymers and surfactants, formation of polymer micelles and the finite sizes of the complexes to develop different biomaterials in the form of nanoparticles, hydrogels and pharmaceutical films as a delivery tool for poorly soluble drugs.

1.6. Gaps in knowledge

Literature is replete of vast concerted multidisciplinary research efforts to optimize the delivery of poorly soluble drugs by the use of nanotechnology and polyelectrolyte complexation techniques as outlined above. However research on amphiphilic drug-polyelectrolyte and polymer-drug-polymer complexation and their influence on the physicochemical behaviour and drug release mechanism of ibuprofen are limited. To our knowledge the influence of cationic polysaccharide on the crystal habit and micromeritic properties of ibuprofen as well as development of pharmaceutical films and hydrogel of Gellan-DEAE-Dextran nanoconjugate for the delivery of ibuprofen have not been reported. Literature reports on the fixed dose nanoparticle hydrogel for extended delivery of ibuprofen are also lacking.

Furthermore most of the techniques used in literature involve the use of high concentrations of toxic chemical crosslinking agents which are subsequently removed by various techniques including evaporation, vacuum drying, spray drying, fluidized bed drying, lyophilization *etc.* making the process more tedious and expensive. Most reports on these techniques did not address the amount of residual crosslinker present in the final product which could be of great safety concerns. There are also concerns about environmental impact of the chemical crosslinkers as well as the reproducibility and scale up difficulties of the technique. Therefore, there is an urgent need to develop new concepts and techniques that can preclude the use of chemical crosslinkers.

1.7. Research intention

The electrostatic interaction of drug molecules with the polymer gel (drug-polymer conjugates) is a relatively new concept of polymer therapeutics where therapeutic agents are covalently attached to a water soluble polymer in order to optimize drug delivery efficiency as well as the therapeutic quality of the final product. As a weak organic acid amphiphile, ibuprofen ionizes at high pH in aqueous environment to facilitate electrostatic interaction and hydrogen bonding with oppositely charged molecules especially hydrophilic cationic polysaccharides with glucosidic backbone.

In the present study, the knowledge of drug-polymer and polymer-drug-polymer solubilization-complexation techniques have been envisioned to prepare bio mimetic nanoconjugate hydrogels and pharmaceutical films without any organic cross linkers for the extended delivery of ibuprofen as a model poorly soluble drug. The study intended to answer whether nanosize dimensions of ibuprofen could be achieved via the drug-polymer complexation technique and to investigate the mechanism of complexation; the structure of the product formed; the complexation efficiency and the impact of complexation on the physicochemical and morphological characteristics; changes in ibuprofen crystal habit and thermal stability as well as mechanism of release of ibuprofen from the nanoconjugate hydrogels and pharmaceutical films. It was hypothesized that this technique would provide extended and predictable dosage delivery.

This technique would overcome the use of various toxic chemical cross linkers which could be harmful and provide foundation knowledge on the characteristics of binary ibuprofen-polymer and ternary polymer-ibuprofen-polymer nanoconjugates as prospective active pharmaceutical ingredients. In the same vein understanding of the change in crystal habit; isothermal stability; micromeritic and spectroscopic properties of the polymer-drug conjugate would shed light on the type of interaction (physical or chemical) and the capacity of the polymer combination to achieve the desired drug payload as well as other features that govern clinical risk-benefit ratio which are key indices to optimization of polymer-drug conjugate design in order to achieve effective delivery of poorly soluble drugs.

1.7.1. Specific Objectives

- To formulate and characterize oppositely charged polymer-polymer nanocomplexes for the delivery of poorly soluble drugs.
- To formulate and characterize drug loaded polymer nanoconjugates.
- To determine the drug encapsulation efficiency of the nanoconjugates.
- To study the in vitro release profile and kinetics of the drug from the nanoconjugates.

- To formulate and characterize nanoconjugate hydrogels.
- To study the *in vitro* release kinetics of ibuprofen from the hydrogels.
- To formulate and characterize pharmaceutical nanoconjugate films.
- To study the *in vitro* release kinetics of ibuprofen from the pharmaceutical films.

1.8. Novelty of research

Development of pharmaceutical nanoconjugate film for the extended delivery of ibuprofen is novel and would have significant application in the management of pain when drug-loaded pharmaceutical films are used to coat medical devices and pharmaceutical implants which could be adapted for contraceptives and Hormone Replacement Therapy. The polymer-drug binary nanoconjugate technique reduced the particle size of ibuprofen significantly thereby enhancing solubility and extended release of ibuprofen while the ternary nanoconjugate provided some controlled release profiles which could be adaptable to solid dosage form design. The enhanced, extended and controlled drug release from these delivery systems could provide reduction in therapeutic doses of ibuprofen with consequent reduced side effects.

1.9. References

1. Connors, R.D. and E.J. Elder, *Delivery of Poorly Soluble or Poorly Permeable Drugs*. 4th ed. 2003, Fall Church, VA: Technology Catalyst International Incorporation.
2. Horter, D. and J.B. Dressman, *Influence of Physicochemical Properties on Dissolution of Drugs in the Gastrointestinal Tract.* Adv Drug Del Rev, 1997. **25**: p. 3-14.
3. Onishi, H., M. Takahashi, and Y. Machida, *PLGA Implant Tablet of Ketoprofen: Comparison of In Vitro and In Vivo Releases.* Biol Pharm Bull, 2005. **28**(10): p. 2011-2015.
4. Bhattamishra, S.D. and R.K. Padhy, *Estimation of Ibuprofen in Cationic and Anionic Surfactant Media Application of Micelle Binding Model.* Ind J Chem Tech, 2009. **16**: p. 426-430.
5. *Current Problems*. 1983, Committee on Safety of Medicines: London.
6. de Waard, H., H.W. Frijlink, and W.L. Hinrichs, *Bottom-Up Preparation Techniques for Nanocrystals of Lipophilic Drugs.* Pharm Res, 2011. **28**(5): p. 1220-1223.
7. Katteboinaa, S., V.S.R. Chandrasekhar, and S. Balaji, *Drug Nanocrystals: A Novel Formulation Approach for Poorly Soluble Drugs.* Int J Pharm Tech Res, 2009. **1**(3): p. 682-694.
8. Jiang, B.H., L. Gao, C. Shen, J., *Ibuprofen-Loaded Nanoparticles Prepared By A Co-Precipitation Method And Their Release Properties* Int J Pharm, 2005. **304**: p. 220-230.
9. Patel, R.P., H.H. Patel, and A.H. Baria, *Formulation and Evaluation of Carbopol Gel Containing Liposomes of Ketoconazole (Part - II).* Int J Drug Del & Tech, 2009. **1**(2): p. 42-45.

10. Akiyoshi, K.K., S. Shichibe, S. Mix, D. Baudys, M. Kim, S. W. Sunamoto, J., *Self - Assembled Hydrogel Nanoparticle of Cholesterol-Bearing Pullulan as a Carrier of Protein Drugs: Complexation and Stabilization of Insulin.* J Control Release, 1998. **54**: p. 313-320.
11. Comission, B.P., *British Pharmacopoeia 2012*. Vol. 1. 2011, Norwich, Great Britain: Stationery Office Books.
12. Higgins, J.D.G., T. P. Martellucci, S. A. Bruce R. D., *Ibuprofen*, in *Analytical Profiles of Drug Substances and Excipients*, H.G. Brittain, Editor. 2001, London Academic Press: San Diego, London. p. 265-300.
13. Hellman, D.B., ed. *Arthritis and Musculoskeletal Disorders*. Current Medical Diagnosis and Treatment, ed. L.M.M. Tierney, S.J. Papadakis, M. A.. 1992, Appleton and Lange: Stamford.
14. Debley, J.S.C., E. R. Gibson, R. L. Rosenfield, M. Redding, G. L., *The Prevalence of Ibuprofen-Sensitive Asthma in Children; a Randomized Controlled Bronchoprovocation Challenge Study.* J Pediatr, 2005. **147**: p. 233-238.
15. Davies, N.M., *Clinical Pharmacokinetics of Ibuprofen. The First 30 years.* Clin Pharmacokinet, 1998. **34**: p. 101-154.
16. Walson, P.D. and M.E. Mortensen, *Pharmacokinetics of Common Analgesics Anti-inflammatory and Antipyretics in Children.* Clin Pharmacokinet, 1989. **17**: p. 116.
17. Avdeef, A., C.M. Berger, and C. Brownell, *pH-Metric Solubility. 2: Correlation Between the Acid-Base Titration and the Saturation Shake-Flask Solubility-pH Methods.* Pharm Res, 2000. **17**(1): p. 85-89.
18. Mizumoto, T.M., Y. Yamamoto, T. Yonemochi, E. Tarada, K., *Formulation Design of a Novel Fast-Disintegrating Tablet.* Int J Pharm, 2005. **306**: p. 83-90.
19. Lakshmi, P.K.K., K. M. Sridharan, A. Bhaskaran, S., *Formulation and Evaluation of Ibuprofen Topical Gel: A Novel Approach For Penetration Enhancement.* Int J Appl Pharm, 2011. **3**(3): p. 25-30.
20. Lindenberg, M., S. Knopp, and J.B. Dressman, *Classification of Orally Administered Drugs on the World Health Organization Model List of Essential Medicines According to the Biopharmaceutics Classification System.* Eur J Pharm Biopharm, 2004. **58**: p. 265-278.
21. Amidon, G.L.L., H. Shah, V. P. Crison, J. R., *A Theoretical Basis for Biopharmaceutic Drug Classification: The Correlation of In Vitro Drug Product Dissolution and In Vivo Bioavailability.* Pharm Res, 1995. **12**(3): p. 413-420.
22. Leuner, C. and J. Dressman, *Improving Drug Solubility For Oral Delivery Using Solid Dispersions.* Eur J Pharm Biopharm, 2000. **50**(1): p. 47-60.
23. Kokot, Z. and H. Zmidzinska, *Solubility and Dissolution Rate of Ibuprofen in Ionic and Non-Ionic Micellar Systems.* Acta Poloniae Pharmaceutica - Drug Res, 2001. **58**(2): p. 117-120.
24. Unit, R.C.o.G.P.-B.R., *Annual Prevalence report 2006*. 2006.
25. Registry, N.J., *4th Annual Report*. 2008, National Joint Registry for England and Wales.
26. Harper, S., *Don't Panic, We Have Nothing to Fear from an Aging Society*, in *The Sunday Times*. 2008, Times Newspaper Limited: London.
27. Underwood, A.M.A., D. Cross, P. Hennesy, E. Letley, L. Martin, J., *"Advice to Use Topical or Oral Ibuprofen for Chronic Knee Pain In Older People: Randomised Controlled Trial and Patient Preference Study".* BMJ, 2008. **336**(7636): p. 138.
28. Lin, J.W.Z., W. Jones, A. Doherty, M., *"Efficacy of Topical Non-Steroidal Anti-Inflammatory Drugs in the Treatment of Osteoarthritis: Meta-Analysis of Randomised Controlled Trials".* BMJ, 2004. **329**(7461): p. 324.
29. Stanos, S.P., *Topical Agents for the Management of Musculoskeletal Pain.* J Pain Symptom Manage, 2007. **33**(3): p. 342-355.
30. Dreiser, R.L., *Topical Antirheumatic Drug Therapy: Current Practise and Future Trends.* Eur J Rheumatol Inflamm, 1994. **14**: p. 3-8.
31. Brown, M.B., G.P. Martin, S.A. Jones, and F.K. Akomeah, *Dermal and Transdermal Drug Delivery Systems: Current and Future Prospects.* Drug Deliv, 2006. **13**(3): p. 175-187.
32. Cevc, G., *Drug Delivery Across the Skin.* Expert Opin Investig Drugs, 1997. **6**(12): p. 1887-1937.
33. Muller, R.H., M. Radtke, and S.A. Wissing, *Solid Lipid Nanoparticles (SLN) and Nanostructured Lipid Carriers (NLC)in Cosmetic and Dermatological Preparations.* Adv Drug Deliv Rev, 2002. **54**: p. S131-S155.
34. Maestrelli, F.G.-F., M. Mura, P. Alonso, M. J., *A New Drug Nanocarrier Consisting of Chitosan and Hydroxypropylcyclodextrin.* Eur J Pharm Biopharm, 2006. **63**: p. 79-86.
35. Cevc, G., *Lipid Vesicles and Other Colloids As Drug Carriers On The Skin* Adv Drug Deliv Rev, 2000. **56**: p. 675-711.

36. Kim, J.-C.S., M-E. Kim, M-J. Lee, E-J. Park, S-K. Rang, M-J. Ahn, H-J, *Preparation and Characterization of Triclosan-Containing Vesicles.* Coll Surf B, 2002. **26**: p. 235-241.
37. Alvarez-Roman, R.N., A. Kalia, Y. N. Guy, R. H. Fessi, H., *Skin Penetration and Distribution of Polymeric Nanoparticles.* J Control Rel, 2004. **99**: p. 53-62.
38. Kiserab, P.F., G. Wilson, and D. Needham, *Lipid-Coated Microgels for Triggered Release of Doxorubicin.* J Control Rel, 2000. **68**: p. 9-22.
39. Lowman, A.M.P., N. A. , *Hydrogels*, in *Encyclopaedia of Controlled Drug Delivery.*, E. Mathiowitz, Editor. 1999, John Wiley and Sons: New York. p. 397-418.
40. Peppas, N.A.B., P. Leobandung, W. Ichikawa, H., *Hydrogels in Pharmaceutical Formulations.* Eur J Pharm Biopharm, 2000. **50**: p. 27-46.
41. Dew, N., T. Bramer, and K. Edsman, *Catanionic Aggregates Formed from Drugs and Lauric or Capric Acids Enable Prolonged Release from Gels.* J Colloid Interface Sci, 2008. **323**(2): p. 386-394.
42. Aggarwal, G., S.L. Ritika, and Harikumar, *Formulation Tactics for the Delivery of Poorly Soluble Drugs.* Int J PharmTech Res, 2012. **4**(3): p. 914-923.
43. Liversidge, G.C., P., *Drug Particle Size Reduction for Decreasing Gastic Irritancy and Enhancing Absorption of Naproxen in Rats.* Int J Pharm, 1995. **125**: p. 309-313.
44. Peters, K.L., S. Diederichs, J. E. Borner, K. Hahn, H. Muller, R. H. Ehlers, S., *Preparation of a Clofazimine Nanosuspension for Intravenous Use and Evaluation of its Therapeutic Efficacy in Murine Mycobacterium avium Infection* J Antimicrob Chemother, 2000. **45**(1): p. 77-83.
45. Velaga, S.P.G., R. Carlfors, J., *Preparation and Characterisation of Hydrocortisone Particles using a Supercritical Fluids Extraction Process.* Int J Pharm, 2002. **231**(2): p. 155-166.
46. Reverchon, E., *Supercritical Antisolvent Precipitation of Micro- and Nano-Particles.* J Supercrit Fluids, 1999. **15**: p. 1-21.
47. Young, T.J.M., S. Johnston, K. P. Henriksen, I. B. Pace, G. W. Mishra, A. K., *Rapid Expansion from Supercritical to aqueous solution to Produce Submicron Suspensions of Water-Insoluble Drugs.* Biotechnol Prog, 2000. **16**(3): p. 402-407.
48. Hu, J.J., K. P. Williams III, R.O., *Spray Freezing into Liquid (SFL) Particle Engineering Technology to Enhance Dissolution of Poorly Water Soluble Drugs: Organic Solvent versus Organic/Aqueous Co-Solvent Systems.* Eur J Pharm Sci, 2003. **20**: p. 295-303.
49. Pathak, P.M., M. J. Desai, T. Sun, Y., *Formation and Stabilization of Ibuprofen Nanoparticle in Supercritical Fluid Processing.* The Journal of Supercritical fluids., 2006. **37**(3): p. 279-286.
50. Kayser, O.O., C. Yardley, V. Kiderten, A. P. Croft, S. L., *Formulation of Amphothericin-B as Nanosuspension for Oral Administration. .* Int J Pharm, 2003. **254**: p. 73-75.
51. Balogh, L.P., *The future of nanomedicine and the future of nanomedicine.* Nanomedicine: NBM, 2009. **5**: p. 1.
52. Cho, K.W., X. Nie, S. Chen, Z.G. Shin D.M., *Therapeutic Nanoparticles For Drug Delivery In Cancer.* Clin Cancer Res, 2008. **14**: p. 1310-1316.
53. Min, K.H.P., K. Kim, Y.S. Bae, S.M. Lee, S. Jo, H.G. Park, R.W. Kim, I.S. Jeong, S.Y. Kim, K. Kwon, I.C., *Hydrophobically Modified Glycol Chitosan Nanoparticles-Encapsulated Campothecin Enhance the Drug Stability and Tumour Targeting in Cancer Therapy.* J. Control. Rel., 2008. **127**(3): p. 208-218.
54. Kreuter, J., *Nanoparticles*, in *Colloidal Drug Delivery Systems*, J. Kreuter, Editor. 1994, Marcel Dekker: New York. p. 219-342.
55. Kreuter, J., *Nanoparticles as Drug Delivery Systems.*, in *Encyclopedia of Nanoscience and Nanotechnology*, H.S. Nalwa, Editor. 2004, American Scientific Publishers: New York. p. 161-180.
56. Soppimath, K.S.A., T. M. Kulkarni, A. R. Rudzinski, W. E., *Biodegradable Polymeric Nanoparticles As Drug Delivery Devices.* J Control Rel, 2001. **70**(1-2): p. 1-20.
57. Anton, N., J.P. Benoit, and S. P., *Design and Production of nanoparticles Formulated from Nano-Emulsion Templates- A Review.* J Control Rel, 2008. **128**: p. 185-199.
58. Mishra, B., B. Bhavesh, Patel, and T. Sanjay, *Colloidal Nanocarriers: A Review on Formulation Technology, Types and Applications Toward Targeted Drug Delivery.* Nanomedicine: NBM, 2009. **6**: p. 9-24.
59. Moinard-Checot, M., Y. Chevalier, S. Briancon, L. Beney, and H. Fessi, *Mechanism of Nanoparticles Formation by the Emulsion-Diffusion Process.* J Coll Int Sci, 2008. **317**: p. 458-468.
60. Lemoine, D. and V. Preat, *Polymerc Nanoparticles as Delivery System for Influenza Virus Glycoproteins.* J. Control. Rel., 1998. **54**: p. 15-27.
61. Rao, J.P. and K.E. Geckeler, *Polymer Naoparticles: Preparation Techniques and Size-Control Parameters.* Prog Polym Sci, 2011. **36**(7): p. 887-913.

62. Allemann, E., R. Gurny, and E. Doelker, *Preparation of Aqueous Polymeric Nanodispersions by a Reversible Salting-Out Process: Influence of Process Parameters on Particle Size.* Int J Pharm, 1992. **87**: p. 247-253.
63. Lambert, G.F., E. Couvreur, P., *Nanoparticulate System for the Delivery of Antisense Oligonucleotides.* Adv Drug Del Rev, 2001. **47**: p. 99-112.
64. Jung, T.K., W. Breintenbach, A. Kaiserling, E. Xiao, J. X. Kissel, T., *Biodegradable Nanoparticles for Oral Delivery of Peptides: is there a Role for Polymers to Affect Mucosal Uptake?* Eur J Pharm Biopharm, 2000. **50**: p. 147-160.
65. Couvreur, P., C. Dubernet, and F. Puisieux, *Controlled drug delivery with nanoparticles: current possibilities and future trends.* Eur J Pharm Biopharm, 1995. **41**: p. 2-13.
66. Fessi, H.P., F. Devissaguet, J. P. Ammoury, N. Benita, S., *Nanocapsule formation by interfacial polymer deposition following solvent displacement.* Int J Pharm, 1989. **55**: p. R1-R4.
67. Yordanov, G.G.D., C. D., *Preparation of Poly(butylcyanocrylate) drug carriers by Nanoprecipitation using a Pre-synthesized Polymer and Different Colloidal Stabilizers.* Colloid Polym Sci, 2010. **288**: p. 1019-1028.
68. Nehilla, B.J.B., M. Popat, K. C. Desai, T. A., *Purified and Surfactant-free Coenzyme Q10-loaded Biodegradable Nanoparticles.* Int J Pharm, 2008. **348**: p. 107-114.
69. Lince, F., D.L. Marchisio, and A.A. Barresi, *Strategies to Control the Particle Size Distribution of Poly-ε–Caprolactone Nanoparticles for Pharmaceutical Applications.* J Coll Int Sci, 2008. **322**: p. 505-515.
70. Barichello, J.M.M., M. Takayama, K. Nagai, T., *Encapsulation of Hydrophilic and Lipophilic Drugs in PLGA Nanoparticles by the Nanoprecipitation Method.* Drug Dev Ind Pharm, 1999. **25**(4): p. 471-476.
71. Leo, E.B., B. Forni, F. Vandelli, M. A., *In vitro Evaluation of PLA Nanoparticles Containing a Lipophilic Drug in Water-Soluble or Insoluble Form.* Int J Pharm, 2004. **278**(1): p. 133-141.
72. Govender, T., S. Stolnik, M.C. Garnett, L. Illum, and S.S. Davis, *PLGA Nanoparticles Prepared by Nanoprecipitation: Drug Loading and Release Studies of a Water Soluble Drug.* J Control Rel, 1999. **57**(2): p. 171-185.
73. Hornig, S., H. Bunjes, and T. Heinze, *Preparation and Characterization of Nanoparticles Based on Dextran-Drug Conjugate.* J Coll Int Sci, 2009. **338**(1): p. 56-62.
74. Hornig, S.H., T., *Nanoscale Structures of Dextran Esters.* Carbohydr Polym, 2006. **68**: p. 280-286.
75. Lee, J.C., E. C. Cho, K., *Incorporation and Release Behaviour of Hydrophobic Drug in Functionalized Poly(D,L-lactide)-block-poly(ethylene oxide) micelles.* J Cont Rel, 2004. **94**: p. 323-335.
76. Bungenberg de Jong, H.G., *Complex Colloid Systems*, in *Colloid Science Vol. II Reversible Systems*, H.R. Kruyt, Editor. 1949, Elsevier: New York.
77. Thickett, S.C. and R.G. Gilbert, *Emulsion Polymerization: State of the Art in Kinetics and Mechanisms.* Polym, 2007. **48**: p. 6965-6991.
78. Garay-Jimenez, J.C.G., D. Young, A. Lim, D.V. Turos, E., *Physical Properties and Biological Activity of Poly(butyl acrylate-styrene) Nanoparticle Emulsions Prepared with Conventional and Polymerizable Surfactants.* Nanomedicine: NBM, 2009. **5**: p. 443-451.
79. Bao, J.Z., A., *Poly(methyl methacrylate) Nanoparticles Prepared through Microwave Emulsion Polymerization.* J Appl Polym Sci, 2004. **93**: p. 2815-2820.
80. O'Neil, M.A., R.R. Selvedran, and V.J. Morris, *Structure of the Acidic Extracellular Gelling Polysaccharide Produced by Pseudonomas elodea.* Carbohydr. Res., 1983. **124**: p. 123-133.
81. Coutinho, D.F.S., S. V. Shin, H. Oliveira, J. T. Gomes, M. E. Neves, N. M. Khademhosseini, A. Reis, R. L., *Modified Gellan Gum Hydrogels with Tunable Physical and Mechanical Properties.* Biomaterials, 2010. **31**: p. 7494-7502.
82. Crescenzi, V.D., M. Coviello, T., *Solution and Gelling Properties of Microbial Polysaccharides of Industrial Interest: the Case of Gellan*, in *Novel Biodegradable Microbial Polymers*, E.A. Dawes, Editor. 1990, Kluwer Academic Publishers, Dordrecht: Boston. p. 227-284.
83. Grasdalen, H.S., O., *Gelation of Gellan Gum.* Carbohydr Polym, 1987. **7**: p. 371-393.
84. Moslemy, P.N., R. J. Millete, D. Guiot, S. R., *Transport of Gellan Gum Microbeads through Sand: An Experimental Evaluation for Encapsulated Cell Bioaugmentation.* J Environ Manage, 2003. **69**(3): p. 249-259.
85. Norton, A.B.C., P. W. Spyropoulos, F., *Acid Gelation of Low Acyl Gellan Gum Relevant to Self-Structuring in the Human Stomach.* Food Hydrocoll, 2011. **25**(5): p. 1105-1111.
86. Lamkey, J.W., *Nonstarch Hydrocolloids*, in *Ingredients in Meat Products: Properties, Functionality and Applications*, R. T., Editor. 2009, Springer Science + Business Media LLC: New York. p. 419.

87. Miyazaki, S.A., H.Kawasaki, N.Kubo, W.Attwood, D., *In Situ Gelling Gellan Formulations as Vehicles for Oral Delivery.* J Control Rel, 1999. **60**: p. 287-295.
88. Yang, F.X., S. Tan, C. Zhang, X., *Preparation and Evaluation of Chitosan-Calcium-Gellan Gum Beads for Controlled Release of Protein.* Eur Food Res Technol, 2013.
89. Rivera-Leyva, J.C.G.-F., M. Valladares-Mendez, A. Orozco-Castellanos, L. M. Martinez-Alfaro, M., *Comparative Studies on the Dissolution Profiles of Oral Ibuprofen Suspension and Commercial Tablets Using Biopharmaceutical Classification System Criteria.* Ind J Pharm Sci, 2012. **74**(4): p. 312-318.
90. Muzarelli, R.A.A., *Chitin*. 1977, Oxford: Pergamon Press. 309.
91. Mao, H.-Q.R., K. Troung-Le, V. L. Janes, K. A. Lin, K. Y. Wang, Y. August, J. T. Leong, K. W. , *Chitosan-DNA Nanoparticles as Gene Carriers: Synthesis, Characterization and Transfection Efficiency.* J Control Rel, 2001. **70**(3): p. 399-421.
92. Chenite, A.B., M. Wang, D. Chaput, C. Kandani, N., *Rheological Characterization of Thermogelling Chitosan/Glycerol-Phosphate Solutions.* Carbohydr Polym, 2001. **46**: p. 39-47.
93. Amin, K.A.M.P., M. I. H., *Polyelectrolyte Complex Materials from Chitosan and Gellan Gum.* Carbohydr Polym, 2011. **86**(1): p. 352-358.
94. Aktas, Y.A., K. Alonso, M. J. Calvo, P. Gursoy, R. N. Couvreur, P. Capan, Y., *Preparation and In Vitro Evaluation of Chitosan Nanoparticles Containing a Caspace Inhibitor* Int J Pharm, 2005. **298**(2): p. 378-383.
95. Agnihotri, S.A., N.N. Mallikarjuna, and T.M. Aminabhavi, *Recent Advances on Chitosan-Based Micro- and Nanoparticles in Drug Delivery.* J Control Rel, 2004. **100**(1): p. 5-28.
96. Duncan, R., *The Dawning Era of Polymer Therapeutics.* Nat Rev Drug Discov, 2003. **2**: p. 347-360.
97. Canal, F.S., J. Vicent, M.J., *Polymer-drug Conjugates as Nano-sized Medicines.* Curr Opin Biotechnol, 2011. **22**: p. 894-200.
98. Duncan, R., *Polymer Conjugates as Anticancer Nanomedicines.* Nat Rev Cancer, 2006. **6**: p. 688-701.
99. Vicent, M.J. and R. Duncan, *Polymer Conjugates: Nanosized Medicines for treating cancer. .* Trends Biotechnol, 2006. **24**: p. 39-47.
100. Greco, F.V., M. J., *Polymer-Drug Conjugates: Current Status and Future Trends.* Front BioSci, 2008. **13**: p. 2744-2756.
101. Li, C. and S. Wallace, *Polymer-Drug Conjugates: Recent Development in Clinical Oncology.* Adv Drug Del Rev, 2008. **60**(8): p. 886-898.
102. Muggia, F.M., *Doxorubicin-Polymer Conjugates: Further Demonstration of the Concept of Enhanced Permeability and Retention.* Clin Cancer Res, 1999. **5**: p. 7-8.
103. Minko, T., *Soluble Polymer Conjugates for Drug Delivery.* Drug Discovery Today: Tech, 2005. **2**(1): p. 15-20.
104. Maeda, H.K., T., ed. *Neocarzinostatin: The Past, Present and Future of an Anticancer Drug*. ed. H.E. Maeda, K. Ishida, N. 1997, Springer-Verlag: Berlin. 227-267.
105. Schmitt, D.A.K., K. Kimura, S. Oka, K. Pollard, R. B. Maeda, H. Suzuki, F., *Antitumour Activity of Orally Administered SMANCS, a Polymer-Conjugated Protein Drug, in Mice Bearing Various Murine Tumors.* Anticancer Res, 1992. **12**(6B): p. 2219-2224.
106. Abuchowski, A.M., J. R. Palczuk, N. C. van Es, T. Davis, F. F., *Effect of Covalent Attachment of Polyethylene Glycol on Immunogenicity and Circulating Life of Bovine Liver Catalase.* J Bio Chem, 1977. **252**: p. 3582-3586.
107. Graham, M.L., *Pegaspargase: A Review of Clinical Studies.* Adv Drug Deliv Rev, 2003. **55**: p. 1293-1302.
108. Delman, K.A.T., M. Ensor, C. M. Holtsberg, F. W. Bomalaski, J. S. Clark, M. A. Curley, S. A., *Phase I/II trial of Pegylated Arginine Deiminase (ADI-PEG20) in Unresectable Hepatocellular Carcinoma.* J Clin Oncol, 2005. **23**(16S): p. 4139.
109. Molineux, G., *The Design and Development of Pegfilgrastin (PEG-rmetHuG-CSF, Neulasta).* Curr Pharm Des, 2004. **10**: p. 1235-1244.
110. Vicent, M.J.G., F. Nicholson, R. I. Paul, A. Griffiths, P. C. Duncan, R., *Polymer Therapeutics Designed for a Combination Therapy of Hormone-dependent Cancer.* Angew Chem Int Ed Engl, 2005. **44**(26): p. 4061-4066.
111. Vicent, M.J., *Polymer-drug conjugates as modulators of cellular apoptosis.* AAPS J, 2007. **9**(2): p. E200-E207.
112. Khandare, J.J.C., P. Wang, Y. Pozharov, V. P. Minko, T., *Novel Polymeric Prodrug with Multivalent Components for Cancer Therapy.* J Pharmacol Exp Ther, 2006. **317**: p. 929-937.

113. Duncan, R.S., L.W. O'Hare, K. B. Flanagan, P.A. Wedge, S. Hume, I.C. Ulbrich, K. Strohalm, J. Subr, V. Spreafico, F. Grandi, M. Ripamonti, M. Farao, M. Suarato, A., *Preclinical Evaluation of Polymer-Bound Doxorubicin.* J Cont Rel, 1992. **19**(1-3): p. 331-346.
114. Williams, C.C.T., S. H. Hantke, T. Vogel, U. Seeberger, P. H. Tsanaktsidis, J. Lepenies, B., *RAFT-derived Polymer-Drug Conjugates: Poly(hydroxypropyl methacrlamide) (HPMA)-7-Ethyl-10-Hydroxycamptothecin (SN-38) Conjugates.* Chem Med Chem, 2012. **7**(2): p. 281-291.
115. Duncan, R., *Development of HPMA Copolymer-Anticancer Conjugates: Clinical Experience and Lessons Learnt.* Adv Drug Del Rev, 2009. **61**(13): p. 1131-1148.
116. Duncan, R.V., M. J., *Do HPMA Copolymer Conjugates have a Future as Clinically Useful Nanomedicines? A Critical Overview of Current Status and Future Opportunities.* Adv Drug Del Rev, 2010. **62**(2): p. 272-282.
117. Duncan, R., *Polymer Therapeutics as Nanomedicines: New Perspectives.* Curr Opin Biotechnol, 2011. **22**(4): p. 492-501.
118. Lankalapalli, S. and V. Kolapalli, *Polyelectrolyte Complexes: A Review of Their Applicability in Drug Delivery Technology.* Ind J Pharm Sci, 2009. **71**(481-487).
119. Overbeek, J.T.V., M. J., *Phase Separation in Polyelectrolyte Solutions: Theory of Complex Coarcevation.* J Cell Physiol Suppl, 1957. **49**(S1): p. 7-26.
120. Chatellier, X.J., J-F., *Adsorption of Polyelectrolyte Solutions on Surface: A Debye-Huckel Theory.* J Phys II France, 1996. **6**(12): p. 1669-1686.
121. Voorn, M.J., *Phase separation in Polymer solutions.* Adv Polym Sci, 1959. **1**: p. 192-233.
122. Etrych, T.L., L. Boustta, M. Vert, M., *Polyelectrolyte Complex Formation and Stability when Mixing Polyanions and Polycations in Salted Media: A Model Study Related to the Case of Body Fluids.* Eur J Pharm Sci, 2005. **2**: p. 281-288.
123. Park, J.H.S., G. Kim, K. Kwon, I.C., *Targeted Delivery of Low Molecular Drugs Using Chitosan and its Derivatives.* Adv Drug Del Rev, 2010. **62**: p. 28-41.
124. Bhattarai, N., J.J. Gunn, and M. Zhang, *Chitosan- Based Hydrogels for Controlled, Localized Drug Delivery.* Adv Drug Del Rev, 2010. **62**: p. 83-99.
125. Genta, I.P., P. Modena, T. Pavanetto, F. Castelli, F. Muzarelli, R. A., *Miconazole-Loaded 6-Oxychitin-Chitosan Microcapsules.* Carboh Polym, 2003. **52**: p. 11-18.
126. Macleod, G.S., J.H. Collett, and J.T. Fell, *The Potential Use of Mixed Films of Pectin, Chitosan and HPMC for Bimodal Drug Release.* J Control Rel, 1999. **58**: p. 303-310.
127. Krone, V.M., M. Walch, A. Groner, A. Hoffman, D., *Pharmacological Composition Containing Polyelectrolyte Complexes in Microparticle Form and at Least on Active Agent.* United States Patent, 1997. **US5700459A**.
128. Hamman, H.J., *Chitosan Based Polyelectrolyte Complexes as Potential Carrier Materials in Drug Delivery Systems.* Mar Drugs, 2010. **8**(4): p. 1305-1322.
129. Arguelles-Monal, W.C., G. Peniche, C. Rinaudo, M., *Conductimetric Study of the Interpolyelectrolyte Reaction Between Chitosan and Polygalacturonic Acid.* Polymer, 2000. **41**: p. 2373-2378.
130. Zhang, L.M., *Synergistic Blends from Aqueous Solutions of Two Cellulose Derivatives.* Coll Polym Sci, 1999. **277**(9): p. 886-890.
131. Takayama, K.N., T., *Application of Interpolymer Complexation of Polyvinylpyrrolidone/Carboxylvinyl Polymer to Control of Drug Release* Chem Pharm Bull, 1987. **35**: p. 4921-4927.
132. Herbert, D., *Light Scattering Studies on Polyelectrolyte Complexes.* Macromol Symp, 2001. **162**: p. 1-22.
133. Anlar, S.C., Y. Guven, O. Gogus, A. Dalkara, T. Hincal, A., *Formulation and In-vitro-in-vivo Evaluation of Buccoadhesive Morphine Sulfate Tablets.* Pharm Res, 1994. **11**: p. 231-236.
134. Jimenez-Kairuz, A.F.L., J. M. Allemandi, D. A. Manzo, R. H., *Swellable Drug-Polyelectrolyte Matrices (SDPM): Characterization and Delivery Properties.* Int J Pharm, 2005. **288**(1): p. 87-99.
135. Liao, I.C.W., A. C. A. Yim, E.K. Leong, K. W., *Controlled Release from Fibers of Polyelectrolyte Complexes.* J Control Rel, 2005. **104**: p. 347-358.
136. Tapia, C.E., Z. Costa, E. Sapag-Hagar, J. Valenzuela, F. Basuatto, C. Gai, M. N. Yazdani-Perdram, M., *Comparative Studies on Polyelectrolyte Complexes and Mixtures of Chitosan-Alginate and Chitosan-Carrageenan as Prolonged Dilitiazem Clorhydrate Release Systems.* . Eur J Pharm Biopharm, 2004. **57**(1): p. 65-75.
137. de la Torre, P.M.E., Y. Torrado, G. Torrado, S., *Release of Amoxicillin from Polyionic Complexes of Chitosan and Poly(acrylic acid): Study of Polymer/Polymer and Polymer/Drug Interactions Within the Network Structure.* Biomaterials, 2003. **24**(8): p. 1499-1506.

138. Win, P.P.S.-y., Y. Hong, K. J. Kajiuchi, T., *Formulation and Characterization of pH Sensitive Drug Carrier Based on Phosphorylated Chitosan (PCS).* Carboh Polym, 2003. **53**: p. 305-310.
139. Rolfes, H.V.D.M., T. L. Truter, P. A., *Method of Making Controlled Release Particles of Complexed Polymers* United States Patent, 2001. **6221399**.
140. Bhaskar, K.M., C. K. Lingam, M. Mohan, S. J. Venkateswarlu, V. Rao, Y. M. Anbu, J. Ravichandran, V., *Development of SLN and NLC Enriched Hydrogels of Transdermal Delivery of Nitrendipine: In Vitro and In Vivo Characteristics.* Drug Dev Ind Pharm, 2009. **35**(1): p. 98-113.
141. Patel, V.R. and M.M. Amiji, *Preparation and Characterization of Freeze-dried Chitosan-Poly(ethylene oxide) Hydrogels for Site-Specific Antibiotic Delivery in the Stomach.* Pharm Res, 1996. **13**(4): p. 588-593.

CHAPTER TWO

2.0. Formulation and characterization of Ibuprofen – Polymer nano conjugates

2.1. Introduction

Ibuprofen is a weak organic acid amphiphile that is soluble in high pH aqueous environment in its ionized form [1]. This ionized species has propensity for electrostatic interaction with oppositely charged molecules. Hydrophilic cationic polysaccharides with glucosidic backbone have a particularly adequate structure to interact with amphiphilic molecules like ibuprofen and the presence of charged or hydrophilic groups in their substituents provides strong affinity for the oppositely charged molecule or hydrogen bonding capacity [2]. A combination of spontaneous electrostatic and hydrophobic interactions between polyelectrolyte and the ionized drug underpins the formation of amphiphile-polyelectrolyte complexes of various structures and sizes depending on the type of amphiphile [3-4]. Literature is replete of reports on the role of polyelectrolyte-ionic surfactant (amphiphile) complexation in solubilization of poorly soluble drugs in a review by Langevin [5] however research on amphiphilic drug-polyelectrolyte complexation is limited. Few reports found in literature include elucidation of the factors underpinning the complexation of amitriptyline, chlorpromazine and doxepin to polyelectrolyte in aqueous phase however the drug delivery and nanoscale applications were not evident from the report [6-8]. Hughert and Sunderlof studied the effect of polyelectrolyte counterion specificity, charge density and conformation on the interaction between carrageenan/furcelleran and amitriptyline by means of dialysis equilibrium technique but did not give a report on its drug delivery potentials [8]. Persson *et al.* studied the interaction of dextran sulphate and hydrophobicity of cationic amphiphiles in the order doxepin-HCl < amitriptyline HCl < chlorpromazine-HCl [7]. The data reported indicated that the polyelectrolyte-amphiphile interaction depended on both the hydrophobicity of the amphiphile and the charge

density of dextran sulphate. The amorphous forms of highly water insoluble drugs are known to exhibit higher saturation solubility, enhanced dissolution and bioavailability as well as nanoscale formulation than the crystalline form [9]. Cheow and Hadinomoto prepared freeze-dried amorphous ciprofloxacin-dextran sulfate nanoplex via drug-polyelectrolyte complexation. The nanoplex powders exhibited about twice the dissolution rate (50% at 1 h) and solubility (0.3 mg/mL) when compared with raw ciprofloxacin crystals (25% at 1 h and 0.14 mg/mL respectively) [9]. The authors however acknowledged that the rapid crystallization of ciprofloxacin from the supersaturated solution could erode its solubility advantage. Therefore, to prolong the supersaturation period, crystallization inhibitors such as polyvinylpyrrolidone (PVP) have to be included.

Polymer-surfactant complexes have been reported to form nanoscopic core-shell structures above the critical micelle concentration (CMC) [10]. In this case poorly soluble drugs are entrapped in the hydrophobic core while the hydrophilic part serves as the interface between the bulk aqueous phase and the hydrophobic domain. The polymeric micelles therefore serve as nanoscopic depot or stabilizers for poorly water soluble drugs [11]. Barreiro-Iglesias *et al.* studied the capability of pluronic conjugated with poly (acrylic acid) to enhance the solubility and stability of camptothecin [10]. The authors found that camptothecin solubility in polymer micellar solution was three to four-folds higher than in water at pH 5. A review of drug loaded polymeric micelles for the enhancement of the solubility of the drug has been presented by Jones and Leroux [12].

The present study aims to investigate a novel drug-polyelectrolyte complexation technique of preparing amorphous ibuprofen nanoconjugate. This technique entails using various techniques to solubilize ibuprofen, including alkaline solubilization at pH above its pK_a 4.5; melt solubilization above melting point of ibuprofen; micellar solubilization using non ionic surfactant and hydrotropic complexation. The respective solutions were mixed with a solution of oppositely charged polyelectrolyte to initiate drug-polymer interaction. Charge neutralization leads to spontaneous precipitation and formation of nanoscale drug-polyelectrolyte complex. The combination of strong electrostatic interactions between the drug and the polyelectrolyte as well as the spontaneous

precipitation prevent the drug from reverting back into the ordered crystalline form hence amorphous drug-polyelectrolyte nanocomplex is formed. The cationic polyelectrolytes employed in this study are Diethylaminoethyl-Dextran (DEAE-Dextran) and chitosan which are natural biocompatible and biodegradable polycations. The high positive charge in the chitosan backbone has been reported to interact with negatively charged biomolecules [13].

Melt solubilization technique is usually preferred when the starting materials are crystalline (solid dispersions) [14]. Sekiguchi and Obi prepared the first solid dispersions consisting of sulphathiazole and urea as matrix by the fusion method [15]. The physical mixture at the eutectic composition was melted and cooled with a simultaneous crystallization of drug and matrix obtained during the cooling step. In this method, a poorly soluble drug is dispersed in a highly soluble hydrophilic matrix which enhances the solubility of the drug. Limitations of fusion method include incompatibility between the drug and matrix at the heating temperature which can lead to inhomogeneous solid dispersion with two liquid phases or a suspension being observed in the heated mixture [16]. Greenhalgh *et al.* prepared solid dispersions of ibuprofen and xylitol by fusion method [16]. The authors reported that large solubility parameter differences existed between the drug and carrier, laying evidence for possible incompatibilities. Another drawback is phase separation which can occur during cooling when the drug miscibility of the drug-matrix miscibility changes. Slow cooling yielded crystalline drug while fast cooling gave amorphous solid dispersions in the preparation of nifedipine-polyethylene glycol solid dispersions [17]. The third drawback is the possibility of degradation of the drug or matrix occurring during heating to temperatures required to fuse drug and matrix.

Alkaline solubilization involved the use of sodium hydroxide (NaOH) as solvent in the enhancement of solubility of ibuprofen. Ibuprofen was solubilized in alkaline medium (NaOH) above its pK_a 4.5 to form a solution of anionic species and was mixed with positively charged polyelectrolyte solution to initiate drug-polymer interaction and the concurrent charge neutralization giving rise to spontaneous precipitation and formation drug-polyelectrolyte complex in the nanometre range.

Surfactant solubilization is one of the important methods of formulating by solubilizing in surfactant solution above the critical micelle concentration (CMC) of 0.02 mM in the case of tween 80 [18]. Surfactants tend to lower the surface tension and improve the dissolution of hydrophobic drugs in aqueous medium. Micelles are formed when the concentration of surfactants exceeds their critical micelle concentration. In this study, tween 80 also known as polysorbate 80, a non-ionic surfactant was used to entrap the drug within the micelle. Seedher and Kanojia studied the enhancement of solubility of seven antidiabetic drugs such as glicazide and glyburide using cationic (cetyl trimethylammonium bromide-CTAB), anionic (sodium dodecyl sulphate-SDS), non-ionic surfactants (tween 80) and their mixtures [19]. The authors found that the non-ionic surfactant (tween 80) could be a better solvent as compared to ionic surfactants. In this study, polymers (DEAE-Dextran and chitosan) were used to control the rheology of the formulations and surfactant (tween 80) was used to control the surface properties or wettability.

Hydrotropy is a molecular phenomenom whereby adding a second solute (the hydrotrope) results in an increase in the aqueous solubility of poorly soluble drugs. Nicotinamide aggregates via self assembly distinct from the surfactant self assembly since hydrotropes form planar or open-layer structures distinct from spheroids formed by surfactants [20-21]. Hydrotropy is considered to be superior to other solubilization methods such as surfactant or micellar solubilization [22]. In this study nicotinamide was used as the hydrotropic agent and tween 80 as surfactant in addition to the ibuprofen-polyion nano conjugate.

The intention of this research was to maximize the solubility of ibuprofen in order to ensure fixed dose and control its release using varying complexation techniques based on electrostatic interaction. It is expected that understanding of the intrinsic capacity of polymer-drug conjugates in terms of phase solubility behaviour of poorly soluble drugs, conjugation efficiency, physicochemical characteristics and thermal stability would shed light on the type of interaction (physical or chemical/agonist or synergistic), the best polymer-drug ratio, the capacity of the polymer to achieve the desired drug payload and other features that govern clinical risk-benefit ratio which are key

indices to optimization of polymer-drug conjugate design and a consequent effective and efficient drug delivery. Presently there is not sufficient research information on the quantitative contribution of drug–polyion nanoconjugates to the biopharmaceutical characteristics of poorly soluble drugs justifying the need for this study to be carried out. Therefore the aim of this phase was to prepare a stabilized amorphous *ibuprofen-polyion nanoconjugate* using a fast, minimum energy and organic solvent-free technique.

2.2. Materials and Methods

2.2.1. Materials

Ibuprofen was purchased from Fagron, UK while gellan gum (Phytagel®), chitosan (low molecular weight), DEAE-Dextran hydrochloride, nicotinamide, tween 80 and pluronic F-68 were purchased from Sigma-Aldrich, UK. They were all used as received without further modification. Other reagents such as glacial acetic acid, hydrochloric acid, sodium hydroxide were of analytical grade.

2.2.2. Formulation of drug-polymer nanoconjugates

2.2.2.1. Melt solubilization

Co-precipitation technique previously reported by Jiang *et al.* [23] was adapted with modifications. Varying amount of DEAE-Dextran was dissolved and made up to 50 mL with 0.1% w/v pluronic solution to produce double strength of the required ratio ranging from 0.2 to 3.2% w/v solutions and heated to 80 ^{o}C under magnetic stirring on a hot plate (Jenway 1000 stirrer). 4 mg/mL ibuprofen (double strength) dispersion was also prepared in 0.1% w/v pluronic solution and heated to 80 ^{o}C under magnetic stirring. Equal volume of the melted ibuprofen dispersion was added drop-wisely into the DEAE-Dextran solution at the same temperature under magnetic stirring for 10 min. The Ibuprofen-DEAE-Dextran nanoconjugates produced contain a final ibuprofen concentration of 2 mg/mL and Ibuprofen-DEAE-Dextran ratios of 1:0, 1:0.5, 1:1, 1:2, 1:4 and 1:8 labelled as IbMelt-control, IbD1Melt, IbD2Melt, IbD3Melt, IbD4Melt and IbD5Melt respectively.

The pH of the drug polymer complex mixture was adjusted to 6.0 with the Mettler Toledo pH meter using 1 M NaOH [23]. The nanosuspension obtained was dialysed in distilled water through Visking dialysis tube (Visking Medicell, London UK) with molecular weight cut off 12000 for 24 h. The distilled water was changed three times within 24 h. The nanosuspension was kept at room temperature prior to particle size and zeta potential analysis. The process was repeated in the preparation of Ibuprofen-Chitosan nanoconjugates however chitosan was hydrated in 1% glacial acetic acid and was adjusted to pH 5.0 using 1 N HCl [24] as precipitation of chitosan occurred above pH of 6.2. Also the final drug-polymer ratio were 1:0.125, 1:0.25, 1:0.5, 1:1, 1:2 as gelatinous mass was formed beyond ratio 1:2. They were labelled as IbMelt-control, IbCh1Melt, IbCh2Melt, IbCh3Melt, IbCh4Melt and IbCh5Melt respectively.

2.2.2.2. Alkaline Solubilization

The concentrations of ibuprofen, DEAE-Dextran and Ibuprofen-DEAEDextran ratio are same as presented in section 2.2.2.1. 200 mg ibuprofen was dissolved in 10 mL of 0.2 M NaOH, made up to 50 mL with 0.1% w/v pluronic solution and added drop-wisely into equal volume of the varying concentrations of DEAEDextran in pluronic solution at room temperature under continuous magnetic stirring for 10 min (Jenway 1000 hotplate and stirrer). The pH of the drug polymer complex mixture was adjusted to 6.0 (Mettler Toledo pH meter) using 1 N HCl [23]. The Ibuprofen-DEAE-Dextran nanoconjugate prepared were dialysed as described in section 2.2.2.1 and labelled as IbNaOH-control, IbD1NaOH, IbD2NaOH, IbD3NaOH, IbD4NaOH and IbD5NaOH respectively. The nanosuspension formed was kept at room temperature prior to analysis. The process was repeated in the preparation of Ibuprofen-Chitosan nanoconjugates however chitosan was hydrated with 1% glacial acetic acid and adjusted to pH 5.0 [24] with 1 N HCl. The final drug-polymer ratio were 1:0, 1:0.125, 1:0.25, 1:0.5, 1:1, 1:2 drug-polymer ratio labelled as IbNaOH-control, IbCh1NaOH, IbCh2NaOH, IbCh3NaOH, IbCh4NaOH and IbCh5NaOH respectively.

2.2.2.3. Surfactant Solubilization

The concentrations of ibuprofen, DEAE-Dextran and Ibuprofen-DEAE-Dextran ratio are same as presented in section 2.2.2.1. 200 mg ibuprofen was dissolved in 10 mL of tween 80, made up to 50 mL with 0.1% w/v pluronic solution and added drop-wisely into equal volume of the varying concentrations of DEAE-Dextran in 0.1% w/v pluronic solution at room temperature under continuous magnetic stirring for 10 min (Jenway 1000 hotplate and stirrer). The pH of the drug polymer complex mixture was adjusted to 6.0 (Mettler Toledo pH meter) using 1 M NaOH [23]. The Ibuprofen-DEAE-Dextran nanoconjugate prepared were dialysed as described in section 2.2.2.1 and labelled as IbTw80-control, IbD1Tw80, IbD2Tw80, IbD3Tw80, IbD4Tw80 and IbD5Tw80 respectively. The nanosuspension formed was kept at room temperature prior to analysis. The process was repeated in the preparation of Ibuprofen-Chitosan nanoconjugates however chitosan was hydrated with 1% glacial acetic acid and adjusted to pH 5.0 [24] with 1 N HCl. The final drug-polymer ratio were 1:0, 1:0.125, 1:0.25, 1:0.5, 1:1, 1:2 drug-polymer ratio labelled as IbTw80-control, IbCh1Tw80, IbCh2Tw80, IbCh3Tw80, IbCh4Tw80 and IbCh5Tw80 respectively.

2.2.2.4. Hydrotropic Complexation

The concentrations of ibuprofen, DEAE-Dextran and Ibuprofen-DEAE-Dextran ratio are same as presented in section 2.2.2.1. 200 mg ibuprofen was dissolved in 10 mL of 10% w/v nicotinamide solution, made up to 50 mL with 0.1% pluronic solution and heated up to 60 ^{o}C on a hot plate (Jenway 1000 hotplate and stirrer, UK). It was added drop-wisely into equal volume of the varying concentrations of DEAE-Dextran in 0.1% w/v pluronic solution at the same temperature under continuous magnetic stirring for 10 min (Jenway 1000 hotplate and stirrer). The pH of the drug polymer complex mixture was adjusted to pH 6.0 (Mettler Toledo pH meter) with 1 M NaOH [23]. The Ibuprofen-DEAE-Dextran nanoconjugate prepared were dialysed as described in section 2.2.2.1 and labelled as IbNic-control, IbD1Nic, IbD2Nic, IbD3Nic, IbD4Nic and IbD5Nic respectively. The nanosuspension formed was kept at room temperature prior to analysis. The process was repeated in the preparation of Ibuprofen-Chitosan nanoconjugates however chitosan was hydrated with 1%

glacial acetic acid and adjusted to pH 5.0 [24] with 1 N HCl. The final drug-polymer ratio were 1:0, 1:0.125, 1:0.25, 1:0.5, 1:1, 1:2 drug-polymer ratio labelled as IbNic-control, IbCh1Nic, IbCh2Nic, IbCh3Nic, IbCh4Nic and IbCh5Nic respectively.

The composition of ibuprofen-DEAE-Dextran and ibuprofen-chitosan conjugates was presented in Tables 1 and 2.

Table 1 Composition of ibuprofen-DEAE-Dextran conjugates

Formulation	Drug-Polymer Ratio	Ibuprofen (%w/v)	DEAE-Dextran (%w/v)
IbMelt-control	1:0	0.2	-
IbD1Melt	1:0.5	0.2	0.1
IbD2Melt	1:1	0.2	0.2
IbD3Melt	1:2	0.2	0.4
IbD4Melt	1:4	0.2	0.8
IbD5Melt	1:8	0.2	1.6

Table 2 Composition of ibuprofen-chitosan conjugates

Formulation	Drug-Polymer Ratio	Ibuprofen (%w/v)	Chitosan (%w/v)
IbMelt-control	1:0	0.2	-
IbCh1Melt	1:0.125	0.2	0.025
IbCh2Melt	1:0.25	0.2	0.05
IbCh3Melt	1:0.5	0.2	0.1
IbCh4Melt	1:1	0.2	0.2
IbCh5Melt	1:2	0.2	0.4

2.2.3. Preparation of plain and drug loaded polymeric nanoconjugates

2.2.3.1. Formulation of plain polymer-polymer binary nanoconjugates

The DEAE-dextran-gellan complex was prepared by modifying the ionic gelation technique previously described by Santucci *et al.* [25]. 0.1% w/v of gellan was prepared in 0.1% w/v pluronic solution in distilled water and adjusted to pH 6.0 with 1 M NaOH. The dispersion was heated up to above 90 ˚C until solution became clear. It was added dropwise to 0.1% aqueous solution of DEAE-Dextran in 0.1% pluronic and adjusted to pH 6.0 with 1 M NaOH using Mettler Toledo pH meter [23] at the same temperature under continuous magnetic stirring (Jenway 1000 hotplate and stirrer) for 10 min. The DEAE-Dextran-Gellan nanoconjugate prepared was dialysed as described in section 2.2.2.1 and were labelled appropriately. The nanoconjugates were collected by centrifugation (Denley BS 400 Crompton) at 5000 rpm for 1 h and dried in the oven at 40 ˚C overnight. The weight ratios of DEAE-

Dextran to gellan were 0:100, 25:75, 50:50, 75:25 and 100:0. The same process was repeated for the chitosan-gellan complex with 0.1% aqueous solution chitosan prepared in 1% glacial acetic acid containing 0.1% pluronic (adjusted to pH 5.0 with 1 M NaOH) [24] used in place of DEAE-Dextran. The weight ratios of chitosan to gellan were 0:100, 25:75, 50:50, 75:25 and 100:0.

2.2.3.2. Formulation of polymer-drug-polymer ternary nanoconjugates with drug

The method described by Santucci *et al.* [25] was adapted and modified as presented in section 2.2.3.1. 100 mg ibuprofen (4.85 mM) was dispersed in 0.1% aqueous solution of gellan in 0.1% w/v pluronic solution with continuous stirring and adjusted to pH 6 with 1 M NaOH [23]. The dispersion was heated up to above 90 ˚C (Jenway 1000 hotplate and stirrer) until solution became clear. The solution was added dropwisely into varying concentrations of aqueous solution of DEAE-Dextran at the same temperature to give final polymer-polymer ratios of 0:100, 25:75, 50:50, 75:25 and 100:0 and adjusted to pH 6.0 with 1 M NaOH on Mettler Toledo pH meter under continuous magnetic stirring (Jenway 1000 hotplate and stirrer) for 10 min. The DEAE-Dextran-ibuprofen-Gellan nanoconjugate prepared was dialysed as described in section 2.2.2.1 and were labelled appropriately. The nanoconjugates were collected by centrifugation (Denley BS 400 Crompton) at 5000 rpm for 1 h and dried in the oven at 40 ˚C overnight. The control was prepared by dispersing 0.1% ibuprofen in distilled water adjusted to pH 6.0 and heated up to above 90 ˚C. The same process was repeated for the chitosan-gellan complex with 0.1% aqueous solution chitosan prepared in 1% glacial acetic acid containing 0.1% pluronic (adjusted to pH 5.0 with 1 M NaOH) [24] used in place of DEAE-Dextran. The weight ratios of chitosan to gellan were 0:100, 25:75, 50:50, 75:25 and 100:0.

2.2.4. Characterization of Ibuprofen nanoconjugates

2.2.4.1. Measurement of Conductivity

The conductivity measurements of the nanoconjugates were performed on the nanoconjugate suspensions before centrifugation using conductivity meter (Oakton CON 110 Series) with a cell

constant of 1 cm^{-1} at 25 ˚C. The conductivity measurements were an average of at least six determinations.

2.2.4.2. Surface tension determination

The torsion balance for surface and interfacial tension measurements with rings of circumference 4 cm (White Elec. Inst, Co. Ltd) was used to determine the surface tension at 20 ˚C. The method involved measurement of the force required to detach a platinum wire ring immersed at the liquid surface, which was proportional to the surface tension [26]. The surface tension measurements were an average of at least six determinations.

2.2.4.3. Measurement of Viscosity

Viscosity of the nanoconjugates was measured by SV 10 Vibro Viscometer (A&D Company Ltd Japan). Viscosity was measured at 25 ˚C. 10.0 g of the sample was poured into the cup until the surface reached between the level gauges. The cup was attached on the table along guides. The grips were pinched and the sensor was gently lowered above the sample surface. The lever was lowered to secure the sensor plates. The knob of the table was turned so as to adjust the surface of the narrow part of sensor plates. The start key was pressed to start the viscosity measurement till 25 ˚C was reached and the reading was taken. The viscosities obtained were the average of at least six determinations.

2.2.4.4. Measurement of Transmittance/Turbidity

The absorbance/transmittance of the nanoconjugates was measured at 420 nm (ThermoFischer Evolution 60S UV Spectrophotometer) against a blank of distilled water. The measurements obtained were the average of at least six determinations.

2.2.4.5. Determination of particle size and zeta potential of nanoconjugates

The mean particle size and zeta potential of the nanoconjugates were determined by ZetaPlus Zeta Potential Analyser (Brookhaven Instruments Corporation). Samples were diluted appropriately with distilled water and injected into the sample cell. Particle size measurements were carried out at a

scaling angle of 90° and a temperature of 25 °C. Apparent z-average hydrodynamic diameter and polydispersity index (PDI) were obtained. Zeta potential was determined by measuring the electrophoretic mobility of the dispersed particles in a charged field. Zeta potential measurements were done in aqueous solutions at 25 °C and the electric field strength was about 14.95 V/cm. All measurements of individual samples were a mean of six determinations for particle size and 10 runs for zeta potential.

2.2.4.6. Drug conjugation capacity/efficiency

Conjugation efficiency (equation 1) is the mass percentage of ibuprofen that forms the Ibuprofen complex relative to the initial amount of ibuprofen added. The amount of ibuprofen that forms the ibuprofen complex was calculated as the difference between the amount of ibuprofen added and the amount of non-conjugated ibuprofen in the supernatant after centrifugation. The ibuprofen concentration was measured by UV (ThermoFischer Evolution 60 UV Spectrophotometer, UK) after passing it through 0.45 µm filter (Sartorius, Germany) at 264 nm wavelength [27]. All measurements were an average of six determinations.

$$Conjugation\ efficiency = \frac{M_0 - M_i}{M_0} * 100\% \qquad (1)$$

Where M_0 is the initial amount of ibuprofen added and M_i is the amount of nonconjugated ibuprofen in the supernatant after centrifugation.

2.2.4.7. Morphology and size- Scanning electron microscopy

The surface characteristics of the reference compound and nanoconjugates were examined by Carl Zeiss SEM EVO High Definition 15 Scanning Electron Microscope (Carl Zeiss, Germany) using variable pressure technology at low voltages with beam deceleration and high definition backscattered electron (BSE) imaging. The samples were mounted on double sided carbon tabs that were previously secured to aluminium stubs and then analysed at different magnifications and a pressure of 10 Pa. The accelerating voltage was 10 KV with probe current of 400 pA. The particle sizes of the reference compounds and the nanoconjugate images were determined.

2.2.4.8. Spectroscopic analysis - Fourier Transform Infra-red

FTIR was conducted using Perkin-Elmer Precisely Spectrum One FTIR Spectrometer and a Universal ATR Sampling Accessory (Perkin Elmer, USA). The samples were mounted directly on the diamond surface and the arm was placed over it by applying enough pressure in the range of 100 to 120 units. The spectrum was recorded in the wavelength region of 4000 to 650 cm^{-1}. All spectra were then collected at an average of 16 scans at a resolution of 4 cm^{-1}. All measurements were taken in replicates of four determinations.

2.2.4.9. Nuclear Magnetic Resonance (NMR) Spectroscopy

All Proton Nuclear Magnetic Resonance (^{1}H-NMR) studies were performed on the Bruker AV-400 (Ultrashield, Germany) spectrometer equipped with a pulsed field gradient accessory (490 mT m^{-1} z-field gradient) at 25 ^{o}C (298 K) using a probe tuned at 5.13 MHz. The samples were prepared in Dimethyl sulfoxide (DMSO) and equilibrated in the probe for about 30 min at 25 ^{o}C before the NMR experiments. ^{1}H-NMR spectra of the pure ibuprofen; ibuprofen loaded Dextran-Gellan and Chitosan-Gellan nanoconjugates were studied in 5 mm quadruple nucleus probe (QNP) (1H/15) tubes and recorded at room temperature; frequency 399.94 MHz; 45^{o} pulse; relaxation delay of 1 sec; acquisition time of 7.9168 sec and spectra width of 8.278 kHz. One hundred and twenty eight scans were recorded for each sample. ^{13}C-NMR analysis was also performed on the same set of samples at frequency of 399.94 MHz; acquisition time of 1.3665 sec and spectra width of 23.980 kHz. All chemical shifts were assigned relative to Tetramethylsilane (TMS) as external reference. One thousand and twenty four scans were recorded for each sample.

2.2.4.10. Thermal studies

2.2.4.10.1. Differential scanning calorimetry

DSC was performed using Perkin Elmer Precisely Jade DSC machine with a Perkin Elmer Intracooler SP cooling Accessory (Perkin Elmer, USA) to study the thermal behaviour of the pure ibuprofen, DEAE-Dextran, chitosan, physical mixtures and ibuprofen nano-conjugates. The sample sizes in the

range of 8 to 10 mg were heated in hermetically sealed aluminium pans under nitrogen flow (40mL/min) using a scanning rate of 20 ˚C/min from -50 to 300 ˚C. Empty aluminium pan was used as a reference. Indium was used as the standard reference material to calibrate the DSC instrument. All measurements were an average of four determinations and expressed as mean ± S.D.

2.2.4.10.2. Thermogravimetric analysis

TGA was performed using Perkin Elmer Pyris 1 Thermogravimetric Analyser (Perkin Elmer, USA) to monitor the mass of the pure starting materials and nanoconjugates as a function of temperature or time as the sample specimen is subjected to a controlled temperature program at atmospheric pressure. The weight of the empty reference pan placed in the crucible was zeroed and then removed. Samples of known weight in the range of 18 to 25 mg were placed in aluminium pans and measurements performed at a scanning rate of 10 ˚C/min in the range of 25 to 500 ˚C. All measurements were an average of four determinations and expressed as mean ± S.D.

2.2.5. Dissolution and drug release studies

Calibration curve (Figure 156 in the Appendix) was constructed by using pure ibuprofen reference standard (secondary standard) dissolved in buffer solution (pH 7.4) within the concentration range 1.56 and 50 µg/mL (7.56 to 242.39 mM). The correlation was linear (r^2 = 0.9953) and the measurements at six levels of concentration were reproducible with limit of quantification (LOQ = 10 x standard error of the intercept/slope) of 0.37 µg/mL (1.79 mM). The concentrations of ibuprofen were derived from this calibration curve. Thereafter the dissolution profile of the ibuprofen-loaded nanoconjugates was studied using the USP dissolution method. 90 mL of the ibuprofen-DEAE-Dextran and ibuprofen-chitosan nanoconjugates (Melt, NaOH, Tween 80 and nicotinamide batches) containing 1 mg/mL ibuprofen was put in a dialysis tubing (Visking Medicell Ltd London UK with diameter 18/32" and exclusion size 12000 to 14000 Da). Both ends were tied. The dialysis tubing was suspended in 900 mL of PBS pH 7.4, rotated at 50 rpm and maintained at 37 ± 0.5 ˚C using Pharma Test PT DT7 USP Apparatus II Dissolution Test Instrument - paddle method (Pharma Test Ltd,

Germany). At pre-determined time intervals 10, 20, 30, 60 min, 1, 2, 4, 6 and 24 h, 5 mL aliquots were withdrawn and replaced with 5 mL PBS pH 7.4. Drug concentrations were quantified using UV (ThermoFischer Evolution 60 UV-Visible Spectrophotometer, UK) after filtering through 0.45 µm filter (Sartorius, Germany) at 264 nm. All measurements were an average of four determinations and expressed as mean ± S.D. This procedure was repeated for ternary nanoconjugates. A calibration curve was produced using a series of dilution of reference standard ibuprofen in PBS pH 7.4 and analysed by UV at 264 nm shown in the Appendix I (Figure 156). The calibration curve was linear at concentrations between 1.56 and 50 µg/mL with R^2 value of 0.99. The absorbance values obtained from the drug release of the complexes were correlated with the calibration curve and the amount of ibuprofen released was determined.

2.2.6. Drug release kinetics

Data obtained from in vitro release studies were fitted to various kinetic equations. The kinetic models used are zero order, first order and Higuchi equation.

The zero order rate equation (2) describes the systems were the drug release rate is independent of its concentration [28]. The cumulative % drug release vs. time plot is made.

$$C = K_0 t \qquad (2)$$

Where k_0 is zero order rate constant expressed in units of concentration/time and t is the time.

The first order rate equation (3) describes the release from the systems where release rate is concentration dependent [29]. The log cumulative % drug release vs. time plot is made.

$$Log\ C = Log\ C_0 - Kt/2.303 \qquad (3)$$

Where C_0 is the initial concentration of drug and K is first order constant.

Higuchi described the release of drugs from insoluble matrix as a square root of time dependent process based on Fickian diffusion: equation (4) [30]. The cumulative % drug release vs. square root of time is made.

$$Q = Kt^{1/2} \quad (4)$$

Where K, is the constant and it reflects the design variables of the system.

Korsemeyer *et al.* derived a simple relationship which described drug release from a polymeric system: equation (5). To find out the mechanism of drug release, first 60 % drug release data was fitted in Korsemeyer-Peppas model:

$$M_t/M_\infty = Kt^n \quad (5)$$

Where M_t/M_∞ is a fraction of drug released at time t, K is the rate constant and n is the release exponent. The n value is used to characterize different release mechanisms [31]. The log cumulative % drug release vs. log time plot is made. The criterion for selecting the appropriate model is the highest R^2 value which indicates linearity of dissolution data [32].

2.2.7. Similarity factors

The similarity fit factor denoted f_2 was used to compare the dissolution profiles of the drug–polymer conjugates (test) and ibuprofen control (reference). The similarity f_2 factor is defined by equation (6) proposed by Moore and Flanner [33]:

$$f_{2=50\ Log}\left\{(1+\frac{1}{n}\sum_{t=1}^{n}\left(R_t - T_t\right)^2)^{-0.5}\times 100\right\} \quad (6)$$

Where n is the number of dissolution sample times, and R_t and T_t are the individual or mean percent dissolved at each time point, t, for the reference and test dissolution profiles, respectively. The f_2 value greater than 50 suggests that the two profiles are similar. The f_2 value of 100 suggests that the test and the reference profiles are identical and as the value becomes smaller the dissimilarity between release profiles increases [34].

2.2.8. Statistical analysis

Quantitative data are presented as mean ± standard deviation. The significance of the differences between means was assessed using Analysis of Variance (ANOVA) and Post hoc Tukey Test with a statistical significance level set at $p < 0.05$ using IBM SPSS (Statistical Package for Social Science) 20.

2.3. Results and Discussions

2.3.1. Formulation and optimization of Drug-Polymer nanoconjugates

Process optimization was based on preliminary studies carried out (results not presented) to determine the optimal formulation variables such as pH, concentration of polymers and drug, drug-polymer and polymer-polymer mixing ratio, mixing time, mixing speed, temperature, salt concentration and the order of polymer addition. Physicochemical properties of the drug, polymers and their binary and ternary conjugates such as surface tension, conductivity, contact angle, turbidity, viscosity and pH were evaluated to determine the critical association concentration and polymer saturation point which in turn was used to determine the appropriate polymer-polymer and drug-polymer ratio for the formulation of the nanoconjugates. The direct effect of the polymeric ingredients on the physicochemical characteristics, solubility, and dissolution profile of ibuprofen-polyelectrolyte nanoconjugates was also investigated.

Two polycation (chitosan and DEAE-Dextran) and two polyanion (sodium alginate and gellan) polymers were used in the pre-formulation study. The final pH chosen for DEAE-Dextran and chitosan formulations based on the preliminary studies was pH 6.0 and 5.0 respectively. In a similar study Jiang *et al.* prepared ibuprofen nanoparticles stabilized by DEAE-Dextran by co-precipitation method at pH 6.0 [23]. Arora *et al.* also reported the use of pH 5.0 for the chitosan solution in the preparation of chitosan-alginate nanoparticles based on ionotropic gelation process [24]. They noted that the nanoparticles obtained at pH 5.0 in chitosan solutions did not aggregate. However, precipitation occurred beyond pH 5.0, particularly when the pK_a value of chitosan (6.5) is approached.

The binary conjugates (Ibuprofen-DEAEDextran and Ibuprofen-Chitosan) were prepared by melt solubilization, solubilization (ibuprofen solubilized in NaOH or Tween 80) and hydrotropic complexation methods. The intention was to design a technique that can dissolve ibuprofen completely to facilitate maximum interaction with cationic polymer and ensure formation of conjugates of nano size dimension with predictable fixed dose as well as complete release. Further interaction with anionic polymer (ternary conjugate) is expected to reinforce the conjugate with a view to controlling and extending the drug release. The use of stainless steel homogenizer during preparation of the conjugates shed some silvery colour contaminants into the sample at high temperature hence magnetic stirrer was used throughout the study.

Reddy and Gudsookar prepared gliclazide-Polyethylene glycol conjugate using the solid dispersion by solvent method [35]. The authors reported a reduction in particle size resulting in enhancement of surface area and increase in gliclazide wettability. However this method involved the use of solvent-ethanol to dissolve the drug and polymer followed by evaporation of the solvent. The method used in this study avoided the use of organic solvents due to safety issues and the increasing need to deliver safe drugs to patients. It also avoids the laborious process of evaporation.

Alkaline solubilization and surfactant solubilization were adapted to enhance the propensity of interaction between ibuprofen and the respective polymers. Hydrotropic complexation was also carried out to solubilize ibuprofen using 10% w/v nicotinamide. The research intention is to enhance the solubility of ibuprofen by the combined advantage of hydrotropic solubilization and the solubilization effect of the polymeric carrier. Hydrotropic agents have been reported to enhance the aqueous solubility of various poorly water-soluble compounds due to the presence of large amount of additives such as sodium benzoate, sodium-o-hydroxy benzoate, sodium-p-hydroxy benzoate, sodium salicylate, urea, nicotinamide, sodium citrate and sodium acetate [37]. They also increase the number of hydrogen bridges in the water clusters making the water more hydrophobic, therefore a better solvent for the poorly soluble drug or due to change in solvent character known as hydrotrope solubilization phenomenon [38]. Ahuja *et al.* prepared urea with nicotinamide as

hydrotrope in varied proportions by hydrotropy solid dispersion method to enhance the dissolution of rofecoxib [39].

DEAE-Dextran was prepared in distilled water containing pluronic used as stabilizer to prevent aggregation. It is well documented that the use of appropriate stabilizers can prevent the induction of agglomeration or aggregation of the drug particles due to the high surface energy of the nanoparticles yielding physically stable formulations by providing steric or ionic barriers [40].

Chitosan solution was prepared under acidic condition due to its poor solubility in neutral and alkaline pH conditions. Ibuprofen can either interact (electrostatic) with the end groups of chitosan or DEAE-Dextran or can be encapsulated in the interior of the polymers (weak interactions) [23]. It is expected that the ibuprofen with a carboxylic group may form a complex with the amine ($–NH_2$) groups of DEAE-Dextran or chitosan.

2.3.2. Preparation of polymer-polymer, polymer-drug-polymer nanoconjugates

DEAE-Dextran-Ibuprofen-Gellan conjugates and Chitosan-Ibuprofen-Gellan conjugates were prepared by modified ionic gelation method. On addition of ibuprofen dispersed in gellan solution to DEAE-Dextran solution, the mixture became turbid instantly indicating the occurrence of electrostatic interaction. A similar reaction was observed when ibuprofen-loaded gellan was added to chitosan solution. Low molecular weight chitosan was used in this study since it has been suggested that it reacts more completely with polyanions compared with chitosan of higher molecular weight [41]. For optimum interaction and polyelectrolyte complex formation, the amine group of chitosan and DEAE-Dextran have to be protonated and the carboxyl group of gellan ionized [42]. This was ensured by keeping the final pH of chitosan, gellan and DEAE-Dextran solutions at pH 5.0, 6.0 and 6.0 respectively.

2.3.3. Physicochemical characteristics of nanoconjugates

2.3.3.1. Conductivity

Conductimetry has been used in the study of transport process in electrolytic solutions due to its high accuracy [44] hence it has been used to investigate the potential ibuprofen-polymer interaction in this study. The conductivity measurements of ibuprofen in distilled water from preliminary studies ranged from 0.10 to 0.50 mS/cm decreasing with increasing concentration (2.5 to 40.0 µg/mL) of ibuprofen. The critical micelle concentration of ibuprofen was obtained from the plot of conductivity as a function of drug concentration. The cmc values were taken as the break point intercepts of the linear portions on the graph. In the presence of the DEAE-Dextran, increase in concentration of the polymer increased specific conductivity with one or more break points depending on the method of preparation (Figure 6). The melt and surfactant (tween 80) solubilization techniques showed two break points which signify two types of aggregation phenomena. The first break at lower DEAE-Dextran concentration was assigned the critical association concentration (*cac*) of DEAE-Dextran where the interaction between ibuprofen and DEAE-Dextran starts while the second break point was assigned the critical micelle concentration (*cmc*) which is attributed to the saturation of the polymer with the drug (polymer saturation point, *psp*). As concentration of the drug increases beyond the *psp* polymer-free aggregates are formed. It was noted that the presence of DEAE-Dextran decreased the *cac* of ibuprofen significantly in all the four techniques used in this study ($p < 0.05$, $n = 6$) confirming the interaction between DEAE-Dextran and ibuprofen in all the techniques studied. However the melt solubilization technique showed the lowest *cac* at 1.0 mg/mL and *cmc* at 3.76 mg/mL compared with *cac* at 2.34 mg/mL and *cmc* at 8.0 mg/mL respectively for Tween 80. Sodium hydroxide solubilization and nicotinamide hydrotropic complexation showed only one break point at 0.95 mg/mL and 1.32 mg/mL respectively within the studied concentrations of DEAE-Dextran. It was opined that alkaline solubilization and hydrotropic complexation may reduce the amphiphilic properties of ibuprofen. In a similar research, Khan *et al.* [43] reported that a cationic polymer, hydroxyethyl cellulose ethoxylate quaternized (HECEQ), reduced the *cac* of ibuprofen sodium and

was credited to strong affinity for ibuprofen and evidence of interaction between them. Therefore the electrostatic interaction between DEAE-Dextran and ibuprofen was evident.

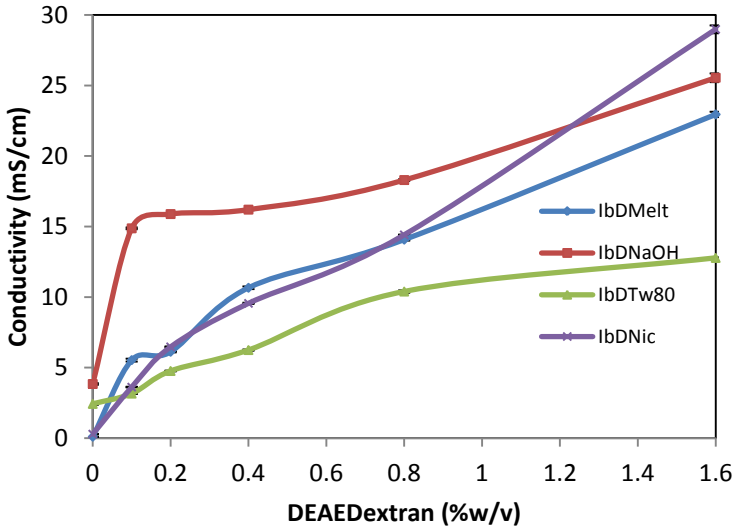

Figure 6 Conductivity of IbDMelt, IbDNaOH, IbDTw80 and IbDNic conjugates based on DEAE-Dextran content in the conjugates. Each data point represents mean ± SD (n = 6).

Table 3 Conjugation efficiency, conductivity, surface tension; viscosity and absorbance/transmittance of ibuprofen-DEAE-Dextran conjugates (melt solubilization). Each value represents mean ± SD (n = 6).

Formulation	Conjugation Efficiency (%)	Conductivity (mS/cm)	Surface tension (dynes/cm)	Viscosity (mPaS)	Absorbance/Transmittance
IbMelt-control	-	0.1±0.001	56.60±1.15	1.28±0.01	0.009±0.0005
IbD1Melt	98.82±1.37	5.53±0.1	36.75±1.12	1.72±0.02	0.011±0.001
IbD2Melt	98.40±1.08	6.12±0.04	32.15±1.06	1.82±0.01	0.014±0.001
IbD3Melt	98.23±1.22	10.66±0.09	34.88±1.48	2.86±0.03	0.003±0.001
IbD4Melt	98.47±1.35	14.08±0.07	36.03±1.25	4.29±0.03	0.015±0.001
IbD5Melt	98.40±1.76	22.95±0.19	37.35±0.83	6.61±0.02	0.008±0.001

Table 4 Conjugation efficiency, conductivity, surface tension, viscosity and absorbance/transmittance of ibuprofen-DEAE-Dextran conjugates (solubilization). Each value represents mean ± SD (n = 6).

Formulation	Conjugation Efficiency (%)	Conductivity (mS/cm)	Surface tension (dynes/cm)	Viscosity (mPaS)	Absorbance/Transmittance
IbNaOH-control	-	3.84±0.06	62.38±1.32	1.38±0.03	0.001±0.001
IbD1NaOH	97.37±0.97	14.88±0.06	36.88±1.09	1.52±0.01	0.016±0.001
IbD2NaOH	97.90±1.05	15.89±0.05	33.43±0.98	1.74±0.01	0.017±0.001
IbD3NaOH	98.14±1.87	16.20±0.04	35.78±0.99	2.09±0.01	0.014±0.001
IbD4NaOH	98.05±1.92	18.30±0.06	33.00±0.80	3.06±0.08	0.017±0.001
IbD5NaOH	97.88±1.73	25.55±0.31	33.95±1.57	5.44±0.03	0.015±0.001

Table 5 Conjugation efficiency, conductivity, surface tension, viscosity and absorbance/transmittance of ibuprofen-DEAE-Dextran conjugates (solubilization). Each value represents mean ± SD (n = 6).

Formulation	Conjugation Efficiency (%)	Conductivity (mS/cm)	Surface tension (dynes/cm)	Viscosity (mPaS)	Absorbance/Transmittance
IbTw80-control	-	2.43±0.07	47.25±1.22	2.39±0.05	0.075±0.001
IbD1Tw80	90.26±0.95	3.16±0.02	38.30±1.00	3.04±0.01	0.056±0.002
IbD2Tw80	90.26±1.03	4.76±0.03	39.68±1.04	4.01±0.02	0.047±0.004
IbD3Tw80	89.05±0.91	6.25±0.04	37.78±1.09	5.09±0.02	0.033±0.003
IbD4Tw80	91.30±1.35	10.40±0.08	40.65±0.39	7.57±0.03	0.033±0.003
IbD5Tw80	96.34±1.46	12.78±0.04	39.58±0.81	11.83±0.16	0.030±0.003

Table 6 Conjugation efficiency, conductivity, surface tension, viscosity and absorbance/transmittance of ibuprofen-DEAE-Dextran conjugates (hydrotropy). Each value represents mean ± SD (n = 6).

Formulation	Conjugation Efficiency (%)	Conductivity (mS/cm)	Surface tension (dynes/cm)	Viscosity (mPaS)	Absorbance/Transmittance
IbNic-control	-	0.29±0.01	50.63±1.07	1.12±0.03	0.000±0.000
IbD1Nic	95.68±1.32	3.62±0.02	34.70±0.37	1.80±0.01	0.001±0.0005
IbD2Nic	95.64±1.47	6.47±0.03	30.78±0.65	2.12±0.01	0.005±0.001
IbD3Nic	95.48±1.56	9.56±0.03	34.08±1.27	2.92±0.02	0.010±0.0005
IbD4Nic	95.61±1.65	14.42±0.02	36.70±0.79	4.73±0.02	0.005±0.002
IbD5Nic	95.54±1.67	28.98±0.28	38.23±0.70	7.01±0.02	0.005±0.002

The specific conductivity profile of ibuprofen in the presence of chitosan is presented in Tables 7 to 10 and Figure 7. Conductivity also increased with increasing concentration of chitosan to a maximum value. All the four techniques have one break point each at the same concentration of chitosan in the range of 0.25 to 0.27 mg/mL which is relatively lower than the *cac* of ibuprofen alone in pure aqueous solution but significantly lower than the DEAE-Dextran values ($p < 0.05$, $n = 6$). There was no significant difference among the four techniques ($p > 0.05$, $n = 6$). Therefore it could be deduced that DEAE-Dextran has more affinity and stronger interaction towards ibuprofen than chitosan. It was opined that larger amount of ibuprofen is required to saturate DEAE-Dextran compared with chitosan hence the interaction may be stronger than in ibuprofen-chitosan conjugates. Although the values of *cac* in chitosan are smaller than in DEAE-Dextran, a decrease in *cac* compared with ibuprofen alone was evident which is a good indication of drug-polymer interaction. The stronger interaction in DEAE-Dextran may be due to its greater hydrophobic characteristics or possible Coulombic repulsion among the counterions of ibuprofen and the cationic DEAE-Dextran. In a similar study, Polyvinyl pyrrolidone (PVP) which is more hydrophobic than polyethylene glycol (PEG) has been reported to exhibit stronger interaction with amphiphilic drugs

[43]. Rodriguez *et al.* [2] also reported that the presence of apolar regions and ammonium groups in the cationic polysaccharides increases the intensity of interactions with aromatic ring and hydrophilic carboxylic acid group of NSAIDs hence the interaction involves both hydrophobic association and electrostatic interaction. The presence of these groups in DEAE-Dextran explains its stronger interaction with ibuprofen than chitosan.

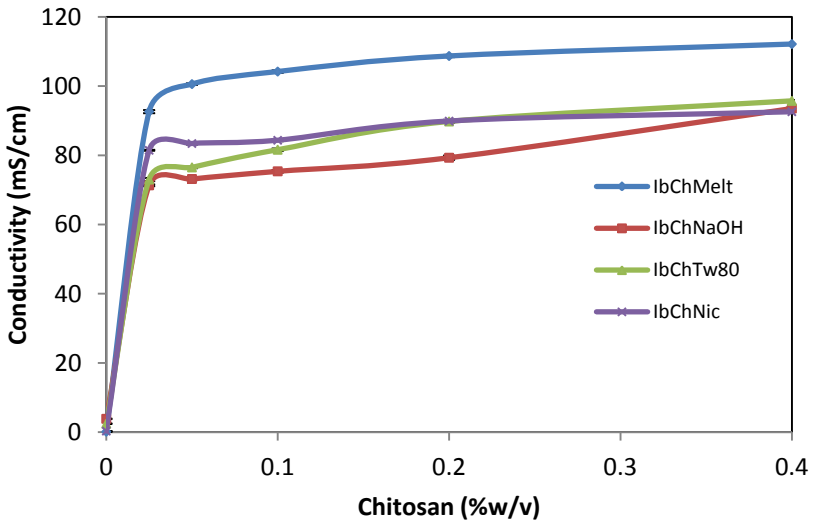

Figure 7 Conductivity of IbChMelt, IbChNaOH, IbChTw80 and IbChNic conjugates based on chitosan content in the conjugates. Each data point represents mean ± SD (n = 6).

Table 7 Conjugation efficiency, conductivity, surface tension; viscosity and absorbance/transmittance of ibuprofen-chitosan conjugates (melt solubilization). Each value represents mean ± SD (n = 6).

Formulation	Conjugation Efficiency (%)	Conductivity (mS/cm)	Surface tension (dynes/cm)	Viscosity (mPaS)	Absorbance/ Transmittance
IbMelt-control	-	0.1 ±0.001	56.60 ±1.15	1.28 ±0.01	0.009 ±0.0005
IbCh1Melt	99.49 ±1.88	92.63 ±0.45	45.53 ±0.46	1.47 ±0.01	0.001 ±0.0005
IbCh2Melt	98.87 ±1.65	100.58 ±0.22	45.00 ±0.91	1.64 ±0.03	0.005 ±0.0005
IbCh3Melt	98.73 ±1.93	104.20 ±0.37	46.5 ±2.16	2.27 ±0.02	0.008 ±0.001
IbCh4Melt	98.09 ±1.27	108.70 ±0.32	41.55 ±0.71	2.90 ±0.01	0.015 ±0.0006
IbCh5Melt	98.04 ±1.36	112.15 ±0.26	48.38 ±0.85	3.22 ±0.02	0.022 ±0.001

Table 8 Conjugation efficiency, conductivity, surface tension, viscosity and absorbance/transmittance of ibuprofen-chitosan conjugates (solubilization). Each value represents mean ± SD (n = 6).

Formulation	Conjugation Efficiency (%)	Conductivity (mS/cm)	Surface tension (dynes/cm)	Viscosity (mPaS)	Absorbance/ Transmittance
IbNaOH-control	-	3.84±0.06	62.38±1.32	1.38±0.03	0.001±0.001
IbCh1NaOH	98.68 ±1.35	71.33 ±0.25	36.63 ±0.63	1.55 ±0.03	0.055 ±0.004
IbCh2NaOH	98.56 ±1.48	73.15 ±0.31	37.38 ±1.41	1.70 ±0.01	0.082 ±0.003
IbCh3NaOH	98.51 ±1.37	75.38 ±0.39	41.55 ±1.21	1.71 ±0.01	0.123 ±0.003
IbCh4NaOH	98.38 ±1.28	79.30 ±0.61	40.15 ±0.53	2.29 ±0.02	0.167 ±0.002
IbCh5NaOH	97.98 ±1.32	93.53 ±0.25	41.43 ±0.83	3.33 ±0.02	0.219 ±0.002

Table 9 Conjugation efficiency, conductivity, surface tension, viscosity and absorbance/transmittance of ibuprofen-chitosan conjugates (solubilization). Each value represents mean ± SD (n = 6).

Formulation	Conjugation Efficiency (%)	Conductivity (mS/cm)	Surface tension (dynes/cm)	Viscosity (mPaS)	Absorbance/ Transmittance
IbTw80-control	-	2.43±0.07	47.25±1.22	2.39±0.05	0.075±0.001
IbCh1Tw80	90.26 ±0.94	73.00 ±0.61	43.78 ±0.96	2.49 ±0.03	0.021 ±0.001
IbCh2Tw80	89.74 ±0.96	76.50 ±0.22	40.15 ±1.08	2.58 ±0.01	0.021 ±0.001
IbCh3Tw80	89.74 ±0.99	81.60 ±0.22	40.35 ±1.30	2.96 ±0.02	0.027 ±0.002
IbCh4Tw80	89.74 ±1.02	89.76 ±0.17	40.80 ±0.57	3.34 ±0.01	0.025 ±0.001
IbCh5Tw80	89.22 ±0.89	95.73 ±0.17	42.30 ±0.57	4.84 ±0.04	0.038 ±0.001

Table 10 Conjugation efficiency, conductivity, surface tension, viscosity and absorbance/transmittance of ibuprofen-chitosan conjugates (hydrotropy). Each value represents mean ± SD (n = 6).

Formulation	Conjugation Efficiency (%)	Conductivity (mS/cm)	Surface tension (dynes/cm)	Viscosity (mPaS)	Absorbance/ Transmittance
IbNic-control	-	0.29±0.01	50.63±1.07	1.12±0.03	0.000±0.000
IbCh1Nic	91.99 ±1.03	81.45 ±0.13	43.50±0.91	1.65 ±0.01	0.001 ±0.00
IbCh2Nic	91.30 ±0.98	83.40 ±0.29	48.55 ±0.66	1.77 ±0.02	0.005 ±0.0005
IbCh3Nic	90.95 ±0.87	84.35 ±0.29	45.93 ±0.81	1.80 ±0.01	0.006 ±0.0005
IbCh4Nic	90.78 ±0.92	89.90 ±0.37	44.00 ±0.91	2.29 ±0.01	0.013 ±0.0005
IbCh5Nic	90.26 ±0.85	92.58 ±0.22	44.25 ±1.32	3.49 ±0.01	0.028 ±0.001

The physical properties of binary polymer-polymer [DEAE-Dextran-Gellan (DG), Chitosan-Gellan (CG)] and ternary polymer-drug-polymer [DEAE-Dextran-Ibuprofen-Gellan (DGIb); Chitosan-Ibuprofen-Gellan (CGIb)] conjugates are shown in Tables 11 to 14. Effective release of active pharmaceutical substances from polymeric materials requires that the concentration of the drug should be high enough at the site of action to facilitate therapeutic effect at the same time it should not be too high to elicit undesirable side effects. However the general drawback of polysaccharides as a delivery system is low complexation efficiency consequently a significantly high amount of water soluble polymers are frequently needed to solubilize small amount of poorly soluble drugs. Ribeiro *et al.* reported a dramatic improvement in drug solubility when a suitable third component (α-hydroxy-acids and water-soluble polymers) was added to cyclodextrin followed by heating [45]. Therefore, oppositely charged polymers were combined to reinforce the initial drug-cationic polymer conjugate so that the release of the solubilized ibuprofen can be enhanced, controlled, extended and complete. Extended and complete release could also allow for dose reduction and consequently reduced side effects without compromising the therapeutic values. Therefore choosing the

appropriate polymer-polymer ratio would be of great value to achieving efficient release profile from the polymer combinations.

Interaction between DEAE-Dextran and Gellan revealed characteristic pattern in each of the parameter studied (Table 11 and Figure 8) exhibiting break points at critical conjugation concentration ratio of the polymers. Break point was prominent at DEAE-Dextran/Gellan ratio 50:50 for conductivity, surface tension and viscosity while turbidity exhibited two breakpoints at ratio 25:75 and 50:50. The Chitosan/Gellan profile was similar to the DEAE-Dextran/Gellan exhibiting critical conjugation at ratio 50:50 for surface tension and viscosity while break point was observed at Chitosan/Gellan ratio 25:75 for conductivity and turbidity. It was concluded that ratio 50:50 is the critical conjugation concentration for both DEAE-Dextran/Gellan and Chitosan/Gellan interaction. Therefore in order to optimize the conjugation process in the presence of ibuprofen DEAE-Dextran/Gellan and Chitosan/Gellan ratio of 2:1 was used in this study to account for the ibuprofen-DEAE-Dextran or Ibuprofen-Chitosan interaction.

Table 11 Conductivity, surface tension, viscosity and absorbance/transmittance of DEAE-Dextran-gellan conjugates. Each value represents mean ± SD (n = 6).

Formulation	Conductivity (µS/cm)	Surface tension (dynes/cm)	Viscosity (mPaS)	Absorbance/Transmittance
DG 0:100	142.23±1.05	55.27±0.25	3.61±0.02	0.008±0.001
DG 25:75	194.43±1.21	54.17±0.15	1.70±0.01	0.771±0.006
DG 50:50	235.75±1.08	52.73±0.64	1.39±0.01	0.756±0.001
DG 75:25	254.13±0.67	54.33±0.42	1.83±0.01	0.039±0.001
DG 100:0	286.83±0.75	54.50±0.50	2.02±0.02	0.001±0.000

Table 12 Conductivity, surface tension, viscosity and absorbance/transmittance of chitosan-gellan conjugates. Each value represents mean ± SD (n = 6).

Formulation	Conductivity (mS/cm)	Surface tension (dynes/cm)	Viscosity (mPaS)	Absorbance/Transmittance
CG 0:100	0.15±0.001	55.23±0.25	3.78±0.03	0.006±0.001
CG25:75	2.50±0.018	54.07±0.12	1.98±0.06	0.243±0.011
CG50:50	4.28±0.026	53.50±0.87	1.60±0.01	0.214±0.002
CG75:25	5.84±0.010	53.67±0.58	1.30±0.01	0.105±0.003
CG 100:0	7.55±0.019	52.77±0.25	1.58±0.02	0.001±0.000

Physical characteristics and conjugation efficiency of the ibuprofen loaded conjugates are presented in Table 13. Breakpoints for surface tension and viscosity of DEAE-Dextran/Ibuprofen/Gellan were at DEAE-Dextran/Gellan ratio 50:50 while conductivity and turbidity were at 75:25 and 25:75 respectively. It showed that the requirement for cationic polymer increased in the presence of ibuprofen especially in the conductivity experiment. However the difference between polymer-polymer ratios in the plain and ibuprofen-loaded nanoconjugate was not statistically significant ($p > 0.05$, $n = 6$).

Table 13 Conjugation efficiency, conductivity, surface tension, viscosity and absorbance/transmittance of ibuprofen-DEAE-Dextran-gellan conjugates (ternary). Each value represents mean ± SD (n = 6).

Formulation	Conjugation Efficiency (%)	Conductivity (µS/cm)	Surface tension (dynes/cm)	Viscosity (mPaS)	Absorbance/Transmittance
IbDW-pH6	-	307.17±1.47	52.33±1.04	1.32±0.01	0.015±0.001
DG0:100	98.57±0.89	175.22±0.17	49.00±0.5	3.29±0.02	0.164±0.005
DG25:75	98.73±0.84	186.10±0.36	47.67±0.76	1.48±0.01	1.162±0.006
DG50:50	97.71±0.82	199.55±0.39	40.17±0.58	1.41±0.01	0.472±0.004
DG75:25	98.22±0.76	211.00±3.34	43.50±1.00	1.75±0.01	0.177±0.003
DG100:0	99.10±0.92	255.15±0.80	47.83±0.58	2.43±0.02	0.062±0.004

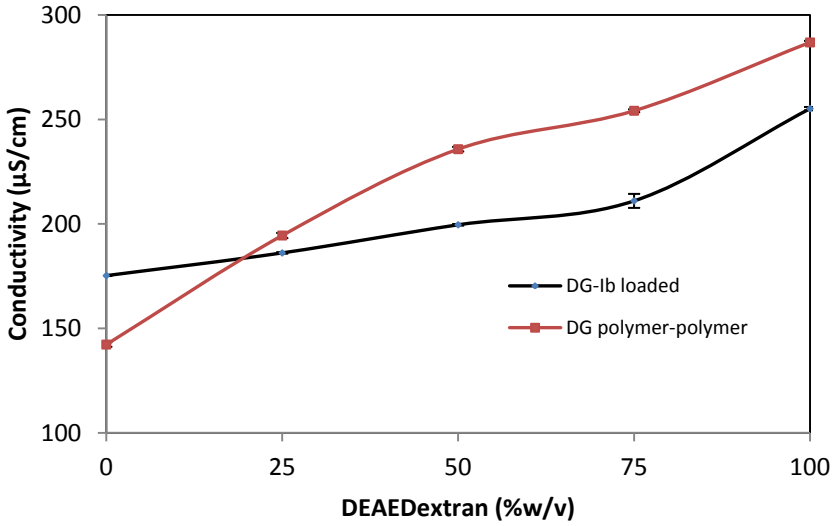

Figure 8 Conductivity of DG polymer-polymer complexes and ibuprofen loaded DG-Ib based on DEAE-Dextran content in the complexes. Each data point represents mean ± SD (n = 6).

Conductivity measurements showed that the DG polymer-polymer and DG-Ib loaded complexes exhibited increase in conductivity values as the DEAE-Dextran content increased: DG 100:0 > DG 75:25 > DG 50:50 > DG 25:75 > DG 0:100. However the rate of increase in conductivity was faster in

the plain than the drug loaded conjugates (Figure 8). The plain conjugate exhibited breakpoint at DEAE-Dextran/Gellan ratio 50:50 while the drug loaded conjugates exhibited breakpoint at 75:25. It was opined that the presence of ibuprofen reduced the affinity between DEAE-Dextran and Gellan probably due to preferential affinity of ibuprofen for DEAE-Dextran because of its higher hydrophobicity. It is well documented in literature that the amphiphilic drugs like ibuprofen have ability to self-associate in aqueous solutions and be adsorbed onto polymer backbone through hydrophobic and electrostatic bonds [2]. Also considering the lowest ibuprofen concentration used in this study (1 mg/mL) which is 4.85 mM, the molar ratio of the carboxylic acid group to quarternary ammonium polymer group on the maximum DEAE-Dextran concentration (0.02 mM) was 242.5 (greater than 1). It follows that there are sufficient ibuprofen molecules in all the systems to neutralize all the cationic groups on DEAE-Dextran. This explains the initial high conductivity of the drug loaded conjugate however as the concentration of DEAE-Dextran increased further interaction occurred probably displacing gellan which can form association below its cmc leading to the observed lowered break point. In a similar study, Rodriguez *et al.* reported that near *cmc* ibuprofen caused phase separation of ethylhydroxyethyl cellulose (EHEC) dispersions because of a strong hydrophobic interaction that shrinks the polymer chain and its micelle solubilised the hydrophobic part of the polymer above *cmc*. This reaction is possible between ibuprofen and the Diethylaminoethyl- (hydrophobic) group of DEAE-Dextran and explains the difference between the plain and drug loaded conjugates.

Table 14 Conjugation efficiency, conductivity, surface tension, viscosity and absorbance/transmittance of ibuprofen-chitosan-gellan conjugates (ternary). Each value represents mean ± SD (n = 6).

Formulation	Conjugation Efficiency (%)	Conductivity (mS/cm)	Surface tension (dynes/cm)	Viscosity (mPaS)	Absorbance/Transmittance
IbDW-pH5	-	0.31±0.001	52.33±1.04	1.32±0.01	0.015±0.001
CG0:100	98.94±0.84	0.16±0.003	47.83±1.15	4.61±0.04	0.158±0.006
CG25:75	98.97±0.75	2.33±0.02	47.67±0.76	1.54±0.01	0.104±0.004
CG50:50	97.01±0.90	4.07±0.01	46.17±0.58	1.33±0.01	0.297±0.001
CG75:25	98.60±0.89	5.71±0.01	47.17±0.58	1.54±0.01	0.120±0.003
CG100:0	98.47±0.91	6.95±0.01	44.33±0.76	1.58±0.02	0.077±0.003

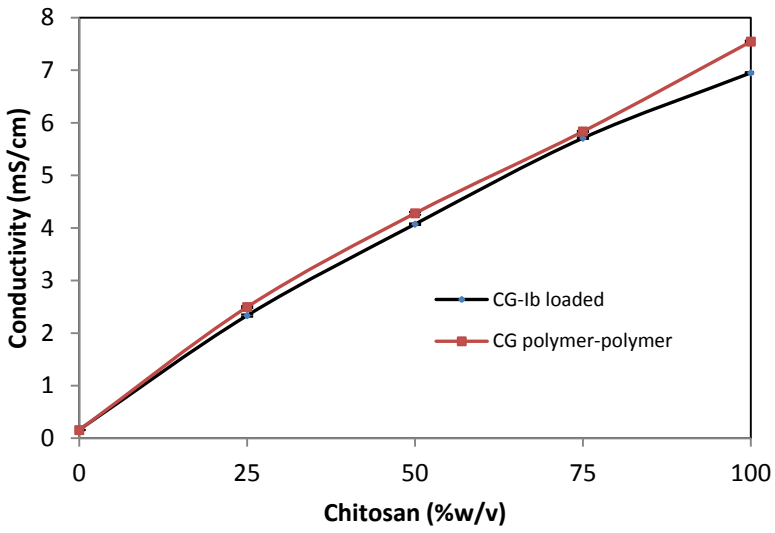

Figure 9 Conductivity of CG polymer-polymer complexes and ibuprofen loaded CG-Ib based on chitosan content in the complexes. Each data point represents mean ± SD (n = 6).

Conductivity measurements showed that the CG polymer-polymer and CG-Ib complexes exhibited in the order CG 100:0 > CG 75:25 > CG 50: 50 > CG 25:75 > CG 0:100. Conductivity increased with increase in chitosan content shown in Figure 9. Li and co-workers reported the conductivity behaviours of chitosan solution showed that there is transforming process of chitosan solution conformation and charge conduction mechanism in 0.1 M acetic acid solution with the increase of chitosan concentrations [46]. The specific electrolytic conductivity increased as chitosan concentration increased and more complexes are formed.

As an amphiphilic substance, ibuprofen can form micelles or micelle-like aggregates above a critical micelle concentration and can interact with polymers in a similar way to surfactant-polymer interaction [43].

2.3.3.2. Surface tension

The surface activity of the drug-polymer was studied by the evaluation of the surface tension measurements of the nanoconjugates as a function of polymer concentration. The surface tension of ibuprofen in distilled water obtained from preliminary studies ranged from 49.20 to 53.99 N/m decreasing with increasing concentration (2.5 to 40.0 µg/mL) of ibuprofen. The surface tension

behaviour of Ibuprofen with cationic DEAE-Dextran is shown in Figure 10. Surface tension measurements showed that the IbDMelt ranged from 32.15 to 37.35 N/m, exhibiting lower surface tension than the control (56.6 N/m). The profile showed an initial decrease till minima was reached at IbD2Melt (0.2% DEAE-Dextran), this was followed by a little increase which remained constant over the increasing concentration of DEAE-Dextran. Addition of DEAE-Dextran caused a reduction in surface tension at the air/water interface indicating its ability to adsorb at the air/water interface in preference to the bulk of the medium. In theory, when surface active agents adsorb at the water interface they replace some water molecules thereby reducing the intermolecular (cohesive) forces of attraction between water molecules hence surface tension is reduced.

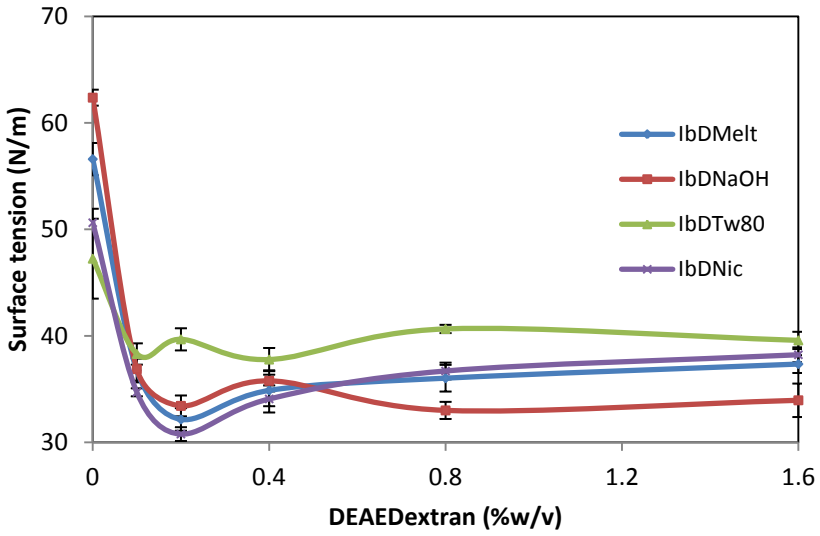

Figure 10 Surface tension of IbDMelt, IbDNaOH, IbDTw80 and IbDNic conjugates based on DEAE-Dextran content in the conjugates. Each data point represents mean ± SD (n = 4).

The amount of DEAE-Dextran present at the water surface, in excess of those in the bulk for the melt solubilization technique was 1.97 x 10^{-4} mol/dm^3 as calculated using the Gibbs equation (equation 7):

$$\Gamma = -\frac{C}{RT}\left(\frac{d\gamma}{dC}\right) \qquad (7)$$

In which Γ is the surface excess concentration of DEAE-Dextran; R is the Gas constant (8.314 J $mol^{-1}K^{-1}$; T is the temperature in kelvin; C is the concentration of DEAE-Dextran in mol/dm^3; dγ is the change in surface tension and dC is the change in concentration. The surface excess of DEAE-Dextran

for alkaline solubilization, Tween 80 (non ionic surfactant) solubilization and hydrotropic complexation are 2.34 x 10^{-4}; 7.23 x 10^{-5} and 1.60 x 10^{-4} mol/dm^3 respectively. Comparing the four processes used in this study the surface excess of DEAE-Dextran was in the order alkaline solubilization > melt solubilization > hydrotropic complexation > non ionic surfactant solubilization technique. It was also observed that the *cmc* of DEAE-Dextran was same in three of the methods (0.004 mM) but lower in the surfactant solubilization technique (0.002 mM). Two break points were also observed in this technique while there was only one in the others. It was opined that the adsorption of Tween 80 was preferentially favoured until the surface was saturated leading to the first *cmc* at lower concentration of DEAE-Dextran. The effect of DEAE-Dextran became prominent afterwards however the *cac* was increased to 0.008 mM. Contrary to this finding, Lee *et al.* have noted that micelle formation of polymers can compete with surface adsorption and that polymer/surfactant combination is often considered to have synergistic effect due to co-adsorption [47].

The surface tension behaviour of Ibuprofen with cationic chitosan is shown in Figure 11. Surface tension measurements showed that the IbChMelt ranged from 41.55 to 48.38 N/m, exhibiting lower surface tension than the control (56.6 N/m). The profile showed an initial decrease till minima was reached at IbCh2Melt (0.2% chitosan), this was followed by a little increase, a decrease and a final increase over the increasing concentration of chitosan.

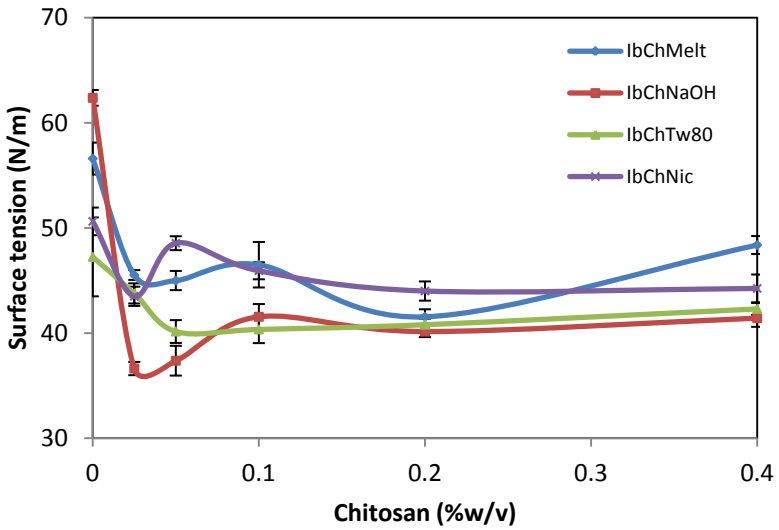

Figure 11 Surface tension of IbChMelt, IbChNaOH, IbChTw80 and IbChNic conjugates based on chitosan content in the conjugates. Each data point represents mean ± SD (n = 4).

The IbChNaOH nanoconjugates ranged from 36.63 to 41.55 N/m, exhibiting lower surface tension than the control (62.38 N/m). The profile showed an initial decrease till minima was reached at IbCh1NaOH (0.1% chitosan), this was followed by an increase, then a decrease which remained constant over the increasing concentration of chitosan.

The IbChTw80 nanoconjugates ranged from 40.15 to 43.78 N/m exhibiting lower surface tension than the control (62.38 N/m). The profile showed an initial decrease till minima was reached at IbD1Tw80 (0.1% DEAE-Dextran), this was followed by a little increase, then a decrease and a final increase which was followed by a decrease over the increasing concentration of chitosan.

While IbChNic nanoconjugates from 43.50 to 48.55 N/m conjugates exhibited lower surface tension than the ibuprofen control (56.6 N/m). No predictable pattern was observed in the trend based on the increasing concentration of chitosan. However the surface excess for melt solubilization; alkaline solubilization; surfactant solubilization and hydrotropic complexation are 9.36 x 10^{-5}; 2.08 x 10^{-4}; 1.79 x 10^{-4} and 1.06 x 10^{-4} mol/dm^3 respectively. The highest surface excess was present in the alkaline solubilization which also had very low *cmc* (0.025% ie 0.0005 mM) while the melt solubilization had the lowest amount with *cmc* of 0.05% (0.001 mM). Tween 80 did not show any visible effect on the surface activity of chitosan unlike DEAE-Dextran and the chitosan surface excess

was 2.5 times the amount of DEAE-Dextran in the presence of Tween 80. It was evident that both DEAE-Dextran and chitosan showed surface activity and were adsorbed significantly at the water surface with high probability of forming micelles and reducing the surface free energy of the system which in turn could facilitate solubility.

Surface tension measurements showed that the DG polymer-polymer loaded complexes exhibited in the order DG 0:100 > DG 100:0 > DG 75:25 > DG 25:75 > DG 50:50 (Table 11). Figure 12 showed the surface tension plot with an initial decrease in surface tension with increasing concentration of DEAE-Dextran up to DG 50:50 exhibiting the minima; beyond which it increased till it reached a constant surface tension value.

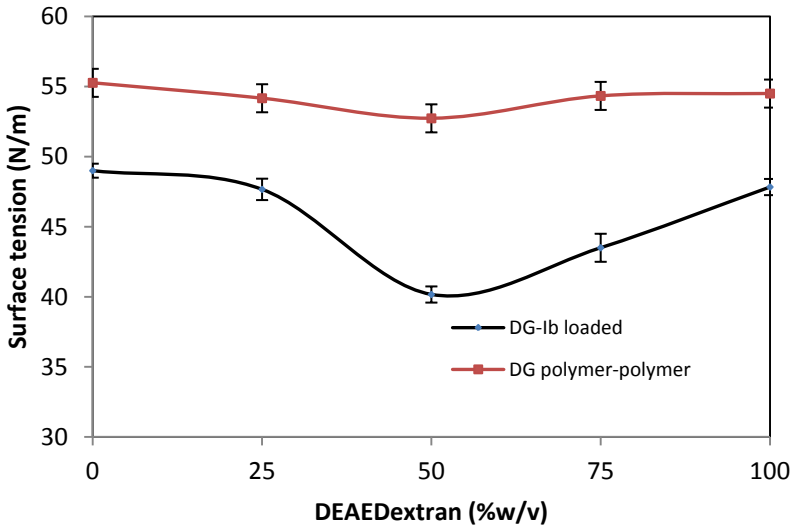

Figure 12 Surface tension of DG polymer-polymer and ibuprofen loaded DG-Ib complexes based on DEAE-Dextran content in the complexes. Each data point represents mean ± SD (n = 4).

Surface tension measurements showed that the DG-Ib loaded complexes exhibited lower surface tension than the ibuprofen control in the order: Ibuprofen control > DG 0:100 > DG 100:0 > DG 25:75 > DG 75:25 > DG 50:50 (Table 13). Figure 12 showed the surface tension plot with DG 50:50 exhibiting the minima.

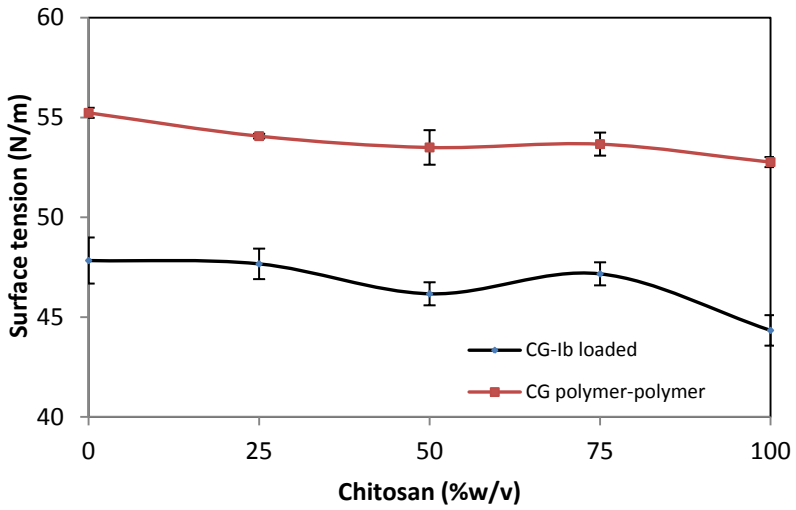

Figure 13 Surface tension of CG polymer-polymer and ibuprofen loaded CG-Ib complexes based on chitosan content in the complexes. Each data point represents mean ± SD (n = 4).

Surface tension measurements showed that the CG complexes exhibited in the order CG 0:100 > CG 25:75 > CG 75:25 > CG 50:50 > CG 100:0 (Table 12). The surface tension plot showed a decrease, a minima (CG 50:50) followed by a maxima (CG 75:25) and a further decrease in surface tension in Figure 13. Surface tension measurements showed that the ibuprofen loaded CG complexes exhibited lower surface tension than the ibuprofen control in the order: ibuprofen control > CG 0:100 > CG 25:75 > CG 75:25 > CG 50:50 > CG 100:0 (Table 14). The surface tension plot showed a decrease, a minima (CG 50:50) followed by a maxima (CG 75:25) in Figure 13. This *cmc* of DEAE-Dextran: Gellan conjugate (50:50) coincides with its *cac* indicating conjugation equilibrium at the weight ratio.

2.3.3.3. Viscosity

The viscosity of the drug-polymer solutions is an important parameter due to its association with the hydrodynamic stabilization of the particles formed [48]. The viscosity of ibuprofen in distilled water obtained from preliminary studies ranged from 1.12 to 1.17 mPas decreasing with increasing concentration (2.5 to 40.0 µg/mL) of ibuprofen. The viscosity of DEAE-Dextran in distilled water ranged from 1.2 to 1.41 mPaS increasing slowly with increasing concentration (0.005 to 0.1% w/v). The viscosity behaviour of the drug-polymer nanoconjugates was studied by the evaluation of the viscosity measurements of the nanoconjugates as a function of polymer concentration. Viscosity

measurements in Table 4 showed that the IbDMelt nanoconjugates from 1.72 to 6.61 mPas, exhibiting higher viscosity than the control 1.28 mPas. Viscosity increased gradually with increasing concentration of DEAE-Dextran in Figure 14.

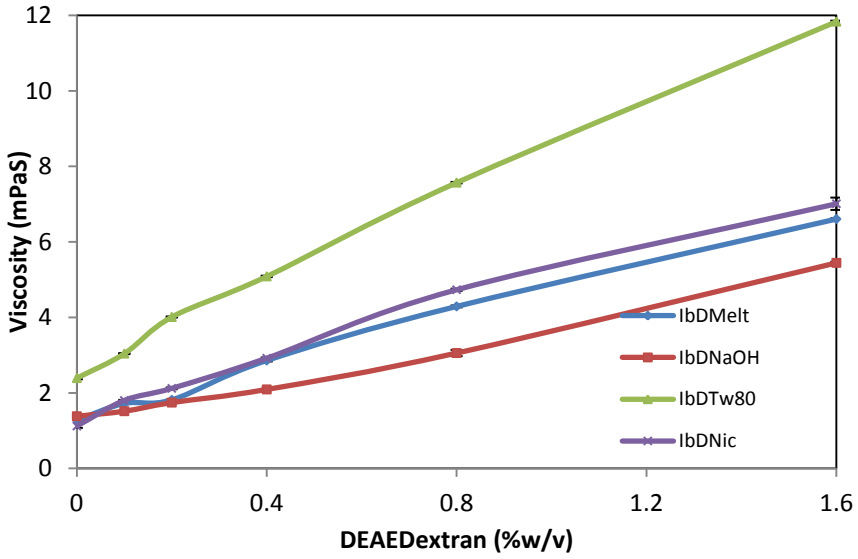

Figure 14 Viscosity of IbDMelt, IbDNaOH, IbDTw80 and IbDNic conjugates based on DEAE-Dextran content in the conjugates. Each data point represents mean ± SD (n = 6).

The IbDNaOH nanoconjugates in Table 5 ranged from 1.52 to 5.44 mPas, exhibiting higher viscosity than the control (1.38 mPas). The IbDTw80 nanoconjugates in Table 6 ranged from 3.04 to 11.83 mPas, exhibiting higher viscosity than the control (2.39 mPas). While IbDNic nanoconjugates in Table 7 ranged from 1.80 to 7.00 mPaS conjugates exhibiting higher viscosity values than the ibuprofen control (1.21 mPas). Viscosity increased with increase in DEAE-Dextran concentration for all the batches. The intrinsic viscosity of IbDMelt, IbDNaOH, IbDTw80 and IbDNic were 1.36 (R^2 = 0.99), 1.21 (R^2 = 0.99), 2.63 (R^2 = 0.99) and 1.4 (R^2 = 0.99) mPas respectively. The intrinsic viscosity of IbDTw80 batch was considerably higher when compared to the other techniques in the order: IbDTw80 > IbDNic > IbDMelt > IbDNaOH.

The viscosity of chitosan in glacial acetic acid ranged from 1.16 to 17.7 mPaS, increasing with increasing concentration (0.005 to 1% w/v) of chitosan. The viscosity measurements in Table 8 showed that the IbChMelt ranged from 1.47 to 3.22 mPas, exhibiting higher viscosity than the

control (1.28 mPas). Viscosity increased with increase in chitosan concentration, gradually reaching a constant in Figure 15.

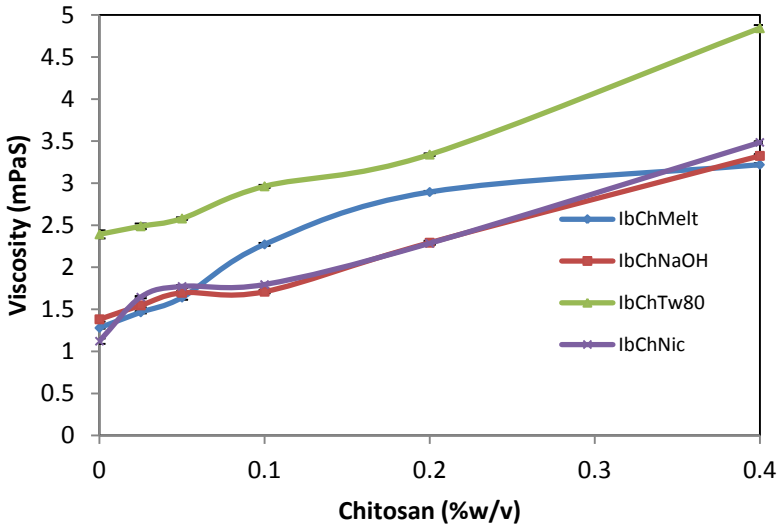

Figure 15 Viscosity of IbChMelt, IbChNaOH, IbChTw80 and IbChNic conjugates based on chitosan content in the conjugates. Each data point represents mean ± SD (n = 6).

The IbChNaOH nanoconjugates in Table 9 ranged from 1.55 to 3.33 mPas, exhibiting higher viscosity than the control (1.38 mPas). The IbChTw80 nanoconjugates in Table 10 ranged from 2.49 to 4.84 mPas, exhibiting higher viscosity than the control (2.39 mPas). While IbChNic nanoconjugates in Table 11 ranged from 1.65 to 3.49 mPas exhibiting higher viscosity values than the ibuprofen control (1.12 mPas). Viscosity increased with increase in chitosan concentration for all the batches. The intrinsic viscosity of IbChMelt, IbChNaOH, IbChTw80 and IbChNic were 1.49 (R^2 = 0.88), 1.38 (R^2 =0.99), 2.31 (R^2 = 0.99) and 1.34 (R^2 = 0.96) respectively. The intrinsic viscosity of IbChTw80 batch was considerably higher when compared to the other techniques in the order IbChTw80 > IbChMelt > IbChNaOH > IbChNic.

Viscosity measurements showed that the DG complexes exhibited a decrease in viscosity in the order DG 0:100 > DG 100:0 > DG 75:25 > DG 25: 75 > DG 50:50. It was obvious that gellan is more viscous than DEAE-Dextran by a factor of 1.8. The binary conjugate of the two showed a steady decrease in viscosity to a minimum value of 1.39 ± 0.01 mPaS at DEAE-Dextran/Gellan conjugate ratio 50:50 which also coincides with the conjugation concentration. The viscosity increased again

beyond the minimum value. The viscosity curve of the plain and ibuprofen loaded conjugates crossed at DEAE-Dextran/Gellan 50:50 hence, it was concluded that process of conjugation accounted for the reduction in viscosity (Figure 16) and that the addition of ibuprofen in the conjugate did not interfere with the process of conjugation. Although the viscosity profile of the ibuprofen-loaded conjugates was slightly lower than the plain, the difference was not statistically significant ($p > 0.05$, $n = 6$).

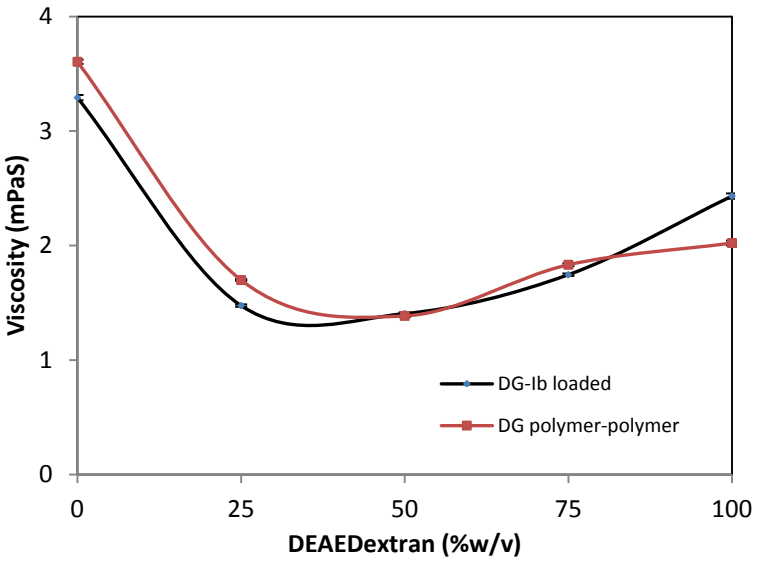

Figure 16 Viscosity of DG polymer-polymer and ibuprofen loaded DG-Ib complexes based on DEAE-Dextran content in the complexes. Each data point represents mean ± SD (n = 6).

Figure 17 shows the viscosity profle of plain and ibuprofen loaded chitosan-gellan conjugate. Viscosity measurements decreased in the order CG 0:100 > CG 25:75 > DG 50:50 > CG 100:0 > CG 75:25 (Table 12). The viscosity plot showed an initial decrease to a minimum followed by a slight increase with increasing concentration of chitosan similar to DEAE-Dextran. Ibuprofen-loaded chitosan-gellan conjugates exhibited higher viscosity than the ibuprofen control in the order CG 0:100 > CG 100:0 > CG 75:25 > CG 25:75 > DG 50:50 > ibuprofen control (Table 14). However, the viscosity decreased to almost a constant value as the chitosan content increased. The minimum viscosity of the drug loaded conjugates was lower than the plain conjugates (Figure 17).

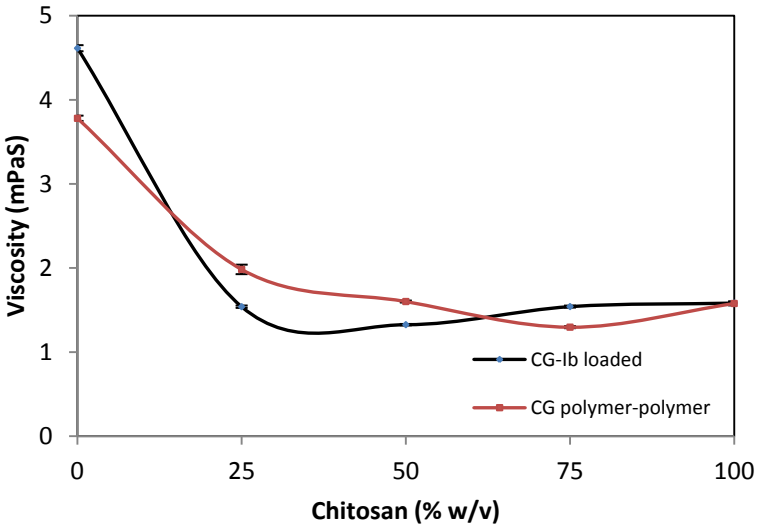

Figure 17 Viscosity of CG polymer-polymer and ibuprofen loaded CG-Ib complexes based on chitosan content in the complexes. Each data point represents mean ± SD (n = 6).

2.3.3.4. Turbidity

Turbidity is used to measure polyelectrolyte complex formation. The turbidity profile of the Ibuprofen-DEAE-Dextran nanoconjugates is shown in Figure 18 and Tables 4 to 7. Turbidity profile of surfactant solubilized Ibuprofen-DEAE-Dextran conjugates decreased steadily to constant value of 0.033 at 0.4% DEAE-Dextran concentration while others exhibited a net increase of turbidity to a maximum (Figure 18). The melt solubilized Ibuprofen-DEAE-Dextran conjugates showed two inflection points indicating multiple complex phenomena. The low turbidity values in Tables 4, 5 and 7; and Figure 18 for IbDMelt, IbDNaOH and IbDNic respectively may indicate formation of soluble complexes which are often reversible and unstable while the ones with higher turbidity values may indicate formation of insoluble complexes which are usually irreversible.

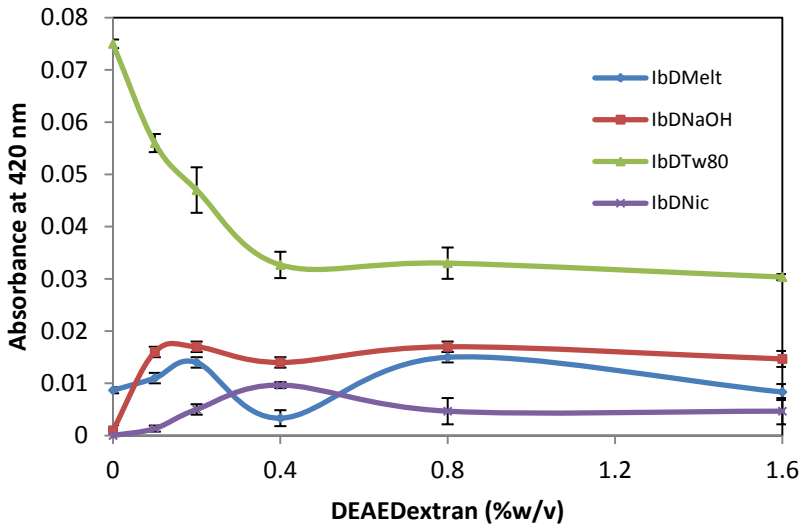

Figure 18 Absorbance at 420 nm of IbDMelt, IbDNaOH, IbDTw80 and IbDNic conjugates based on DEAE-Dextran content in the conjugates. Each data point represents mean ± SD (n = 6).

The turbidity profile of the Ibuprofen-Chitosan nanoconjugates is shown in Figure 19 and Tables 8 to 11. Turbidity profile of IbChNaOH increased steadily as the concentration of chitosan increased while others exhibited a net decrease to a minimum in Figure 19. The IbChNaOH exhibited high turbidity due to its cloudiness when compared to the other techniques. The low turbidity in other techniques may be due to formation of soluble complexes which are reversible.

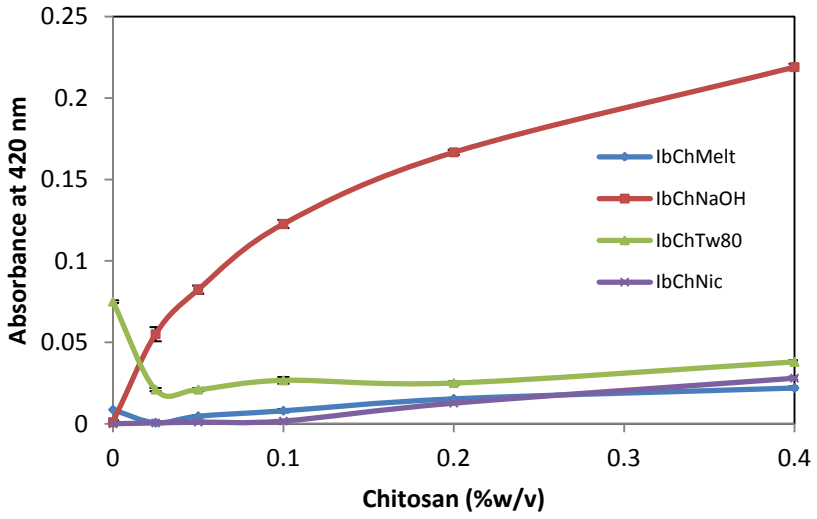

Figure 19 Absorbance at 420 nm of IbChMelt, IbChNaOH, IbChTw80 and IbChNic conjugates based on chitosan content in the conjugates. Each data point represents mean ± SD (n = 6).

Turbidity values for the DG complexes ranged between 0.001 and 0.771. The order of increase in turbidity: DG 25:75 > DG 50:50 > DG 75:25 > DG 0: 100 > DG 100:0. Maximum turbidity was achieved by DG 25:75 shown by the maxima in Figure 20.

Turbidity values for the ibuprofen loaded DG complexes ranged between 0.062 and 1.162 much higher than the control formulation. The order of increase in turbidity: DG 25:75 > DG 50:50 > DG 75:25 > DG 0:100 > DG 100:0 > ibuprofen control. Maximum turbidity was achieved by DG 25:75 shown by the maxima in Figure 20. It was noted that the plain conjugates exhibited a normal distribution shape while the drug-loaded conjugates was skewed to lower concentration of DEAE-Dextran indicating that smaller quantities of DEAE-Dextran is required to achieve conjugation equilibrium in the presence of ibuprofen. It follows that the addition of a third component may have synergistic effect in this case. The area under the curve (AUC) measures the extent of complexation. The AUC of the plain DEAE-Dextran/Gellan conjugate (31.6 unit^2) was less than that of the ibuprofen-loaded conjugates (57.5 unit^2). This finding corresponds to the stronger interaction between DEAE-Dextran and ibuprofen due to a combination of hydrophobic and electrostatic interaction as discussed under conductivity and surface tension.

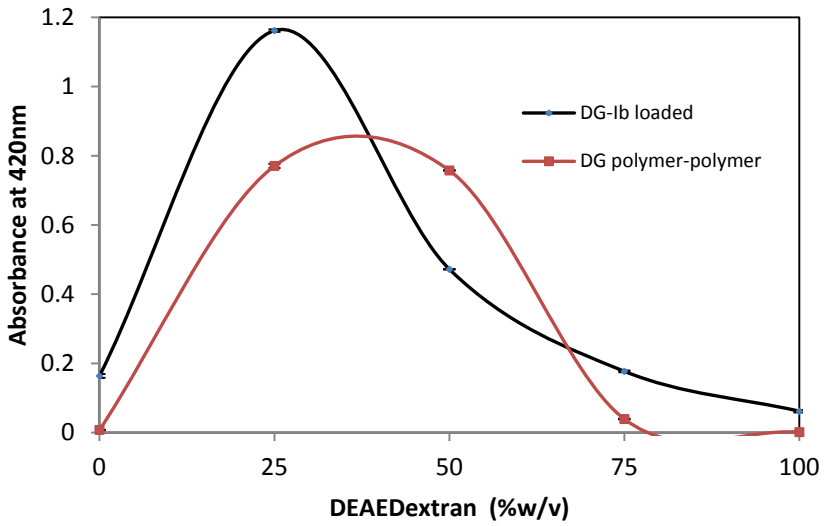

Figure 20 Absorbance at 420 nm of DG polymer-polymer and ibuprofen loaded DG-Ib complexes based on DEAE-Dextran content in the complexes. Each data point represents mean ± SD (n = 6).

Turbidity measurements showed that CG complexes ranged between 0.001 and 0.243 in the order: CG 25:75 > CG 50:50 > CG 75:25 > CG 0:100 > CG 100: 0. The turbidity plot showed an initial decrease followed by maxima and then a decrease as the chitosan content increased. Maximum turbidity was achieved by CG 25:75 shown by the maxima in Figure 21.

The ibuprofen loaded CG complexes showed higher turbidity than the ibuprofen control in the order: CG 50:50 > CG 0:100 > CG 75:25 > CG 25:75 > CG 100:0 > ibuprofen control. The turbidity plot showed an initial decrease followed by maxima shown by CG 50:50 and then a decrease as the chitosan content increased in Figure 21. The plain and the drug-loaded conjugates exhibited slightly skewed conjugate distribution with AUC of 12.5 and 15 unit^2 respectively which are significantly lower than the DEAE-Dextran conjugates ($p < 0.05$, $n = 6$). The plain conjugate was skewed to the lower concentration of chitosan while the drug-loaded type was near normal distribution. In contrary to the DEAE-Dextran conjugates, the plain binary chitosan-gellan mixture formed conjugates at lower concentration of chitosan than the drug-loaded type. It was opined that addition of a third reacting component delayed the process of conjugation and may have antagonistic effect.

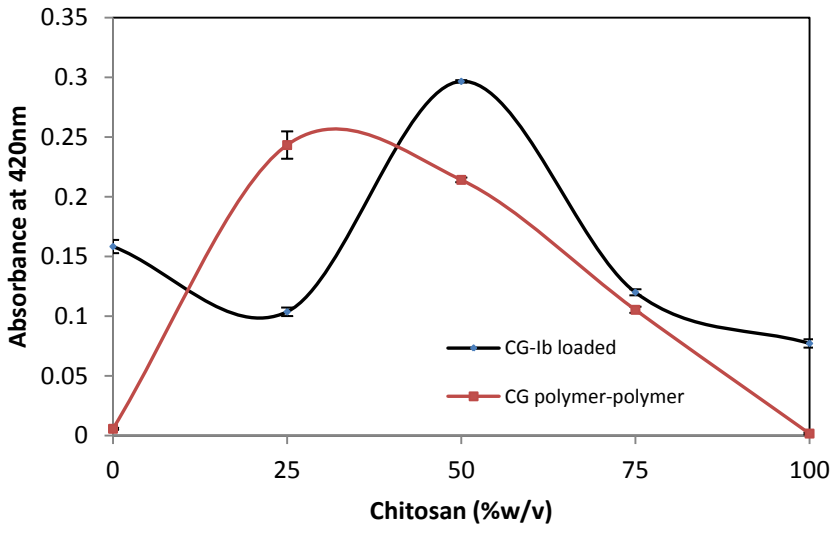

Figure 21 Turbidity at 420 nm of CG polymer-polymer and ibuprofen loaded CG-Ib complexes based on chitosan content in the complexes. Each data point represents mean ± SD (n = 6).

2.3.3.5. Particle size, poly-dispersity index and zeta potential

Poorly soluble drugs are commonly associated with critical problems of slow dissolution and erratic absorption with a consequent low and variable bioavailability. Preparation of dosage forms with particle size of less than 1 µm (nano-medicines) has been identified as an approach to enhance the dissolution as well as the rate and extent of absorption for poorly soluble drugs [49]. Literature is replete of particle size reduction techniques to enhance drug dissolution and hence the bioavailability of poorly soluble drugs [50-51] by increasing the effective surface area [52]. The relationship between rate of solution and surface area has been described by the Noyes Whitney equation (equation 8):

$$\frac{dC}{dT} = kS\ (C_s - C_t) \qquad (8)$$

where dC/dT is the rate of dissolution (concentration with respect to time), k is the dissolution rate constant, S is the surface area of the particles, C_s is the concentration of the drug in the immediate proximity of the dissolving particle (solubility of the drug) and C_t is the concentration of the drug in the bulk [53].

The particle size of ibuprofen control (processed without polymer) was found to be 2.87 µm (Table 15). Miyadai *et al.* reported that raw ibuprofen has a mean particle size of 27 µm [54]. This shows that the process of melt solubilization alone reduced the particle size significantly by a factor of 9 ($p < 0.05$, $n = 6$). Introduction of DEAE-Dextran at 0.1% (2.0 x 10^{-3} mM) concentration formed conjugates with further 14-fold size reduction to 203.25 nm. Drug-polymer nanoconjugates of size range 203.25 to 321.42 nm were obtained with DEAE-Dextran concentrations of 2.0 x 10^{-3} to 8.0 x 10^{-3} mM. Further increase in DEAE-Dextran concentration increased the conjugate size steadily up to 2351.68 nm at 1.6% (3.2 x 10^{-2} mM) (Table 15, Figure 22). In a similar study Lemarchand *et al.* reported smaller nanoparticle size of 104 nm and 165 nm from coprecipitation and emulsion polymerization of DEAE-Dextran with iron oxide and polyalkylcyanoacrylate (PACA) respectively however the amount of the polysaccharide at the surface was not quantified [55]. It was opined that

the smaller particle size in the complexation of DEAE-Dextran with metallic ion (FeO) may be due to formation of stronger bond than DEAE-Dextran with ibuprofen used in this study. Hornig *et al.*[56] also prepared dextran-ibuprofen conjugates by *in situ* activation of the carboxylic acid group with *N,N'*-carbonyldiimidazole (CDI), they obtained nanoparticles in the range of 102 to 287 nm. Nonetheless it was remarkable to note that nanoparticles could be prepared from DEAE-Dextran-Ibuprofen conjugate without any addition of surfactants or activators which are generally required for the preparation of polymeric nanoparticles. The increase in particle size at higher concentrations of DEAE-Dextran in this study was attributed to increase in the coating layer of DEAE-Dextran on ibuprofen. Jiang *et al.* [23] found that hydrodynamic diameter of ibuprofen particles decreased slowly with increase in pH values as ibuprofen was solubilized with NaOH in this study. The surfactant solubilized technique produced the smallest particle sizes ranging from 13.02 to 122.17 nm (Table 17 and Figure 22). Also unlike the other techniques used in this study, the nanoconjugate size decreased steadily to a minimum (13.02 nm) with increase in concentration of DEAE-Dextran confirming the synergistic effect of polymer surfactant combination which is consistent with surface tension findings in section 2.3.3.2. Hydrotropic complexation with nicotinamide also produced nanoconjugates at all concentrations of DEAE-Dextran used in this study as shown in Table 18 and Figure 22. The nanoconjugate sizes ranged from 77.92 to 994.27 nm and the size increased with increase in DEAE-Dextran concentrations. Comparing the four techniques, the initial conjugate size produced at the lowest concentration of DEAE-Dextran (2.0×10^{-3} mM) was in the order melt solubilization (203.25 nm) > alkaline solubilization (185.68 nm) > surfactant (Tween 80) solubilization (122.17 nm) > hydrotropic (nicotinamide) complexation (77.92 nm). The impact of hydrotropic complexation on particle size reduction was statistically significant ($p < 0.05$, $n = 12$) compared with other techniques. Sanghvi *et al.* [57] have reported the use of nicotinamide as potent solubility enhancing agent for poorly soluble drugs. They reported significant improvement in solubility up to 4000-fold (Benzophenyl urea derivative) with 20% nicotinamide however the effect on particle size was not investigated. The only NSAID on the list of the drugs they investigated was ketoprofen with

solubility enhancement of 12-fold. 10% w/v nicotinamide was used in this study based on the preliminary study which showed that the *cmc* of nicotinamide is 10% w/v, it was opined that higher concentrations could lead to self-association which could interfere with the conjugation process.

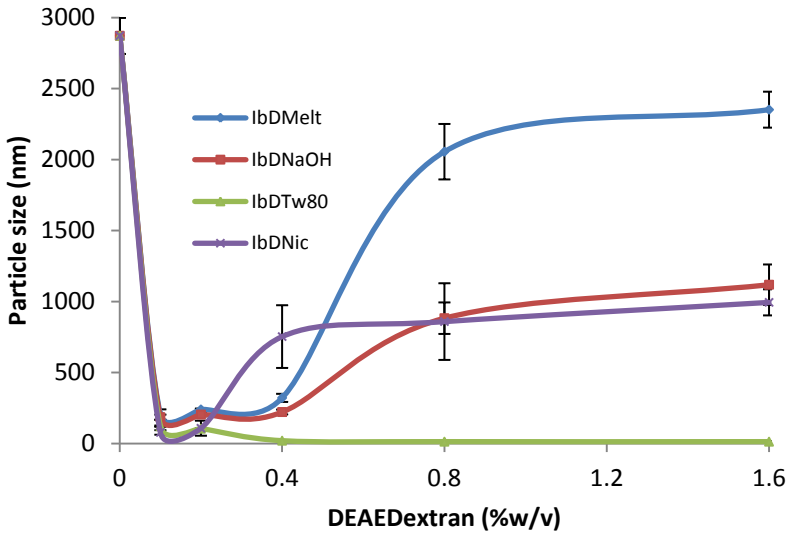

Figure 22 Effect of DEAE-Dextran concentration on particle sizes of the drug-polymer conjugates.

Polydispersity index (PDI) is the size or width of particle size distribution of the sample and has a scale which ranges from 0 to 1. PDI value of 0.1 to 0.25 which has been assigned to a narrow size distribution while PI value greater than 0.5 indicates a very wide or broad size distribution [40, 58]. High PI values indicate less homogenous size distribution hence PDI should be as low as possible for the long term stability of formulations.

The PDI of ibuprofen control was 0.67 (Tables 15 to 18) which indicated a broad and non homogeneous size distribution. The PDI of nanoconjugates in the melt solubilization technique (IbDMelt conjugates) ranged from 0.35 to 0.42 (Table 15, Figure 23) which indicated a medium homogeneous size distribution. Also the PDI of nanoconjugates in alkaline solubilization (IbDNaOH); surfactant solubilisation (IbDTw80) and hydrotropic complexation (IbDNic) ranged from 0.29 to 0.39; 0.15 to 0.37 and 0.23 to 0.55 respectively (Figure 23) which indicated a net medium homogeneous size distribution. This suggests that all the techniques used in this study exhibited semi homogenous size distribution which may translate to medium stabilization of the particles formed. However at

higher concentrations of DEAE-Dextran (1.6 x 10^{-2} and 3.2 x 10^{-2} mM), the surfactant solubilization technique produced PDI of 0.16 and 0.15 respectively indicating narrow particle size distribution, high homogeneity and stabilization. The hydrotropic complexation technique also produced PDI of 0.23 at DEAE-Dextran concentration of 3.2 x 10^{-2} mM suggesting narrow particle size distribution and high homogeneity.

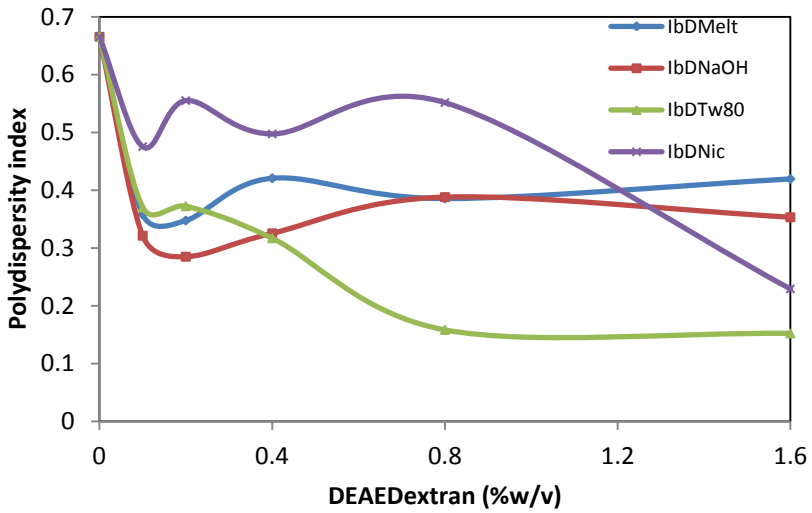

Figure 23 Effect of DEAE-Dextran on polydispersity indices of drug-polymer conjugates.

Zeta potential is a measure of the charge of the particle which is an index for particle stability. It is the potential difference between the dispersion medium and the stationary layer of fluid attached to the dispersed particle. The minimum zeta potential of ±30 mV is required and can be used to assure the stability by electrostatic repulsion of nanoparticulate suspensions [59]. However, if stability is based on electrostatic and steric stabilizer, the zeta potential of ±20 mV suffices [60]. Low zeta potential values can lead to decrease in electrostatic repulsion between the particles thereby increasing the propability of particle aggregation [61]. The aim of this study is to reduce the particle size of ibuprofen using the four techniques to increase the dissolution rate of ibuprofen.The particle size, polydispersity index values and zeta potential for the four methods of preparing the drug-polymer conjugates were presented in Tables 15 to Table 22.

The zeta potential of the ibuprofen/DEAE-Dextran nanoconjugates increased from -7.251 mV in the control batch to steady maximum values of +4.79; -1.18; +3.45 and +13.87 mV in melt solubilization, alkaline solubilization, surfactant solubilization and hydrotropic complexation techniques respectively (Figure 24, Tables 15 to 18) however the overall profile showed low values close to neutrality in all the four techniques used in this study. The negative zeta potential in the ibuprofen control indicates electrostatic repulsion between ibuprofen molecules and therefore higher physical stability of the colloidal suspension in the absence of DEAE-Dextran. The positive values of zeta potentials suggest surface modification of the nanoparticles by the cationic DEAE-Dextran. It was noted that zeta potential in the hydrotropic complexation technique tended to reduce towards neutrality after attaining the maximum value (Figure 24) probably because of aggregation of the nano conjugates which may occur when the particles overcome the energy barrier of electrostatic repulsion and approach each other to form bigger aggregates. Plakkot *et al.* [49] suggested that if the kinetic energy or velocity of the particles is sufficiently high they will collide with a consequent growth in particle size. This may explain the increase in conjugate size with increasing concentration of DEAE-Dextran except in the surfactant solubilization technique where conjugate sizes decreased steadily from 122.17 to 13.2 nm with a corresponding decrease in zeta potential from 3.45 to 1.02 mV respectively. The values of zeta potential observed in this study were relatively low (-3.04 to +13.87 mV) indicating low repulsion stabilization probably because stabilization of the nanoconjugates is by steric effect rather than electrostatic repulsion as reported by Plakkot *et al*. [49].

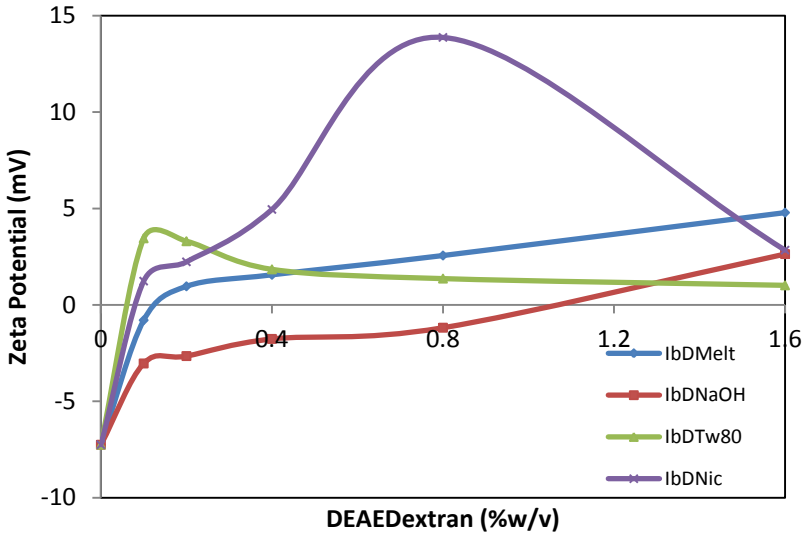

Figure 24 Effect of DEAE-Dextran on zeta potential measurements of drug-polymer conjugates.

Table 15 Particle size, polydispersity index and zeta potential for melt (IbDMelt) nanoconjugates. Each value represents mean ± SD (n = 6).

Formulation	Ibuprofen (%w/v)	DEAE-Dextran (%w/v)	Particle size (nm)	Polydispersity Index	Zeta Potential (mV)
IbMelt-control	0.2	-	2872.12±128.9	0.67±0.08	-7.251±1.3
IbD1Melt	0.2	0.1	203.25±3.7	0.36±0.05	-0.79±0.11
IbD2Melt	0.2	0.2	239.80±6.34	0.35±0.02	0.96±0.24
IbD3Melt	0.2	0.4	321.42±2.86	0.42±0.05	1.56±0.23
IbD4Melt	0.2	0.8	2055.58±19.5	0.39±0.09	2.56±0.26
IbD5Melt	0.2	1.6	2351.68±12.6	0.42±0.07	4.79±0.24

Table 16 Particle size, polydispersity index and zeta potential of solubilised (IbDNaOH) nanoconjugates. Each value represents mean ± SD (n = 6).

Formulation	Ibuprofen (%w/v)	DEAE-Dextran (%w/v)	Particle size (nm)	Polydispersity Index	Zeta Potential (mV)
IbNaOH-control	0.2	-	2872.12±128.9	0.67±0.08	-7.25±1.3
IbD1NaOH	0.2	0.1	185.68±17.61	0.32±0.04	-3.04±2.39
IbD2NaOH	0.2	0.2	203.90±12.78	0.29±0.03	-2.65±1.97
IbD3NaOH	0.2	0.4	204.48±17.02	0.33±0.03	-1.76±0.03
IbD4NaOH	0.2	0.8	882.77±110.8	0.39±0.03	-1.18±0.17
IbD5NaOH	0.2	1.6	1118.55±142.57	0.35±0.04	2.64±0.30

Table 17 Particle size, polydispersity index and zeta potential of tween 80 (IbDTw80) nanoconjugates. Each value represents mean ± SD (n = 6).

Formulation	Ibuprofen (%w/v)	DEAE-Dextran (%w/v)	Particle size (nm)	Polydispersity Index	Zeta Potential (mV)
IbTw80-control	0.2	-	2872.12±128.9	0.67±0.08	-7.251±1.3
IbD1Tw80	0.2	0.1	122.17±4.65	0.37±0.02	3.45±0.2
IbD2Tw80	0.2	0.2	104.08±4.99	0.37±0.01	3.30±0.46
IbD3Tw80	0.2	0.4	19.92±1.59	0.32±0.04	1.84±0.12
IbD4Tw80	0.2	0.8	13.02±0.92	0.16±0.14	1.37±0.16
IbD5Tw80	0.2	1.6	13.02±1.19	0.15±0.14	1.02±0.21

Table 18 Particle size, polydispersity index and zeta potential of hydrotrope (IbDNic) nanoconjugates. Each value represents mean ± SD (n = 6).

Formulation	Ibuprofen (%w/v)	DEAE-Dextran (%w/v)	Particle size (nm)	Polydispersity Index	Zeta Potential (mV)
IbNic-control	0.2	-	2872.12±128.9	0.67±0.08	-7.251±1.3
IbD1Nic	0.2	0.1	77.92±1.61	0.48±0.03	1.24±0.42
IbD2Nic	0.2	0.2	107.75±5.28	0.56±0.09	2.23±0.59
IbD3Nic	0.2	0.4	753.12±22.19	0.50±0.09	4.95±0.26
IbD4Nic	0.2	0.8	858.47±27.21	0.55±0.13	13.87±0.23
IbD5Nic	0.2	1.6	994.27±91.85	0.23±0.02	2.84±0.18

Similar to DEAE-Dextran, initial concentration (5.0×10^{-4} mM) reduced the particle size of ibuprofen from 2872.12 nm to 216.7, 502.93, 10.70 and 336.93 nm in melt solubilization; alkaline solubilization; surfactant (Tween 80) solubilization and hydrotropic (nicotinamide) complexation techniques respectively (Tables 19 to 22; Figure 25). The greatest impact of initial concentration of chitosan was observed in the surfactant solubilization technique where particle size was reduced from 2872.12 to 10.70 nm (268-fold reduction) at lower concentration suggesting a more potent synergism with surfactant (Tween 80) compared with DEAE-Dextran. All the techniques used in this study produced nanoconjugates (below 1000 nm) except the alkaline solubilization technique which produced greater than 4000 nm particles at chitosan concentration of 8.0×10^{-3} mM (Table 20). It was noted that the nanoconjugate sizes decreased to a minimum value (*cac*) at chitosan concentration of 0.05% (1.0×10^{-4} mM) in all the four techniques used in this study suggesting that method of preparation did not affect the critical association concentration of ibuprofen/chitosan nanoconjugates (ratio of 1:0.5). Beyond this ratio, chitosan nanoconjugates exhibited steady increase in size with increasing chitosan concentration. This similar trend was reported by Gan *et al.* in their investigation of chitosan-tripolyphosphate nanoparticles where a linear relationship was exhibited between the size and the concentration of chitosan within the tested range (0.05 to 3%) [61]. The authors suggested that the increase in particle size may be due to the dense spatial distance among chitosan molecules at higher concentration which led to the formation of larger particles.

Unlike the DEAE-Dextran, the conjugate size increased after *cac* in the surfactant solubilization technique. In a similar study polyalkylcyanoacrylate (PACA) and poly (lactic acid) (PLA) nanoparticles were coated with chitosan using emulsion polymerization and adsorption respectively to achieve 60 and 500 nm sizes respectively [55]. However the effect of different nanoparticularization technique was not evaluated.

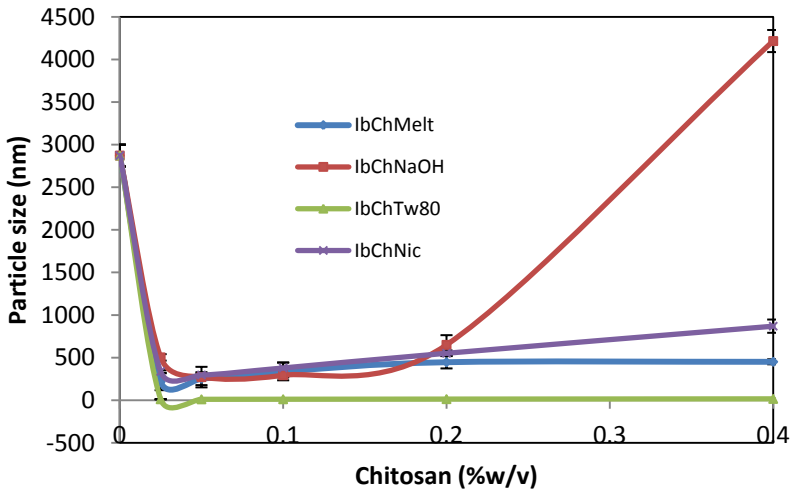

Figure 25 Effect of chitosan concentration on particle sizes of drug-polymer conjugates.

Table 19 Particle size, polydispersity index and zeta potential of melt (IbChMelt) nanoconjugates. Each value represents mean ± SD (n = 6).

Formulation	Ibuprofen (%w/v)	Chitosan (%w/v)	Particle size (nm)	Polydispersity Index	Zeta Potential (mV)
IbMelt-control	0.2	-	2872.12±128.9	0.67±0.08	-7.251±1.3
IbCh1Melt	0.2	0.025	216.7±99.15	0.51±0.17	1.89±0.59
IbCh2Melt	0.2	0.05	252.92±75.78	0.62±0.25	2.27±0.33
IbCh3Melt	0.2	0.1	338.15±104.76	0.57±0.2	2.51±0.08
IbCh4Melt	0.2	0.2	446.07±73.15	0.35±0.09	2.84±0.24
IbCh5Melt	0.2	0.4	450.83±29.69	0.45±0.09	3.03±0.21

Table 20 Particle size, polydispersity index and zeta potential of solubilised (IbChNaOH) nanoconjugates. Each value represents mean ± SD (n = 6).

Formulation	Ibuprofen (%w/v)	Chitosan (%w/v)	Particle size (nm)	Polydispersity Index	Zeta Potential (mV)
IbNaOH-control	0.2	-	2872.12±128.90	0.67±0.08	-7.251±1.3
IbCh1NaOH	0.2	0.025	502.93±37.93	0.41±0.10	0.42±0.22
IbCh2NaOH	0.2	0.05	271.05±12.06	0.69±0.20	1.27±0.18
IbCh3NaOH	0.2	0.1	292.81±25.80	0.65±0.06	1.88±0.02
IbCh4NaOH	0.2	0.2	649.50±11.39	0.42±0.08	2.07±0.02
IbCh5NaOH	0.2	0.4	4216.70±129.70	0.53±0.11	2.68±0.03

Table 21 Particle size, polydispersity index and zeta potential of surfactant solubilization (IbChTw80) nanoconjugates. Each value represents mean ± SD (n = 6).

Formulation	Ibuprofen (%w/v)	Chitosan (%w/v)	Particle size (nm)	Polydispersity Index	Zeta Potential (mV)
IbTw80-control	0.2	-	2872.12±128.90	0.67±0.08	-7.25±1.30
IbCh1Tw80	0.2	0.025	10.70±0.97	0.25±0.07	1.27±0.20
IbCh2Tw80	0.2	0.05	9.93±2.19	0.35±0.06	2.05±0.62
IbCh3Tw80	0.2	0.1	10.90±1.58	0.41±0.20	2.11±0.04
IbCh4Tw80	0.2	0.2	12.40±1.20	0.28±0.11	2.13±0.02
IbCh5Tw80	0.2	0.4	15.13±2.40	0.33±0.08	2.33±0.03

Table 22 Particle size, polydispersity index and zeta potential of hydrotrope (IbChNic) nanoconjugates. Each value represents mean ± SD (n = 6).

Formulation	Ibuprofen (%w/v)	Chitosan (%w/v)	Particle size (nm)	Polydispersity Index	Zeta Potential (mV)
IbNic-control	0.2	-	2872.12 ±128.9	0.67 ±0.08	-7.25 ±1.30
IbCh1Nic	0.2	0.025	336.93 ±15.3	0.30 ±0.04	2.57 ±0.18
IbCh2Nic	0.2	0.05	295.82 ±18.01	0.33 ±0.06	2.69 ±0.28
IbCh3Nic	0.2	0.1	378.55 ±62.97	0.32 ±0.03	2.74 ±0.03
IbCh4Nic	0.2	0.2	551.27 ±33.51	0.33 ±0.01	3.11 ±0.17
IbCh5Nic	0.2	0.4	869.17 ±77.9	0.31 ±0.033	4.39 ±1.54

The PDI of ibuprofen/chitosan nanoconjugates are presented in Tables 19 to 22; Figure 26. The PDI of IbChMelt; IbChNaOH; IbChTw80 and IbChNic was in the range of 0.35 to 0.62; 0.41 to 0.69; 0.25 to 0.41 and 0.30 to 0.33 repectively with no specific pattern with respect to concentration of chitosan. This suggests medium to broad and non homogeneous particle size distribution with low probability of stabilization.

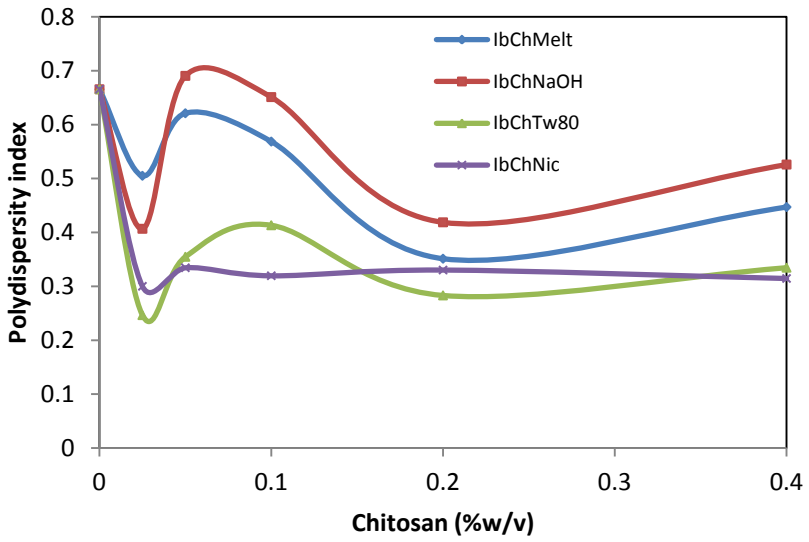

Figure 26 Effect of chitosan concentration on polydispersity indices of drug-polymer conjugates.

Similar to the ibuprofen/DEAE-Dextran nanoconjugates, the zeta potential of ibuprofen/chitosan nanoconjugates exhibited relatively low values but the values increased to a maximum with increasing concentrations of chitosan (Figure 27). The zeta potential of IbChMelt; IbChNaOH; IbChTw80 and IbChNic was in the range of 1.89 to 3.03; 0.42 to 2.68; 1.27 to 2.33 and 2.57 to 4.39 repectively (Tables 19 to 22). The presence of positive charge in the nanoconjugates also suggests modification of the nanoconjugate surface with chitosan and the low zeta potential values indicates high probability of particle aggregation. However the stabilization of the nanoconjugates may be due to steric effect rather than electrostatic repulsion. The difference between the zeta potentials of ibuprofen/DEAE-Dextran and ibuprofen/chitosan nanoconjugates was not statistically significant ($p > 0.05$, $n = 24$).

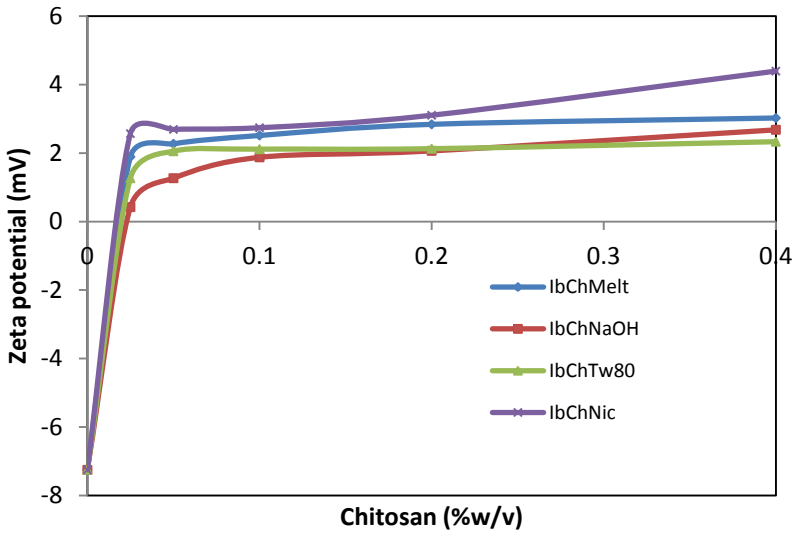

Figure 27 Effect of chitosan on zeta potential measurements of drug-polymer conjugates.

The preliminary studies showed that DEAE-Dextran and Chitosan interacted individually with gellan to form colloidal DEAE-Dextran-Gellan complex and Chitosan-Gellan complex. Therefore ternary DEAE-Dextran-Ibuprofen-Gellan conjugates were prepared, characterized and evaluated for controlled release potentials. The particle size, polydispersity index and zeta potential for ibuprofen loaded DEAE-Dextran-gellan and chitosan-gellan ternary conjugates are presented in Tables 23 and 24 respectively. The mean particle size of ibuprofen/DEAE-Dextran control conjugate was 4.23 µm

while those of ibuprofen loaded DEAE-Dextran-gellan complexes ranged from 552.87 to 972.38 nm in the order DG 50:50 < DG 75:25 < DG 25:75 < DG 0:100 < DG 100:0 < Ib-control (Table 23 and Figure 28). It was obvious that the mean particle size of the ternary DEAE-Dextran-Ibuprofen-Gellan nanoconjugate was significantly higher than the binary DEAE-Dextran-Ibuprofen nanoconjugates ($p < 0.05$, $n = 6$). For instance at ibuprofen/DEAE-Dextran ratio 1:1, the nanoconjugate size was 203.25 nm (Table 15) and 552.87 nm (Table 23) for the binary and ternary nanoconjugates respectively. It was opined that addition of anionic polyelectrolyte (gellan) could reduce the zeta (repulsion) potential of DEAE-Dextran-ibuprofen nanoconjugates leading to particle aggregation and growth. Gellan may also coat the nanoconjugate to increase the particle size. Wang *et al.* have reported the unique characteristics of gellan which include temperature-dependent hydrogen bonding and cation-induced electrostatic incorporation [62]. Since high temperature was used in the presence of cationic polymer during the preparation of ternary nanoconjugates, both electrostatic interaction and hydrogen bonding which might have occurred could increase the particle size. Increasing concentration of DEAE-Dextran decreased conjugate size steadily to a minimum value of 552.87 nm at critical conjugation DEAE-Dextran concentration of 1×10^{-3} mM (DEAE-Dextran/Gellan weight ratio 50:50), suggesting a single complexation phenomenon. Higher concentrations of DEAE-Dextran increased the conjugate size steadily (Figure 28).

Table 23 Particle size, polydispersity index and zeta potential for ibuprofen loaded DEAE-Dextran-gellan complexes. Each value represents mean ± SD (n = 6).

Formulation	Particle size (nm)	Polydispersity Index	Zeta Potential (mV)
Ib-control	4233.33±154.7	0.13±0.04	-0.97±0.28
DG 0:100	924.35±96.43	0.41±0.05	-32.14±3.75
DG 25:75	721.07±35.40	0.34±0.06	-30.31±8.10
DG 50:50	552.87±28.00	0.22±0.03	34.15±2.10
DG 75:25	635.98±29.69	0.19±0.02	44.63±2.17
DG 100:0	972.38±48.34	0.38±0.05	47.23±2.92

Table 24 Particle size, polydispersity index and zeta potential for ibuprofen loaded chitosan-gellan complexes. Each value represents mean ± SD (n = 6).

Formulation	Particle size (nm)	Polydispersity Index	Zeta Potential (mV)
Ib-control	4233.33±154.7	0.13±0.04	-0.97±0.28
CG 0:100	869.07±64.40	0.72±0.09	-30.36±3.00
CG 25:75	725.66±42.68	0.27±0.04	-24.81±2.73
CG 50:50	783.40±36.55	0.31±0.06	29.67±3.88
CG 75:25	1017.3±42.10	0.04±0.01	31.22±6.96
CG 100:0	1046.33±134.69	0.20±0.01	32.16±2.98

Similar results were obtained for ibuprofen loaded chitosan-gellan complexes as shown in Table 24 and Figure 28. The ternary conjugate sizes ranged from 725.66 to 1046.33 nm in the order CG 25:75 < CG 50:50 < CG 0:100 < CG 75:25 < CG 100:0 < Ib-control. The mean particle size of the ternary Chitosan-Ibuprofen-Gellan nanoconjugate was also significantly higher than the binary Chitosan-Ibuprofen nanoconjugates ($p < 0.05$, $n = 6$). For instance at ibuprofen/chitosan ratio 1:1, the nanoconjugate size was 338.15 nm (Table 19) and 783.40 nm (Table 24) for the binary and ternary nanoconjugates respectively. The conjugate size also decreased to a minimum value of 725.66 nm at chitosan concentration of 5×10^{-4} mM (Figure 29) suggesting a mono complexation phenomenon.

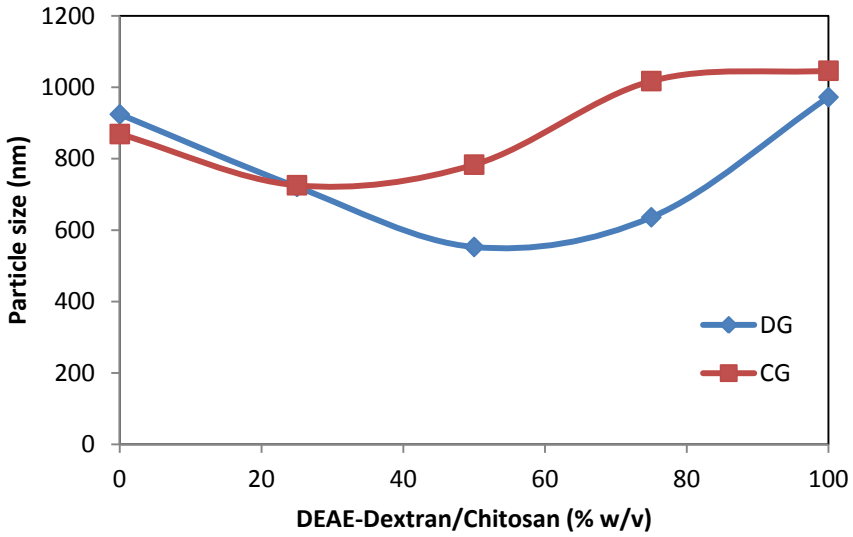

Figure 28 Effect of DEAE-Dextran and chitosan concentration on particle sizes of ibuprofen loaded DEAE-Dextran-gellan and chitosan-gellan complexes.

The PDI for DEAE-Dextran ternary conjugates exhibited only one breakpoint (*cac*) at 1.5×10^{-3} mM of DEAE-Dextran while chitosan ternary conjugates exhibited two breakpoints at 5×10^{-4} and 1.5×10^{-3} mM of chitosan indicating mono- and multiple-complexation phenomena respectively. Ibuprofen control has a PDI of 0.13 while those of ibuprofen loaded DEAE-Dextran-gellan and chitosan-gellan complexes ranged from 0.19 to 0.41 (Figure 29) and 0.04 to 0.72 (Figure 29) respectively. The PDI for DEAE-Dextran-ibuprofen-gellan conjugates decreased steadily to a minimum value of 0.19 with increase in DEAE-Dextran concentration indicating homogeneous monodispersed particle size. Further increase in DEAE-Dextran concentration beyond the *cac* increased PDI steadily indicating

polydispersed system at higher concentrations. On the other hand chitosan-ibuprofen-gellan conjugates exhibited two inflection points (Figure 29) with increasing concentration of chitosan indicating multiple complexation and polydisperse systems.

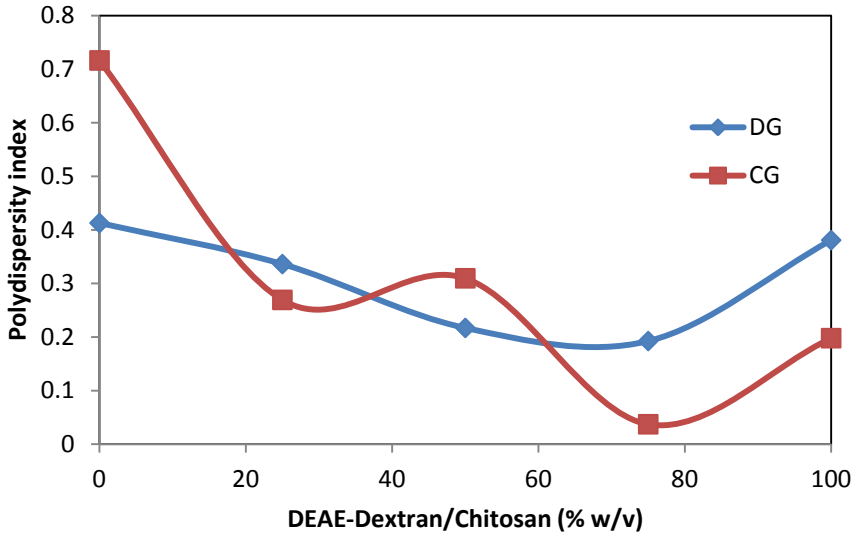

Figure 29 Effect of DEAE-Dextran and chitosan concentration on polydispersity indices of ibuprofen loaded DEAE-Dextran-gellan and chitosan-gellan complexes.

The zeta potential of ibuprofen is -0.97 mV while those of ternary ibuprofen loaded DEAE-Dextran-gellan complexes ranged from -30.31 to 47.23 mV (Figure 30). The zeta potential of the ternary nanoconjugates were significantly higher ($p < 0.05$, $n = 6$) than those of binary nanoconjugates (Figures 24 and 27) suggesting high repulsion potential and better physical stability of the ternary nanoconjugates. The increased stability was ascribed to the interaction between cationic (DEAE-Dextran) and anionic (gellan) polyelectrolytes. Similar zeta potential was observed with chitosan-ibuprofen-gellan conjugates ranging from -30.36 to 32.16 mV (Figure 33) which was also higher than the corresponding zeta potentials for binary chitosan/ibuprofen nanoconjugates (Figure 27). The enhanced stability was ascribed to the presence of gellan.

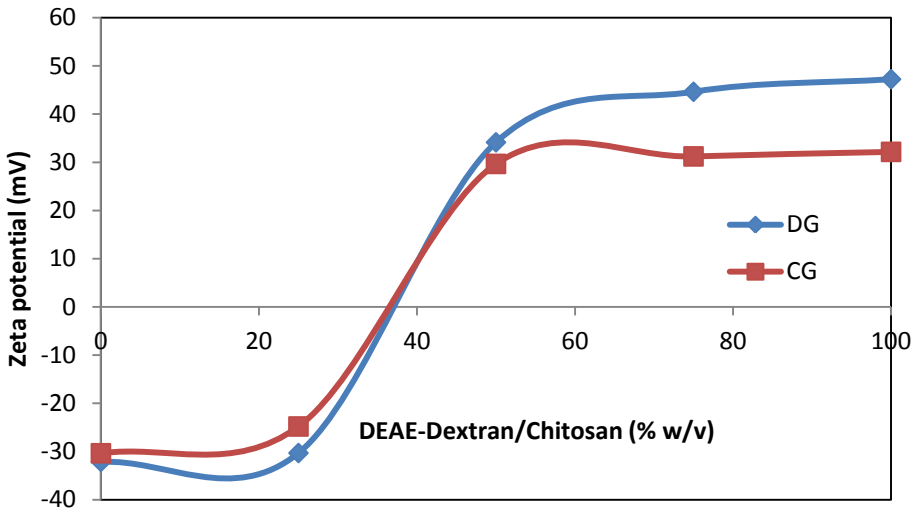

Figure 30 Effect of DEAE-Dextran and chitosan concentration on zeta potential of ibuprofen loaded DEAE-Dextran-gellan and chitosan-gellan complexes.

2.3.3.6. Drug conjugation capacity/efficiency

The efficiency of attaching drugs to the polymer carrier is very important for the success of polymer therapeutics. It is desirable to achieve higher conjugation efficiency for clinical applications. The drug conjugation efficiency of the nano-conjugates is shown in Table 3 toTable 10. The conjugation efficiency of IbDMelt conjugates was in the range of 98.22 to 98.81%; IbDNaOH conjugates 97.38 to 98.14%; IbDTw80 conjugates 89.05 to 96.33% and IbDNic conjugates from 95.48 to 95.68%. It appeared that the concentration of DEAE-Dextran did not affect the conjugation efficiency of the four techniques studied. The conjugation efficiency was relatively constant, thus independent of DEAE-Dextran concentration. High conjugation efficiency was achieved by all the method studied. This was higher than the findings of Jiang *et al.* which stated a maximum entrapment efficiency of 72.20% for ibuprofen-DEAE-Dextran complex [23].

The conjugation efficiency of IbChMelt conjugates was in the range of 98.03 to 98.73%; IbChNaOH conjugates 97.98 to 98.68%; IbChTw80 conjugates 89.21 to 90.26% and IbChNic conjugates from 90.26 to 91.99%. High conjugation efficiency was achieved by all the methods studied.

The conjugation efficiency of the ibuprofen-DEAE-Dextran-gellan complex was found to be between 97.35 and 99.1% in the order DG 100:0 > DG 25:75 > DG 0:100 > DG 75:25 > DG 50:50 as shown in Table 11. The conjugation efficiency was highest for DG 100:0.

The conjugation efficiency of the ibuprofen-chitosan-gellan complex was found to be in the range of 97.01 and 98.97% in the order CG 25:75 > CG 0:100 > CG 75:25 > CG 100:0 > CG 50:50 in Table 12. CG 25:75 complex showed the highest conjugation efficiency.

2.3.3.7. Morphology and size – Scanning electron microscopy

The SEM micrographs of ibuprofen, DEAE-Dextran, chitosan and the respective nanoconjugates are presented in Figures 31 to 38. Ibuprofen had a distinct long needle-like crystalline structure and rough surface with particle size of 145.08 ± 56.63 x 32.82 ± 12.06 µm and aspect ratio (length to width of 4.42) in Figure 31G. This was similar to the SEM image of ibuprofen crystals reported by Plakkot *et al.* with aspect ratio range of 4 to 6 [49]. While DEAE-Dextran, had rough surface and irregular structures in Figure 31H. The surface morphology of ibuprofen control showed almost spherical shaped particles in aggregates (Figure 31F).

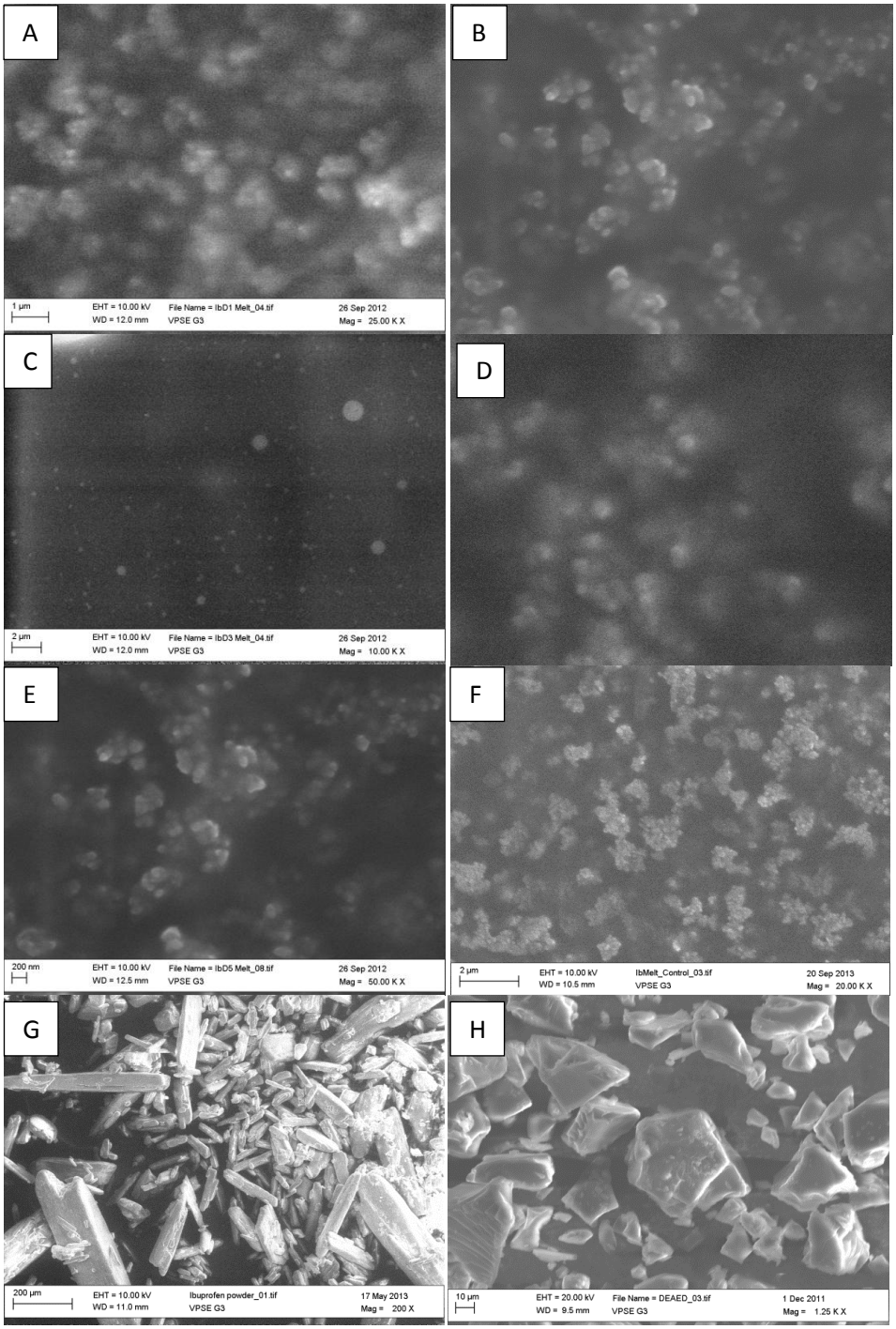

Figure 31 Scanning electron micrographs of ibuprofen-DEAE-Dextran conjugates (melt solubilization) (A) IbD1Melt, (B) IbD2Melt, (C) IbD3Melt, (D) IbD4Melt, (E) IbD5Melt, (F) IbMelt-control, (G) ibuprofen powder-reference and (H) DEAE-Dextran powder-reference.

All the four techniques produced particles of nano-size dimensions. The nanoparticles where observed to be either distinct, spherical particles or as clusters/aggregates. All the IbDMelt conjugates showed spherical particles in aggregates with particle size range of 122.7 to 807.1 nm except IbD3Melt which was spherical and appeared singly with particle size of 315.3 nm in Figure

31A to Figure 31E. They appeared to be homogenous in size under the SEM. The particle sizes increased with increasing concentration of DEAE-Dextran with the exception of IbD5Melt which exhibited the smallest particle size (Table 100 in the Appendix). It was observed that raw ibuprofen powder changed from a needle like shape to spherical particles in the processed ibuprofen (IbMelt control) and drug polymer (IbDMelt) nanoconjugates.

All the particle sizes measurements from the SEM images of the IbDMelt conjugates were in the nanometre range. This is in contrast with the particle size analyzer measurements which showed that the IbD4Melt and IbD5Melt were in the micrometer range. The discrepancy between the particle size measurement by SEM and particle size analyzer has been justified by Prabha *et al.* to be due to the fact that particle size analyzer measures the apparent size (hydrodynamic radius) of a particle, and this includes the hydrodynamic layers composed of the polymers formed around the hydrophilic particle, causing an overestimation of nanoparticles size [63].

IbD1NaOH and IbD3NaOH showed single spherical shaped particles with two concentric rings with particle sizes 364.9 nm and 249.73 nm respectively, while IbD2NaOH, IbD4NaOH and IbD5NaOH showed spherical shaped particles in aggregates with particle sizes 109.1 nm, 89.9 nm and 60.4 nm respectively in Figure 32A to 32E. The particle sizes were all in the nanometre range, which decreased with increasing concentration of DEAE-Dextran.

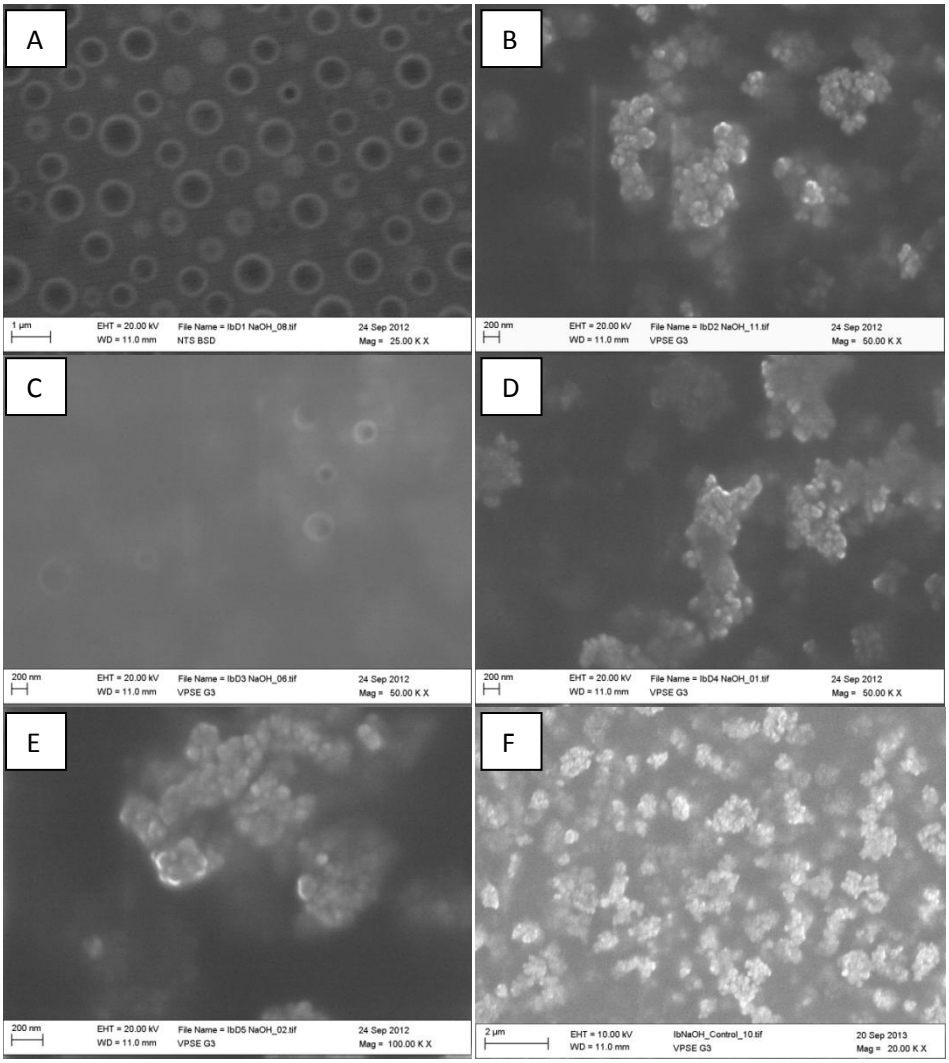

Figure 32 Scanning electron micrographs of ibuprofen-DEAE-Dextran conjugates (solubilization) (A) IbD1NaOH, (B) IbD2NaOH, (C) IbD3NaOH, (D) IbD4NaOH, (E) IbD5NaOH and (F) IbNaOH-control.

The surface morphologies of IbDTw80 conjugates were all spherical in shape and in aggregates (Figures 33A to 33E). The particle sizes decreased with increasing concentration of DEAE-Dextran in the range of 38.76 to 111.6 nm. This was comparable to that observed with the particle size analyzer in this study. It was observed that the surfactant solubilization technique exhibited the highest tendency to coalesce when compared to other techniques.

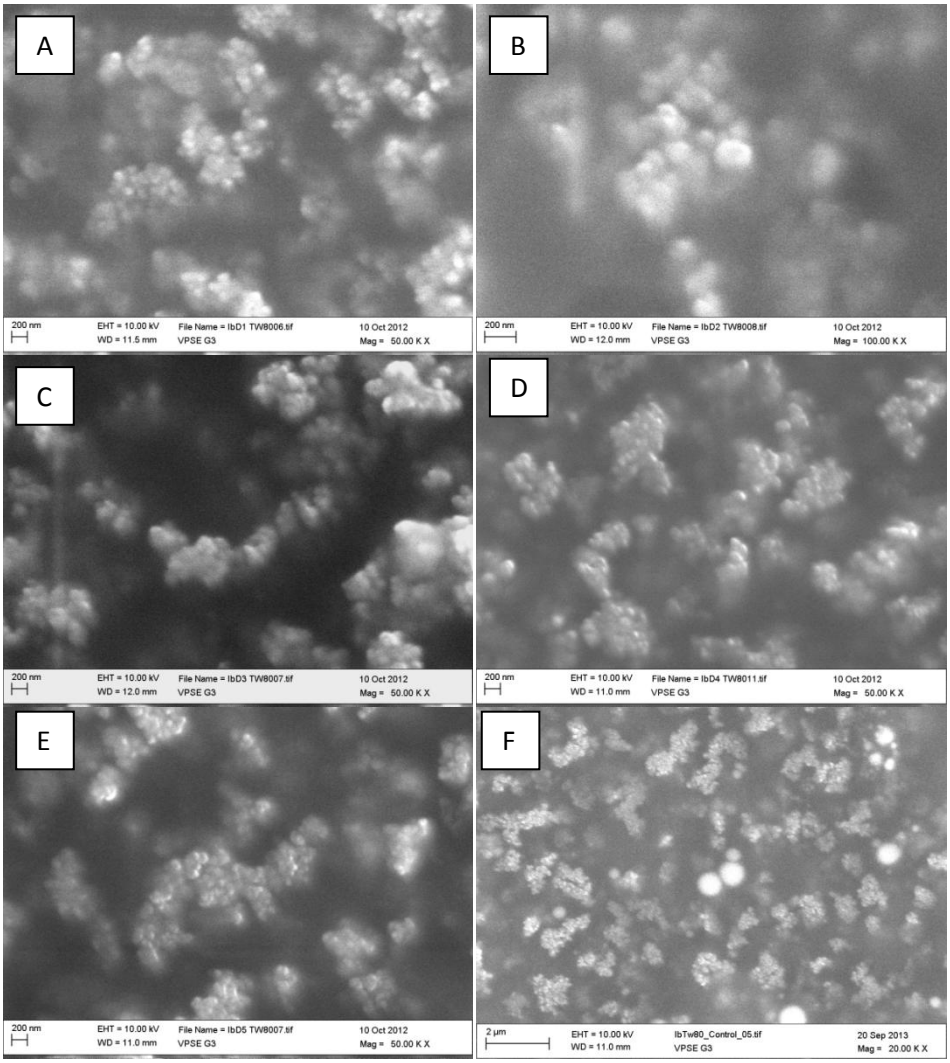

Figure 33 Scanning electron micrographs of ibuprofen-DEAE-Dextran conjugates (solubilization) (A) IbD1Tw80, (B) IbD2Tw80, (C) IbD3Tw80, (D) IbD4Tw80, (E) IbD5Tw80 and (F) IbTw80-control.

The surface morphology of IbDNic conjugates were single and spherical in Figure 34A to 34E. The particle sizes increased with increasing concentration of DEAE-Dextran in the range of 77.52 to 162.7 nm. The values of the particle sizes were smaller when compared to the particle size analyzer measurements.

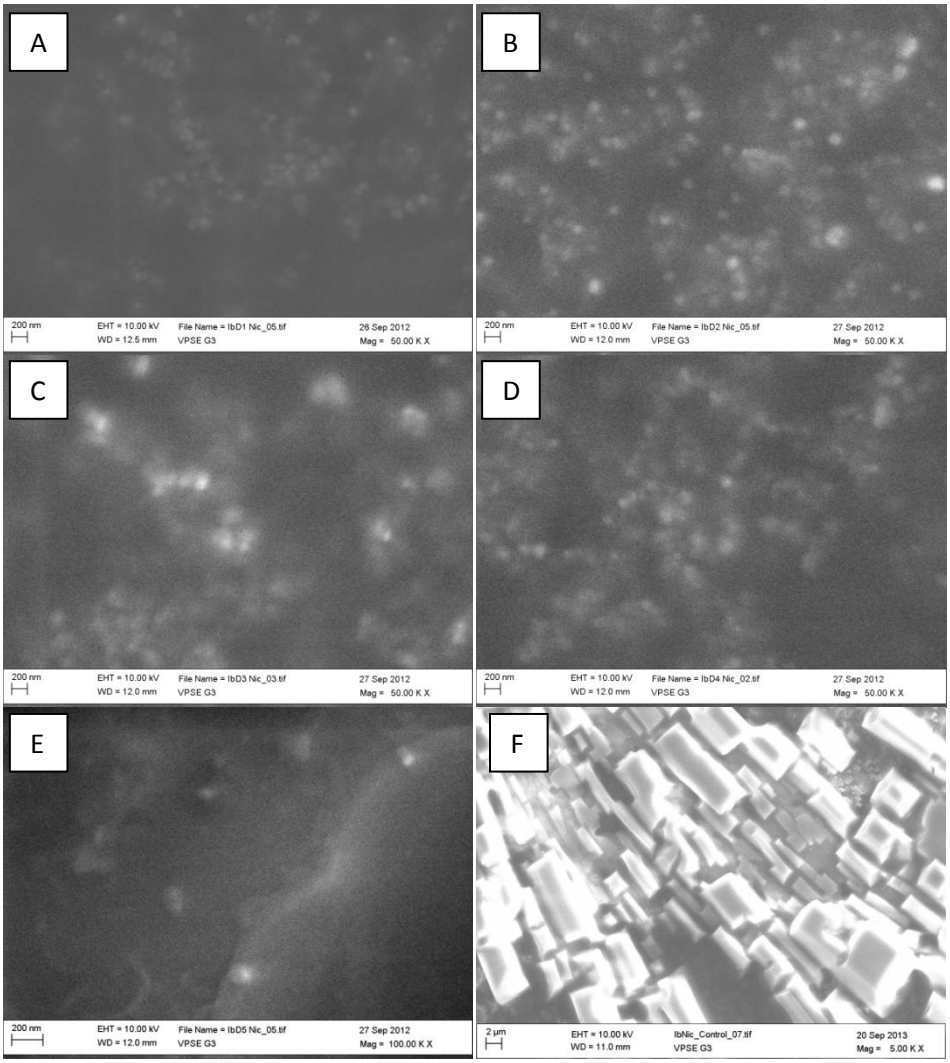

Figure 34 Scanning electron micrographs of ibuprofen-DEAE-Dextran conjugates (hydrotropy) (A) IbD1Nic, (B) IbD2Nic, (C) IbD3Nic, (D) IbD4Nic, (E) IbD5Nic and (F) IbNic-control.

The surface morphology of IbCh1Melt was almost spherical, IbCh2Melt, IbCh3Melt and IbCh5Melt were spherical and in aggregates while IbCh4Melt showed spherical particles on interconnected strands in Figure 35A to Figure 35E. The particle sizes increased with increasing chitosan concentration were in the range of 261.3 to 602.37 nm (Table 101 in Appendix I). This was comparable to the particle size analyzer measurements.

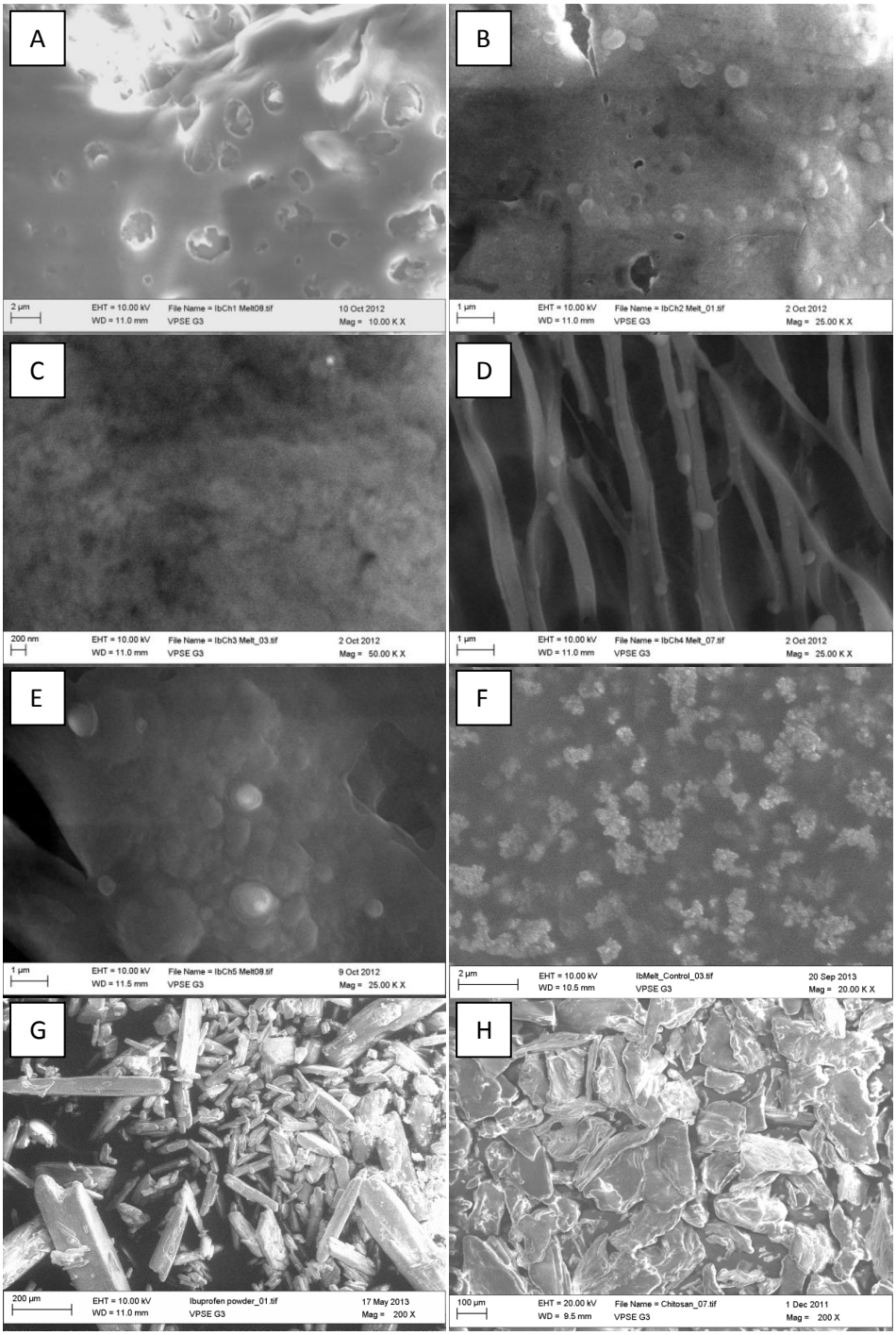

Figure 35 Scanning electron micrographs of ibuprofen-chitosan conjugates (melt solubilization) (A) IbCh1Melt, (B) IbCh2Melt, (C) IbCh3Melt, (D) IbCh4Melt, (E) IbCh5Melt, (F) IbMelt-control, (G) ibuprofen powder-reference and (H) chitosan powder-reference.

The surface morphology of IbChNaOH conjugates showed single and near spherical particles in Figure 36A to Figure 36E. The particle sizes increased with increasing concentration of chitosan with the exception of IbCh2NaOH in the range of 2.3 to 9.84 µm. The particle sizes were within the

micrometre range compared with the nanometre range obtained from the particle size analyzer measurements.

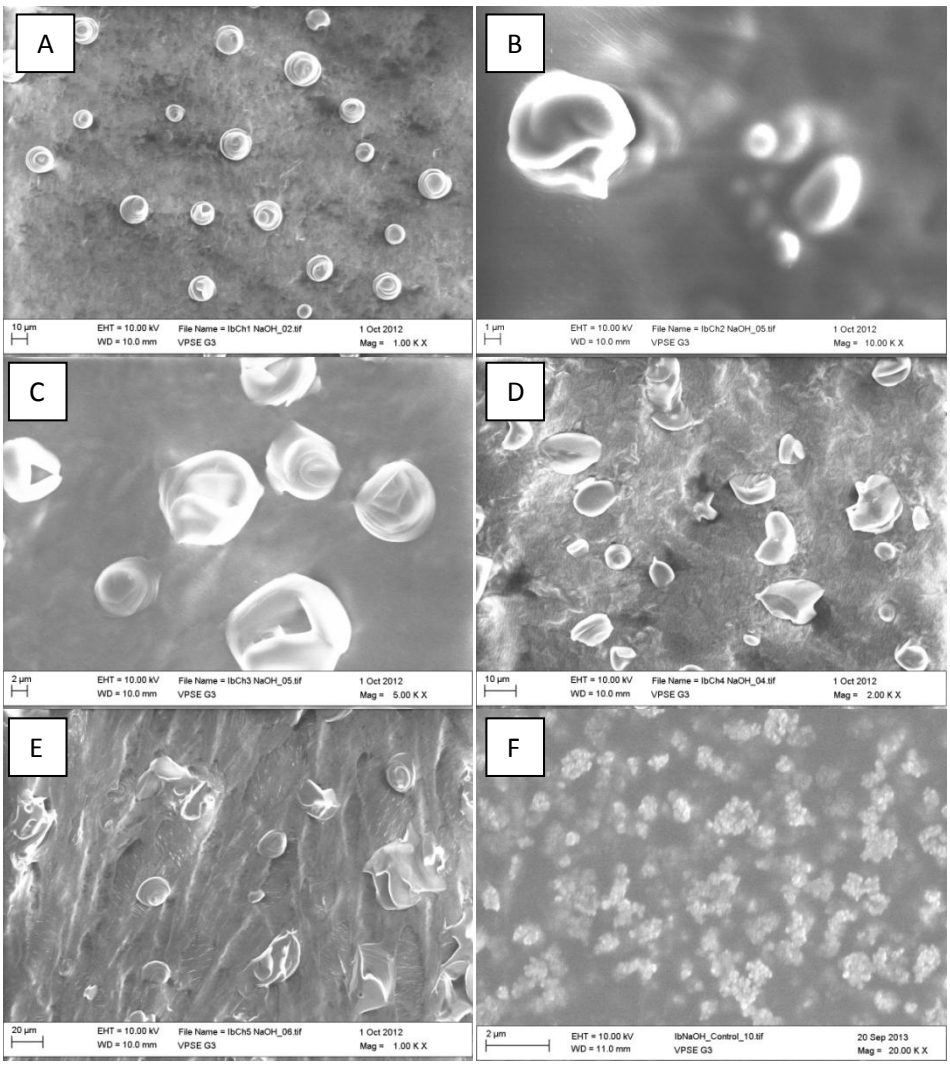

Figure 36 Scanning electron micrographs of ibuprofen-chitosan conjugates (solubilization) (A) IbCh1NaOH, (B) IbCh2NaOH, (C) IbCh3NaOH, (D) IbCh4NaOH, (E) IbCh5NaOH and (F) IbNaOH-control.

The surface morphology of IbChTw80 conjugates showed spherical and monodisperse particles in Figure 37A to 37E. The particle sizes increased with increasing chitosan concentration in the range of 166.2 to 498.9 nm. The sizes were larger than the measurements obtained from the particle size analyzer.

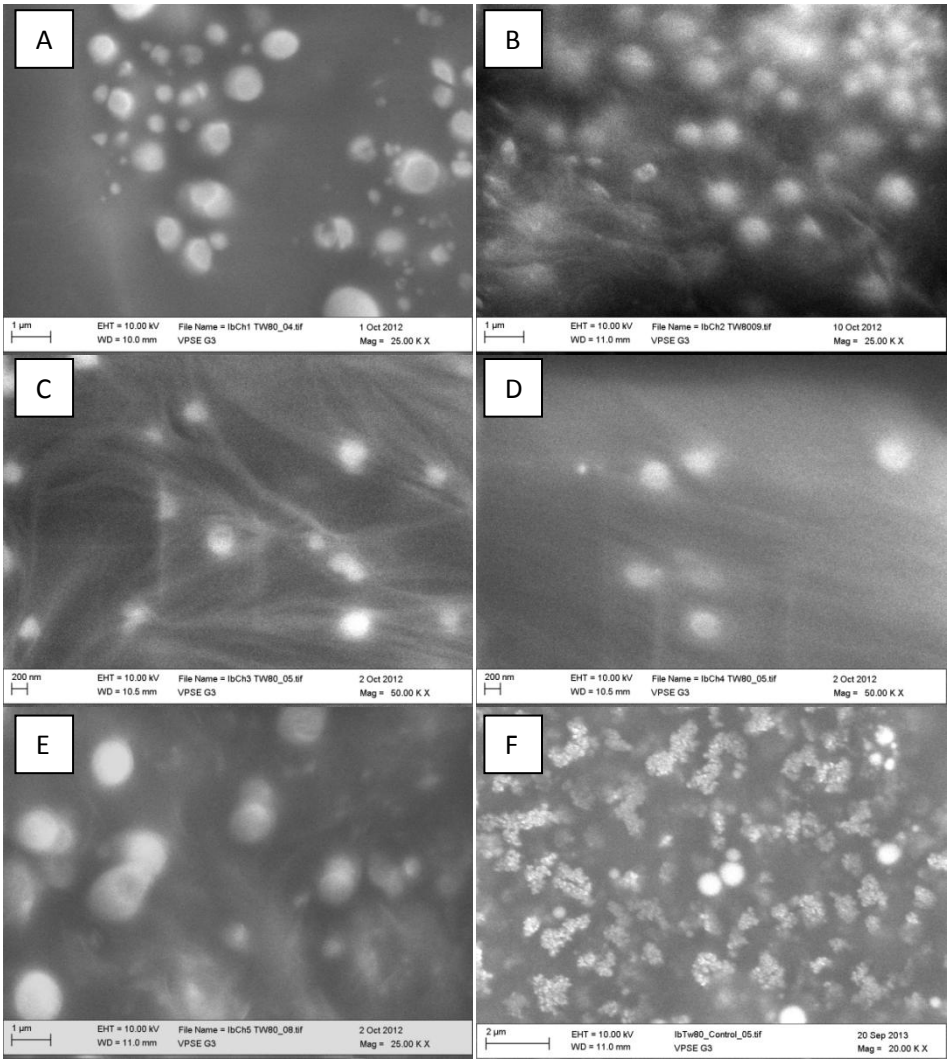

Figure 37 Scanning electron micrographs of ibuprofen-chitosan conjugates (solubilization) (A) IbCh1Tw80, (B) IbCh2Tw80, (C) IbCh3Tw80, (D) IbCh4Tw80, (E) IbCh5Tw80 and (F) IbTw80-control.

The surface morphology of IbChNic conjugates showed spherical particles in aggregates (Figures 38A to 38E). The particle sizes increased with increasing chitosan concentration in the range of 114.8 nm to 2.6 µm with IbCh5Nic in the micrometer range. The particle sizes were all in the nanometre range for particle size analyzer measurements.

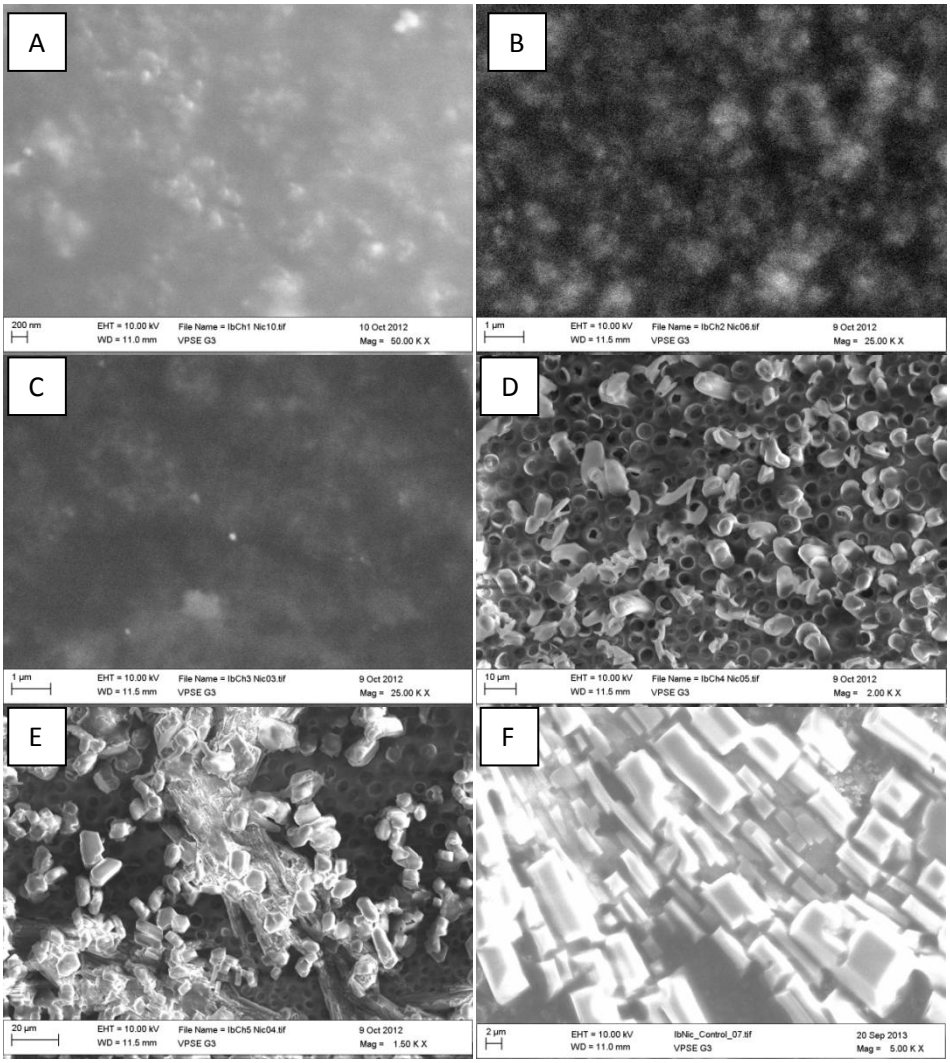

Figure 38 Scanning electron micrographs of ibuprofen-chitosan conjugates (hydrotropy) (A) IbCh1Nic, (B) IbCh2Nic, (C) IbCh3Nic, (D) IbCh4Nic, (E) IbCh5Nic and (F) IbNic-control.

The surface morphology of gellan, DEAE-Dextran and chitosan exhibited particles with irregular form and sharp edges in Figures 39 and 40. The surface morphology of binary complexes DG 0:100, DG 25:75, DG 50:50, DG 75:25 and DG 100:0 showed that the complexes were spherical and appeared singly.

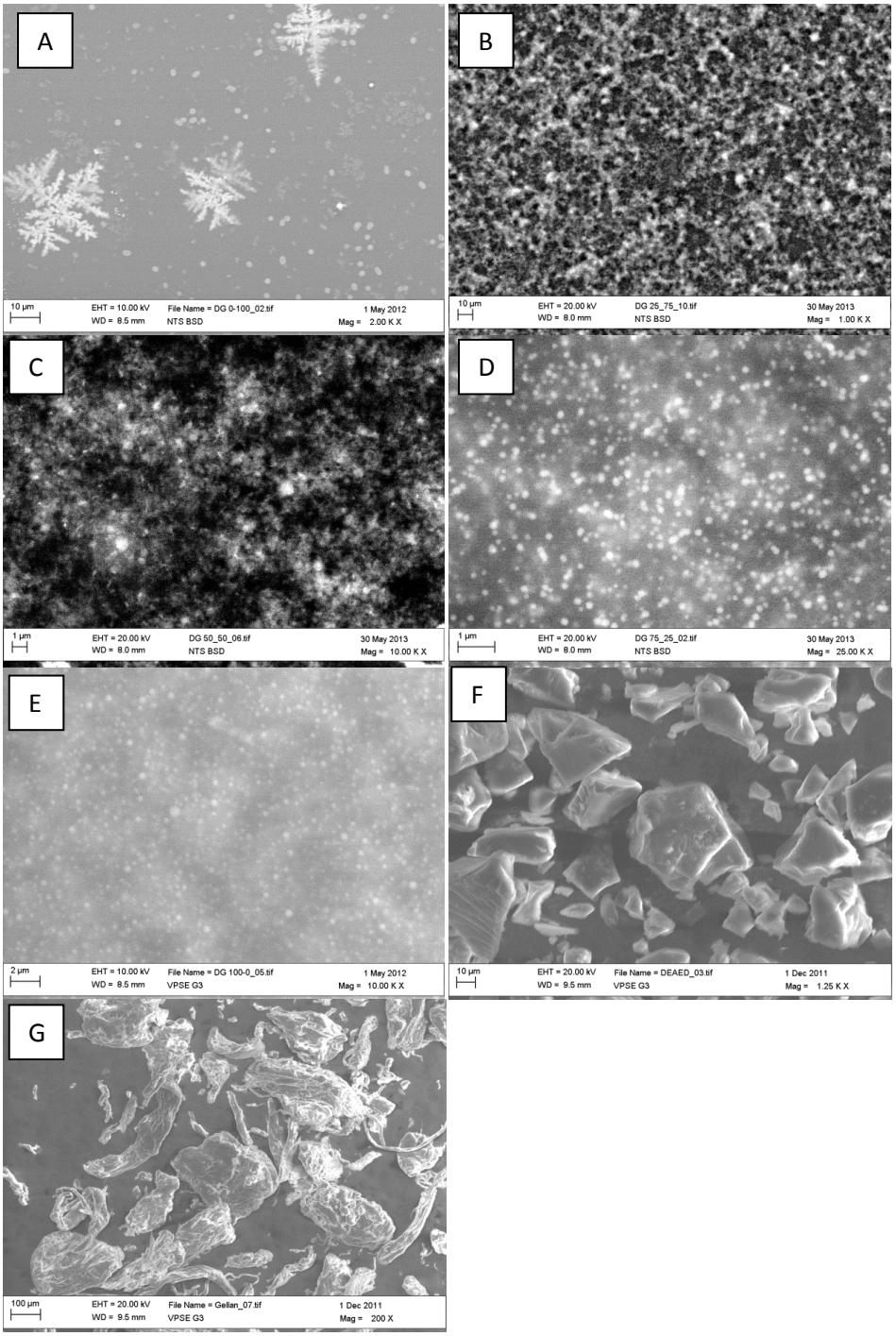

Figure 39 Scanning electron micrographs of DEAE-Dextran-gellan conjugates (binary) (A) DG 0:100, (B) DG 25:75, (C) DG 50:50, (D) DG 75:25, (E) DG 100:0, (F) DEAE-Dextran powder-reference and (G) Gellan powder-reference.

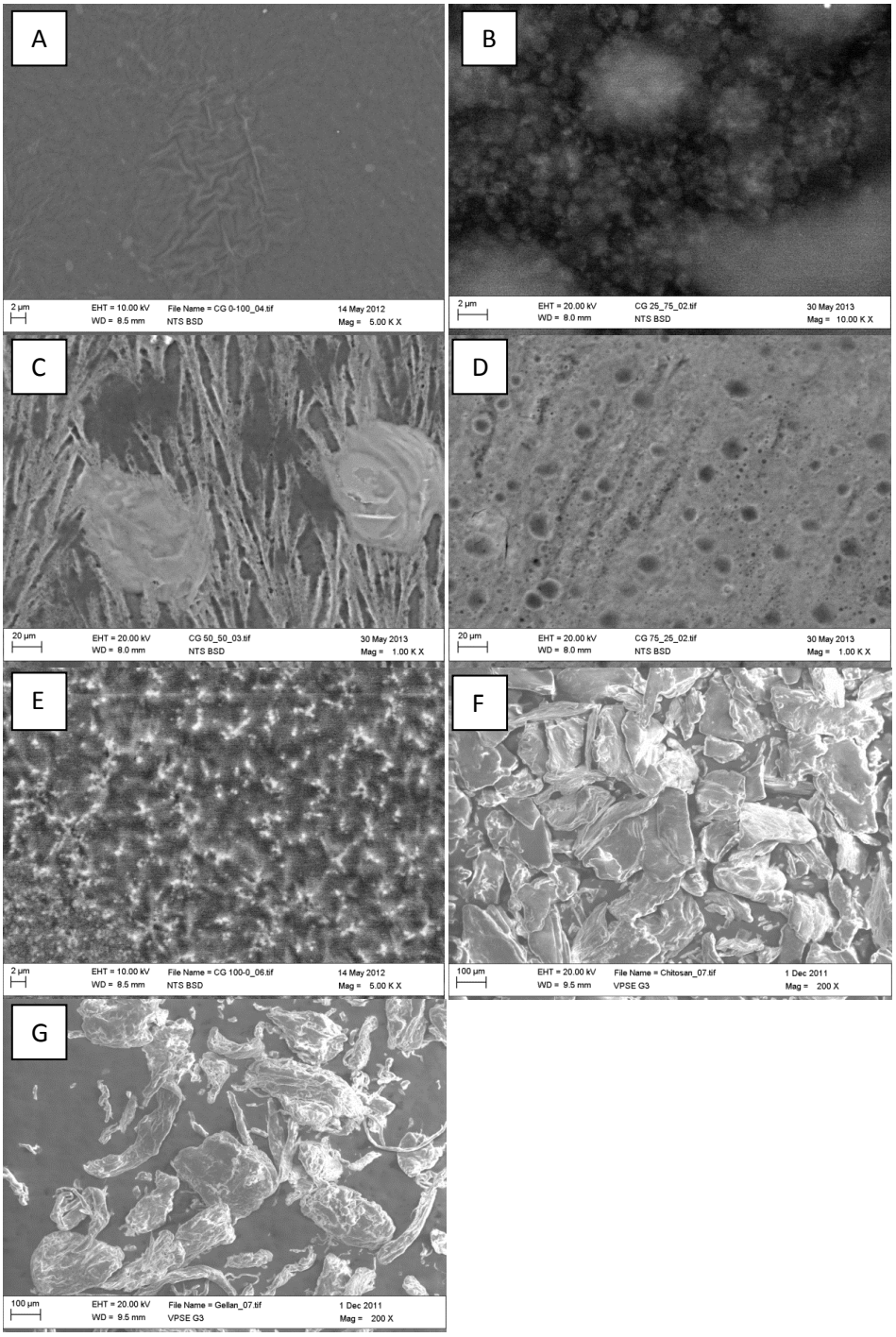

Figure 40 Scanning electron micrographs of gellan conjugates (binary) (A) CG 0:100, (B) CG 25:75, (C) CG 50:50, (D) CG 75:25, (E) CG 100:0, (F) Chitosan powder-reference and (G) Gellan powder-reference.

The surface morphology of binary complexes CG 0:100, CG 25:75, CG 50:50, CG 75:25 and CG 100:0 showed that the complexes were spherical and appeared singly (Figure 40).

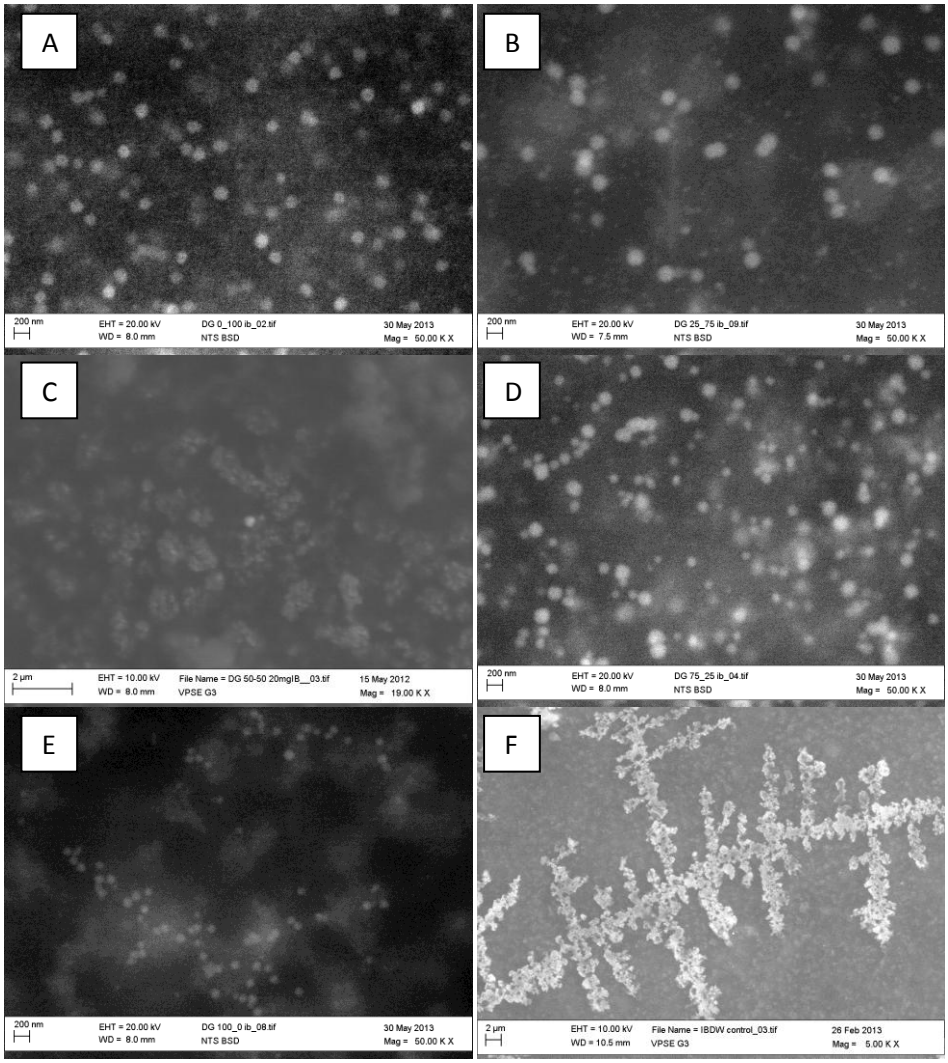

Figure 41 Scanning electron micrographs of ibuprofen-DEAE-Dextran-gellan conjugates (ternary) (A) DG 0:100, (B) DG 25:75, (C) DG 50:50, (d) DG 75:25, (E) DG 100:0 and (F) ibuprofen control.

The surface morphology of ibuprofen loaded DG 0:100, DG 25:75, DG 50:50, DG 75:25 and DG100:0 were found to be spherical and monodisperse. IbDW (processed ibuprofen in distilled water), the control formulation showed that ibuprofen remained crystalline and angular shaped arranged in cross pattern in Figure 41. The particle sizes were in the range of 171.4 to 499.5 nm exhibiting initial increase with increasing concentration of DEAE-Dextran in the DG weight ratio up to DG 50:50 beyond which there was a decrease in particle sizes.

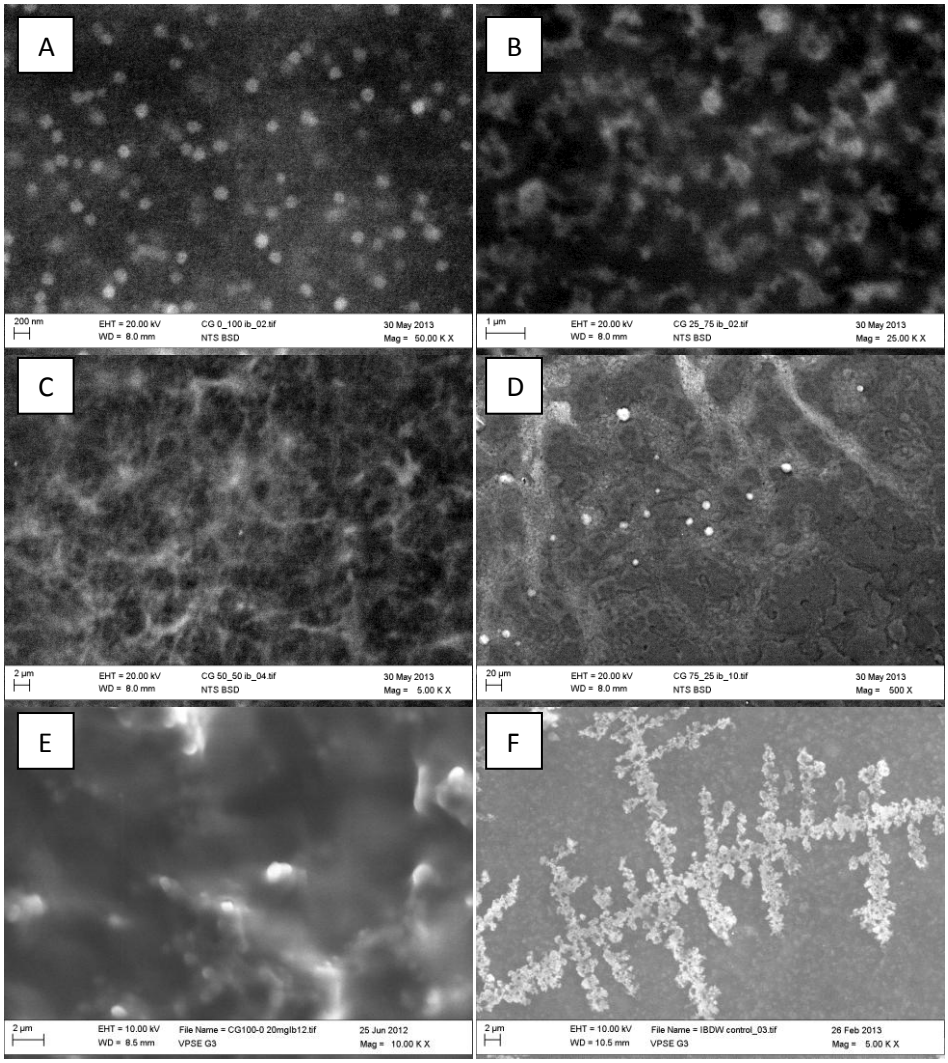

Figure 42 Scanning electron micrographs of ibuprofen-chitosan-gellan conjugates (ternary) (A) CG 0:100, (B) CG 25:75, (C) CG 50:50, (D) CG 75:25, (E) CG 100:0 and (F) ibuprofen-control.

For the ibuprofen-gellan-chitosan complexes shown in Figure 42, CG 0:100, CG 25:75, CG 50:50, CG 75:25 and CG 100:0 complexes were spherical and appeared singly. IbDW, the control formulation showed that ibuprofen remained crystalline and angular shaped arranged in cross pattern. The particle sizes ranged from 162.1 nm to 1.45 µm with the CG 75:25 only in the micrometer range.

2.3.3.8. Spectroscopic studies- Fourier Transform Infrared

FTIR is the preferred method of infrared spectroscopy due to its highly accurate and reproducible frequency determinations. The resulting spectrum represents the molecular absorption and transmission, creating a molecular fingerprint of the sample. Like a fingerprint, no two unique molecular structures produce the same infrared spectrum. This makes infrared spectroscopy useful

for several types of analysis including drug formulations. The unique fingerprint is required in this study to readily dinstinguish the absorption patterns of all drug-polymer nanoconjugate samples in comparison to pure references of drugs and polymers.

FTIR spectra of the samples were generated to identify any potential intrinsic molecular interaction between functional groups of ibuprofen and DEAE-Dextran; Chitosan; Gellan or any local disturbances to the basic backbone spectrum of their structure due to neighbouring electrostatic effects. The assignments of peaks of drug and polymers used are summarized in Table 25 and the changes in peak positions and intensities of absorption bands are summarized in Tables 26 to 35 and Figures 43 to 52. The spectra of raw ibuprofen showed characteristic broad absorption peaks at 3020 and 2954 cm^{-1} corresponding to OH group usually from carboxylic acid which has strong tendency to form hydrogen bonded dimers and methyl CH-stretching respectively. Broad absorption bands at 3500 to 2500 cm^{-1} have been ascribed to OH group from carboxylic acid [64]. The hydrogen bonded dimer is also evident between 3309 and 2632 cm^{-1} (Figure 43). This was consolidated by strong and sharp C-O stretching at 1230 cm^{-1} as well as strong and sharp carbonyl band absorption peak at 1706 cm^{-1} with high intensity due to large dipole moment of the carbonyl bond (C = O) stretching of the carboxylic acid (COOH) group. Major band in the region of 1750 to 1700 cm^{-1} have been reported to correspond to substances containing simple carbonyl compounds such as aldehyde, ketone, ester or carboxylic acid [65]. It also includes absorption peaks at 2954 cm^{-1}, 2923 cm^{-1} and 2859 cm^{-1} which are characteristic for linear aliphatic C-H stretching as well as the presence of aromatic ring vibration (C = C) observed at bands 1507 cm^{-1} which supports the presence of aromatic structure of ibuprofen. DEAE-Dextran spectra contain characteristic broad absorption band at 3295 cm^{-1} corresponding to normal polymeric –OH stretching [65]. The N-H deformation vibration at 1641 cm^{-1} was assigned to tertiary amine (NH bend: 1650 to 1550 cm^{-1}) and C-N stretching at 1342 cm^{-1} (1340 to 1250 cm^{-1}). Chitosan showed characteristic amine absorption peak at 3279 cm^{-1} accompanied with NH- bending at 1651 cm^{-1} while gellan exhibited OH- stretching, CH- stretching and carboxyl stretching at 3306 cm^{-1}, 2897 cm^{-1} and 1602 cm^{-1} respectively. In the FT-IR spectrum of 1:1 physical mixture of

ibuprofen and DEAE-Dextran (Figure 43, Table 26) the band features correspond to the bands in the individual components of the mixture however the carbonyl group peak at 1706 cm^{-1} shifted to 1716 cm^{-1} and a new peak appeared at 1844 cm^{-1} indicating a possible intermolecular interaction in solid state. Also absorption peaks at 3610, 3749 and 3902 cm^{-1} corresponds to monomeric hydroxyl groups which indicate a strong tendency to form intermolecular hydrogen bonding. The Ibuprofen-DEAE-Dextran nanoconjugates obtained from melt solubilization exhibited only two peaks at 3309 to 3334 cm^{-1} and 1634 to 1639 cm^{-1} at all concentrations of DEAE-Dextran (Figure 43). The characteristic aromatic and the fingerprint features completely disappeared while the hydroxyl group became a broad Gaussian-shaped peak at around 3334 cm^{-1} indicating intermolecular hydrophobic and hydrogen-bonded hydroxyl interactions respectively. Also the carbonyl group at 1706 cm^{-1} disappeared and a new peak appeared at 1634 cm^{-1} which corresponds to amide functional group as reported by Coates (1680 to 1630 cm^{-1}) [65]. It was hypothesized that melt solubilization of ibuprofen (-COOH) in the presence of cationic DEAE-Dextran ($-N^{+}HR_2$) produced an amide probably through condensation reaction.

The nanoconjugates prepared by alkaline solubilization technique showed similar peaks to the melt solubilization process showing broad Gaussian-shaped hydroxyl and CH-stretching absorption peak at 3335 to 3324 cm^{-1} as well as amide group at 1635 cm^{-1}. However a new peak appeared at 2149 to 2111 cm^{-1} which increased to a maximum of 2149 cm^{-1} at ibuprofen/DEAE-Dextran ratio 1:2 (Figure 44). Harwood and Claridge have assigned sharp absorption peaks at around 3300 cm^{-1} accompanied by absorption around 2100 cm^{-1} which was due to disubstituted alkynes stretching [64]. This may not be applicable in this case because the peak was particularly broad and intense due to the strong tendency of carboxylic acids to form hydrogen-bonded dimers. The broad hydroxyl absorption peaks shifted to higher values in the physical mixture and nanoconjugates, this has been linked with hydrogen bond interaction or amorphous transformation by Coates [65] although the shift in the peaks was not statistically significant ($p > 0.05$, $n = 4$). All the characteristic bands for secondary amine and polymeric hydroxyl groups on DEAE-Dextran also disappeared from all the treated

samples which supports the potential interaction of the $–R_2NH$ groups of DEAE-Dextran with ibuprofen. Amino groups (present on DEAE-Dextran) have been reported to have strong propensity to form hydrogen bond network with carboxylic groups (present on ibuprofen) due to the van der Waals forces of attraction which forces the hydrophobic organic molecules to interact during the process of crystallization to produce multiple layered crystals [66]. In corollary, only the tertiary amine group of the DEAE-Dextran with pK_a 9.5 is totally protonated [67] at the formulation pH (6.0) and can interact with ibuprofen. The tertiary amine with pKa 5.5 has little or no protonation while the quaternary amine group with pK_a of 14 could protonate but is not very accessible due to steric hindrance effects. Complex formation between ibuprofen and DEAE-Dextran involving electrovalent as well as hydrogen bonding was therefore hypothesized.

Table 25 Functional groups and vibrations assigned to the major peaks of pure components observed in the FTIR spectra displayed in Figures 46 to 53.

Material	Assignment / group	Group frequency Wave number/ cm^{-1}
Ibuprofen	Aromatic C-H asymmetric stretching	3088 and 3040
	Hydroxyl O-H stretching	3020
	Methyl –CH stretch	2954
	Methylene C-H stretching	2923
	Methyne C-H stretching	2859
	Carboxylic acid C=O stretching	1706
	Aromatic ring C=C-C stretching	1563, 1507, 1461 and 1450
	Methyl –CH bend	1462, 1450 and 1442
	Methyne C-H bending	1320
	Skeletal C-C vibration	1268, 1230, 1183
	Aromatic C-H in plane bending	1183, 1168, 1123, 1091, 1073, 1007 and 969
	Aromatic C-H bend out of plane bending	880, 865, 849, 834, 820, 779, 746 and 690
DEAE-Dextran	N-H stretching, O-H stretching	3295
	C-H stretching	2921
	N-H bending (C=O in amide group)	1641
	C-C stretching	1456
	Methyne C-H bending	1342
	C-O-C stretching	1144
	C-N stretching	1007
	C-O stretching	915
	C-Cl stretching	760
Chitosan	O-H stretching	3279
	NH stretching	3279
	Methyl C-H symmetrical stretch	2873
	N-H bending (C=O in amide group)	1651
	Amine $–NH_2$ (NH_2 in amino group)	1583
	Methyl C-H symmetrical bending	1300
	C-O-C stretching	1161
	C-N stretching	1025
	C-C stretching	672
Gellan	O-H stretching	3306
	C-H stretching	2897
	Aromatic carboxyl COO- stretching	1602
	C-O-C stretching for alkyl ether	1191
	C-O stretching	1020
	C-C stretching	672

DEAE-Dextran showed peaks at 3295 cm^{-1} (NH and OH), 2921 cm^{-1} (CH), 1641 cm^{-1} (NH), 1456 cm^{-1} (C-C), 1342 cm^{-1} (C-H), 1144 cm^{-1} (C-O-C), 1007 cm^{-1} (C-N), 915 cm^{-1} (C-O) and 760 cm^{-1} (C-Cl). Dermibilek and Dinc reported similar peaks for DEAE-Dextran at 3394 cm^{-1}, 2926 cm^{-1}, 1643 cm^{-1}, 1467 cm^{-1}, 1157 cm^{-1}, 1013 cm^{-1}, 918 cm^{-1} and 765 cm^{-1} [68]. The bands assigned as the finger prints of ibuprofen in literature include 2992 cm^{-1} (CH), 1706 cm^{-1} (C=O), 1230 cm^{-1} (C-C) and 779 cm^{-1} (CH) [69-70]. Ibuprofen-DEAE-Dextran physical mixture showed peaks at 3610 cm^{-1} (OH), 2921 cm^{-1} (CH), 1716 cm^{-1} (CO), 1646 cm^{-1} (NH), 1319 cm^{-1} (CH), 1230 cm^{-1} (C-C), 1007 cm^{-1} (CN) and 778 cm^{-1} (CH)

which are basically a combination of peaks present in ibuprofen and DEAE-Dextran with slight variations.

Table 26 FTIR spectral characteristics at various wavelengths for ibuprofen-DEAE-Dextran conjugates (melt solubilization) ibuprofen control, ibuprofen-reference, DEAE-Dextran-reference and ibuprofen-DEAE-Dextran physical mixture.

Formulation	Position of absorption band (Wavenumber) / cm^{-1}					
Ibuprofen-reference	3089	2954	2542	1507	1305	969
	3045	2923	1911	1462	1268	934
	3020	2859	1804	1450	1231	880
	2992	2727	1706	1442	1183	865
	2980	2632		1418	1168	849
				1379	1123	834
				1365	1091	820
				1329	1073	779
				1321	1007	746
						690
DEAE-Dextran-reference	3295	2921		1641	1144	760
				1456	1007	
				1342	915	
Ibuprofen-DEAE-Dextran physical mixture	3902	3610	1844	1675	1542	1319
	3749	2921	1716	1646	1524	1230
				1555	1456	1007
						778
IbMelt-control (IbD 1:0)	3309			1634		
IbD1Melt (IbD 1:0.5)	3324			1635		
IbD2Melt (IbD 1:1)	3327			1635		
IbD3Melt (IbD 1:2)	3324			1635		
IbD4Melt (IbD 1:4)	3334			1639		
IbD5Melt (IbD 1:8)	3334			1634		

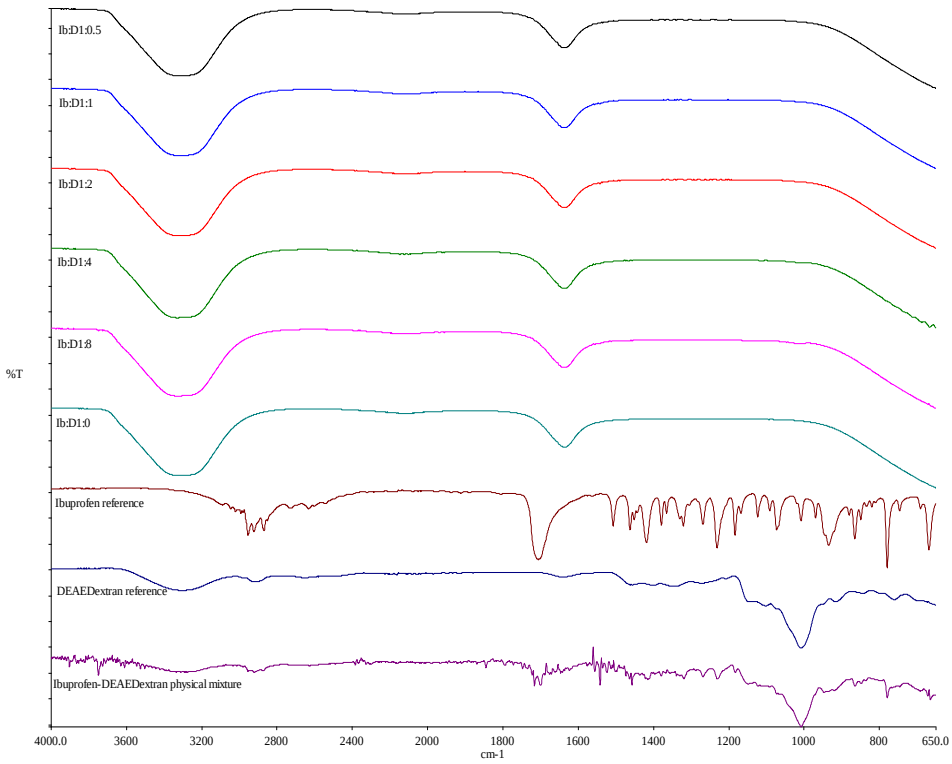

Figure 43 The FTIR spectra of ibuprofen-DEAE-Dextran conjugates (melt solubilization) ibuprofen control, ibuprofen-reference, DEAE-Dextran-reference and ibuprofen-DEAE-Dextran physical mixture.

Table 27 FTIR spectral characteristics at various wavelengths for ibuprofen-DEAE-Dextran conjugates (solubilization) ibuprofen control, ibuprofen-reference, DEAE-Dextran-reference and ibuprofen-DEAE-Dextran physical mixture.

Formulation	Position of absorption band (Wavenumber) / cm^{-1}					
Ibuprofen-reference	3089	2859	1507	1329	1123	865
	3045	2727	1462	1321	1091	849
	3020	2632	1450	1305	1073	834
	2992	2542	1442	1268	1007	820
	2980	1911	1418	1231	969	779
	2954	1804	1379	1183	934	746
	2923	1706	1365	1168	880	690
DEAE-Dextran-reference	3295	2921	1641	1342	1007	760
			1456	1144	915	
Ibuprofen-DEAE-Dextran physical mixture	3902	3610	1844	1646	1524	1230
	3749	2921	1716	1555	1456	1007
			1675	1542	1319	778
IbNaOH-control (IbD 1:0)	3288	2122		1635		
IbD1NaOH (IbD 1:0.5)	3325	2132		1635		
IbD2NaOH (IbD 1:1)	3322	2144		1634		
IbD3NaOH (IbD 1:2)	3324	2140		1635		
IbD4NaOH (IbD 1:4)	3335	2125		1635		
IbD5NaOH (IbD 1:8)	3326	2111		1635		

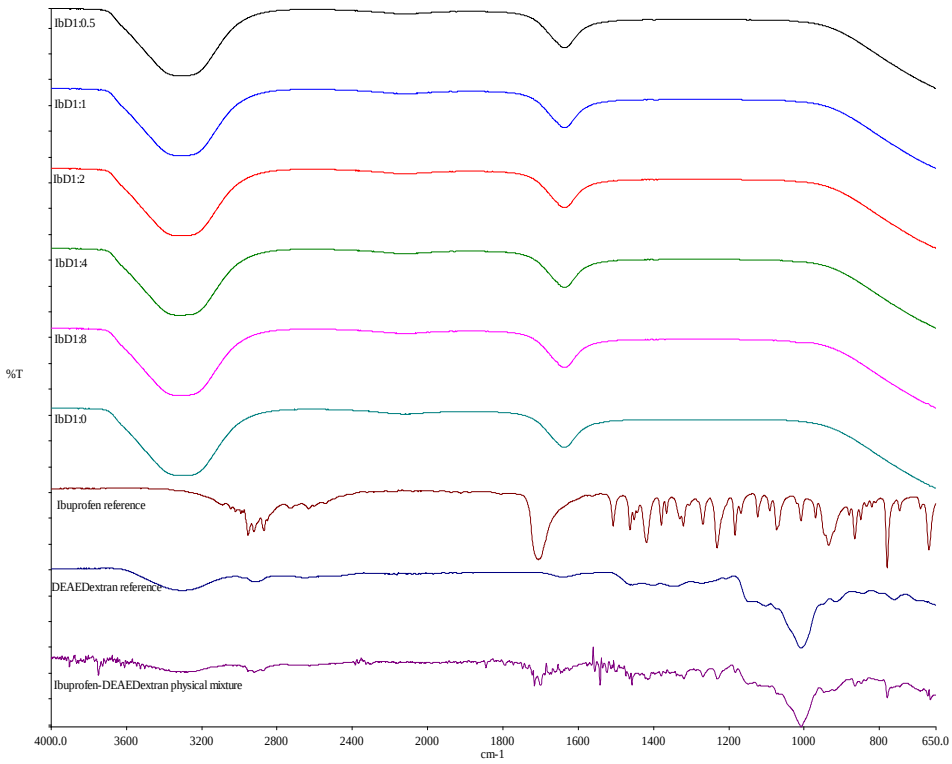

Figure 44 The FTIR spectra of ibuprofen-DEAE-Dextran conjugates (solubilization) ibuprofen control, ibuprofen-reference, DEAE-Dextran-reference and ibuprofen-DEAE-Dextran physical mixture.

Table 28 FTIR spectral characteristics at various wavelengths for ibuprofen-DEAE-Dextran conjugates (solubilization) ibuprofen control, ibuprofen-reference, DEAE-Dextran-reference and ibuprofen-DEAE-Dextran physical mixture.

Formulation	Position of absorption band (Wavenumber) / cm^{-1}					
Ibuprofen-reference	3089	2859	1507	1329	1123	865
	3045	2727	1462	1321	1091	849
	3020	2632	1450	1305	1073	834
	2992	2542	1442	1268	1007	820
	2980	1911	1418	1231	969	779
	2954	1804	1379	1183	934	746
	2923	1706	1365	1168	880	690
DEAE-Dextran-reference	3295	2921	1641	1342	1007	760
			1456	1144	915	
Ibuprofen-DEAE-Dextran physical mixture	3902	3610	1844	1646	1524	1230
	3749	2921	1716	1555	1456	1007
			1675	1542	1319	778
IbTw80-control (IbD 1:0)	3496	2922	1735	1436	1296	946
		2836	1643	1349	1248	845
					1095	712
IbD1Tw80 (IbD 1:0.5)	3336			1635	1087	
IbD2Tw80 (IbD 1:1)	3337			1635	1086	
IbD3Tw80 (IbD 1:2)	3335			1635	1086	
IbD4Tw80 (IbD 1:4)	3342			1635	1086	
IbD5Tw80 (IbD 1:8)	3343			1639	1086	

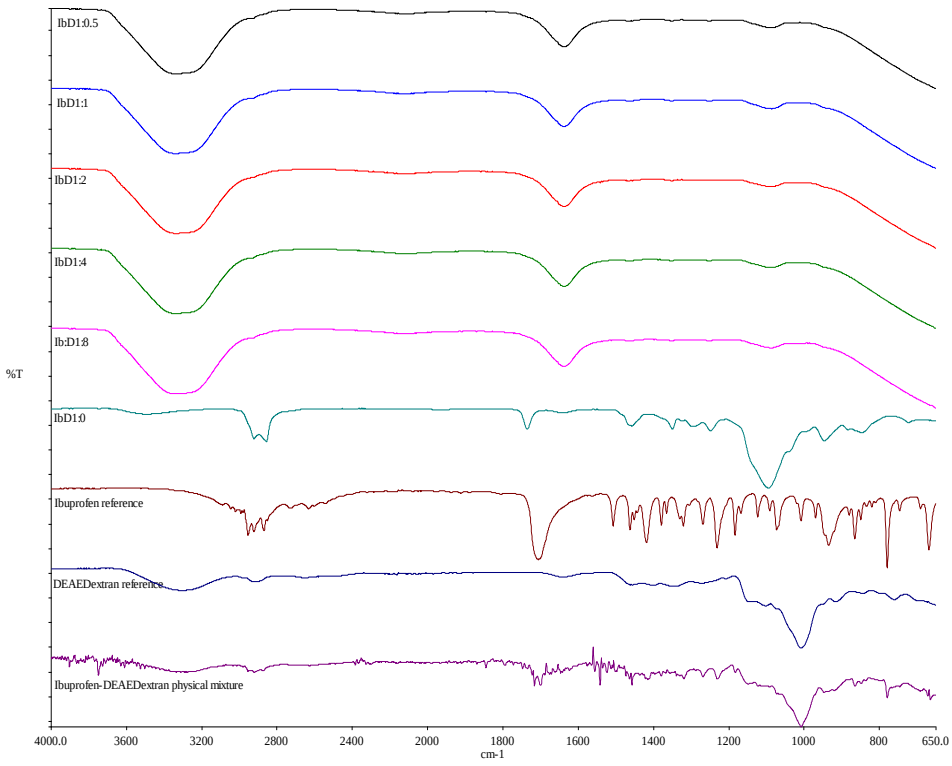

Figure 45 The FTIR spectra of ibuprofen-DEAE-Dextran conjugates (solubilization) ibuprofen control, ibuprofen-reference, DEAE-Dextran-reference and ibuprofen-DEAE-Dextran physical mixture.

Nanoconjugates derived from the surfactant (Tween 80) solubilization technique; exhibited similar FT-IR absorption profile to the melt and alkaline solubilization techniques. However in the absence of DEAE-Dextran, the broad hydroxyl absorption became very weak and the aromatic as well as the fingerprint peaks of ibuprofen was more prominent (Figure 45). This effect was attributed to Tween 80, the non ionic surfactant. Also the intensity of the amide peak reduced and shifted to 1643 cm^{-1} while the carbonyl peak reappeared at 1735 cm^{-1} which may indicate the formation of ester or six-membered ring lactone [65]. A new peak also appeared at 1350 cm^{-1} suggesting the formation of carboxylic acid salt (carboxylate). It was opined that carboxylic acid salt, ester and amide as well as hydrogen bonding were formed during surfactant solubilization of ibuprofen in the absence of DEAE-Dextran.

Table 29 FTIR spectral characteristics at various wavelengths for ibuprofen-DEAE-Dextran conjugates (hydrotropy) ibuprofen control, ibuprofen-reference, DEAE-Dextran-reference and ibuprofen-DEAE-Dextran physical mixture.

Formulation	Position of absorption band (Wavenumber) / cm^{-1}					
Ibuprofen-reference	3089	2954	2542	1462	1268	934
	3045	2923	1911	1450	1231	880
	3020	2859	1804	1442	1183	865
	2992	2727	1706	1418	1168	849
	2980	2632	1507	1379	1123	834
				1365	1091	820
				1329	1073	779
				1321	1007	746
				1305	969	690
DEAE-Dextran-reference	3295	2921	1641	1342	1007	760
			1456	1144	915	
Ibuprofen-DEAE-Dextran physical mixture	3902	3610	1844	1646	1524	1230
	3749	2921	1716	1555	1456	1007
			1675	1542	1319	778
IbNic-control (IbD 1:0)	3382	2127		1635		
IbD1Nic (IbD 1:0.5)	3326	2100		1635		
IbD2Nic (IbD 1:1)	3321	2090		1635		
IbD3Nic (IbD 1:2)	3327	2143		1635		
IbD4Nic (IbD 1:4)	3324	2147		1635		
IbD5Nic (IbD 1:8)	3324	2149		1635		

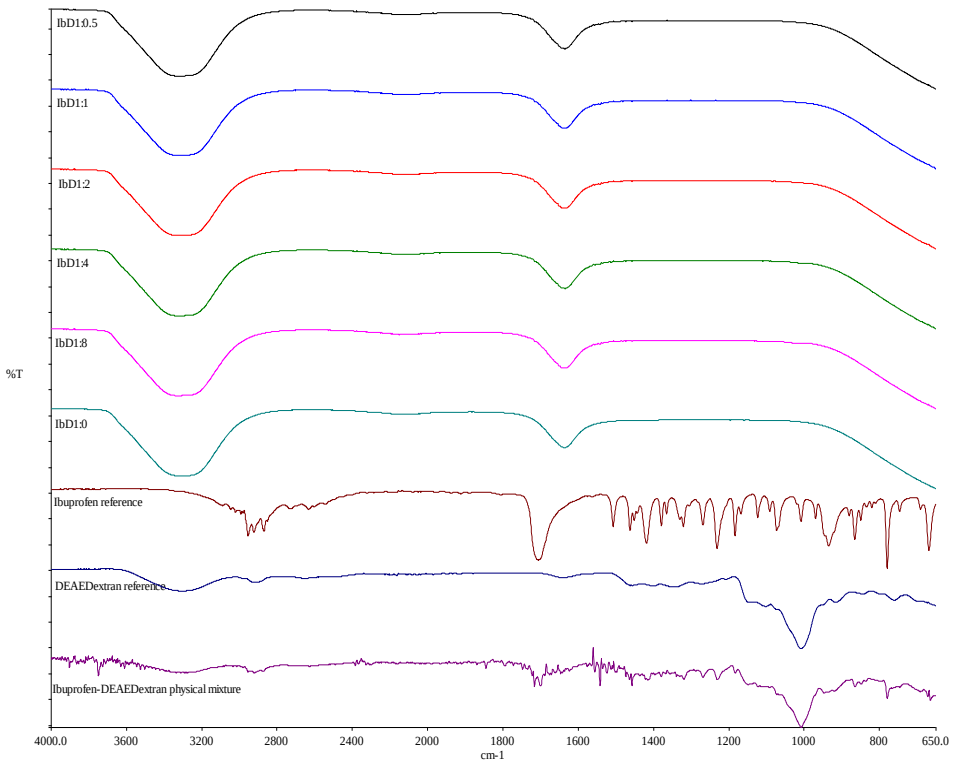

Figure 46 The FTIR spectra of ibuprofen-DEAE-Dextran conjugates (hydrotropy) ibuprofen control, ibuprofen-reference, DEAE-Dextran-reference and ibuprofen-DEAE-Dextran physical mixture.

Ibuprofen/DEAE-Dextran nanoconjugates prepared by hydrotropic complexation technique exhibited three peaks at 3327 to 3312 cm^{-1}; 2149 to 2090 cm^{-1} and 1635 cm^{-1} corresponding to hydrogen bonding, transition metal carbonyls (2100 to 1800 cm^{-1}) and amide respectively (Figure

46). The disappearance of the carbonyl peak also suggests its involvement in electrostatic interacton with the DEAE-Dextran. Similar to other techniques hydrogen bonding and formation of amide was evident.

The FTIR spectra of ibuprofen/chitosan nanoconjugates (Figure 47) prepared by melt solubilization were quite similar to the ibuprofen/DEAE-Dextran nanoconjugates (Figure 46) producing only two peaks at 3335 cm^{-1} and 1635 cm^{-1} corresponding to hydrogen bonding and amide respectively. The ibuprofen/chitosan physical mixture also reflected the spectra of the components and the disappearance of the N-H stretching absorption peak at 3279 cm^{-1} as well as the broadness of the hydroxyl peak suggest hydrogen bonding.

Table 30 FTIR spectral characteristics at various wavelengths for ibuprofen-chitosan conjugates (melt solubilization) ibuprofen control, ibuprofen-reference, chitosan-reference and ibuprofen-chitosan physical mixture.

Formulation	Position of absorption band (Wavenumber) / cm^{-1}					
Ibuprofen-reference	3089	2859	1507	1329	1123	865
	3045	2727	1462	1321	1091	849
	3020	2632	1450	1305	1073	834
	2992	2542	1442	1268	1007	820
	2980	1911	1418	1231	969	779
	2954	1804	1379	1183	934	746
	2923	1706	1365	1168	880	690
Chitosan-reference	3279	2918	1583	1300	1161	672
Ibuprofen-Chitosan physical mixture	3902	2954	1542	1320	1091	865
	3854	2922	1508	1268	1072	849
	3749	2868	1462	1229	1008	820
		2631	1418	1183	969	779
		1715	1379	1167	935	746
		1555	1365	1122	880	690
						667
IbMelt-control (IbCh 1:0)	3309			1634		
IbCh1Melt (IbCh 1:0.125)	3333			1635		
IbCh2Melt (IbCh 1:0.25)	3335			1635		
IbCh3Melt (IbCh 1:0.5)	3326			1634		
IbCh4Melt (IbCh1:1)	3324			1639		
IbCh5Melt (IbCh 1:2)	3324			1635		

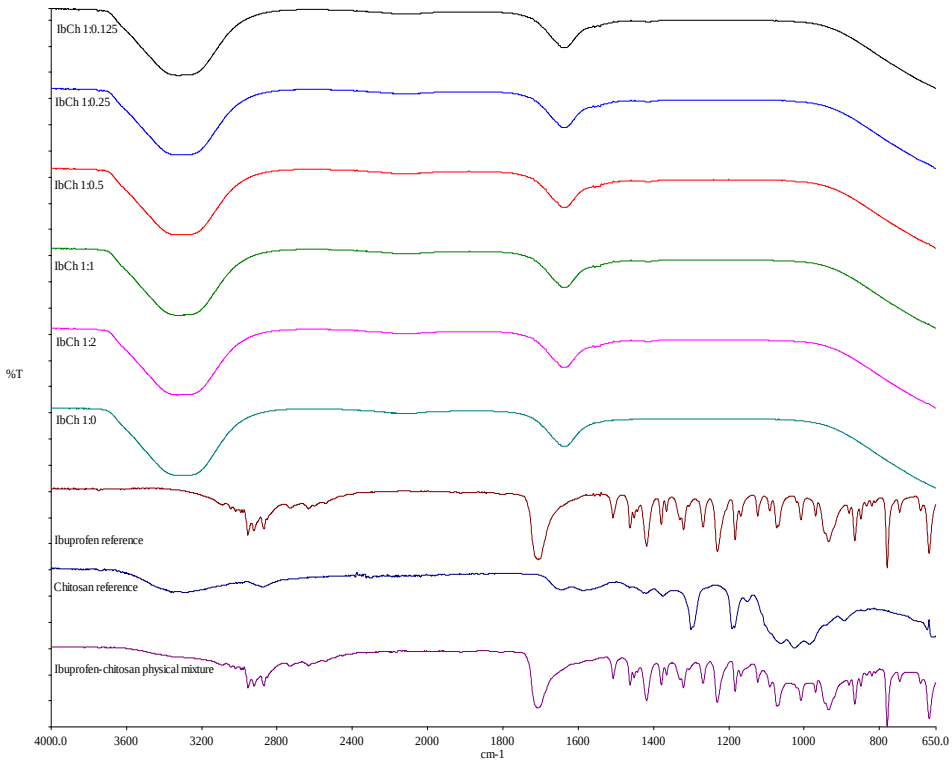

Figure 47 The FTIR spectra of ibuprofen-chitosan conjugates (melt solubilization) ibuprofen control, ibuprofen-reference, chitosan-reference and ibuprofen-chitosan physical mixture.

The FTIR spectra of ibuprofen/chitosan nanoconjugates prepared by alkaline solubilization were similar to the ibuprofen/DEAE-Dextran nanoconjugates. Three characteristic new peaks appeared at a range of 3324 to 3325 cm^{-1} ascribed to bonded hydroxyl group, 2099 to 2149 cm^{-1} ascribed to cyanide and 1635 cm^{-1} ascribed to amide for IbChNaOH nanoconjugates in Figure 48. There was a shift of peak at 1418 cm^{-1} in ibuprofen and DEAE-Dextran to 1412 cm^{-1} in the IbChNaOH nanoconjugates. The C=O and C-C stretching peak at 1706 cm^{-1} and 1230 cm^{-1} for pure ibuprofen disappeared in the spectra of IbChNaOH nanoconjugates.The disappearance in peaks suggested there is a possible interaction between the polymer and the drug. Hydrogen bonding and formation of amide was evident.

Table 31 FTIR spectral characteristics at various wavelengths for ibuprofen-chitosan conjugates (solubilization) ibuprofen control, ibuprofen-reference, chitosan-reference and ibuprofen-chitosan physical mixture.

Formulation	Position of absorption band (Wavenumber) / cm^{-1}					
Ibuprofen-reference	3089	2954	2542	1507	1305	969
	3045	2923	1911	1462	1268	934
	3020	2859	1804	1450	1231	880
	2992	2727	1706	1442	1183	865
	2980	2632		1418	1168	849
				1379	1123	834
				1365	1091	820
				1329	1073	779
				1321	1007	746
						690
Chitosan-reference	3279	2918		1583	1161	672
				1300		
Ibuprofen-Chitosan physical mixture	3902	2954	2631	1555	1229	880
	3854	2922	1715	1542	1183	865
	3749	2868		1508	1167	849
				1462	1122	820
				1418	1091	779
				1379	1072	746
				1365	1008	690
				1320	969	667
				1268	935	
IbNaOH-control (IbCh 1:0)	3288	2122		1635		
IbCh1NaOH (IbCh 1:0.125)	3324	2099		1635	1412	
IbCh2NaOH (IbCh 1:0.25)	3324	2122		1635		
IbCh3NaOH (IbCh 1:0.5)	3324	2115		1635	1412	
IbCh4NaOH (IbCh 1:1)	3325	2147		1635	1412	
IbCh5NaOH (IbCh 1:2)	3324	2149		1634	1412	

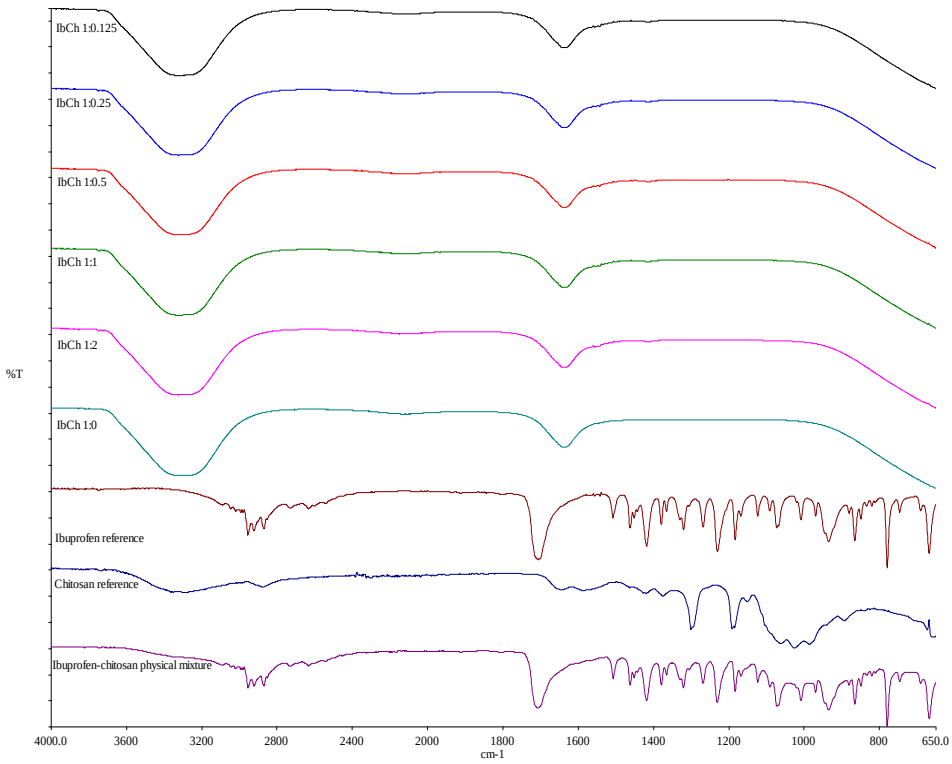

Figure 48 The FTIR spectra of ibuprofen-chitosan conjugates (solubilization) ibuprofen control, ibuprofen-reference, chitosan-reference and ibuprofen-chitosan physical mixture.

The FTIR spectra of ibuprofen/chitosan nanoconjugates were also similar to the corresponding ibuprofen/DEAE-Dextran nanoconjugates. Four characteristic peaks appeared in the range of 3335 to 3337 cm^{-1} ascribed to bonded hydroxyl group, 2100 to 2149 cm^{-1} ascribed to cyanide, 1635 cm^{-1} ascribed to amide and 1086 to 1092 cm^{-1} ascribed to aromatic C-H in plane bend for IbChTw80 nanoconjugates in Figure 49. The C=O and C-C stretching peak at 1706 cm^{-1} and 1230 cm^{-1} for pure ibuprofen disappeared in the spectra of IbChTw80 conjugates. The disappearance in peaks suggested there is a possible interaction between the polymer and the drug.

Table 32 FTIR spectral characteristics at various wavelengths for ibuprofen-chitosan conjugates (solubilization) ibuprofen control, ibuprofen-reference, chitosan-reference and ibuprofen-chitosan physical mixture.

Formulation	Position of absorption band (Wavenumber) / cm^{-1}					
Ibuprofen-reference	3089	2859	1507	1329	1123	865
	3045	2727	1462	1321	1091	849
	3020	2632	1450	1305	1073	834
	2992	2542	1442	1268	1007	820
	2980	1911	1418	1231	969	779
	2954	1804	1379	1183	934	746
	2923	1706	1365	1168	880	690
Chitosan-reference	3279	2918	1583	1300	1161	672
Ibuprofen-Chitosan physical mixture	3902	2631	1418	1183	969	779
	3854	1715	1379	1167	935	746
	3749	1555	1365	1122	880	690
	2954	1542	1320	1091	865	667
	2922	1508	1268	1072	849	
	2868	1462	1229	1008	820	
IbTw80-control (IbCh 1:0)	3496	2836	1643	1349	1248	946
	2922	1735	1436	1296	1095	845
						712
IbCh1Tw80 (IbCh 1:0.125)	3337	2100	1635	1555	1086	
IbCh2Tw80 (IbCh 1:0.25)	3337	2149	1635		1091	
IbCh3Tw80 (IbCh 1:0.5)	3337	2147	1635	1555	1088	
IbCh4Tw80 (IbCh1:1)	3336	2146	1639	1555	1456	1091
IbCh5Tw80 (IbCh 1:2)	3335	2145	1639	1555	1092	

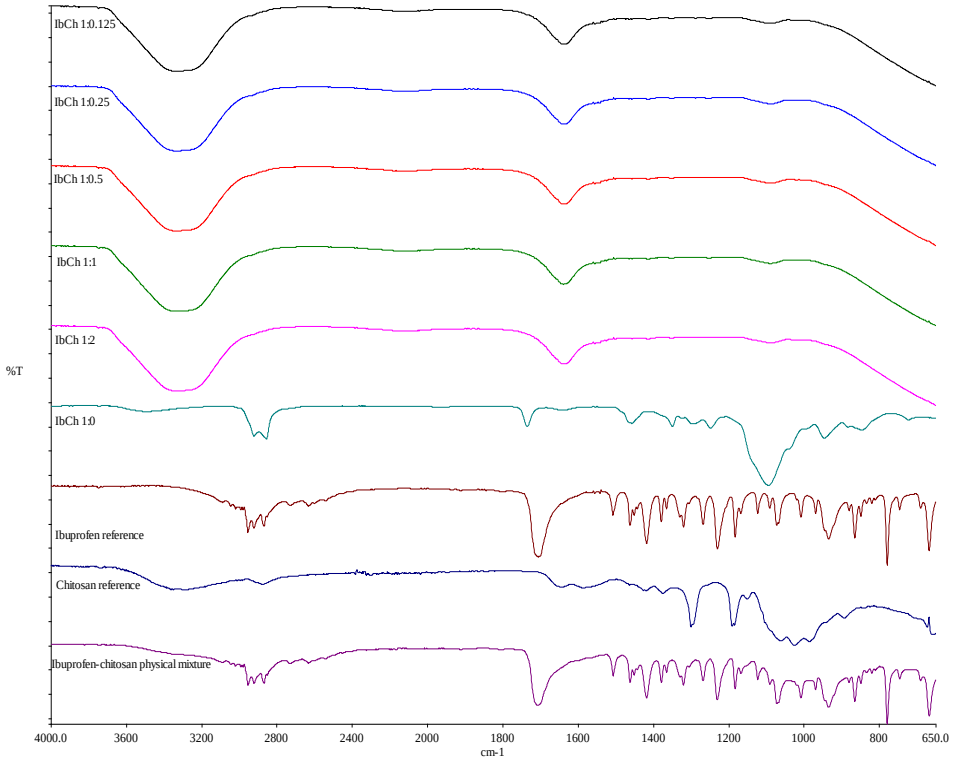

Figure 49 The FTIR spectral characteristics at various wavelengths for ibuprofen-chitosan conjugates (solubilization) ibuprofen control, ibuprofen-reference, chitosan-reference and ibuprofen-chitosan physical mixture.

Three characteristic peaks appeared at a range of 3310 cm^{-1} to 3336 cm^{-1} ascribed to bonded hydroxyl group, 2090 to 2146 cm^{-1} ascribed to cyanide and 1635 cm^{-1} ascribed to amide for IbChNic

nanoconjugates in Figure 50. There was a shift of peak at 1418 cm^{-1} in ibuprofen to 1412 cm^{-1} in the IbChNic nanoconjugates. The C=O and C-C stretching peak at 1706 cm^{-1} and 1230 cm^{-1} for pure ibuprofen disappeared in the spectra of IbChNic nanoconjugates. The disappearance in peaks suggested there is a possible interaction between the amino group of the polymer and the -COOH group of the drug.

Table 33 FTIR spectral characteristics at various wavelengths for ibuprofen-chitosan conjugates (hydrotropy) ibuprofen control, ibuprofen-reference, chitosan-reference and ibuprofen-chitosan physical mixture.

Formulation	Position of absorption band (Wavenumber) / cm^{-1}					
Ibuprofen-reference	3089	2954	2542	1507	1305	969
	3045	2923	1911	1462	1268	934
	3020	2859	1804	1450	1231	880
	2992	2727	1706	1442	1183	865
	2980	2632		1418	1168	849
				1379	1123	834
				1365	1091	820
				1329	1073	779
				1321	1007	746
						690
Chitosan-reference	3279	2918		1583	1161	672
				1300		
Ibuprofen-Chitosan physical mixture	3902	2954	2631	1555	1229	880
	3854	2922	1715	1542	1183	865
	3749	2868		1508	1167	849
				1462	1122	820
				1418	1091	779
				1379	1072	746
				1365	1008	690
				1320	969	667
				1268	935	
IbNic-control (IbCh 1:0)	3382	2127		1635		
IbCh1Nic (IbCh 1:0.125)	3310	2116		1634	1555	
IbCh2Nic (IbCh 1:0.25)	3336	2146		1635	1555	1412
IbCh3Nic (IbCh 1:0.5)	3335	2091		1634		1412
IbCh4Nic (IbCh1:1)	3310	2090		1635	1555	1412
IbCh5Nic (IbCh 1:2)	3312	2114		1634		1412

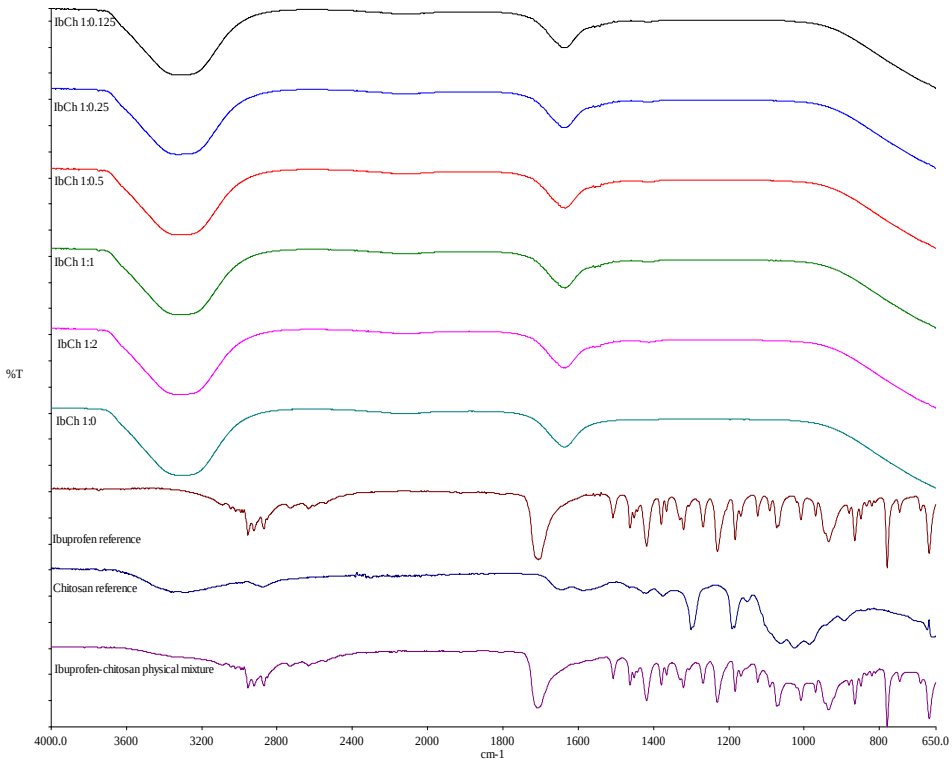

Figure 50 The FTIR spectral characteristics at various wavelengths for ibuprofen-chitosan conjugates (hydrotropy) ibuprofen control, ibuprofen-reference, chitosan-reference and ibuprofen-chitosan physical mixture.

The FTIR spectra of ibuprofen-DEAE-Dextran-gellan complex, pure ibuprofen, gellan gum, DEAE-Dextran, chitosan are shown in Figures 51 and 52; and Tables 34 and 35. Gellan showed significant peaks at 3306 cm^{-1}, 1602 cm^{-1} 1408 cm^{-1} and 1020 cm^{-1}. The peaks at 1602 cm^{-1} and 1408 cm^{-1} are assigned to the characteristic absorption band of carboxyl in gellan gum [71]. The peak assignments of gellan has also been described by Sudhamani *et al.* [72]. They reported significant absorption peaks of gellan at 3273 cm^{-1}, 1611 cm^{-1} and 1035 cm^{-1}. The peak at 3306 cm^{-1} is assigned to hydroxyl stretching. Gellan gum has hydroxyl and carboxyl groups in its structure capable of undergoing a nucleophilic substitution reaction with DEAE-Dextran as described for the methacrylation of gellan gum (GG-MA) with the most favourable reaction being with the carboxyl group [73]. FTIR spectrum of the complexes DG 25:75, DG 50:50 and DG 75:25 showed the disappearances of 1641 cm^{-1} peak of DEAE-Dextran, 1602 cm^{-1} in gellan and slight shift of 1706 cm^{-1} ibuprofen peak to a range of 1710 to 1713 cm^{-1} in the complexes which appeared to be of lesser intensities. The characteristic peaks of ibuprofen were present in the complexes with slight variations. This confirms the chemical stability of ibuprofen in the DEAE-Dextran-gellan complex. Since ibuprofen interacted with DEAE-Dextran in a

binary mixture (Figures 43 to 46) it was opined that polyelectrolyte complexation between DEAE-Dextran and gellan was favoured in the ternary mixture rather than the ibuprofen/DEAE-Dextran conjugation.

Table 34 FTIR spectral characteristics at various wavelengths for ibuprofen incorporated into DEAE-Dextran-gellan conjugate in ratios, DG 0:100, DG 25:75, DG 50:50, DG 75:25 and DG 100:0; pure ibuprofen, gellan and DEAE-Dextran.

Formulation	Position of absorption band (Wavenumber) / cm^{-1}					
Ibuprofen-reference	3089	2859	1507	1329	1123	865
	3045	2727	1462	1321	1091	849
	3020	2632	1450	1305	1073	834
	2992	2542	1442	1268	1007	820
	2980	1911	1418	1231	969	779
	2954	1804	1379	1183	934	746
	2923	1706	1365	1168	880	690
Gellan-reference	3306	1602	1300	1191	1020	672
DEAE-Dextran-reference	3295	2921	1641	1342	1007	760
			1456	1144	915	
IbDW-pH6	2954	1712	1365	1123	934	779
	2921	1507	1268	1092	880	746
	2868	1462	1230	1073	865	691
	2727	1451	1183	1007	849	667
	2631	1379	1168	969	820	
DG 0:100	3089	2727	1461	1329	1091	849
	3046	2632	1450	1320	1072	834
	3020	2542	1442	1268	1008	820
	2954	1911	1418	1230	969	746
	2922	1701	1379	1183	935	690
	2869	1507	1365	1168	880	667
				1122	865	
DG 25:75	2991	2727	1451	1268	1072	849
	2980	2632	1418	1230	1008	834
	2954	1710	1379	1183	969	819
	2922	1507	1365	1168	935	746
	2868	1462	1321	1122	880	690
				1091	865	668
DG 50:50	2992	2922	1462	1268	1073	849
	2980	2869	1451	1230	1008	834
	2954	2727	1418	1183	969	820
		2632	1379	1168	935	746
		1713	1365	1123	880	690
		1507	1321	1091	866	668
DG 75:25		2991	2868	1507	1375	1230
		2980	2725	1461	1365	1122
		2954	2631	1450	1320	1091
		2922	1711	1418	1268	1072
DG 100:0	3020	2980	1703	1329	1122	865
	2992	2954	1507	1321	1091	849
		2923	1462	1230	1072	834
		2868	1450	1305	1008	820
		2727	1418	1268	934	746
		2632	1379	1183	880	690
		1910	1365	1168	969	668

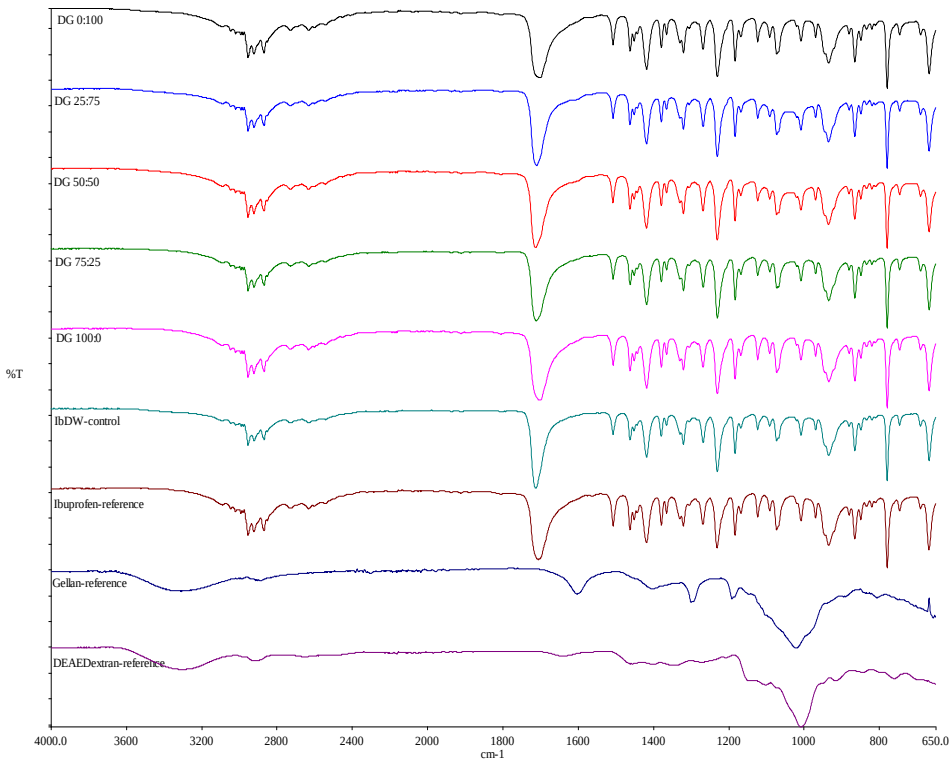

Figure 51 The FTIR spectra of ibuprofen incorporated into DEAE-Dextran-gellan conjugate in ratios: DG 0:100, DG 25:75, DG 50:50, DG 75:25 and DG 100:0; pure ibuprofen, gellan and DEAE-Dextran powder references.

Chitosan showed significant peaks at 3279 cm^{-1}, 2918 cm^{-1}, 1583 cm^{-1} and 1300 cm^{-1}. Chitosan exhibits main characteristic band O-H and N-H stretching at 3279 cm^{-1} and methyl C-H symmetrical stretch at 2981 cm^{-1} (Figure 52). The band at 1583 cm^{-1} is due to the NH_3^+ absorption band. The band at 1300 cm^{-1} is due to the methyl C-H symmetrical bend. The band at 1025 cm^{-1} is attributed to the alkyl substituted ether C-O-C. Gellan peaks at 3306 cm^{-1} and 1602 cm^{-1} disappeared in the complexes. Chitosan peaks at 3279 cm^{-1} and 1583 cm^{-1} disappeared in the complexes. The absence of the absorption band at 3279 cm^{-1} indicated that hydroxyl and amino groups are apparently substituted on the monosaccharide units of the chitosan chains. FTIR spectra of the CG 25:75, CG 75:25 and CG 100:0 complexes showed a new peak at a region of 1557 to 1563 cm^{-1} which was absent in CG 50:50 and CG 0:100 suggesting the formation of carboxylate salt. The characteristic peaks of ibuprofen were present in the complexes with slight variations. This confirms the chemical stability of ibuprofen in the chitosan-gellan complex and a preferential interaction between chitosan and gellan.

Table 35 FTIR spectra at various wavelengths for ibuprofen incorporated into chitosan-gellan conjugate in ratios, CG 0:100, CG 25:75, CG 50:50, CG 75:25 and CG 100:0; pure ibuprofen, gellan and chitosan.

Formulation	Position of absorption band (Wavenumber) / cm^{-1}					
Ibuprofen-reference	3089	2859	1507	1329	1123	865
	3045	2727	1462	1321	1091	849
	3020	2632	1450	1305	1073	834
	2992	2542	1442	1268	1007	820
	2980	1911	1418	1231	969	779
	2954	1804	1379	1183	934	746
	2923	1706	1365	1168	880	690
Gellan-reference	3306	1602	1300	1191	1020	672
Chitosan-reference	3279	2918	1583	1300	1161	672
IbDW-pH5	2954	2631	1379	1123	934	779
	2921	1712	1365	1092	880	746
	2868	1507	1268	1073	865	691
	2727	1462	1230	1007	849	667
		1451	1168	969	820	
CG 0:100	3020	2767	1450	1305	1091	865
	2992	2632	1418	1268	1072	849
	2980	1910	1379	1230	1008	834
	2954	1705	1365	1183	969	820
	2922	1507	1329	1168	934	746
	2869	1462	1321	1123	880	690
						667
CG 25:75	3089	2991	1910	1379	1168	880
	3045	2979	1710	1364	1122	865
	3019	2954	1557	1321	1091	849
		2922	1507	1305	1072	834
		2868	1461	1268	1020	819
		2727	1451	1230	1007	746
		2632	1418	1183	969	690
					934	667
CG 50:50		2992	2727	1462	1183	880
		2954	2632	1450	1167	865
		2922	1708	1418	1122	849
		2868	1507	1379	1091	834
				1365	1072	820
				1320	1008	746
				1268	969	690
				1230	935	667
CG 75:25	3019	2631	1450	1267	1072	865
	2991	1910	1418	1229	1020	849
	2954	1705	1379	1183	1007	834
	2922	1563	1365	1167	969	819
	2868	1507	1320	1122	934	746
	2725	1461	1304	1091	880	690
						667
CG 100:0	3019	2991	1706	1320	1091	849
		2954	1563	1305	1072	834
		2922	1507	1268	1007	820
		2868	1461	1230	969	746
		2727	1451	1183	934	690
		2632	1418	1167	880	667
		1910	1379	1122	865	

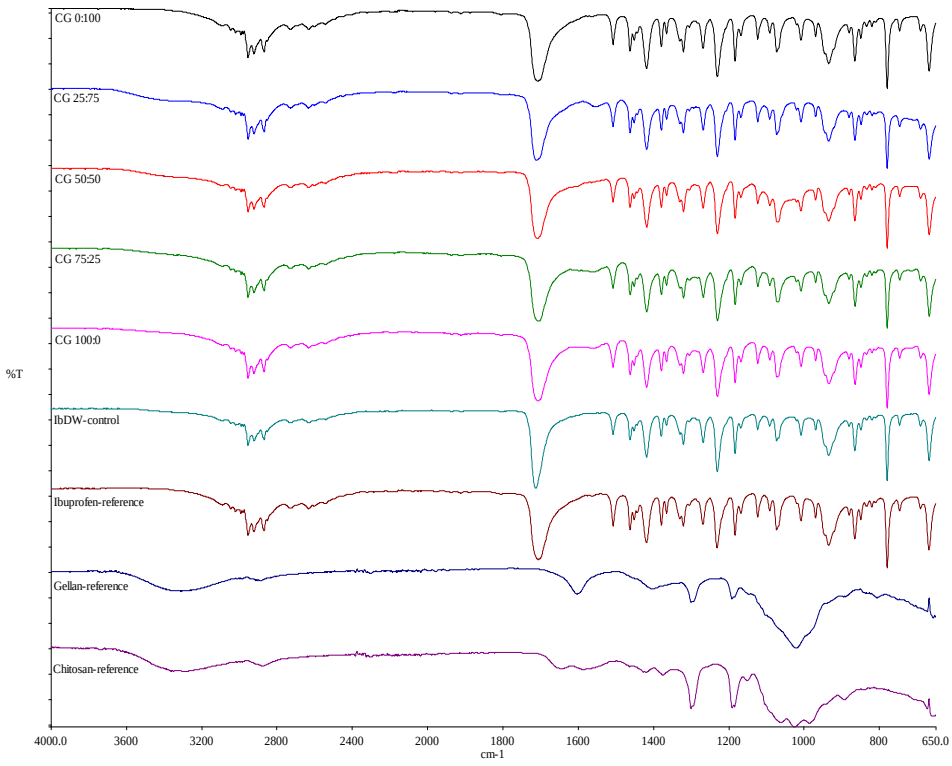

Figure 52 The FTIR spectra of ibuprofen incorporated into chitosan-gellan conjugate in ratios: CG 0:100, CG 25:75, CG 50:50, CG 75:25, CG 100:0; pure ibuprofen, gellan and chitosan powder references.

2.3.3.9. ^{1}H- and ^{13}C- Nuclear Magnetic Resonance

^{1}H NMR technique was chosen to confirm the suspected interaction between ibuprofen and DEAE-Dextran/Chitosan. The ^{1}H NMR spectra of the pure ibuprofen, DEAE-Dextran, chitosan and their ternary nanoconjugate assembly are presented in Figure 55. Pure ibuprofen exhibited typical signals of the isopropyl methyl protons (C10 and C11); methyl doublet proton (C3); nonet CH proton (C9); doublet CH proton (C8); quartet CH proton (C2) and the aromatic ring proton (C4 to C7) which were detected at 0.87; 1.36; 1.65; 2.51; 3.66 and 7.21 ppm respectively (Figure 55). Complete ^{1}H and ^{13}C chemical shifts assigned to pure ibuprofen, DEAE-Dextran-ibuprofen-gellan and Chitosan-ibuprofen-gellan nanoconjugates are presented in Table 36. The ^{1}H-NMR spectra of DEAE-Dextran showed signals in both anomeric (4.4 to 5.5 ppm) region indicating the presence of amines ($-R_3N^{+}H$) and RCH_2O- group as well as the bulk (3.0 to 4.2 ppm) proton resonance regions in chitosan suggesting the presence of amino (RNH_2) groups. The OH-signal detected at 12.24 ppm from the pure ibuprofen is characteristic of the proton from carboxylic acid group. The peak was completely absent from the binary ibuprofen-DEAE-Dextran and ibuprofen-chitosan nanoconjugates but was present in

ibuprofen-gellan mixture (Figure 53). This confirms the interaction between the carbonyl group of ibuprofen and the cationic polyelectrolytes but no visible interaction with gellan which is an anionic polymer. The OH-signal from the carbonyl group was also completely absent in all the ternary DEAE - Dextran-ibuprofen-gellan and Chitosan-ibuprofen-gellan nanoconjugates prepared in this study confirming electrostatic interaction that involved the carboxylic acid group of ibuprofen and the amino group of the cationic polymers. Ibuprofen-DEAE-Dextran conjugate exhibited an exceptionally broad multiplet signals between 3.0 and 5.5 ppm which overlapped the quartet CH proton signal on C2 indicating the presence of amino group from DEAE-Dextran and formation of hydrogen bond. Proton chemical shift of δ 6.9, 7.9 and 8.4 ppm was also observed in the ibuprofen-DEAE-Dextran nanoconjugates which indicate the formation of amide (δ 4.0 to 8.5 ppm) [74]. It was evident that electrovalent interaction between ibuprofen and DEAE-Dextran occurred confirming the FTIR data that an amide was formed from the interaction between Ibuprofen and DEAE-Dextran. Multiplicity (splitting and duplication) of signals were also observed at the isopropyl methyl protons (C10 and C11); methyl doublet proton (C3); doublet CH proton (C8) and quartet proton (C2) which overlapped with the signals of the DEAE-Dextran suggesting hydrophobic interaction or formation of hydrogen bonding network with the carboxylic groups due to van der Waals forces of attraction. Multiplicity (or duplication) of proton signals of racemic enantiomers of ibuprofen has been reported in the presence of chiral cyclodextrin [66]. The authors assert that this phenomenon underpins the spatial arrangement of ibuprofen molecules and formation of inclusion complex with β-cyclodextrin. Similar proton signal multiplicity and absence of the hydroxyl group were observed for the ibuprofen-chitosan nanoconjugates indicating electrovalent and hydrogen bonding interaction between ibuprofen and chitosan. The amide proton signals from the ibuprofen-chitosan nanoconjugates were more prominent and stronger (δ 7.89, 8.08 and 8.46 ppm) than ibuprofen-DEAE-Dextran nanoconjugates (δ 6.99, 7.38, 7.91 and 8.38 ppm). There was no visible interaction between the proton signals of ibuprofen and gellan however the ^{13}C NMR of binary mixtures of ibuprofen with each of the three polymers including gellan exhibited extensive carbon multiplicity and split of peaks

into singlets with varying chemical shifts (Figure 54) suggesting dipole-dipole interaction within racemic ibuprofen molecule and confirms the result of FT-IR analysis in this regard [66]. The ternary DEAE-Dextran-ibuprofen-gellan and ibuprofen-chitosan-gellan nanoconjugates prepared with varying weight ratios of DEAE-Dextran/Gellan and chitosan/gellan exhibited increased intensities of amide proton signals with increasing concentrations of the cationic polymers. There was no noticeable shift in the resonance of the H- bonded proton of the aromatic portion of ibuprofen (Figure 55). It was opined that the aromatic proton signal of ibuprofen may not be involved in the complexation reaction however it was evident that the amino groups on DEAE-Dextran and chitosan interacted with the carbonyl group of ibuprofen in agreement with the FT-IR data.

The ^{13}C-NMR spectra and assignments of pure ibuprofen and the ibuprofen-DEAE-Dextran nanoconjugates are presented in Table 36 and Figure 56. The peak assignment of chemical shifts (δ) for pure ibuprofen with a signal at 175.44 ppm corresponding to the carbonyl group was prominent in all the binary nanconjugates but the ibuprofen-DEAE-Dextran and ibuprofen-chitosan nanoconjugates shifted downfields to δ 175.68 and 176.39 ppm respectively. An upfield chemical shift was also observed at δ 172.77 ppm in ibuprofen-chitosan nanoconjugates (Figure 54). Multiplicity of the aromatic carbon (δ: 127 to 147 ppm) and aliphatic carbons (δ: 18.50 to 44.25 ppm) of ibuprofen was very prominent in ibuprofen-chitosan nanoconjugates with upfield and downfield chemical shifts. This suggests that both aliphatic and aromatic carbon atoms of ibuprofen experienced reduced freedom of rotation due to complexation with DEAE-Dextran or chitosan. Similar findings have been reported for ibuprofen complexation with hyperbranched polymers and cyclodextrin [75]. This confirms the ^{1}H NMR and FT-IR findings and that complexation of ibuprofen with DEAE-Dextran and chitosan respectively was evident.

Table 36 ^{1}H and ^{13}C chemical shift assignments for ibuprofen and Ibuprofen nanoconjugates.

Carbon No.	Proton Type	Ibuprofen		DEAE-Dextran-Ibuprofen-Gellan Nanoconjugates		Chitosan-Ibuprofen-Gellan Nanoconjugates	
		^{1}H Chemical Shift	***^{13}C Chemical Shift***	***^{1}H Chemical Shift***	***^{13}C Chemical Shift***	***^{1}H Chemical Shift***	***^{13}C Chemical Shift***
1	COOH	12.24	175.44	-	**195.38**	-	175.64
2	CH	3.66	44.26	3.64; 3.52	44.42; 69.75	3.68; 3.58; 3.56; 3.52	44.58; 69.76
3	CH_3	1.36	18.50	1.35; 1.24	18.57	1.35; 1.32; 1.24; 1.11; 1.10	18.65
4	C	-	138.46	-	138.65	-	138.87; **146.63**
5, 5'	CH	7.11	127.07	7.11	127.08	7.09	127.09
6, 6'	CH	7.20	128.93	7.20	128.89	7.21	128.84
7	C	-	139.51	-	139.43	-	139.32
8	CH_2	2.43	44.26	2.42	44.42	2.42	44.58
9	CH	1.85	40.11	1.83; 1.91	40.11	1.84; 1.89	40.11
10	CH_3	0.85	18.50	0.85	18.57	0.85; 0.71; 0.69	18.65
11	CH_3	0.87	22.14	0.87	22.15	0.85; 0.87; 0.94; 0.92	22.15

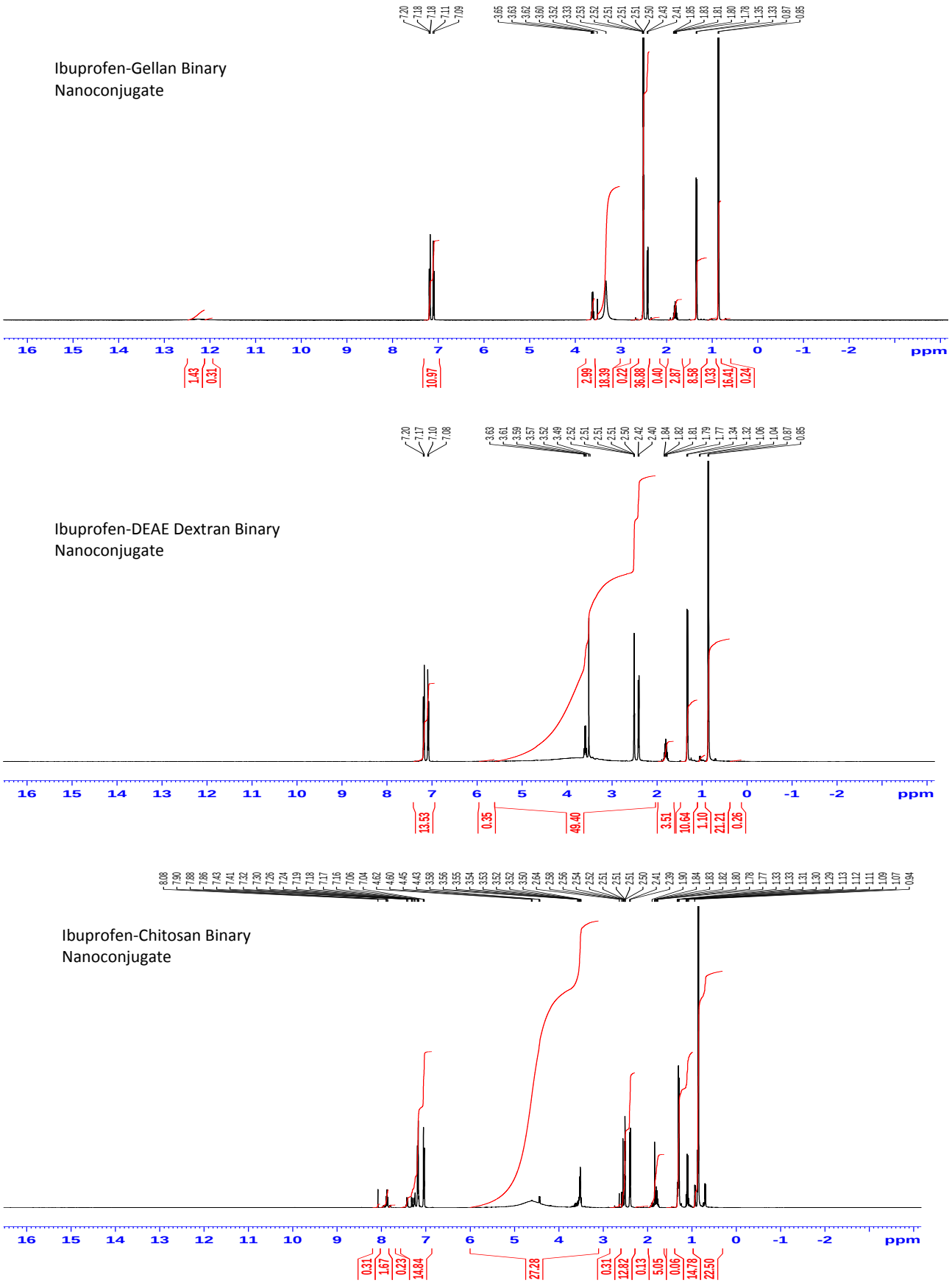

Figure 53 ^{1}H NMR spectra of binary nanoconjugates of Ibuprofen.

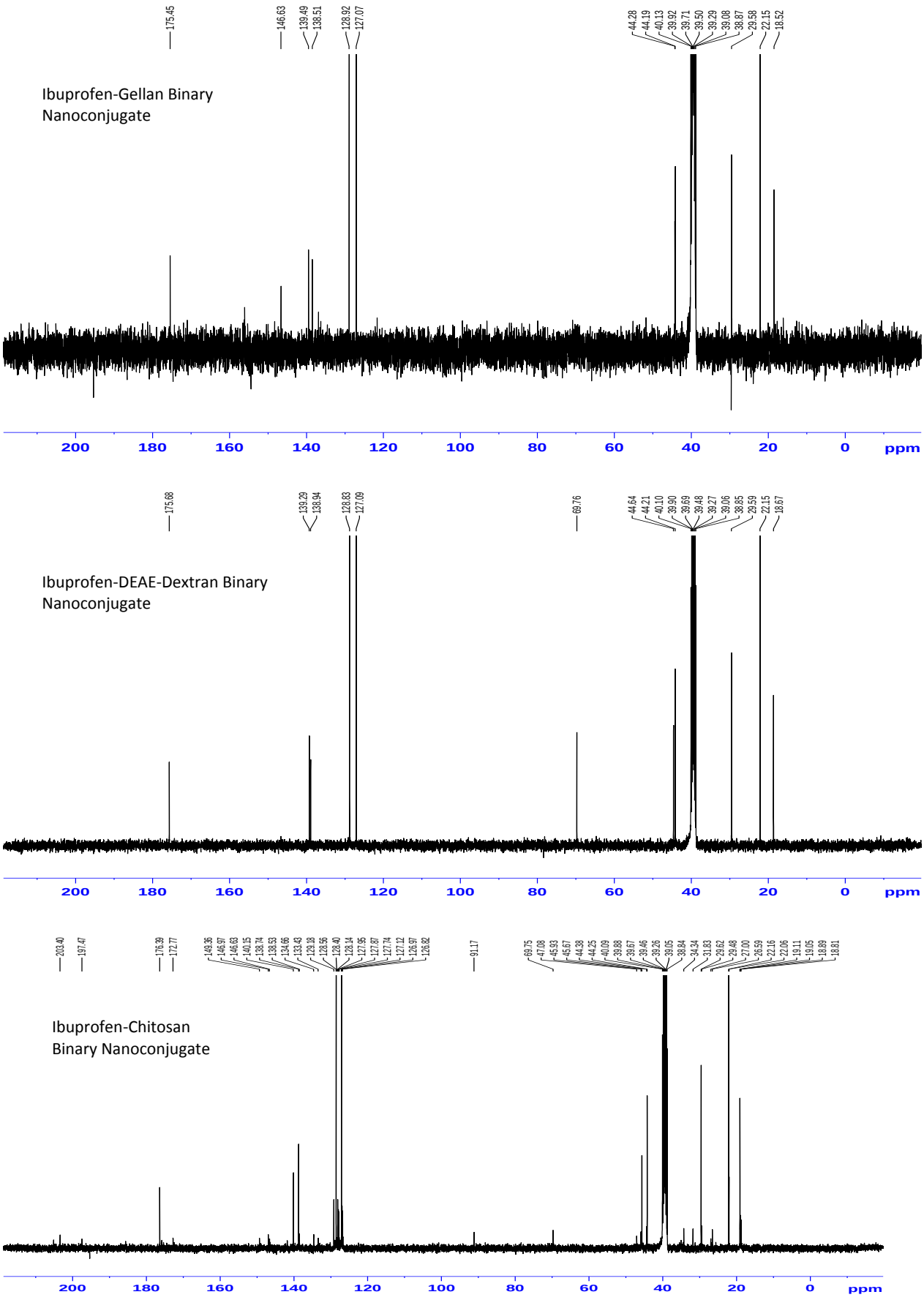

Figure 54 ^{13}C- NMR spectra of binary nanoconjugates of Ibuprofen.

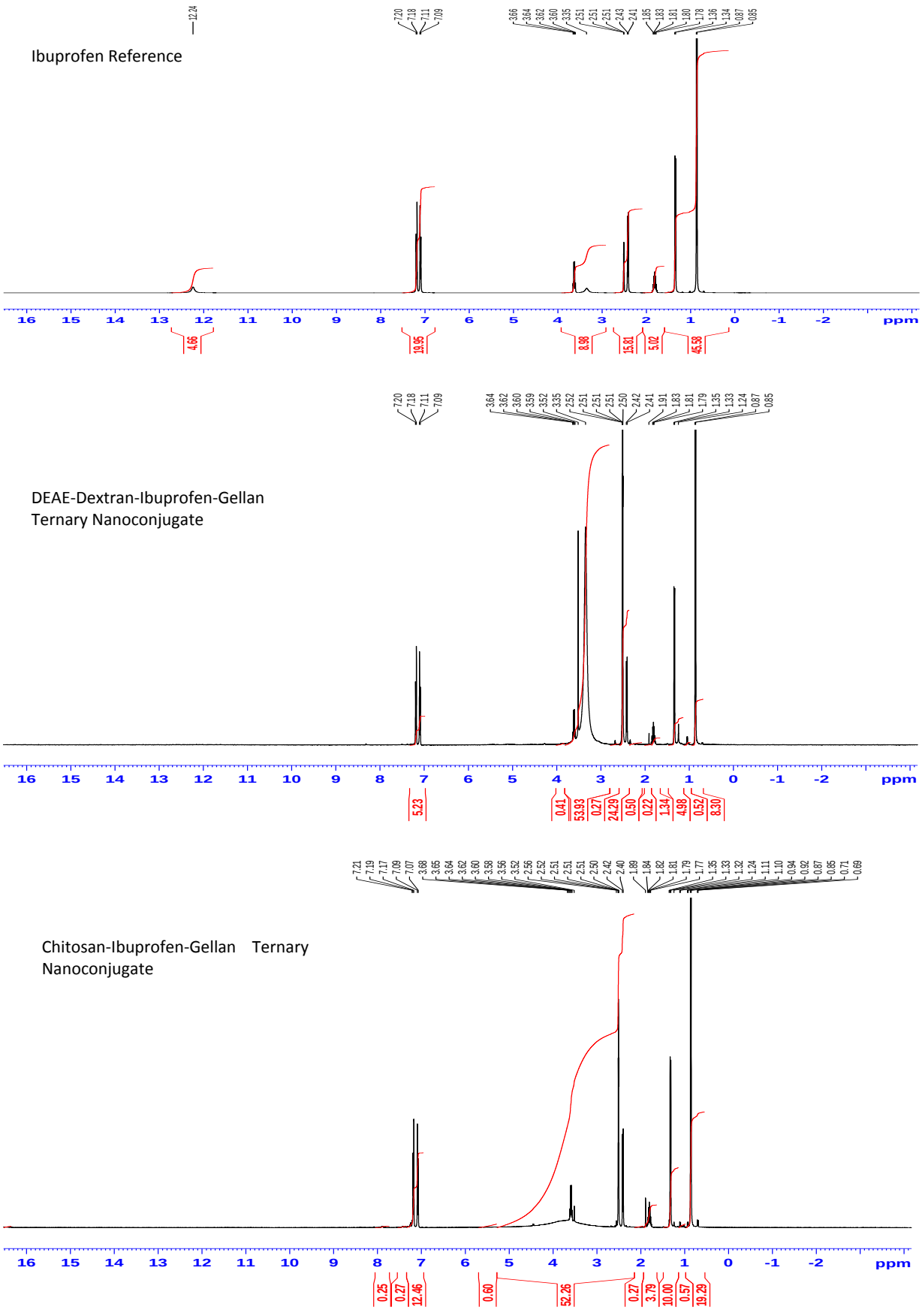

Figure 55 ^{1}H NMR spectra of ternary nanoconjugates of Ibuprofen.

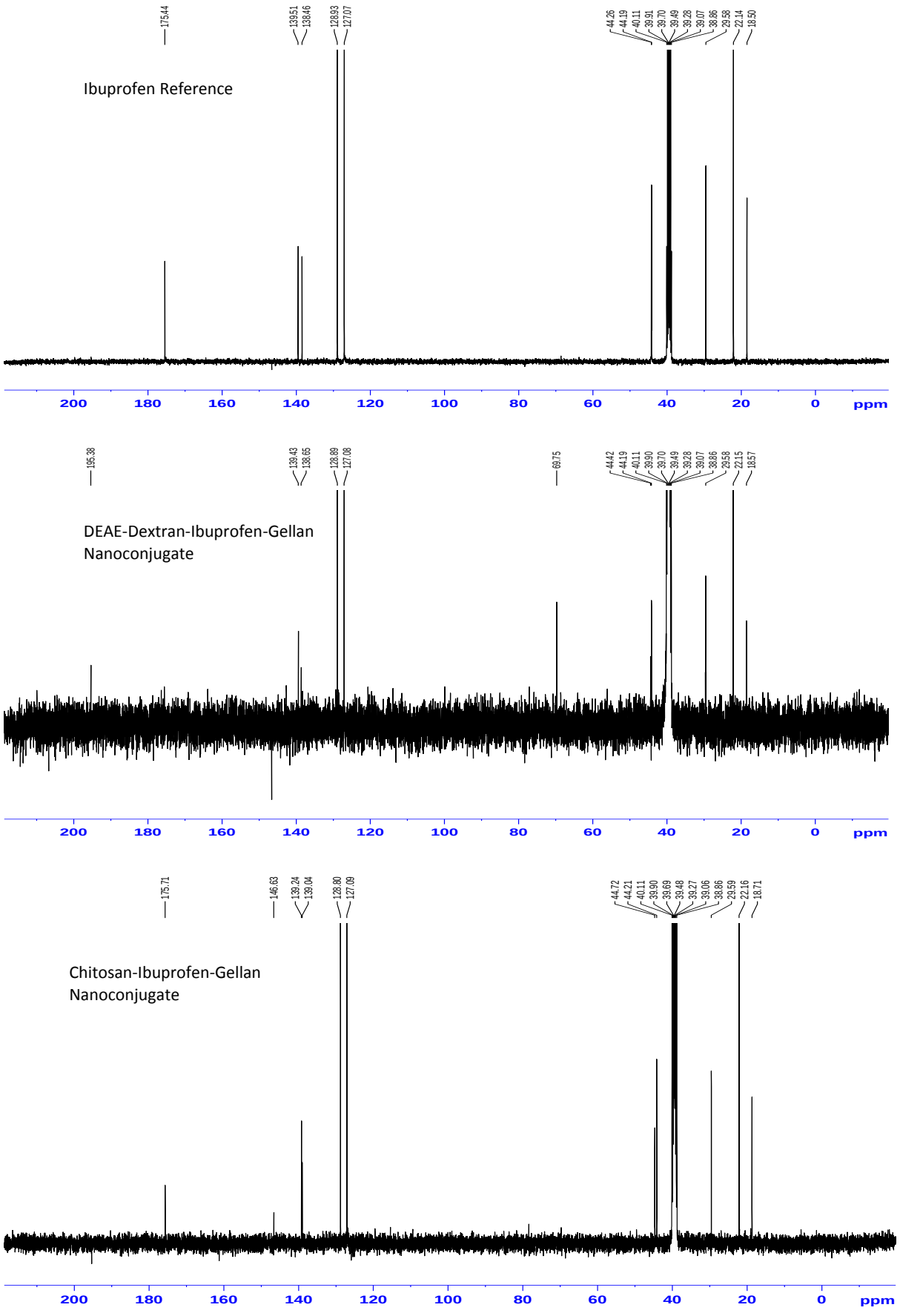

Figure 56 ^{13}C- NMR spectra of ternary nanoconjugates of Ibuprofen.

2.3.3.10. Thermal studies

2.3.3.10.1. Differential scanning calorimetry

Differential Scanning Calorimetry (DSC) is a well established rapid thermal analytical technique commonly used for the evaluation of potential physical and chemical interactions between drugs and excipients during preformulation studies stage of product development [76]. It has also found wide applications in detection of polymorphism, incompatibility between drugs and excipients of a dosage form, measurement of interaction and decomposition kinetics [77], and more recently in the determination of the solubility of Active Pharmaceutical Ingredients (API) within semi-solid and solid matrix systems [78] as well as estimating the binding or complexation parameters in multiligand binding proteins [79]. DSC measures the differences in heat flow into a substance compared with a reference as a function of controlled sample temperature and heat (enthalpy) capacity [80]. It was intended to use DSC technique to evaluate the complexation between ibuprofen and DEAE-Dextran or chitosan in binary conjugates as well as the ternary DEAE-Dextran-ibuprofen-gellan and chitosan-ibuprofen-gellan nanoconjugates.

The DSC thermograms of the nanoconjugates and their components are presented in Tables 37 to 44 and Figures 57 to 66. The DSC thermograms of Ibuprofen showed characteristic sharp endothermic peak at 80.07 °C suggesting its crystallinity, with enthalpy of fusion of 118.64 J/g in Figure 56. This melting peak is higher than the literature value for pure ibuprofen in the range of 75 to 78 °C [81]. This could be due to some impurity in the ibuprofen sample however in a similar study, Kumar *et al.* reported that the melting peak of ibuprofen was 82.76 °C [82]. The second peak of the pure ibuprofen was ascribed to the degradation of ibuprofen at 237.51 °C with enthalpy of fusion 2241.34 J/g. DEAE-Dextran showed a glass transition temperature (Tg) at 57.26 °C; a broad endothermic melting peak at 124.05 °C due to its amorphous characteristic; a small peak was noted at 201.21 °C probably due to the semi crystalline component of the polymer and a final peak at 268.50 °C attributed to the decomposition of DEAE-Dextran. The physical mixture of DEAE-Dextran and

Ibuprofen showed peaks at 59.58 °C, 79.99 °C, 116.86 °C, 200.58 °C and 237.63 °C which represented peaks from individual components (ibuprofen and DEAE-Dextran). It was observed that the Tg of DEAE-Dextran increased by 2.32 °C in the physical mixture while the melting peak of ibuprofen did not change to any great extent (79.99 °C). However, the melting peak of the DEAE-Dextran decreased by 5.80% while the degradation peaks remained almost constant.

The melt solubilization technique produced nanoconjugates (IbDMelt) with only three endothermic peaks which did not correspond to any of the peaks in the physical mixture. The new peaks exhibited significantly lower melting temperatures (5.42 to 9.69 °C; 39.24 to 85.98 °C and 92.49 to 105.48 °C) compared with five peaks in the physical mixture which ranged from 59.58 to 237.63 °C (Table 37; Figure 58). The appearance of new multiple endothermic peaks suggests formation of multiple complexes and the reduced melting temperatures indicates the existence of the newly formed product in amorphous state. The peak at the lowest temperature decreased to a minimum of 5.42 °C at ibuprofen/DEAE-Dextran weight ratio 1:1 and increased steadily beyond this ratio (Figure 59) indicating the critical complexation concentration of DEAE-Dextran. It was opined that this peak may be attributed to the melt of water ice crystals since the DSC temperature range was -50 to 300 °C. The Tg of ibuprofen has been reported to be -42.3 °C [83] hence the process of melt solubilization may have increased the Tg of ibuprofen. The second peak of each of the nanoconjugate (39.24 to 85.98 °C) was broad and diffuse due to loss of residual water. This peak also decreased to a minimum of 39.24 °C at ibuprofen/DEAE-Dextran weight ratio 1:1 and increased steadily beyond this concentration confirming the critical complexation concentration of DEAE-Dextran. The increase in the melting temperature of the third peak (92.49 to 108.16 °C) suggests increased isothermal stability of the nanoconjugate. These peaks increased with increasing concentration of DEAE-Dextran to a maximum of 108.16 °C at ibuprofen/DEAE-Dextran weight ratio 1:4. The degradation peak of pure ibuprofen at 237.51 °C disappeared completely in all the IbDMelt nanoconjugates suggesting the isothermal stability of the nanoconjugates.

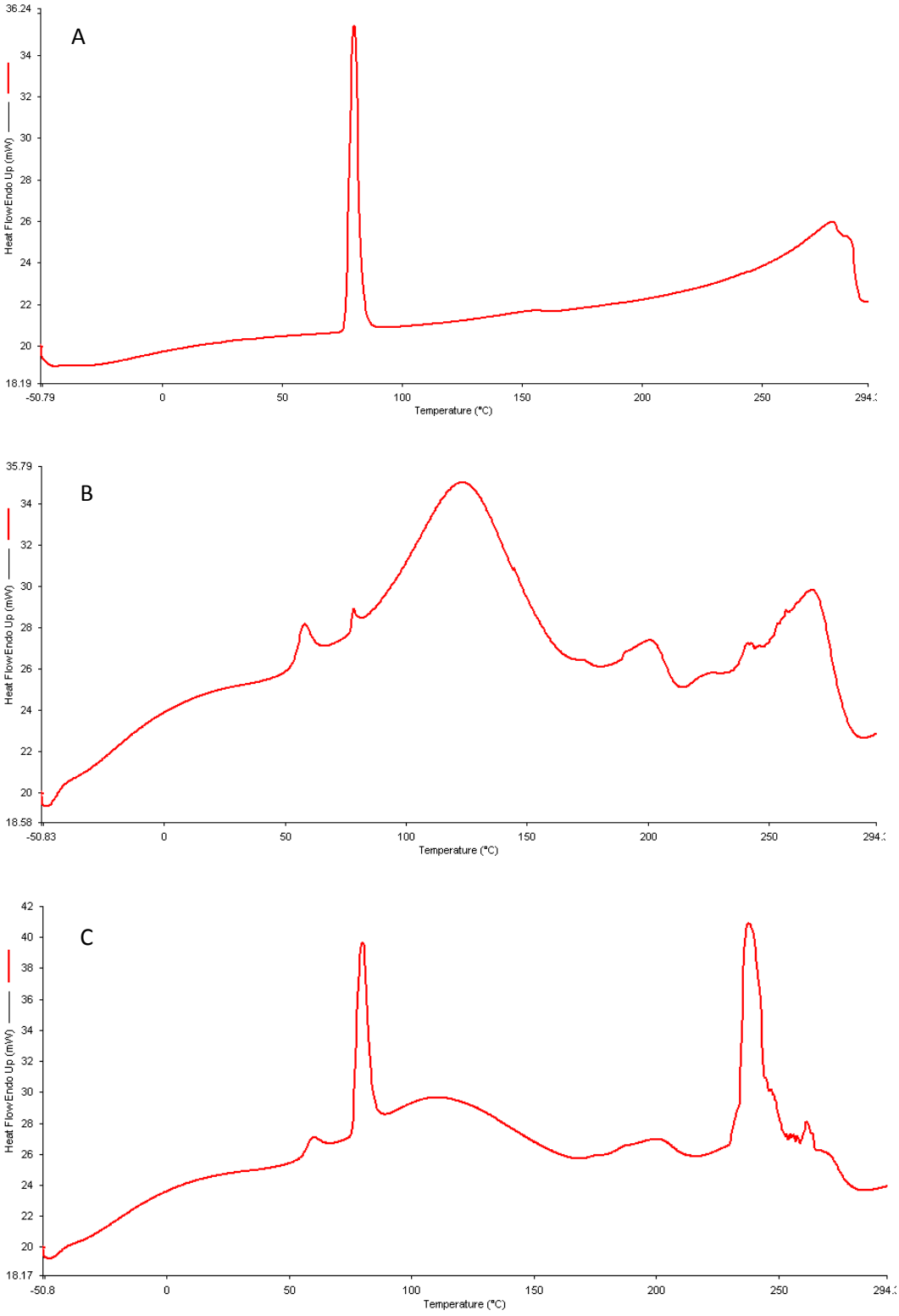

Figure 57 DSC thermograms of (A) ibuprofen (B) DEAE-Dextran (C) Ibuprofen-DEAE-Dextran physical mixture.

Table 37 DSC of ibuprofen-DEAE-Dextran conjugates (melt solubilization) and ibuprofen control. Each value represents mean ± SD (n = 4).

Formulation	Onset (°C)	Peak (°C)	End (°C)	Delta H (J/g)	Area (mJ)
Ibuprofen-reference	76.52±1.42	80.07±1.94	83.23±1.78	118.64±0.96	949.15±38.72
	193.66±7.73	237.51±9.93	243.03±9.57	2241.34±51.03	309.29±11.21
DEAE-Dextran-reference	53.55±0.85	57.86±0.76	63.97±0.92	5.10±0.08	35.16±0.41
	87.43±1.22	124.05±4.16	158.87±5.34	139.17±5.64	960.30±40.48
	187.42±8.23	201.54±10.58	210.60±11.45	12.72±0.84	87.74±1.25
	245.83±12.74	268.50±11.78	281.53±13.66	70.84±0.92	488.852±21.22
Ibuprofen-DEAE-Dextran physical mixture	55.30±0.76	59.58±0.92	66.17±0.88	3.37±0.02	20.57±0.43
	75.83±1.40	79.99±1.84	83.83±1.91	31.48±0.95	192.03±9.47
	90.83±1.35	116.86±2.76	154.50±5.58	37.13±0.86	226.48±10.82
	179.65±7.43	200.58±10.68	211.36±10.54	10.93±0.22	66.68±0.81
	233.64±10.75	237.63±10.96	245.06±10.84	67.67±0.81	412.78±18.64
IbMelt-control (IbD 1:0)	1.57±0.04	8.31±0.23	12.93±0.58	193.68±7.3	1278.28±52.78
	52.64±1.08	89.00±2.32	97.04±2.64	1220.79±38.22	8057.21±105.77
IbD1Melt (IbD 1:0.5)	2.13±0.04	5.57±0.18	8.94±0.30	139.69±6.48	391.12±11.65
	29.59±0.88	56.44±1.33	63.39±1.45	566.35±20.14	1585.78±58.69
	84.99±1.98	92.49±2.25	95.40±2.37	39.94±0.85	111.82±4.07
IbD2Melt (IbD 1:1)	2.69±0.02	5.42±0.07	8.53±0.15	32.67±0.61	127.40±1.36
	28.67±0.65	39.24±0.84	44.00±0.96	76.29±0.81	297.51±12.18
	91.75±1.32	99.53±1.62	103.06±1.74	71.65±0.76	279.44±11.23
IbD3Melt (IbD 1:2)	1.92±0.03	8.75±0.22	13.05±0.58	124.21±4.35	1179.95±51.57
	51.78±1.27	81.16±1.95	91.03±2.14	567.13±22.18	5387.69±68.74
	102.06±2.65	106.63±3.78	110.39±3.32	64.56±2.09	613.29±25.22
IbD4Melt (IbD 1:4)	1.93±0.04	8.78±0.28	13.56±0.69	158.72±5.77	1460.15±61.54
	46.45±1.01	81.81±1.96	89.81±2.05	10.04±35.44	7452.36±96.38
	101.63±2.24	108.16±3.02	110.91±3.21	98.97±2.52	910.49±38.34
IbD5Melt (IbD 1:8)	2.07±0.05	9.69±0.35	14.66±0.77	212.46±7.22	1763.41±65.22
	51.26±1.11	85.98±2.08	94.90±2.33	1277.84±48.23	10606.04±130.78
	101.36±2.55	105.34±2.98	107.65±3.11	28.75±0.96	238.63±7.63

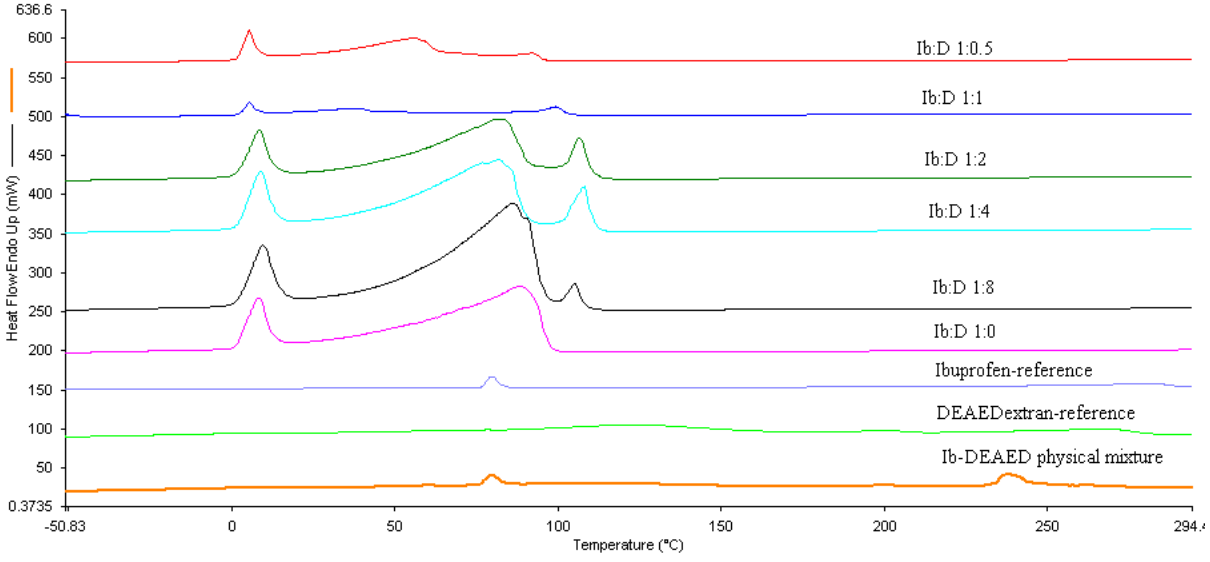

Figure 58 DSC thermograms of ibuprofen-DEAE-Dextran conjugates (melt solubilization), ibuprofen control, pure ibuprofen, DEAE-Dextran and physical mixture of ibuprofen and DEAE-Dextran.

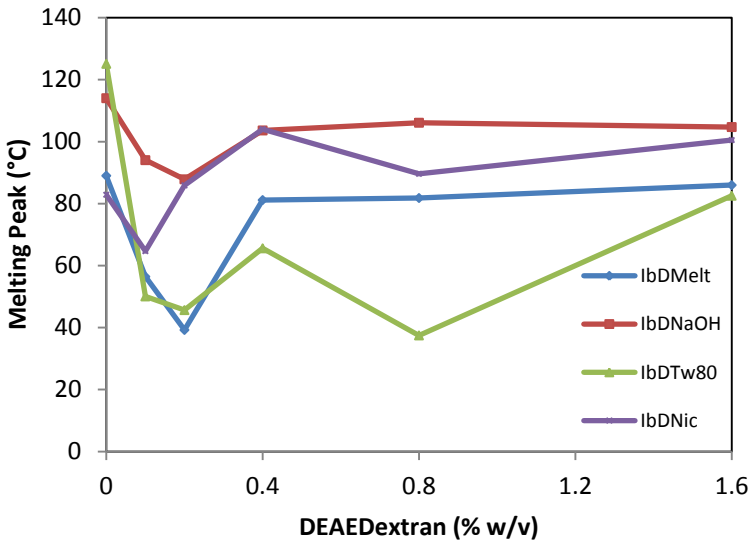

Figure 59 The DSC melting peak profile of IbDMelt, IbDNaOH, IbDTw80 and IbDNic nanoconjugates.

The nanoconjugates obtained from the alkaline solubilization technique (IbDNaOH nanoconjugates) exhibited similar profile with the melt solubilization technique. However only two endothermic peaks were shown (in the range of 3.16 to 11.06 °C and 70.16 to 104.71 °C) except IbD4NaOH which showed three peaks (Table 38). The peak with the lowest melting temperature did not show any particular pattern with increasing concentration of the DEAE-Dextran however low values of 3.16 °C and 2.78 °C were observed at ibuprofen/DEAE-Dextran weight ratios of 1:1 and 1:2 respectively. It was opined that nanoconjugates were formed at similar ratio of ibuprofen/DEAE-Dextran as in the melt solubilization technique. The second peak also decreased to a minimum of 87.85 °C at ibuprofen/DEAE-Dextran weight ratio of 1:1 beyond which it became unpredictable. It was opined that the endothermic melting peak of pure ibuprofen which appeared at 80.07 °C had shifted to higher temperatues ranging from 87.85 to 106.10 °C for IbDNaOH nanoconjugates (Figure 60). The thermal decomposition peak of pure ibuprofen at 237.51 °C also disappeared in all the IbDNaOH nanoconjugates. All the endothermic peaks shown in this technique were broad with higher melting temperatues than the melt solubilization technique suggesting the existence of the nanoconjugates formed in the amorphous state with better isothermal stability. It was concluded that multiple complexes were also formed in this technique.

Table 38 DSC of ibuprofen-DEAE-Dextran conjugates (solubilization), ibuprofen control, pure ibuprofen, DEAE-Dextran and physical mixture of ibuprofen and DEAE-Dextran. Each value represents mean ± SD (n = 4).

Formulation	Onset (°C)	End (°C)	Peak (°C)	Area (mJ)	DeltaH (J/g)
Ibuprofen-reference	76.52±1.42	83.23±1.78	80.07±1.94	949.15±38.72	118.64±0.96
	193.66±7.73	243.03±9.57	237.51±9.93	309.29±11.21	2241.34±51.03
DEAE-Dextran-reference	53.55±0.85	63.97±0.92	57.86±0.76	35.16±0.41	5.10±0.08
	87.43±1.22	158.87±5.34	124.05±4.16	960.30±40.48	139.17±5.64
	187.42±8.23	210.60±11.45	201.54±10.58	87.74±1.25	12.72±0.84
	245.83±12.74	281.53±13.66	268.50±11.78	488.852±21.22	70.84±0.92
Ibuprofen-DEAE-Dextran physical mixture	55.30±0.76	66.17±0.88	59.58±0.92	20.57±0.43	3.37±0.02
	75.83±1.40	83.83±1.91	79.99±1.84	192.03±9.47	31.48±0.95
	90.83±1.35	154.50±5.58	116.86±2.76	226.48±10.82	37.13±0.86
	179.65±7.43	211.36±10.54	200.58±10.68	66.68±0.81	10.93±0.22
	233.64±10.75	245.06±10.84	237.63±10.96	412.78±18.64	67.67±0.81
IbNaOH-control (IbD 1:0)	0.54±0.04	10.48±0.58	5.91±0.23	966.66±42.78	322.22±14.30
	101.07±1.18	119.18±1.37	114.02±1.41	5166.17±58.77	1722.07±35.37
IbD1NaOH (IbD 1:0.5)	1.87±0.03	16.17±0.82	11.06±0.42	2262.32±70.58	128.90 ±7.22
	59.58±1.18	106.33±2.28	94.04±1.92	14792.58±128.09	842.88 ±1.21
IbD2NaOH (IbD 1:1)	1.28±0.04	5.52±0.13	3.16±0.09	96.06±1.93	16.85 ±0.61
	70.37±1.52	92.39±1.90	87.85±1.86	317.06±17.48	55.62±1.21
IbD3NaOH (IbD 1:2)	0.50±0.01	5.65±0.15	2.78±0.78	129.03±3.25	14.34±0.58
	99.10±2.08	108.41±2.37	103.62±2.41	614.60±22.17	68.29±1.26
IbD4NaOH (IbD 1:4)	1.98±0.05	9.47±0.36	6.06±0.17	614.08±22.84	45.55±0.93
	52.34±1.11	78.18±1.54	70.16±1.58	3448.78±69.87	255.84±8.74
	101.53±2.27	109.22±2.58	106.10±2.11	332.35±18.66	24.66±0.85
IbD5NaOH (IbD 1:8)	0.69±0.02	6.56±0.25	3.60±0.14	234.80±8.22	14.14±0.64
	100.48±2.58	108.72±2.61	104.71±2.33	757.37±35.47	45.62±0.98

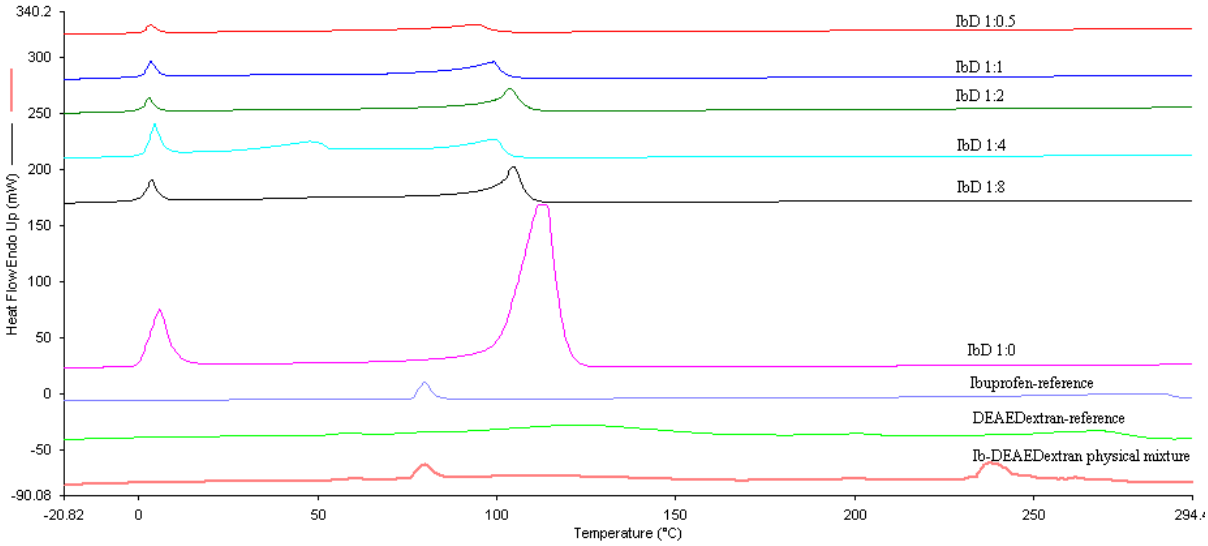

Figure 60 DSC thermograms of ibuprofen-DEAE-Dextran conjugates (alkaline solubilization), ibuprofen control, pure ibuprofen, DEAE-Dextran and physical mixture of ibuprofen and DEAE-Dextran.

Nanoconjugates obtained from the surfactant solubilization technique (IbDTw80) showed three peaks in the range of -14.15 to 8.64 °C; 37.47 to 82.55 °C and 104.45 to 106.31 °C (Table 39). The melting temperature of the first peak was observed at -14.00 °C in the absence of DEAE-Dextran but increased with increasing concentration of DEAE-Dextran to a maximum value of 6.35 °C at

ibuprofen/DEAE-Dextran weight ratio of 1:2 beyond which it became unpredictable. The second peak did not show any particular pattern with increase in the concentration of DEAE-Dextran but exhibited two minima values of 45.65 °C and 37.47 °C at ibuprofen/DEAE-Dextran weight ratios 1:1 and 1:4 respectively suggesting formation of multiple complexes. The broad and diffused peaks with reduced melting temperatures of the nanoconjugates produced in this technique also signify the amorphous state of the new product. There was a shift of melting peak of ibuprofen to a range of 37.47 to 82.55 °C for IbDTw80 conjugates in Figure 61. The thermal decomposition peak of ibuprofen at 237.51 °C also disappeared in all the IbDTw80 nanoconjugates suggesting isothermal stability.

Table 39 DSC of ibuprofen-DEAE-Dextran conjugates (solubilization), ibuprofen control, pure ibuprofen, DEAE-Dextran and physical mixture of ibuprofen and DEAE-Dextran. Each value represents mean ± SD (n = 4).

Formulation	Onset (^{o}C)	End (^{o}C)	Peak (^{o}C)	Area (mJ)	Delta H (J/g)
Ibuprofen-reference	76.52±1.42	83.23±1.78	80.07±1.94	949.15±38.72	118.64±0.96
	193.66±7.73	243.03±9.57	237.51±9.93	309.29±11.21	2241.34±51.03
DEAE-Dextran-reference	53.55±0.85	63.97±0.92	57.86±0.76	35.16±0.41	5.10±0.08
	87.43±1.22	158.87±5.34	124.05±4.16	960.30±40.48	139.17±5.64
	187.42±8.23	210.60±11.45	201.54±10.58	87.74±1.25	12.72±0.84
	245.83±12.74	281.53±13.66	268.50±11.78	488.852±21.22	70.84±0.92
Ibuprofen-DEAE-Dextran physical mixture	55.30±0.76	66.17±0.88	59.58±0.92	20.57±0.43	3.37±0.02
	75.83±1.40	83.83±1.91	79.99±1.84	192.03±9.47	31.48±0.95
	90.83±1.35	154.50±5.58	116.86±2.76	226.48±10.82	37.13±0.86
	179.65±7.43	211.36±10.54	200.58±10.68	66.68±0.81	10.93±0.22
	233.64±10.75	245.06±10.84	237.63±10.96	412.78±18.64	67.67±0.81
IbTw80-control (IbD 1:0)	-25.29±0.14	-7.35±0.22	-14.15±0.23	207.06±12.13	28.76±0.53
	120.42±1.08	131.83±3.64	125.11±3.32	262.84±11.77	36.51±0.52
IbD1Tw80 (IbD 1:0.5)	1.35±0.01	6.75±0.02	4.18±0.02	275.97±10.89	28.99±0.41
	42.00±0.88	58.59±1.03	50.06±0.97	844.64±39.65	88.72±1.86
	100.49±5.24	109.91±5.87	105.48±5.43	961.77±43.28	101.03±5.73
IbD2Tw80 (IbD 1:1)	1.68±0.02	6.92±0.03	4.45±0.02	249.69±9.75	36.72±0.58
	24.29±0.76	55.30±1.07	45.65±0.92	1019.52±50.20	149.92±6.23
	100.03±4.83	108.68±5.22	104.45±5.08	921.83±40.22	135.56±7.52
IbD3Tw80 (IbD 1:2)	2.14±0.02	9.70±0.04	6.35±0.03	428.72±20.21	47.63±0.90
	34.29±0.81	72.05±1.33	65.58±1.24	2930.03±90.14	325.56±16.13
	100.89±3.86	109.35±5.41	105.11±5.18	505.03±27.82	56.11±0.90
IbD4Tw80 (IbD 1:4)	1.33±0.02	6.28±0.03	3.71±0.02	170.09±7.88	17.54±0.63
	18.09±0.62	46.77±0.80	37.47±0.76	562.83±28.74	58.02±1.21
	100.21±4.37	109.30±5.11	104.63±5.03	565.57±25.38	58.31±1.08
IbD5Tw80 (IbD 1:8)	1.47±0.01	12.98±0.06	8.64±0.04	1390.84±48.95	144.88±7.79
	49.74±0.82	92.35±3.25	82.55±2.87	8995.74±110.68	937.06±43.66
	99.63±4.73	110.33±5.36	106.31±5.06	952.14±48.21	98.18±4.01

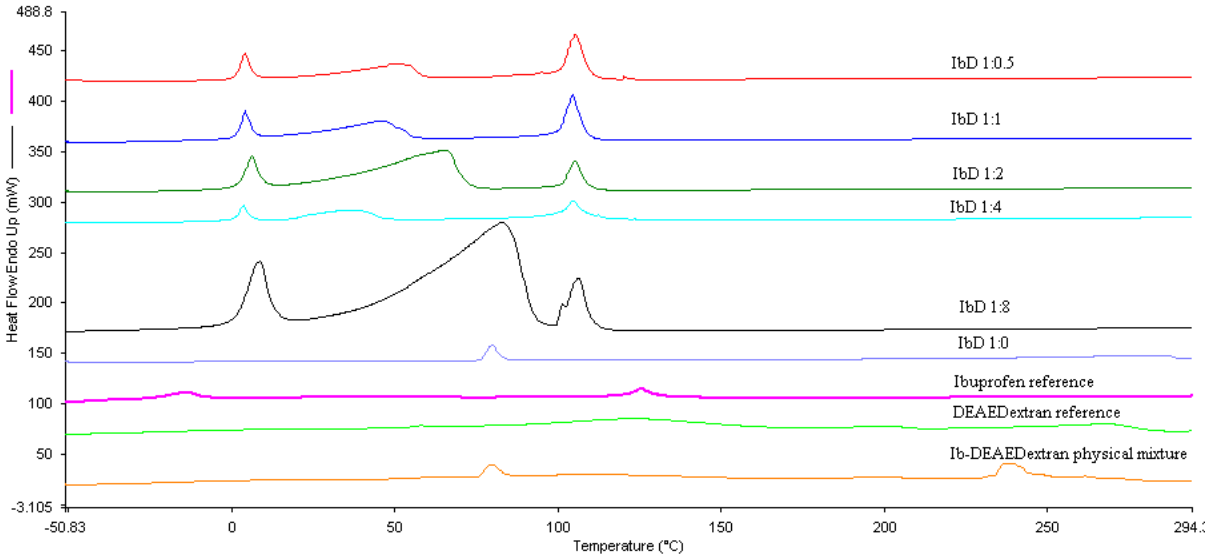

Figure 61 DSC thermograms of ibuprofen-DEAE-Dextran conjugates (surfactant solubilization), ibuprofen control, pure ibuprofen, DEAE-Dextran and physical mixture of ibuprofen and DEAE-Dextran.

The DSC thermograms of the nanoconjugates obtained from the hydrotropic complexation technique exhibited three peaks at ibuprofen/DEAE-Dextran weight ratios 1:0.5; 1:1 and 1:4 while other weight ratios studied exhibited only two peaks as presented in Table 40 and Figure 62. The first peak exhibited two minima values of 7.34 °C and 3.62 °C at ibuprofen/DEAE-Dextran weight ratio 1:0.5 and 1:2 respectively suggesting formation of multiple complexes. The second peak which was assigned to melting point of ibuprofen decreased to a minimum value of 64.67 °C at ibuprofen/DEAE-Dextran ratio of 1:0.5 beyond which it increased steadily. It was opined that lower concentration of DEAE-Dextran was required for complexation in this technique and the lower melting peak for ibuprofen indicates the amorphous state of the nanoconjugates formed. The absence of ibuprofen peaks at weight ratios 1:2 and 1:8 may indicate the formation of eutectic mixture as well as formation of multiple complexes. The melting point of nicotinamide was reported to be in the range of 128 to 131 °C [84]. The third peak did not vary significantly with increase in concentration of DEAE-Dextran. The thermal decomposition peak of ibuprofen at 237.51 °C disappeared in all the IbDNic nanoconjugates however the ibuprofen melting peak exhibited higher values indicating isothermal stability of the nanoconjugates.

Table 40 DSC of ibuprofen-DEAE-Dextran conjugates (hydrotropy), ibuprofen control, pure ibuprofen, DEAE-Dextran and physical mixture of ibuprofen and DEAE-Dextran. Each value represents mean ± SD (n = 4).

Formulation	Onset (°C)	End (°C)	Peak (°C)	Area (mJ)	Delta H (J/g)
Ibuprofen-reference	76.52±1.42	83.23±1.78	80.07±1.94	949.15±38.72	118.64±0.96
	193.66±7.73	243.03±9.57	237.51±9.93	309.29±11.21	2241.34±51.03
DEAE-Dextran-reference	53.55±0.85	63.97±0.92	57.86±0.76	35.16±0.41	5.10±0.08
	87.43±1.22	158.87±5.34	124.05±4.16	960.30±40.48	139.17±5.64
	187.42±8.23	210.60±11.45	201.54±10.58	87.74±1.25	12.72±0.84
	245.83±12.74	281.53±13.66	268.50±11.78	488.852±21.22	70.84±0.92
Ibuprofen-DEAE-Dextran physical mixture	55.30±0.76	66.17±0.88	59.58±0.92	20.57±0.43	3.37±0.02
	75.83±1.40	83.83±1.91	79.99±1.84	192.03±9.47	31.48±0.95
	90.83±1.35	154.50±5.58	116.86±2.76	226.48±10.82	37.13±0.86
	179.65±7.43	211.36±10.54	200.58±10.68	66.68±0.81	10.93±0.22
	233.64±10.75	245.06±10.84	237.63±10.96	412.78±18.64	67.67±0.81
IbNic-control (IbD 1:0)	0.64±0.04	14.33±0.58	9.54±0.13	1663.60±32.78	186.92±7.57
	54.37±1.11	95.45±2.72	82.88±2.32	10631.82±105.77	1194.58±58.22
IbD1Nic (IbD 1:0.5)	1.62±0.02	10.77±0.48	7.34±0.26	703.17±28.21	93.76±2.44
	38.21±0.83	75.17±1.99	64.67±1.34	3805.28±187.35	507.37±22.16
	86.46±2.25	99.88±2.92	96.09±2.68	249.29±9.56	33.24±0.74
IbD2Nic (IbD 1:1)	2.29±0.02	15.30±0.58	9.97±0.35	1383.84±50.14	168.76±8.02
	51.61±1.10	92.58±2.54	85.90±2.11	7964.04±103.22	971.22±48.11
	102.24±5.24	109.64±5.36	105.41±5.38	267.82±10.29	32.66±0.41
IbD3Nic (IbD 1:2)	0.97±0.01	6.48±0.23	3.62±0.03	213.20±9.22	28.81±0.31
	96.06±4.87	107.98±5.65	104.03±5.23	805.64±29.22	108.87±5.79
IbD4Nic (IbD 1:4)	1.44±0.01	14.59±0.54	9.99±0.38	1781.70±58.36	209.61±8.76
	54.27±1.14	95.56±2.73	89.64±2.03	10695.82±185.48	1258.33±49.83
	102.37±5.10	107.01±5.76	104.51±5.32	62.53±1.21	7.36±0.25
IbD5Nic (IbD 1:8)	1.38±0.01	15.84±0.67	10.90±0.42	2111.71±84.63	224.65±9.78
	57.01±1.14	106.89±4.23	100.52±5.10	14607.10±212.23	1153.93±47.36

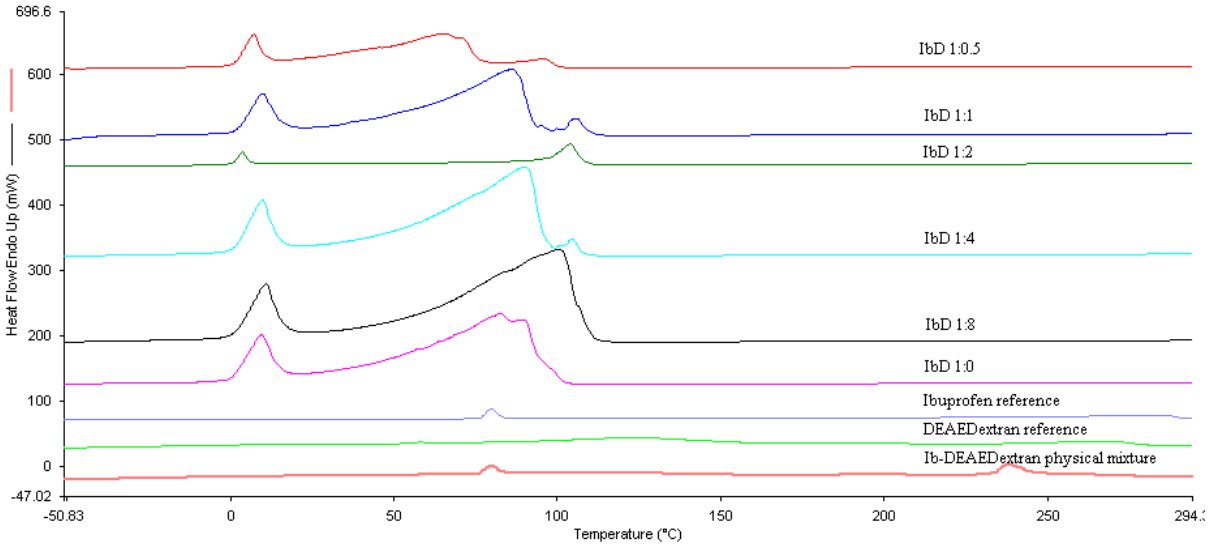

Figure 62 DSC thermograms of ibuprofen-DEAE-Dextran conjugates (hydrotropy), ibuprofen control, pure ibuprofen, DEAE-Dextran and physical mixture of ibuprofen and DEAE-Dextran.

The thermo-analytical profile of ibuprofen/chitosan nanoconjugates was similar to that of ibuprofen/DEAE-Dextran nanoconjugates. Chitosan exhibited a broad melting peak at 115.44 °C with enthalpy of 301.02 J/g and an exothermic peak at 318.29 °C with enthalpy of -201.91 J/g. These

correspond to the values reported by Silva *et al.* [85]. They observed the endothermic melting peak of chitosan at 112.00 °C while the exothermic peak was at about 311.00 °C which was attributed to chitosan degradation. The ibuprofen-chitosan physical mixture exhibited melting peaks at 81.34 °C, 126.56 °C and 250.30 °C corresponding to the individual components of the nanoconjugates. The first peak increased to a maximum value of 9.52 °C at ibuprofen/chitosan weight ratio of 1:0.5 beyond which it decreased steadily indicating the critical complexation concentration of chitosan. IbCh2Melt and IbCh3Melt conjugates showed two endothermic peaks while IbCh1Melt, IbCh4Melt and IbCh5Melt showed three peaks (Table 41). The melting peak of ibuprofen in the nanoconjugates shifted to higher values in this technique ranging from 80.00 to 93.17 °C with minima values of 80.00 °C and 80.71 °C at ibuprofen/chitosan weight ratios 1:0.125 and 1:1 respectively suggesting formation of multiple complexes (Figures 63 and 64).

Table 41 DSC of ibuprofen-chitosan conjugates (melt solubilization), ibuprofen control, pure ibuprofen, chitosan and physical mixture of ibuprofen and chitosan. Each value represents mean ± SD (n = 4).

Formulation	Onset (^{o}C)	End (^{o}C)	Peak (^{o}C)	Area (mJ)	Delta H (J/g)
Ibuprofen-	76.52±1.42	83.23±1.78	80.07±1.94	949.15±38.72	118.64±0.96
reference	193.66±7.73	243.03±9.57	237.51±9.93	309.29±11.21	2241.34±51.03
Chitosan-reference	60.44±1.02	155.57±6.2	115.44±4.32	2077.04±45.38	301.02±9.75
	299.84±7.95	339.81±10.85	318.39±10.68	-1938.38±42.56	-201.91±9.21
Ibuprofen-Chitosan	75.45±1.30	85.47±1.88	81.34±1.54	581.56±17.56	67.62±1.12
physical mixture	104.95±2.94	153.00±5.96	126.56±3.68	111.01±3.02	12.91±0.49
	250.30±9.82	267.84±10.11	262.48±10.35	59.29±1.14	6.89±0.23
IbMelt-control	1.57±0.04	12.93±0.58	8.31±0.23	1278.28±52.78	193.68±7.3
(IbCh 1:0)	52.64±1.08	97.04±2.64	89.00±2.32	8057.21±105.77	1220.79±38.22
IbCh1Melt	0.47±0.02	11.59±0.54	7.82±0.36	1107.72±35.47	246.16±7.85
(IbCh 1:0.125)	45.37±1.57	87.06±3.58	80.00±3.65	6566.20±80.69	1459.16±58.32
	98.39±4.62	108.96±5.84	104.85±5.22	350.41±18.72	77.87±2.65
IbCh2Melt	0.34±0.01	13.01±0.61	8.55±0.33	1473.09±40.12	196.41±7.24
(IbCh 1:0.25)	52.50±1.97	93.89±3.86	85.49±2.06	10899.12±120.33	1453.22±38.62
IbCh3Melt	0.62±0.02	13.92±0.69	9.52±0.42	1759.81±66.85	219.98±7.72
(IbCh 1:0.5)	61.71±2.08	101.44±4.36	93.17±2.55	12833.43±115.46	1604.18±60.31
IbCh4Melt	1.13±0.03	12.50±0.65	8.26±0.37	1024.83±32.63	133.09±6.12
(IbCh 1:1)	45.10±0.97	89.17±2.24	80.71±1.98	6245.46±85.30	811.10±31.26
	101.56±4.01	109.35±4.74	104.90±4.32	237.54±11.25	30.85±0.68
IbCh5Melt	0.06±0.01	10.31±0.41	6.30±0.27	1050.81±34.08	134.72±5.96
(IbCh 1:2)	72.84±2.14	98.17±3.82	89.20±2.78	6174.67±82.33	791.62±25.68
	103.68±3.78	110.83±4.52	107.92±4.31	193.70±6.55	24.83±0.85

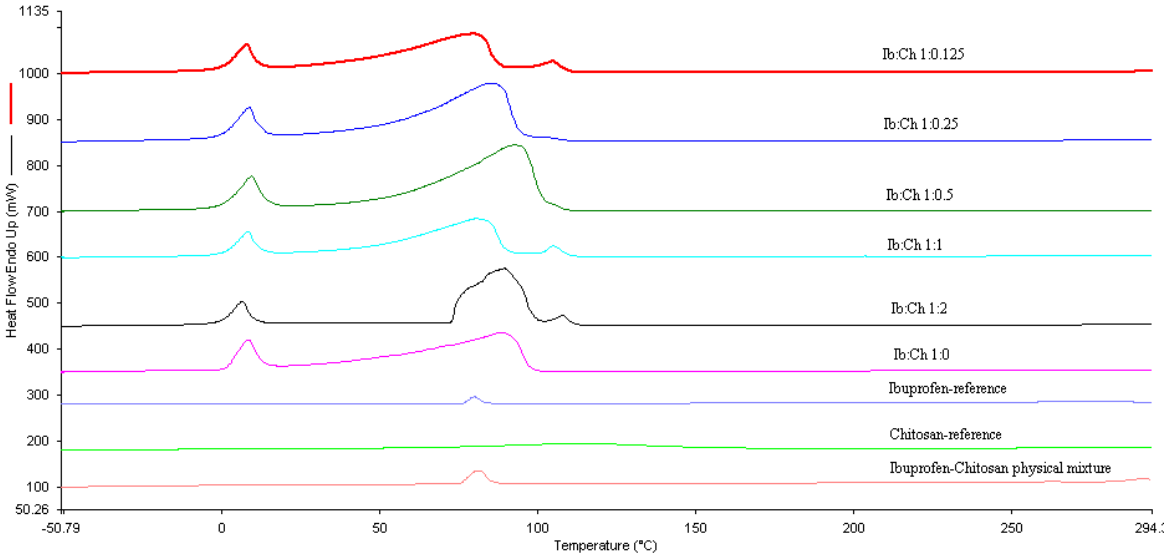

Figure 63 DSC thermograms of ibuprofen-chitosan conjugates (melt solubilization), ibuprofen control, pure ibuprofen, chitosan and physical mixture of ibuprofen and chitosan.

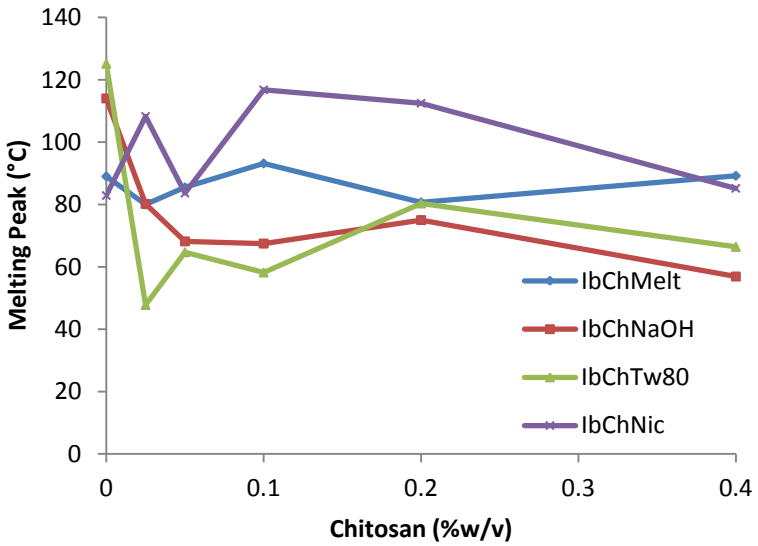

Figure 64 DSC melting peak profiles of IbChMelt, IbChNaOH, IbChTw80 and IbChNic nanoconjugates

The nanoconjugates obtained from the alkaline solubilization technique (IbChNaOH) showed three peaks in the range of 2.93 to 6.95 °C; 56.90 to 80.17 °C and 104.35 to 105.20 °C (Table 41 and Figure 65). The first peak exhibited two minima values of 4.66 °C and 2.93 °C at ibuprofen/chitosan weight ratio of 1:2 and 1:8 respectively suggesting formation of multiple complexes. The melting peak of ibuprofen shifted to a range of 56.90 to 80.17 °C with minima values of 67.47 °C and 56.90 °C at ibuprofen/chitosan weight ratios 1:2 and 1:8 respectively (Figure 65).

Table 42 DSC of ibuprofen-chitosan conjugates (solubilization), ibuprofen control, pure ibuprofen, chitosan and physical mixture of ibuprofen and chitosan. Each value represents mean ± SD (n = 4).

Formulation	Onset (°C)	End (°C)	Peak (°C)	Area (mJ)	Delta H (J/g)
Ibuprofen-reference	76.52±1.42	83.23±1.78	80.07±1.94	949.15±38.72	118.64±0.96
	193.66±7.73	243.03±9.57	237.51±9.93	309.29±11.21	2241.34±51.03
Chitosan-reference	60.44±1.02	155.57±6.2	115.44±4.32	2077.04±45.38	301.02±9.75
	299.84±7.95	339.81±10.85	318.39±10.68	-1938.38±42.56	-201.91±9.21
Ibuprofen-Chitosan physical mixture	75.45±1.30	85.47±1.88	81.34±1.54	581.56±17.56	67.62±1.12
	104.95±2.94	153.00±5.96	126.56±3.68	111.01±3.02	12.91±0.49
	250.30±9.82	267.84±10.11	262.48±10.35	59.29±1.14	6.89±0.23
IbNaOH-control (IbCh 1:0)	0.54±0.04	10.48±0.58	5.91±0.23	966.66±42.78	322.22±14.30
	101.07±1.18	119.18±1.37	114.02±1.41	5166.17±58.77	1722.07±35.37
IbCh1NaOH (IbCh 1:0.5)	0.15±01	10.19±0.45	6.26±0.21	1001.42±35.14	126.76±5.98
	39.85±0.79	86.27±2.43	80.17±1.98	6364.10±58.39	805.58±25.67
	98.72±5.21	111.61±5.76	105.10±4.89	251.75±7.96	31.87±0.69
IbCh2NaOH (IbCh 1:1)	0.61±0.03	7.43±0.22	4.67±0.14	502.64±17.21	67.02±1.42
	39.63±0.73	76.68±1.81	68.17±1.27	3108.43±42.36	414.46±15.64
	100.91±4.72	110.43±5.66	104.42±5.03	318.21±9.63	42.43±0.85
IbCh3NaOH (IbCh 1:2)	0.46±0.02	7.78±0.26	4.66±0.18	520.83±18.69	70.38±1.59
	41.07±0.88	75.41±1.58	67.47±1.13	3367.61±46.39	455.04±17.03
	99.12±5.06	110.19±5.21	104.45±5.36	278.46±8.76	37.63±0.85
IbCh4NaOH (IbCh1:4)	0.57±0.02	10.53±0.41	6.95±0.16	885.60±28.36	150.10±6.32
	46.89±0.96	81.30±1.95	75.01±1.38	4552.84±59.36	771.67±29.56
	98.09±4.36	109.82±5.01	105.20±4.98	440.24±16.38	74.62±1.52
IbCh5NaOH (IbCh 1:8)	1.02±0.01	5.39±0.12	2.93±0.06	279.13±8.21	31.01±0.65
	39.93±0.76	64.06±1.32	56.90±1.20	1530.97±42.58	170.11±5.98
	100.68±4.43	108.98±4.65	104.35±5.01	441.81±15.21	49.10±0.87

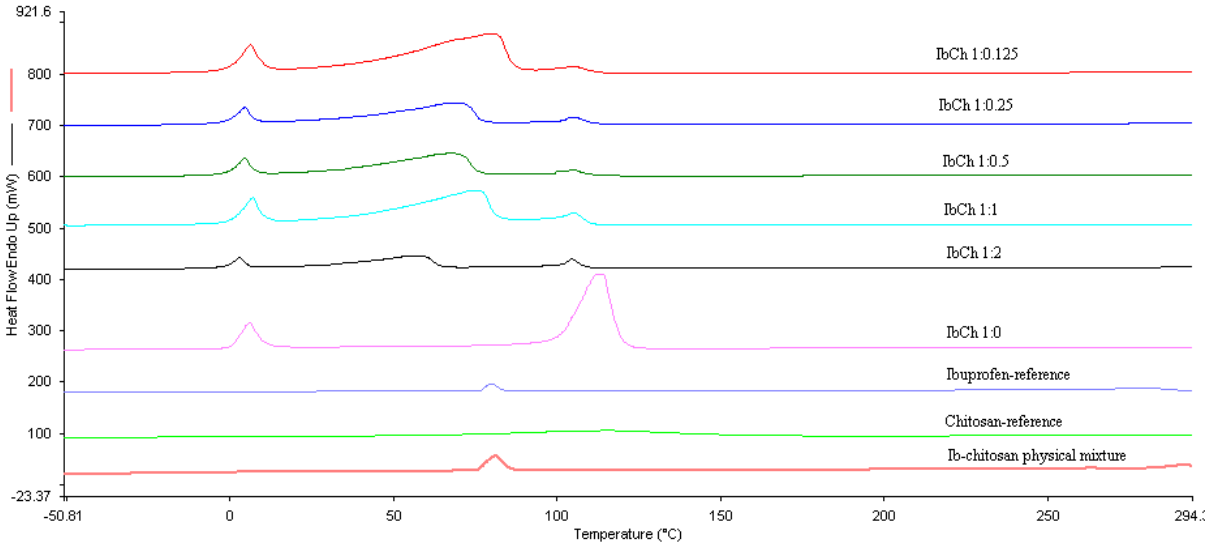

Figure 65 DSC thermograms of ibuprofen-chitosan conjugates (alkaline solubilization), ibuprofen control, pure ibuprofen, chitosan and physical mixture of ibuprofen and chitosan.

The nanoconjugates obtained from the surfactant solubilization technique (IbChTw80) showed three peaks in the range of 2.71 to 6.66 °C; 47.77 to 80.31 °C and 103.92 to 105.87 °C (Table 43 and Figure 66). The first peak increased to two maxima values of 5.54 °C and 6.66 °C at ibuprofen/chitosan weight ratios 1:0.5 and 1:1 respectively indicating the formation of multiple complexes. The melting

peak of ibuprofen shifted to a range of 47.77 to 80.31 °C in IbChTw80 conjugates with two minima values of 47.77 °C and 58.19 °C at ibuprofen/chitosan weight ratios 1:0.125 and 1:0.5 respectively (Figure 66). All the nanoconjugates except IbCh4Tw80 exhibited broad and diffuse peaks with lower melting points than raw ibuprofen suggesting the existence of nanoconjugates in the amorphous state.

Table 43 DSC of ibuprofen-chitosan conjugates (solubilization), ibuprofen control, pure ibuprofen, chitosan and physical mixture of ibuprofen and chitosan. Each value represents mean ± SD (n = 4).

Formulation	Onset (°C)	End (°C)	Peak (°C)	Area (mJ)	Delta H (J/g)
Ibuprofen-reference	76.52±1.42	83.23±1.78	80.07±1.94	949.15±38.72	118.64±0.96
	193.66±7.73	243.03±9.57	237.51±9.93	309.29±11.21	2241.34±51.03
Chitosan-reference	60.44±1.02	155.57±6.2	115.44±4.32	2077.04±45.38	301.02±9.75
	299.84±7.95	339.81±10.85	318.39±10.68	-1938.38±42.56	-201.91±9.21
Ibuprofen-Chitosan physical mixture	75.45±1.30	85.47±1.88	81.34±1.54	581.56±17.56	67.62±1.12
	104.95±2.94	153.00±5.96	126.56±3.68	111.01±3.02	12.91±0.49
	250.30±9.82	267.84±10.11	262.48±10.35	59.29±1.14	6.89±0.23
IbTw80-control (IbCh 1:0)	-25.29±0.14	-7.35±0.22	-14.15±0.23	207.06±12.13	28.76±0.53
	120.42±1.08	131.83±3.64	125.11±3.32	262.84±11.77	36.51±0.52
IbCh1Tw80 (IbCh 1:0.125)	0.15±0.01	4.97±0.09	2.71±0.02	152.93±5.98	17.11±0.78
	25.20±0.58	54.66±1.36	47.77±1.25	695.81±18.33	77.83±1.52
	101.36±4.65	108.74±5.11	103.92±5.05	291.34±7.84	32.59±0.81
IbCh2Tw80 (IbCh 1:0.25)	0.44±0.01	8.88±0.19	5.54±0.16	363.79±13.65	43.31±1.14
	46.28±1.08	75.82±1.36	64.67±1.09	2562.82±64.32	305.10±12.66
	101.19±4.98	111.26±5.09	105.87±4.86	507.23±16.58	60.38±1.25
IbCh3Tw80 (IbCh 1:0.5)	0.09±0.01	6.43±0.15	3.36±0.82	251.42±7.21	30.29±0.75
	33.59±0.82	69.19±1.65	58.19±1.24	1595.91±53.69	192.28±6.18
	100.67±5.06	110.34±5.22	104.42±5.17	303.26±13.25	36.54±0.81
IbCh4Tw80 (IbCh1:1)	0.01±0.00	10.50±0.32	6.66±0.18	1000.08±47.25	123.47±5.23
	46.77±1.01	88.32±1.69	80.31±1.72	7070.51±92.03	872.90±35.67
	102.43±4.98	109.93±5.02	104.74±4.61	142.63±5.36	17.61±0.85
IbCh5Tw80 (IbCh 1:2)	0.05±0.01	8.11±0.26	4.87±0.12	533.82±17.48	100.72±4.86
	33.02±0.87	77.09±1.59	66.42±1.23	3942.72±76.38	743.91±23.54
	101.15±5.01	110.17±5.14	104.87±4.86	420.53±15.42	79.35±1.52

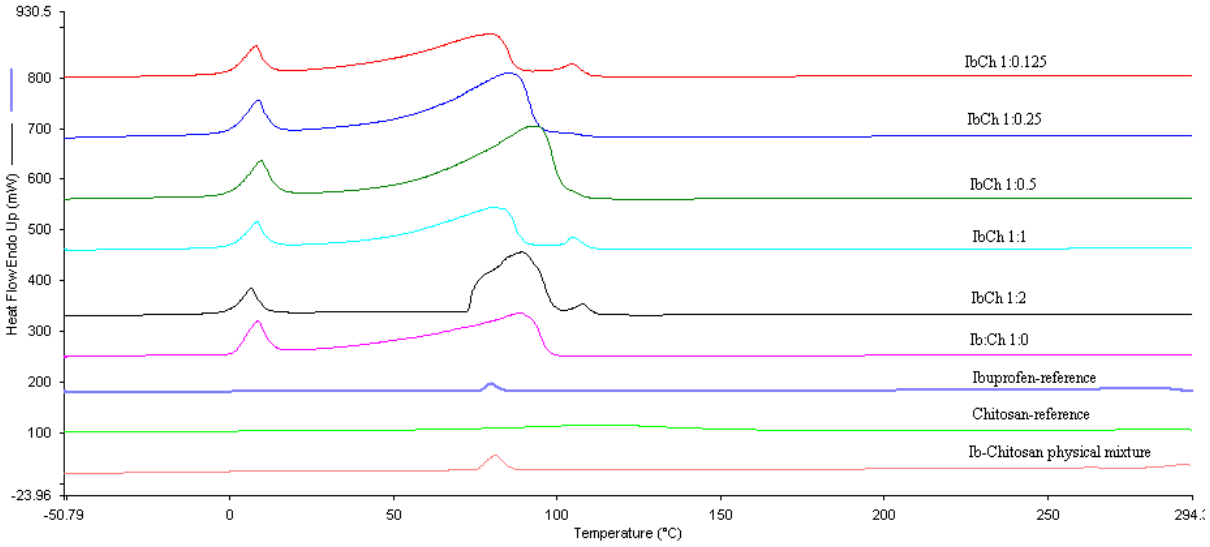

Figure 66 DSC thermograms of ibuprofen-chitosan conjugates (surfactant solubilization), ibuprofen control, pure ibuprofen, chitosan and physical mixture of ibuprofen and chitosan.

Nanoconjugates obtained from the hydrotropic complexation technique showed two peaks (IbCh1Nic and IbCh3Nic) however the IbCh2Nic, IbCh4Nic and IbCh5Nic exhibited three peaks as presented in Table 44 and Figure 67. The first peak exhibited two minimal values of 3.84 °C and 6.26 °C at ibuprofen/chitosan weight ratios 1:0.125 and 1:1 respectively suggesting formation of multiple complexes. The melting peak of ibuprofen shifted to 83.65 °C and 85.17 °C at ibuprofen/chitosan weight ratios 1:0.25 and 1:2 respectively but did not appear at other weight ratios. It was observed that the weight ratios without the ibuprofen melting peak exhibited broad and diffuse second peak with higher values indicating the formation of stable amorphous product (Figure 64). Similar complexation was reported by Oberoi *et al.* in the preparation of ibuprofen-nicotinamide suspensions by solvent evaporation method [84].

Table 44 DSC of ibuprofen-chitosan conjugates (solubilization), ibuprofen control, pure ibuprofen, chitosan and physical mixture of ibuprofen and chitosan. Each value represents mean ± SD (n = 4).

Formulation	Onset (°C)	End (°C)	Peak (°C)	Area (mJ)	Delta H (J/g)
Ibuprofen-reference	76.52±1.42	83.23±1.78	80.07±1.94	949.15±38.72	118.64±0.96
	193.66±7.73	243.03±9.57	237.51±9.93	309.29±11.21	2241.34±51.03
Chitosan-reference	60.44±1.02	155.57±6.2	115.44±4.32	2077.04±45.38	301.02±9.75
	299.84±7.95	339.81±10.85	318.39±10.68	-1938.38±42.56	-201.91±9.21
Ibuprofen-Chitosan physical mixture	75.45±1.30	85.47±1.88	81.34±1.54	581.56±17.56	67.62±1.12
	104.95±2.94	153.00±5.96	126.56±3.68	111.01±3.02	12.91±0.49
	250.30±9.82	267.84±10.11	262.48±10.35	59.29±1.14	6.89±0.23
IbNic-control (IbCh 1:0)	0.64±0.04	14.33±0.58	9.54±0.13	1663.60±32.78	186.92±7.57
	54.37±1.11	95.45±2.72	82.88±2.32	10631.82±105.77	1194.58±58.22
IbCh1Nic (IbCh 1:0.125)	0.83±0.04	6.90±0.25	3.84±0.15	404.29±20.36	134.76±5.36
	101.97±4.93	113.79±5.26	108.24±4.73	1190.10±33.56	396.70±8.22
IbCh2Nic (IbCh 1:0.25)	0.19±0.01	11.27±0.52	7.14±0.31	832.41±35.22	163.22±6.58
	51.84±0.95	91.33±4.01	83.65±4.32	5428.98±72.34	1064.51±42.33
	99.90±4.97	111.68±5.21	105.07±4.65	254.57±11.25	49.92±0.85
IbCh3Nic (IbCh 1:0.5)	0.44±0.02	11.03±0.51	7.41±0.21	1369.36±38.74	273.87±10.58
	101.18±4.89	127.10±5.87	116.75±5.74	8548.60±73.42	1709.72±37.28
IbCh4Nic (IbCh1:1)	1.53±0.05	10.51±0.48	6.26±0.20	563.89±22.64	281.95±8.15
	108.19±5.18	116.72±5.29	112.47±5.37	3258.61±67.85	1162.7±32.55
IbCh5Nic (IbCh 1:2)	0.28±0.01	10.25±0.43	6.66±0.18	946.50±43.17	182.10±6.39
	48.98±0.92	92.02±2.23	85.17±1.82	5861.76±72.36	1127.26±35.42
	101.94±4.72	109.59±5.16	105.57±5.06	216.32±7.23	41.60±0.95

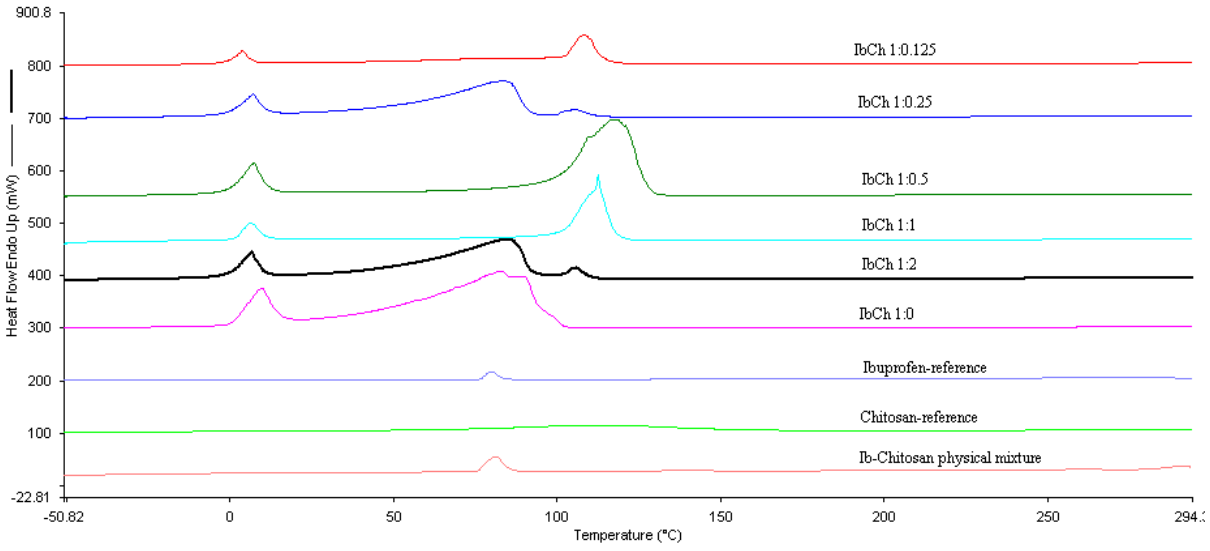

Figure 67 DSC thermograms of ibuprofen-chitosan conjugates (hydrotropy), ibuprofen control, pure ibuprofen, chitosan and physical mixture of ibuprofen and chitosan.

The DSC thermograms of ibuprofen-DEAE-Dextran-gellan complex, IbDW-control, pure ibuprofen, gellan, DEAE-Dextran and chitosan are shown in Figures 68 and 69; Tables 45 and 46. Pure ibuprofen showed a sharp melting peak at 80.37 °C due to the melting of the drug and the second peak at 237.51 °C due to its decomposition. Gellan and DEAE-Dextran powders exhibited broad melting peaks at 127.86 °C and 124.05 °C respectively. The melting peak of ibuprofen decreased in the

ternary conjugates to a minimum value of 77.06 °C with decreased intensity at DEAE-Dextran/Gellan weight ratio of 75:25 however, the peaks were still broad and diffuse suggesting the amorphous nature of the nanoconjugates. The second endothermic peaks observed in the complexes correspond to the step of inflection in the thermograms, confirming that the peak was due to the decomposition of the complex.

Table 45 DSC of ibuprofen incorporated into DEAE-Dextran-gellan conjugate in ratios, DG 0:100, DG 25:75, DG 50:50, DG 75:25 and DG 100:0; pure ibuprofen, gellan and DEAE-Dextran. Each value represents mean ± SD (n = 4).

Formulation	Onset (°C)	End (°C)	Peak (°C)	Area (mJ)	Delta H (J/g)
Ibuprofen-reference	76.52±1.42	83.23±1.78	80.07±1.94	949.15±38.72	118.64±0.96
	193.66±7.73	243.03±9.57	237.51±9.93	309.29±11.21	2241.34±51.03
Gellan-reference	77.70±1.55	186.32±8.76	127.86±7.43	1043.54±52.70	168.31±8.81
	246.56±12.37	270.88±12.86	264.02±12.75	-803.81±40.22	-129.64±6.5
DEAE-Dextran-reference	53.55±0.85	63.97±0.92	57.86±0.76	35.16±0.41	5.10±0.08
	87.43±1.22	158.87±5.34	124.05±4.16	960.30±40.48	139.17±5.64
	187.42±8.23	210.60±11.45	201.54±10.58	87.74±1.25	12.72±0.84
	245.83±12.74	281.53±13.66	268.50±11.78	488.852±21.22	70.84±0.92
IbDW-pH6	75.89±1.54	84.31±1.78	80.67±1.58	333.87±15.64	104.33±5.04
	184.30±8.59	224.45±10.36	219.59±10.32	602.20±27.79	188.18±8.37
DG 0:100	74.47±1.41	80.92±1.62	77.54±1.48	349.49±16.76	116.49±5.21
	184.16±8.26	219.04±10.04	204.63±9.78	289.15±12.97	96.38±4.02
DG 25:75	73.51±1.22	81.80±1.48	78.40±1.17	293.49±13.05	97.83±4.18
	244.98±11.21	252.38±10.97	246.90±11.04	133.84±5.26	44.61±0.54
DG 50:50	73.39±1.17	80.51±1.40	77.38±1.29	270.97±11.33	87.41±1.73
	240.91±10.87	255.61±11.81	248.64±11.32	39.52±0.54	12.74±0.27
DG 75:25	73.27±1.35	80.21±1.26	77.06±1.02	286.55±12.71	92.43±3.31
	240.15±11.58	250.12±11.42	244.27±10.80	148.00±5.07	47.74±0.62
DG 100:0	76.20±1.21	82.76±1.54	79.52±1.37	373.05±18.95	109.72±4.78
	177.36±7.07	229.66±10.86	221.93±11.31	711.26±32.45	209.19±10.52

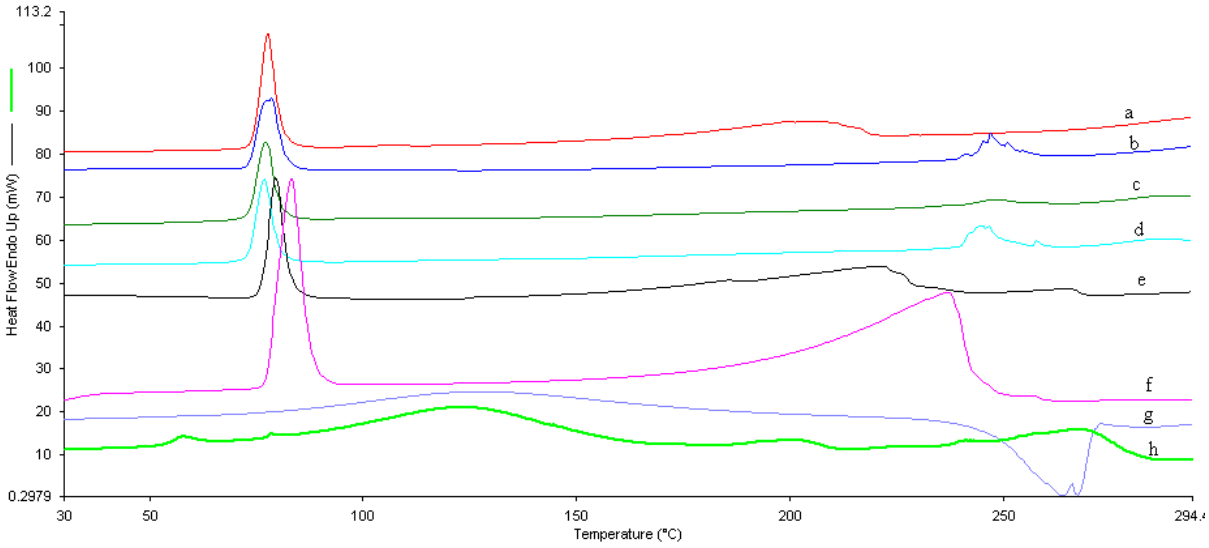

Figure 68 DSC thermograms of ibuprofen incorporated into DEAE-Dextran-gellan conjugate in ratios (a) DG 0:100, (b) DG 25:75, (c) DG 50:50, (d) DG 75:25, (e) DG 100:0, (f) pure ibuprofen-reference, (g) gellan-reference and (h) DEAE-Dextran-reference.

The ternary chitosan-ibuprofen-gellan nanoconjugates showed a decrease in the melting peak of ibuprofen ranging from 67.01 to 77.18 °C indicating the formation of amorphous nanoconjugates (Table 46 and Figure 68). Chitosan exhibited broad melting peak at 115.44 °C.

Table 46 DSC of ibuprofen incorporated into chitosan-gellan conjugate in ratios, CG 0:100, CG 25:75, CG 50:50, CG 75:25 and CG 100:0; pure ibuprofen, gellan and chitosan. Each value represents mean ± SD (n = 4).

Formulation	Onset (°C)	End (°C)	Peak (°C)	Area (mJ)	Delta H (J/g)
Ibuprofen-reference	76.52±1.42	83.23±1.78	80.07±1.94	949.15±38.72	118.64±0.96
	193.66±7.73	243.03±9.57	237.51±9.93	309.29±11.21	2241.34±51.03
Gellan-reference	77.70±1.55	186.32±8.76	127.86±7.43	1043.54±52.70	168.31±8.81
	246.56±12.37	270.88±12.86	264.02±12.75	-803.81±40.22	-129.64±6.5
Chitosan-reference	60.44±1.02	155.57±6.2	115.44±4.32	2077.04±45.38	301.02±9.75
	299.84±7.95	339.81±10.85	318.39±10.68	-1938.38±42.56	-201.91±9.21
IbDW-pH5	75.89±1.54	84.31±1.78	80.67±1.58	333.87±15.64	104.33±5.04
	184.30±8.59	224.45±10.36	219.59±10.32	602.20±27.79	188.18±8.37
CG 0:100	76.91±1.21	84.06±1.62	77.18±1.58	353.92±13.78	104.09±4.73
	184.16±8.26	219.04±10.04	204.63±9.78	289.15±12.97	96.38±4.02
CG 25:75	57.96±0.78	77.22±1.36	71.33±1.07	158.73±6.26	52.91±0.65
	193.22±6.62	220.19±11.03	197.88±8.26	66.28±1.04	22.09±0.21
CG 50:50	71.92±1.15	81.24±1.65	77.15±1.14	297.75±13.32	85.07±1.87
	167.83±6.03	202.65±10.84	192.73±6.54	42.71±0.72	12.20±0.14
CG 75:25	58.78±0.73	76.74±1.18	71.63±1.12	215.44±10.76	61.55±0.74
	163.49±5.92	277.93±12.36	206.37±10.96	81.36±1.32	23.24±0.28
CG 100:0	57.33±0.86	73.25±1.10	67.01±0.92	68.31±0.96	17.51±0.21
	167.95±6.34	260.09±12.25	221.99±11.23	451.40±16.13	115.74±5.62

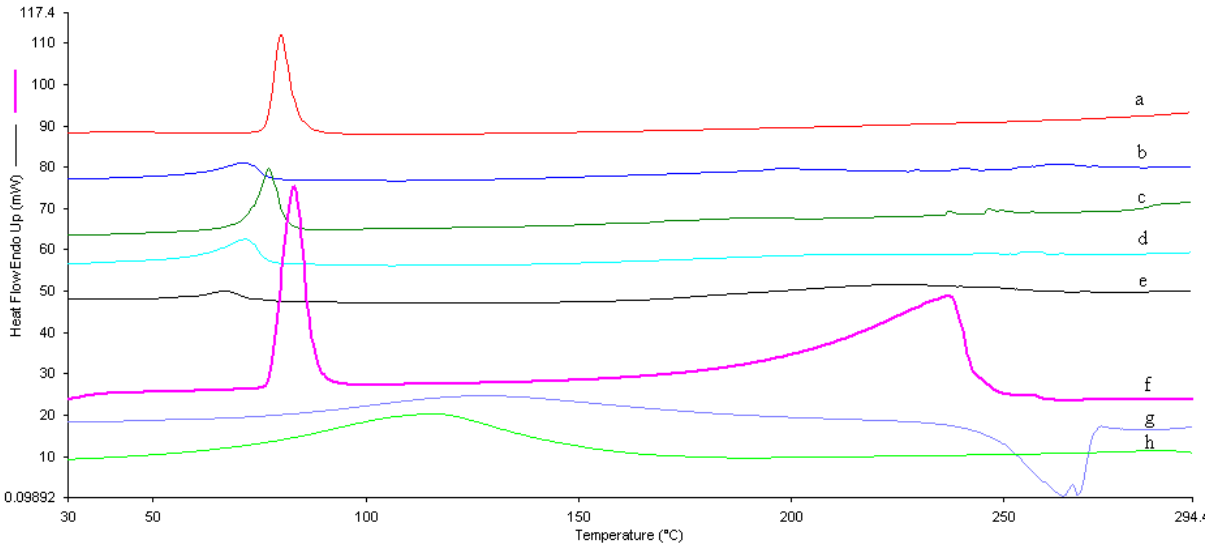

Figure 69 DSC thermograms of ibuprofen incorporated into chitosan-gellan conjugate in ratios (a) CG 0:100, (b) CG 25:75, (c) CG 50:50, (d) CG 75:25, (e) CG 100:0, (f) pure ibuprofen-reference, (g) gellan-reference and (h) chitosan-reference.

2.3.3.10.2. Thermogravimetric analysis (TGA)

Thermogravimetric analysis (TGA) is a useful thermal analysis technique which measures the changes in physical and chemical properties of material as a function of increasing temperature or

time. TGA measures the mass of a sample as a function of sample temperature or time. It is used to evaluate the mass loss or gain of polymers due to decomposition, oxidation or loss of moisture. The thermal stability of the pure reference compounds and nanoconjugates can be interpreted from the TGA thermograms.

The TGA thermograms of pure ibuprofen and ibuprofen control (processed ibuprofen without polymer) showed one step of weight loss of 99.5% and 99.3% at 240.76 °C and 104.52 °C respectively in Figure 70. DEAE-Dextran showed two steps of weight loss of 6.94% and 67.61% at 24.94 °C and 272.15 °C respectively while the ibuprofen-DEAE-Dextran physical mixture showed three steps of weight loss of 4.13%, 47.92% and 36.17% at 126.01 °C, 218.05 °C and 253.12 °C respectively. The pure ibuprofen exhibited almost 100% degradation. DEAE-Dextran exhibited 88.2% degradation, a residue of 11.88% remained after degradation. The IbDMelt conjugates showed one step of weight loss of 97.40 to 99.77% at temperatures below 150 °C in the range of 97.17 to 140.34 °C which has been attributed to weight loss due to free or loosely bound water in the conjugate structure [86] in Table 47. The step of inflection decreased with increasing concentration of DEAE-Dextran up to 0.8%, followed by a final increase. The absence of the decomposition step in the TGA curve confirmed the absent decomposition peaks in the DSC thermograms of the nanoconjugates.

Table 47 TGA of ibuprofen-DEAE-Dextran conjugates (melt solubilization) ibuprofen control, ibuprofen-reference, DEAE-Dextran-reference and ibuprofen-DEAE-Dextran physical mixture. Each value represents mean ± SD (n = 4).

Formulation	Onset (°C)	End (°C)	Step of inflection (°C)	Delta Y (%)
Ibuprofen-reference	207.81±11.23	247.08±11.87	240.76±12.32	99.50±1.95
DEAE-Dextran-reference	47.16±0.47	106.74±4.32	77.47±1.47	6.94±0.12
	261.20±11.43	301.16±15.72	272.15±12.62	67.61±0.98
Ibuprofen-DEAE-Dextran physical mixture	115.93±5.32	129.68±5.68	126.01±.47	4.13±0.02
	192.74±8.65	223.95±12.04	218.05±11.95	47.92±0.52
	248.94±12.12	270.55±12.69	253.12±12.48	36.17±0.34
IbMelt-control (IbD 1:0)	71.42±0.57	106.88±1.95	104.52±1.87	99.32±1.21
IbD1Melt (IbD 1:0.5)	93.08±2.68	138.59±5.07	135.77±4.98	96.35±2.78
IbD2Melt (IbD 1:1)	82.57±2.53	124.39±4.36	121.14±4.21	98.91±2.54
IbD3Melt (IbD 1:2)	76.53±0.89	114.96±4.51	112.34±4.23	97.40±2.10
IbD4Melt (IbD 1:4)	66.01±0.64	104.38±2.43	97.17±2.17	97.44±2.23
IbD5Melt (IbD 1:8)	96.68±1.82	142.55±4.88	140.34±4.58	99.72±1.18

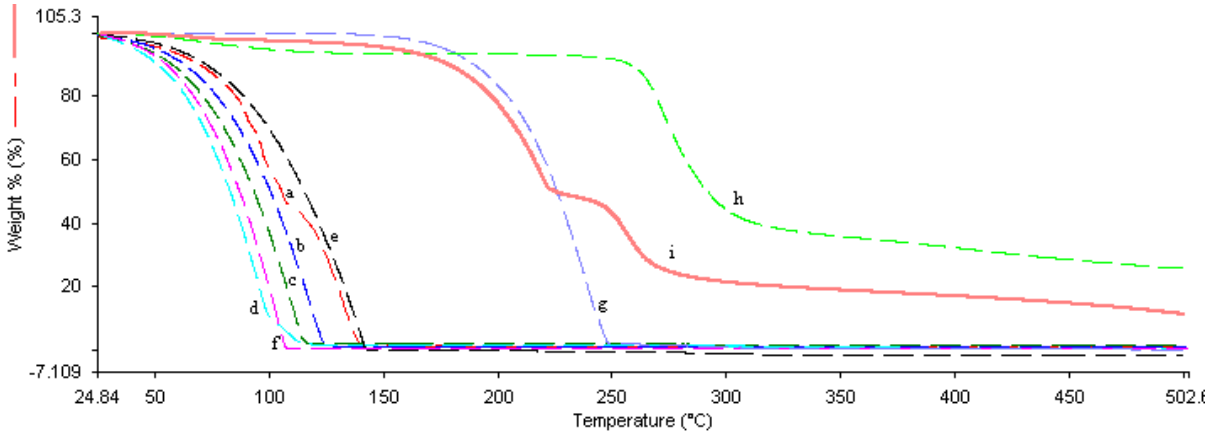

Figure 70 TGA thermogram of ibuprofen-DEAE-Dextran conjugates (melt solubilization) (a) IbD1Melt, (b) IbD2Melt, (c) IbD3Melt, (d) IbD4Melt, (e) IbD5Melt, (f) IbMelt-control, (g) ibuprofen-reference, (h) DEAE-Dextran-reference and (i) ibuprofen-DEAE-Dextran physical mixture.

Nanoconjugates obtained from the alkaline solubilization technique (IbDNaOH) showed one step of weight loss in the range of 97.78 to 99.16% at temperatures below 150 °C which indicated weight loss due to free water in the conjugates in Table 48 and Figure 71 [87]. The step of inflection initially increased, followed by decrease with increasing DEAE-Dextran concentration. The rate of moisture loss was faster in nanoconjugates than the physical mixture.

Table 48 TGA of ibuprofen-DEAE-Dextran conjugates (solubilization) ibuprofen control, ibuprofen-reference, DEAE-Dextran-reference and ibuprofen-DEAE-Dextran physical mixture. Each value represents mean ± SD (n = 4).

Formulation	Onset (°C)	End (°C)	Step of inflection (°C)	Delta Y (%)
Ibuprofen-reference	207.81±11.23	247.08±11.87	240.76±12.32	99.50±1.95
DEAE-Dextran-reference	47.16±0.47	106.74±4.32	77.47±1.47	6.94±0.12
	261.20±11.43	301.16±15.72	272.15±12.62	67.61±0.98
Ibuprofen-DEAE-Dextran physical mixture	115.93±5.32	129.68±5.68	126.01±.47	4.13±0.02
	192.74±8.65	223.95±12.04	218.05±11.95	47.92±0.52
	248.94±12.12	270.55±12.69	253.12±12.48	36.17±0.34
IbNaOH-control (IbD 1:0)	71.42±0.57	106.88±1.95	104.52±1.87	99.32±1.21
IbD1NaOH (IbD 1:0.5)	72.96±0.12	110.94±3.16	106.69±3.34	99.16±0.46
IbD2NaOH (IbD 1:1)	85.01±1.42	134.02±5.04	130.45±4.65	98.40±2.82
IbD3NaOH (IbD 1:2)	74.43±1.08	111.17±3.48	108.50±3.21	98.73±2.64
IbD4NaOH (IbD 1:4)	69.91±0.98	105.33±2.82	102.08±2.64	97.78±2.16
IbD5NaOH (IbD 1:8)	72.80±1.02	109.08±2.66	106.07±2.48	98.22±2.38

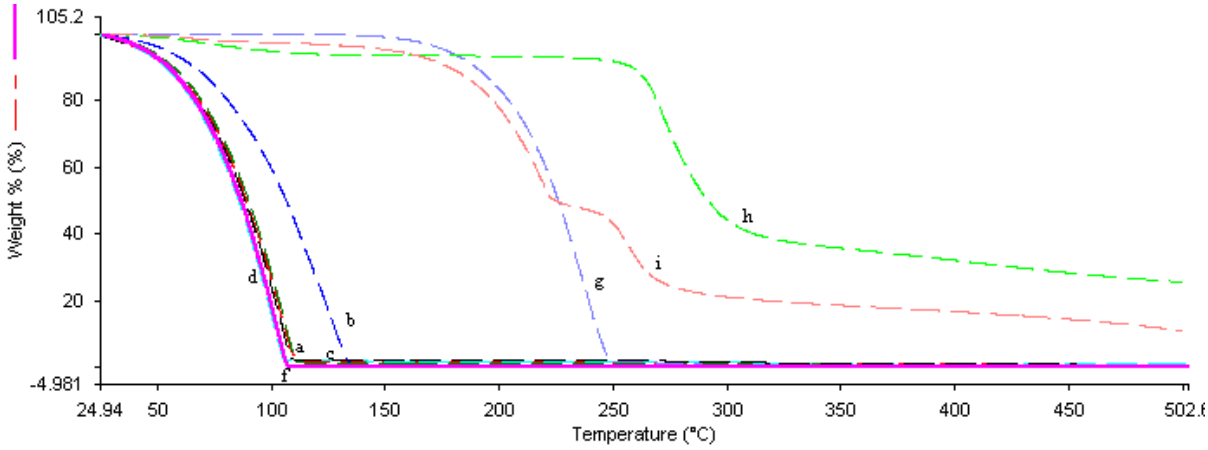

Figure 71 TGA thermograms of ibuprofen-DEAE-Dextran conjugates (solubilization) (a) IbD1NaOH, (b) IbD2NaOH, (c) IbD3NaOH, (d) IbD4NaOH, (e) IbD5NaOH, (f) IbNaOH-control, (g) ibuprofen-reference, (h) DEAE-Dextran-reference and (i) ibuprofen-DEAE-Dextran physical mixture.

TGA thermograms of nanoconjugates obtained from surfactant solubilization technique are presented in Table 49 and Figure 72. The IbDTw80 conjugates showed two steps of weight loss at a range of 104.34 to 130.96 °C and 379.29 to 405.62 °C which was close to 429.7 °C, the reported weight loss temperature due to decomposition of Tween 80 [88]. The IbDTw80 conjugates showed two steps of weight loss at a range of 104.34 to 130.96 °C and 379.29 to 405.62 °C (Table 49). The first weight loss was due to the loss of free water in the conjugates while the second weight loss was due to the decomposition of the conjugates [87]. The higher temperature of decomposition of the IbDTw80 conjugates compared to ibuprofen was due to the effect of Tween 80 on the conjugates.

Table 49 TGA of ibuprofen-DEAE-Dextran conjugates (solubilization) ibuprofen control, ibuprofen-reference, DEAE-Dextran-reference and ibuprofen-DEAE-Dextran physical mixture. Each value represents mean ± SD (n = 4).

Formulation	Onset (°C)	End (°C)	Step of inflection (°C)	Delta Y (%)
Ibuprofen-reference	207.81±11.23	247.08±11.87	240.76±12.32	99.50±1.95
DEAE-Dextran-reference	47.16±0.47	106.74±4.32	77.47±1.47	6.94±0.12
	261.20±11.43	301.16±15.72	272.15±12.62	67.61±0.98
Ibuprofen-DEAE-Dextran physical mixture	115.93±5.32	129.68±5.68	126.01±.47	4.13±0.02
	192.74±8.65	223.95±12.04	218.05±11.95	47.92±0.52
	248.94±12.12	270.55±12.69	253.12±12.48	36.17±0.34
IbTw80-control (IbD 1:0)	71.42±0.57	106.88±1.95	104.52±1.87	99.32±1.21
IbD1Tw80	86.58±1.55	131.43±4.88	126.01±3.78	91.30±1.94
(IbD 1:0.5)	335.07±14.36	412.37±20.14	379.29±16.64	8.74±0.03
IbD2Tw80	86.95±1.46	130.25±5.34	125.56±4.68	89.23±1.32
(IbD 1:1)	378.00±15.48	420.20±22.42	405.62±21.06	9.31±0.04
IbD3Tw80	90.44±1.94	135.16±5.16	130.96±4.82	90.25±1.87
(IbD 1:2)	380.89±16.00	419.07±21.04	403.18±20.64	8.36±0.04
IbD4Tw80	72.31±0.81	107.79±4.21	104.34±4.23	88.44±1.64
(IbD 1:4)	372.36±17.61	415.63±20.18	403.77±21.21	10.21±0.05
IbD5Tw80	76.39±0.74	114.47±4.98	111.45±5.21	88.65±1.58
(IbD 1:8)	376.17±16.89	416.36±22.54	402.06±21.08	9.80±0.04

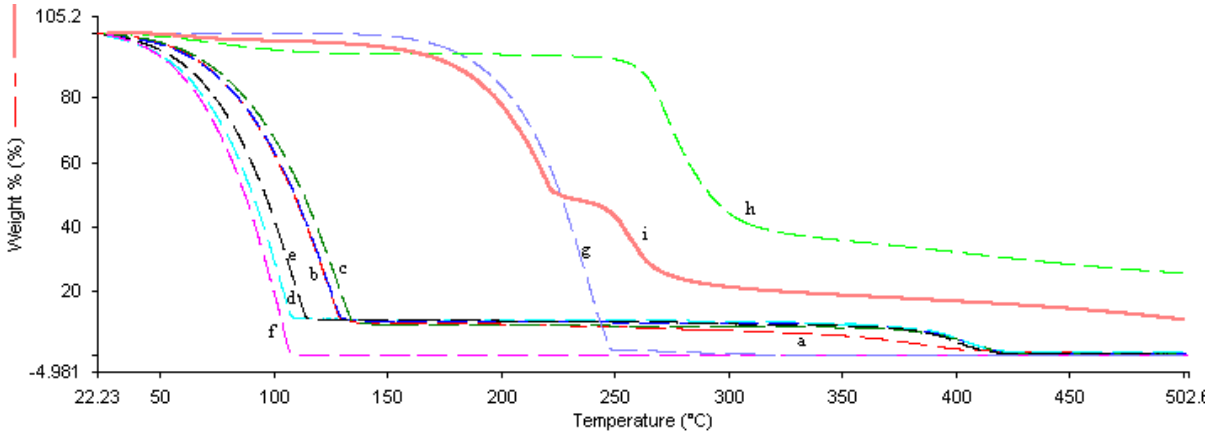

Figure 72 TGA thermograms of ibuprofen-DEAE-Dextran conjugates (solubilization) (a) IbD1Tw80, (b) IbD2Tw80, (c) IbD3Tw80, (d) IbD4Tw80, (e) IbD5Tw80, (f) IbTw80-control, (g) ibuprofen-reference, (h) DEAE-Dextran-reference and (i) ibuprofen-DEAE-Dextran physical mixture.

The TGA thermograms of nanoconjugates obtained from the hydrotropic complexation technique are presented in Table 50 and Figure 73. The IbDNic conjugates showed one step of weight loss at temperatures below 150 °C which indicated weight loss due to free water in the conjugates in Table 50 and Figure 73 [87]. The step of inflection decreased with increasing concentration of DEAE-Dextran. The decomposition step was absent in three of the four techniques (except tween 80 nanoconjugates) suggesting isothermal stability of the nanoconjugates.

Table 50 TGA of ibuprofen-DEAE-Dextran conjugates (hydrotropy) ibuprofen control, ibuprofen-reference, DEAE-Dextran-reference and ibuprofen-DEAE-Dextran physical mixture. Each value represents mean ± SD (n = 4).

Formulation	Onset (°C)	End (°C)	Step of inflection (°C)	Delta Y (%)
Ibuprofen-reference	207.81±11.23	247.08±11.87	240.76±12.32	99.50±1.95
DEAE-Dextran-reference	47.16±0.47	106.74±4.32	77.47±1.47	6.94±0.12
	261.20±11.43	301.16±15.72	272.15±12.62	67.61±0.98
Ibuprofen-DEAE-Dextran physical mixture	115.93±5.32	129.68±5.68	126.01±5.47	4.13±0.02
	192.74±8.65	223.95±12.04	218.05±11.95	47.92±0.52
	248.94±12.12	270.55±12.69	253.12±12.48	36.17±0.34
IbNic-control (IbD 1:0)	71.42±0.57	106.88±1.95	104.52±1.87	99.32±1.21
IbD1Nic (IbD 1:0.5)	90.14±2.04	134.40±4.16	129.34±4.64	99.75±2.68
IbD2Nic (IbD 1:1)	75.15±0.86	114.82±4.34	110.43±4.26	99.86±2.42
IbD3Nic (IbD 1:2)	80.94±0.90	123.78±5.42	118.57±5.32	100.88±2.74
IbD4Nic (IbD 1:4)	80.46±0.72	120.45±5.36	117.26±5.06	98.30±2.48
IbD5Nic (IbD 1:8)	81.60±0.84	124.16±5.32	120.10±5.18	97.34±2.16

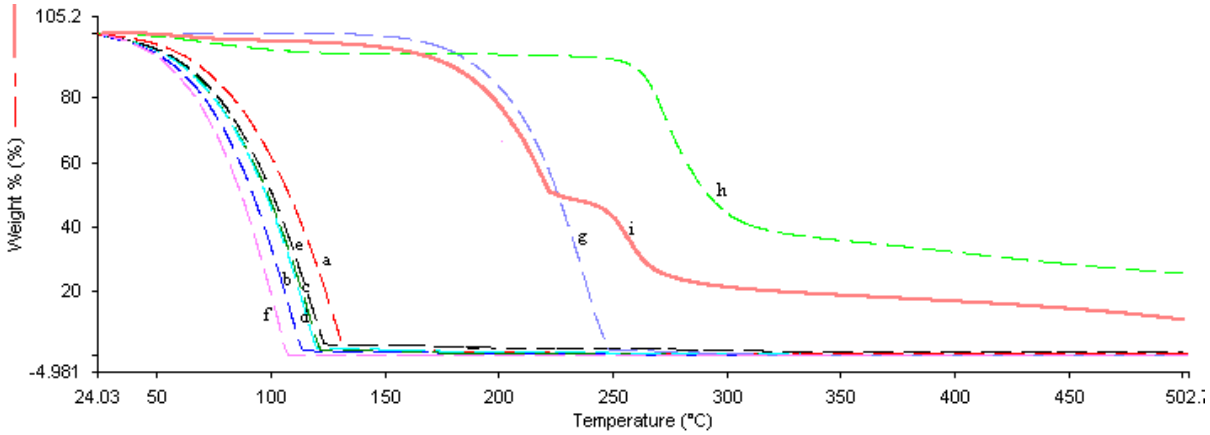

Figure 73 TGA thermograms of ibuprofen-DEAE-Dextran conjugates (hydrotropy) (a) IbD1Nic, (b) IbD2Nic, (c) IbD3Nic, (d) IbD4Nic, (e) IbD5Nic, (f) IbNic-control, (g) ibuprofen-reference, (h) DEAE-Dextran-reference and (i) ibuprofen-DEAE-Dextran physical mixture.

The TGA thermograms of ibuprofen/chitosan nanoconjugates are similar to the ibuprofen/DEAE-Dextran. The thermograms of pure chitosan showed two steps of weight loss of 9.65% and 47.65% (total weight loss of 57.00 %) at 57.48 °C and 311.76 °C in Table 50. The 43.00% residue remaining could be assigned to the part of chitosan that did not undergo decomposition. The first weight loss was due to the loss of free water in the conjugates while the second weight loss was due to the decomposition of the conjugates [87]. The ibuprofen-chitosan physical mixture showed three steps of weight loss at 27.81 °C, 233.76 °C and 311.89 °C in Figure 74. The first weight loss was due to the loss of free water in the conjugates while the second and third weight loss was due to the decomposition of the ibuprofen and chitosan components in the physical mixture [87]. The nanoconjugates obtained from melt solubilization technique (IbChMelt) showed one step of weight loss below 150 °C which indicated weight loss due to free water in the conjugates.

Table 51 TGA of ibuprofen-chitosan conjugates (melt solubilization) ibuprofen control, ibuprofen-reference, chitosan-reference and ibuprofen-chitosan physical mixture. Each value represents mean ± SD (n = 4).

Formulation	Onset (°C)	End (°C)	Step of inflection (°C)	Delta Y (%)
Ibuprofen-reference	207.81±11.23	247.08±11.87	240.76±12.32	99.50±1.95
Chitosan-reference	36.14±0.37	92.94±0.85	57.48±0.45	9.65±0.08
	291.90±14.28	338.75±16.72	311.76±15.24	47.65±0.32
Ibuprofen-Chitosan physical mixture	27.81±0.22	63.05±0.58	27.81±0.22	3.26±0.01
	203.02±10.55	235.31±11.23	233.76±11.45	61.41±0.44
	293.87±15.21	342.21±16.34	311.89±15.22	20.35±0.18
IbDW-pH6 (IbCh 1:0)	71.42±0.57	106.88±1.95	104.52±1.87	99.32±1.21
IbCh1Melt (IbCh 1:0.125)	76.36±1.10	116.36±3.21	111.87±2.05	96.76±1.58
IbCh2Melt (IbCh 1:0.25)	82.58±1.36	126.70±3.45	121.25±3.27	98.12±1.89
IbCh3Melt (IbCh 1:0.5)	75.02±1.06	114.54±2.32	110.03±2.21	98.00±1.88
IbCh4Melt (IbCh 1:1)	75.90±1.12	114.94±2.26	110.90±2.32	95.56±1.74
IbCh5Melt (IbCh 1:2)	90.43±1.86	136.67±4.73	131.13±4.56	97.29±1.65

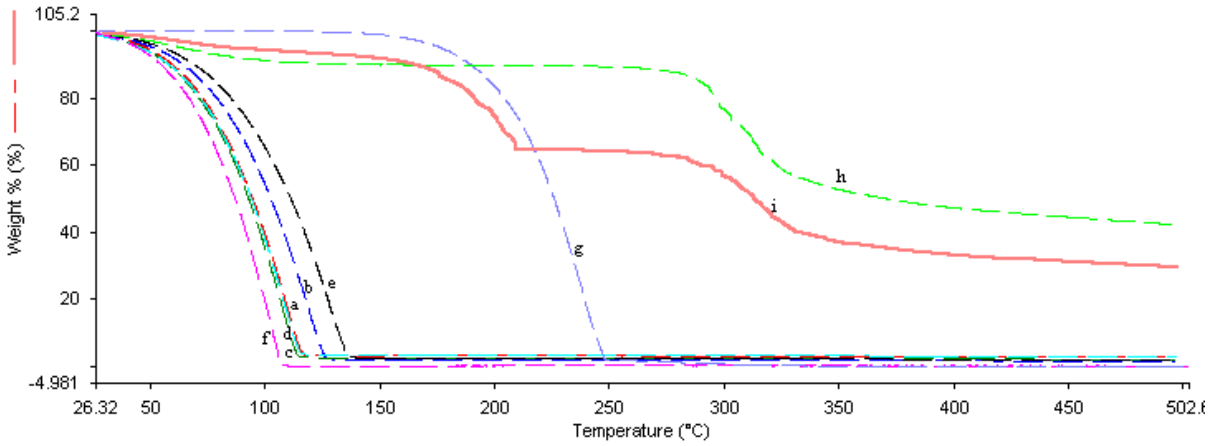

Figure 74 TGA thermograms of ibuprofen-chitosan conjugates (melt solubilization) (a) IbCh1Melt, (b) IbCh2Melt, (c) IbCh3Melt, (d) IbCh4Melt, (e) IbCh5Melt, (f) IbMelt-control, (g) ibuprofen-reference, (h) chitosan-reference and (i) ibuprofen-chitosan physical mixture.

The nanoconjugates obtained from alkaline solubilization technique (IbChNaOH) showed one step of weight loss in the range of 114.07 to 126.91 °C (below 150 °C) which indicated weight loss due to free water in the conjugates in Figure 75 [87].

Table 52 TGA of ibuprofen-chitosan conjugates (solubilization) ibuprofen control, ibuprofen-reference, chitosan-reference and ibuprofen-chitosan physical mixture. Each value represents mean ± SD (n = 4).

Formulation	Onset (°C)	End (°C)	Step of inflection (°C)	Delta Y (%)
Ibuprofen-reference	207.81±11.23	247.08±11.87	240.76±12.32	99.50±1.95
Chitosan-reference	36.14±0.37	92.94±0.85	57.48±0.45	9.65±0.08
	291.90±14.28	338.75±16.72	311.76±15.24	47.65±0.32
Ibuprofen-Chitosan physical mixture	27.81±0.22	63.05±0.58	27.81±0.22	3.26±0.01
	203.02±10.55	235.31±11.23	233.76±11.45	61.41±0.44
	293.87±15.21	342.21±16.34	311.89±15.22	20.35±0.18
IbNaOH-control (IbCh 1:0)	71.42±0.57	106.88±1.95	104.52±1.87	99.32±1.21
IbCh1NaOH (IbCh 1:0.125)	77.45±0.76	119.65±3.54	114.56±2.98	98.08±1.88
IbCh2NaOH (IbCh 1:0.25)	76.77±0.89	119.00±3.24	114.07±3.26	98.57±1.98
IbCh3NaOH (IbCh 1:0.5)	80.63±1.14	123.00±3.08	119.17±3.02	97.54±1.95
IbCh4NaOH (IbCh 1:1)	78.87±0.89	119.89±2.98	116.00±2.89	97.93±1.84
IbCh5NaOH (IbCh 1:2)	87.37±1.06	132.01±3.25	126.91±3.14	97.84±1.92

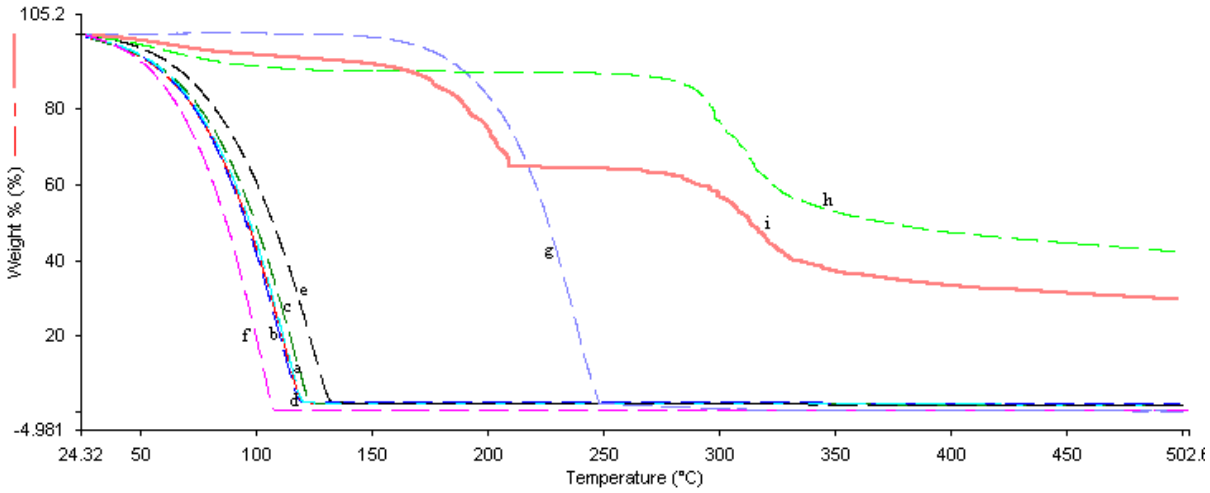

Figure 75 TGA thermograms of ibuprofen-chitosan conjugates (melt solubilization) (a) IbCh1NaOH, (b) IbCh2NaOH, (c) IbCh3NaOH, (d) IbCh4NaOH, (e) IbCh5NaOH, (f) IbNaOH-control, (g) ibuprofen-reference, (h) chitosan-reference and (i) ibuprofen-chitosan physical mixture.

The IbChTw80 conjugates showed two steps of weight loss at the range of 108.92 to 129.53 °C and 378.81 to 385.25 °C in Table 53. The first weight loss (range of 90.15 to 90.69%) was due to the loss of free water in the conjugates while the second weight loss (range of 6.20 to 7.81%) was due to the decomposition of the conjugates in Figure 76. The higher temperature of decomposition of the IbChTw80 conjugates compared to ibuprofen showed that the conjugates had a better isothermal stability than the pure ibuprofen.

Table 53 TGA of ibuprofen-chitosan conjugates (solubilization) ibuprofen control, ibuprofen-reference, chitosan-reference and ibuprofen-chitosan physical mixture. Each value represents mean ± SD (n = 4).

Formulation	Onset (°C)	End (°C)	Step of inflection (°C)	Delta Y (%)
Ibuprofen-reference	207.81±11.23	247.08±11.87	240.76±12.32	99.50±1.95
Chitosan-reference	36.14±0.37	92.94±0.85	57.48±0.45	9.65±0.08
	291.90±14.28	338.75±16.72	311.76±15.24	47.65±0.32
Ibuprofen-Chitosan physical mixture	27.81±0.22	63.05±0.58	27.81±0.22	3.26±0.01
	203.02±10.55	235.31±11.23	233.76±11.45	61.41±0.44
	293.87±15.21	342.21±16.34	311.89±15.22	20.35±0.18
IbTw80-control (IbCh 1:0)	71.42±0.57	106.88±1.95	104.52±1.87	99.32±1.21
IbCh1Tw80	73.63±0.65	113.93±3.06	108.92±2.89	90.19±1.72
(IbCh 1:0.125)	351.03±14.32	404.40±18.32	378.81±18.64	6.67±0.05
IbCh2Tw80	87.35±0.87	136.05±3.26	129.53±3.45	90.64±1.72
(IbCh 1:0.25)	369.44±16.54	398.49±18.02	385.25±17.22	7.55±0.05
IbCh3Tw80	77.05±0.68	120.01±3.24	113.28±2.98	90.32±1.72
(IbCh 1:0.5)	361.06±17.04	399.38±16.58	384.69±16.54	7.81±0.05
IbCh4Tw80	76.04±0.70	116.75±2.89	109.73±3.12	90.15±1.65
(IbCh 1:1)	340.46±16.54	397.47±17.68	378.88±15.45	7.64±0.05
IbCh5Tw80	77.60±0.72	118.05±3.08	112.83±2.54	90.69±1.74
(IbCh 1:2)	357.90±17.84	391.47±17.45	379.49±16.88	6.20±0.06

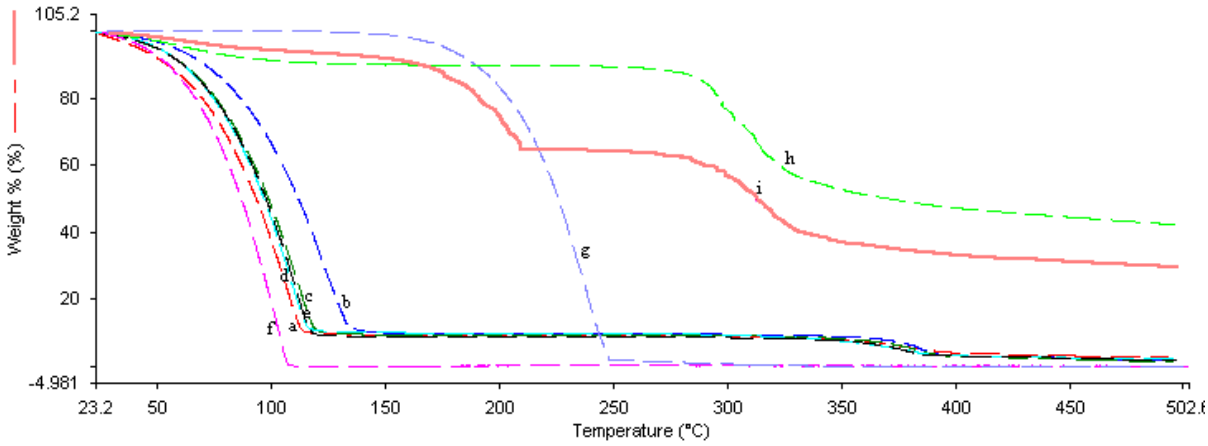

Figure 76 TGA thermogram of ibuprofen-chitosan conjugates (melt solubilization) (a) IbCh1Tw80, (b) IbCh2Tw80, (c) IbCh3Tw80, (d) IbCh4Tw80, (e) IbCh5Tw80, (f) IbTw80-control, (g) ibuprofen-reference, (h) chitosan-reference and (i) ibuprofen-chitosan physical mixture.

The hydrotropic nanoconjugates (IbChNic) showed one step of weight loss in the range of 105.81 to 122.85 °C (below 150 °C) which indicated weight loss due to free water in the conjugates in Table 54 and Figure 76.

Table 54 TGA of ibuprofen-chitosan conjugates (hydrotropy) ibuprofen control, ibuprofen-reference, chitosan-reference and ibuprofen-chitosan physical mixture. Each value represents mean ± SD (n = 4).

Formulation	Onset (°C)	End (°C)	Step of inflection (°C)	Delta Y (%)
Ibuprofen-reference	207.81±11.23	247.08±11.87	240.76±12.32	99.50±1.95
Chitosan-reference	36.14±0.37	92.94±0.85	57.48±0.45	9.65±0.08
	291.90±14.28	338.75±16.72	311.76±15.24	47.65±0.32
Ibuprofen-Chitosan physical mixture	27.81±0.22	63.05±0.58	27.81±0.22	3.26±0.01
	203.02±10.55	235.31±11.23	233.76±11.45	61.41±0.44
	293.87±15.21	342.21±16.34	311.89±15.22	20.35±0.18
IbNic (IbCh 1:0)	71.42±0.57	106.88±1.95	104.52±1.87	99.32±1.21
IbCh1Nic (IbCh 1:0.125)	75.80±1.17	116.45±2.76	111.32±2.85	96.50±1.72
IbCh2Nic (IbCh 1:0.25)	81.77±1.28	126.54±3.18	120.35±3.22	98.76±1.99
IbCh3Nic (IbCh 1:0.5)	83.08±1.36	128.76±3.10	122.85±3.15	97.60±1.86
IbCh4Nic (IbCh1:1)	80.31±1.25	123.97±3.02	118.37±2.98	97.21±1.73
IbCh5Nic (IbCh 1:2)	71.00±0.62	111.55±2.32	105.89±1.93	98.16±1.61

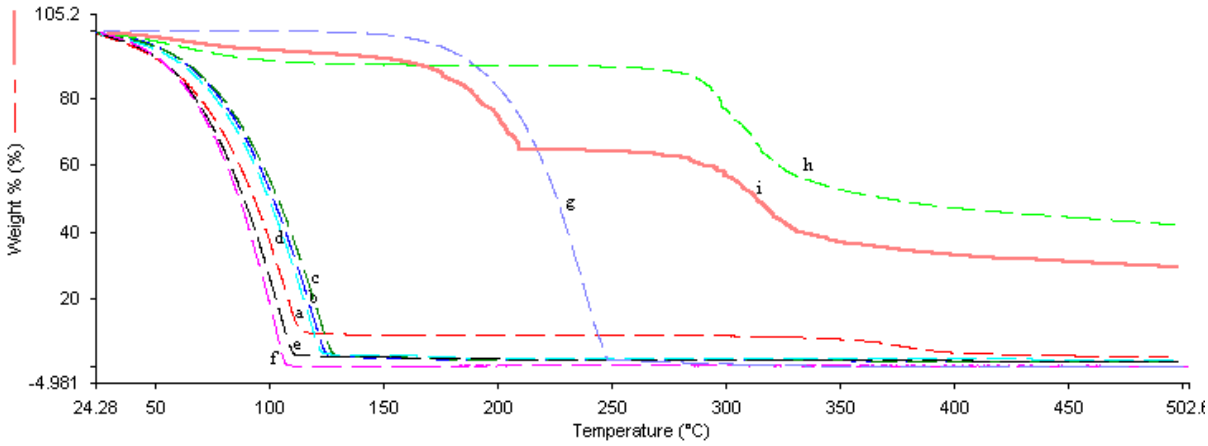

Figure 77 TGA thermograms of ibuprofen-chitosan conjugates (hydrotropy) (a) IbCh1Nic, (b) IbCh2Nic, (c) IbCh3Nic, (d) IbCh4Nic, (e) IbCh5Nic, (f) IbNic-control, (g) ibuprofen-reference, (h) chitosan-reference and (i) ibuprofen-chitosan physical mixture.

The TGA thermograms of ibuprofen-DEAE-Dextran-gellan complex, IbDW-control, pure ibuprofen, gellan, DEAE-Dextran and chitosan are shown in Figures 78 and 79; Tables 55 and 56. Ibuprofen and gellan powders showed one step of weight loss of 99.5% and 67.4%, at 240.76 °C and 264.91°C respectively, predominantly caused by the thermal decomposition of the molecular structure. DEAE-Dextran showed two steps of weight loss of 6.94% and 67.61% at 24.94 °C and 272.15 °C respectively. However, DG 25:75, DG 50:50 and DG 75:25 showed two steps of inflection or weight loss after 150 °C predominantly caused by the thermal decomposition of the molecular structure. DG 0:100 and DG 100:0 with gellan-ibuprofen and DEAE-Dextran-ibuprofen complex respectively showed one step weight loss of 99.8% and 99.7% at 206.01 °C and 205.05 °C respectively. It was obvious that the nanoconjugates lost moisture faster the the reference ibuprofen and the physical mixture however the ternary nanoconjugates retained moisture than the corresponding binary nanoconjugates.

Table 55 TGA of ibuprofen incorporated into DEAE-Dextran-gellan conjugate in ratios, DG 0:100, DG 25:75, DG 50:50, DG 75:25 and DG 100:0; pure ibuprofen, gellan and DEAE-Dextran. Each value represents mean ± SD (n = 4).

Formulation	Onset (°C)	End (°C)	Step of inflection (°C)	Delta Y (%)
Ibuprofen-reference	207.81±11.23	247.08±11.87	240.76±12.32	99.50±1.95
DEAE-Dextran-reference	47.16±0.47	106.74±4.32	77.47±1.47	6.94±0.12
	261.20±11.43	301.16±15.72	272.15±12.62	67.61±0.98
Gellan-reference	43.99±0.65	131.17±4.72	90.39±3.15	7.85±0.08
	257.79±12.21	282.29±12.74	264.91±12.10	59.67±0.93
IbDW-pH6	186.84±7.24	218.10±11.42	214.74±11.25	99.87±2.13
DG0:100	180.43±8.03	210.96±11.67	206.01±11.22	99.80±2.01
DG25:75	181.23±8.15	215.41±10.55	206.72±10.39	97.11±1.78
DG50:50	173.32±8.23	205.13±10.21	199.87±9.69	77.93±1.12
	241.29±11.65	277.11±12.24	250.51±11.40	18.49±0.15
DG75:25	167.06±7.30	201.80±9.87	197.68±8.32	79.19±1.06
	238.16±11.14	283.19±12.98	249.20±11.17	17.03±0.12
DG100:0	179.80±8.45	207.68±10.66	205.05±10.24	99.70±2.03

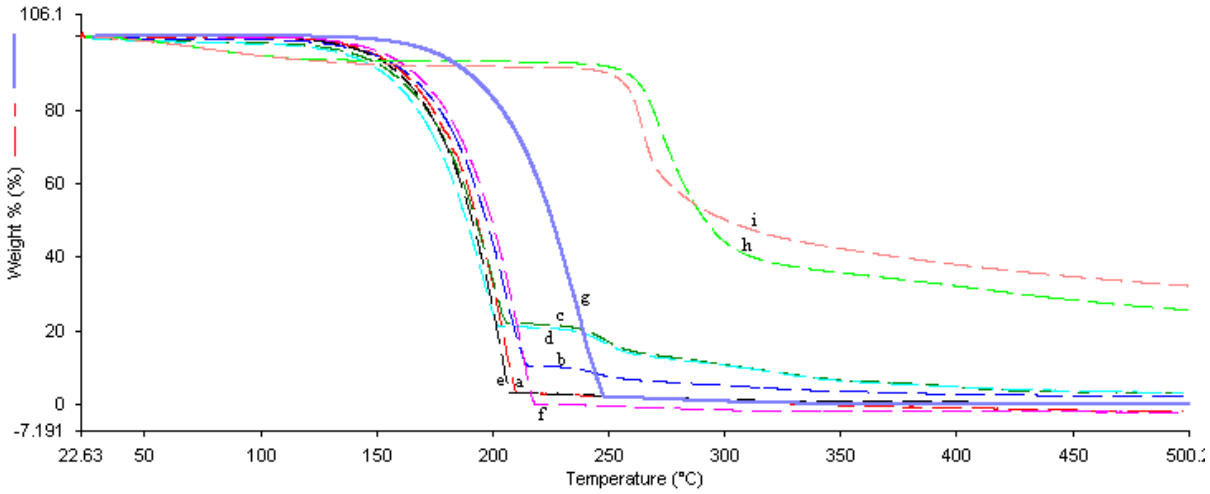

Figure 78 TGA thermograms of ibuprofen incorporated into DEAE-Dextran-gellan conjugate in ratios,(a) DG 0:100, (b) DG 25:75,(c) DG 50:50, (d) DG 75:25, (e) DG 100:0, (f) IbDW-pH6 control, (g) pure ibuprofen-reference, (h) DEAE-Dextran-reference and (i) gellan-reference.

The TGA thermograms of Chitosan-ibuprofen-gellan ternary nanoconjugates are presented in Table 56 and Figure 79. Pure chitosan reference, showed two steps of weight loss. The first step of weight loss of 9.65% at 57.48 °C may be due to loss of free water in the polymer. The second weight loss of 47.65% observed at 311.76 °C may be attributed to the decomposition of the polymer. CG 0:100, CG25:75, CG 50:50 and CG 75:25 showed one step of weight loss after 150 °C, due to the decomposition of the molecular structure of the complexes in Figure 79. CG 100:0 showed two steps of weight loss of 86.89% and 9.60% at 201.33 °C and 456.51 °C respectively, due to the decomposition of the molecular structure. The chitosan-ibuprofen-gellan nanoconjugates lost

moisture faster than the pure ibuprofen and the physical mixture however they retained moisture than the corresponding binary nanoconjugates.

Table 56 TGA of ibuprofen incorporated into chitosan-gellan conjugate in ratios, CG 0:100, CG 25:75, CG 50:50, CG 75:25 and CG 100:0; pure ibuprofen, gellan and chitosan. Each value represents mean ± SD (n = 4).

Formulation	Onset (°C)	End (°C)	Step of inflection (°C)	Delta Y (%)
Ibuprofen-reference	207.81±11.23	247.08±11.87	240.76±12.32	99.50±1.95
Chitosan-reference	36.14±0.37	92.94±0.85	57.48±0.45	9.65±0.08
	291.90±14.28	338.75±16.72	311.76±15.24	47.65±0.32
Gellan-reference	43.99±0.65	131.17±4.72	90.39±3.15	7.85±0.08
	257.79±12.21	282.29±12.74	264.91±12.10	59.67±0.93
IbDW-pH5	186.84±7.24	218.10±11.42	214.74±11.25	99.87±2.13
CG 0:100	177.59±6.87	210.62±10.94	205.30±10.77	99.36±1.84
CG 25:75	159.65±5.86	239.46±11.02	197.16±10.48	90.53±1.73
CG 50:50	170.87±6.62	212.06±10.71	200.98±10.43	98.59±1.85
CG 75:25	165.00±6.01	243.87±11.32	203.05±10.76	88.87±1.03
CG 100:0	170.88±6.44	215.94±10.52	201.33±10.73	86.89±1.27
	436.82±18.32	468.94±18.45	456.51±18.21	9.60±0.05

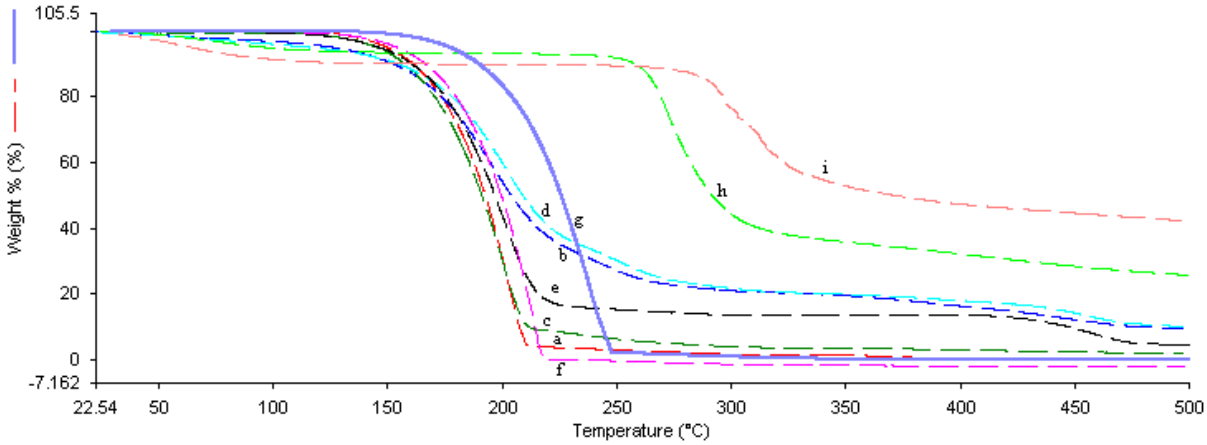

Figure 79 TGA thermograms of ibuprofen incorporated into chitosan-gellan conjugate in ratios, (a) CG 0:100, (b) CG 25:75, (c) CG 50:50, (d) CG 75:25, (e) CG 100:0, (f) IbDW-pH6 control, (g) pure ibuprofen-reference, (h) chitosan-reference and (i) gellan-reference.

2.3.4. Drug release studies

The *in vitro* release profiles of Ibuprofen-DEAE-Dextran conjugates and ibuprofen control in PBS pH 7.4 at 37 °C are shown in Figure 80 toFigure 83. The release of Ibuprofen from IbDMelt was in the range of 37.40 to 65.76%, which was significantly higher ($p < 0.05$, $n = 4$) than the release by ibuprofen control (30.72%) as shown in Figure 80. Increasing concentration of DEAE-Dextran increased rate of ibuprofen release to 65.77 % at 0.2% w/v followed by a decrease up to 45.93 % at 0.8% w/v with a further increase at higher concentrations of DEAE-Dextran. The order of release of

ibuprofen from IbDMelt conjugates at the end of 24 h is as follows: IbD2Melt > IbD5Melt > IbD3Melt > IbD4Melt > IbD1Melt > IbMelt-control as shown in Appendix I (Figure 158). The dissolution of ibuprofen from the solid dispersion is dependent on the preparation method, proportion and the properties of the carriers used in the formulation [90]. Esnaashari *et al.* studied the drug release rates along with the polymer dissolution rates of ibuprofen-polyvinylpyrrolidone (PVP) solid dispersions [91]. The authors found that ibuprofen dissolution was greatly enhanced by the formation of a solid dispersion (1:4 ratio) with 100% of the drug dissolving within 60 min compared with 12.26 and 45.94% at 1 and 24 h respectively in this study. The low dissolution rate in this study was ascribed to the strong electrostatic interaction between ibuprofen and DEAE-Dextran which retarded the release.

Two theories have been proposed to justify the higher dissolution rates of solid dispersions. Firstly, formation of higher energy metastable states of the components as a function of the carrier system and the proportion of the carriers present enhance the dissolution rates [92]. The formation of a solid solution of the drug affects the dissolution was the second theory. The melt solubilization technique as well as the decrease in particle size to nano dimensions as shown previously (section 2.3.3.5) suggests a combination of these literature principles. However the stronger affinity between ibuprofen and DEAE-Dextran retarded the dissolution rate within 24 h of study.

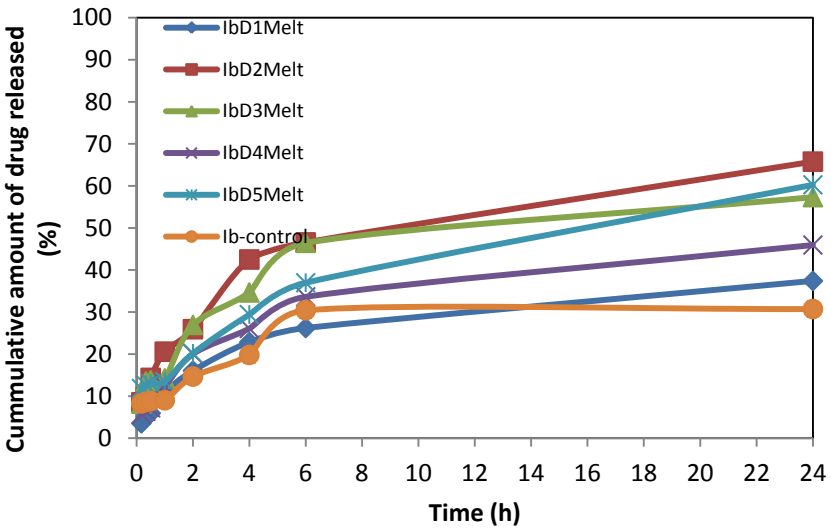

Figure 80 Release profile of ibuprofen from DEAE-Dextran conjugate (melt solubilization). Each data point represents mean ± SD (n = 4).

The release of Ibuprofen from IbDNaOH was in the range of 59.63 to 70.78%, which was significantly higher than the release by ibuprofen control (30.72%) in Figure 81. The order of release of ibuprofen from IbDNaOH conjugates at 24 h is as follows: IbD3NaOH > IbD2NaOH > IbD1NaOH > IbD4NaOH > IbD5NaOH > IbNaOH-control as shown in Appendix I (Figure 158). Dissolution studies of ibuprofen polymer conjugates showed an increase in dissolution due to the reduction of the particle size from the micrometer range to the nanometer range (section 2.3.3.5), which has been previously reported for other poorly soluble drugs such as nitrendipine [93] and deacety mycoepoxydiene [94]. Alkaline solubilization of ibuprofen at higher pH values could also contribute to the enhanced dissolution rate.

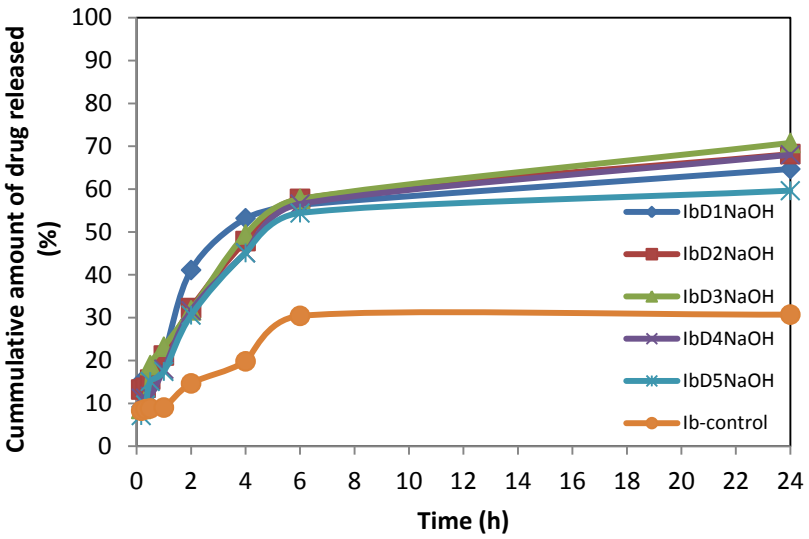

Figure 81 Release profile of ibuprofen from DEAE-Dextran conjugates (solubilization). Each data point represents mean ± SD (n = 4).

The release of Ibuprofen from IbDTw80 conjugates was in the range of 74.67 to 85.53%, which was significantly higher ($p < 0.05$, $n = 4$) than the release by ibuprofen control (30.72%) at the end of 24 h in Figure 82. The order of release of ibuprofen from IbDTw80 conjugates at 24 h is as follows: IbD4Tw80 > IbD2Tw80 > IbD5Tw80 > IbD3Tw80 > IbD1Tw80 > IbTw80-control as shown in Appendix I (Figure 158). Increasing concentration of DEAE-Dextran increased the release of ibuprofen from 74.67 to 85.53%. However the increase was not statistically significant ($p > 0.05$, $n = 20$). Purcaru *et al.* studied the drug release of nimesulide from Tween 80 solutions in combination with buffer (pH 7.4) [95]. They reported that the release from 1% Tween 80 was instantaneous with drug release of 78 to 79% after 60 min. However, in this study the release of ibuprofen from tween 80 conjugates was 17% after 60 min. It was opined that the affinity between the DEAE-Dextran and ibuprofen retarded the release. The solubilizing effect of tween 80 may have been hindered by increased degree of disorderliness (entropy) in the mixture due to the presence of the conjugates.

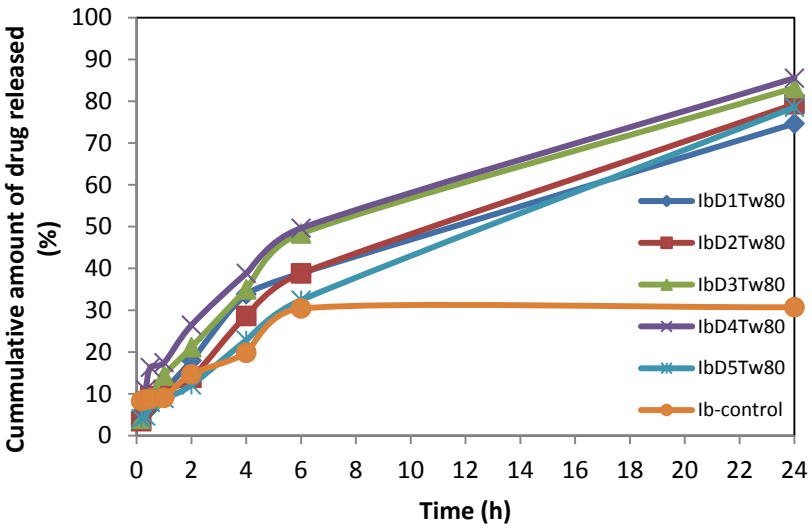

Figure 82 Release profile of ibuprofen from DEAE-Dextran conjugates (solubilization). Each data point represents mean ± SD (n = 4).

The release of Ibuprofen from IbDNic conjugates was in the range of 86.53 to 99.72%, which was significantly higher ($p < 0.05$) than the release by ibuprofen control (30.72%) in Figure 83. The order of release of ibuprofen from IbDNic conjugates at 24 h is as follows: IbD1Nic > IbD2Nic > IbD4Nic > IbD5Nic > IbD3Nic > IbNic-control as shown in Appendix I (Figure 158). Increasing concentration of DEAE-Dextran significantly increased ($p < 0.05$, $n = 20$) the release of ibuprofen from the conjugate. Nicotinamide acts as water structure disruptors by increasing the solubility which destroys clusters of associated water molecules releasing water of solvation [96]. It was opined that the structure disruptors (nicotinamide) prevented self aggregation of ibuprofen which led to increase in solubility of ibuprofen. In a similar study, Ahuja *et al.* reported that higher drug release of rofecoxib was observed with urea and nicotinamide systems via their ability to destroy water structure and complex formation [39] supporting the findings in this study.

From the foregoing, it was obvious that the influence of the four different techniques on the *in vitro* release of ibuprofen from the conjugates is in the following order: IbDNic > IbDTw80 > IbDNaOH > IbDMelt with maximum release of 99.71, 85.53, 70.78 and 65.77% respectively.

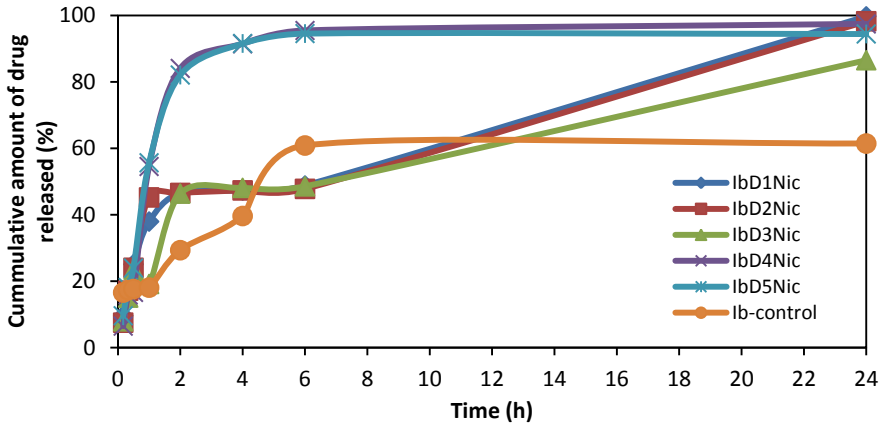

Figure 83 Release profile of ibuprofen from DEAE-Dextran conjugates (hydrotropy). Each data point represents mean ± SD (n = 4).

The *in vitro* release profiles of ibuprofen-chitosan conjugates and dissolution profile of ibuprofen control in PBS 7.4 at 37 ^{o}C are shown in Figure 84 to Figure 87. The release of Ibuprofen from IbChMelt conjugates was in the range of 32.83 to 59.10%, which was significantly higher ($p < 0.05$, $n = 4$) than the release by ibuprofen control (30.72%) in Figure 84. The order of release of ibuprofen from IbChMelt conjugates at 24 h is as follows: IbCh4Melt > IbCh5Melt > IbCh2Melt > IbCh3Melt > IbCh1Melt > IbMelt-control as shown in Appendix I (Figure 159). Increasing concentration of chitosan significantly increased ($p < 0.05$, $n = 20$) the release of ibuprofen from the conjugates. Portero *et al.* studied the effect of chitosan and chitosan glutamate enhancing the dissolution properties of nifedipine [97]. Chitosan significantly increased the dissolution of nifedipine. The effect was dependent on the polymer: drug mixing weight ratio, the chitosan type and the method employed in dispersing the drug in the polymer.

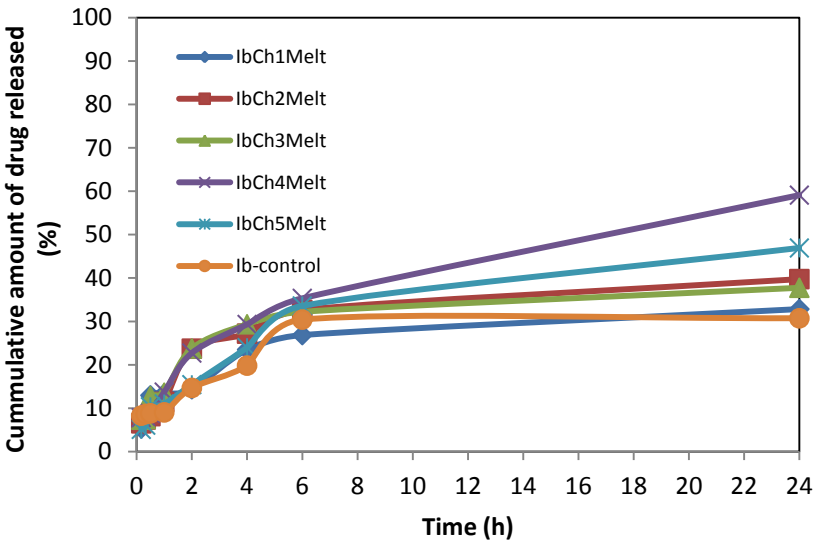

Figure 84 Release profile of ibuprofen from chitosan conjugates (melt solubilization). Each data point represents mean ± SD (n = 4).

The release of Ibuprofen from IbChNaOH conjugates was in the range of 57.68 to 66.87%, which was significantly higher ($p < 0.05$, $n = 4$) than the release by ibuprofen control (30.72%) in Figure 85. The order of release of ibuprofen from IbChNaOH conjugates at 24 h is as follows: IbCh1NaOH > IbCh2NaOH > IbCh3NaOH > IbCh4NaOH > IbCh5NaOH > IbNaOH-control. There was insignificant decrease ($p > 0.05$, $n = 20$) in the release of ibuprofen from the conjugates with increase in chitosan content.

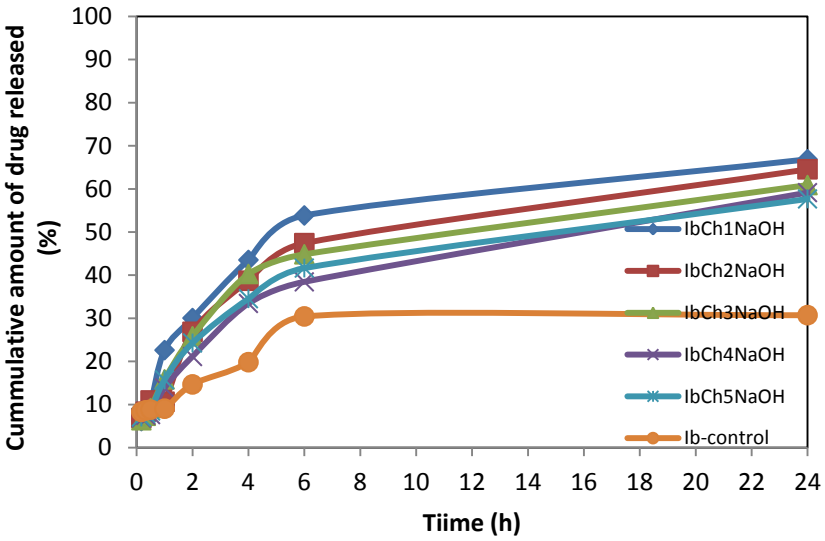

Figure 85 Release profile of ibuprofen from chitosan conjugates (solubilization). Each data point represents mean ± SD (n = 4).

The release of Ibuprofen from IbChTw80 conjugates was in the range of 52.01 to 55.93%, which was significantly higher ($p < 0.05$, $n = 4$) than the release by ibuprofen control (30.72%) in Figure 86. The order of release of ibuprofen from IbChTw80 conjugates at 24 h is as follows: IbCh4Tw80 > IbCh1Tw80 > IbCh5Tw80 > IbCh2Tw80 > IbCh3Tw80 > IbTw80-control. Chitosan did not significantly change ($p > 0.05$, $n = 20$) the release of ibuprofen as the concentration of ibuprofen increased.

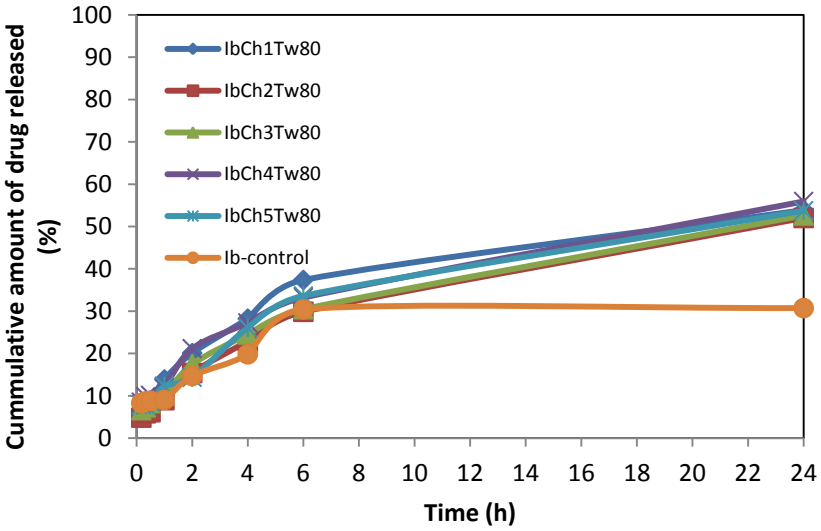

Figure 86 Release of ibuprofen from chitosan conjugates (solubilization). Each data point represents mean ± SD (n = 4).

The release of Ibuprofen from IbChNic conjugates was in the range of 97.31 to 99.28%, which was significantly higher ($p < 0.05$, $n = 4$) than the release by ibuprofen control (30.72%) in Figure 87. The order of release of ibuprofen from IbChNic conjugates at 24 h is as follows: IbCh4Nic > IbCh2Nic > IbCh3Nic > IbCh1Nic > IbCh5Nic > Ibuprofen control. Chitosan did not significantly ($p > 0.05$, $n = 20$) change the ibuprofen release with increasing concentration. The initial burst release has been reported to be mainly due to weakly bound or adsorbed drug to the large surface of the nanoparticles [98]. The solubility and dissolution characteristics are altered by the complexation of drugs to suitable carriers due to high solubility of the carrier [99].

Overall, the effect of the four different techniques on the *in vitro* release of ibuprofen from the conjugates is in the following order: IbChNic > IbChNaOH > IbChMelt> IbChTw80 with maximum release of 99.28, 66.87, 59.10 and 55.94% respectively.

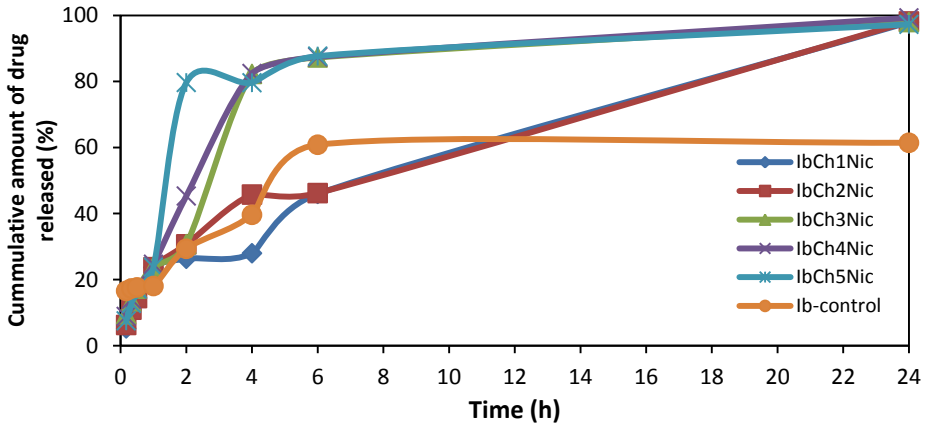

Figure 87 Release profile of ibuprofen from chitosan conjugates (hydrotropy). Each data point represents mean ± SD (n = 4).

The release profile of the complexes and dissolution profile of ibuprofen control in PBS pH 7.4 at 37 ^{o}C are shown in Figure 88. The release of Ibuprofen from DEAE-Dextran-gellan complexes was in the range of 56.83 to 95.49%, which was significantly higher ($p < 0.05$, $n = 4$) than the release by ibuprofen control (30.91%). The order of release of ibuprofen from the DEAE-Dextran-gellan complexes at 48 h is as follows: DG 100:0 > DG 0:100 > DG 75:25 > DG 50:50 > DG 25:75 > ibuprofen control. The drug release significantly increased ($p < 0.05$, $n = 20$) with increase in DEAE-Dextran concentration. The individual polymers (DEAE-Dextran and chitosan) gave greater release of 95.49 and 95.33% respectively than the ternary conjugates (56.83 to 90.38%). Increasing concentration of DEAE-Dextran increased the release to an initial maximum followed by an extended release as shown in Appendix I (Figure 160). Ternary conjugate containing DG 75:25 weight ratio exhibited the highest release of 90.38% (3-fold) compared with ibuprofen control.

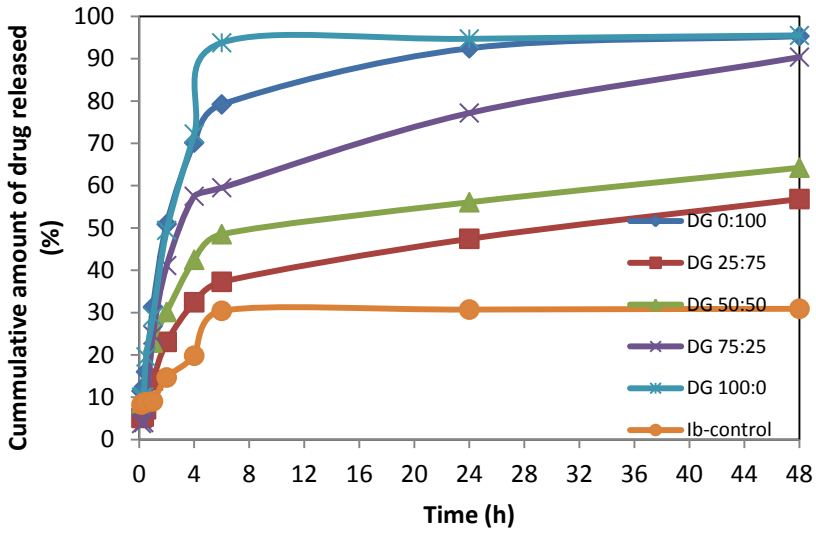

Figure 88 Release profile of ibuprofen from DEAE-Dextran-Gellan conjugates (ternary). Each data point represents mean ± SD (n = 4).

The release profile of the complexes and dissolution profile of ibuprofen control in PBS pH 7.4 at 37 ^{o}C are shown in Figure 89. The release of Ibuprofen from chitosan-gellan complexes was in the range of 45.33 to 96.59%, which was significantly higher ($p < 0.05$, $n = 4$) than the release by ibuprofen control (30.91%). The order of release of ibuprofen at 48 h is as follows: CG 100:0 > CG 0:100 > CG 75:25 > CG 50:50 > CG 25:75 > ibuprofen control. The ibuprofen release significantly increased ($p < 0.05$, $n = 20$) with increase in chitosan concentration as shown in Appendix I (Figure 160).

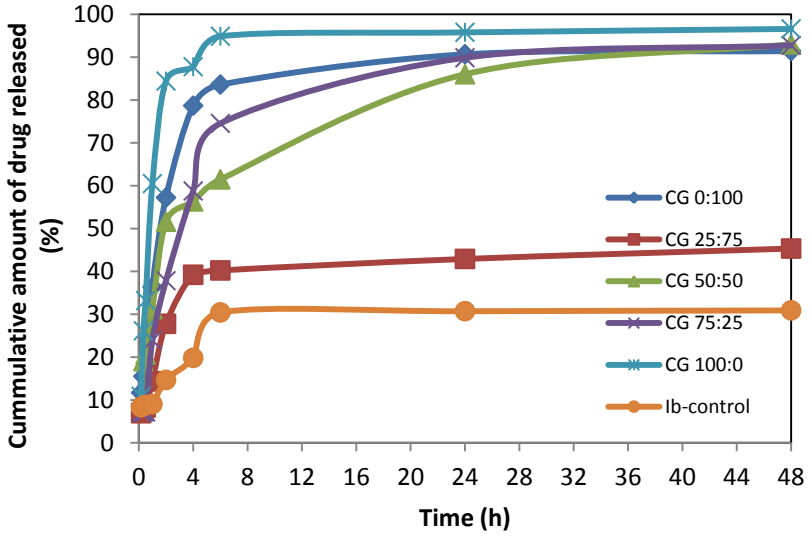

Figure 89 Release profile of ibuprofen from Chitosan-Gellan conjugates (ternary). Each data point represents mean ± SD (n = 4).

2.3.5. Drug release kinetics

Kinetic or mathematical models are model – dependent methods useful in comparing in vitro dissolution profiles. Methods of drug release from nanoparticles include desorption of drug bound to the surface; diffusion through the nanoparticle matrix; diffusion through the polymer wall of nanocapsules; nanoparticle matrix erosion; or a combined erosion-diffusion process. To analyze the drug release mechanism in the complexes, the release data was fitted into different kinetic models: zero order, first order, Higuchi plot and Korsemeyer-Peppas (first 60% release) [31]. The parameters of the models were obtained by linear regression.

The drug release kinetics showed that the data were best fitted with the Korsemeyer-Peppas kinetic models for ibuprofen control and the IbDMelt conjugates except IbD5Melt which was best fitted with the Higuchi plot. Based on Korsemeyer-Peppas equation, values of n = 0.5 refers to Fickian diffusion which indicates drug release by diffusion and n = 1 refers to Case II transport which indicates drug release by the process of swelling [100]. Values of n between 0.5 and 1 refer to anomalous transport mechanism which indicates the superposition of diffusion and swelling processes. These extreme values of n are valid for slab geometry (thin films). For spheres which represent the particles in this study, different n values have been derived [101-102]. Values of $n < 0.43$ refers to Fickian diffusion; $0.43 < n < 0.85$ refers to anomalous transport; while n = 0.85 refers to Case II transport.

The the n values obtained (Table 57) indicated that for the conjugates IbD3Melt, IbD5Melt and ibuprofen control had $n < 0.43$, exhibiting Fickian diffusion. For IbD1Melt, IbD2Melt and IbD4Melt, the release mechanism was anomalous (non-Fickian) diffusion where diffusion exponent (n) is $0.43 < n < 0.85$. This can be attributed to presence of unbound drug on the surface of the nanoconjugates.

Table 57 Regression coefficient (r) values of different kinetic models and diffusion exponent (n) of Korsemeyer-Peppas models for the release of ibuprofen from DEAE-Dextran conjugates (melt solubilization).

Formulation	Zero order	First Order	Higuchi	Korsemeyer-Peppas	
	R^2	R^2	R^2	R^2	n
IbMelt-control (IbD 1:0)	0.61	0.56	0.80	0.88	0.32
IbD1Melt (IbD 1:0.5)	0.75	0.51	0.93	0.97	0.51
IbD2Melt (IbD 1:1)	0.76	0.54	0.93	0.99	0.50
IbD3Melt (IbD 1:2)	0.56	0.46	0.78	0.92	0.43
IbD4Melt (IbD 1:4)	0.76	0.54	0.93	0.98	0.54
IbD5Melt (IbD 1:8)	0.81	0.67	0.94	0.84	0.28

The data were best fitted with Korsemeyer-Peppas kinetic models for Ibuprofen control and all the IbDNaOH conjugates. The n values obtained (Table 58) indicated that for IbD1NaOH, IbD3NaOH, IbD4NaOH and IbD5NaOH, the release mechanism was anomalous diffusion where diffusion exponent (n) is $0.43 < n < 0.85$. IbD2NaOH and Ibuprofen control had n values less than 0.43 exhibiting Fickian diffusion.

Table 58 Regression coefficient (r) values of different kinetic models and diffusion exponent (n) of Korsemeyer-Peppas models for the release of ibuprofen from DEAE-Dextran conjugates (solubilization).

Formulation	Zero order	First Order	Higuchi	Korsemeyer-Peppas	
	R^2	R^2	R^2	R^2	n
IbNaOH-control (IbD 1:0)	0.61	0.56	0.80	0.88	0.32
IbD1NaOH (IbD 1:0.5)	0.56	0.46	0.78	0.92	0.44
IbD2NaOH (IbD 1:1)	0.67	0.53	0.87	0.96	0.37
IbD3NaOH (IbD 1:2)	0.67	0.48	0.67	0.98	0.54
IbD4NaOH (IbD 1:4)	0.68	0.52	0.87	0.94	0.51
IbD5NaOH (IbD 1:8)	0.58	0.44	0.81	0.94	0.47

The data were best fitted with Higuchi kinetic models for all the IbDTw80 conjugates. The n values obtained (Table 589) indicated that for all the IbDTw80 nanoconjugates, the release mechanism was anomalous (non-Fickian) diffusion where diffusion exponent (n) is $0.43 < n < 0.85$.

Table 59 Regression coefficient (r) values of different kinetic models and diffusion exponent (n) of Korsemeyer-Peppas models for the release of ibuprofen from DEAE-Dextran conjugates (solubilization).

Formulation	Zero order	First Order	Higuchi	Korsemeyer-Peppas	
	R^2	R^2	R^2	R^2	n
IbTw80-control (IbD 1:0)	0.61	0.56	0.80	0.88	0.32
IbD1Tw80 (IbD 1:0.5)	0.91	0.65	0.99	0.96	0.60
IbD2Tw80 (IbD 1:1)	0.95	0.66	0.99	0.93	0.60
IbD3Tw80 (IbD 1:2)	0.89	0.59	0.99	0.98	0.65
IbD4Tw80 (IbD 1:4)	0.89	0.58	0.99	0.96	0.56
IbD5Tw80 (IbD 1:8)	0.98	0.74	0.98	0.96	0.57

The data were best fitted with the Higuchi kinetic models for IbD1Nic, IbD2Nic and IbD3Nic conjugates (lower concentrations of DEAE-Dextran) while IbD4Nic, IbD5Nic and ibuprofen control were best fitted with Korsemeyer-Peppas kinetic models.The n values obtained (Table 60) indicated that for IbD1Nic, IbD2Nic and IbD3Nic conjugates, the release mechanism was anomalous (non Fickian) diffusion where diffusion exponent (n) is $0.43 < n < 0.85$, while for IbD4Nic and IbD5Nic a Super Case II transport mechanism (where $n > 0.85$) was exhibited.

Table 60 Regression coefficient (r) values of different kinetic models and diffusion exponent (n) of Korsemeyer-Peppas models for the release of ibuprofen from DEAE-Dextran conjugates (hydrotropy).

Formulation	Zero order	First Order	Higuchi	Korsemeyer-Peppas	
	R^2	R^2	R^2	R^2	n
IbNic-control (IbD 1:0)	0.61	0.56	0.80	0.88	0.32
IbD1Nic (IbD 1:0.5)	0.86	0.53	0.94	0.86	0.44
IbD2Nic (IbD 1:1)	0.81	0.45	0.90	0.79	0.48
IbD3Nic (IbD 1:2)	0.79	0.51	0.92	0.88	0.49
IbD4Nic (IbD 1:4)	0.35	0.26	0.59	0.95	1.15
IbD5Nic (IbD 1:8)	0.34	0.27	0.58	0.99	0.98

The data were best fitted with the Korsemeyer-Peppas kinetic models for all the IbChMelt conjugates except IbCh4Melt which fitted the Higuchi kinetic model. The n values obtained (Table 61) indicated that for IbCh2Melt, IbCh3Melt, IbCh4Melt and IbCh5Melt nanoconjugates, the release mechanism was anomalous (non Fickian) diffusion where diffusion exponent (n) is $0.43 < n < 0.85$. The IbCh1Melt nanoconjugate and ibuprofen control had n values less than 0.43 exhibiting Fickian diffusion.

Table 61 Regression coefficient (r) values of different kinetic models and diffusion exponent (n) of Korsemeyer-Peppas models for the release of ibuprofen from chitosan conjugates (melt solubilization).

Formulation	Zero order	First Order	Higuchi	Korsemeyer-Peppas	
	R^2	R^2	R^2	R^2	n
IbMelt-control (IbCh 1:0)	0.61	0.56	0.80	0.88	0.32
IbCh1Melt (IbCh 1:0.125)	0.67	0.47	0.86	0.91	0.37
IbCh2Melt (IbCh 1:0.25)	0.64	0.48	0.84	0.93	0.51
IbCh3Melt (IbCh 1:0.5)	0.58	0.44	0.81	0.94	0.47
IbCh4Melt (IbCh 1:1)	0.87	0.63	0.98	0.94	0.47
IbCh5Melt (IbCh 1:2)	0.81	0.59	0.95	0.97	0.51

The data were best fitted with the Korsemeyer-Peppas kinetic models for ibuprofen control and all the IbChNaOH conjugates.The n values obtained (Table 62) indicated that for all the IbChNaOH conjugates,the release mechanism was anomalous (non Fickian) diffusion where diffusion exponent (n) is $0.43 < n < 0.85$.

Table 62 Regression coefficient (r) values of different kinetic models and diffusion exponent (n) of Korsemeyer-Peppas models for the release of ibuprofen from Chitosan conjugates (solubilization).

Formulation	Zero order	First Order	Higuchi	Korsemeyer-Peppas	
	R^2	R^2	R^2	R^2	n
IbNaOH-control (IbCh 1:0)	0.61	0.56	0.80	0.88	0.32
IbCh1NaOH (IbCh 1:0.125)	0.67	0.45	0.87	0.98	0.65
IbCh2NaOH (IbCh 1:0.25)	0.74	0.54	0.91	0.94	0.57
IbCh3NaOH (IbCh 1:0.5)	0.71	0.50	0.90	0.96	0.52
IbCh4NaOH (IbCh 1:1)	0.81	0.58	0.95	0.96	0.50
IbCh5NaOH (IbCh 1:2)	0.76	0.54	0.93	0.96	0.49

The data were best fitted with the Higuchi kinetic models for IbCh2Tw80, IbCh3Tw80, IbCh4Tw80 and IbCh5Tw80 conjugates while IbCh1Tw80 was best fitted with Korsemeyer-Peppas kinetic models. The n values obtained indicated that for IbCh1Tw80, IbCh2Tw80, IbCh3Tw80 and IbCh5Tw80 conjugates, the release mechanism was anomalous (non Fickian) diffusion where diffusion exponent (n) is $0.43 < n < 0.85$. The IbCh4Tw80 conjugate had $n < 0.43$ exhibiting Fickian diffusion.

Table 63 Regression coefficient (r) values of different kinetic models and diffusion exponent (n) of Korsemeyer-Peppas models for the release of ibuprofen from Chitosan conjugates (solubilization).

Formulation	Zero order	First Order	Higuchi	Korsemeyer-Peppas	
	R^2	R^2	R^2	R^2	n
IbTw80-control (IbCh 1:0)	0.61	0.56	0.80	0.88	0.32
IbCh1Tw80 (IbCh 1:0.125)	0.82	0.59	0.96	0.99	0.46
IbCh2Tw80 (IbCh 1:0.25)	0.90	0.65	0.99	0.97	0.54
IbCh3Tw80 (IbCh 1:0.5)	0.90	0.68	0.99	0.98	0.46
IbCh4Tw80 (IbCh 1:1)	0.89	0.68	0.99	0.95	0.41
IbCh5Tw80 (IbCh 1:2)	0.88	0.69	0.98	0.96	0.43

The data were best fitted with the Higuchi kinetic models for IbCh1Nic and IbCh2Nic conjugates (lower concentrations of DEAE-Dextran), while IbCh3Nic, IbCh4Nic, IbCh5Nic and ibuprofen control were best fitted with Korsemeyer-Peppas kinetic models.The n values obtained (Table 64) indicated that for all the IbChNic conjugates, the dominant release mechanism was anomalous (non Fickian) diffusion where diffusion exponent (n) is $0.43 < n < 0.85$.

Table 64 Regression coefficient (r) values of different kinetic models and diffusion exponent (n) of Korsemeyer-Peppas models for the release of ibuprofen from Chitosan conjugates (hydrotropy).

Formulation	Zero order	First Order	Higuchi	Korsemeyer-Peppas	
	R^2	R^2	R^2	R^2	n
IbNic-control (IbCh 1:0)	0.61	0.56	0.80	0.88	0.32
IbCh1Nic (IbCh 1:0.125)	0.95	0.64	0.98	0.91	0.53
IbCh2Nic (IbCh 1:0.25)	0.91	0.59	0.99	0.97	0.56
IbCh3Nic (IbCh 1:0.5)	0.57	0.47	0.78	0.99	0.48
IbCh4Nic (IbCh 1:1)	0.57	0.43	0.79	0.99	0.64
IbCh5Nic (IbCh 1:2)	0.45	0.35	0.67	0.98	0.65

Drug release kinetics showed that the data were best fitted with the Korsemeyer-Peppas models for all the ibuprofen-DEAE-Dextran-gellan complexes and ibuprofen control. The n values obtained (Table 65) indicated that for the complexes (DG 0:100, DG 25:75 and DG 100:0) and ibuprofen control, the release mechanism was anomalous (non-Fickian) diffusion where diffusion exponent (n) is $0.43 < n < 0.85$; DG 50:50 exhibited Fickian diffusion ($n < 0.43$) while DG 75:25 exhibited Super case II transport ($n > 0.85$).

Table 65 Regression coefficient (r) values of different kinetic models and diffusion exponent (n) of Korsemeyer-Peppas models for the release of ibuprofen from DEAE-Dextran-Gellan conjugates.

Formulation	Zero order	First Order	Higuchi	Korsemeyer-Peppas	
	R^2	R^2	R^2	R^2	n
IbDW-control	0.54	0.34	0.74	0.85	0.81
DG 0:100	0.54	0.39	0.75	0.96	0.64
DG 25:75	0.71	0.47	0.88	0.92	0.47
DG 50:50	0.62	0.43	0.81	0.89	0.41
DG 75:25	0.64	0.36	0.83	0.94	0.90
DG 100:0	0.47	0.36	0.69	0.96	0.68

Drug release kinetics showed that the data were best fitted with the Korsemeyer-Peppas models for all the ibuprofen-chitosan-gellan complexes. The n values obtained (Table 66) indicated that for the

complexes CG 0:100, CG 50:50 and CG 75:25, the release mechanism was by anomalous (non-Fickian) diffusion where diffusion exponent (n) is 0.5 < n < 1; CG 25:75 was by Fickian diffusion (n < 0.43), while CG 100:0 exhibited Super case II transport (n > 0.85).

Table 66 Regression coefficient (r) values of different kinetic models and diffusion exponent (n) of Korsemeyer-Peppas models for the release of ibuprofen from Chitosan-Gellan conjugates.

Formulation	Zero order	First Order	Higuchi	Korsemeyer-Peppas	
	R^2	R^2	R^2	R^2	n
IbDW-control	0.54	0.34	0.74	0.85	0.82
CG 0:100	0.45	0.34	0.66	0.96	0.68
CG 25:75	0.46	0.36	0.67	0.86	0.39
CG 50:50	0.67	0.44	0.86	0.95	0.51
CG 75:25	0.60	0.40	0.80	0.91	0.78
CG 100:0	0.31	0.23	0.52	0.98	0.95

2.3.6. Similarity factor

The f_2 similarity factor was used to compare the drug release profiles of processed ibuprofen control (reference) with ibuprofen-DEAE-Dextran or ibuprofen-chitosan nanoconjugates (tests) and the mean f_2 data was presented in Tables 102 and 103. The f_2 values were in the range of 45.27 to 79.53 for the IbDMelt nanoconjugates. Three nanoconjugates IbD1Melt, IbD3Melt and IbD4Melt were higher than the limit value of 50, suggesting a similarity between the test and reference drug release profiles. The IbD2Melt and IbD5Melt were lower than the limit value of 50 suggesting dissimilarity between the drug release profiles. The f_2 values obtained for the IbDNaOH conjugates were lower than limit value of 50 (f_2 values in the range of 42.38 to 49.41) suggesting dissimilarity of the drug release profiles of IbDNaOH conjugates compared to the control. The f_2 values obtained for the IbDTw80 conjugates were lower than limit value of 50 (f_2 values in the range of 35.60 to 40.38) suggesting dissimilarity of the drug release profiles of IbDTw80 conjugates compared to the control. This implied that the nanoconjugates were not identical with the control. The f_2 values obtained for the IbDNic conjugates were lower than limit value of 50 (f_2 values in the range of 30.61 to 35.21) suggesting dissimilarity of the drug release profiles of IbDNic conjugates compared to the control.

The f_2 values obtained were higher than limit value of 50 (f_2 values in the range of 49.81 to 95.17) except IbCh4Melt suggesting similarity of the drug release profiles of IbChMelt conjugates compared

to the control. The f_2 values obtained were lower than limit value of 50 (f_2 values in the range of 44.60 to 50.92) except IbCh5NaOH (higher concentration of chitosan) suggesting dissimilarity of the drug release profiles of IbChNaOH conjugates compared to the control. The f_2 values obtained were higher than limit value of 50 (f_2 values in the range of 52.35 to 55.96) suggesting similarity of the drug release profiles of IbChTw80 conjugates compared to the control. The f_2 values obtained were lower than limit value of 50 (f_2 values in the range of 30.75 to 31.38) suggesting dissimilarity of the drug release profiles of IbChNic conjugates compared to the control.

For the ibuprofen loaded DEAEDextran-Gellan nanoconjugates, all the similarity f_2 values obtained were lower than the limit value of 50 except DG 25:75 (f_2 = 53.02) suggesting dissimilarity of the drug release profiles of the conjugates compared with ibuprofen control shown in Table 104. All the similarity f_2 factor values obtained for the ibuprofen loaded Chitosan-Gellan nanocongates were lower than the limit value of 50 except CG 25:75 (f_2 = 65.46) suggesting dissimilarity of the drug release profiles of the conjugates compared with ibuprofen control (Table 104).

2.4. Conclusion

Ibuprofen-polymer binary and ternary nanoconjugates have been prepared from ibuprofen and DEAE-Dextran or chitosan and gellan respectively using five techniques. The nanoconjugates were characterized using particle size analysis and zeta potential, SEM, FTIR, NMR, DSC and TGA. It was evident that conjugation occurred between ibuprofen and each of the polymers via electrostatic and hydrophobic interaction as well as hydrogen bonding. The conjugation efficiency was above 89% in all techniques employed. All the techniques used in this study decreased the particle size of ibuprofen to nanometre ranges in the order IbDTw80 < IbDNic < IbDNaOH < IbDMelt; IbChTw80 < IbChMelt < IbChNic < IbChNaOH. The conjugates where spherical particles presented either as discrete, or in aggregates with particle sizes within nanometre range and a few in the micrometre range as evidenced by the SEM micrographs. The DSC thermograms of the conjugates revealed that

lower concentrations (up to 1:1 weight ratio) of the polymer reduced the crystallinity of the ibuprofen to 50.99% with respect to melting peaks suggesting increased solubility of the conjugates.

The hydrotropic conjugation technique exhibited almost complete release profile (99.71 and 99.28%) at 0.1% DEAE-Dextran and 0.2% chitosan respectively. The least release profile was exhibited by the melt solubilization technique for DEAE-Dextran and surfactant solubilization for chitosan. Fickian and non-Fickian anomalous mechanisms were deduced for the drug release of ibuprofen from the conjugates. In conclusion the five techniques used in this study, successfully reduced the particle size of ibuprofen to nanometre range and enhanced the *in vitro* drug release of ibuprofen without the use of organic solvents.

2.5. References

1. Raffa, R.B., *Analgesic, Antipyretic and Anti-inflammatory Drugs.*, in *Remington: The Science and Practise of Pharmacy*, D.B. Troy, Editor. 2005, Lippincott, Williams & Wilkins: Philadelphia, PA. p. 2393.
2. Rodriguez, R., C. Alvarez-Lorenzo, and A. Concheiro, *Interactions of Ibuprofen with Cationic Polysaccharides in Aqueous Dispersions and Hydrogels. Rheological and Diffusional Implications.* Eur J Pharm Sci, 2003. **20**(4-5): p. 429-438.
3. Ramos, L.S., M. Luan, Y. Mohwald, H. Brezesinski, G., *Electrostatic Interactions Between Polyelectrolyte and Amphiphiles in Two and Three-Dimensional Systems.* Coll Surf A, 2007. **303**: p. 79-88.
4. Taylor, D.J.F., R.K. Thomas, and J. Penfold, *Polymer/Surfactant Interactions at the Air/Water Interface.* Adv Colloid Interface Sci, 2007. **132**: p. 69-110.
5. Langevin, D., *Complexation of Oppositely Charged Polyelectrolytes and Surfactants in Aqueous Solutions. A Review.* Adv Coll Int Sci, 2009. **147-148**: p. 170-177.
6. Caram-Lelham, N.H., F. Sundelof, L. O., *Adsorption of Charged Amphiphiles to Oppositely Charged Polysaccharides - A Study of the Influence of Polysaccharide Structure and Hydrophobicity of the Amphiphile Molecule.* Biopolyms, 1997. **41**(7): p. 765-772.
7. Persson, B.H., A. Caram-Lelham, N. Sundelof, L. O., *Dextran Sulfate-Amphiphile Interaction: Effect of polyelectrolyte Charge Density and Amphiphile Hydrophobicity.* Langmuir, 2000. **16**(2): p. 313-317.
8. Hugerth, A. and L.O. Sundelof, *The Effect of Polyelectrolyte Counterion Specificity, Charge Density, and Conformation on Polyelectrolyte-Amphiphile Interaction: The Carrageenan/Furcelleran-Amitriptyline System.* Biopolyms, 2001. **58**(2): p. 186-194.
9. Cheow, W.S. and K. Hadinoto, *Self-Assembled Amorphous Drug-Polyelectrolyte Nanoparticle Complex with Enhanced Dissolution Rate and Saturation Solubility.* J Coll Int Sci, 2012. **367**: p. 518-526.
10. Barreiro-Iglesias, R.B., L. Temchenko, M. Hatton, T. A. Concheiro, A. Alvarez-Lorenzo, C., *Solubilization and Stabilization of Camptothecin in Micellar Solutions of Pluronic-g-poly(acrylic acid) Copolymers.* J Cont Rel, 2004. **97**(3): p. 537-549.
11. Adams, M.L.L., A. Kwon, G. S., *Amphiphilic Block Copolymers for Drug Delivery.* J Pharm Sci, 2003. **92**: p. 1343-1355.
12. Jones, M.-C. and J.-C. Leroux, *Polymeric Micelles-A New Generation of Colloidal Drug Carriers.* Eur J Pharm Biopharm, 1999. **48**(2): p. 101-111.
13. Motornov, M.R., Y. Tokarev, I. Minko, S., *Stimuli-Responsive Nanoparticles, Nanogels and Capsules for Integrated Multifunctional Intelligent Systems.* Prog Polym Sci, 2010. **35**(1-2): p. 174-211.

14. Dhirendra, K.L., S. Udupa, N. Atin, K., *Solid Dispersions: A Review.* J Pharm Sci, 2009. **22**(2): p. 234-246.
15. Sekiguchi, K. and N. Obi, *Studies on Absorption of Eutectic Mixture. I. A Comparison of the Behaviour of Eutectic Mixture of Sulfathiazole and that of Ordinary Sulfathiazole in Man.* Chem Pharm Bull, 1961. **9**: p. 866-872.
16. Greenhalgh, D.J.W., A. C. Timmins, P. York, P, *Solubility Parameters as Predictors of Miscibility in Solid Dispersions.* J Pharm Sci, 1999. **88**(11): p. 1182-1190.
17. Save, T. and P. Venkitachalam, *Studies on Solid Dispersions of Nifedipine.* Drug Dev Ind Pharm, 1992. **18**(15): p. 1663-1679.
18. Attwood, D. and A.T. Florence, *Surfactant Systems*. 1983, New York: Chapman and Hall Ltd. 779.
19. Seedher, N. and M. Kanojia, *Micellar Solubilization of Some Poorly Soluble Antidiabetic Drugs: A Technical Note.* AAPS PharmSciTech, 2008. **9**(2): p. 431-436.
20. Jayesh, M.T.H., P. Nirav, P. Prassana, P. Umesh, U., *A Review on Hydrotropy: A Novel Concept For Solubility Enhancement.* Int J Pharm Res Dev, 2012. **4**(5): p. 103-110.
21. Kumar, S.T.G., N. N., *A Study on the Properties of Hydrotrope Solutions for the Enhancement of Solubility of P-aminobenzoic Acid through Hydrotropy.* Int J Pharm Pharm Sci, 2012. **4**(4).
22. Ooya, T.M.H., K. Saitoh, M. Tamiya, E. Park K., *Self Assembly of Cholesterol-Hydrotropic Dendrimer Conjugates into Micelle-Like Structure: Preparation and Hydrotropic Solubilization of Paclitaxel.* Sci Technol Adv Mater, 2005. **6**: p. 452-456.
23. Jiang, B.H., L. Gao, C. Shen, J., *Ibuprofen-Loaded Nanoparticles Prepared By A Co-Precipitation Method And Their Release Properties* Int J Pharm, 2005. **304**: p. 220-230.
24. Arora, S.G., S. Narang, R. K. Budhiraja, R. D., *Amoxicillin Loaded Chitosan-Alginate Polyelectrolyte Complex Nanoparticles as Mucopenetrating Delivery System for H. Pylori.* Sci Pharm, 2011. **79**(3): p. 673-694.
25. Santucci, E.A., F. Carafa, M. Coviello, T. Murtas, E. Riccieri, F. M., *Gellan for the Formulation of Sustained Delivery Beads.* J Cont Rel, 1996. **42**: p. 157-164.
26. Huh, C. and S.G. Mason, *Rigorous Theory of Ring Tensiometry.* Colloid Polym Sci, 1975. **253**: p. 566-580.
27. Cheow, W.S. and K. Hadinoto, *Factors Affecting Drug Encapsulation and Stability of Lipid-Polymer Hybrid Nanoparticles.* Coll Surf B, 2011. **85**: p. 214-220.
28. Hadjiioannou, T.P., G.D. Cristian, M.A. Kouparris, and P.E. Macheras, *Quantitative Calculations in Pharmaceutical Practise and Research*. 1993, New York: VCH Publishers Inc.
29. Bourne, D.W.A., *Pharmacokinetics*, in *Modern Pharmaceutics*, G.S. Banker and C.T. Rhodes, Editors. 2002, Marcel Dekker Inc: New York. p. 94-144.
30. Higuchi, T., *Mechanism of Sustained-Action Medication. Theoretical Analysis of Rate of Release of Solid Drugs Dispersed in Solid Matrices.* J Pharm Sci, 1963. **52**(12): p. 1145-1149.
31. Korsemeyer, R.W., R. Gurny, E. Doelker, P. Buri, and N.A. Peppas, *Mechanism of Solute Release from Porous Hydrophilic Polymers.* Int J Pharm, 1983. **15**(1): p. 25-35.
32. Thakkar, V.T.S., P. A. Soni, T. G. Parmar, M. Y. Gohel M. C. Ghandi, T. R., *Goodness-of-fit Model-Dependent Approach for Release Kinetics of Levofloxacin Hemihydrates Floating Tablet.* Dissolution Technol, 2009. **1**: p. 35-39.
33. Moore, J.W., *Mathematical Comparison of Dissolution Profiles.* Drug Dev Ind Pharm, 1996. **12**: p. 969-992.
34. Pillay, J. and R. Fassihi, *Evaluation and Comparison of Dissolution Data Derived from Different Modified Release Dosage Forms: an Alternative Method.* J Control Release, 1998. **1998**: p. 45-55.
35. Reddy, S.J. and V.R. Gudsoorkar, *Solid Dispersions of Gliclazide.* The Indian Pharmacist, 2005. **32**: p. 82-84.
36. Dubey, R., *Pure Drug Nanosuspensions-Impact of Nanosuspension Technology on Drug Discovery and Development.* Drug Deliv Tech, 2006. **6**: p. 65-71.
37. Saharan, V.A.K., V. Kataria, M. Gera, M. Choudhury, P. K., *Dissolution Enhancements of Drugs Part II: Effect of Carriers.* Int J Health Res, 2009. **2**(2): p. 207-223.
38. Maheshwari, R.K., *Application of Hydrotropic Solubilization Phenomenon in Spectrophotometric Estimation of Norfloxacin in Tablets.* J Pharm Biomed Anal, 2006. **40**: p. 237-240.
39. Ahuja, N.K., O. P. Singh, B., *Studies on Dissolution Enhancement and Mathematical Modelling of Drug Release of a Poorly Water-Soluble Drug Using Water-Soluble Carriers.* Eur J Pharm Biopharm, 2007. **65**(1): p. 26-38.

40. Patravale, V.B.D., A. A. Kulkarni, R. M., *Nanosuspensions: A Promising Drug Delivery Strategy.* J Pharm Pharmacol, 2004. **56**(7): p. 827-840.
41. Yan, X., E. Khor, and L. Lim, *Chitosan-Alginate Films Prepared with Chitosans of Different Molecular Weights.* J Biomed Mater Res (Appl Biomater), 2001. **58**: p. 358.
42. Douglas, K.L. and M.J. Tabrizian, *Effect of Experimental Parameters on the Formation of Alginate-Chitosan Nanoparticles and Evaluation of their Potential Application as DNA Carrier.* J Biomater Sci Polym Ed, 2005. **16**(1): p. 43-56.
43. Khan, I.A.A., K. Ali, M. S. Kabir-ud, D, *A Comparative Study of Interaction of Ibuprofen with Biocompatible Polymers. .* Colloids Surf B Biointerfaces, 2011. **88**(1): p. 72-77.
44. Vink, H., *Conductivity of Polyelectrolytes in Very Dilute Solutions.* J Chem Soc- Faraday Trans 1, 1981. **77**: p. 2439-2449.
45. Ribeiro, L.C., R. A. Ferreira, D. C. Veiga, F. J. B., *Multicomponent Complex Formation Between Vinpocetine, Cyclodextrins, Tartaric Acid and Water-Soluble Polymers Monitored by NMR and Solubility Studies.* Eur J Pharm Sci, 2004. **24**: p. 1-13.
46. Li, Q.-X.S., B-Z. Yang, Z-Q. Fan, H-L., *Electrolytic Conductivity Behaviors and Solution Conformations of Chitosan in Different Acid Solutions.* Carboh Polym, 2006. **63**(2): p. 272-282.
47. Lee, J.C., J. Y. Park, C.H., *Characteristics of Polymer Enabling Nano-comminution of Water-Insoluble Drugs.* Int J Pharm, 2008. **355**: p. 328-336.
48. Galindo-Rodriguez, S.A., E. Fessi, H. Doelker, E., *Physicochemical Parameters Associated with Nanoparticle Formation in the Salting-out, Emulsification-Diffusion, and Nanoprecipitation Methods.* Pharm Res, 2004. **21**(8): p. 1428-1439.
49. Plakkot, S.D.M., M. York, P. Saunders, M. Sulaiman, B., *Comminution of Ibuprofen to Produce Nano-particles for Rapid Dissolution.* Int J Pharm, 2011. **415**: p. 307-314.
50. Liversidge, G.G. and K.C. Cundy, *Particle Size Reduction for Improvement of Oral Bioavailability of Hydrophobic Drugs: Absolute Oral Bioavailability of Nanocrystalline Danzol in Beagle Dogs.* Int J Pharm, 1995. **122**: p. 35.
51. Mosharraf, M. and C. Nystorm, *The Effect of Particle Size and Shape on the Specific Dissolution Rate of Micronized Practically Insoluble Drugs.* Int J Pharm, 1995. **122**: p. 35-47.
52. Newa, M.B., K. H. Kim, J. O. Im, J. S. Yoo, B. K. Woo, J. S. Choi, H. G. Yong, C. S., *Enhancement of Solubility, Dissolution and Bioavailability of Ibuprofen in Solid Dispersion Systems.* Chem Pharm Bull, 2008. **56**(4): p. 569-574.
53. Allen, L.V.P., N. Ansel, H. C., *Ansel's Pharmaceutical Dosage Forms and Drug Delivery Systems*. 9th ed. Dosage Form Design: Biopharmaceutical and Pharmacokinetic Considerations, ed. D.B. Troy. 2011, Baltimore: Lippincott Williams & Wilkins. 738.
54. Miyadai, N.H., K. Moribe, K. Yamamoto, K., *Optimization and Characterization of Direct Coating for Ibuprofen Particles using a Composite Fluidized Bed.* Adv Pow Tech, 2012. **23**(1): p. 40-45.
55. Lemarchand, C.G., R. Couvreur, P., *Polysaccharide-Decorated Nanoparticles.* Eur J Pharm Biopharm, 2004. **58**: p. 327-341.
56. Hornig, S., H. Bunjes, and T. Heinze, *Preparation and Characterization of Nanoparticles Based on Dextran-Drug Conjugate.* J Coll Int Sci, 2009. **338**(1): p. 56-62.
57. Sanghvi, R., D. Evans, and S.H. Yalkowsky, *Stacking Complexation by Nicotinamide: A Useful Way of Enhancing Drug Solubility.* Int J Pharm, 2007. **336**: p. 35-41.
58. Ali, H.S.Y., P. Blangden, N., *Preparation of Hydrocortisone Nanosuspension through a Bottom-Up Nanoprecipitation Technique Using Microfluidic Reactors.* Int J Pharm, 2009. **375**(1-2): p. 107-113.
59. Motwani, S.K., S. Chopra, S. Talegaonkar, K. Kohli, F.J. Ahmad, and R.K. Khar, *Chitosan-Sodium Alginate Nanoparticles as Submicroscopic Reservoirs for Ocular Delivery: Formulation, Optimization and In Vitro Characterization.* Eur J Pharm Biopharm, 2007. **68**: p. 513-525.
60. Arunkumar, N.D., M. Rani, C., *Nanosuspension Technology and its Applications in Drug Delivery.* Asian J Pharm, 2009. **3**(3): p. 168-173.
61. Gan, Q.W., T. Cochrane, C. McCarron, P., *Modulation of Surface Charge, Particle Size and Morphological Properties of Chitosan-TPP Nanoparticles Intended for Gene Delivery.* Colloids Surf B Biointerfaces, 2005. **44**(2-3): p. 65-73.
62. Wang, C.G., Y. Lin, Y. Shen, J. Wang, D., *A Novel Gellan Gel-Based Microcarrier for Anchorage-Dependent Cell Delivery.* Acta Biomater, 2008. **4**: p. 1226-1234.
63. Prabha, S., W.Z. Zhou, J. Panyam, and V. Labhasetwar, *Size-Dependency of Nanoparticle-Mediated Gene Transfer: Studies with Fractionated Nanoparticles.* Int J Pharm, 2002. **244**: p. 105-115.

64. Harwood, L.M. and T.D.W. Claridge, *Introduction to Organic Spectroscopy*. 1999, New York: Oxford University Press Inc.
65. Coates, J., *Interpretation of Infrared Spectra, A Practical Approach*, in *Encyclopedia of Analytical Chemistry*, R.A. Meyers, Editor. 2000, John Wiley and Sons Ltd: Chichester, UK. p. 10815-10837.
66. Kyle, J., *The Basis of the Hydrophobic Effect.* Biophys Chem, 2003. **100**(1-3): p. 193-203.
67. Huguet, M.L., R.J. Neufeld, and E. Dellacherie, *Calcium Alginate Beads Coated with polycationic polymers: Comparison of Chitosan and DEAE-Dextran.* Process Biochem, 1996. **31**(4): p. 347-356.
68. Demirbilek, C. and C.O. Dinc, *Synthesis of Diethylaminoethyl Dextran Hydrogel and its Heavy Metal Ion Adsorption Characteristics.* Carbohydr Polym, 2012. **90**(2): p. 1159-1167.
69. Matkovic, S.R., G.M. Valle, and L.E. Briand, *Quantitative Analysis of Ibuprofen in Pharmaceutical formulations through FTIR Spectroscopy.* Lat Am Appl Res, 2005. **35**(3): p. 189-195.
70. Nokhodchi, A.A., O. Jelvehgari, M., *Physico-Mechanical and Dissolution Behaviours of Ibuprofen Crystals Crystallized in the Presence of Various Additives.* DARU, 2010. **18**(2): p. 74-83.
71. Xu, L.L., B.Kennedy, J. F.Xie, B. J.Huang, M., *Characterization of Konjac Glucomannam-Gellan Gum Blend Films and their Sutaibility for Release of Nisin Incorporated Therein.* Carboh Polym, 2007. **70**: p. 192-197.
72. Sudhamani, S.R., M.S. Prasad, and K. Udaya Sankar, *DSC and FTIR studies on Gellan and Polyvinyl Alcohol (PVA) blend Films.* Food Hydrocoll, 2003. **17**: p. 245-250.
73. Silva-Correia, J.O., J. M. Caridade, S. G. Oliveira, J. T. Sousa, R. A. Mano, J. F. Reis, R. L., *Gellan Gum-Based Hydrogels for Intervertebral Disc Tissue-Engineering Applications.* J Tissue Eng Regen Med, 2011. **5**: p. e97-e107.
74. Macomber, R.S., *A Complete Introduction to Modern NMR Spectroscopy.* 1998, New York: John Wiley and Sons Inc.
75. Oh, I.L., M. Lee, Y. Shin, S. Park, I., *Spectroscopic Characterization of Ibuprofen / 2-hydroxypropyl-β-Cyclodextrin Inclusion Complex.* Int J Pharm, 1998. **175**(215-223).
76. Mora, P.C., M. Cirri, and P. Mura, *Differential Scanning Calorimetry as a Screening Technique in Compatibility Studies of DHEA Extended release Formulations.* J Pharm Biomed Anal, 2006. **42**: p. 3-10.
77. Coleman, N.J. and D.Q.M. Craig, *Modulated Temperature Differential Scanning Calorimetry: A Novel Approach to Pharmaceutical Thermal Analysis.* Int J Pharm, 1996. **135**: p. 13-29.
78. Gramaglia, D.C., B. R. Kett, V. L. Malcolm, R. K. Batchelor, H. K., *High Speed DSC (hyper-DSC) as a Tool to Measure the Solubility of a Drug Within a Solid or Semi-Solid Matrix.* Int J Pharm, 2005. **301**: p. 1-5.
79. Celej, M.S.D., S. A. Gonzalez, M. Bianconi, L. M. Fidelio, G. D., *Differential Scanning Calorimetry as a Tool to Estimate Binding Parameters in Multiligand Binding Proteins.* Anal Biochem, 2006. **350**: p. 277-284.
80. Gabbott, P., ed. *A Practical Introduction to Differential Scanning Calorimetry*. 1st ed. The Principles and Applications of Thermal Analysis., ed. P. Gabbott. 2007, Blackwell Publishing Ltd: Oxford. 459.
81. Commission, B.P., *British Pharmacopoeia 2012*. Vol. 1. 2011, Norwich, Great Britain: Stationery Office Books.
82. Kumar, D.P.S., D. C. Subrata, C. Soumen, R, *Formulation and Evaluation of Solid Lipid Nanoparticles of A Poorly Water Soluble Model Drug, Ibuprofen.* Int Res J Pharm, 2012. **3**(12): p. 132-137.
83. Lee, D.-G., S. Lee, and I.W. Kim, *Effects of Humidity and Surfaces on the Melt Crystallization of Ibuprofen.* Int J Mol Sci, 2012. **13**: p. 10296-10304.
84. Oberoi, L.M.A., K. S. Riga, A. T., *Study of Interaction Between Ibuprofen and Nicotinamide Using Differential Scanning Calorimetry, Spectroscopy, and Microscopy and Formulation of a Fast-acting and Possibly Better Ibuprofen Suspension for Osteoarthritis Patients.* J Pharm Sci, 2005. **94**(1): p. 93-101.
85. Silva, C.L.P., J. C. Ramalho, A. Pais, A. A. C. C. Sousa, J. J. S., *Films Based on Chitosan Polyelectrolyte Complexes for Skin Drug Delivery: Development and Characterization.* J Memb Sci, 2008. **320**(1-2): p. 268-279.
86. Kittur, F.S.H.P., K. V. Udaya Sankar, K. Tharanathan, R. N., *Characterization of Chitin, Chitosan and their Carboxymethyl Derivatives by Differential Scanning Calorimetry.* Carbohydr Polym, 2002. **49**: p. 185-193.
87. Bottom, R., ed. *Thermogravimetric Analysis*. Principles and Applications of Thermal Analysis, ed. P. Gabbott. 2008, Blackwell Publishing Ltd: Oxford. 484.
88. Cardenas, G. and S.P. Miranda, *FTIR and TGA Studies of Chitosan Composite Films.* J Chil Chem Soc, 2004. **49**(4): p. 291-295.

89. Chopra, S., G.V. Patil, and S.K. Motwani, *Release Modulating Hydrophilic Matrix Systems of Lorsatan Potassium: Optimisation of Formulation Using Statistical Experimental Design.* Eur J Pharm Biopharm, 2007. **66**: p. 73-82.
90. Corrigan, O.I., *Mechanisms of Dissolution of Fast Release Solid Dispersions.* Drug Dev Ind Pharm, 1985. **11**(2-3): p. 697-724.
91. Esnaashari, S.J., Y. Batchelor, H. K. Conway, B. R., *The Use of Microviscometry to Study Polymer Dissolution from Solid Dispersion Drug Delivery Systems.* Int J Pharm, 2005. **292**: p. 227-230.
92. Simonelli, A.P.M., S. C. Higuchi, W.I., *Dissolution Rates of High Energy Polyvinylpyrrolidone-Sulfathiazole Co-precipitates. .* J. Pharm. Sci., 1969. **58**(5): p. 538-549.
93. Xia, D.Q., P. Piao, H. Sun, S. Yin, Y. Cui, F., *Preparation of Stable Nitrendipine Nanosuspensions Using the Precipitation-Ultrasonication Method for Enhancement of Dissolution and Oral Bioavailability.* Eur J Pharm Sci, 2010. **40**(4): p. 325-334.
94. Wang, Y.L., Z. Zhang, D. Duan, C. Jia, L. Feng, F. Huang, Y. Shen, Y. Zhang, Q., *Development and In Vitro Evaluation of Deacety Mycoepoxydiene Nanosuspension.* Colloids Surf B Biointerfaces, 2011. **83**(2): p. 189-197.
95. Purcaru, S.-O.I., M. Raneti, C. Anuta, V. Mircioiu, I. Belu, I., *Study of Nimesulide Release from Solid Pharmaceutical Formulations in Tween 80 Solutions.* Curr Health Sci J, 2010. **36**(1).
96. Muller, B.W. and E. Albers, *Effect of Hydrotropic Substances on the Complexation of Sparingly Soluble Drugs with Cyclodextrin Derivatives and the Influence of Cyclodextrin Complexation on the Pharmacokinetics of the Drugs.* J Pharm Sci, 1991. **80**: p. 599-604.
97. Portero, A.L., R. Jato J. L. V., *Effect of Chitosan Glutamate Enhancing the Dissolution Properties of the Poorly Water Soluble Drug Nifedipine.* Int J Pharm, 1998. **175**: p. 75-84.
98. Chen, Y.M., V. J. Parkin, J. E., *Chitosan-Dextran Sulfate Nanoparticles for Delivery of an Anti-Angiogenesis Peptide.* Lett Peptide Sci, 2003. **10**(5): p. 621-629.
99. Saharan, V.A.K., V. Kataria, M. Gera, M., *Dissolution Enhancement of Drugs. Part 1: Technologies and Effect of Carriers.* Int J Health Res, 2009. **2**(2).
100. Siepmann, J. and N.A. Peppas, *Modeling of Drug Release from Delivery Systems based on Hydroxypropyl Methylcellulose (HPMC).* Adv Drug Deliv Rev, 2001. **48**: p. 139-157.
101. Ritger, P.L. and N.A. Peppas, *A Simple Equation For Description of Solute Release. I. Fickian and non-Fickian Release from Non-Swellable Devices in the Form of Slabs, Spheres, Cylinders or Discs.* J Cont Rel, 1987. **5**: p. 23-36.
102. Ritger, P.L. and N.A. Peppas, *A Simple Equation for Description of Solute Release. II. Fickian and Anomalous Release from Swellable Devices.* J Cont Rel, 1987. **5**: p. 37-42.

CHAPTER THREE

3.0. Formulation and characterization of Ibuprofen – Polymer ternary nanoconjugate hydrogels

3.1. Introduction

Hydrogels are three-dimensional hydrophilic polymeric networks with tendency to absorb large quantity of water or biological fluids and thus resembling biological tissues [1]. The polymeric networks are made up of homopolymers or copolymers and the presence of chemical or physical crosslinks renders them insoluble. They exhibit thermodynamic compatibility with water which aids their swelling in aqueous media [1].They are classified based on the nature of their side groups as neutral or ionic and based on the physical structures of their networks as amorphous, semicrystalline, hydrogen bonded or supermolecular structures [1-2]. Other categories include: physiologically responsive hydrogels whose polymer complexes can be broken or networks swollen due to changing external environment such as pH, ionic strength, changes in concentration of glucose, temperature and electromagnetic radiation [3]. Environmental sensitive hydrogels are also referred to as 'intelligent' or 'smart' hydrogels [4]. They are ideal candidates for developing self regulated drug delivery systems [5]. The disadvantage of these smart hydrogels is their slow response time; therefore fast acting gels are necessary.

Hydrogels may require crosslinking to prevent matrix erosion which may affect their solubility. Chemical hydrogels are formed by irreversible covalent crosslinking. Crosslinking reagents in trace quantities are toxic (glutaraldehyde, epichlorohydrin) [6] and if drug is added before the cross linking step, the crosslinker can affect the integrity of the drug entrapped. This has led to the crosslinker being replaced by polyelectrolyte complexes since they crosslink by ionic linkages or direct physical interactions [7]. Various forces such as van der Waals, electrostatic attraction and hydrogen have been reported to be responsible for the physical interaction of polymer chains. These physical

hydrogels or polyelectrolyte complex gels are formed by the interaction of positively charged polymer with an oppositely charged polyelectrolyte. Positively charged chitosan has been used to form polyelectrolyte complex gels by electrostatic interaction with negatively charged polyelectrolytes [8]. Saleem *et al.* reported a non-Fickian diffusion mechanism first order release of diltiazem hydrochloride from chitosan-carboxymethylcellulose sodium PEC hydrogel [8].

Hydrogels have been used extensively for the controlled release of drugs, bioadhesives and targetable devices of therapeutic agents [7]. Hydrogels are used as delivery devices to various sites such as oral, ocular, nasal, gastrointestinal tract, transdermal and subcutaneous applications. Patel and Amiji developed cationic hydrogels composed of freeze-dried chitosan-poly (ethylene oxide) (PEO) semi-interpenetrating polymeric network (IPN) loaded with amoxicillin and metronidazole for site specific antibiotic delivery [9]. A fast release of the entrapped antibiotics was achieved from simulated gastric fluid (SGF) of more than 65% and 59% of amoxicillin and metronidazole respectively from the hydrogels after 2 h in SGF. However, potential applications of polyelectrolyte complex hydrogels for controlled drug release are still limited [10].

Gellan gum is a linear anionic polysaccharide gelling agent produced by *Sphingomonas elodea*. It consists of tetrasaccharide repeating units of glucose, glucuronic acid and rhamnose in the 2:1:1 ratio [11]. Gellan can form solid transparent gels at concentrations as low as 0.1% [12]. Gelation of gellan is either temperature dependent or cation induced. As temperature decreases, there is a coil to double helix transition forming a gel based on pH and ionic strength of the solution. The process of gelation starts with the gellan coil molecules forming double helices with the reduction in temperature; and helices aggregate subsequently forming junction zones, leading to system gelation [13]. Diethylaminoethyl-Dextran (DEAE-Dextran) is a water soluble polycationic derivative of Dextran produced by reacting diethylaminoethyl chloride with Dextran. There is no report showing that DEAE-Dextran form gels or films.

Gellan gum has been used in controlled release hydrogel with scleroglucan [14]. Theophylline was used as the model poorly soluble drug in the preparation of the gellan/scleroglucan hydrogel. The controlled delivery system formed exhibited the capability of responding to different environmental conditions with potentials for specific applications such as implants for drug delivery. However, little information has been focussed on the preparation and characterization of gellan gum and DEAE-Dextran complex gel. The purpose of this research was to design and develop hydrogel by polyelectrolyte complexation of gellan gum and DEAE-Dextran. Poorly soluble drug ibuprofen was incorporated as the model drug, to form drug-polymer conjugate and drug-polymer-polymer conjugate.

Ibuprofen is a non-steroidal anti-inflammatory drug used in the treatment of rheumatoid arthritis. It is an anionic drug with poor water solubility. Oral delivery of ibuprofen gives side effects such as gastric ulceration and bleeding, therefore, topical and transdermal delivery could be alternative routes to minimize the gastrointestinal side effects of ibuprofen. Topical (gels) and transdermal (dermal patches) improve patient compliance due to reduced dosage frequency. The poor permeability of ibuprofen at the skin surface due to the formidable barrier property of the stratum corneum may be overcome by the use of drug carriers and penetration enhancers. In this work, a series of polymer complexes were prepared in form of hydrogels as carriers for incorporating the poorly soluble drug. The complexes were fully characterized and the in vitro drug release evaluated.

The aim of this study was to develop and characterize a novel PEC hydrogel from gellan gum and DEAE-Dextran as a drug carrier for ibuprofen. This research also intends to investigate the effect of the PEC on the physicochemical and drug release of ibuprofen from the hydrogel.

3.2. Materials and methods

3.2.1. Materials

Ibuprofen (purchased from Fagron, UK), gellan gum (Phytagel®) and DEAE-Dextran hydrochloride (purchased from Sigma-Aldrich, UK), were used as supplied in this study.

3.2.2. Preparation of binary and ternary nanoconjugate hydrogels

Gellan reference hydrogel (**G**) was prepared by dispersing 2% gellan powder in distilled water while under magnetic stirring until homogeneous and heated up to 90 °C. The pH was adjusted to 6 with NaOH (Mettler Toledo pH meter) and left to cool.

The plain binary hydrogel was prepared by dispersing 2% gellan in distilled water while stirring until homogeneous and heated up to 90 °C (Jenway 1000 hotplate and stirrer). The gellan solution was transferred into DEAE-Dextran solution at different mixing ratios (2:0.125, 2:0.25, 2:0.5 and 2:1) at the same temperature under continuous magnetic stirring. The resulting composite polyelectrolyte complex hydrogels were adjusted to pH 6 (Mettler Toledo pH meter) with NaOH and further left to cool. These samples will be referred to **GDD 2:0.125, GDD 2:0.25, GDD 2:0.5** and **GDD 2:1** (Table 67). The samples were stored at room temperature until analysis.

Table 67 Composition of plain gellan and gellan-DEAE-Dextran hydrogels.

Sample	Gellan (%w/v)	DEAE-Dextran (%w/v)
G	2.0	-
GDD 2:0.125	2.0	0.125
GDD 2:0.25	2.0	0.25
GDD 2:0.5	2.0	0.5
GDD 2:1	2.0	1.0

All samples were made up to 100 g with distilled water.

The drug loaded reference hydrogel was prepared by solubilizing 1% ibuprofen in 1 M NaOH. This solution was added drop-wisely to a 2% gellan dispersed in distilled water while under magnetic stirring at 90 °C (Jenway 1000 hotplate and stirrer).The pH was adjusted to 6 with NaOH (Mettler Toledo pH meter). The mixture was continuously stirred and left to cool and referred to as **Glb**.

The drug loaded ternary hydrogel was prepared by solubilizing 1% of ibuprofen in 5 mL NaOH. It was added drop wise to 2% gellan dispersed in distilled water while stirring at 90 °C (Jenway 1000 hotplate and stirrer). This was transferred into DEAE-Dextran solution at different mixing ratios (2:0.125, 2:0.25, 2:0.5 and 2:1) at the same temperature under continuous magnetic stirring. The resulting polyelectrolyte complex (loaded with ibuprofen) hydrogels were adjusted to pH 6 (Mettler Toledo pH meter) with NaOH (referred to as **GIbDD 2:0.125, GIbDD 2:0.25, GIbDD 2:0.5** and **GIbDD**

2:1 shown in Table 68. The mixture was continuously stirred and left to cool. The samples were stored at room temperature until analysis.

Table 68 Composition of ibuprofen loaded gellan and gellan-DEAE-Dextran gels.

Sample	Ibuprofen (%w/v)	Gellan (%w/v)	DEAE-Dextran (%w/v)
GIb	-	2.0	-
GIbDD 2:0.125	1.0	2.0	0.125
GIbDD 2:0.25	1.0	2.0	0.25
GIbDD 2:0.5	1.0	2.0	0.5
GIbDD 2:1	1.0	2.0	1.0

All samples were made up to 100 g with distilled water.

3.2.3. Physicochemical characterization of the plain and drug loaded hydrogels

3.2.3.1. pH

One gram (1 g) of gel was dispersed in 100 mL of distilled water and stirred for 2 h. The pH of each formulation was determined by a pH meter (Mettler Toledo). All measurements were an average of four determinations and expressed as mean ± S.D.

3.2.3.2. Morphology and size – Scanning electron microscopy

The surface morphologies of the polymeric hydrogels were examined by a Carl Zeiss SEM EVO High Definition 15 (Carl Zeiss, Germany) scanning electron microscope using variable pressure technology at low voltages with beam deceleration and high definition backscattered electron (BSE) imaging. The hydrogel samples were mounted on double sided carbon tabs that were previously secured to aluminium stubs and then analysed at different magnifications and a pressure of 10 Pa. The accelerating voltage was 10 KV with probe current of 400 pA.

3.2.3.3. Spectroscopic analysis - Fourier Transform Infra-red

The spectra of samples were acquired by a Precisely Spectrum One FTIR spectrometer (PerkinElmer, USA) fitted with a Universal ATR Sampling Accessory. The hydrogels were mounted directly on the diamond surface and the arm was placed over it by applying enough pressure in the range of 100 to 120 units. The spectrum was recorded in the wavelength region of 4000 to 650 cm^{-1}. All spectra

were then collected at an average of 16 scans at a resolution of 4 cm^{-1}. All measurements were taken in replicates of four determinations.

3.2.3.4. Thermal studies

3.2.3.4.1. Differential scanning calorimetry

DSC was performed using Perkin Elmer Jade DSC machine in conjunction with a Perkin Elmer Intracooler SP cooling Accessory (Perkin Elmer, USA) to study the thermal characteristics of polymeric hydrogels. The polymeric hydrogel samples of mass 3 mg (±0.5 mg) were heated in hermetically sealed aluminium pans under nitrogen flow (40 mL/min) at a scanning rate of 20 ˚C/min from 30 to 300 ˚C. Empty aluminium pan was used as a reference pan. Zinc and indium were used as the standard reference materials to calibrate the DSC instrument. All measurements were an average of four determinations and expressed as mean ± S.D.

3.2.3.4.2. Thermogravimetric analysis

Mass changes as a function of temperature in a controlled chamber were studied using Pyris 1 Thermogravimetric Analyser (Perkin Elmer, USA). The weight of the empty reference pan placed in the crucible was zeroed and then removed. Samples of known weight 17 mg (±3 mg) were placed in aluminium pans and measurements performed at a scanning rate of 10 ˚C/min in the range of 25 to 500 ˚C. All measurements were an average of four determinations and expressed as mean ± S.D.

3.2.4. Rheological studies of hydrogels

3.2.4.1. Oscillatory measurements

Dynamic rheological properties of the plain and drug loaded polymeric complex hydrogels were evaluated using a Physica MCR501 rheometer (Anton Paar, Austria) using cone and plate geometry (CP50 with 1° angle) in oscillatory mode at 32 °C. Tests were conducted in controlled strain amplitude performed within the linear viscoelastic region (LVR) so that the storage (G') and loss (G") moduli were independent of strain. A strain sweep measurement between 0.1 and 100% was

conducted first at a frequency of 1 Hz for plain and 1% w/v ibuprofen loaded gellan and gellan-DEAE-Dextran complex hydrogels at a strain value which was within the linear viscoelastic region for both samples was selected for the subsequent frequency sweeps. The strain value selected for all polymeric complex hydrogels was 1%. Frequency sweeps at this constant strain were then conducted between 0.01 to 50 Hz and a solvent trap was used to prevent sample dehydration during the test. All tests were done in replicate of four determinations using fresh sample for each test and expressed as mean ± S.D. The rheological parameters examined were processed with pre-installed Physica software provided with the rheometer. The flow test was also conducted.

3.2.4.2. Determination of sol-gel temperature

The dynamic rheological characterisation of the plain and drug loaded polymeric hydrogel samples was evaluated using Physica MCR 501 Rheometer (Anton Paar, Austria) using cone and plate geometry (CP50 with 1^{o} angle) in oscillatory mode. Tests were conducted in controlled strain amplitude performed within the linear viscoelastic range (LVR) so that the storage (G') and loss (G") moduli were independent of strain. The tests were carried out at low oscillation frequency of 1 Hz. The polymeric complex hydrogel solutions were analysed just after preparation at 90 °C. The hot polymeric complex hydrogel solutions were transferred onto the rheometer plate which was preheated to 90 °C.The polymeric complex hydrogel solution tests started with the cooling step from 90 to 15 °C at the rate 2 °C/min. The thermo reversibility of the gels was also studied by increasing the temperature from 15 to 90 °C the heating step followed the cooling step at the same conditions in the temperature range 15 to 90 °C also at the rate 2 °C/min. A solvent trap was used to prevent sample dehydration during the test. All tests were done in replicate of four determinations using fresh sample for each test and expressed as mean ± S.D. The data acquired was analysed with pre-installed Physica software provided with the rheometer.

3.2.5. Swelling kinetics

About 500 mg of polymeric complex hydrogel was carefully weighed and dried in an oven at 60 °C till constant weight was achieved. The dried polymeric gel was accurately weighed and immersed in 5ml of PBS (pH 7.4) at 37 °C (B Braun Certomat WR Shaker Waterbath, Germany). At predetermined intervals, swollen gels were taken out, and the excess surface water removed by blotting with filter paper. This was then weighed on a balance. The following equation (equation 1) was used to determine the swelling ratio of the gel.

$$Swelling\ ratio = (W_s - W_d)/W_d \qquad (1)$$

Where W_d is the weight of dry gel and W_s is the weight of the swollen gel. All measurements were an average of four determinations and expressed as mean ± S.D.

3.2.6. Drug release from the binary and ternary nanoconjugate hydrogels

Franz cell (Permegear, USA) with diameter 11.28 mm, surface area 1.00 cm^2 and receptor volume of 8 mL was used in this study. Polymeric complex hydrogel of mass 0.5 g was placed into the donor chamber on the stratum corneum of the excised pig abdominal skin, with the dermal side facing the receptor compartment. The pig abdominal skin was obtained from freshly killed animals in a local slaughterhouse (Leicester, UK). After cleaning, full thickness, non-dermatomed skin (about 1.1 mm) was removed with a scapel, cut into squares (2.5 x 2.5 cm) were kept in sealed plastic bags then stored at -20 °C until ready for use. The samples were thawed 2 h prior to the experiment [15]. The pig abdominal skin was conditioned by immersing in receptor medium (PBS with pH 7.4) for 30 min and blotted dry prior to use. At a constant temperature of 32 °C (±0.5 °C) which corresponds to the skin surface temperature in vivo, 0.2 mL samples were withdrawn at specified collection intervals from the receptor fluid via the sampling port over a period of 24 h. 0.2 mL of the receptor fluid was replaced via the sampling port to the receptor chamber. The top of the donor compartment of the Franz diffusion cells were occluded with Parafilm® to minimise evaporation. The concentrations of the active drug released from the gel were determined by UV (ThermoFischer Evolution 60 UV-

Visible Spectrophotometer, UK) after appropriate dilutions at 264 nm wavelength and passing through 0.45 µm filter (Sartorius, Germany). All measurements were an average of four determinations and expressed as mean ± S.D.

3.2.7. Drug release kinetics

Data obtained from in vitro release studies were fitted to various kinetic equations. The kinetic models used are zero order, first order, Higuchi and Korsemeyer-Peppas equation.

The zero order rate equation (2) describes the systems were the drug release rate is independent of its concentration [16]. The cumulative % drug release vs. time plot is made.

$$C = K_0 t \qquad (2)$$

Where k_0 is zero order rate constant expressed in units of concentration/time and t is the time.

The first order rate equation (3) describes the release from the systems where release rate is concentration dependent [17]. The log cumulative % drug release vs. time plot is made.

$$Log\ C = Log\ C_0 - Kt/2.303 \qquad (3)$$

Where C_0 is the initial concentration of drug and K is first order constant.

Higuchi described the release of drugs from insoluble matrix as a square root of time dependent process based on Fickian diffusion: equation (4) [18]. The cumulative % drug release vs. square root of time is made.

$$Q = Kt^{1/2} \qquad (4)$$

Where K, is the constant and it reflects the design variables of the system.

Korsemeyer *et al.* derived a simple relationship which described drug release from a polymeric system: equation (5). To find out the mechanism of drug release, first 60 % drug release data was fitted in Korsemeyer-Peppas model:

$$M_t/M_\infty = Kt^n \qquad (5)$$

Where M_t/M_∞ is a fraction of drug released at time t, K is the rate constant and n is the release exponent. The n value is used to characterize different release mechanisms [19]. The log cumulative % drug release vs. log time plot is made. The criterion for selecting the appropriate model is the highest R^2 value which indicates linearity of dissolution data [20].

3.2.8. Similarity factors

The similarity fit factor denoted f_2 was used to compare the dissolution profiles of the ibuprofen loaded gellan-DEAE-Dextran (GIbDD) complex hydrogels (test) and GIb hydrogel (reference). The similarity f_2 factor is defined by equation 6 proposed by Moore and Flanner [21]:

$$f_{2=50\ Log}\left\{(1+\frac{1}{n}\sum_{t=1}^{n}\left(R_t-T_t\right)^2)^{-0.5}\times 100\right\} \qquad (6)$$

Where n is the number of dissolution sample times, and R_t and T_t are the individual or mean percent dissolved at each time point, t, for the reference and test dissolution profiles, respectively. The f_2 value greater than 50 suggests that the two profiles are similar. The f_2 value of 100 suggests that the test and the reference profiles are identical and as the value becomes smaller the dissimilarity between release profiles increases [22].

3.2.9. Statistical analysis

Quantitative data are presented as mean ± standard deviation. The significance of the differences between means was assessed using Analysis of Variance (ANOVA) and Post hoc Tukey Test with a statistical significance level set at $p < 0.05$ using IBM SPSS® (Statistical Package for Social Science) 20.

3.3. Results and Discussions

3.3.1. Preparation and optimization of plain and drug loaded binary and ternary hydrogels

The hydrogel formulations were optimized in the preliminary studies with respect to polymer concentration, mixing ratio, ibuprofen concentration, pH and temperature. The choice of 2% gellan was based on preliminary studies results of its comparison with 1% gellan gel. Polymer concentration has been reported to influence the helix content in gellan solutions with increased concentration forming stronger physical crosslinking [23]. Gellan gum has the ability to undergo physical gelation. It swells when dispersed in water and on application of heat up to 90 °C; forming a clear and transparent solution (sol). Subsequent decrease in temperature transformed the sol to gel, thus gellan gel was formed. When the temperature of the gellan solution is decreased, the gellan chains undergo a conformational thermo-reversible change from random coil to double helices [24]. The aggregation of the double helices forms a three dimensional network by hydrogen bonding with water. DEAE-Dextran solution, a positively charged polymer, was added to gellan solution (negatively charged polymer) at 90 °C to form polyelectrolyte complex GDD gels of different mixing ratios. It was observed that after the addition of DEAE-Dextran, the GDD hydrogels were still formed in response to temperature decrease.

Ibuprofen was initially dissolved in sodium hydroxide NaOH (basic medium) to form anionic drug solute. The ionized drug solution was mixed with negatively charged gellan polyelectrolyte solution at 90 °C. This mixture was added to an oppositely charged DEAE-Dextran solution forming drug-polyelectrolyte electrostatic complex gels.

Pure gellan hydrogel (G) prepared had the highest transparency when visualized and smoothness. On addition of ibuprofen to gellan gel, the GIb gels remained transparent. The plain and drug loaded polyelectrolyte complex (PEC) gels formed opaque gels. The opacity of the gel increased with increasing concentration of oppositely charged DEAE-Dextran. All the gels were uniform in

consistency and showed no appreciable particulate matter (free from grittiness). It is important for any topical formulation to be free from grittiness.

3.3.2. Physicochemical characteristics of plain and drug loaded nanoconjugate hydrogels

3.3.2.1. pH

The pH of plain and ibuprofen loaded gellan polymeric complex gels was presented in Figure 90 and Table 105 in the Appendix I.

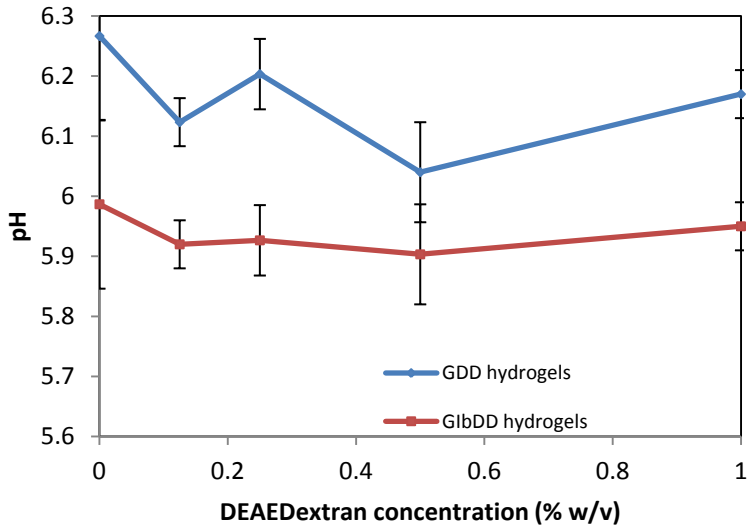

Figure 90 The pH of plain and ibuprofen loaded polymeric complex hydrogels. Each data point represents mean ± SD (n = 4).

It is important for the gels to be maintained at a stable pH to achieve the homogeneous distribution of ibuprofen in the gel matrix. The pH of pure gellan gel (G) was 6.27 and it ranged from 6.04 to 6.20 for Gellan-DEAE-Dextran complex gels. While the pH ranged from 5.90 to 5.95 for the ibuprofen loaded Gellan-DEAE-Dextran complex gels and 5.99 for GIb gels. The addition of ibuprofen caused a little decrease in pH. The pH of the final gels was adjusted to pH 6, which explains why all the gels were about pH 6.

3.3.2.2. Morphology and size – Scanning electron microscopy

The morphology of plain and drug loaded hydrogels was analyzed by SEM. The surface micrographs of plain and ibuprofen loaded Gellan-DEAE-Dextran PEC hydrogels are presented in Figure 91 and 92. The micrograph of plain gellan reference (G) gel showed strand-like smooth compact structured surface while the GDD gels showed crinkled rough surfaces in Figure 91.

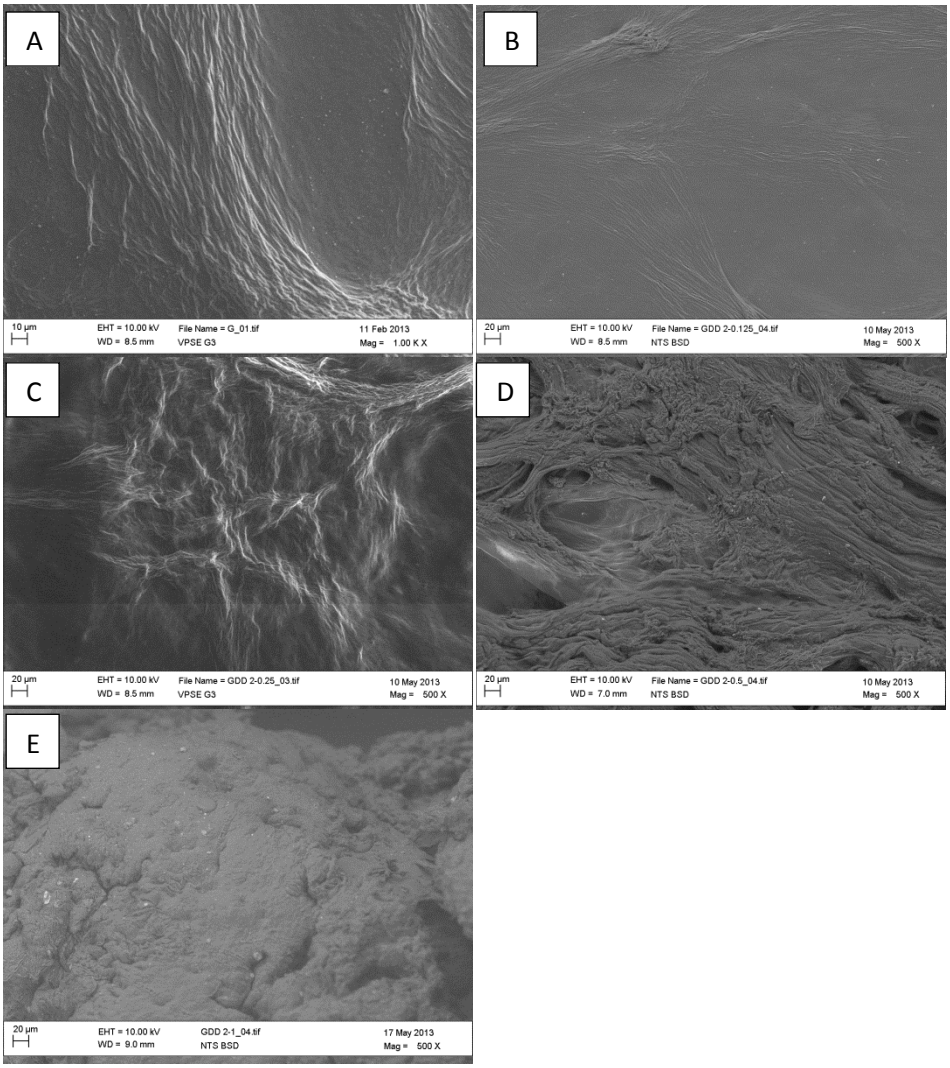

Figure 91 Scanning electron micrograph of gellan and gellan-DEAE-Dextran complex gels (A) plain gelan G, (B) gellan-DEAE-Dextran complex gel GDD 2:0.125, (C) GDD 2:0.25, (D) GDD 2:0.5 and (E) GDD 2:1

The ibuprofen loaded gellan GIb gel showed whitish ibuprofen dispersed through the gel while the GIbDD complex gels showed almost sphere-like shapes on the surface of their meshwork in Figure 92. The complex aggregate observed was due to the presence of ibuprofen and DEAE-Dextran in the gel matrix. The spherical patches increased in size and sphericalness in the micrometre range with

increasing concentration of DEAE-Dextran. The spherical patch sizes exhibited were 43.67 ± 9.13 µm (GIbDD 2:0.125), 33.26 ± 9.27 µm (GIbDD 2:0.25), 42.58 ± 6.68 µm (GIbDD 2:0.5) and 82.85 ± 8.13 µm (GIbDD 2:1).

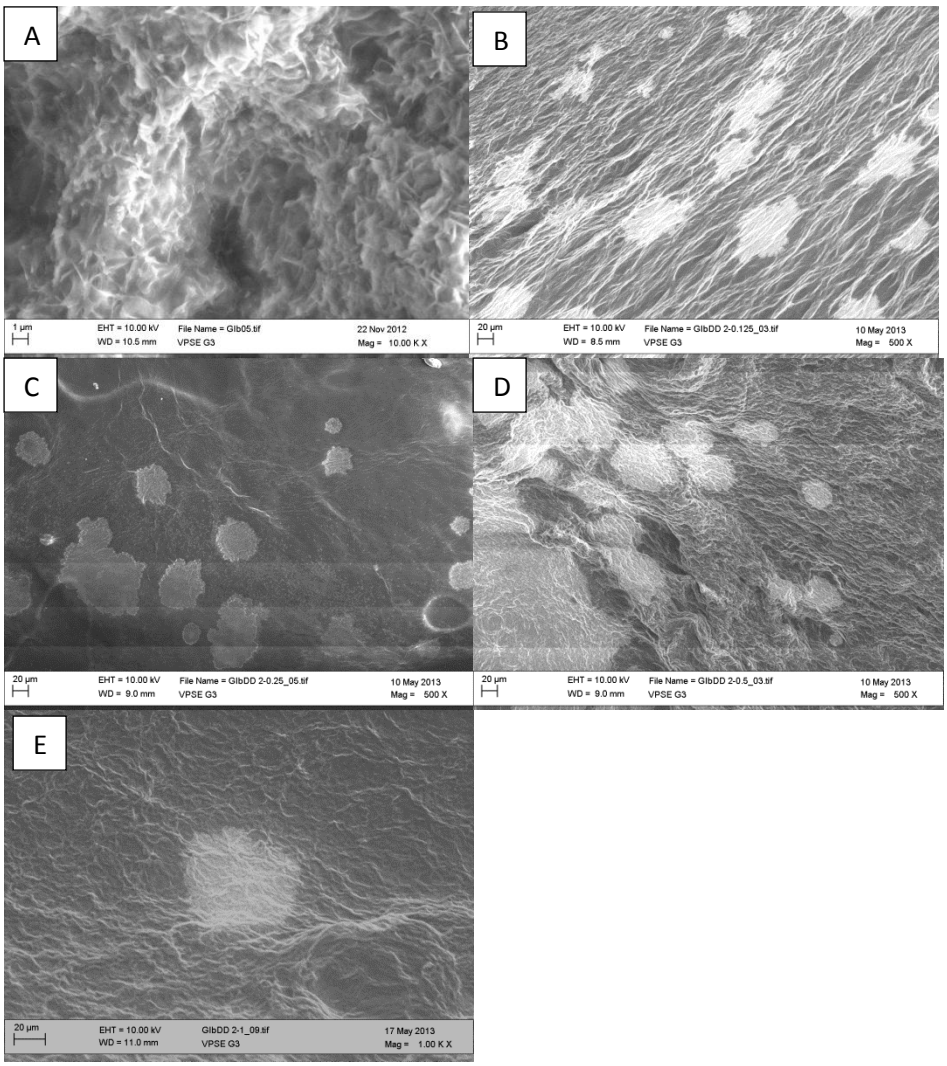

Figure 92 Scanning electron micrographs of ibuprofen loaded gellan and gellan-DEAE-Dextran complex gels (A) ibuprofen loaded GIb, (B) ibuprofen loaded gellan-DEAE-Dextran GIbDD 2:0.125, (C) GIbDD 2:0.25, (D) GIbDD 2:0.5, (E) GIbDD 2:1.

3.3.2.3. Spectroscopic studies – Fourier Transform Infra-Red (FTIR)

The FTIR spectra of pure ibuprofen, gellan gum, DEAE-Dextran, and the complex gel formulations were obtained and shown in Figure 93 and 94 with band positions shown in Table 69 and 70.

Gellan showed significant peaks at 3306 cm^{-1}, 1602 cm^{-1}, 1408 cm^{-1} and 1020 cm^{-1}. The peak assignments of gellan has also been described by Sudhamani *et al.* [25]. The peak at 3306 cm^{-1} is

assigned to hydroxyl stretching. Gellan gum has hydroxyl and carboxyl groups in its structure capable of undergoing a nucleophilic substitution reaction with DEAE-Dextran as described for the methacrylation of gellan gum (GG-MA) with the most favourable reaction being with the carboxyl group [26]. The peaks at 1602 cm^{-1} and 1408 cm^{-1} are assigned to the characteristic absorption band of carboxyl group in gellan gum [27]. The peak at 1020 cm^{-1} is assigned to C-O stretching. Pure DEAE-Dextran showed significant peaks at 3295 cm^{-1}, 2921 cm^{-1}, 1641 cm^{-1}, 1342 cm^{-1} and 1007 cm^{-1}. Pure DEAE-Dextran showed N-H deformation vibration at 1641 cm^{-1}. This peak is assigned to the free N-H group present on DEAE-Dextran. The peaks at 2921 cm^{-1} and 3295 cm^{-1} are assigned to N-H stretching and C-H stretching vibrations. The peaks at 1342 cm^{-1} and 1007 cm^{-1} are assigned to methyne C-H bending and C-N stretching respectively. The peaks at 3318 cm^{-1}, 2163 cm^{-1}, 2080 cm^{-1} and 1601 cm^{-1} in pure gellan shifted to 3285 cm^{-1}, 2214 cm^{-1}, 2108 cm^{-1} and 1638 cm^{-1} in the plain gellan reference G hydrogel. The peaks at 2897 cm^{-1}, 2324 cm^{-1}, 2018 cm^{-1}, 1974 cm^{-1}, 1403 cm^{-1}, 1295 cm^{-1}, 1198 cm^{-1}, 1021 cm^{-1}, 891 cm^{-1}, 836 cm^{-1} and 806 cm^{-1} in gellan disappeared in the gellan reference G hydrogel.

The -OH stretching peak at 3318 cm^{-1} in pure gellan and at 3309 cm^{-1} in DEAE-Dextran shifted to a range of 3277 to 3285 cm^{-1} in the GDD hydrogels. The N-H deformation peak at 1644 cm^{-1} in DEAE-Dextran and carboxyl group peak at 1601 cm^{-1} in gellan shifted to a range of 1631 to 1638 cm^{-1} in GDD gels. Additional peak at 1491 cm^{-1} was exhibited in GDD 2:0.125 and GDD 2:0.25 hydrogels. The C-C stretching peak at 1456 cm^{-1} in DEAE-Dextran shifted to 1491 cm^{-1} in the hydrogels with lower concentrations of DEAE-Dextran. The peak at 1491 cm^{-1} disappeared in GDD complex hydrogels with high concentrations of DEAE-Dextran in GDD 2:0.5 and GDD 2:1 hydrogels. Features of DEAE-Dextran became increasingly prominent in the complex gels with increasing concentration of DEAE-Dextran. GDD 2:0.5 and GDD 2:1 showed additional peaks at 1071 cm^{-1}, 1238 cm^{-1}, 1293 cm^{-1}, 1370 cm^{-1} and 1411 cm^{-1} contributed by gellan and DEAE-Dextran powders. The C-H stretching peak at 2922 cm^{-1} in DEAE-Dextran shifted to 2929 cm^{-1} and 2941 cm^{-1} in GDD 2:0.5 and GDD 2:1 hydrogels. The shifts and disappearances in peak suggest an interaction between gellan and DEAE-Dextran.

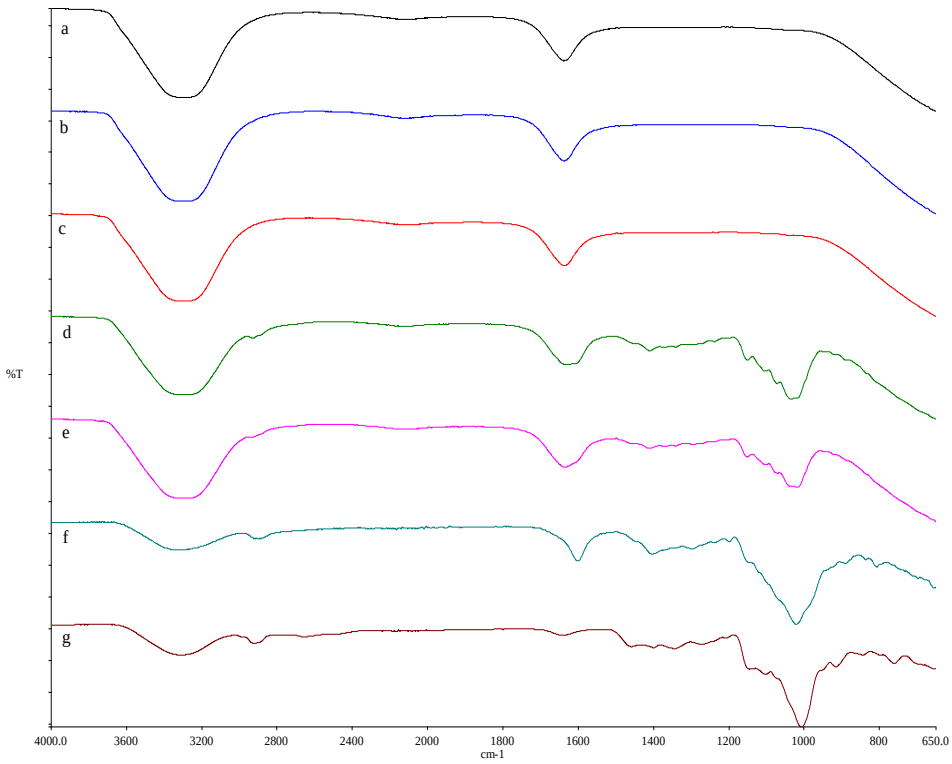

Figure 93 The FTIR spectra gellan and gellan-DEAE-Dextran PEC gels (a) plain gellan gel G (b) gellan-DEAE-Dextran gel GDD 2:0.125 (c) GDD 2:0.25 (d) GDD 2:0.5 (e) GDD 2:1 (f) gellan powder-reference (g) DEAE-Dextran powder-reference.

Table 69 FTIR spectral characteristics of gellan and plain gellan-DEAE-Dextran complex gels.

Formulation	Position of absorption band (Wavenumber) / cm^{-1}					
Gellan-reference	3318	2897	2080	1601	1198	891
		2324	2018	1403	1019	836
		2163	1974	1295		806
DEAE-Dextran reference	3309	2922	2161	1981	1269	915
		2656	2145	1644	1144	844
		2487	2081	1456	1102	797
		2287	2018	1399	1007	760
		2245	2010	1343		
G	3285	2214	2108	1638		
GDD 2:0.125	3285	2099	1988	1638	1491	
		2003				
GDD 2:0.25	3286	2213	2100	1638	1491	
		2170	1988			
GDD 2:0.5	3277	2929	2170	1631	1293	1071
		2382	2099	1410	1238	1035
		2322	1964	1370	1150	946
				1340	1103	920
GDD 2:1	3902	2941	2147	1634	1293	1071
	3284	2382	2113	1411	1238	1017
			1988	1369	1151	
				1340	1103	

The bands assigned as the finger prints of ibuprofen in literature include 2992 cm^{-1}, 1706 cm^{-1} (carboxylic acid), 1230 cm^{-1} and 779 cm^{-1} [28-29]. The peak at 2992 cm^{-1} is assigned to the C-H stretching. The peak at 1706 cm^{-1} is assigned to strong carbonyl band absorbance which corresponds

to the carboxyl group present in ibuprofen. The peaks at 1230 cm^{-1} and 779 cm^{-1} are assigned to skeletal C-C vibration and aromatic C-H bending. The other peaks in the region 1200 to 1000 cm^{-1} are contributions from the benzene ring. All these major peaks in ibuprofen were absent in the GIb and GIbDD gels. Ibuprofen loaded gellan gel GIb exhibited new peaks at 3902 cm^{-1}, 3749 cm^{-1},2383 cm^{-1}, 2126 cm^{-1}, 1637 cm^{-1} and 1491 cm^{-1}. The C=O, C=C and C-C stretching peaks at 1710 cm^{-1} (carbonyl), 1563 cm^{-1} and 1229 cm^{-1} for pure ibuprofen disappeared in the spectra of ibuprofen loaded GIb and GIbDD hydrogels. This suggests a new product has been formed based on interaction of ibuprofen with the polymers as confirmed by the DSC thermograms of the complex gels exhibiting a single melting peak.

The peaks at 3318 cm^{-1} in pure gellan and at 3309 cm^{-1} DEAE-Dextran shifted to a range of 3296 to 3320 cm^{-1} in the GIbDD gels.The N-H deformation peak at 1644 cm^{-1} in DEAE-Dextran and carboxyl peak at 1601 cm^{-1} in gellan shifted to a range of 1635 to 1637 cm^{-1} in the GIbDD hydrogels.

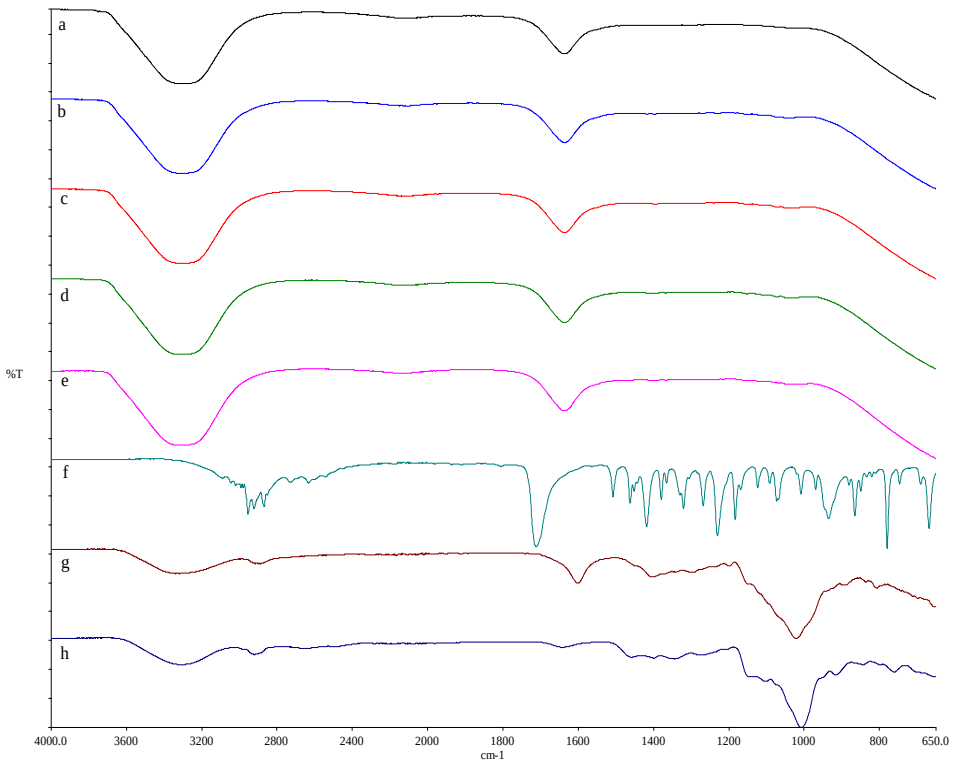

Figure 94 The FTIR spectra of ibuprofen incorporated into polymer complex gels (a) ibuprofen loaded gellan gel GIb (b) ibuprofen gellan-DEAE-Dextran complex gel GIbDD 2:0.125 (c) GIbDD 2:0.25 (d) GIbDD 2:0.5 (e) GIbDD 2:1 (f) Ibuprofen powder-reference (g) gellan powder-reference (h) DEAE-Dextran powder-reference.

Table 70 Spectral characteristics at various wavelengths for gellan, DEAE-Dextran and ibuprofen complex GIbDD hydrogels.

Formulation	Position of absorption band (Wavenumber) / cm^{-1}					
Ibuprofen-reference	3088	2954	2144	1451	1183	865
	3044	2922	2115	1442	1168	849
	3015	2868	2079	1418	1123	834
	2991	2851	1911	1379	1092	820
	2980	2728	1887	1365	1073	810
		2631	1803	1329	1068	779
		2601	1706	1321	1008	746
		2542	1563	1305	969	690
		2203	1507	1268	935	667
		2163	1461	1229	880	
Gellan-reference	3318	2897	2080	1601	1198	891
		2324	2018	1403	1019	836
		2163	1974	1295		806
DEAE-Dextran reference	3309	2656	2145	1644	1144	915
	2922	2487	2081	1456	1102	844
		2287	2018	1399	1007	797
		2240	2010	1343		760
		2161	1981	1269		
GIb	3902	3284	2126	1637	1473	1368
	3749	2383		1491	1396	
GIbDD 2:0.125	3314	2147	1984	1635	1396	1152
		2109	1974	1461	1230	1041
GIbDD 2:0.25	3305	2128		1635	1396	1105
				1459	1151	1042
GIbDD 2:0.5	3296	2362		1635	1151	1041
		2109		1397		
GIbDD 2:1	3320	2150	1957	1637	1151	1015
				1396		

3.3.2.4. Thermal analysis

3.3.2.4.1. Differential scanning calorimetry

The DSC thermal characteristics of plain (G) and binary (GDD) hydrogels were compared with pure gellan and DEAE-Dextran and presented in Figure 137 and Table 90. Pure gellan powder exhibited a broad melting peak at 127.86 °C and exothermic decomposition peak at 254.84 °C. DEAE-Dextran showed a small peak at 57.26 °C which indicated its glass transition endotherm (Tg); a broad endothermic peak at 124.05 °C due to its amorphous characteristic; a small peak at 201.21 °C and a final peak at 268.50 °C attributed to the decomposition of DEAE-Dextran.

The DSC thermograms of hydrogels exhibited one endothermic melting peak for plain reference gellan hydrogel (G) at 114.2 °C and the GDD hydrogels ranged from 99.8 to 115.3 °C shown in Table 71 which indicated that the two polymers merged into one peak. This was a shift to lower values

from the melting peak shown by gellan powder reference at 127.9 °C, DEAE-Dextran powder reference at 124.1 °C which suggested the miscibility or compatibility of gellan and DEAE-Dextran.

Table 71 DSC of plain gellan and gellan - DEAE-Dextran PEC gels. Each value represents mean ± SD (n = 4).

Formulation	Onset (°C)	Peak (°C)	End (°C)	Delta H (J/g)	Area (mJ)
Gellan-reference	77.70±1.55	127.86±7.43	186.32±8.76	168.31±8.81	1043.54±52.70
	246.56±12.37	264.02±12.75	270.88±12.86	-129.64±6.5	-803.81±40.22
DEAE-Dextran-reference	53.55±0.85	57.86±0.76	63.97±0.92	5.10±0.08	35.16±0.41
	87.43±1.22	124.05±4.16	158.87±5.34	139.17±5.64	960.30±40.48
	187.42±8.23	201.54±10.58	210.60±11.45	12.72±0.84	87.74±1.25
	245.83±12.74	268.50±11.78	281.53±13.66	70.84±0.92	488.852±21.22
G	98.13±3.21	114.15±5.17	119.56±4.78	1392.94± 57.51	3900.23±208.43
GDD 2:0.125	101.62±4.32	115.26±4.96	121.60±6.38	1535.61±74.38	5067.50±312.19
GDD 2:0.25	101.68±4.28	112.11±4.35	120.70±5.86	1324.11±43.10	4237.14±261.76
GDD 2:0.5	101.89±3.84	114.94±5.08	128.60±5.45	1092.03±41.22	3494.47±188.73
GDD 2:1	70.75±1.67	99.83±3.36	113.26±4.20	299.34±18.78	927.96±38.04

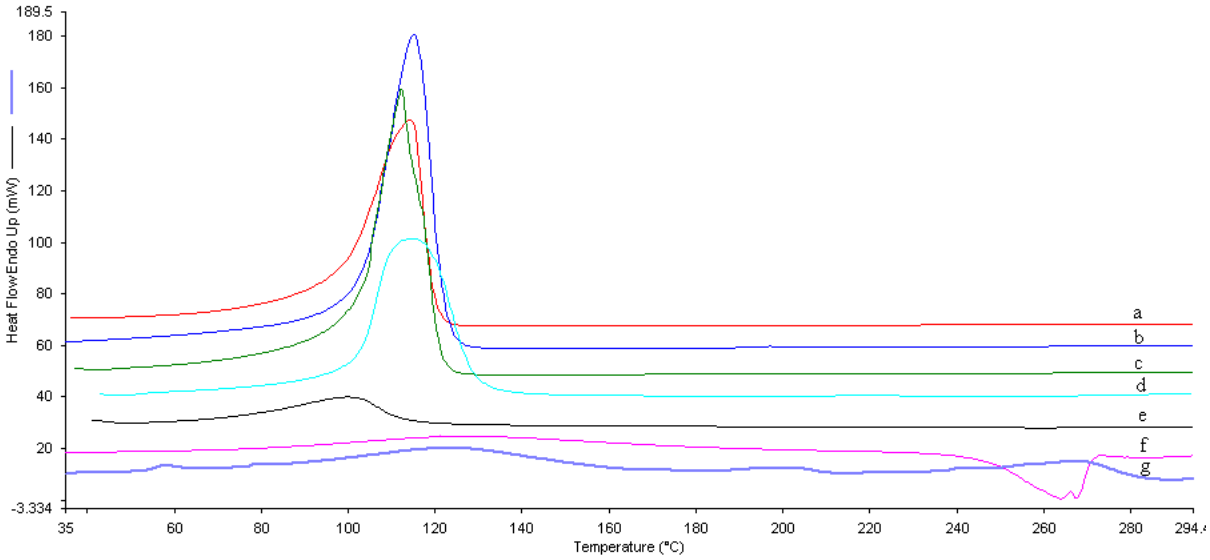

Figure 95 DSC thermograms of gellan and gellan-DEAE-Dextran PEC gels (a) plain gellan reference G (b) GDD 2:0.125 (c) GDD 2:0.25 (d) GDD 2:0.5 (e) GDD 2:1 (f) gellan powder-reference (g) DEAE-Dextran powder-reference.

The melting peak and enthalpy change profiles of plain and ibuprofen loaded binary and ternary hydrogels were presented in Figures 96 and 97 respectively. The melting peak profile of GDD hydrogels exhibited two maxima values at 0.125 and 0.5% of DEAE-Dextran with increasing DEAE-Dextran concentration. While the melting peak profile of GIbDD hydrogels initially increased to maximum value at 0.125% DEAE-Dextran and then decreased with increasing DEAE-Dextran concentration. The DSC enthalpy profiles of GDD and GIbDD hydrogels initially increased to maximum values at 0.125% and then decreased steadily with increasing DEAE-Dextran concentration.

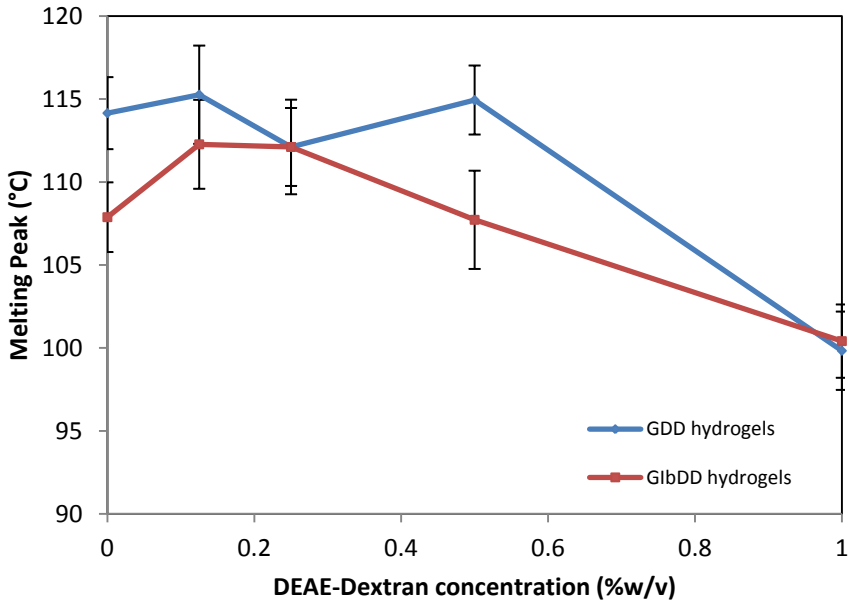

Figure 96 DSC melting peak profile of plain and ibuprofen loaded gellan and gellan - DEAE-Dextran PEC gels. Each data point represents mean ± SD (n = 4).

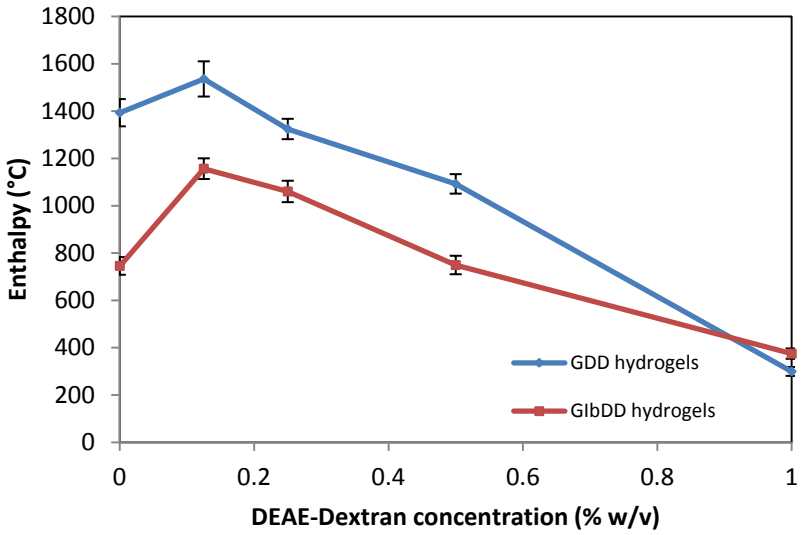

Figure 97 DSC enthalpy profile of plain and ibuprofen loaded gellan and gellan - DEAE-Dextran PEC gels. Each data point represents mean ± SD (n = 4).

DSC thermograms of ibuprofen loaded gellan, gellan-DEAE-Dextran hydrogels were presented in Figure 142 and Table 9272. The DSC thermograms of Ibuprofen showed characteristic sharp endothermic peak at 80.07 °C suggesting its crystallinity, with enthalpy of fusion of 118.64 J/g. This melting peak is higher than the literature value for pure ibuprofen in the range of 75 to 78 °C [30]. This could be due to some impurity in the ibuprofen sample however in a similar study, Kumar *et al.*

reported that the melting peak of ibuprofen was 82.76 °C [31], while gellan and DEAE-Dextran showed endothermic peaks at 127.86 °C and 124.05 °C respectively. The endothermic peaks were exhibited by GIb at 107.9 °C and the GIbDD gels ranged from 100.4 to 112.3 °C as shown in Table 72. The sharp endothermic peak exhibited by ibuprofen at 82.7 °C corresponding to its melting point completely disappeared in the ibuprofen loaded gellan GIb and GIbDD complex hydrogels shown in Figure 98 suggesting an interaction between the drug and the polymer.

Table 72 DSC of ibuprofen loaded polymer complex (Gellan-DEAE-Dextran) gels. Each value represents mean ± SD (n = 4)

Formulation	Onset (°C)	Peak (°C)	End (°C)	Delta H (J/g)	Area (mJ)
Ibuprofen-reference	76.85±0.64 236.27±11.36	82.69±2.46 264.63±19.41	86.79±3.27 273.47±17.20	92.90±4.32 203.71±18.79	826.37±55.04 1753.15±74.65
Gellan-reference	77.70±1.55 246.56±12.37	127.86±7.43 264.02±12.75	186.32±8.76 270.88±12.86	168.31±8.81 -129.64±6.5	1043.54±52.70 -803.81±40.22
DEAE-Dextran-reference	53.55±0.85 87.43±1.22 187.42±8.23 245.83±12.74	57.86±0.76 124.05±4.16 201.54±10.58 268.50±11.78	63.97±0.92 158.87±5.34 210.60±11.45 281.53±13.66	5.10±0.08 139.17±5.64 12.72±0.84 70.84±0.92	35.16±0.41 960.30±40.48 87.74±1.25 488.852±21.22
GIb	95.14±3.87	107.88±4.10	115.67±4.75	745.30±37.45	2161.36±91.94
GIbDD 2:0.125	101.64±4.06	112.27±4.68	119.57±5.32	1156.40±43.70	3469.19±188.52
GIbDD 2:0.25	101.87±4.62	112.11±4.85	118.52±5.41	1060.11±45.25	2968.32±146.37
GIbDD 2:0.5	96.45±3.82	107.72±4.96	114.36±4.96	749.15±39.04	2172.54±112.74
GIbDD 2:1	78.66±1.79	100.41±4.21	107.72±4.65	374.65±21.96	1086.49±48.36

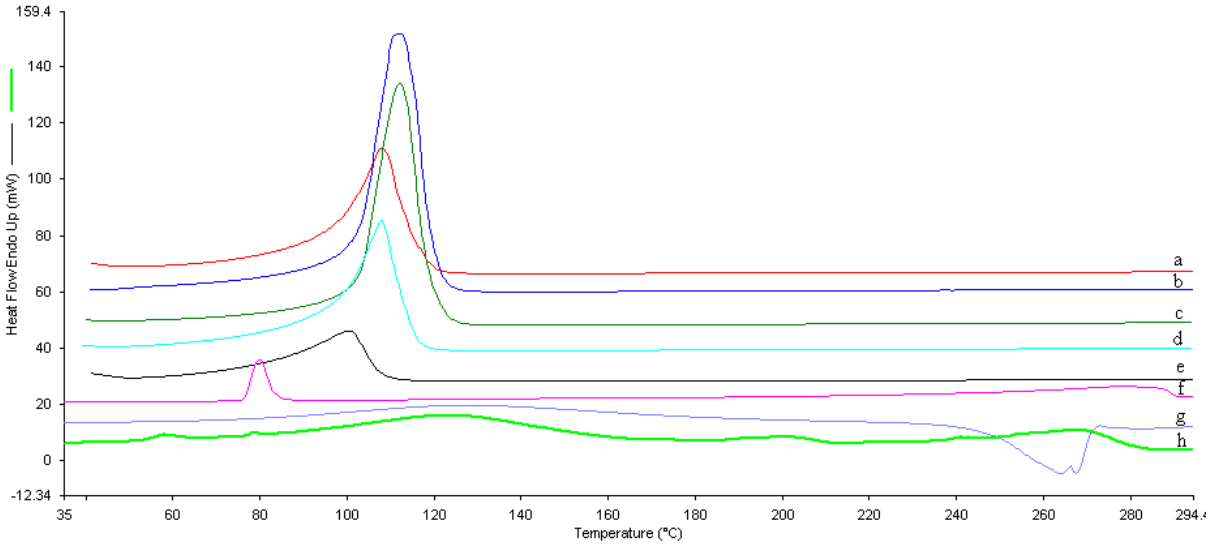

Figure 98 DSC thermograms of ibuprofen incorporated into polymer complex gels (a) ibuprofen loaded gellan GIb (b) ibuprofen loaded gellan-DEAE-Dextran GIbDD 2:0.125 (c) GIbDD 2:0.25 (d) GIbDD 2:0.5 (e) GIbDD 2:1 (f) Ibuprofen powder-reference (g) gellan powder-reference (h) DEAE-Dextran powder-reference.

3.3.2.4.2. Thermogravimetric analysis

TGA analysis was conducted to examine the thermal stability of the polymer gels as presented in Figure 99 and 100; Table 73 andTable 74. Gellan powder showed two steps of inflection at 90.4 °C and 264.9 °C with corresponding weight losses of 7.9% and 59.7%. DEAE-Dextran showed two steps of inflection at 77.47 °C and 272.15 °C with corresponding weight losses of 6.94% and 67.61%. The first weight loss below 150 °C was attributed to loss of free or loosely bound water while the second weight loss was due to the decomposition of the polymers. The plain gellan reference G hydrogel showed two steps of inflection at 100 °C and 257 °C with corresponding weight losses of 97.17%, and 2.14% respectively. The GDD gels also exhibited two steps of inflection ranging from 106.5 °C to 108.7 °C and 251.8 °C to 258.3 °C; with corresponding weight losses ranging from 97.20 to 97.70% and from 2.00 to 2.80%. The total weight loss exhibited by G hydrogel was 99.30% and for GDD gels was in the range of 99.60 to 100%. The prepared hydrogels lost their high moisture content faster when compared to the individual polymer powders. It showed that the hydrogels main constituent was water. The plain gellan G gel was able to withstand more heat when compared to the GDD complex gels.

Table 73 TGA of plain gellan and gellan-DEAE-Dextran PEC hydrogels. Each value represents mean ± SD (n = 4).

Formulation	Onset (°C)	End (°C)	Step of inflection (°C)	Delta Y (%)
Gellan-reference	43.99 ±0.65	131.17 ±4.72	90.39 ±3.15	7.85 ±0.08
	257.79 ±12.21	282.29 ±12.74	264.91 ±12.10	59.67 ±0.93
DEAE-Dextran-reference	47.16 ±0.47	106.74 ±4.32	77.47 ±1.47	6.94 ±0.12
	261.20 ±11.43	301.16 ±15.72	272.15 ±12.62	67.61 ±0.98
G	59.47 ±0.56	133.66 ±2.07	100.00 ±3.78	97.17 ±3.12
	253.10 ±12.11	280.60 ±13.18	257.03 ±12.65	2.14 ±0.01
GDD 2:0.125	69.75 ±1.05	122.59 ±5.13	107.86 ±4.19	97.34 ±3.24
	237.64 ±12.25	281.77 ±13.65	251.77 ±13.18	2.37 ±0.01
GDD 2:0.25	71.78 ±1.13	116.47 ±4.62	107.14 ±4.02	97.18 ±2.98
	241.82 ±12.54	280.15 ±12.68	251.68 ±12.95	2.43 ±0.01
GDD 2:0.5	70.79 ±1.05	116.12 ±4.55	108.69 ±4.18	97.70 ±2.66
	233.80 ±11.63	293.20 ±12.76	254.19 ±12.74	2.76 ±0.02
GDD 2:1	71.59 ±1.12	115.74 ±4.31	106.51 ±3.94	97.74 ±3.40
	235.33 ±10.86	299.01 ±12.84	258.31 ±12.46	2.02 ±0.01

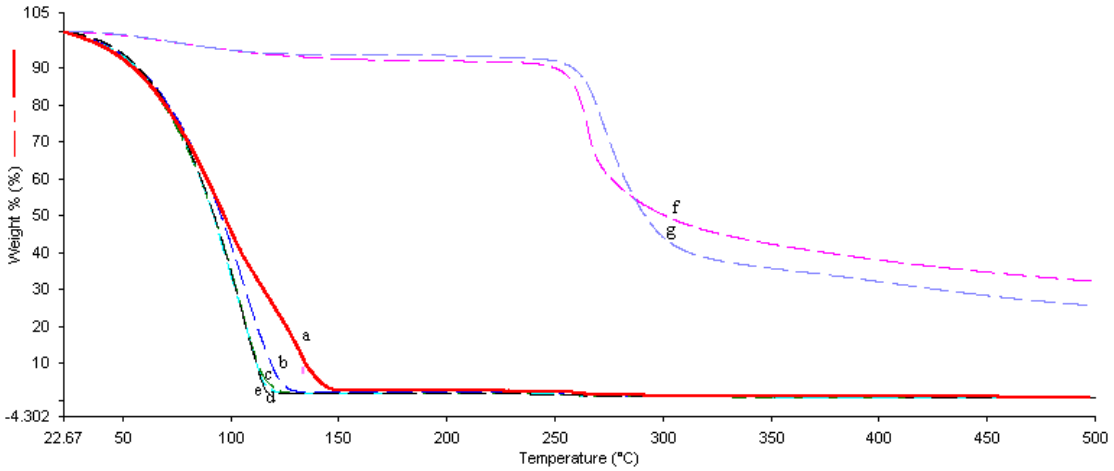

Figure 99 TGA thermogram of plain gellan and gellan-DEAE-Dextran PEC gels (a) plain gellan reference G (b) gellan-DEAE-Dextran complex GDD 2:0.125 (c) GDD 2:0.25 (d) GDD 2:0.5 (e) GDD 2:1 (f) gellan powder-reference (g) DEAE-Dextran powder-reference.

Ibuprofen exhibited one step of inflection at 240.76 ˚C attributed to the heat of decomposition of the drug or disintegration of the molecular chains with a complete weight loss of 99.50%; while gellan and DEAE-Dextran powder reference exhibited two steps of inflection with a total weight loss of 67.52% and 74.55% respectively. The ibuprofen loaded gellan GIb gel showed two steps of inflection at 91.9 °C, and 282.8 °C with corresponding weight losses of 94.60%, and 4.10% respectively. The GIbDD gels also exhibited two steps of inflection ranging from 86.4 to 109.6 °C and 246.8 to 256.5 °C; with corresponding weight losses ranging from 94.60 to 96.70% and from 2.60 to 4.00%. The first high percentage weight loss was due to loss of loosely bound water in the hydrogel while the second low percentage weight loss was due to decomposition of the polymer complexes. The GIb hydrogel was able to withstand more heat than the GIbDD complex hydrogels.

Table 74 TGA of ibuprofen incorporated into gellan and gellan-DEAE-Dextran PEC hydrogels. Each value represents mean ± SD (n = 4).

Formulation	Onset (°C)	End (°C)	Inflection step (°C)	Delta Y (%)
GIb	55.94 ±0.82	105.00 ±3.96	91.86 ±3.14	94.58 ±3.06
	270.43 ±12.31	303.73 ±13.66	282.82 ±12.75	4.11 ±0.02
GIbDD 2:0.125	60.09 ±0.74	131.44 ±4.87	101.47 ±3.78	95.44 ±3.12
	228.55 ±11.16	275.73 ±12.25	249.75 ±11.62	2.36 ±0.01
GIbDD 2:0.25	67.81 ±0.71	120.64 ±4.62	103.04 ±3.22	95.60 ±2.98
	236.72 ±11.40	274.85 ±12.14	254.67 ±11.70	2.90 ±0.01
GIbDD 2:0.5	52.61 ±0.61	127.61 ±4.88	86.44 ±2.35	96.67 ±2.86
	231.68 ±11.24	294.82 ±12.67	246.79 ±10.94	3.28 ±0.02
GIbDD 2:1	69.06 ±0.66	119.75 ±4.32	109.63 ±3.47	94.56 ±2.74
	209.81 ±11.10	358.79 ±13.48	256.52 ±11.02	4.04 ±0.02
Ibuprofen-reference	207.81 ±11.23	247.08 ±11.87	240.76 ±12.32	99.50 ±1.95
Gellan-reference	43.99 ±0.65	131.17±4.72	90.39 ±3.15	7.85 ±0.08
	257.79 ±12.21	282.29±12.74	264.91 ±12.10	59.67 ±0.93
DEAE-Dextran-reference	47.16 ±0.47	106.74 ±4.32	77.47 ±1.47	6.94 ±0.12
	261.20 ±11.43	301.16 ±15.72	272.15 ±12.62	67.61 ±0.98

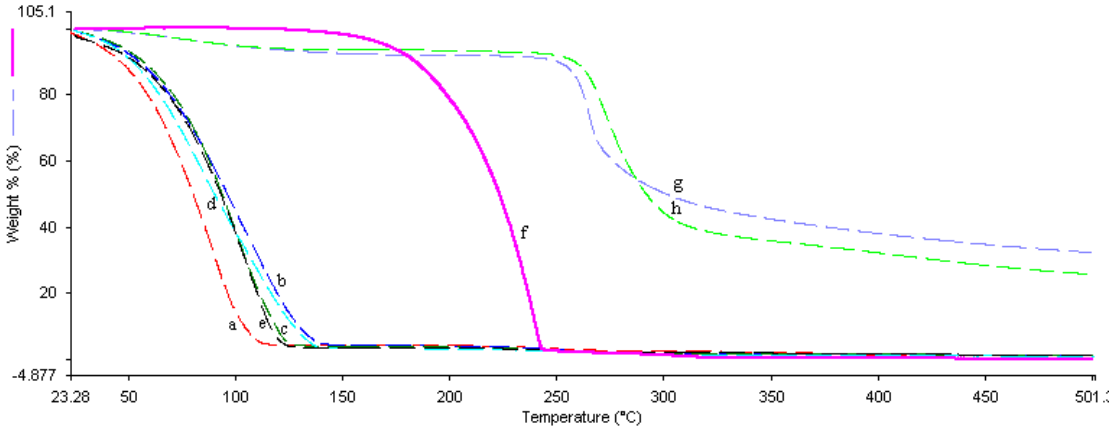

Figure 100 TGA thermograms of ibuprofen incorporated into polymer complex gels (a) ibuprofen loaded gellan GIb (b) ibuprofen loaded gellan-DEAE-Dextran GIbDD 2:0.125 (c) GIbDD 2:0.25 (d) GIbDD 2:0.5 (e) GIbDD 2:1 (f) Ibuprofen powder-reference (g) gellan powder-reference (h) DEAE-Dextran powder-reference.

3.3.3. Rheological studies

3.3.3.1. Oscillatory measurements

Rheology is the science of the deformation and flow of matter. It is useful in the monitoring of gelation (crosslinking) and microstuctural changes in a material allowing materials to be probed in 'at rest' conditions without disruption of the microstructure [32]. Rheological studies were carried out on all formulations of gellan, plain GDD complex and ibuprofen loaded polymer GIbDD complex hydrogels. It measured the viscoelastic response of the gels to an applied strain.

Rheological properties are used to describe the flow characteristics and textural behaviour of materials. The storage modulus – elastic part (G'), loss modulus - viscous part (G"), complex viscosity

(η*) and loss tangent (δ) were measured in oscillation mode. The storage or elastic modulus is the measure of how structured a material is and its ability of the material to store energy. The loss or viscous modulus is the ability of the material to dissipate energy. The loss tangent is the ratio of energy lost to energy stored, in the cyclic deformation (the ratio of G"/ G'). When tan δ < 1 (because G' > G") means a prevalent elastic behaviour and or gel state.

The strain amplitude values were verified to ensure that all the rheological measurements were performed within the viscoelastic range, with the storage (G') and the loss (G") moduli being independent of the strain [33]. The linear viscoelastic region can be observed in Figure 101 where G' and G" are both linear across the strain range 0.1 to 50% suggesting that a strain of 1% could be used for all gellan hydrogel formulations measurements. G' and G" are linear up to about 50%. Beyond the linear viscoelastic (LVE) range, the G' and G" abruptly decreased indicating that the structural breakdown occurred as a consequence of large deformations imposed [34]. The results showed that G' > G" for all samples in the LVE range exhibiting prevalence of the elastic behaviour over the viscous behaviour.

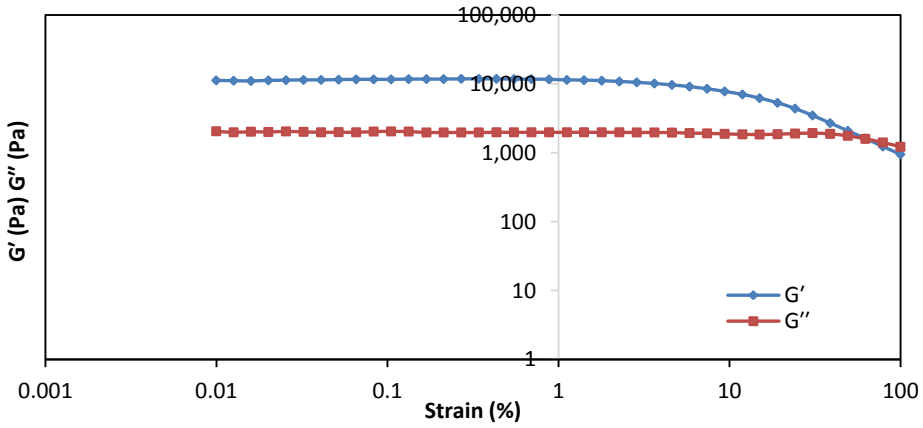

Figure 101 Strain amplitude sweeps of G' and G" with linearity at strain of 1% for plain gellan reference G hydrogel.

After the gels linear viscoelastic range was defined by a strain sweep, the gels were further characterized using frequency sweep. Figures 102 to 105 below showed the behaviour of viscoelastic parameters G', G", η* and tan δ when subjected to frequency oscillation sweep across a frequency

range of 0.1 to 50 Hz at a strain of 1% at 32 °C for plain gellan gel, gellan-DEAE-Dextran GDD complex gels and ibuprofen loaded GIbDD complex gels. Figures 102 and 103 showed an increase in G' and G" of the hydrogels as the frequency increased across the frequency range. The storage modulus G' solid-like characteristics of all the hydrogels tested; predominated over the loss modulus G" liquid-like characteristics.

The GDD complex gels exhibited an increase in G' (elastic modulus) in ascending order through G < GDD 2:1 < GDD 2:0.125 < GDD 2:0.25 < GDD 2:0.5 with GDD 2:0.5 exhibiting the highest G' value (elasticity) at frequency of 1 Hz mid way through the frequency sweep shown in Figure 102A. Across the frequency range, G' increased sharply from 0.05 to 1 Hz (at low frequency) and slowly increased till 50 Hz for G, GDD 2:0.125 and GDD 2:0.25 gels; while G' increased steadily across the frequency range for GDD 2:0.5 and GDD 2:0.1. The plain gellan G, GDD 2:0.125 and GDD 2:0.25 (lower concentrations of DEAE-Dextran) hydrogels required a higher frequency to assume the solid-like state characterized by the sharp increase in G' to achieve a similar response when compared to the GDD 2:0.5 and GDD 2:0.1 (higher concentrations of DEAE-Dextran) hydrogels.

Addition of ibuprofen to plain gellan G gel, the G' of GIb gel was higher when compared to plain G gel at low frequency from 0.05 to 1 Hz, and the G' of GIb gel became lower than G gel at higher frequency between 1 and 50 Hz. While with GIbDD complex gel, the G' increased across the frequency range of 0.05 to 50 Hz in ascending order through GIb < GIbDD 2:0.125 < GIbDD 2:0.25 < GIbDD 2:0.5 < GIbDD2:1 shown in Figure 102B. The addition of DEAE-Dextran increased the elasticity of the gels as the concentration of DEAE-Dextran increased which suggests the enhancement of their elasticity and a clear indication of the improvement on the three dimensional network stability. The formulations with lesser G' showed a less solid-like behaviour, hence are less elastic in viscoelastic character. A near plateau was achieved for all the hydrogels towards the end of the frequency range (50 Hz) suggesting a stable polymer network.

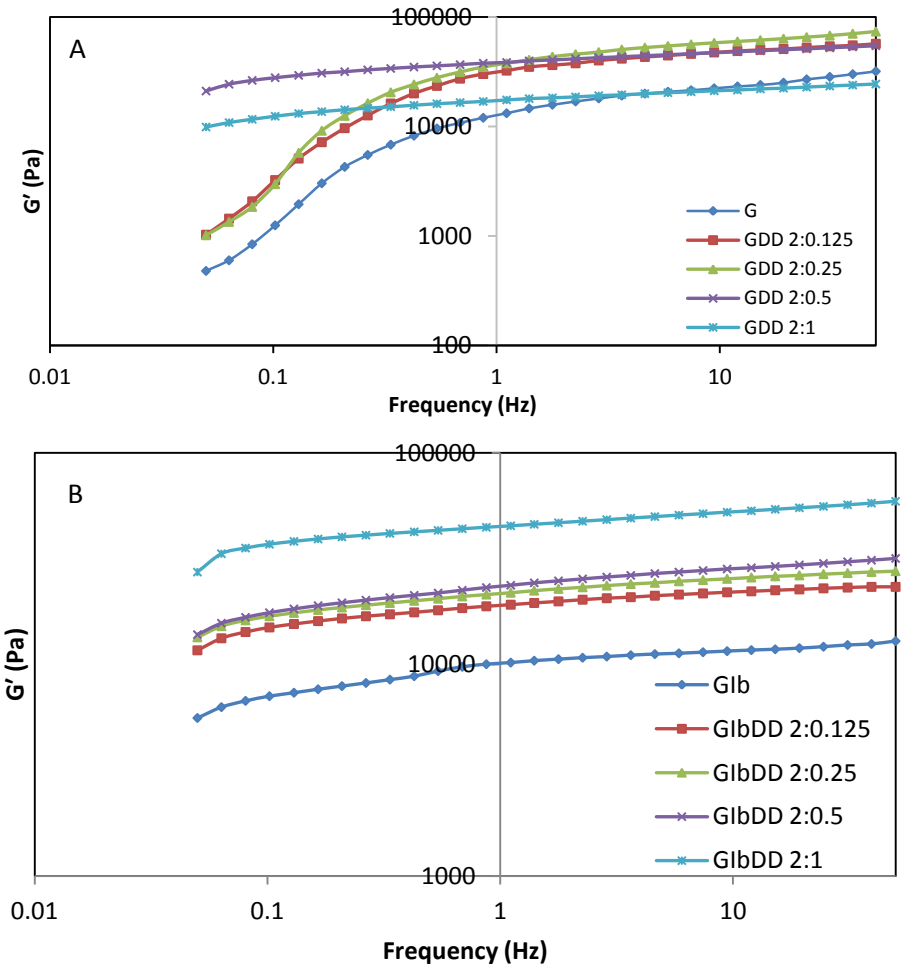

Figure 102 Storage modulus profiles across a frequency range of 0.01 to 50 Hz at 32°C for (A) plain gellan G and GDD complex gels and (B) Ibuprofen loaded gellan GIb and GIbDD complex gels. Each data point represents mean ± S.D (n = 4).

The GDD complex gels exhibited an increase in G" in ascending order through G < GDD 2:1 < GDD 2:0.125 < GDD 2:0.25 < GDD 2:0.5; with GDD 2:0.5 exhibiting the highest G" value (viscous) at frequency of 1 Hz shown in Figure 103A. Across the frequency range, G" increased sharply from 0.05 to 1Hz and slowly increased till 50 Hz for G, GDD 2:0.125 and GDD 2:0.25 gels; while G" increased steadily across the frequency range for GDD 2:0.5 and GDD 2:1. In the GIbDD complex gels, the G" increased slowly across the frequency range of 0.05 to 50Hz in ascending order through G < GIbDD 2:0.125 < GIbDD 2:0.25 < GIbDD 2:0.5 < GIbDD2:1 shown in Figure 103B. The addition of DEAE-Dextran increased the storage moduli of ibuprofen loaded GIbDD complex gels with increasing concentration of DEAE-Dextran.

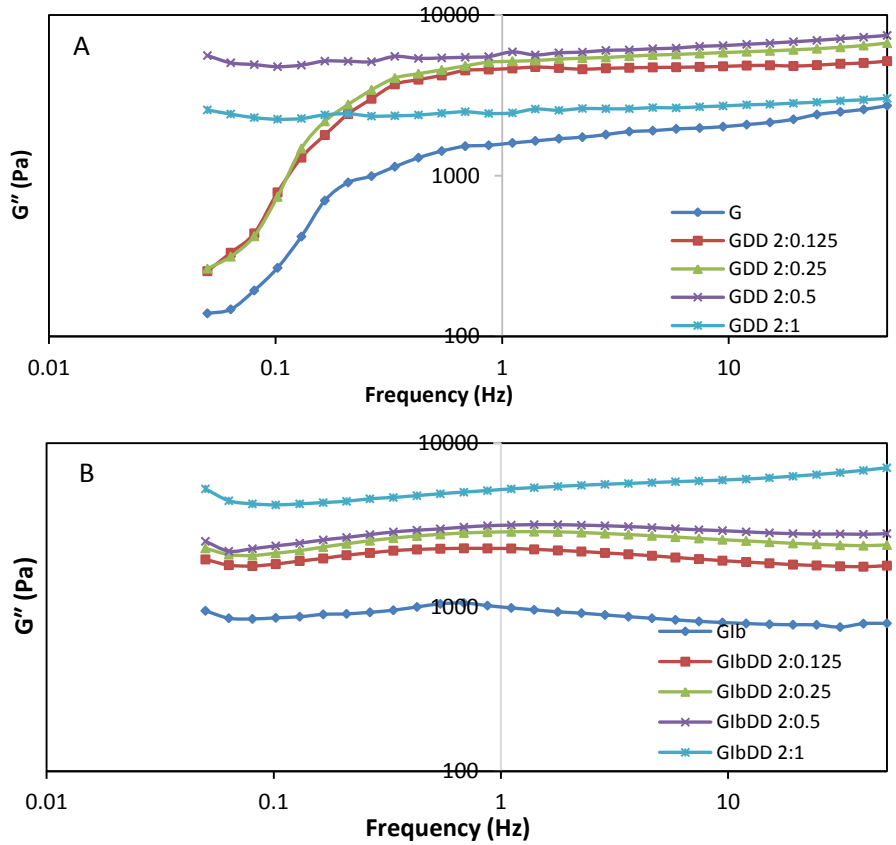

Figure 103 Loss modulus profiles across a frequency range of 0.01 to 50 Hz at 32 °C for (A) plain gellan G and GDD complex gels and (B) Ibuprofen loaded gellan Glb and GlbDD complex gels. Each data point represents mean ± S.D (n=4).

The flow behaviour of the gels in Figure 104A and 104B showed that for G, and low concentrations of DEAE-Dextran GDD 2:0.125 and GDD 2:0.25 gels, there was an initial increase in complex viscosity followed by a decrease across the frequency range while complex viscosity for GDD 2:0.5, GDD 2:1 and GlbDD gels decreased steadily across the frequency, suggesting pseudoplastic behaviour.

With reference to GDD complex gels, complex viscosity increased in ascending order through G < GDD 2:1 < GDD 2:0.125 < GDD 2:0.25 < GDD 2:0.5; with GDD 2:0.5 exhibiting the highest complex viscosity trend shown in Figure 104A. Complex viscosity decreased across the frequency range in ibuprofen loaded GlbDD complex gels. In GlbDD complex gels, complex viscosity increased in ascending order through Glb < GlbDD 2:0.125 < GlbDD 2:0.25 < GlbDD 2:0.5 < GlbDD 2:1; with GlbDD 2:1 exhibiting the highest complex viscosity trend shown in Figure 104B. These results showed an increase in the complex viscosity frequency sweep profiles as DEAE-Dextran content was increased.

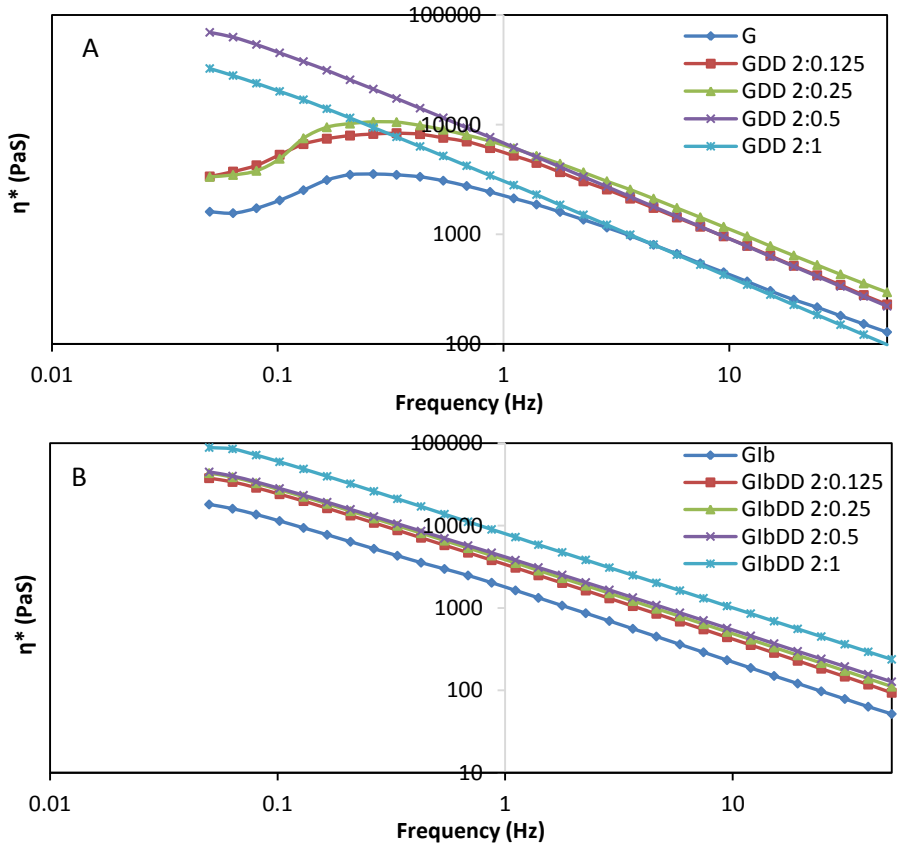

Figure 104 Complex viscosity profiles across a frequency range of 0.01 to 50 Hz at 32 °C for (A) plain gellan G and GDD complex gels and (B) Ibuprofen loaded gellan GIb and GIbDD gels. Each data point represents mean ± S.D (n = 4).

Tan delta (δ) is the ratio of energy loss to energy stored which gives the overall viscoelasticity of the sample [35]. Therefore as tan δ becomes smaller, the elasticity of the material increases, but the viscous behaviour is reduced [36].

The tan δ frequency sweep profiles for all the formulations were below 1 (Figure 105A and Figure 105B) indicating that all samples were gels with dominant elastic (solid like) behaviour [37]. Tan δ remained almost constant near 0.1 for all the plain and ibuprofen loaded gellan-DEAE-Dextran complex gels. Addition of DEAE-Dextran slightly increased the tan δ values of GDD and GIbDD gels as the concentration of DEAE-Dextran increased. This indicated a more solid-like state resulting in a decrease in tan δ. Generally, frequency sweeps of the tested plain and ibuprofen loaded complex gels showed typical gel behaviour [38] with G' greater than G" and tan δ well below 1.

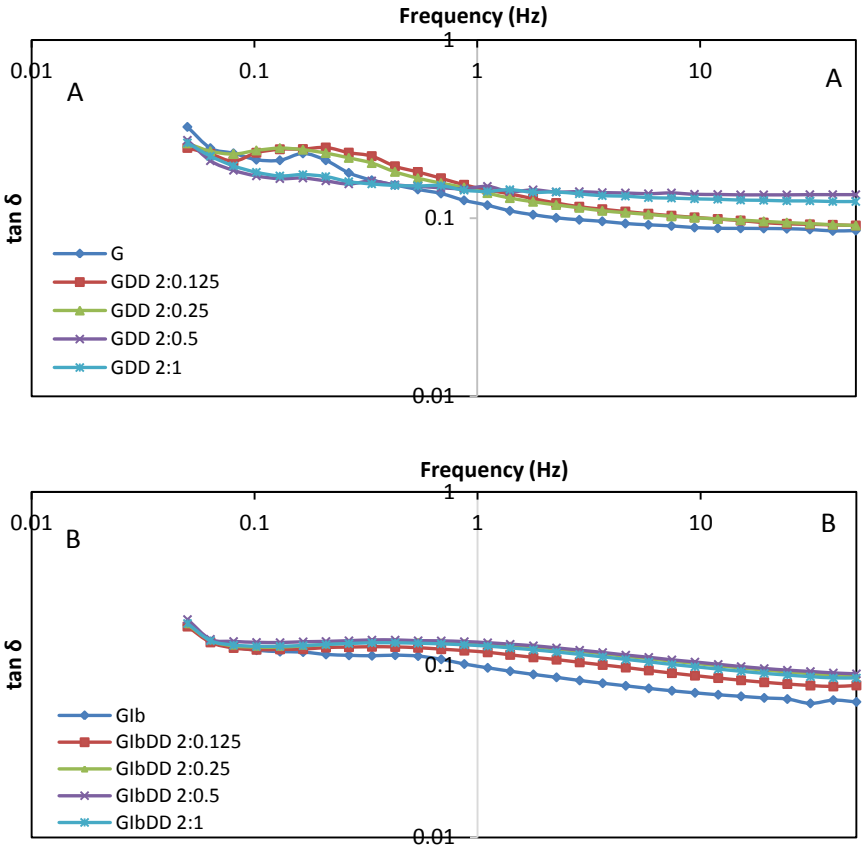

Figure 105 Tan delta profiles across a frequency range of 0.01 to 50 Hz at 32°C for (A) Gellan G and GDD complex gels and (B) Ibuprofen loaded gellan GIb and GIbDD complex gels. Each data point represents mean ± S.D (n = 4).

The flow behaviour of plain gellan G hydrogel is shown in Figure 106. The viscosity of gellan G hydrogel decreased with increase in shear rate which indicated a pseudoplastic behaviour (shear thinning). The plain gellan G gel gave a flow like behaviour with increasing shear rate exhibiting hysteresis (thixotropy) on return, this suggests that the structures of the samples were broken and did not fully recover to the original state. The increase in shear rate permanently destroyed the sample structures. This was observed in all the batches including the reference gel formulations. The area between the curves is an indication of the extent of thixotropy. The larger the curve, the more thixotropic the sample is. Thixotropic materials lose their structure during shear, and rebuild it on standing. This behaviour is an important parameter in the ability of the gel to be easily applied to a surface (through structure breakdown in spreading) and then rebuild its structure and viscosity so that it does not drip and run.

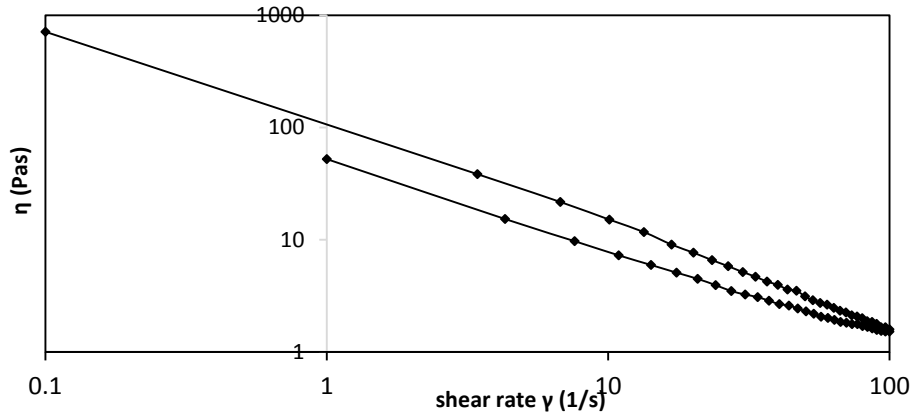

Figure 106 Viscosity curve against shear rate with hysteresis (thixotropy) for plain gellan G hydrogel.

3.3.3.2. Determination of sol-gel temperature

A gel is a three dimensional network formed once the polymer reaches the critical gelation concentration. Polymer gel formed was monitored from the viscoelastic functions (G′, G″ and tan δ) of the material developed at the gel point. Sol-gel transition point such as a particular temperature or volume concentration is an important parameter used in characterizing gel formation. In physical gels, the sol-gel transition is often reversible due to van der Waals forces or hydrogen bonding being employed in binding polymer chains together to form a gel network [39]. Existence of hysteresis in the melting process of reversible physical gels complicates the investigation of the gelation process and gel structure [40]. To determine the sol-gel transition point, the sudden loss of flow is the most common indication since the viscoelastic property change abruptly from liquid like state to a solid like state at gelation point [41]. Therefore the sol-gel transition is determined from rheological characterization since it coincides with the point at which G′ intersects G″. It can also be determined based on Winter-Chambon criterion [42], where the gel point is the time at which G′(ω) and G″(ω) follow the power law $G' = k' \omega^n$ and $G'' = k'' \omega^n$ (G′ and G″ were proportional to ω^n over a wide range of temperature and frequency). Here, n denotes the exponent, ω is the angular frequency, k′ and k″ are proportionality constants. Four ways from which the gelling time can be determined was also described by Ross-Murphy [43]: (i) when viscosity becomes infinite in a steady shear test (ii) when G′ diverges from a characteristic “signal noise”, (iii) when G″ shows a maximum, and (iv) when G′ = G″ (tan δ = 1.0) during time evolution of both moduli in gel cure experiment.

Gellan gum forms strong gels at very low concentrations (0.05% w/v) [44]. Gellan gelation can be induced by increasing the temperature of the concentrated gellan gum solution up to 90 °C. A decrease in temperature to 32.5 ± 2.5 °C leads to a conformational change of the chains from random coils to double helices (coil-helix transition). The rearrangement of the double helices occurs which leads to the formation of ordered junction zones (sol-gel-transition) [24]. Ultimately, a thermo-reversible hydrogel is formed. Addition of mono and divalent cations to gel solutions gives a much stronger physical thermo-reversible gel [45]. The gel formed is heat resistant and its gel strength is less dependent on pH compared to other common polysaccharides [46]. Gellan forms Ca^{2+} mediated junction zones by cross linking two double helices [47].

Gellan solutions undergo thermally induced sol-gel transition. The solution is a sol at high temperature and a gel when the solution is cooled. The traditional mechanism proposed for the sol-gel transition of gellan gum is based on a 'random coil' to 'double helix' transition followed by 'helix to helix aggregation', involving weak interactions such as Van der Waals forces and hydrogen bonds [48]. Existence of thermal hysteresis between gelation and melting was reported since aggregation stabilizes the helices to temperatures higher than those at which they form on cooling [49].

Figures 107 to 110 showed the temperature sweep profile of G' and G" with cooling from 90 to 15 °C and heating from 15 to 90 °C for G, GIb, GDD, GIbDD gels. During the cooling cycle for plain gellan G gel in Figure 107, the gels generally exhibited an increase in G' and G" from 90 to 76.8 °C until a plateau was reached.

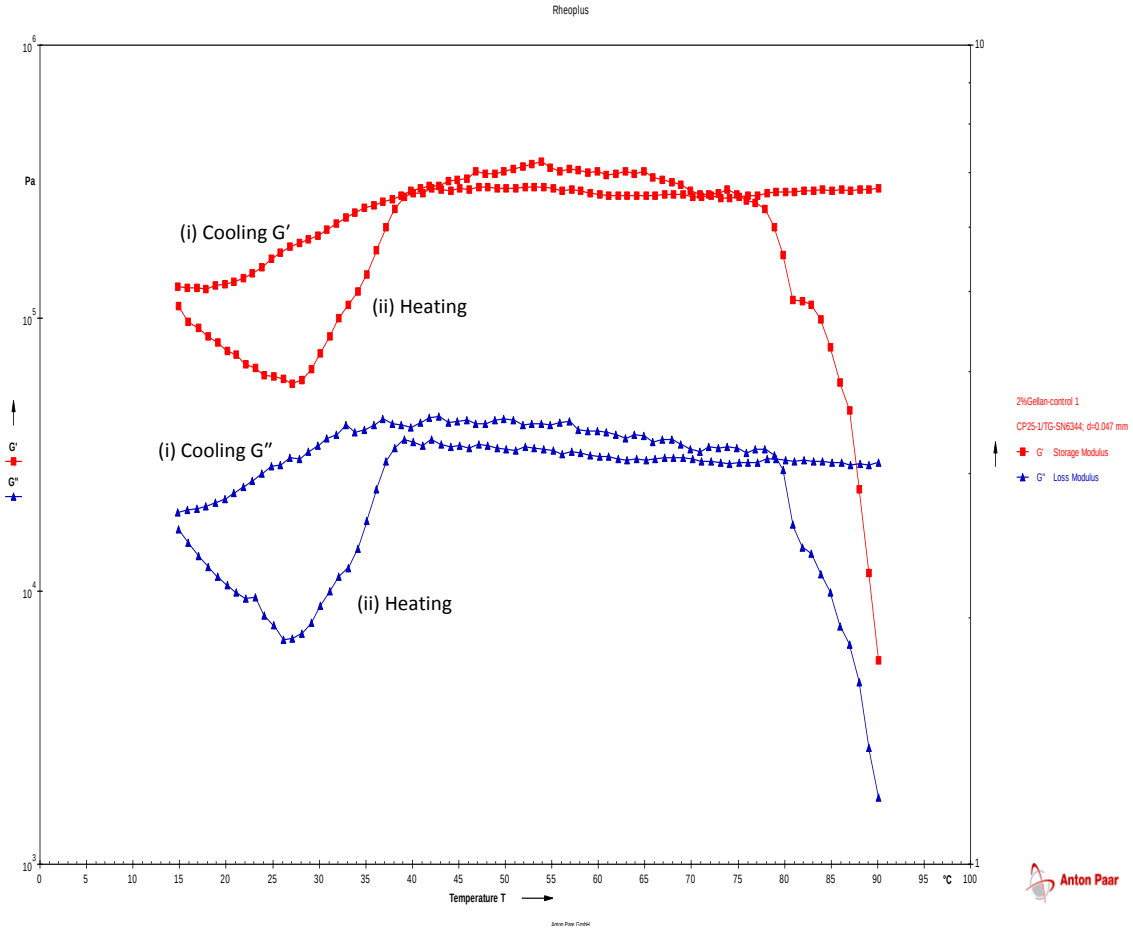

Figure 107 Temperature sweep profile of heating and cooling curves of plain gellan G hydrogel.

The plateau was maintained across a large temperature range from 76.8 to 38.8 °C until a lower temperature was reached, then the elastic and storage modulus started to decrease from 37.8 °C, until they reached the values (15 °C) close to the value recorded at the beginning of the heating cycle. This indicated that the liquid solution turned into solid-like gel in the vicinity of 38 °C.

During the heating cycle, the gels generally exhibited a decrease in G' and G" from 15 to 27.1 °C. This was followed by a sharp increase from 27.1 to 39.1 °C, until a plateau is reached and the values are maintained till the end of the heating cycle at 90 °C. The sharp increase of the moduli at 27 °C, indicated thermoreversibility with a tendency of the gel to return to liquid state.This similar observation was reported by Moura *et al.* in the rheological study of chitosan solution at physiological pH exhibiting gelation at 50 °C which was thermoreversible [34]. G' and G" crossover was not observed during the heating and cooling cycles of the complex gels. This was expected

because G’ > G” throughout the cycles and the elastic properties dominated. For cross-linked gels, G’ and G” are very high and are nearly parallel to each other [50]. This was observed for G, GIb in Figure 108, GDD and GIbDD complex hydrogels in Figure 109 and Figure 110 respectively, which indicated that they are hydrogels with highly cross-linked polymer networks.

Gels cross-linked with genipin also showed this rheological pattern [50]. Hysteresis effect was observed when the gels where first subjected to the cooling phase and then the heating phase. This indicated an irreversible break down in structure of the gels.

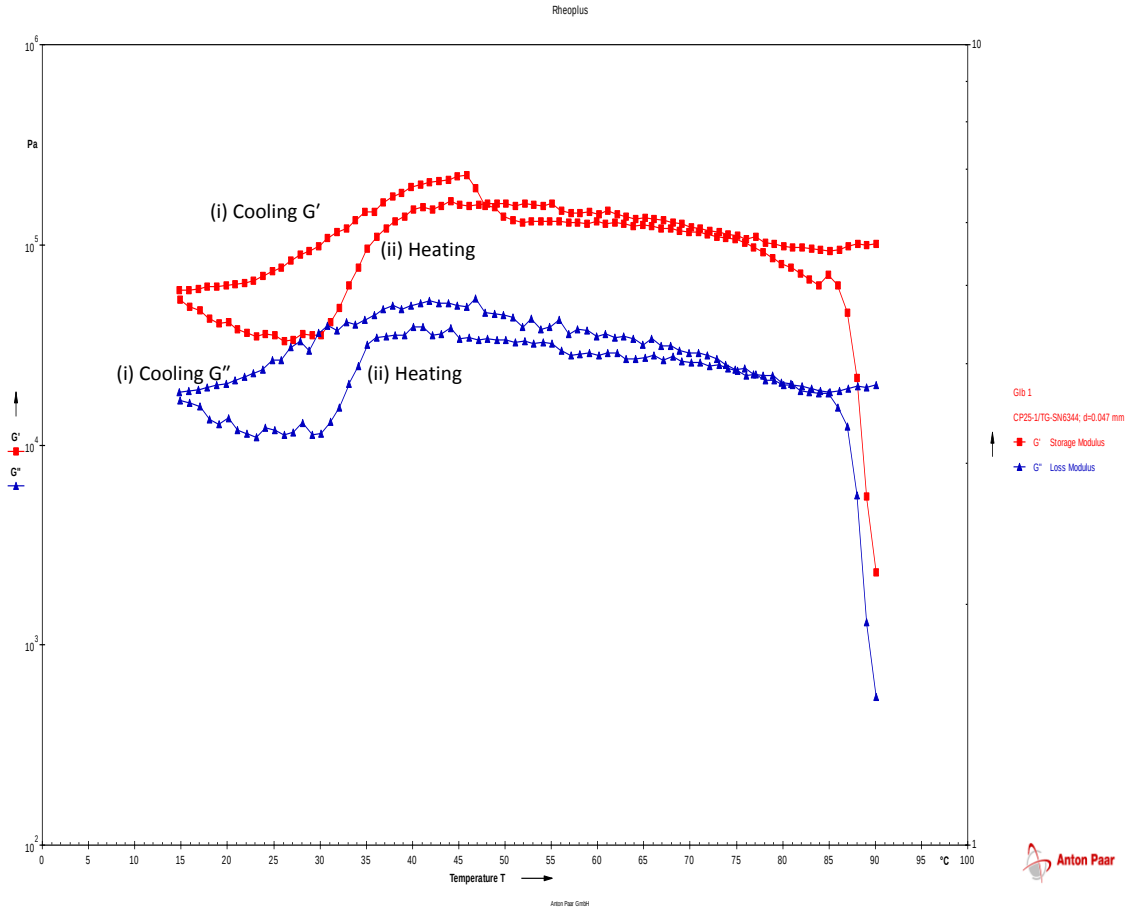

Figure 108 Temperature sweep profile of heating and cooling curves of GIb hydrogel.

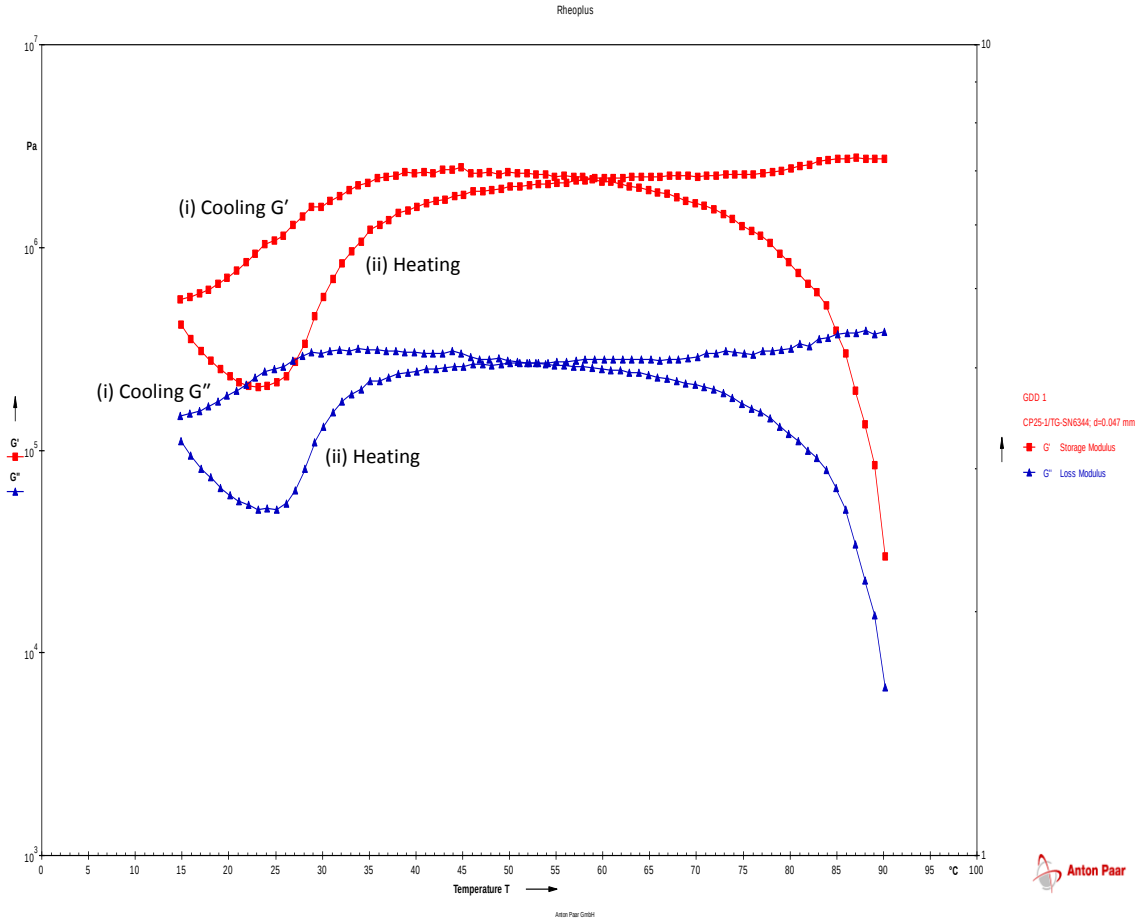

Figure 109 Temperature sweep profile of heating and cooling curves of GDD hydrogel

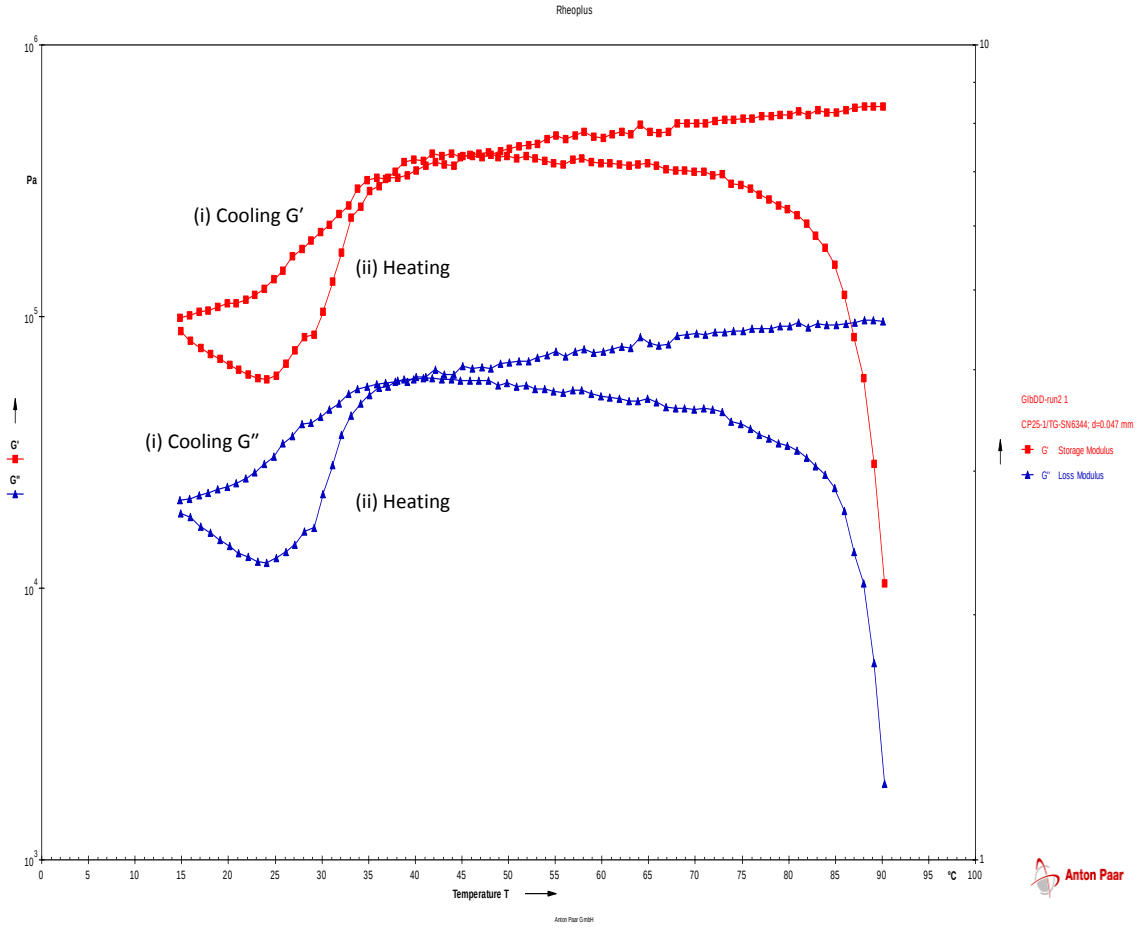

Figure 110 Temperature sweep profile of heating and cooling curves of GIbDD hydrogel.

3.3.4. Swelling kinetics

The swelling behaviour of the hydrogels was assessed by immersing the hydrogels in PBS (pH 7.4) at 37 °C. Hydrogels are crosslinked macromolecular network with swelling capabilities in aqueous media or biological fluids. Due to the high water content of the hydrogel formulations and their ability to retain great quantities of water, the gels were initially weighed and dried to constant weight before starting the swelling tests.

Plain gellan reference G gel increased in swelling with increasing contact time in PBS pH 7.4 up to 0.47 times its dried weight without losing its physical integrity at the end of 48 h in Figure 111. The general trend is that the swelling increased with time and the swelling ratio of the gels reached equilibrium at 6 h. The swelling ratio ranged from 0.53 to 0.59 times its dried weight in PBS pH 7.4 at 37 °C for the GDD gels. The addition of DEAE-Dextran to gellan GDD complex gels significantly

increased ($p < 0.05$, $n = 4$) swelling ratio when compared to the plain gellan reference G gel. The swelling behavioural pattern showed a steady increase in swelling ratio in the GDD complex as the concentration of DEAE-Dextran increased. Therefore, the swelling ratio was increased by the addition of DEAE-Dextran.

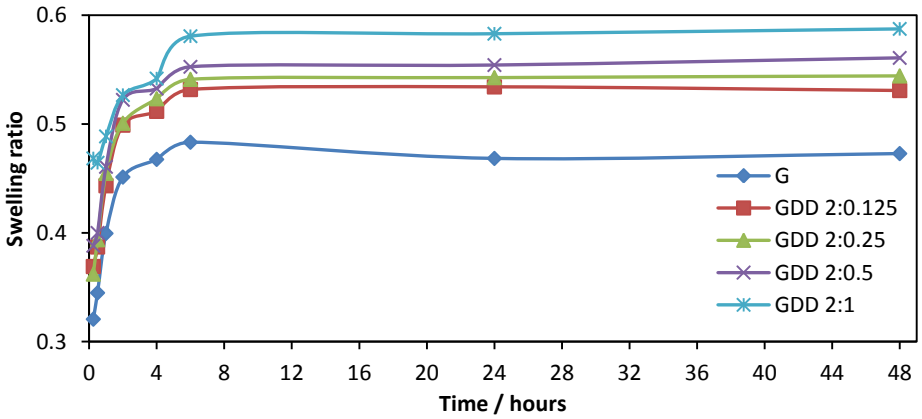

Figure 111 The swelling kinetics of gellan and gellan-DEAE-Dextran complex gels. Each data point represents mean ± S.D (n = 4).

The ibuprofen loaded plain gellan GIb had a swelling ratio of 0.52, while for the GIbDD complex gels the swelling ratio ranged from 0.77 to 1.61 times its dried weight in PBS pH 7.4 at 37 °C in Figure 112. The addition of DEAE-Dextran to GIb gel (GIbDD complex gels) significantly increased ($p < 0.05$, $n = 4$) swelling ratio when compared to the GIb gel. The swelling behavioural pattern showed that a steady increase in swelling ratio in GIbDD complex gels as the concentration of DEAE-Dextran increased. The incorporation of ibuprofen (GIb and GIbDD complex gels) significantly increased ($p < 0.05$, $n = 4$) the swelling of the gels when compared with G and GDD gels without ibuprofen. The swollen hydrogels maintained their gel integrity till the end of 48 h.

The swelling of hydrogels has been reported to be affected by crosslinking ratio. Highly cross-linked hydrogels exhibit tighter structure with less swelling when compared with lower cross-linked hydrogels [7]. The swelling ratio is thus lowered by the hindering of the polymer chains by crosslinking. Plain gellan reference G gel exhibited the highest physical crosslinking of its polymer network when compared with GDD complex and ibuprofen loaded complex GIbDD gels. The addition

of DEAE-Dextran and ibuprofen lowered the crosslinking ratios of the polymer network of the plain gellan G hydrogels.

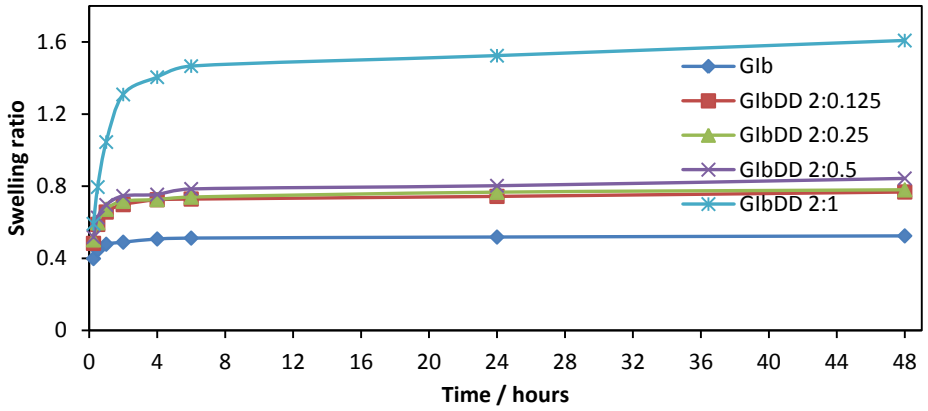

Figure 112 The swelling kinetics of ibuprofen loaded gellan and gellan-DEAE-Dextran complex gels. Each data point represents mean ± S.D (n = 4).

3.3.5. Drug release from the binary and ternary nanoconjugate hydrogels

The release of drug from hydrogels is governed by its ability to act as a permeable membrane or matrix. The release profile of ibuprofen from gellan, gellan-DEAE-Dextran complex GIbDD hydrogels and commercial ibuprofen gel was presented in Figure 113.

The drug release profile of ibuprofen from the hydrogels was divided into three phases. Within the first hour, there was a steady rate of release of ibuprofen from GIb (31.98%), GIbDD gels (34.58 to 67.18%) and commercial ibuprofen gel (40.44%) shown in Figures 161 to 163 in the Appendix. The release rate reduced between 1 and 4 h. There was a similar trend of release between 4 and 48 h. The drug release profile showed that the maximum ibuprofen released from GIb gels was 85.67%; ranged from 94.33% to 97.13% for GIbDD gels and 77.17% for commercial ibuprofen gel (Figure 113). Ibuprofen release from commercial ibuprofen gel was significantly reduced ($p < 0.05$, $n = 4$) when compared to plain gellan GIb gel and gellan-DEAE-Dextran GIbDD complex gels. At 48 h, the release exhibited were in the increasing order from commercial ibuprofen gel < GIb < GIbDD 2:1 < GIbDD 2:0.5 < GIbDD 2:0.25 < GIbDD 2:0.125 with GIbDD 2:0.125 showing the highest drug release. The DEAE-Dextran concentration that gave the highest release was 0.125%. DEAE-Dextran initially increased then decreased the release of ibuprofen from the hydrogels at the rate of 2.97% per unit

weight (R^2 = 0.97) shown in Figure 114. The combination of gellan and DEAE-Dextran influenced the drug release of ibuprofen which suggested a synergistic effect of the two polymers.

The drug release pattern showed an initial burst release up to 6 h and slower release rate up to 48 h. The initial burst effect may be attributed to the diffusion of the drug caused by rapid gel swelling and also the release of the drug adsorbed towards the surface of the gel matrix [51]. The formation of polyelectrolyte complex hydrogels (PEC) could have enhanced the release of ibuprofen over time. The degree of swelling of the hydrogels influenced the diffusional properties of the solute through the hydrogel. This was confirmed by the drug release studies which showed a significantly higher ($p < 0.05$, n = 20) drug release for the GIbDD complex gels when compared to GIb gel.

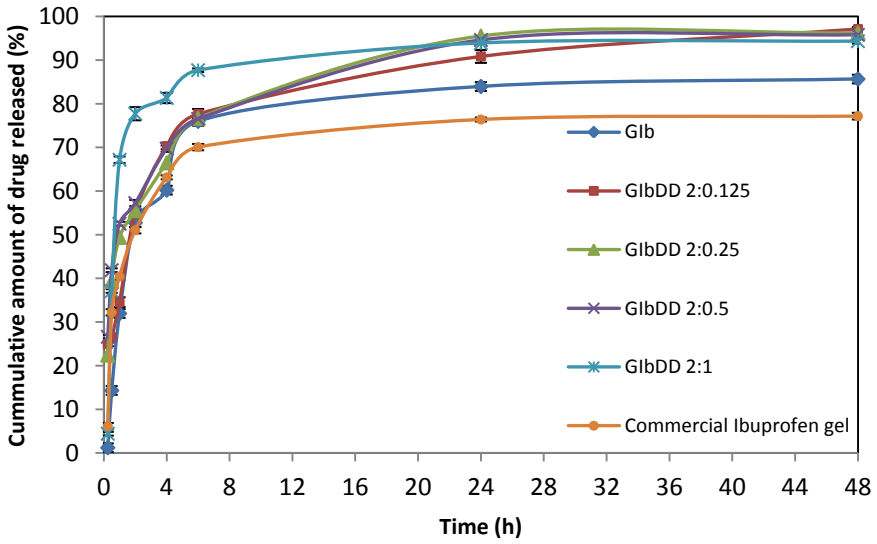

Figure 113 Ibuprofen release from gellan, gellan-DEAE-Dextran complex and commercial ibuprofen gels. Each data point represents mean ± S.D (n = 4).

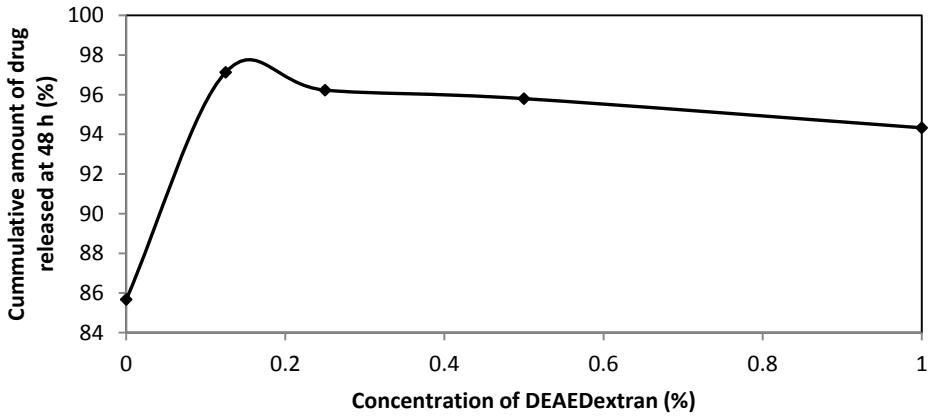

Figure 114 Effect of DEAE-Dextran on the release profile of ibuprofen from the conjugate hydrogels. Each data point represents mean ± S.D (n = 4).

3.3.6. Drug release kinetics

The drug release kinetics data based on the kinetic models is shown in Table 75. The data was best fitted with the Korsemeyer-Peppas models for GIb, GIbDD and commercial ibuprofen gels. The classification of diffusional exponent (n) based on release behaviour of bioactive agent from the hydrogel systems described by Lowman is as follows: Fickian diffusion (n = 0.5); anomalous transport system - Fickian diffusion and polymer relaxation (0.5 < n < 1); case II transport system - polymer relaxation (n = 1); super case II transport system – zero order release and plasticization at gel layer (n > 1) [52]. The n values obtained shown in Table 75 indicated that for GIbDD 2:0.125, GIbDD 2:0.25 and GIbDD 2:0.5 (where n < 0. 5) Fickian diffusion was exhibited, for commercial ibuprofen gel the release mechanism was anomalous (non-Fickian) diffusion where diffusion exponent (n) is 0. 5 < n < 1, while in the absence of DEAE-Dextran, GIb and GIbDD 2:1 gels (higher concentration of DEAE-Dextran) the release mechanism was a Super Case II transport mechanism (where n > 1). The Super Case II release kinetics of GIb and GIbDD 2:1 gel is a strong indication of zero order release mechanism. In controlled drug release, zero order is the ideal with advantage of delivering drug at a constant rate which gives a predictable bioavailabilty.

Table 75 Regression coefficient (r) values of different kinetic models and diffusion exponent (n) of Korsemeyer-Peppas models for the ibuprofen loaded gellan, gellan-DEAE-Dextran complex gels and branded ibuprofen gel.

Formulation	Zero order	First Order	Higuchi	Korsemeyer-Peppas	
	R^2	R^2	R^2	R^2	n
GIb	0.47	0.21	0.67	0.81	1.31
GIbDD 2:0.125	0.60	0.47	0.79	0.90	0.38
GIbDD 2:0.25	0.62	0.45	0.81	0.89	0.43
GIbDD 2:0.5	0.61	0.47	0.80	0.91	0.23
GIbDD 2:1	0.30	0.15	0.47	0.90	1.96
Commercial Ibuprofen gel	0.42	0.22	0.61	0.76	0.74

3.3.7. Similarity of drug release profiles (Similarity factor f_2)

All the similarity (f_2) values of GIbDD complex hydrogels were higher than the limit value of 50 (f_2 values ranging from 68.97 to 74.60 in Table 106) suggesting a similarity between the ibuprofen loaded (GIbDD ternary) complex and the ibuprofen loaded plain gellan (GIb binary) hydrogels. The f_2 values increased with increase in concentration of DEAE-Dextran in the complex.

3.4. Conclusion

Polyelectrolyte complex nanoconjugate hydrogels were prepared by *in situ* interaction between gellan gum and different concentrations of oppositely charged DEAE-Dextran. The plain PEC hydrogels were further loaded with solubilized ibuprofen. The DSC thermograms exhibited the disappearance of the melting peak of ibuprofen suggesting an interaction between ibuprofen and the polymers. This was confirmed by the FTIR spectra, where the major peaks of ibuprofen were absent. The TGA of the hydrogels showed that the the binary GIb (282.8 °C) had higher decomposition temperature than the ternary GIbDD complex (246.8 to 256.5 °C) gels suggesting greater thermal stability. The release of ibuprofen from the gels increased steadily with time to 100% at the end of 48 hours. This correlates with the rheological findings which showed pseudoplastic behaviour. The lowest concentration of DEAE-Dextran (GIbDD 2:0.125) used in this study, increased the release of ibuprofen by 13.4%. Higher concentrations of DEAE-Dextran decreased the release profile steadily. It follows that DEAE-Dextran has potentials in the formulation of modified (extended) release of hydrogels. The drug release kinetics fitted into different models

suggests a combination of mechanisms of release including Fickian, anomalous and Super Case II transport. However, diffusion from the hydrogel is more dominant than discrete particle dissolution mechanism.

3.5. References

1. Peppas, N.A. and A.G. Mikos, *Preparation methods and structure of hydrogels*, in *Hydrogels in Medicine and Pharmacy*, N.A. Peppas, Editor. 1986, CRC Press: Boca Raton, Florida. p. 1-25.
2. Brannon-Peppas, L., *Preparation and Characterization of Crosslinked Hydrophilic Networks*, in *Absorbent Polymer Technology*, L. Brannon-Peppas and R.S. Harland, Editors. 1990, Elsevier: Amsterdam. p. 45-66.
3. Peppas, N.A., *Physiologically Responsive Gels.* J Bioact Compat Polym, 1991. **6**: p. 241-246.
4. Park, K. and H. Park, *Smart Hydrogels*, in *Concise Polymeric Materials Encyclopedia*, J.C. Salamone, Editor. 1999, CRC Press: Boca raton. p. 1476-1478.
5. Qiu, Y. and K. Park, *Environment-sensitive Hydrogels for Drug Delivery.* Adv Drug Deliv Rev, 2001. **53**: p. 321-339.
6. Hennink, J.D. and C.F. Van Nostrum, *Novel Crosslinking Methods to Design Hydrogels.* Adv. Drug Deliv. Rev., 2002. **54**: p. 13-36.
7. Peppas, N.A.B., P. Bures, W. Leobandung and H. Ichikawa, , *Hydrogels in Pharmaceutical Formulations.* Eur J Pharm Biopharm, 2000. **50**: p. 27-46.
8. Saleem, M.A.A., S. K. Ali, S. Patil, C. C., *Studies on Different Chitosan Polyelectrolyte Complex Hydrogels for Modified Release of Diltiazem Hydrochloride.* Int J Pharm Pharm Sci, 2010. **2**(4): p. 64-67.
9. Patel, V.R. and M.M. Amiji, *Preparation and Characterization of Freeze-dried Chitosan-Poly(ethylene oxide) Hydrogels for Site-Specific Antibiotic Delivery in the Stomach.* Pharm Res, 1996. **13**(4): p. 588-593.
10. Prado, H.J.M., M. C. Matulewicz, P. R. Bonelli and A. L. Cukierman, *Preparation and Characterization of Controlled Release Matrices Based on Novel Seaweed Interpolyelectrolyte Complexes.* Int J Pharm, 2012. **429**: p. 12-21.
11. O'Neil, M.A., R.R. Selvedran, and V.J. Morris, *Structure of the Acidic Extracellular Gelling Polysaccharide Produced by Pseudonomas elodea.* Carbohydr. Res., 1983. **124**: p. 123-133.
12. Rodriguez-Hernadez, A.I.D., S. Garnier, C. Tecante, A. Doublier, J. L., *Rheology-Structure Properties of Gellan Systems:Evidence of Network formation at Low Gellan Concentration.* Food Hydrocoll, 2003. **17**: p. 621-628.
13. Yuguchi, Y., H. Urakawa, and K. Kajiwara, *Structural Characteristics of Crosslinking Domain in Gellan Gum Gel.* Macromol Symp, 1997. **120**: p. 77-89.
14. Coviello, T.D., M. Rambone, G. Desideri, P. Carafa, M. Murtas, E. Riccieri, F. M. Alhaique, F., *A Novel Co-Crosslinked Polysaccharide: Studies for a Controlled Delivery Matrix.* J Control Release, 1998. **55**(1): p. 57-66.
15. Kurul, E. and S. Hekimoglu, *Skin Permeation of Two Different Benzophenone Derivatives from Various Vehicles.* Int J Cosmet Sci, 2001. **23**: p. 211-218.
16. Hadjiioannou, T.P., G.D. Cristian, M.A. Kouparris, and P.E. Macheras, *Quantitative Calculations in Pharmaceutical Practise and Research*. 1993, New York: VCH Publishers Inc.
17. Bourne, D.W.A., *Pharmacokinetics*, in *Modern Pharmaceutics*, G.S. Banker and C.T. Rhodes, Editors. 2002, Marcel Dekker Inc: New York. p. 94-144.
18. Higuchi, T., *Mechanism of Sustained-Action Medication. Theoretical Analysis of Rate of Release of Solid Drugs Dispersed in Solid Matrices.* J Pharm Sci, 1963. **52**(12): p. 1145-1149.
19. Korsemeyer, R.W., R. Gurny, E. Doelker, P. Buri, and N.A. Peppas, *Mechanism of Solute Release from Porous Hydrophilic Polymers.* Int J Pharm, 1983. **15**(1): p. 25-35.
20. Thakkar, V.T.S., P. A. Soni, T. G. Parmar, M. Y. Gohel M. C. Ghandi, T. R., *Goodness-of-fit Model-Dependent Approach for Release Kinetics of Levofloxacin Hemihydrates Floating Tablet.* Dissolution Technol, 2009. **1**: p. 35-39.

21. Moore, J.W., *Mathematical Comparison of Dissolution Profiles.* Drug Dev Ind Pharm, 1996. **12**: p. 969-992.
22. Pillay, J. and R. Fassihi, *Evaluation and Comparison of Dissolution Data Derived from Different Modified Release Dosage Forms: an Alternative Method.* J Control Release, 1998. **1998**: p. 45-55.
23. Dai, L.L., X. X. Liu, Y. L. Tong, Z., *Concentration Dependence of Critical Exponents for Gelation in Gellan Gum Aqueous Solutions Upon Cooling.* Eur Polym J, 2008. **44**(12): p. 4012-4019.
24. Miyoshi, E., T. Takaya, and K. Nishinari, *Rheological and Thermal Studies of Gel-Sol Transition in Gellan Gum Aqueous Solutions.* Carbohydr Polym, 1996. **30**: p. 109-119.
25. Sudhamani, S.R., M.S. Prasad, and K. Udaya Sankar, *DSC and FTIR studies on Gellan and Polyvinyl Alcohol (PVA) blend Films.* Food Hydrocoll, 2003. **17**: p. 245-250.
26. Silva-Correia, J.O., J. M. Caridade, S. G. Oliveira, J. T. Sousa, R. A. Mano, J. F. Reis, R. L., *Gellan Gum-Based Hydrogels for Intervertebral Disc Tissue-Engineering Applications.* J Tissue Eng Regen Med, 2011. **5**: p. e97-e107.
27. Xu, L.L., B.Kennedy, J. F.Xie, B. J.Huang, M., *Characterization of Konjac Glucomannam-Gellan Gum Blend Films and their Sutaibility for Release of Nisin Incorporated Therein.* Carboh Polym, 2007. **70**: p. 192-197.
28. Matkovic, S.R., G.M. Valle, and L.E. Briand, *Quantitative Analysis of Ibuprofen in Pharmaceutical formulations through FTIR Spectroscopy.* Lat Am Appl Res, 2005. **35**(3): p. 189-195.
29. Nokhodchi, A.A., O. Jelvehgari, M., *Physico-Mechanical and Dissolution Behaviours of Ibuprofen Crystals Crystallized in the Presence of Various Additives.* DARU, 2010. **18**(2): p. 74-83.
30. Commission, B.P., *British Pharmacopoeia 2012*. Vol. 1. 2011, Norwich, Great Britain: Stationery Office Books.
31. Kumar, D.P.S., D. C. Subrata, C. Soumen, R, *Formulation and Evaluation of Solid Lipid Nanoparticles of A Poorly Water Soluble Model Drug, Ibuprofen.* Int Res J Pharm, 2012. **3**(12): p. 132-137.
32. Pai, V.S., M. Khan, S, A., *Evolution of Microstructure and Rheology in Mixed Polysaccharide Systems.* Macromolecules, 2002. **35**(5): p. 1699-1707.
33. Chenite, A.B., M. Wang, D. Chaput, C. Kandani, N., *Rheological Characterization of Thermogelling Chitosan/Glycerol-Phosphate Solutions.* Carbohydr Polym, 2001. **46**: p. 39-47.
34. Moura, M., J. Figueiredo, M. M. Gil, M. H., *Rheological Study of Genipin Cross-Linked Chitosan Hydrogels.* Biomacromolecules, 2007. **8**: p. 3823-3829.
35. Ferry, J.D., *Viscoelastic Properties of Polymer.* 1980, New York: Wiley & Sons. 641.
36. Montembault, A., C. Viton, and A. Domard, *Rheometric Study of the Gelation of Chitosan in a Hydroalcoholic Medium.* Biomaterials, 2005. **26**: p. 1633-1643.
37. Madsen, F., K. Eberth, and J.D. Smart, *A Rheological Examination of Mucoadhesive/Mucus Interaction: The Effect of Mucoadhesive Type and Concentration.* J Control Rel, 1999. **50**: p. 167-178.
38. Nishinari, K., *Rheological and DSC Study of Sol-Gel Transition in Aqueous Dispersions of Industrially Important Polymers and Colloids.* Coll Polym Sci, 1997. **275**: p. 1093-1107.
39. Almdal, K.D., J. Hvidt, S. Kramer, O, *Towards a Phenomenological Definition of the Term 'Gel'.* Polym Gels Networks, 1993. **1**: p. 5-17.
40. Zhao, Y.C., Y. Yang, Y. Wu, C., *Rheological Study of the Sol-Gel Transition of Hybrid Gels.* Macromol 2003. **36**: p. 855-859.
41. Yoon, P.J. and C.D. Han, *Effect of Thermal History on the Rheological Behaviour of Thermoplastic Polyurethane.* Macromolecules, 2000. **33**: p. 2171-2183.
42. Winter, H.H. and F. Chambon, *Analysis of Viscoelasticity of a Cross-Linking Polymer at the Gel Point.* J Rheol, 1986. **30**: p. 367-382.
43. Ross-Murphy, S.B., *Incipient Behaviour of Gelatin Gels* Rheol Acta, 1991. **30**: p. 401-411.
44. Sworn, G., *Gellan gum*, in *Handbook of Hydrocolloids*, G.O. Phillips and P.A. Williams, Editors. 2000, Woodhead Publishing Limited: Cambridge. p. 117-135.
45. Sanderson, G.R. and R.C. Clark, *Gellan Gum.* Food Technol, 1983. **37**: p. 63-70.
46. Sanderson, G.R., *Food Gels*, ed. P. Harris. 1990, London and New York: Elsevier Applied Science.
47. Chandrasekaran, R. and A. Radha, *Molecular Architectures and Functional Properties of Gellan Gum and Related Polysaccharides.* Trends Food Sci Tech, 1995. **6**: p. 143-147.
48. Garcia, M.C.A., M.C. Calero, N. Munoz, J., *Influence of Gellan Gum Concentration on the Dynamic Viscoelasticity and Transient Flow of Fluid Gels.* Biochem. Eng. J, 2011. **55**(2): p. 73-81.
49. Morris, E.R., K. Nishinari, and M. Rinaudo, *Gelation of Gellan- A Review.* Food Hydrocoll, 2012. **28**: p. 373-411.

50. Brummer, R., *Rheology Essentials of Cosmetic and Food Emulsions*, ed. H.G.P. Barth, H. 2006, Berlin Heidelberg: Springer. 177.
51. Shanta, K.L.H., D. R. K., *Preparation and In-Vitro Evaluation of Poly(N-vinyl-2-pyrrolidone-polyethylene glycol diacrylate)-Chitosan Interpolymeric pH-Responsive.* Int J Pharm, 2000. **207**(1): p. 65-70.
52. Shi, D., *Biomedical Devices and their Applications.* 2005, Berlin: Springer.

CHAPTER FOUR

4.0. Preparation and characterization of composite and bilayer polymer films

4.1. Introduction

There is ongoing research on the preparation of films using natural and synthetic polymers to improve their bioavailability and expand their use as biomaterials. Biodegradable polymer films are made from biopolymers which include polysaccharides, lipids and proteins. These films have been exploited for their controlled drug release potential based on softness, absorbency and high surface area characteristics [1]. Due to their biodegradability, biocompatibility and non-toxicity, they have advantages over synthetic polymers and are fast replacing them. The release profile of naproxen from the three polymers (poly (lactide-co-glycolide) PLGA, poly (D, L-lactide) PDLLA and poly (ε-caprolactone) PCL studied, exhibited two-stage release model: release by diffusion followed by zero order release due to polymer erosion. Polymer films and coatings have been used to modulate surface properties of biomaterials and a reservoir for drug [1].

Methods developed for fabrication of polymer films include solvent evaporation method used in the development of curcumin loaded hydroxyl propyl methylcellulose - ethyl cellulose polymeric films [2] and layer-by-layer method in the preparation of gentamicin and cefazolin loaded poly-L-lysine/poly-L-(glutamic acid) multilayer nanofilms [3]. Solvent casting is the most popular and an old film making technique which dates back up to a century ago. It involves the suspension or dissolution of Active Pharmaceutical Ingredients (APIs) in a solution of polymers, plasticizers and other excipients in a volatile solvent such as water or ethanol, casting on a surface and drying to remove the solvent. Layer-by-Layer (LbL) films were first developed by Decher [4]. He proposed a method for the preparation of thin films based on alternate and repeated adsorption of polycations and polyanions on the surface of a solid substrate from the solution with washing steps. LbL is not

only based on electrostatic forces but also hydrogen bonding, covalent bonding and biological affinity [5]. Polyelectrolyte multi layer films has been developed for drug delivery with advantages which include: drug molecules acting as functional drugs or components of the film, with the tendency to form stable crosslinking structure with other film components; possibility of achieving sustained drug release; potential of protecting drug molecules from losing their biological activities; simplicity of the film preparation process which can be automated [3]. Kawashima *et al.* developed a polyelectrolyte (PEC) film by reacting theophylline granules coated with sodium tripolyphosphate and chitosan [6]. Drug release from the coated granules followed zero order kinetics with significant reduction compared with that of original granules. Pang *et al.* fabricated ibuprofen loaded PLGA polymeric films dissolved in tetrahydrofuran solvent by spreading PLGA-ibuprofen solution on non solvent surface [7]. The films with higher concentrations of ibuprofen prepared had convex patterned surfaces due to surface tension when the phase separation moved to the surface of the polymer solution.

Gellan gum is a water soluble polysaccharide consisting of a tetrasaccharide repeat units of two D-glucose, one L-rhamnose and one D-glucuronic acid connected by glycosidic bonds [8]. It is produced by the fermentation of *Sphingomonas elodea* ATCC 31461 [9] (formerly referred to as *Pseudomonas elodea*). Gellan gum is finding increasing applications in the pharmaceutical and biotechnology industry based on its good film-forming properties [10] exhibited by the preparation of gellan-gelatin composite films with improved mechanical properties and potential to be used as packing or coating materials; and drug release [11]. Agnihotri *et al.* prepared cephalexin loaded gellan gum beads with spherical shaped beads with average size of 925 to 1183 µm and higher release rates achieved by beads prepared in acidic pH media [11]. The authors found that it was important to use the combination of calcium and zinc cations to give uniform sized beads with sustained drug release.

Gellan gum has been found to be of use in oral sustained delivery in the formulation of cimetidine loaded gellan *in situ* gel with *in vitro* release profile following root-time kinetics over a period of 6 h [12], in the development of methylprednisolone loaded gellan based systems for sustained release

for ophthalmic drug delivery [13], in the preparation of amoxicillin loaded gellan beads prepared by ionic gelation with the release kinetics following the diffusion model [14] and floating in situ gelling for controlled delivery of ramipril with good fit to the zero order and Korsemeyer Peppas model exhibiting Fickian diffusion mechanism [15]. The mechanical and water vapour properties of edible gellan films have been investigated [16]. It was found that the mechanical properties of the film were adversely affected by high water activity. Gellan film has been used to produce regenerative barrier membrane with the 2% gellan film exhibiting better film integrity in the bone defect in rats healing after two months and good cell separation ability [17]. The choice of exploiting gellan further is based on its cheapness, biodegradable, easy gel and film forming characteristics

Diethylaminoethyl-Dextran (DEAE-Dextran) is a polycationic derivative of Dextran produced by reacting diethylaminoethyl chloride with Dextran. It is freely soluble in water and salt solutions and biodegradable [18]. There is no report showing that DEAE-Dextran form films or gels but have been found to possess bioadhesive properties in the preparation of laminin treated DEAE-Dextran where laminin binds readily with it [19]. Its polycationic nature is being explored in this study in combination with gellan at different mixing ratio without the use of crosslinking agents and toxic solvents with potential to form polyelectrolyte films with the desired properties.

In this study, single, composite and bilayer gellan - DEAE-Dextran films; and ibuprofen-loaded films were prepared and characterized with the objective of its future application of biodegradable films in the transdermal delivery of ibuprofen. The synergistic potential of incorporating DEAE-Dextran into gellan in view of improving their physicochemical properties was exploited and the mode of preparation (composite and electrostatic layer-by-layer) where compared. The *in vitro* drug release study of ibuprofen from gellan films and its polyelectrolyte complex and bilayer composite films were evaluated.

4.2. Materials and methods

4.2.1. Materials

Ibuprofen (purchased from Fagron, UK), gellan (Phytagel®), DEAE-Dextran hydrochloride and glycerol (all purchased from Sigma-Aldrich, UK) were used as supplied.

4.2.2. Preparation of plain composite and bilayer films

The method of preparing composite gellan films by Yang and Paulson was modified in this study. 2% w/v of gellan was dispersed in distilled water and 3% v/v of glycerol (at 60% w/w plasticizer/(plasticizer + polymer) [16] was added under magnetic stirring and heated at 80 to 90°C until it became a transparent solution coded G film. Gellan-glycerol solution was added to DEAE-Dextran solution at different mixing ratios (2:0.125, 2:0.25, 2:0.5 and 2:1) under magnetic stirring and heated up to 90 ˚C until homogenous mix was achieved. The resulting binary composite polyelectrolyte complex film forming mixtures were adjusted to pH 6.0 (Mettler Toledo pH meter) with sodium hydroxide NaOH coded GDD 2:0.125, GDD 2:0.25, GDD 2:0.5 and GDD 2:1 shown in Table 76.

The hot film forming mixtures of gellan and gellan - DEAE-Dextran composite polyelectrolyte complexes were placed individually under vacuum for 30 sec to remove air bubbles and 30 g was immediately poured into a 12 cm square petri dish (casting method). The petri dishes were placed in the oven overnight at 40 ˚C. The dried films were peeled out from the plates and stored in a desiccator prior to analysis.

Bilayer polyelectrolyte complex films were formed with gellan films as base component. Already prepared gellan films were immersed into varying concentrations of oppositely charged DEAE-Dextran solutions for about 5 min on each side and dried again overnight in the oven (layer by layer immersion) coded G/DDB 2:0.125, G/DDB 2:0.25, G/DDB 2:0.5 and G/DDB 2:1 shown in Table 77. The DEAE-Dextran solutions were kept at room temperature while being used as immersion liquid.

Table 76 Composition of gellan and gellan-DEAE-Dextran composite films.

Sample	Gellan (%w/v)	DEAE-Dextran (%w/v)	Glycerol (%v/v)	Distilled Water (%)
G	2.0	-	3.0	to 100
GDD 2:0.125	2.0	0.125	3.0	to 100
GDD 2:0.25	2.0	0.25	3.0	to 100
GDD 2:0.5	2.0	0.5	3.0	to 100
GDD 2:1	2.0	1.0	3.0	to 100

Table 77 Composition of gellan-DEAE-Dextran bilayer films.

Sample	Gellan (%w/v)	DEAE-Dextran (%w/v)	Glycerol (%v/v)	Distilled Water (%)
G/DDB 2:0.125	2.0	0.125	3.0	to 100
G/DDB 2:0.25	2.0	0.25	3.0	to 100
G/DDB 2:0.5	2.0	0.5	3.0	to 100
G/DDB 2:1	2.0	1.0	3.0	to 100

4.2.3. Preparation of drug loaded composite and bilayer films

2% w/v of gellan was dispersed in distilled water and 3% v/v of glycerol (at 60% w/w plasticizer/(plasticizer + polymer) [16] was added under magnetic stirring and heated between 80 and 90 ˚C until it became a transparent solution. 1% w/v of ibuprofen was dissolved in 5 mL of 1 M NaOH, added to the polymer solution at same temperature, adjusted to pH 6.0 and coded GIb film. 2% w/v of gellan and 3% w/v of glycerol in 50 mL distilled water under stirring and heated between 80 and 90 ˚C until it became a transparent solution. 1% w/v of ibuprofen was dissolved in 5mL of 1 M NaOH and added to the hot solution. 1% w/v of DEAE-Dextran was dispersed in 25 mL of distilled water, adjusted to pH 6 with NaOH and heated up to 90 ˚C. The gellan-ibuprofen solution was transferred into the DEAE-Dextran solution at different mixing ratios of gellan to DEAE-Dextran (2:0.125, 2:0.25, 2:0.5 and 2:1) under continuous magnetic stirring until homogenous mix was achieved. The resulting composite polyelectrolyte complex (loaded with ibuprofen) film forming solutions were adjusted to pH 6 (Mettler Toledo pH meter) with NaOH coded GIbDD 2:0.125, GIbDD 2:0.25, GIbDD 2:0.5 and GIbDD 2:1 shown in Table 78.

The hot film forming solutions of gellan and gellan - DEAE-Dextran composite polyelectrolyte complexes loaded with ibuprofen were placed under vacuum for 30 sec to remove air bubbles and

30 g was immediately transferred into a 12 cm square petri dish (casting method). The petri dishes were placed in the oven overnight at 40˚C. The dried films were peeled out from the plates and stored in a desiccator.

Bilayer polyelectrolyte complex films were formed with gellan loaded with ibuprofen films as base component. Already prepared gellan-ibuprofen films were immersed into varying concentrations of oppositely charged DEAE-Dextran solutions adjusted to pH 6 (Mettler Toledo pH meter) for about 5 min on each side and dried again overnight in the oven (layer by layer immersion) coded GIb/DDB 2:0.125, GIb/DDB 2:0.25, GIb/DDB 2:0.5 and GIb/DDB 2:1 shown in Table 79. The DEAE-Dextran solutions were kept at room temperature while being used as immersion liquid.

Table 78 Composition of ibuprofen loaded gellan and gellan-DEAE-Dextran composite films.

Code	Ibuprofen (%w/v)	Gellan (%w/v)	DEAE-Dextran (%w/v)	Glycerol (%v/v)	Distilled Water (%)
GIb	-	2.0	-	3.0	to 100
GIbDD 2:0.125	1.0	2.0	0.125	3.0	to 100
GIbDD 2:0.25	1.0	2.0	0.25	3.0	to 100
GIbDD 2:0.5	-	2.0	0.5	3.0	to 100
GIbDD 2:1	1.0	2.0	1.0	3.0	to 100

Table 79 Composition of ibuprofen loaded gellan and gellan-DEAE-Dextran bilayer films.

Code	Ibuprofen (%w/v)	Gellan (%w/v)	DEAE-Dextran (%w/v)	Glycerol (%v/v)	Distilled Water (%)
GIb/DDB 2:0.125	1.0	2.0	0.125	3.0	to 100
GIb/DDB 2:0.25	1.0	2.0	0.25	3.0	to 100
GIb/DDB 2:0.5	1.0	2.0	0.5	3.0	to 100
GIb/DDB 2:1	1.0	2.0	1.0	3.0	to 100

4.2.4. Physicochemical characterization of the composite and bilayer films

4.2.4.1. Morphology and size studies

4.2.4.1.1. Scanning electron microscopy

The surface and cross-sectional morphologies of gellan (pure and blend) films and ibuprofen loaded films were observed by a Carl Zeiss SEM EVO High Definition 15 scanning electron microscope (Carl Zeiss, Germany) using variable pressure technology at low voltages with beam deceleration and high definition backscattered electron (BSE) imaging. The film samples were mounted on double sided

carbon tabs that were previously secured to aluminium stubs and then analysed at different magnifications and a pressure of 10 Pa. The accelerating voltage was 10 KV with probe current of 400 pA. The particle sizes on the surface and cross section of the films were determined.

4.2.4.1.2. Atomic force microscopy

The surface topographies of the films were observed using an Agilent Technologies 5420 Scanning Probe Microscope/ Atomic Force Microscopy (Agilent Technologies Inc., USA). The AFM mapping was performed in a contact mode with a cantilever. The measurements were carried out in ambient conditions at a scan speed of 10.01 lines/second, and a resolution of 256 µm together with the scan area of size 20 x 20 µm.

4.2.4.2. Film thickness measurements

The thickness of the film samples was measured using a thickness micrometer screw gauge (Draper Expert, UK) micrometer to the nearest 0.01 mm. Thickness measurements were taken at six different locations on each sample and the average value was taken as the mean thickness of the film.

4.2.4.3. Mechanical properties of films

Tensile strength (TS), percentage tensile elongation (TE) at break and elastic modulus (EM) of the film were determined at 21 ± 1˚C using Zwick Roell Materials Tester (Zwick GmbH & Co AG Ulm, Germany) according to ASTM standard method D882 [21]. Strips of dimension 10 x 2.5 cm were cut from films and mounted between the grips of the machine. The initial grip separation and cross head speed were set to 80 mm and 40 mm/min respectively. A computer with Zwick TestXpert II software was used to record the stress-strain curves. Elastic modulus, tensile strength and elongation were calculated from the slope of the linear part of the stress-strain curve, the maximum stress and percentage elongation at break respectively. All measurements were an average of four determinations and expressed as mean ± S.D.

4.2.5. Spectroscopic analysis - Fourier Transform Infrared

FTIR was conducted using Perkin-Elmer Precisely Spectrum One FTIR Spectrometer and a Universal ATR Sampling Accessory (Perkin Elmer, USA). The films were mounted directly on the diamond surface and the arm was placed over it by applying enough pressure in the range of 100 to 120. The spectrum was recorded in the wavelength region of 4000 to 650 cm^{-1}. All spectra were then collected at an average of 16 scans at a resolution of 4 cm^{-1}. All measurements were taken in replicates of four determinations.

4.2.6. Thermal analysis

4.2.6.1. Differential scanning calorimetry

DSC was performed using Perkin Elmer Jade DSC machine in conjunction with a Perkin Elmer Intracooler SP cooling Accessory (Perkin Elmer, USA) to study the thermal behaviour of the ibuprofen powder, polymer powders and polymer films. The samples were prepared from several pieces cut from the polymer film to a mass ranging between 5 to 10 mg. The samples were heated in hermetically sealed aluminium pans under nitrogen flow (40 mL/min) at a scanning rate of 20˚C/min from 30 to 300 ˚C. Empty aluminium pan was used as a reference pan. Indium was used as the standard reference material to calibrate the DSC instrument. All measurements were an average of four determinations and expressed as mean ± S.D.

4.2.6.2. Thermogravimetric analysis

TGA was performed using Perkin Elmer Pyris 1 Thermogravimetric Analyser (Perkin Elmer, USA) to monitor the mass of the films as a function of temperature or time as the sample specimen is subjected to a controlled temperature program in a controlled atmosphere. The weight of the empty reference pan placed in the crucible was zeroed and then removed. The samples of known weight between 5 to 10 mg were placed in aluminium pans and measurements performed at a scanning rate of 10 ˚C/min from 25 to 500 ˚C. All measurements were an average of four determinations and expressed as mean ± S.D.

4.2.7. Swelling kinetics

Dried films (1.5 x 1.5 cm) were carefully weighed and immersed in 5mL of PBS 7.4 at 37 ˚C (B Braun Certomat WR Shaker Waterbath Germany). At predetermined intervals, swollen films were taken out, and the excess was blotted with filter paper at the surface. This was then weighed on a balance. The swelling ratio of the film was determined using the following equation (equation 1):

$$Swelling\ ratio = (W_s - W_d)/W_d \qquad (1)$$

Where W_d is the weight of dry film and W_s is the weight of the swollen film. All data were averages of four independent experiments expressed as mean ± S.D.

4.2.8. Drug release profile from bilayer films

The concentration of pure ibuprofen (secondary standard) was derived from a calibration model constructed with the average of six independent measurements. The concentrations of ibuprofen were derived from this calibration curve. Thereafter, the dissolution profile of the ibuprofen-loaded films was studied using the USP dissolution method.

Dried films (4 x 4 cm) were placed in 900 mL of PBS pH 7.4, rotated at 50 rpm and maintained at 32 ± 0.5 °C using Pharma Test PT DT7 USP Apparatus II Dissolution Test Instrument – paddle method (Pharma Test Ltd, Germany). At pre-determined time intervals 5, 10, 15, 20, 30, 60, 90, 120 min, 4, 6 and 24 h, 5 mL aliquots were withdrawn and replaced with 5 mL PBS pH 7.4. Drug concentrations were quantified using UV (ThermoFischer Evolution 60S UV-Visible Spectrophotometer, UK) at 264 nm wavelength after passing through 0.45 µm filter (Sartorius, Germany). All measurements were an average of four determinations and expressed as mean ± S.D.

4.2.9. Drug release kinetics

Data obtained from in vitro release studies were fitted to various kinetic equations. The kinetic models used are zero order, first order, Higuchi and Korsemeyer Peppas equation.

The zero order rate equation (2) describes the systems were the drug release rate is independent of its concentration [22]. The cumulative % drug release vs. time plot is made.

$$C = K_0 t \qquad (2)$$

Where k_0 is zero order rate constant expressed in units of concentration/time and t is the time.

The first order rate equation (3) describes the release from the systems where release rate is concentration dependent [23]. The log cumulative % drug release vs. time plot is made.

$$Log\ C = Log\ C_0 - Kt/2.303 \qquad (3)$$

Where C_0 is the initial concentration of drug and K is first order constant.

Higuchi described the release of drugs from insoluble matrix as a square root of time dependent process based on Fickian diffusion: equation (4) [24]. The cumulative % drug release vs. square root of time is made.

$$Q = Kt^{1/2} \qquad (4)$$

Where K, is the constant and it reflects the design variables of the system.

Korsemeyer *et al.* derived a simple relationship which described drug release from a polymeric system: equation (5). To find out the mechanism of drug release, first 60 % drug release data was fitted in Korsemeyer-Peppas model:

$$M_t/M_\infty = Kt^n \qquad (5)$$

Where M_t/M_∞ is a fraction of drug released at time t, K is the rate constant and n is the release exponent. The n value is used to characterize different release mechanisms [25]. The log cumulative

% drug release vs. log time plot is made. The criterion for selecting the appropriate model is the highest R^2 value which indicates linearity of dissolution data [26].

4.2.10. Similarity factors

The similarity fit factor denoted f_2 was used to compare the dissolution profiles of the ibuprofen loaded gellan - DEAE-Dextran (GIbDD) composite or bilayer (GIb/DDB) films (test) and GIb binary film (reference). The similarity f_2 factor is defined by equation 6 proposed by Moore and Flanner [27]:

$$f_{2=50\,Log}\left\{(1+\frac{1}{n}\sum_{t=1}^{n}\left(R_t-T_t\right)^2)^{-0.5}\times 100\right\} \qquad (6)$$

Where n is the number of dissolution sample times, and R_t and T_t are the individual or mean percent dissolved at each time point, t, for the reference and test dissolution profiles, respectively. The f_2 value greater than 50 suggests that the two profiles are similar. The f_2 value of 100 suggests that the test and the reference profiles are identical and as the value becomes smaller the dissimilarity between release profiles increases [28].

4.2.11. Statistical analysis

Quantitative data are expressed as mean ± standard deviation (S.D). The significance of the differences between means was assessed using Analysis of Variance (ANOVA) and Post hoc Tukey Test with a statistical significance level set at $p < 0.05$ using IBM SPSS® (Statistical Package for Social Science) 20.

4.3. Results and discussions

4.3.1. Preparation and optimization of plain and drug loaded composite and bilayer films

The basic constituents of films include polymers, solvents, plasticizers and cross-linking agents. Gellan and DEAE-Dextran composite films were prepared by casting method from aqueous solution without the use of organic toxic solvents and cross-linking agents since both polymers are soluble in hot water (above 90 °C) and cold water respectively. The amount of gellan used in the mixing ratio was fixed at 2% based on preliminary optimization studies done. The 2% gellan film was found to have better mechanical properties when compared with the 1% gellan film, hence its selection. A varying concentration range of 0.125 to 1% of DEAE-Dextran was used to study the effect of its increasing concentration on the films formed. Due to the poor mechanical properties of biopolymer films, hydrophobic materials and plasticizers have been incorporated to improve their mechanical properties [16]. Glycerol was incorporated as plasticizer to provide elasticity for the films based on the proposition Yang and Paulson of using 60% w/w plasticizer: (plasticizer + polymer) as the lowest effective concentration, therefore used in this ratio in the formulation 3% glycerol: 2% gellan + 3% glycerol. The authors found that below that proposed concentration, the films were found to be brittle and difficult to handle, while when it exceeds its compatibility limit, it exhibits white residues on the surface. Plasticizers increase the flexibility and workability of the polymers; and degradability of biodegradable polymers in preparation of polymer films [29]. Pure gellan films (G) prepared had the highest transparency when visualized and smoothness. The smoothness is a desired property since the formulation can maintain a smooth and uniform surface when applied to the skin. There was reduced clarity and transparency when gellan solution was reacted with oppositely charged DEAE-Dextran at different mixing ratios to form the polyelectrolyte complex (PEC) composite films (GDD). The increasing concentration of DEAE-Dextran decreased the clarity and transparency of the films. Increased concentration of DEAE-Dextran increased crosslinking efficiency. This was supported by Yang *et al.* report that films with a higher crosslinking degree tend to exhibit an increase in

opacity due to a decrease in polymer inter-chain spacing, which allows less light to pass through it [30].

In the preparation of PEC bilayer films, gellan films were used as the base component since DEAE-Dextran does not form films on its own even at high concentrations from results of preliminary studies. Bilayer films formed by immersing fixed concentration of gellan (2%) films into varying concentrations of DEAE-Dextran were transparent with glossy, smooth but sticky surfaces. The stickiness of the surfaces increased with increasing concentration of DEAE-Dextran solutions. This shows potential bioadhesive properties with potential applications in transdermal patches.

The conformational transition from coil to helix structure could be used to describe the mechanism of formation of gellan films. The choice of heating up to 90 °C is based on the finding that gellan gum is stable at higher temperatures with maintained strength at 90 °C [31]. Sanderson and Clark reported that the melting temperature can be below or above 100 °C, depending on the conditions of gel formation [8]. Brittle films are thus formed by gellan due to tight packing of gellan chains.

When gellan was loaded with ibuprofen solubilized in NaOH (GIb), it remained transparent. The PEC-ibuprofen loaded (GIbDD) changed from opaque film forming mixtures which indicated formation of two-phase structure and turned back to translucent films after evaporation. This similar occurrence was reported by Ma and McHugh in the preparation of PLGA-acetone-naproxen films due to the formation of two-phase structure while opaque and finally reverting back to clear state at the end of the solidification process [32]. Bierhalz *et al.* also reported an increase in film opacity on incorporation of natamycin into alginate/pectin films related to the low water solubility of naproxen [32]. An increase in opacity due to addition of hydrophobic substances was also reported by Yang and Paulson [16]. The authors also opined in their further work that films with a higher crosslinking degree tend to exhibit an increase in opacity due to a decrease in polymer inter-chain spacing which allows less light to pass through [30]. The use of a crosslinker was avoided in this study; rather an

oppositely charged polyelectrolyte (DEAE-Dextran) to gellan was used in the preparation of film which showed an increase in opacity as DEAE-Dextran was increased.

4.3.2. Physicochemical characterization and mechanical properties of plain and Ibuprofen loaded composite and bilayer films

4.3.2.1. Morphology and size studies

4.3.2.1.1. Scanning electron microscopy of plain and Ibuprofen loaded composite and bilayer films

Scanning electron microscopy (SEM) was used to investigate the differences in film morphology due to method of preparation (composite and bilayer) and addition of ibuprofen to plain films. SEM micrographs of the surface and cross sectional of the composite and bilayer films with and without ibuprofen were presented in Figure 115 to 117.

Plain gellan (G) film exhibited a smooth and homogenous surface and cross section with a continuous and compact matrix in Figure 115. Similar report was made by Chang *et al.* about gellan films exhibiting smooth and dense morphological structures required to prevent apical migration of fibroblasts into bony defects in the development of regenerative barrier membrane [17].

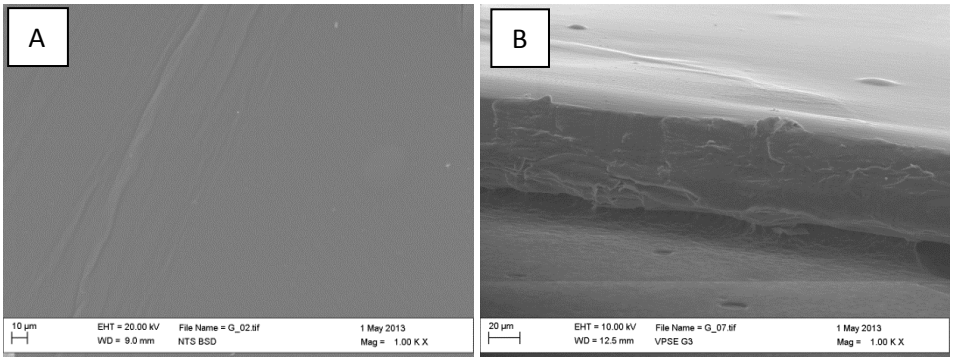

Figure 115 Scanning electron micrographs of gellan films (A) surface of plain gellan G film (B) cross section of G film.

Gellan-DEAE-Dextran (GDD) PEC composite films exhibited increased surface irregularity and cross section morphologies with the addition of increasing concentration of DEAE-Dextran in Figure 116. While the gellan-DEAE-Dextran (G/DDB) PEC bilayer films exhibited smooth and homogenous

surfaces due to the DEAE-Dextran coat on the surface of the films in Figure 117. The cross section of the G/DDB bilayer films was homogenous.

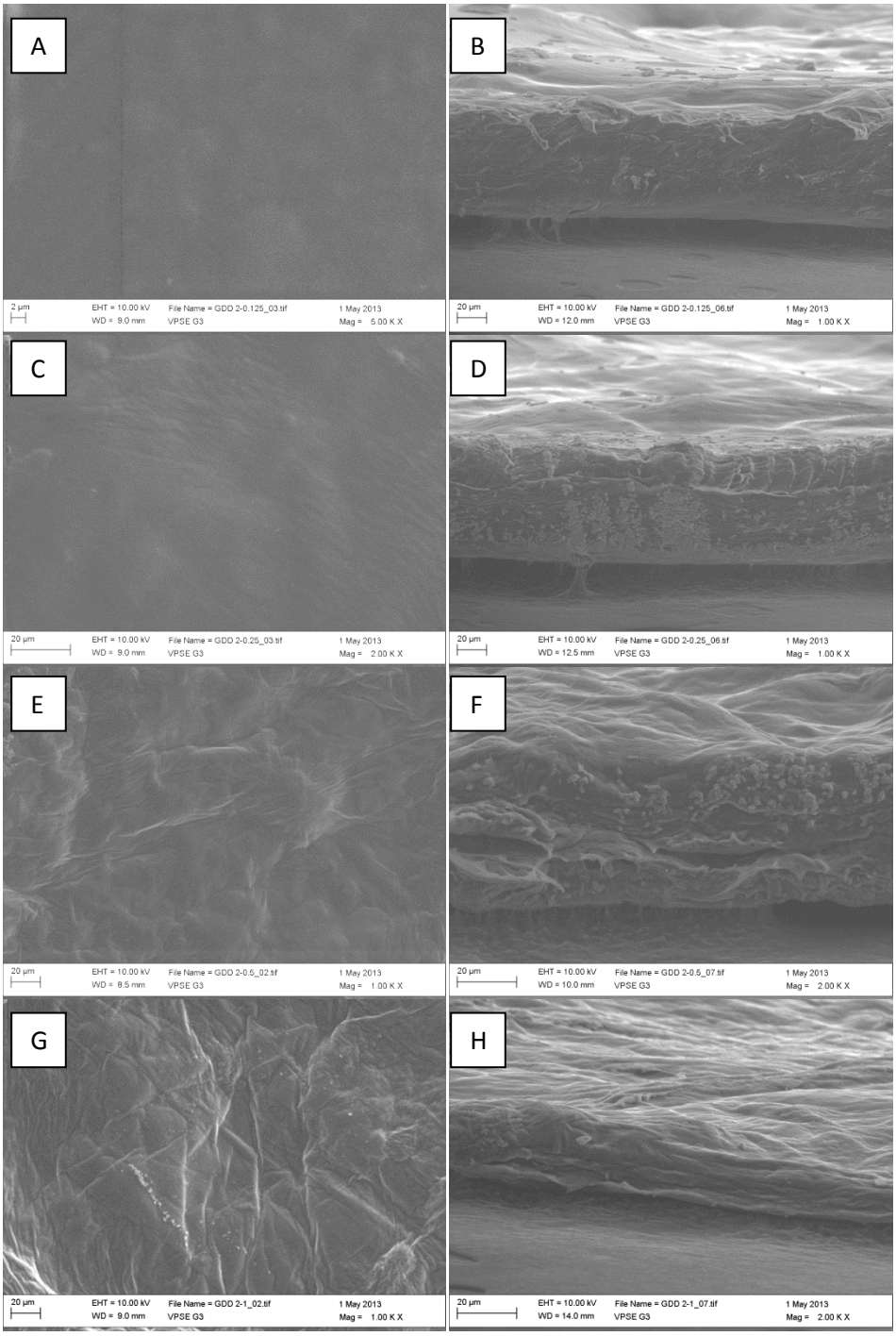

Figure 116 Scanning electron micrographs of gellan-DEAE-Dextran composite films (A) surface of GDD 2:0.125 (B) cross-section of 2:0.125 (C) surface of GlbDD 2:0.25 (D) cross-section of GlbDD 2:0.25 (E) surface of GlbDD 2:0.5 (F) cross-section of GlbDD 2:0.5 (G) surface of GlbDD 2:1 (H) cross-section of GlbDD 2:1.

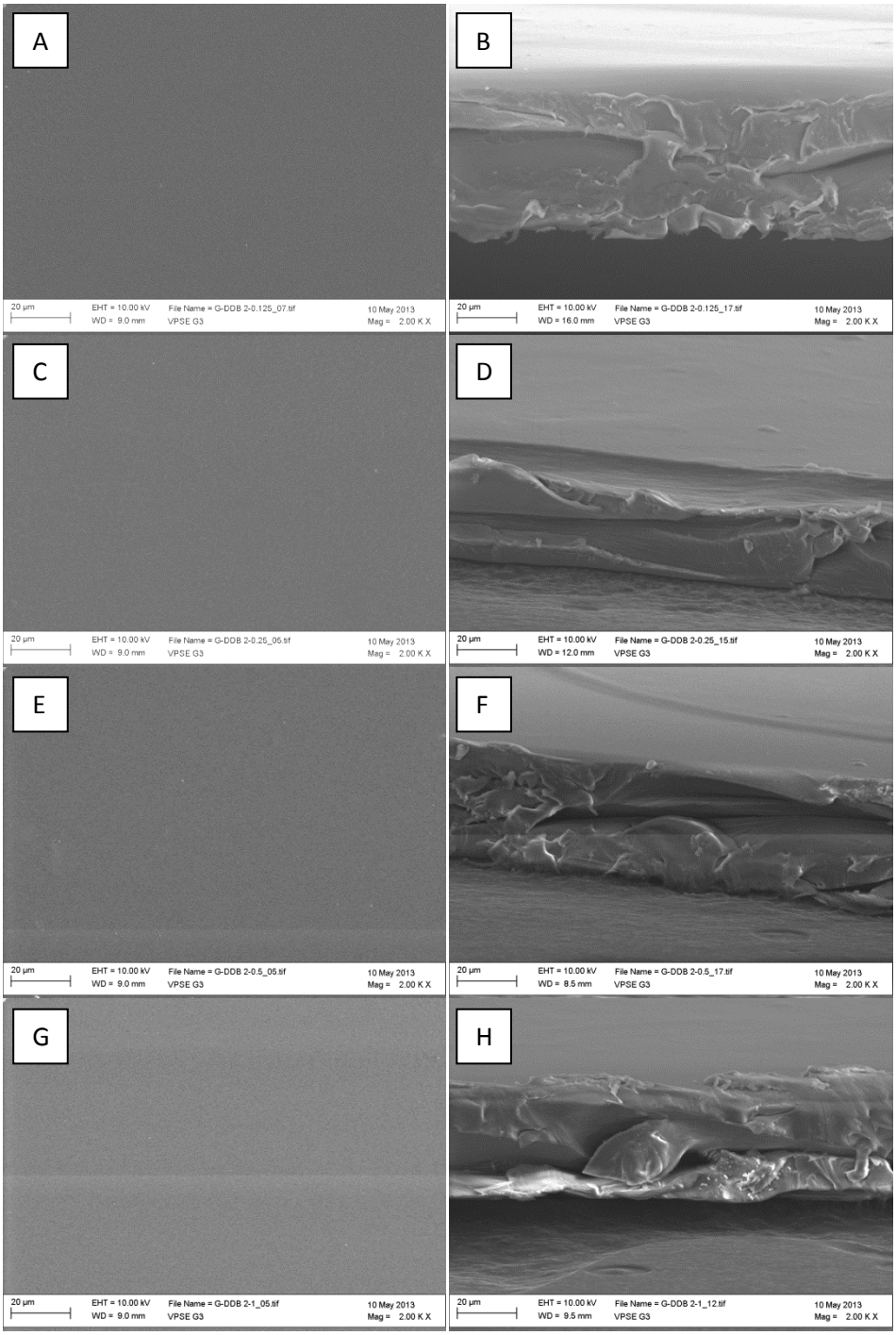

Figure 117 Scanning electron micrographs of gellan-DEAE-Dextran PEC bilayer films (A) surface of G/DDB 2:0.125 (B) cross-section of G/DDB 2:0.125 (C) surface of G/DDB 2:0.25 (D) cross-section of G/DDB 2:0.25 (E) surface of G/DDB 2:0.5 (F) cross-section of G/DDB 2:0.5 (G) surface of G/DDB 2:1 and (H) cross-section of G/DDB 2:1.

The effect of the incorporation of ibuprofen into the films was evaluated by the scanning electron microscopy (SEM). The surface and cross sectional micrographs of the prepared films are presented in Figures 118 to 120.

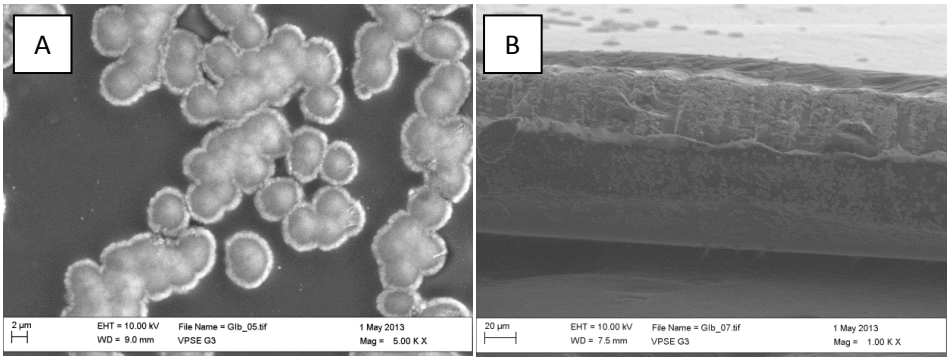

Figure 118 Scanning electron micrographs of ibuprofen loaded gellan binary film (A) surface morphology of GIb (B) cross-section of GIb

The incorporation of ibuprofen caused changes on the film surfaces with GIb and GIbDD showing clearly visible spheres with concentric layers dispersed throughout the film matrix and particle sizes of 7.85 µm and 7.79 to 3.71 µm respectively. The particle sizes of the spheres on the surfaces of the GIbDD films decreased with increasing concentration of DEAE-Dextran. Bierhalz *et al*. reported observing the crystals of natamycin on the film surface compared to the control films which had homogenous film surfaces [33]. There are more concentric layers round the spheres in the ibuprofen loaded complex films (GIbDD) in Figure 119 when compared with GIb films in Figure 118, indicating that extra layers where formed by addition of DEAE-Dextran. The particle sizes of GIbDD films were smaller compared to GIb films. The cross section of the films exhibited spherical patterns disperse along its plane with particle sizes in the range of 2.56 to 4.12 µm. Ibuprofen dissolved completely in sodium hydroxide as molecular state, hence the drug was distributed homogenously in the formed films.

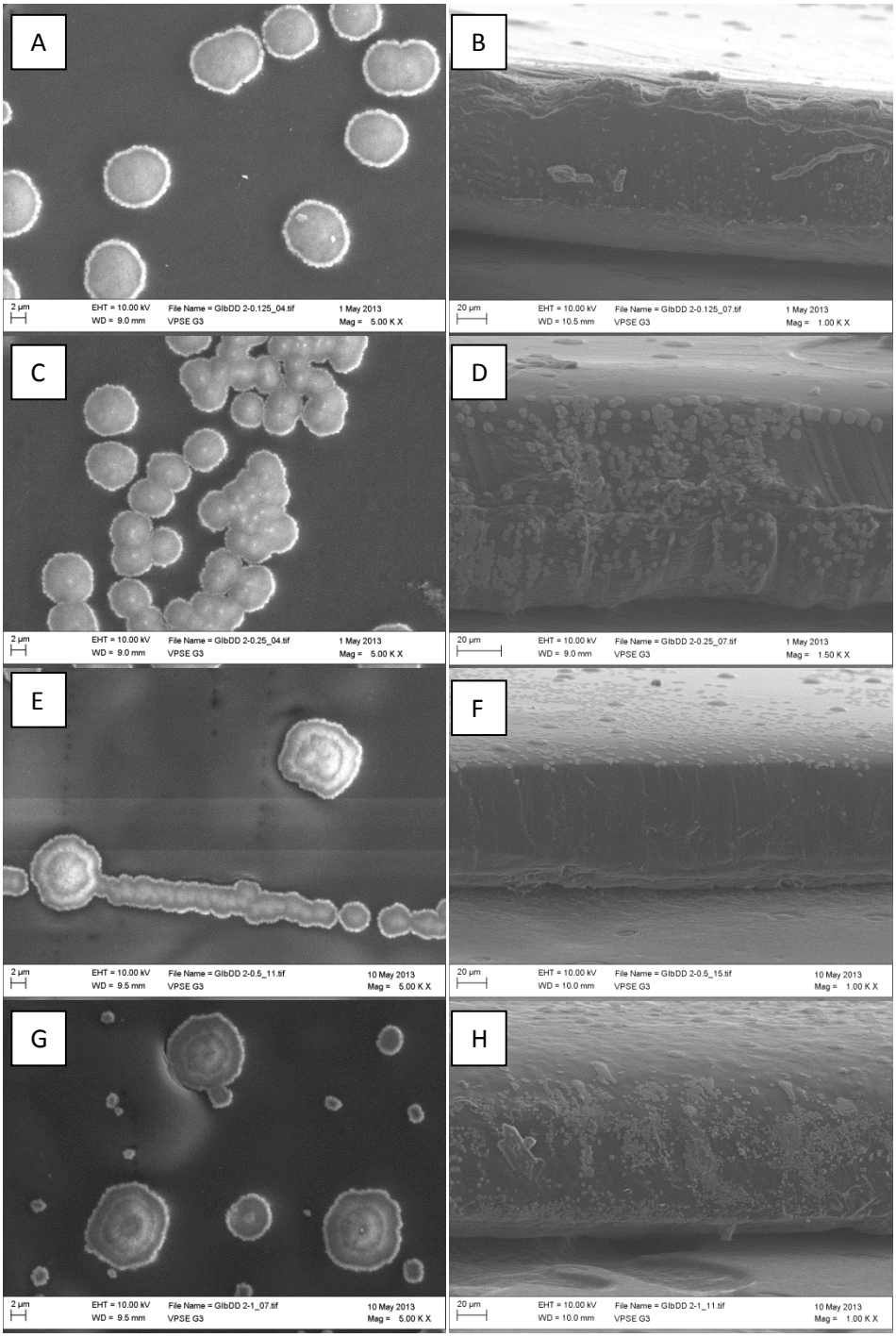

Figure 119 Scanning electron micrographs of ibuprofen loaded gellan-DEAE-Dextran complex composite films (A) surface of GIbDD 2:0.125 (B) cross-section of GIbDD 2:0.125 (C) surface of GIbDD 2:0.25 (D) cross-section of GIbDD 2:0.25 (E) surface of GIbDD 2:0.5 (F) cross-section of GIbDD 2:0.5 (G) surface of GIbDD 2:1 (H) cross-section of GIbDD 2:1.

The GIb/DDB films in Figure 120 showed less spherical patterns on the surface with somewhat empty pores which may have been caused by the diffusion of Ibuprofen out of the gellan base layer while being immersed in DEAE-Dextran solutions. The depletion was also exhibited along the cross section of the Ibuprofen loaded bilayer films. The particle sizes of spheres on the surface of GIb/DDB

films were in the range of 217 to 3446 nm with GIb/DDB film only in the micrometer range. The particle sizes decreased with increasing concentration of DEAE-Dextran.

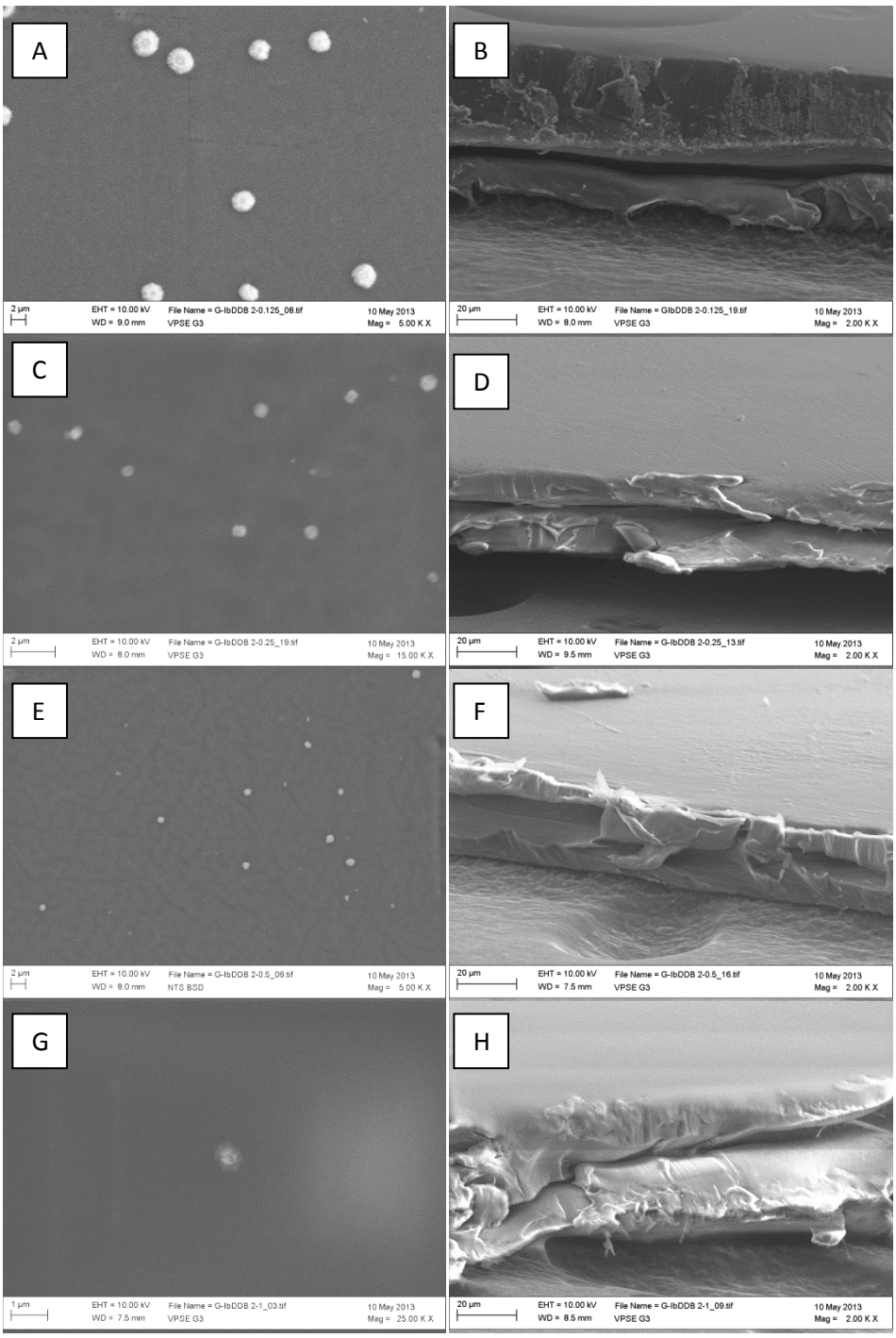

Figure 120 Scanning electron micrographs of ibuprofen loaded gellan-DEAE-Dextran complex bilayer films (A) surface of GIb/DDB 2:0.125 (B) cross-section of GIb/DDB 2:0.125 (C) surface of GIb/DDB 2:0.25 (D) cross-section of GIb/DDB 2:0.25 (E) surface of GIb/DDB 2:0.5 (F) cross-section of GIb/DDB 2:0.5 (G) surface of GIb/DDB 2:1 (H) cross-section of GIb/DDB 2:1.

The particle sizes exhibited on the surfaces of GIb/DDB bilayer films were smaller when compared to particle sizes on GIb and GIbDD composite films. The particle sizes of the composite and bilayer films were significantly reduced ($p < 0.05$, $n = 4$) when compared to raw ibuprofen crystals of 31.42 µm.

4.3.2.1.2. Atomic force microscopy (AFM)

Atomic Force Microscopy (AFM) is a characterization technique that can provide direct spatial mapping of surface topography and surface heterogeneity with nanometer resolution [34]. The AFM imaging of the films was done under contact mode with intrinsic challenges which include: difficulty in achieving ultimate high resolution; transient stick-and-slip caused by lateral force which may lead to sample damage. These problems are overcome by the introduction of Acoustic AC mode which removes the tip or sample degradation effects and makes it a good technique of imaging polymers.

The topography retrace images of G and GDD films are shown in Figures 121 and 122. The G film image exhibited a gellan rich surface while the GDD 2:0.5 film (representative) showed a gellan-DEAE-Dextran rich surface.

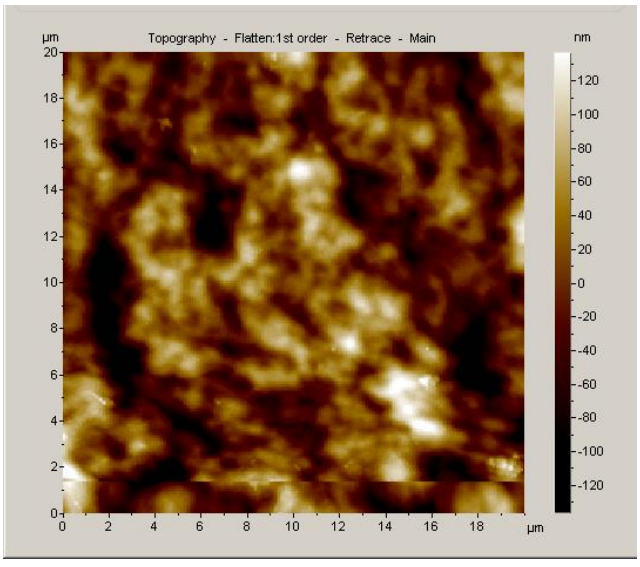

Figure 121 Topography retrace image of plain gellan G film.

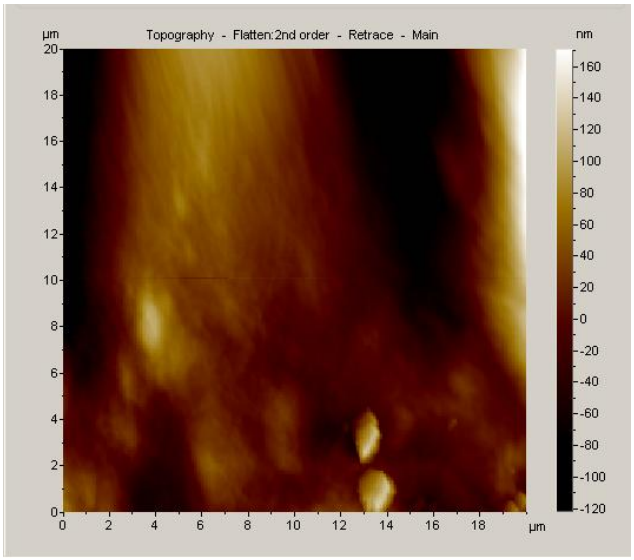

Figure 122 Topography retrace image of gellan-DEAE-Dextran GDD 2:0.5 composite film.

The topography retrace images of GIb and GIbDD 2:0.5 composite films are shown in Figure 123 and 124. The GIb image exhibited one concentric layer (gellan) round the core (ibuprofen) of the sphere formed in the film while two concentric layers were formed round the GIbDD sphere depicting a core (ibuprofen) surrounded by two shells (first is DEAE-Dextran, followed by the gellan coat). These images were similar to those exhibited by SEM micrographs of the films. The topography first trace, amplitude and phase trace images of the films were presented in Figures 164 to 166 in the Appendix I.

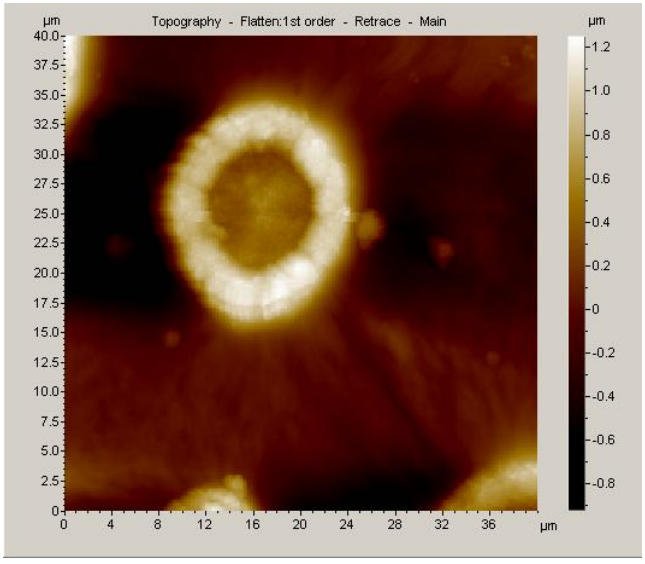

Figure 123 Topography retrace image of ibuprofen loaded gellan GIb film.

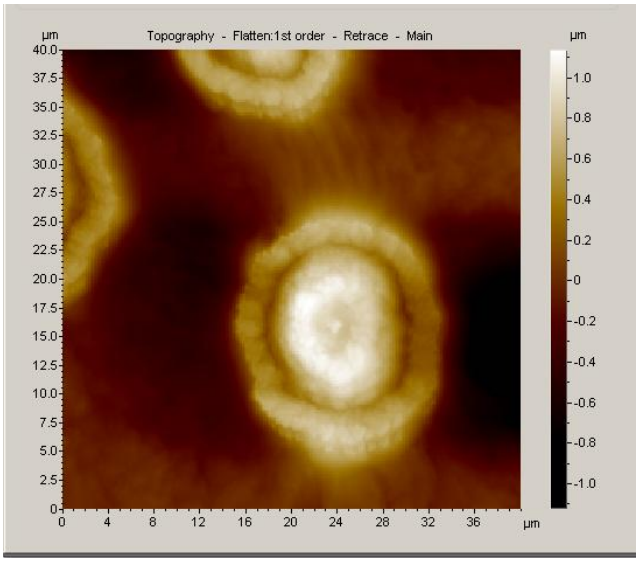

Figure 124 Topography retrace image of ibuprofen loaded gellan-DEAE-Dextran GIbDD 2:0.5 composite film.

4.3.2.2. Film thickness

The results of the average film thickness of the plain composite and bilayer films were presented in Table 80. The thickness of plain gellan reference G (2% gellan) film was 0.062 mm. Chang *et al.* reported the thickness of 2% gellan film prepared without plasticizer (glycerol) to be 0.034 mm [17].The thickness of the films prepared ranged from 0.082 to 0.167mm for the composite GDD films. The values indicated that there was a significant increase in thickness of the films on addition of DEAE-Dextran to the formulations. The GDD composite films were thus significantly higher than the plain gellan G film ($p < 0.05$, $n = 6$).

The profile of the thickness of the films was presented in Figure 125. There was an increase in thickness of GDD composite films with increasing DEAE-Dextran concentration and were greater than the baseline G film with thickness 0.062 mm. The increase in thickness is expected as the increase in polymer concentration leads to higher solution viscosity.

The G/DDB PEC bilayer films formed ranged from 0.060 to 0.073 mm. There was an initial increase and a decrease with increasing concentration of DEAE-Dextran. The statistical analysis of the film thickness results showed that the addition of DEAE-Dextran to the plain gellan G film did not

significantly change the thickness of the G/DDB bilayer films ($p > 0.05$, $n = 6$). However, the GDD composite films were significantly thicker than the G/DDB bilayer films ($p < 0.05$, $n = 6$).

Table 80 The thickness of gellan films. Each value represents mean ± S.D (n = 6)

Formulation	Film Thickness (mm) Mean ± S.D
G	0.062±0.004
GDD 2:0.125	0.082±0.004
GDD 2:0.25	0.097±0.008
GDD 2:0.5	0.138±0.010
GDD 2:1	0.167±0.008
G/DDB 2:0.125	0.073±0.008
G/DDB 2:0.25	0.062±0.004
G/DDB 2:0.5	0.060±0.001
G/DDB 2:1	0.065±0.005

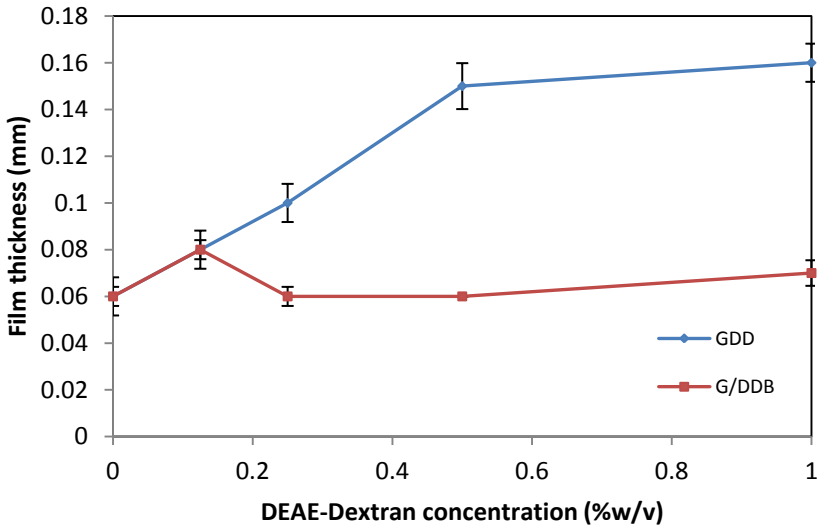

Figure 125 Film thickness of GDD composite and G/DDB bilayer films. Each data point represents mean ± S.D (n = 6).

The profile of the ibuprofen loaded composite and bilayer film thickness was presented in Figure 126. The thickness of the films prepared ranged from 0.097 to 0.117 mm for the ibuprofen loaded composite films shown in Table 81. The thickness of film increased with increasing concentration of DEAE-Dextran in the films except the thickness decreased to a minimum at low concentration of DEAE-Dextran at 2:0.25 gellan-DEAE-Dextran weight ratio. The GIbDD ibuprofen loaded composite films formed were significantly thicker ($p < 0.05$, $n = 6$) than the baseline ibuprofen loaded film (GIb) with thickness of 0.078 mm. The addition of ibuprofen to the formulations changed the thickness of the films significantly. Similar values were reported for gellan films loaded with ascorbic acid with

thickness in the range of 0.085 (±0.005 mm) [35]. The GIb/DDB PEC bilayer films had a thickness of 0.072 (±0.005 mm). The GIb/DDB ibuprofen loaded bilayer films formed were thinner than the single component ibuprofen loaded film (GIb). The GIbDD ibuprofen loaded composite films were significantly thicker ($p < 0.05$, $n = 6$) than the GIb/DDB ibuprofen loaded bilayer films.

Table 81 The thickness of ibuprofen loaded gellan, gellan-DEAE-Dextran composite and bilayer films. Each value represents mean ± S.D (n = 6).

Formulation	Film Thickness (mm)
GIb	0.078±0.004
GIbDD 2:0.125	0.100±0.006
GIbDD 2:0.25	0.097±0.008
GIbDD 2:0.5	0.110±0.006
GIbDD 2:1	0.117±0.005
GIb/DDB 2:0.125	0.077±0.005
GIb/DDB 2:0.25	0.067±0.005
GIb/DDB 2:0.5	0.072±0.007
GIb/DDB 2:1	0.072±0.007

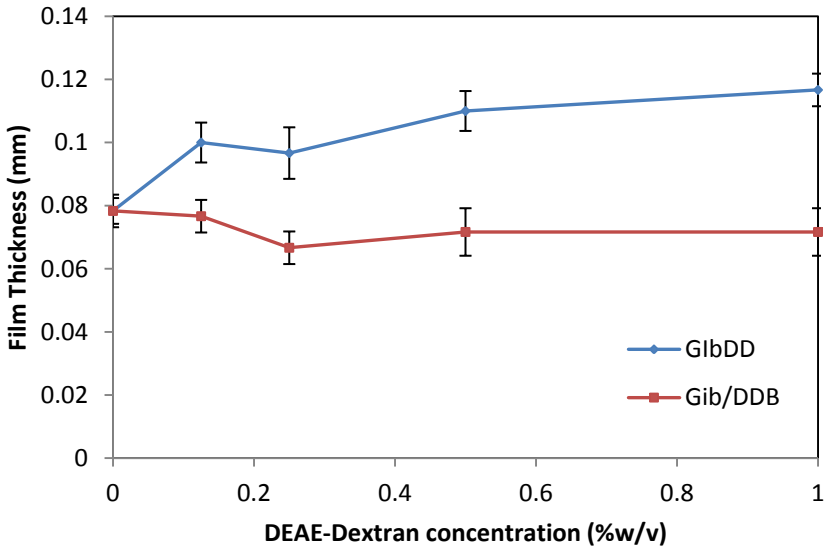

Figure 126 Film thickness of GIbDD composite and GIb/DDB bilayer films. Each data point represents mean ± S.D (n = 6).

4.3.2.3. Mechanical properties

The effects of DEAE-Dextran concentration on the mechanical properties of gellan films were evaluated. The mechanical properties of gellan, gellan-DEAE-Dextran composite and bilayer films were shown in Table 82 and 83.

The tensile strength of the films which indicated the films resistance to abrasion for plain gellan G film was 17.14 MPa, while GDD composite films ranged from 0.60 to 16.26 MPa. The addition of DEAE-Dextran to gellan decreased the tensile strength of the composite blend films. Statistical analysis indicated that lower concentrations of DEAE-Dextran (0.125 and 0.25%) did not cause significant reduction ($p > 0.05$, $n = 4$) in the tensile strength of GDD 2:0.125 and GDD 2:0.25 compared to the plain gellan G film. However, higher concentrations of DEAE-Dextran (0.5 and 1.0 %) caused significant reduction ($p < 0.05$) in the tensile strength of GDD 2:0.5 and GDD 2:1 film. This could be due to the interaction between DEAE-Dextran and gellan which resulted in a more flexible film. Comparable values were reported by Lee *et al.* which ranged from 12.4 to 59 MPa for gellan/gelatin composite films with the tensile strength decreasing linearly as the gelatin ratio increased [10]. The tensile strength of the G/DDB bilayer films ranged from 11.98 to 20.33 MPa with G/DDB 2:0.125 and G/DDB 2:0.5 exhibiting higher tensile strength than G single component film. The addition of DEAE-Dextran in the bilayer method did not significantly change ($p > 0.05$, $n = 4$) the tensile strength of the films when compared to the plain gellan G film. The tensile strength profile in Figure 127 showed that the G/DDB bilayer film exhibited two maxima values at 0.125 and 0.5% DEAE-Dextran as the concentration of DEAE-Dextran increased. The G/DDB bilayer films exhibited significantly higher ($p < 0.05$, $n = 4$) tensile strength than their corresponding GDD composite films.

Table 82 Mechanical properties of gellan and gellan-DEAE-Dextran PEC composite films. Each value represents mean ± SD (n = 4).

Formulation	Tensile strength(MPa)	Percentage Tensile Elongation (%)	Elastic Modulus (MPa)
G	17.14±2.43	19.53±2.35	742.00±40.93
GDD 2:0.125	16.26±2.13	13.90±2.30	480.67±86.64
GDD 2:0.25	10.88±1.74	20.23±1.59	201.33±17.90
GDD 2:0.5	6.32±0.62	18.63±3.45	22.23±4.02
GDD 2:1	0.60±0.07	9.37±0.91	17.80±5.27

Table 83 Mechanical properties of gellan and gellan-DEAE-Dextran PEC bilayer films. Each value represents mean ± SD (n = 4).

Formulation	Tensile strength (MPa)	Percentage Tensile Elongation (%)	Elastic Modulus (MPa)
G	17.14±2.43	19.53±2.35	742.00±40.93
G/DDB 2:0.125	20.33±3.25	2.33±0.10	927.00±105.24
G/DDB 2:0.25	12.91±1.62	1.00±0.05	1206.67±166.23
G/DDB 2:0.5	19.36±2.78	1.37±0.12	1212.00±100.02
G/DDB 2:1	11.98±1.42	0.80±0.06	1261.67±106.89

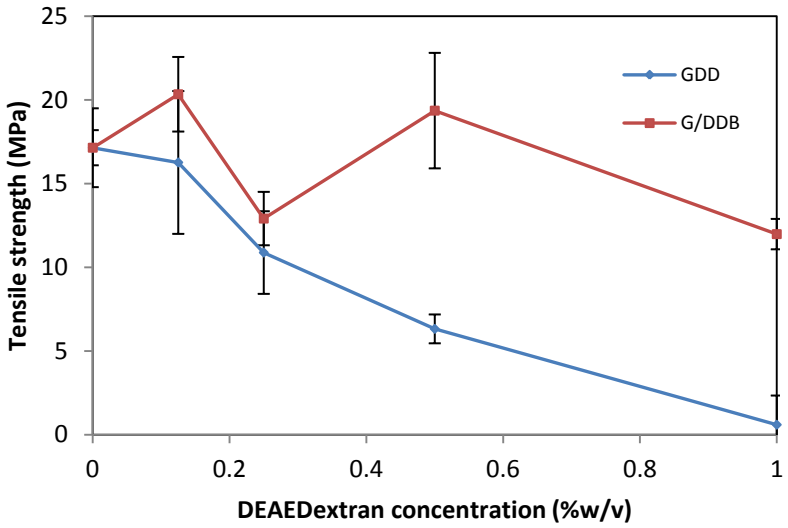

Figure 127 Effect of DEAE-Dextran concentration on the tensile strength of gellan and gellan-DEAE-Dextran PEC composite and bilayer films. Each data point represents mean ± SD (n = 4).

The percentage tensile elongation which indicated the flexibility of the films was 19.53% for G film; ranged from 9.37 to 20.23% for GDD films and from 0.88 to 2.33% for G/DDB films. The addition of DEAE-Dextran to the GDD films did not cause significant change ($p > 0.05$, $n = 4$) except with the higher concentration (GDD 2:1) when compared to plain gellan G film. The GDD 2:0.25 composite film was the only mixing ratio which exhibited a higher tensile elongation than gellan film.

G/DDB bilayer films were less flexible with significantly reduced ($p < 0.05$, $n = 4$) tensile elongation when compared with the GDD composite films. The profile in Figure 128 showed that the tensile elongation of GDD composite film initially decreased then increased and finally decreased as DEAE-Dextran concentration increased. While G/DDB bilayer films decreased as the DEAE-Dextran

increased. This suggests that the incorporation of DEAE-Dextran reduced the flexibility and increased brittleness of gellan composite and bilayer films.

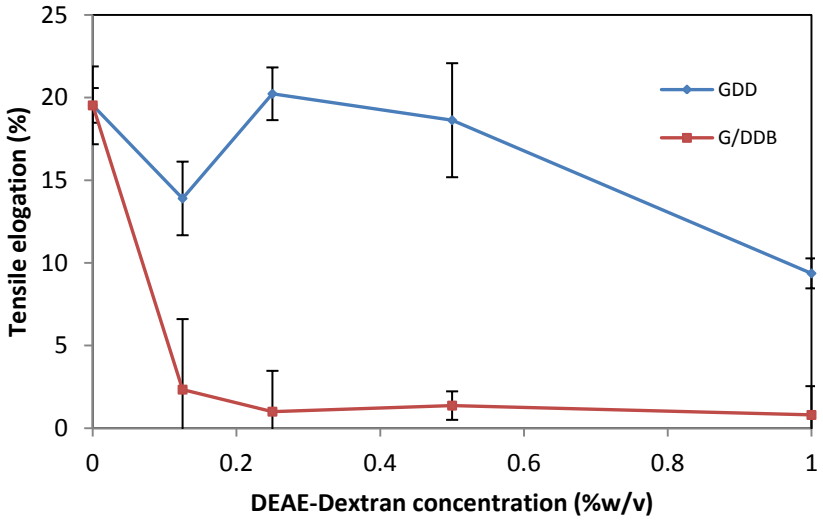

Figure 128 Effect of DEAE-Dextran concentration on the percentage tensile elongation of gellan and gellan-DEAE-Dextran PEC composite and bilayer films. Each data point represents mean ± SD (n = 4).

Young's modulus also known as elastic modulus is used to measure the stiffness of an elastic material. Stiffness is the capacity of a material to resist deformation in the elastic range. The elastic modulus was 742 MPa for G film; ranged from 17.80 to 480.67 MPa for GDD films and 927 to 1261.67 MPa for G/DDB films in Figure 129. Lower concentrations of DEAE-Dextran (0.125 and 0.25%) did not cause significant reduction ($p > 0.05$, $n = 4$) in the elastic modulus of GDD 2:0.125 and GDD 2:0.25 compared to the plain gellan G film. However, higher concentrations of DEAE-Dextran (0.5 and 1.0%) caused significant reduction ($p < 0.05$, $n = 4$) in the elastic modulus of GDD 2:0.5 and GDD 2:1 film. The G/DDB films had significantly higher ($p < 0.05$, $n = 4$) elastic modulus values than G and GDD films. The higher elastic modulus values exhibit greater stiffness when compared to lower elastic modulus values characteristic of softer films. The GDD composite films showed the lowest value in tensile strength and elastic modulus but highest percentage tensile elongation. This can be attributed to the presence of DEAE-Dextran; where the gellan-DEAE-Dextran bonds reduced the intermolecular forces along polymer chains, which reduced the elastic modulus and increased the percentage tensile elongation. The GDD composite films were weaker and more flexible when

compared to G/DDB bilayer films. Mechanical strength is increased by increasing the cross linking density leading to stronger films being formed. However, with increase in cross linking density, there is a decrease in percentage elongation of the films resulting in brittleness.

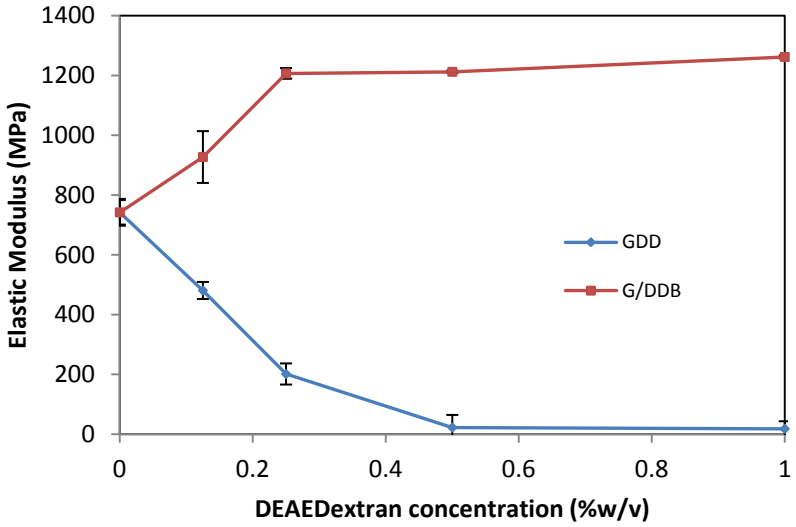

Figure 129 Effect of DEAE-Dextran concentration on the elastic modulus of gellan and gellan-DEAE-Dextran PEC composite and bilayer films. Each data point represents mean ± SD (n = 4).

The mechanical properties of ibuprofen loaded gellan, gellan-DEAE-Dextran composite and bilayer films were shown in Table 84 and 85.

Table 84 Mechanical properties of drug loaded gellan composite films. Each value represents mean ± SD (n = 4).

Formulation	Tensile strength (MPa)	Percentage Tensile Elongation (%)	Elastic Modulus (MPa)
G	17.14±2.43	19.53±2.35	742.00±40.93
GIb	7.61±0.53	21.93±1.05	462.33±44.92
GIbDD 2:0.125	3.31±0.14	20.23±4.27	245.67±22.27
GIbDD 2:0.25	5.62±0.58	18.93±2.47	341.67±45.28
GIbDD 2:0.5	5.24±0.42	20.17±0.86	342.33±36.14
GIbDD 2:1	4.14±0.37	22.4±1.74	185.00±21.63

Table 85 Mechanical properties of drug loaded gellan bilayer films. Each value represents mean ± SD (n = 4).

Formulation	Tensile strength (MPa)	Percentage Tensile Elongation (%)	Elastic Modulus (MPa)
GIb	7.61±0.53	21.93±1.05	462.33±44.92
GIb/DDB 2:0.125	28.66±3.94	5.33±0.15	1149.33±97.08
GIb/DDB 2:0.25	10.91±1.12	1.10±0.35	1142.50±94.00
GIb/DDB 2:0.5	19.69±2.58	2.50±0.70	1036.00±95.66
GIb/DDB 2:1	24.67±2.71	2.63±0.26	179.00±6.57

The tensile strength GIb film was 7.61 MPa, while GIbDD composite films ranged from 3.31 to 5.62 MPa. The incorporation of ibuprofen into gellan significantly decreased ($p < 0.05$, $n = 4$) the tensile strength of the drug loaded gellan (GIb) and GIbDD composite films. The decrease in tensile strength may be due to the incorporated ibuprofen causing changes in the polymeric structure [33]. Bierhalz *et al.* reported a reduction in tensile strength on incorporation of natamycin into alginate/pectin composite films which may be attributed to modifications in the polymeric structure [33]. The tensile strength of the GIb/DDB bilayer films ranged from 10.91 to 28.66 MPa exhibiting significantly higher ($p < 0.05$, $n = 4$) tensile strength than GIb and GIbDD films in Figure 130. The bilayer films may have more linear and organized chain, giving more energetic crosslinking and higher cohesive forces between the chains.

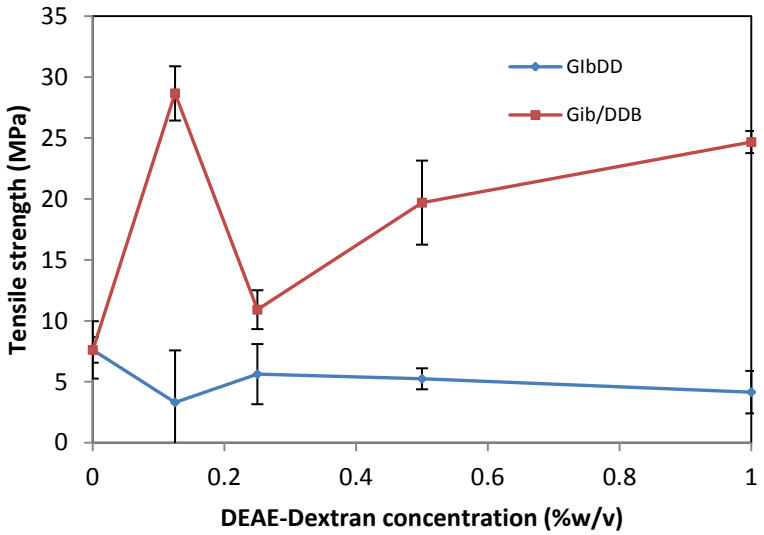

Figure 130 Effect of DEAE-Dextran concentration on the tensile strength of ibuprofen loaded gellan and gellan-DEAE-Dextran PEC composite and bilayer films. Each data point represents mean ± SD (n = 4).

The percentage tensile elongation which indicated the flexibility of the films was 21.93% for GIb film; ranged from 18.93 to 22.40% for GIbDD films and from 1.10 to 5.33% for GIb/DDB films in Figure 131. GIb/DDB films were less flexible than the GIb and the GIbDD films. The brittleness of the GIb/DDB films which was as low as 1.1% may be due to drying of the films twice (double heat treatment) before and after immersion during the bilayer preparation.

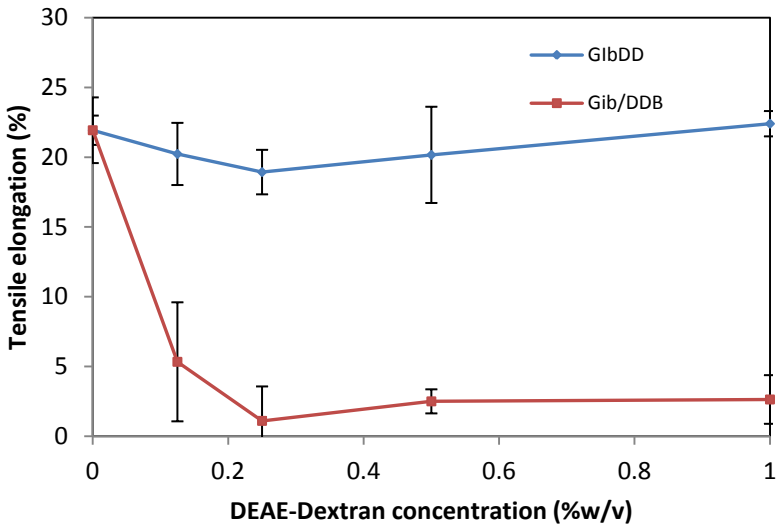

Figure 131 Effect of DEAE-Dextran concentration on the percentage tensile elongation of ibuprofen loaded gellan and gellan-DEAE-Dextran PEC composite and bilayer films. Each data point represents mean ± SD (n = 4).

The elastic modulus was 462.33 MPa for GIb film; ranged from 185.00 to 342.33 MPa for GIbDD films and 179.00 to 1149.33 MPa for GIb/DDB films in Figure 132. The GIb/DDB films except GIb/DDB 2:1 had higher elastic modulus values than GIb and GIbDD films. The addition of ibuprofen resulted in decreased elastic modulus values of GIb and GIbDD 2:0.125 when compared to plain G and GDD 2:0.125 films. However, the effect of addition of ibuprofen on higher mixing ratios of gellan-DEAE-Dextran (GIbDD 2:0.25, GIbDD 2:0.5 and GIbDD 2:1) resulted in significant increase ($p < 0.05$, $n = 4$) in elastic modulus values when compared to the plain GDD films. The mechanical properties of gellan film were improved when loaded with ibuprofen by the bilayer immersion method GIb/DDB films but they exhibited low tensile elongation values caused by the effect of heat during the two drying stages.

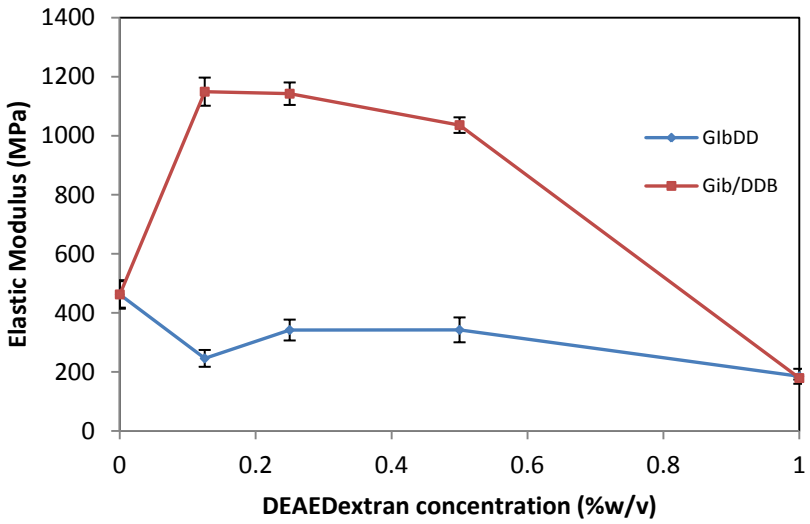

Figure 132 Effect of DEAE-Dextran concentration on the elastic modulus of ibuprofen loaded gellan and gellan-DEAE-Dextran PEC composite and bilayer films. Each data point represents mean ± SD (n = 4).

4.3.3. Spectroscopic studies of plain and ibuprofen loaded composite and bilayer films - Fourier Transform Infrared

To investigate possible chemical or physical interaction between ibuprofen and excipients, the functional groups exhibited by the plain and drug loaded composite and bilayer film were studied by the FTIR spectrometry technique. Figure 133 shows the FTIR spectra of gellan, DEAE-Dextran; gellan and GDD films. Gellan powder showed significant peaks at 3318 cm^{-1}, 2897 cm^{-1}, 1601 cm^{-1} and 1403 cm^{-1} presented in Tables 86 and 87. The broad absorption band at 3318 cm^{-1} is assigned to the stretching –OH groups in gellan. The peak at 2897 cm^{-1} is due to the stretching vibrations of the $–CH_2$ group [11]. The peaks at 1601 cm^{-1} and 1403 cm^{-1} are assigned to the characteristic absorption band of carboxyl group in gellan [36]. Due to the presence of free carboxylate groups in gellan, it becomes anionic with characteristic property of undergoing ionic gelation.

The C-O stretching peak at 1021 cm^{-1} for pure gellan powder shifted to a higher peak at 1030 cm^{-1} in plain gellan G film, from 1027 to 1029 cm^{-1} in GDD films; and from 1016 to 1028 cm^{-1} in G/DDB films shown in Figures 133 and 134.

The N-H deformation peak at 1644 cm^{-1} and 1007 cm^{-1} C-N stretching peak in DEAE-Dextran powder disappeared in the spectra of the GDD PEC composite films and G/DDB bilayer films. A new peak at

1551 cm^{-1} corresponding to secondary -NH_2 group was observed in the GDD 2:0.5 films. The peak at 994 cm^{-1} seen in G and GDD films disappeared in the G/DDB films. The O-H peak at 3318 cm^{-1} in pure gellan and at 3309 cm^{-1} DEAE-Dextran shifted to a range of 3283 cm^{-1} and 3293 cm^{-1} in the GDD films; and a range of 3277 to 3288 cm^{-1} in the G/DDB films. Similar shifts from peak at 3273 cm^{-1} for gellan to a range of 3223 to 3229 cm^{-1} for the blends were reported in gellan and PVA blends suggesting interactions in the blends [37]. Contributions from the components (gellan and DEAE-Dextran) could be easily seen with slight variations in the GDD complex films at a range of 2926 to 2932 cm^{-1} (from 2922 cm^{-1} in DEAE-Dextran), 1966 to 1977 cm^{-1} (from 1981 cm^{-1} in DEAE-Dextran), 1609 cm^{-1} (from 1601 cm^{-1} in gellan), 1408 cm^{-1} (from 1403 cm^{-1} in gellan), 1148 cm^{-1} (from 1144 cm^{-1} in DEAE-Dextran). The shifts and disappearances in peaks show there is a possible interaction between the two polymers.

Table 86 Spectral characteristics of gellan and gellan – DEAE-Dextran PEC composite films.

Formulation	Position of absorption band (Wavenumber) / cm^{-1}					
Gellan-reference	3318	2897	2080	1601	1198	891
		2324	2018	1403	1019	836
		2163	1974	1295		806
DEAE-Dextran-reference	3309	2922	2145	1644	1144	915
		2656	2081	1456	1102	844
		2487	2018	1399	1007	797
		2287	2010	1343		760
		2240	1981	1269		
		2161				
G	3296	2929	2020	1609	1148	922
		2884	1977	1408	1105	847
		2163		1338	1029	812
		2087		1235	993	
GDD 2:0.125	3289	2932	2140	1966	1235	993
		2883	2081	1609	1148	922
		2186	2019	1408	1106	849
		2163	1976	1338	1028	813
GDD 2:0.25	3289	2932	2080	1609	1148	993
		2883	2046	1408	1106	922
		2186	2019	1338	1028	849
		2163	1976	1235		813
			1966			
GDD 2:0.5	3283	2925	2164	1609	1235	994
		2883	2139	1551	1149	922
		2339	2080	1408	1105	849
		2232	1976	1338	1028	812
GDD 2:1	3293	2926	2180	1609	1236	923
		2883	1977	1408	1149	886
		2165		1339	1105	848
					1028	785

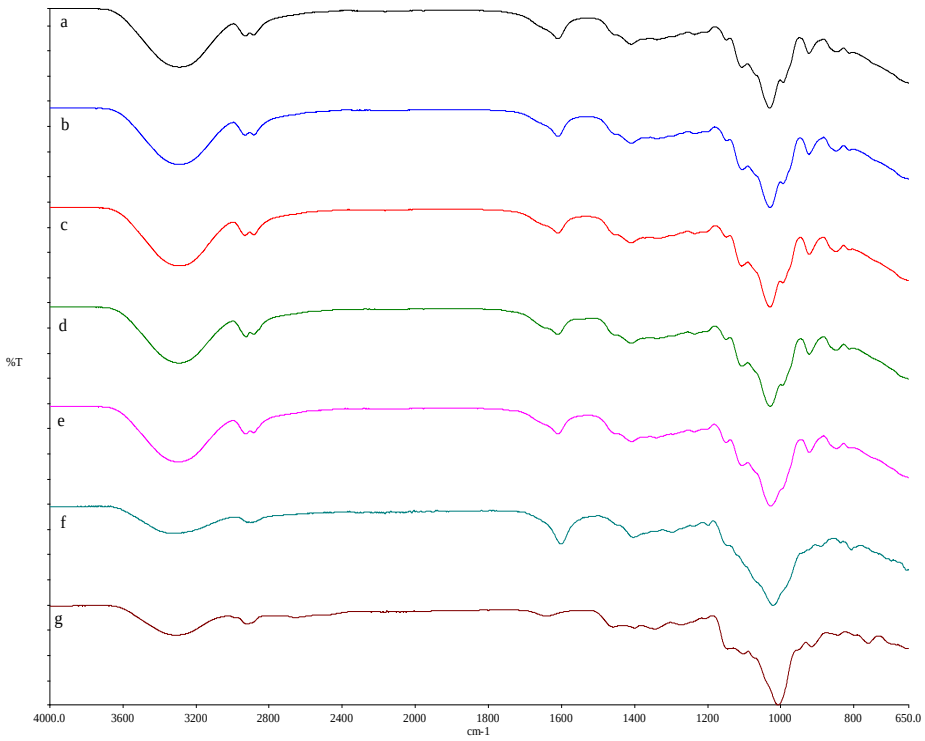

Figure 133 The FTIR spectra of gellan and PEC composite films (a) G , (b) GDD 2:0.125 , (c) GDD 2:0.25, (d) GDD 2:0.5, (e) GDD 2:1, (f) Gellan powder-reference and (g) DEAE-Dextran powder-reference.

Table 87 Spectral characteristics of gellan and gellan – DEAE-Dextran PEC bilayer films.

Formulation	Position of absorption band (Wavenumber) / cm^{-1}					
Gellan-reference	3318	2897	2080	1601	1198	891
		2324	2018	1403	1019	836
		2163	1974	1295		806
DEAE-Dextran-reference	3309	2922	2161	1981	1269	915
		2656	2145	1644	1144	844
		2487	2081	1456	1102	797
		2287	2018	1399	1007	760
		2240	2010	1343		
G	3296	2929	2020	1609	1148	922
		2884	1977	1408	1105	847
		2163		1338	1029	812
		2087		1235	993	
G/DDB 2:0.125	3287	2923	2103	1607	1149	922
		2883	2051	1405	1105	841
		2191	2019	1338	1026	812
		2163	1999	1292		
		2147	1979	1233		
G/DDB 2:0.25	3288	2922	2163	1987	1293	1025
		2884	2136	1967	1234	922
		2323	2115	1606	1148	837
		2195	2048	1405	1101	872
		2175	2015	1338	1069	
G/DDB 2:0.5	3289	2924	2147	1967	1237	922
		2884	2103	1606	1149	840
		2283	2051	1406	1105	812
		2203	2015	1338	1024	
		2164	1987	1293		
G/DDB 2:1	3273	2884	2151	1606	1148	923
	2922	2307	2049	1404	1103	837
		2212	2016	1338	1070	812
		2165	1986	1236	1016	675

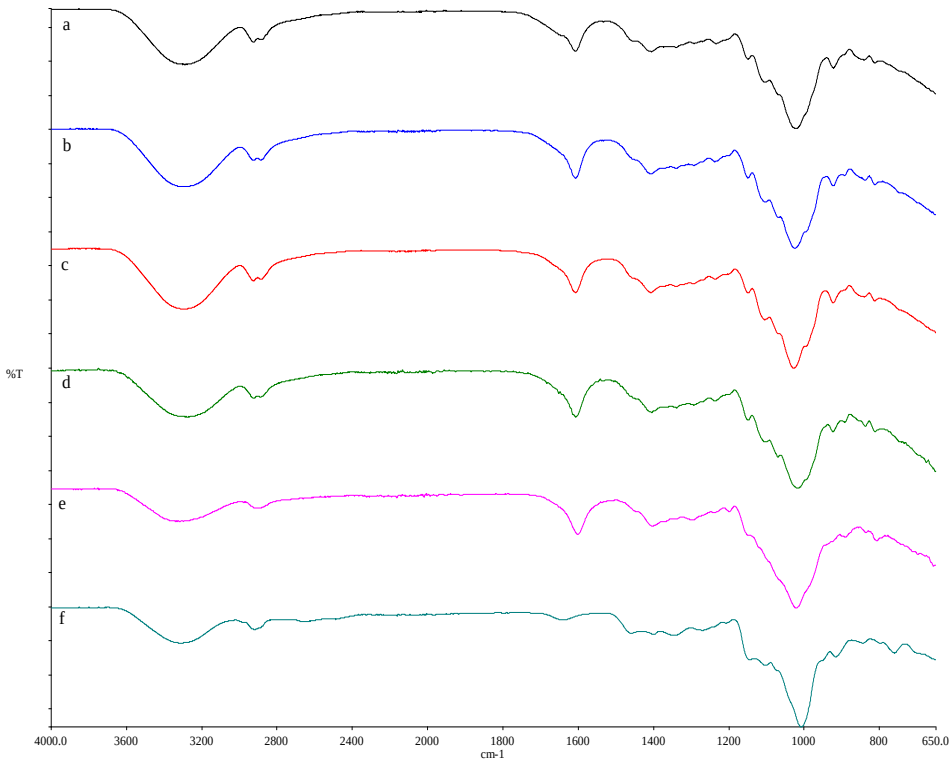

Figure 134 The FTIR spectra of bilayer films (a) G/DDB 2:0.125 , (b) G/DDB 2:0.25, (c) G/DDB 2:0.5, (d) G/DDB 2:1, (e) Gellan powder-reference and (f) DEAE-Dextran powder-reference.

The FTIR spectra of pure ibuprofen, gellan, DEAE-Dextran; ibuprofen loaded gellan - DEAE-Dextran composite and bilayer films is shown in Figures 135 and 136. Gellan showed significant peaks at 3318 cm^{-1}, 2897 cm^{-1}, 1601 cm^{-1} and 1403 cm^{-1} presented in Tables 88 and 89. The broad absorption band at 3318 cm^{-1} is assigned to the stretching –OH groups in gellan. The peak at 2897 cm^{-1} is due to the stretching vibrations of the $–CH_2$ group [11]. Pure DEAE-Dextran showed N-H deformation vibration at 1644 cm^{-1}. This peak is assigned to the free N-H group present on DEAE-Dextran. The peaks at 2921 cm^{-1} and 3295 cm^{-1} are assigned to N-H stretching and C-H stretching vibrations. The peaks at 1606 cm^{-1} and 1408 cm^{-1} are assigned to the characteristic absorption band of carboxyl group in gellan in literature [36]. The bands assigned as the finger prints of ibuprofen in literature include 2992 cm^{-1}, 1706 cm^{-1}, 1230 cm^{-1} and 779 cm^{-1} [38-39]. The FTIR spectra of GIb film showed the disappearances of 1403 cm^{-1} peak of gellan, strong carbonyl absorbance at 1706 cm^{-1} and 1230 cm^{-1} peaks of ibuprofen. Instead, a new $–NH_2$ group peak at 1512 cm^{-1} was observed. Contributions from ibuprofen and gellan were observed in the GIb complex with slight variations. The C-O stretching peak at 1021 cm^{-1} for pure gellan powder shifted to 1028 cm^{-1} in GIb, 1032 cm^{-1} in GIbDD

composite films and a range of 1008 cm^{-1} to 1023 cm^{-1} in GIb/DDB bilayer films. The shifts and disappearances in peaks show there is a possible hydrophobic interaction between gellan and ibuprofen.

The C=O and C-C stretching peak at 1710 cm^{-1} (carbonyl) and 1229 cm^{-1} for pure ibuprofen disappeared in the spectra of ibuprofen loaded films GIbDD composite and GIb/DDB bilayer films which suggests a possible electrostatic interaction forming a carboxylate. The N-H deformation peak at 1644 cm^{-1} in DEAE-Dextran powder disappeared in the spectra of ibuprofen loaded films GIbDD composite and GIb/DDB bilayer films. The peak at 1608 cm^{-1} disappeared in the GIbDD 2:0.125 composite, GIb/DDB 2:0.5 and GIb/DDB 2:1 bilayer films. The peak at 3318 cm^{-1} in pure gellan and 3309 cm^{-1} in DEAE-Dextran shifted to a range of 3299 to 3307 cm^{-1} in the GIbDD films; and a range of 3288 to 3308 cm^{-1}. While in gellan, a peak was observed at 2827 cm^{-1} and in DEAE-Dextran, at 2927 cm^{-1}, GIbDD films exhibited two single peaks at 2927 cm^{-1} and 2881 cm^{-1}. Similar shifts from 2927 cm^{-1} in gellan and 2938 cm^{-1} in PVA to a single peak at 2934 cm^{-1} in the blend were reported in gellan and PVA blends confirming the interaction of different OH groups in the gellan and DEAE-Dextran complex [37].

The new peak at 1512 cm^{-1} may be attributed to the asymmetric stretching vibration of COO^- since carboxylic acid salts exhibit strong characteristic COO^- band in the region of 1650 to 1550 cm^{-1} suggesting the peak of carboxylate ion [40]. This suggests that carboxylate ion may be forming a complex with the amine group of DEAE-Dextran. This result shows that polyelectrolyte complex was formed.

Table 88 Spectral characteristics of ibuprofen loaded gellan and gellan – DEAE-Dextran PEC composite films.

Formulation	Position of absorption band (Wavenumber) / cm^{-1}					
Ibuprofen-reference	3088	2954	2203	1563	1305	935
	3044	2922	2163	1507	1268	880
	3015	2868	2144	1461	1229	865
	2991	2851	2115	1451	1183	849
	2980	2728	2079	1442	1168	834
		2631	1911	1418	1123	820
		2601	1887	1379	1092	810
		2542	1803	1365	1073	779
			1706	1329	1068	746
				1321	1008	690
					969	667
Gellan-reference	3318	2897	2080	1601	1198	891
		2324	2018	1403	1019	836
		2163	1974	1295		806
DEAE-Dextran-reference	3309	2922	2145	1644	1144	915
		2656	2081	1456	1102	844
		2487	2018	1399	1007	797
		2287	2010	1343		760
		2240	1981	1269		
		2161				
GIb	3294	2932	2080	1608	1364	991
		2880	2047	1564	1289	922
		2340	1976	1512	1192	850
		2163		1455	1099	812
				1396	1028	
GIbDD 2:0.125	3307	2928	2163	1563	1364	992
		2872	2079	1512	1287	923
		2344	1981	1456	1195	885
		2187	1906	1395	1099	850
					1032	
GIbDD 2:0.25	3305	2930	2078	1607	1364	992
		2881	2018	1564	1288	922
		2324	1982	1512	1193	887
		2163		1455	1098	849
		2140		1395	1032	814
GIbDD 2:0.5	3307	2927	2108	1607	1395	1032
		2881	2017	1565	1364	922
		2322	1977	1512	1288	889
		2163	1948	1455	1201	849
					1147	812
					1108	
GIbDD 2:1	3299	2928	2079	1607	1363	1106
		2882	2019	1566	1288	1032
		2339	1977	1511	1240	922
		2163	1916	1456	1203	886
				1394	1149	849
						811

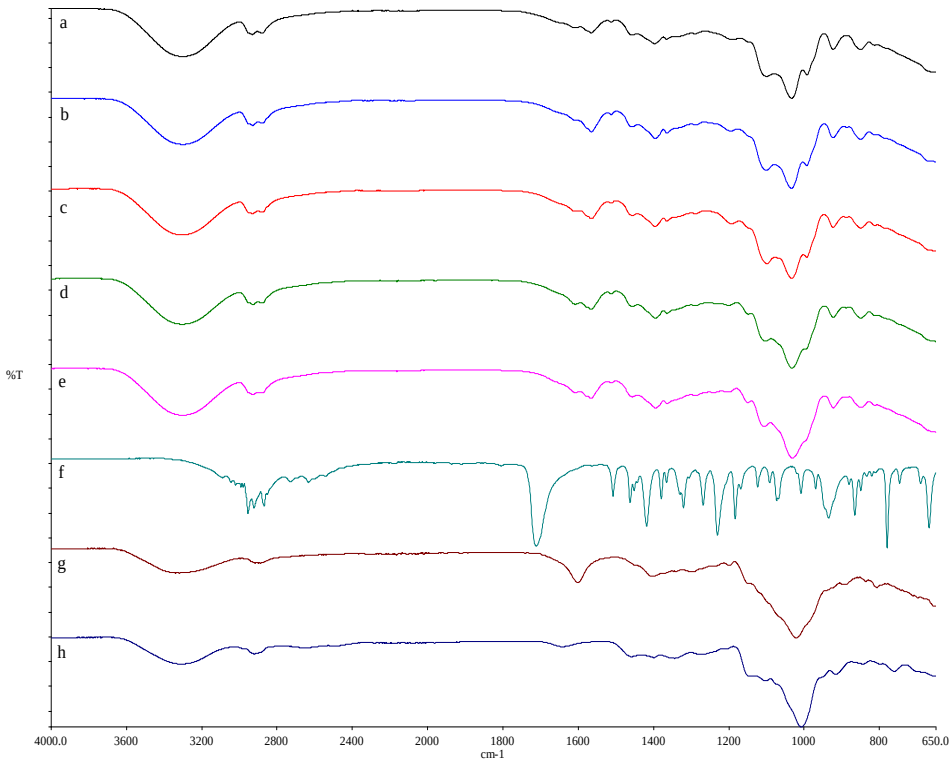

Figure 135 The FTIR spectra ibuprofen loaded composite films (a) GIb , (b) GIbDD 2:0.125, (c) GIbDD 2:0.25, (d) GIbDD 2:0.5, (e) GIbDD 2:1, (f) Ibuprofen powder-reference. (g) Gellan powder-reference and (h) DEAE-Dextran powder-reference.

Table 89 Spectral characteristics of ibuprofen loaded gellan and gellan – DEAE-Dextran PEC bilayer films.

Formulation	Position of absorption band (Wavenumber) / cm^{-1}					
Ibuprofen-reference	3088	2954	2203	1563	1305	935
	3044	2922	2163	1507	1268	880
	3015	2868	2144	1461	1229	865
	2991	2851	2115	1451	1183	849
	2980	2728	2079	1442	1168	834
		2631	1911	1418	1123	820
		2601	1887	1379	1092	810
		2542	1803	1365	1073	779
			1706	1329	1068	746
				1321	1008	690
					969	667
Gellan-reference	3318	2897	2080	1601	1198	891
		2324	2018	1403	1019	836
		2163	1974	1295		806
DEAE-Dextran-reference	3309	2922	2145	1644	1144	915
		2656	2081	1456	1102	844
		2487	2018	1399	1007	797
		2287	2010	1343		760
		2240	1981	1269		
		2161				
GIb	3294	2932	2080	1608	1364	991
		2880	2047	1564	1289	922
		2340	1976	1512	1192	850
		2163		1455	1099	812
				1396	1028	
GIb/DDB 2:0.125	3308	2925	2080	1606	1364	922
		2325	2009	1579	1290	890
		2191	1987	1567	1237	850
		2165	1905	1512	1149	812
		2146		1454	1105	
				1394	1023	
GIb/DD 2:0.25	3301	2927	2064	1606	1362	922
		2285	2009	1510	1290	891
		2162	1987	1454	1238	841
				1394	1150	811
					1106	674
					1019	
GIb/DDB 2:0.5	3302	2953	2145	1567	1393	1012
		2927	2118	1511	1362	921
		2870	2049	1455	1285	887
		2324	2017		1150	853
		2192	1982		1107	673
		2162				
GIb/DDB 2:1	3288	2953	2064	1567	1362	921
		2923	2050	1511	1283	886
		2326	2009	1461	1150	852
		2187	1986	1385	1110	754
		2161	1703		1008	672
		2137				665

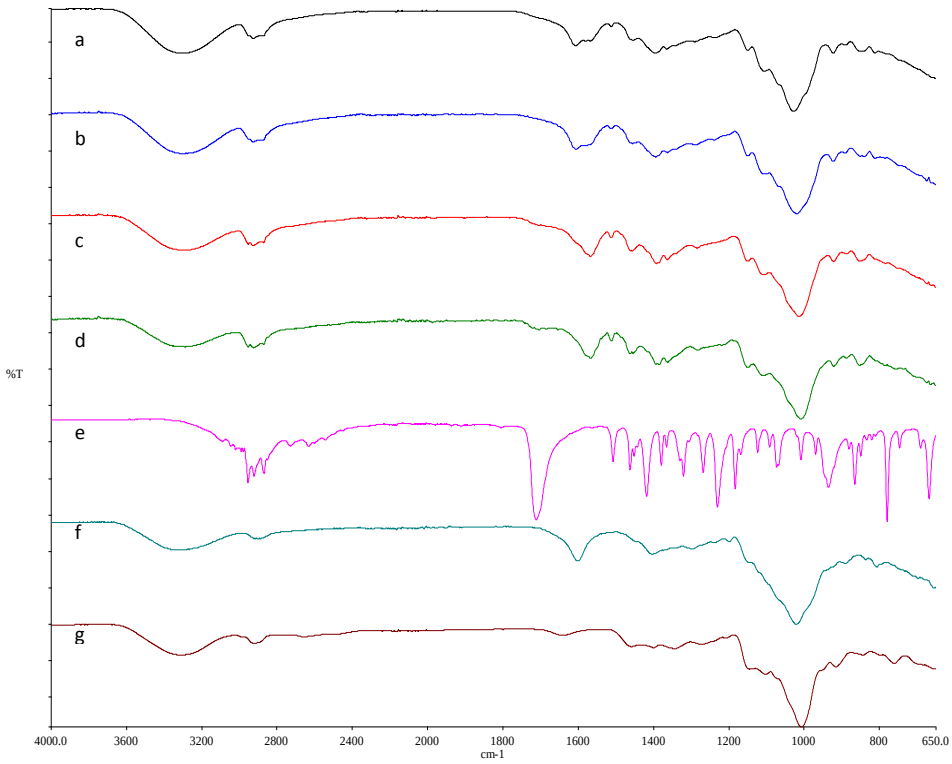

Figure 136 The FTIR spectra of ibuprofen loaded bilayer films (a) GIb/DDB 2:0.125, (b) GIb/DDB 2:0.25, (c) GIb/DDB 2:0.5, (d) GIb/DDB 2:1, (e) Ibuprofen powder-reference, (f) Gellan powder-reference and (g) DEAE-Dextran powder-reference.

4.3.4. Thermal analysis

4.3.4.1. Differential scanning calorimetry (DSC)

DSC analysis was conducted to examine the thermal behaviour of gellan, GDD composite and G/DDB bilayer films and further study polymer-polymer and drug-polymer interaction. Therefore, the DSC thermal characteristics of G, GDD composite and G/DDB bilayer films were compared with pure gellan and DEAE-Dextran and presented in Figure 137; Table 90 and 91. Pure gellan powder exhibited a broad melting peak at 127.86 °C and exothermic decomposition peak at 254.84 °C. DEAE-Dextran showed a glass transition endotherm (Tg) at 57.26 °C; a broad endothermic peak at 124.05 °C due to its amorphous characteristic; a small peak at 201.21 °C and a final peak at 268.50 °C attributed to the decomposition of DEAE-Dextran.

Representative DSC thermograms and their derivatives of G, GDD and G/DDB films were presented in Figure 138. The DSC thermogram exhibited endothermic melting peak for G film at 127.81 ˚C, GDD films ranged from 125.70 to 140.83 ˚C while for G/DDB films, ranged from 125.21 to 135.20 ˚C. The

DSC curve of plain gellan G film exhibited an exothermic peak at 255.89 ˚C which indicated the decomposition of the polymer presented in Figure 138A and this corresponds to the step of inflection on the TGA curve in Figure 146. The GDD films showed exothermic peaks at 254.81 to 261.63 ˚C while G/DDB films ranged from 264.34 to 266.59 ˚C caused by the thermal degradation of the films. The G/DDB films were thermally more stable than the G and GDD films. The DSC melting profile of GDD was presented in Figure 139 with an initial decrease, an increase, a decrease and finally an increase in melting point as the DEAE-Dextran concentration increased. The melting point profile of G/DDB exhibited an initial decrease and then increase with increasing DEAE-Dextran concentration. The enthalpy change profile of GDD in Figure 140 exhibited an initial decrease and a further increased as DEAE-Dextran concentration increased. The enthalpy change profile of G/DDB exhibited a steady increase in enthalpy change as DEAE-Dextran concentration increased.

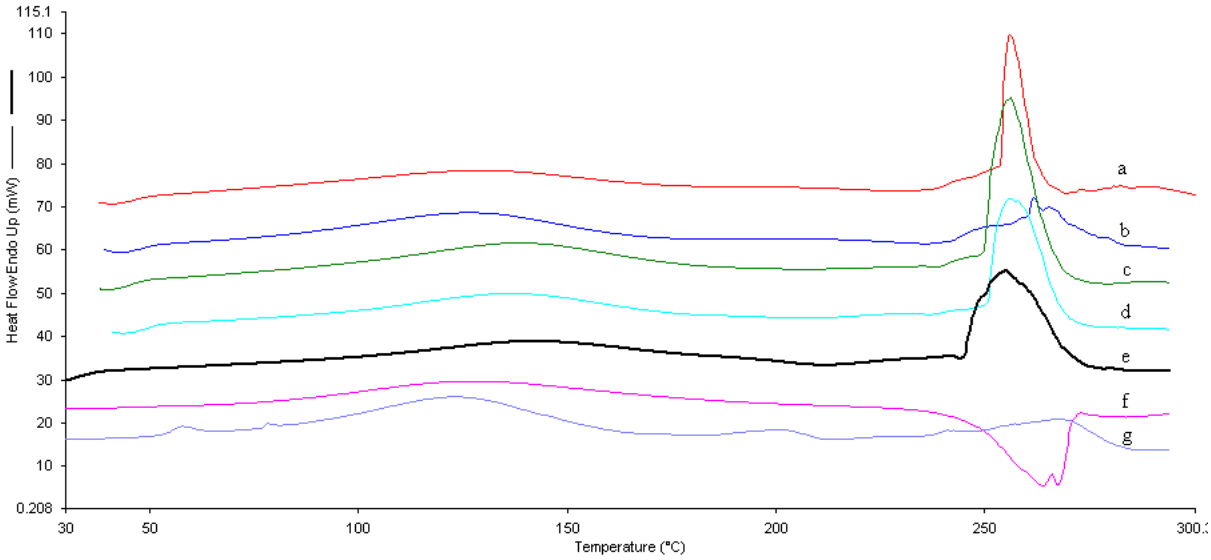

Figure 137 DSC thermograms of gellan and composite films (a) G , (b) GDD 2:0.125 , (c) GDD 2:0.25, (d) GDD 2:0.5, (e) GDD 2:1, (f) Gellan powder-reference and (g) DEAE-Dextran powder-reference.

Table 90 DSC of plain gellan and gellan-DEAE-Dextran PEC composite films. Each value represents mean ± SD (n = 4).

Formulation	Onset (°C)	Peak (°C)	End (°C)	Delta H (J/g)	Area (mJ)
Gellan-reference	77.70±1.55	127.86±7.43	186.32±8.76	168.31±8.81	1043.54±52.70
	246.56±12.37	264.02±12.75	270.88±12.86	-129.64±6.5	-803.81±40.22
DEAE-Dextran-reference	53.55±0.85	57.86±0.76	63.97±0.92	5.10±0.08	35.16±0.41
	87.43±1.22	124.05±4.16	158.87±5.34	139.17±5.64	960.30±40.48
	187.42±8.23	201.54±10.58	210.60±11.45	12.72±0.84	87.74±1.25
	245.83±12.74	268.50±11.78	281.53±13.66	70.84±0.92	488.852±21.22
G	77.66±2.33	127.81±4.27	174.79±7.43	71.60±1.38	862.87±38.36
	253.70±8.23	255.89±10.68	262.69±11.57	137.33±5.14	789.62±31.54
GDD 2:0.125	76.18±1.35	125.70±5.63	166.60±6.86	179.94±6.17	1025.65±52.66
	259.07±8.20	261.63±11.77	267.61±11.48	99.92±2.79	569.50±0.95
GDD 2:0.25	96.24±2.23	138.55±5.33	178.88±6.94	122.06±4.76	805.57±38.73
	249.54±9.44	256.21±12.37	265.88±11.92	207.19±8.13	1367.49±62.46
GDD 2:0.5	90.96±2.15	135.98±5.12	176.05±6.35	125.66±4.48	804.21±35.73
	250.46±8.77	255.88±10.66	267.74±10.93	161.91±5.70	1036.22±58.41
GDD 2:1	93.75±1.11	140.83±5.14	182.79±7.12	116.87±4.66	666.16±22.46
	245.23±9.66	254.84±11.05	270.22±12.11	181.70±6.88	1035.68±14.21

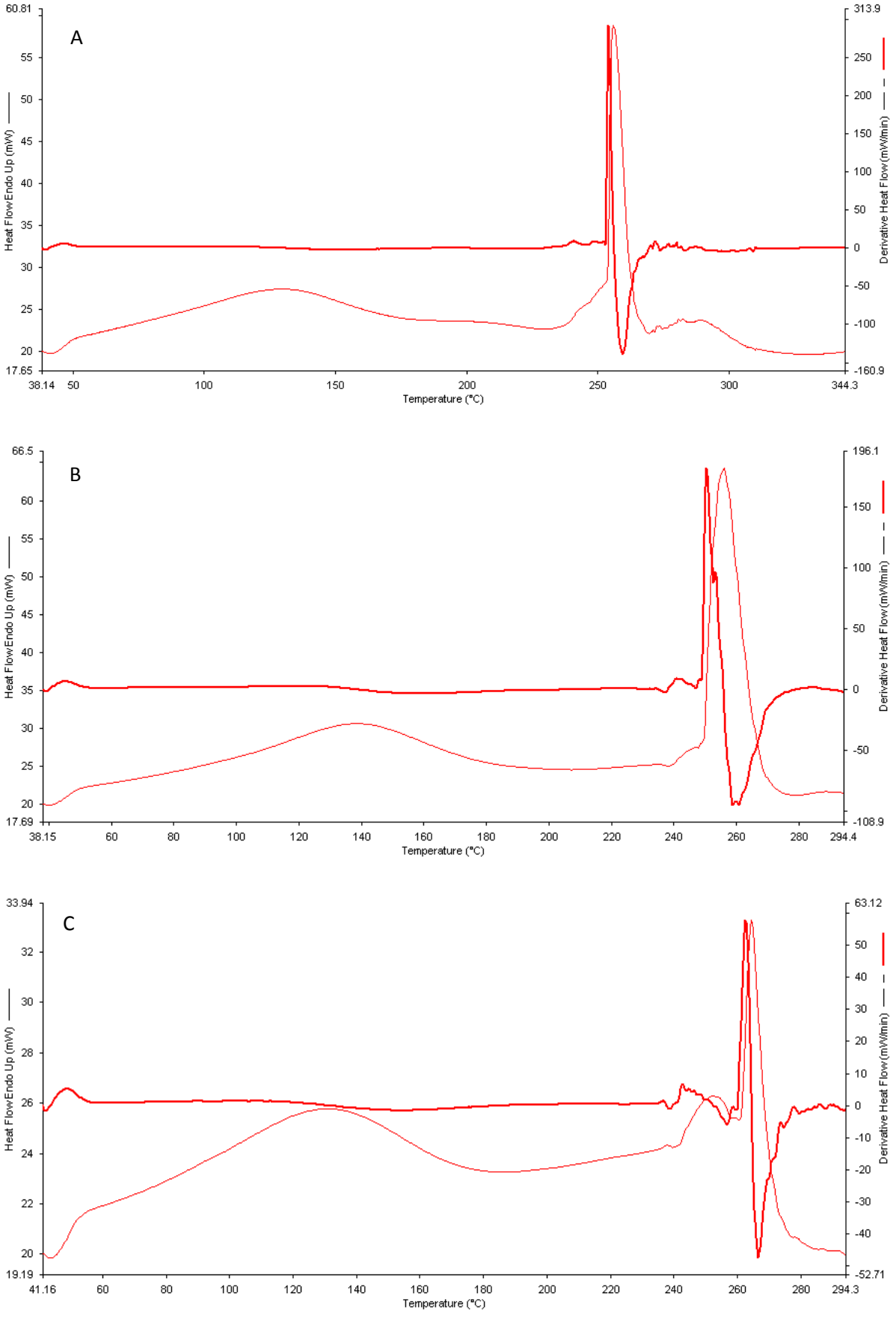

Figure 138 DSC/DTG thermograms of (A) G, (B) GDD and (C) G/DDB films.

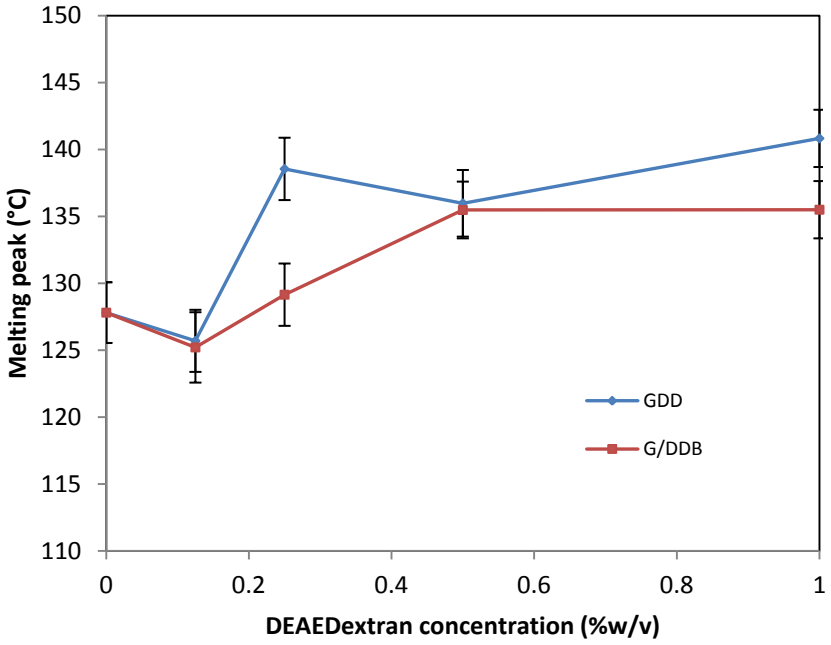

Figure 139 DSC melting peak profiles of GDD and G/DDB films. Each data point represents mean ± S.D (n = 4).

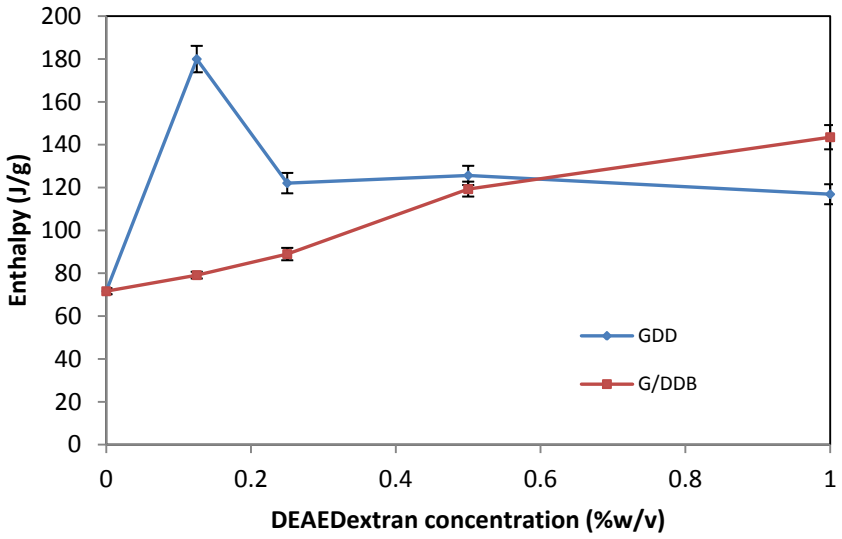

Figure 140 DSC enthalpy change profiles of GDD and G/DDB films. Each data point represents mean ± S.D (n = 4).

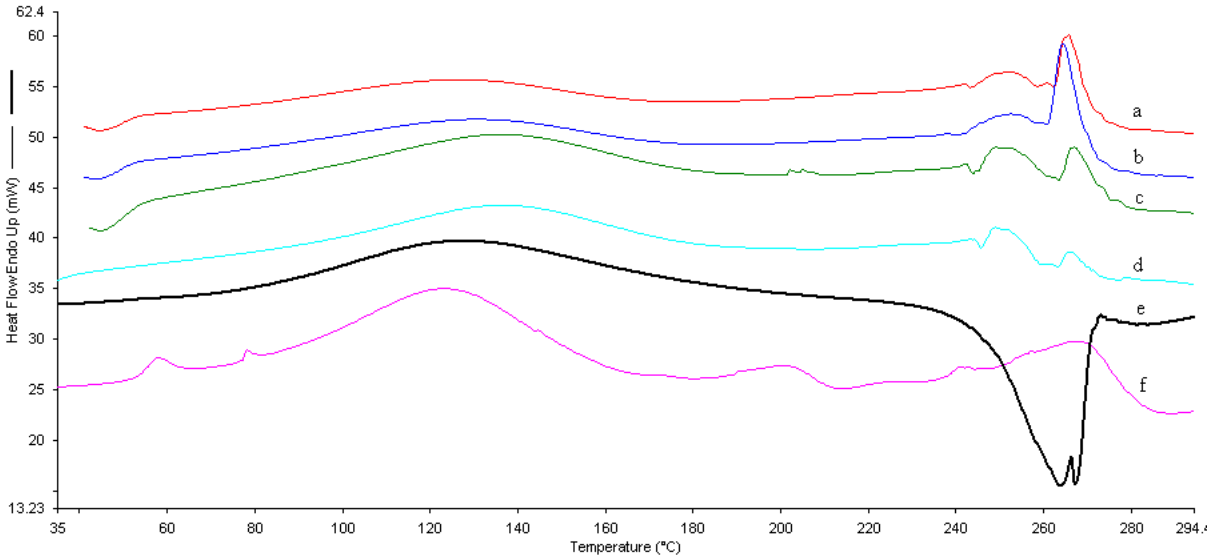

Figure 141 DSC thermograms of bilayer films (a) G/DDB 2:0.125 , (b) G/DDB 2:0.25, (c) G/DDB 2:0.5, (d) G/DDB 2:1, (e) Gellan powder-reference and (f) DEAE-Dextran powder-reference.

Table 91 DSC of plain gellan and gellan-DEAE-Dextran PEC bilayer films. Each value represents mean ± SD (n = 4).

Formulation	Onset (°C)	Peak (°C)	End (°C)	Delta H (J/g)	Area (mJ)
Gellan-reference	77.70±1.55	127.86±7.43	186.32±8.76	168.31±8.81	1043.54±52.70
	246.56±12.37	264.02±12.75	270.88±12.86	-129.64±6.5	-803.81±40.22
DEAE-Dextran-	53.55±0.85	57.86±0.76	63.97±0.92	5.10±0.08	35.16±0.41
reference	87.43±1.22	124.05±4.16	158.87±5.34	139.17±5.64	960.30±40.48
	187.42±8.23	201.54±10.58	210.60±11.45	12.72±0.84	87.74±1.25
	245.83±12.74	268.50±11.78	281.53±13.66	70.84±0.92	488.852±21.22
G	77.66±2.33	127.81±4.27	174.79±7.43	71.60±1.38	862.87±38.36
	253.70±8.23	255.89±10.68	262.69±11.57	137.33±5.14	789.62±31.54
G/DDB 2:0.125	75.51±2.26	125.21±4.32	166.82±6.24	79.12±1.57	419.31±13.89
	244.56±7.08	265.78±10.96	269.95±12.11	14.08±0.07	76.03±1.95
G/DDB 2:0.25	78.39±2.15	129.15±5.33	173.18±6.52	88.94±2.89	498.05±19.73
	261.28±9.31	264.34±12.37	269.46±12.86	25.77±0.58	144.36±5.55
G/DDB 2:0.5	76.63±1.85	135.48±5.49	180.17±7.22	119.26±3.48	878.85±25.73
	245.28±8.77	266.84±12.66	273.21±12.93	10.81±0.07	63.76±1.41
G/DDB 2:1	79.96±1.11	135.50±5.14	181.27±7.58	143.49±5.66	947.02±29.13
	246.51±11.65	266.59±12.05	271.09±13.11	3.75±0.08	24.77±0.21

DSC thermograms of ibuprofen loaded gellan, gellan-DEAE-Dextran composite and bilayer films as presented in Figure 142 and 143; Table 92 and 93. The DSC thermograms of Ibuprofen showed characteristic sharp endothermic peak at 80.07 °C suggesting its crystallinity, with enthalpy of fusion of 118.64 J/g. This melting peak is higher than the literature value for pure ibuprofen in the range of 75 to 78 °C [41]. This could be due to some impurity in the ibuprofen sample however in a similar study, Kumar *et al.* reported that the melting peak of ibuprofen was 82.76 °C [42], while gellan and DEAE-Dextran showed endothermic peaks at 127.86 °C and 124.05 °C respectively. The variation in

the reported ibuprofen melting peak compared to the compedial values could be due to the presence of impurities in the sample.

The ibuprofen peak was not observed in the thermograms of the films, which suggested a complete solubilization of the drug in the polymers with loss of crystallinity. This similar trend was observed by Barriero-Iglesias where the peak of camptothecin completely disappeared in the thermograms of its conjugate films [43]. The melting peak of ibuprofen disappeared in all the film blends incorporated with ibuprofen suggesting an interaction between ibuprofen and gellan (GIb) in the binary conjugate; between ibuprofen, gellan and DEAE-Dextran in the ternary conjugate GIbDD and GIb/DDB (PEC) films. The DSC thermograms of the components of the drug loaded films were shown to be compatible since a single melt peak was observed [44]. It also suggests that ibuprofen was uniformly dispersed in an amorphous state in the film. The melting peak of GIb film was 142.17 ˚C; ranged from 131.87 to 142.40 ˚C for GIbDD films and from 124.28 to 139.16 ˚C for GIb/DDB bilayer films in Table 93 and Figure 145. The presence of DEAE-Dextran increased the melting point of the binary complex GIb film; ternary complexes GIbDD composite and bilayer films when compared with the single component G film. The DSC of gellan and PVA blends exhibiting single melt temperature that shifted to higher temperature with increasing amount of PVA had been reported [37].

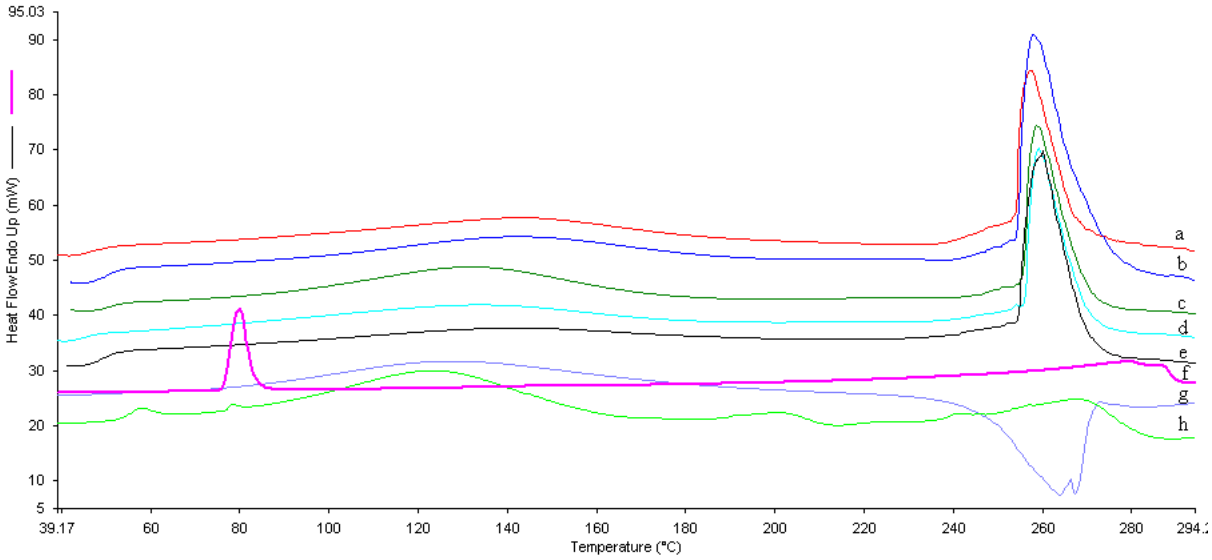

Figure 142 DSC thermograms of ibuprofen loaded composite films (a) GIb, (b) GIbDD 2:0.125, (c) GIbDD 2:0.25, (d) GIbDD 2:0.5, (e) GIbDD 2:1, (f) Ibuprofen powder-reference. (g) Gellan powder-reference and (h) DEAE-Dextran powder-reference.

Table 92 DSC of ibuprofen loaded gellan and gellan-DEAE-Dextran PEC composite films. Each value represents mean ± SD (n = 4).

Formulation	Onset (°C)	Peak (°C)	End (°C)	Delta H (J/g)	Area (mJ)
Ibuprofen-reference	76.85±0.64 236.27±11.36	82.69±2.46 264.63±19.41	86.79±3.27 273.47±17.20	92.90±4.32 203.71±18.79	826.37±55.04 1753.15±74.65
Gellan-reference	77.70±1.55 246.56±12.37	127.86±7.43 264.02±12.75	186.32±8.76 270.88±12.86	168.31±8.81 -129.64±6.5	1043.54±52.70 -803.81±40.22
DEAE-Dextran-reference	87.43±1.22 187.42±8.23 245.83±12.74	124.05±4.16 201.54±10.58 268.50±11.78	158.87±5.34 210.60±11.45 281.53±13.66	139.17±5.64 12.72±0.84 70.84±0.92	960.30±40.48 87.74±1.25 488.852±21.22
G	77.66±2.33 253.70±8.23	127.81±4.27 255.89±10.68	174.79±7.43 262.69±11.57	71.60±1.38 137.33±5.14	862.87±38.36 789.62±31.54
GIb	79.90±1.22 253.62±9.08	142.77±6.36 257.24±10.13	190.10±8.32 268.05±10.21	182.22±5.43 202.21±8.15	902.01±42.76 1000.93±50.89
GIbDD 2:0.125	96.38±3.41 253.95±8.31	142.40±6.64 258.01±11.37	187.59±7.55 270.64±10.86	105.80±3.89 237.38±9.08	677.15±28.73 1519.22±63.55
GIbDD 2:0.25	87.85±2.85 255.41±9.77	131.87±5.49 269.00±12.54	173.03±6.22 258.70±11.93	140.95±4.42 153.02±5.70	817.51±35.73 887.52±38.44
GIbDD 2:0.5	80.83±3.15 255.70±8.65	132.81±5.14 259.25±11.05	176.84±6.59 269.31±12.07	98.15±3.46 149.43±5.34	559.43±27.12 851.76±34.21
GIbDD 2:1	91.08±2.31 254.43±9.38	140.30±4.86 259.98±12.01	192.15±7.55 268.74±13.43	74.21±1.82 156.58±7.31	452.70±25.61 955.19±46.44

The DSC curves of ibuprofen, gellan gum and DEAE-Dextran powders showed exothermic peaks at 264.63 ˚C, 264.02 ˚C and 268.50 ˚C respectively attributed to the disintegration of the molecular chains, which corresponds to the step of inflection on the TGA curve. The GIb film showed exothermic peak at 257.24 ˚C; from 258.01 to 269.00 ˚C for the GIbDD films while G/DDB films ranged from 264.34 to 266.59 ˚C caused by the thermal degradation of the films. The GIbDD and

GIb/DDB films were thermally more stable than the G films since they withstand more heat. The DSC profile of GIbDD films in Figure 143 exhibited a decrease in melting point up to 0.6% followed by increase as DEAE-Dextran concentration increased; and the profile of GIb/DDB exhibited an initial decrease, an increase and then a further increase as DEAE-Dextran concentration increased. The enthalpy change profile of GIbDD in Figure 143 exhibited an initial decrease, increase and a further decrease as DEAE-Dextran concentration increased; and the profile of GIb/DDB exhibited a decrease up to 0.5 % and a further increase as the DEAE-Dextran concentration increased.

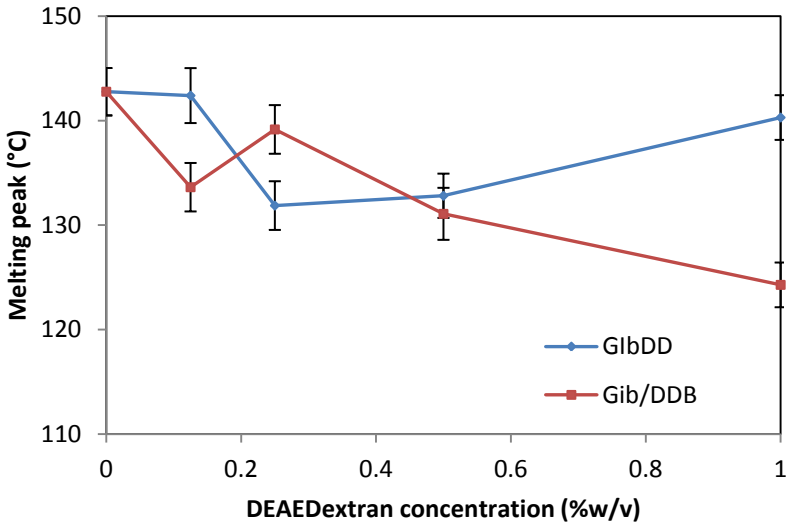

Figure 143 DSC melting peak profiles of GIbDD and GIb/DDB films. Each data point represents mean ± S.D (n = 4).

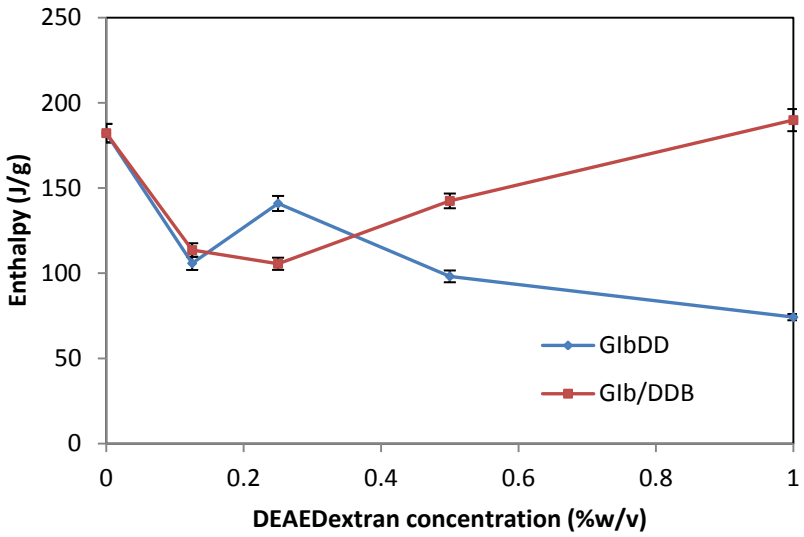

Figure 144 DSC enthalpy changes of GIbDD and GIb/DDB films. Each data point represents mean ± S.D (n = 4).

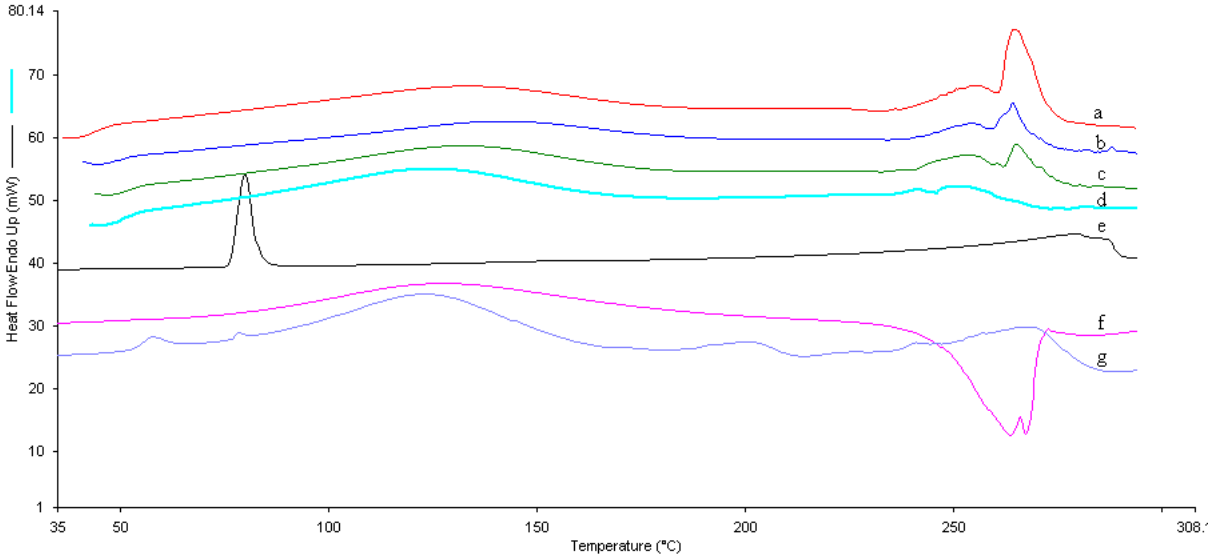

Figure 145 DSC thermograms of ibuprofen loaded bilayer films (a) GIb/DDB 2:0.125, (b) GIb/DDB 2:0.25, (c) GIb/DDB 2:0.5, (d) GIb/DDB 2:1 (e) Ibuprofen powder-reference, (f) Gellan powder-reference and (g) DEAE-Dextran powder-reference.

Table 93 DSC of ibuprofen loaded gellan and gellan-DEAE-Dextran PEC bilayer films. Each value represents mean ± SD (n = 4).

Formulation	Onset (°C)	Peak (°C)	End (°C)	Delta H (J/g)	Area (mJ)
Ibuprofen-reference	76.85±0.64	82.69±2.46	86.79±3.27	92.90±4.32	826.37±55.04
	236.27±11.36	264.63±19.41	273.47±17.20	203.71±18.79	1753.15±74.65
Gellan-reference	77.70±1.55	127.86±7.43	186.32±8.76	168.31±8.81	1043.54±52.70
	246.56±12.37	264.02±12.75	270.88±12.86	-129.64±6.5	-803.81±40.22
DEAE-Dextran-reference	87.43±1.22	124.05±4.16	158.87±5.34	139.17±5.64	960.30±40.48
	187.42±8.23	201.54±10.58	210.60±11.45	12.72±0.84	87.74±1.25
	245.83±12.74	268.50±11.78	281.53±13.66	70.84±0.92	488.852±21.22
GIb	79.90±1.22	142.77±6.36	190.10±8.32	182.22±5.43	902.01±42.76
	253.62±9.08	257.24±10.13	268.05±10.21	202.21±8.15	1000.93±50.89
GIb/DDB 2:0.125	78.77±1.51	133.63±4.72	178.75±7.55	113.58±4.02	681.47±25.65
	260.55±8.89	264.46±10.60	272.68±11.06	96.99±2.97	581.19±23.42
GIb/DDB 2:0.25	81.04±2.62	139.16±5.31	186.14±6.22	105.53±3.58	664.72±25.21
	259.73±9.61	264.10±11.54	269.78±11.68	44.41±0.70	279.78±12.56
GIb/DDB 2:0.5	75.91±1.26	131.08±5.39	176.29±6.42	142.45±4.32	854.69±37.32
	262.58±9.52	265.07±12.38	272.04±12.03	11.88±0.32	71.25±1.53
GIb/DDB 2:1	73.46±1.36	124.28±4.54	167.21±6.35	189.88±6.49	895.30±35.38
	244.80±9.37	252.33±9.38	263.16±11.59	24.91±0.51	139.55±4.71

4.3.4.2. Thermogravimetric analysis

TGA complements the DSC technique since they are both thermal analysis technique useful in the detection of the inter-atomic and inter/-intra- molecular interactions in relation to external change in temperature. The complimentary data obtained allows differentiation between endothermic and exothermic events which have no associated weight loss (melting and crystallization) and those which involve a weight loss (degradation). TGA analysis was conducted to examine the thermal stability and degradation characteristics of the plain composite and bilayer films as presented in Figure 146 and 147; Table 93 and 95. The onset temperature denotes the temperature at which weight loss begins while the step of inflection point indicates the point of the greatest rate of change of the weight loss curve. The G film showed three steps of inflection at 24.99 ˚C, 184.59 ˚C and 250.62 ˚C with corresponding weight losses of 10.17%, 40.41% and 35.27% respectively and total weight loss of 85.85%. The first weight loss was due to the loss of water in the films while the second and third weight loss was due to the decomposition of the films. The third weight loss at 250.62 ˚C can be correlated to its DSC exothermic peak at 255.89 ˚C in Figure 136 which suggests decomposition of the films.

The GDD films in Figure 146 exhibited three steps of inflection denoting three distinct thermal events. The total weight loss in Table 94 was in the range of 80.93 to 88.50% with an initial decrease, an increase and a further decrease with increasing DEAE-Dextran concentration. The residual weight left in the range of 18.07 to 11.50% could be attributed to the residual left from the complex. The temperature at which the films decomposed was in the range of 250.62 to 309.64 ˚C which increased with increasing DEAE-Dextran concentration. It showed that GDD 2:1 with highest concentration was the most thermally stable film. This suggests that addition of DEAE-Dextran increased the thermal stability of the composite films.

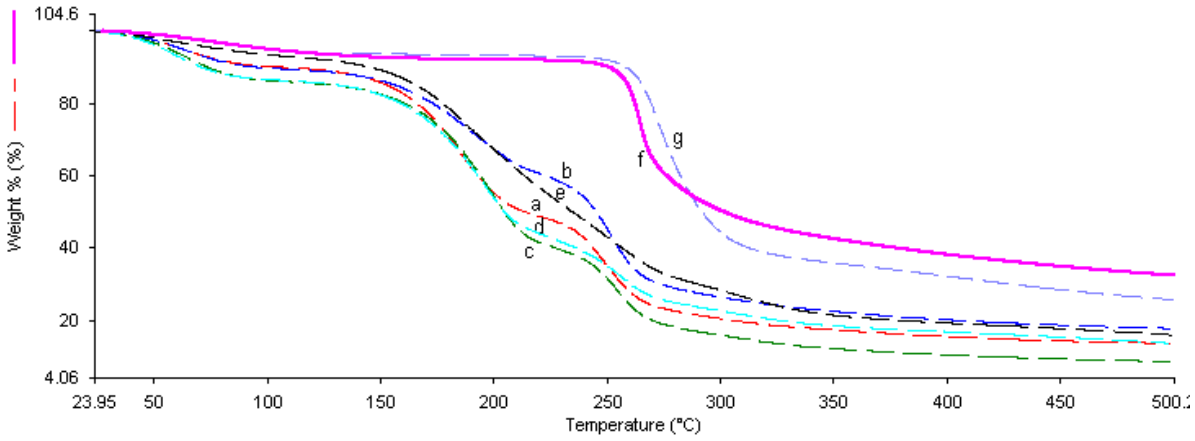

Figure 146 TGA thermograms of gellan and PEC composite films (a) G, (b) GDD 2:0.125, (c) GDD 2:0.25, (d) GDD 2:0.5, (e) GDD 2:1, (f) Gellan powder-reference and (g) DEAE-Dextran powder-reference.

Table 94 TGA of gellan and gellan-DEAE-Dextran PEC composite films. Each value represents mean ± SD (n = 4)

Formulation	Onset (°C)	End (°C)	Step of inflection (°C)	Delta Y (%)
Gellan-reference	43.99±0.65	131.17±4.72	90.39±3.15	7.85±0.08
	257.79±12.21	282.29±12.74	264.91±12.10	59.67±0.93
DEAE-Dextran-reference	47.16±0.47	106.74±4.32	77.47±1.47	6.94±0.12
	261.20±11.43	301.16±15.72	272.15±12.62	67.61±0.98
G	24.99±0.56	176.56±7.31	24.99±0.56	10.17±0.33
	158.64±5.21	204.82±10.32	184.91±8.73	40.41±1.05
	233.83±10.27	275.67±12.53	250.62±11.47	35.27±0.98
GDD 2:0.125	27.37±0.65	133.51±7.65	27.37±0.65	10.46±0.36
	158.66±5.14	211.12±9.52	194.98±9.73	27.89±0.65
	236.20±10.54	274.80±12.18	252.15±11.04	42.48±1.13
GDD 2:0.25	42.73±0.97	85.71±1.93	65.25±1.08	13.67±0.72
	168.02±5.31	214.89±9.66	199.88±9.41	45.79±1.28
	240.42±10.13	278.04±12.38	255.22±11.44	29.39±0.84
GDD 2:0.5	26.26±0.67	126.51±4.43	26.26±0.67	13.38±0.59
	164.13±6.15	214.30±9.32	196.53±8.87	44.75±1.47
	239.73±10.21	292.60±13.58	258.33±11.25	27.47±0.75
GDD 2:1	36.62±0.98	76.68±1.46	40.23±1.04	7.28±0.48
	158.54±5.75	259.18±13.32	189.16±8.96	61.10±1.46
	290.80±13.15	357.26±16.28	309.64±15.81	13.42±0.43

The G/DDB PEC films in Figure 1468 exhibited three steps of inflection denoting three distinct thermal events except G/DDB 2:1 which exhibited two steps. The total weight loss in Table 95 was in the range of 77.16 to 89.26% with a maxima value at 0.25% DEAE-Dextran and a further decrease with increase in DEAE-Dextran concentration. The weight loss in the range of 251.18 to 255.20 °C attributed to decomposition, exhibited increase in weight loss with increase in DEAE-Dextran except G/DDB 2:1 which was least the thermally stable film. This suggests that addition of DEAE-Dextran increased the thermal stability of the films up to 0.8%.

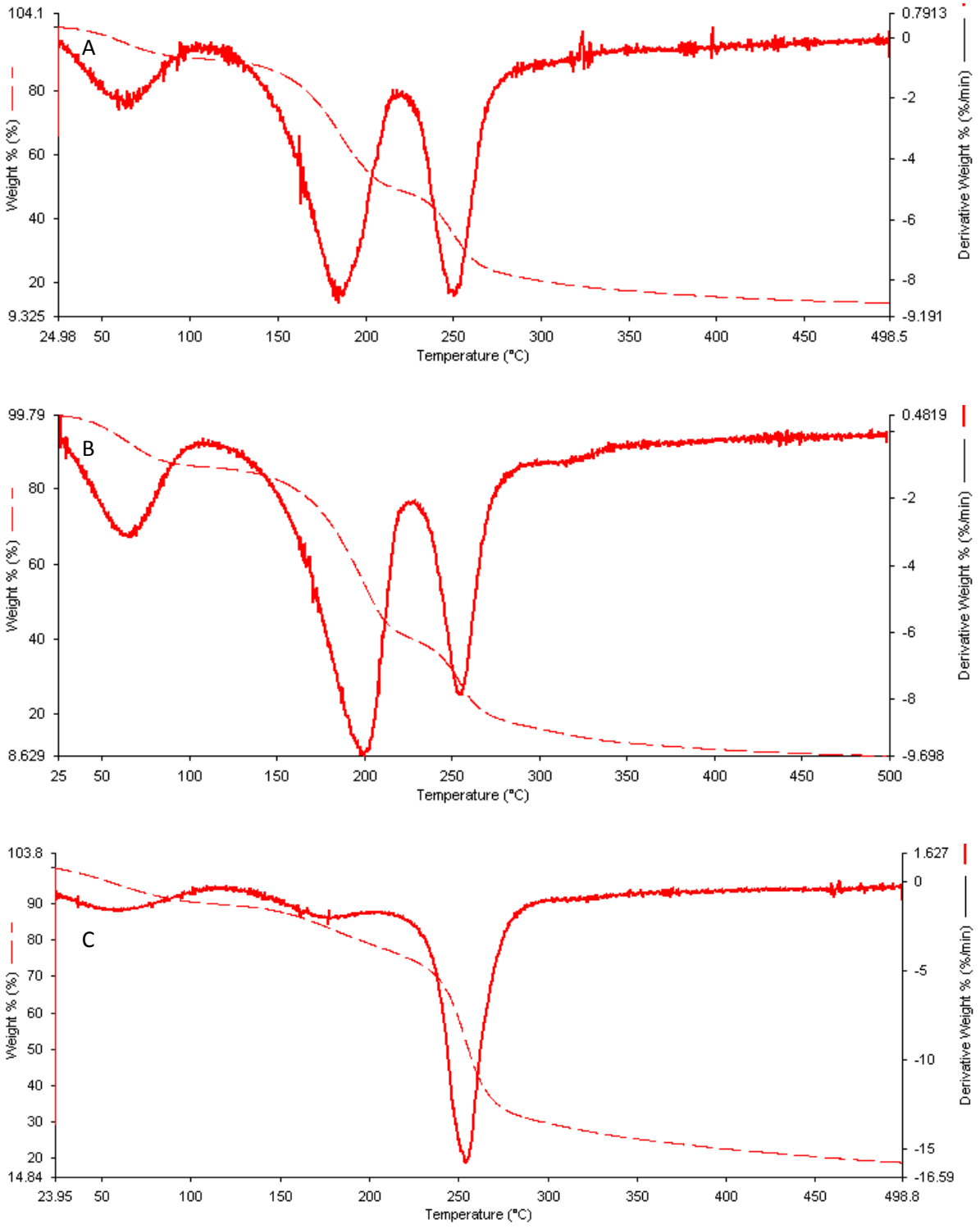

Figure 147 TGA/DTG thermograms of (A) G, (B) GDD and (C) G/DDB Films.

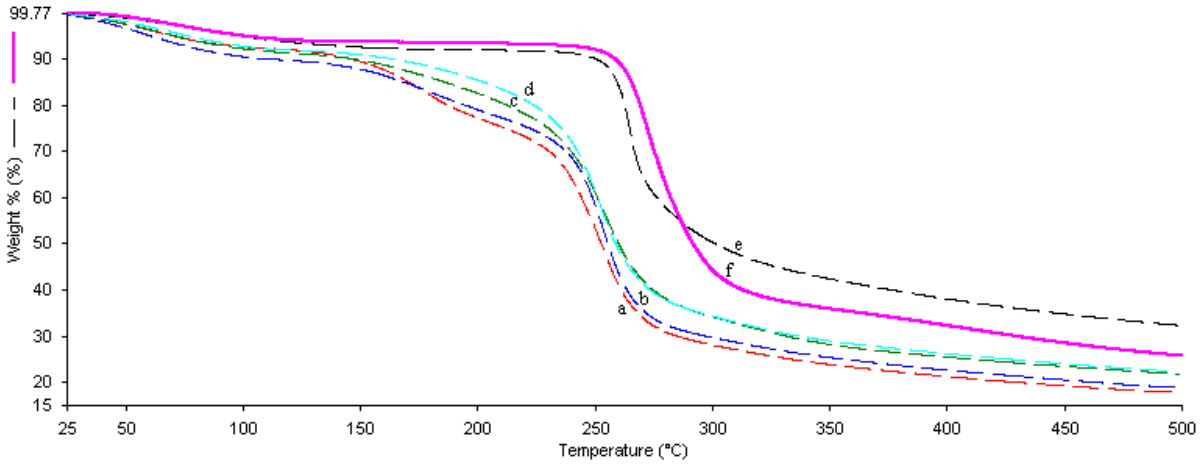

Figure 148 TGA thermograms of bilayer films (a) G/DDB 2:0.125, (b) G/DDB 2:0.25, (c) G/DDB 2:0.5, (d) G/DDB 2:1, (e) Gellan powder-reference and (f) DEAE-Dextran powder-reference.

Table 95 TGA of gellan and gellan-DEAE-Dextran PEC bilayer films. Each value represents mean ± SD (n = 4).

Formulation	Onset (˚C)	End (˚C)	Step of inflection (˚C)	Delta Y (%)
Gellan-reference	43.99±0.65	131.17±4.72	90.39±3.15	7.85±0.08
	257.79±12.21	282.29±12.74	264.91±12.10	59.67±0.93
DEAE-Dextran-reference	47.16±0.47	106.74±4.32	77.47±1.47	6.94±0.12
	261.20±11.43	301.16±15.72	272.15±12.62	67.61±0.98
G	24.99±0.56	176.56±7.31	24.99±0.56	10.17±0.33
	158.64±5.21	204.82±10.32	184.91±8.73	40.41±1.05
	233.83±10.27	275.67±12.53	250.62±11.47	35.27±0.98
G/DDB 2:0.125	26.43±0.97	124.51±5.56	26.43±0.97	6.95±0.21
	148.67±5.32	198.46±9.25	176.14±7.37	16.12±0.56
	233.06±10.45	277.49±12.36	252.17±11.24	58.66±1.23
G/DDB 2:0.25	26.27±0.78	89.46±2.95	34.87±0.86	14.78±0.52
	146.32±5.40	203.89±9.25	180.88±8.32	17.09±0.67
	238.49±10.35	275.23±12.07	253.94±12.03	57.39±1.14
G/DDB 2:0.5	26.33±0.52	149.61±4.12	26.33±0.52	8.29±0.24
	166.90±6.26	210.75±9.73	212.59±9.96	11.69±0.47
	234.53±10.16	284.13±12.85	255.20±11.52	57.18±1.25
G/DDB 2:1	25.59±0.47	151.36±5.87	25.59±0.47	8.69±0.48
	228.95±9.57	277.92±12.23	251.18±10.69	68.68±1.64

TGA thermograms of ibuprofen loaded composite and bilayer films were presented in Figure 149 and 150; Table 97 and 97. Ibuprofen exhibited one step of inflection at 240.76 ˚C attributed to the heat of decomposition of the drug with a complete weight loss of 99.50%; while gellan and DEAE-Dextran powder reference exhibited two steps of inflection with a total weight loss of 67.52% and 74.55% respectively. The GIb film showed two steps of inflection at 41.24 ˚C and 201.63 ˚C with corresponding weight losses of 8.81%, and 78.99% respectively and total weight loss of 87.80% in Table 96. The first weight loss was due to the loss of free water in the films while the second weight loss was due to the decomposition of the films. The addition of Ibuprofen to the film GIb exhibited

lower temperature of decomposition at 201.63 ˚C compared to G film at 250.62 ˚C suggesting reduced thermal stability of the GIb film. The GIbDD films in Figure 149 exhibited three steps of inflection denoting three distinct thermal events in the range of 25.98 to 29.54 ˚C; 195.97 to 199.4 ˚C and 451.62 to 456.20 ˚C. The total weight loss was in the range of 83.15% and 86.65% exhibiting two minima values with increasing DEAE-Dextran concentration. The marked increase in the second decomposition temperature to about 450 ˚C suggests that the addition of DEAE-Dextran to form the ternary complex further increased the thermal stability of GIbDD films greatly.

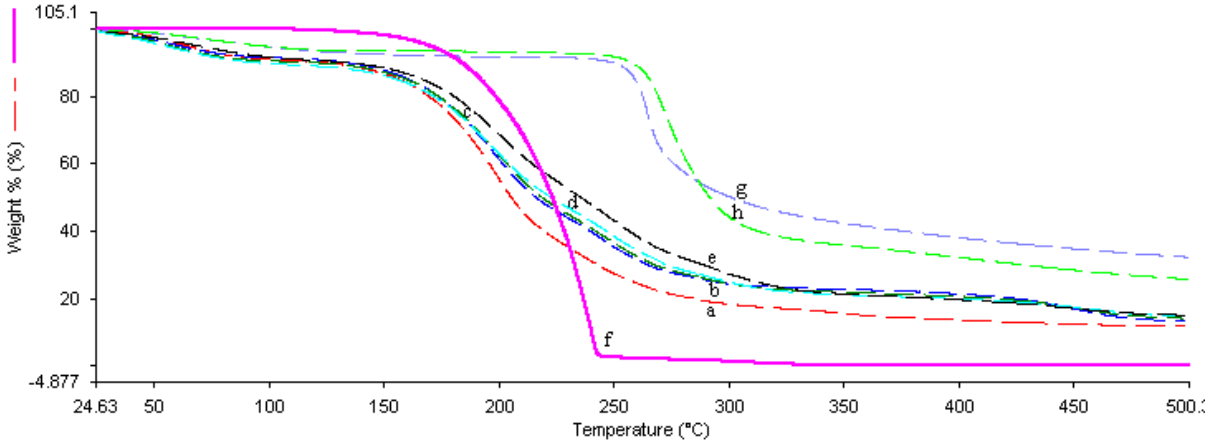

Figure 149 TGA thermograms of ibuprofen loaded composite films (a) GIb, (b) GIbDD 2:0.125, (c) GIbDD 2:0.25, (d) GIbDD 2:0.5, (e) GIbDD 2:1, (f) Ibuprofen powder-reference. (g) Gellan powder-reference and (h) DEAE-Dextran-reference.

Table 96 TGA of ibuprofen loaded gellan and gellan-DEAE-Dextran PEC composite films. Each value represents mean ± SD (n = 4).

Formulation	Onset (˚C)	End (˚C)	Step of inflection (˚C)	Delta Y (%)
Ibuprofen-reference	207.81 ±11.23	247.08±11.87	240.76±12.32	99.50±1.95
Gellan-reference	43.99±0.65	131.17±4.72	90.39±3.15	7.85±0.08
	257.79±12.21	282.29±12.74	264.91±12.10	59.67±0.93
DEAE-Dextran-reference	47.16±0.47	106.74±4.32	77.47±1.47	6.94±0.12
	261.20±11.43	301.16±15.72	272.15±12.62	67.61±0.98
G	24.99±0.56	176.56±7.31	24.99±0.56	10.17±0.33
	158.64±5.21	204.82±10.32	184.91±8.73	40.41±1.05
	233.83±10.27	275.67±12.53	250.62±11.47	35.27±0.98
GIb	39.52±0.87	57.53±1.24	41.24±1.21	8.81±0.27
	167.81±6.45	241.04±11.62	201.63±9.37	78.99±1.06
GIbDD 2:0.125	26.41±0.56	127.47±4.86	26.41±0.56	7.89±0.41
	164.89±5.71	245.20±10.54	199.34±9.47	68.54±1.25
	416.43±33.42	468.12±35.37	455.69±34.32	9.10±0.37
GIbDD 2:0.25	25.98±0.97	122.65±5.21	25.98±0.97	9.61±0.29
	164.74±6.28	252.36±10.73	197.99±10.36	68.34±1.52
	421.21±32.76	475.82±36.74	461.06±35.28	7.89±0.18
GIbDD 2:0.5	26.25±0.61	125.12±5.74	26.25±0.61	10.28±0.37
	162.83±6.45	260.14±14.23	195.97±10.87	69.35±1.12
	413.66±32.31	482.96±37.58	456.20±35.25	7.02±0.22
GIbDD 2:1	29.54±0.73	126.51±4.67	29.54±0.73	8.77±0.43
	167.20±6.75	273.22±12.64	199.17±10.96	68.99±0.21
	404.08±31.03	475.98±37.11	451.62±34.19	5.39±0.12

The GIb/DDB films in Figure 150 exhibited three steps of inflection denoting three distinct thermal events in the range of 22.87 to 26.33 ˚C; 188.50 to 197.99 ˚C and 250.24 to 257.53 ˚C. The total weight loss was in the range of 77.22 to 81.60% which exhibited decrease with increasing DEAE-Dextran concentration.

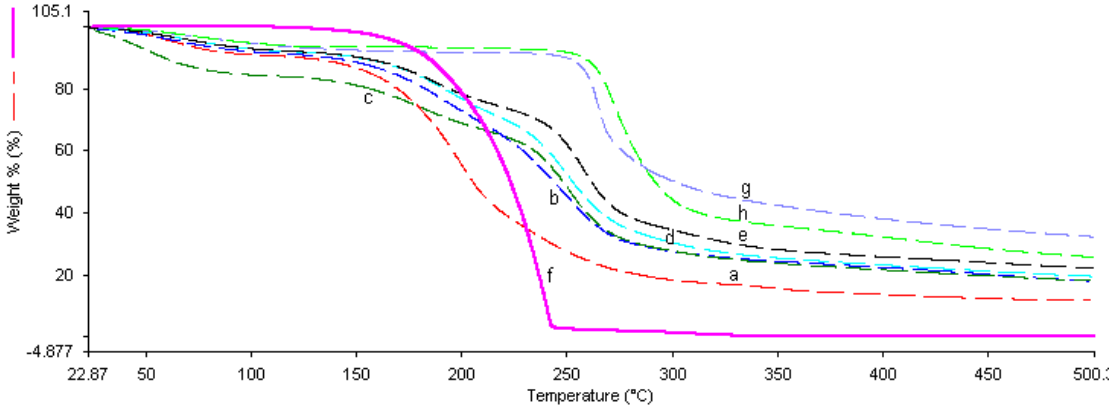

Figure 150 TGA thermograms of ibuprofen loaded bilayer films (a) GIb, (b) GIb/DDB 2:0.125, (c) GIb/DDB 2:0.25, (d) GIb/DDB 2:0.5, (e) GIb/DDB 2:1 (f) Ibuprofen powder-reference, (g) Gellan powder-reference and (h) DEAE-Dextran powder-reference.

Table 97 TGA of ibuprofen loaded gellan and gellan-DEAE-Dextran PEC bilayer films. Each value represents mean ± SD (n = 4).

Formulation	Onset (˚C)	End (˚C)	Step of inflection (˚C)	Delta Y (%)
Ibuprofen-reference	207.81±11.23	247.08±11.87	240.76±12.32	99.50±1.95
Gellan-reference	43.99±0.65	131.17±4.72	90.39±3.15	7.85±0.08
	257.79±12.21	282.29±12.74	264.91±12.10	59.67±0.93
DEAE-Dextran-reference	47.16±0.47	106.74±4.32	77.47±1.47	6.94±0.12
	261.20±11.43	301.16±15.72	272.15±12.62	67.61±0.98
GIb	39.52±0.87	57.53±1.24	41.24±1.21	8.81±0.27
	167.81±6.45	241.04±11.62	201.63±9.37	78.99±1.06
GIb/DDB 2:0.125	24.85±0.78	125.37±4.68	24.85±0.78	8.33±0.41
	192.14±5.71	285.26±12.54	251.30±10.73	73.27±1.21
GIb/DDB 2:0.25	25.98±0.97	122.65±5.21	25.98±0.97	14.78±0.58
	164.74±6.28	252.36±10.73	197.99±10.36	17.09±0.52
	231.17±10.64	281.28±12.47	252.30±10.82	48.44±0.98
GIb/DDB 2:0.5	26.33±0.52	149.61±5.74	26.33±0.52	10.28±0.37
	166.90±6.45	210.75±14.23	194.51±10.87	17.58±0.43
	229.13±10.17	285.99±13.85	250.24±11.27	52.54±0.56
GIb/DDB 2:1	22.87±0.56	42.49±4.67	22.87±0.56	7.30±0.35
	157.68±5.88	207.64±13.71	188.50±9.28	16.89±0.67
	239.93±31.03	285.32±37.11	257.53±14.11	53.03±0.61

4.3.5. Swelling kinetics

An important property of biopolymer film is the swelling ratio which gives the amount of water absorbed by films. The polymer films were subjected to swelling tests in PBS pH 7.4. The results were presented in Figures 151 and 152. Gellan film increased in swelling with increasing contact time in PBS pH 7.4. The hydrophilic nature of gellan polysaccharide makes it readily absorb water

which results in changes of its structure. The films reached equilibrium at 6 h as shown in Figure 151 and 152.

The swelling ratio ranged from 2.65 to 3.27 times its dried weight in PBS pH 7.4 at 37 ˚C for GDD films; 3.59 to 3.98 times for G/DDB films. The average equilibrium swelling ratio (SR) of G film was 2.58 ± 0.03. Statistical analysis showed that the addition of DEAE-Dextran to gellan significantly increased ($p < 0.05$, $n = 4$) the swelling ratio of the GDD and G/DDB films. The swelling ratio increased in the order: GDD 2:0.25 > GDD 2:0.125 > GDD 2:0.5 > GDD 2:1 > G for GDD films. The swelling ratio increased in the order: G/DDB 2:0.25 > G/DDB 2:0.125 > G/DDB 2:0.5 > G/DDB 2:1 > G for G/DDB films. The same trend or profile was observed in the composite and bilayer films. The swelling behavioural pattern showed a higher swelling ratio in the G/DDB complexes when compared with the GDD films indicating a higher capability to retain water. In the G/DDB and GDD complex films, the polymer network is loose with more hydrodynamic free volume with capacity to absorb more water leading to higher swelling.

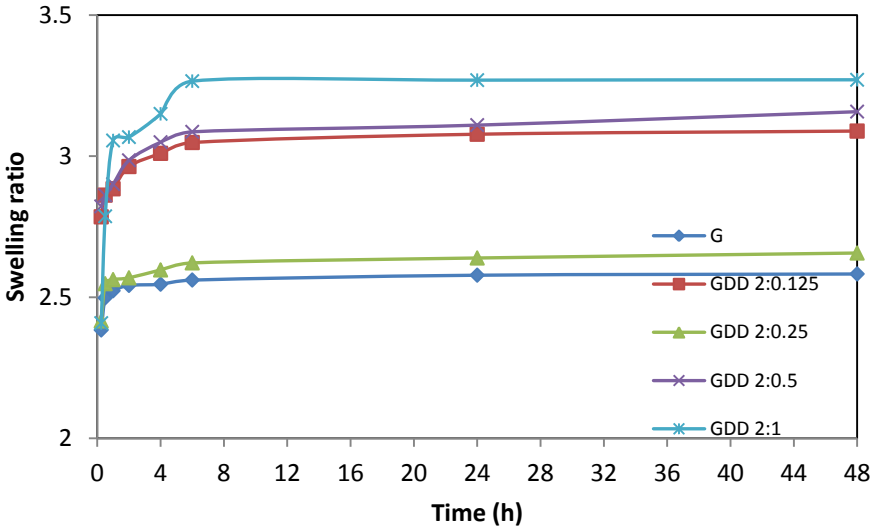

Figure 151 The swelling ratio of gellan and GDD composite films in PBS pH 7.4 at 37°C. Each data point represents mean ± SD (n = 4).

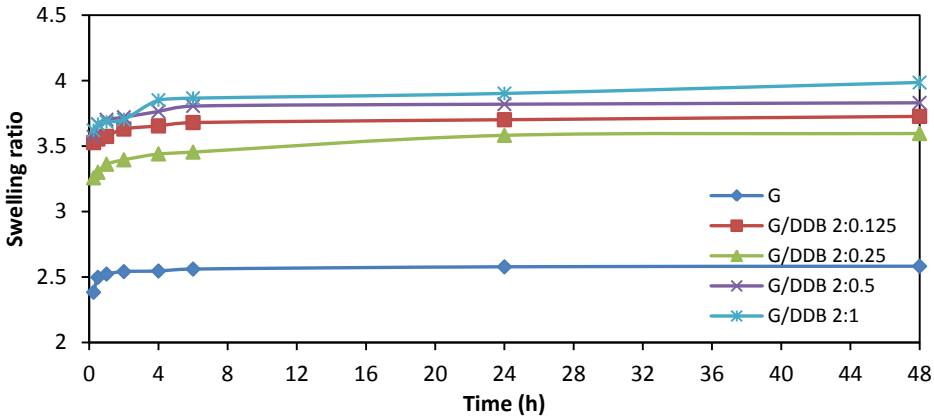

Figure 152 The swelling ratio of gellan and G/DDB bilayer films in PBS pH 7.4 at 37 ˚C. Each data point represents mean ± SD (n = 4).

The swelling of the drug loaded films reached equilibrium at 6 h in Figure 153 and 154. The swelling ratio ranged from 4.37 to 6.84 times its dried weight in PBS pH 7.4 at 37 ˚C for GIbDD films; 4.67 to 5.10 times for GIb/DDB films. The average equilibrium swelling ratio (SR) of GIb film was 2.85 (±0.12). The swelling ratio increased in the order: GIbDD 2:0.25 > GIbDD 2:0.125 > GIbDD 2:0.5 > GIbDD 2:1 > GIb for GIbDD composite films. The swelling ratio increased in the order: GIb/DDB 2:0.25 > GIb/DDB 2:0.125 > GIb/DDB 2:0.5 > GIb/DDB 2:1 > GIb for GIb/DDB bilayer films. The swelling behavioural pattern showed a higher swelling ratio in the GIbDD composite films when compared with the GIb/DDB bilayer films. It also showed that incorporation of ibuprofen significantly increased ($p < 0.05$, $n = 4$) the swelling of the films when compared with films without the drug. In the drug loaded complexes, the polymer network is loose with more hydrodynamic free volume with capacity to absorb more water leading to higher swelling.

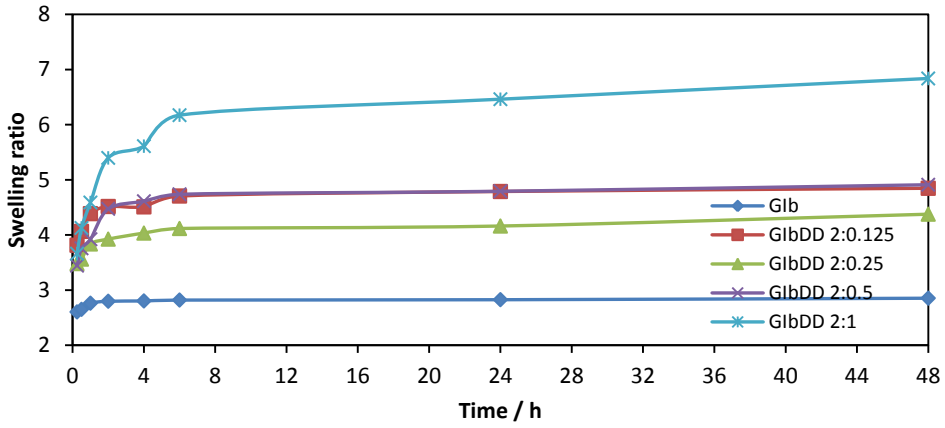

Figure 153 The swelling ratio of ibuprofen loaded gellan and gellan-DEAE-Dextran PEC composite films in PBS pH 7.4 at 37 ˚C. Each data point represents mean ± SD (n = 4).

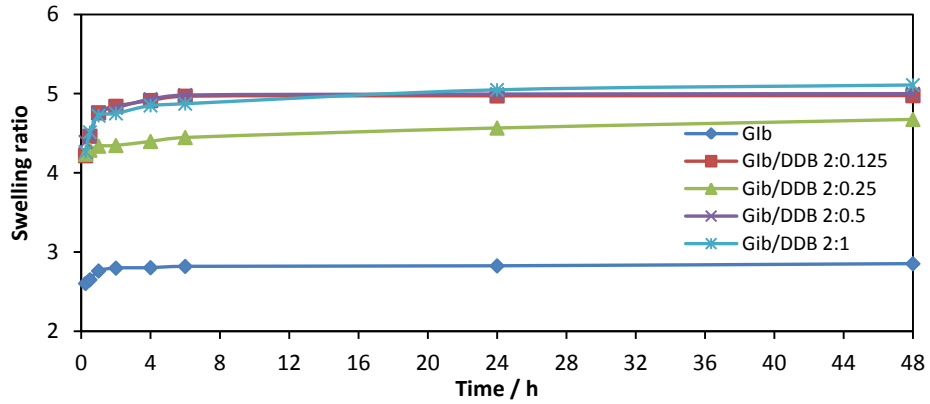

Figure 154 The swelling ratio of ibuprofen loaded gellan and gellan-DEAE-Dextran PEC bilayer films in PBS pH 7.4 at 37˚C. Each data point represents mean ± SD (n = 4).

4.3.6. Drug release from composite and bilayer films

The release profiles of ibuprofen from gellan, gellan-DEAE-Dextran composite and bilayer complex films in PBS pH 7.4 are shown in Figures 155 and 156 respectively. Drug release from matrices is preceded by polymer hydration. Hydration of the polymeric films in the dissolution medium triggered the release of ibuprofen from the film. The drug release profile of ibuprofen from the composite and bilayer films was divided into three phases shown in Figures 166 to 172 in the Appendix I. The cumulative release of ibuprofen from GIb films (50.61%) was lower than the ternary complex GIbDD composite films (69.59 to 79.44%). An increased rate of release was exhibited by the GIbDD films compared with the GIb films within the first 30 min. The GIb films maintained a constant release rate which slowly increased beyond 2 h. The third phase of drug release between 2 and 24 h showed a steady increase from 2 to 4 h and a further constant rate of release up to 24 h. The drug

release profile from the bilayer films within the first 30 min showed a slow release rate which continued till 24 h. The maximum ibuprofen released from GIb films was 71.52%; of the range of 80.49 to 99.76% for GIbDD films of the range 31.8 to 47.37% for GIb/DDB films. The statistical analysis of the drug release profiles indicated that for GIbDD films, the ibuprofen release significantly increased ($p < 0.05$, $n = 4$) with increase in DEAE-Dextran concentration. Bajpai *et al.* studied the release of potassium nitrate from alginate/pectin beads and also observed that the release rate of potassium nitrate increased with increase in pectin concentration [45]. Ibuprofen release from GIb/DDB films was significantly reduced ($p < 0.05$, $n = 4$) when compared to GIb and GIbDD films. In the GIb/DDB films, a considerable amount of ibuprofen was washed out during the bilayer formation process when the films were immersed in DEAE-Dextran solutions. Part of ibuprofen migrated into the DEAE-Dextran solution during the process. This was evident from the SEM micrographs in Figure 119 where empty pores showing depletion of ibuprofen on the surface morphology of the films were observed. The release profiles of the GIb, GIbDD and GIb/DDB films exhibited burst release from the films. The initial burst release could be due to the ibuprofen molecules being physically and chemically entrapped. This similar initial burst release trend was reported by Yan *et al.* where there was burst release of Rhodamine B from nanoporous polymer (N-vinylpyrrolidinone and dipentaerythritol penta/hexa-acrylate) thin film [46]. This may be due to increased swelling ratio of the films and fast dissolution of the weakly incorporated ibuprofen in the film matrix resulting in rapid release of ibuprofen into the buffer medium. The slow ibuprofen release rate in the later stage may be related to the chemical bonding between ibuprofen and DEAE-Dextran, therefore the drug release rate was controlled by the equilibrium between bonding with DEAE-Dextran and dissolution in aqueous medium. At the last plateau stage, the release was quite slow and maintained the release up to 24 h.

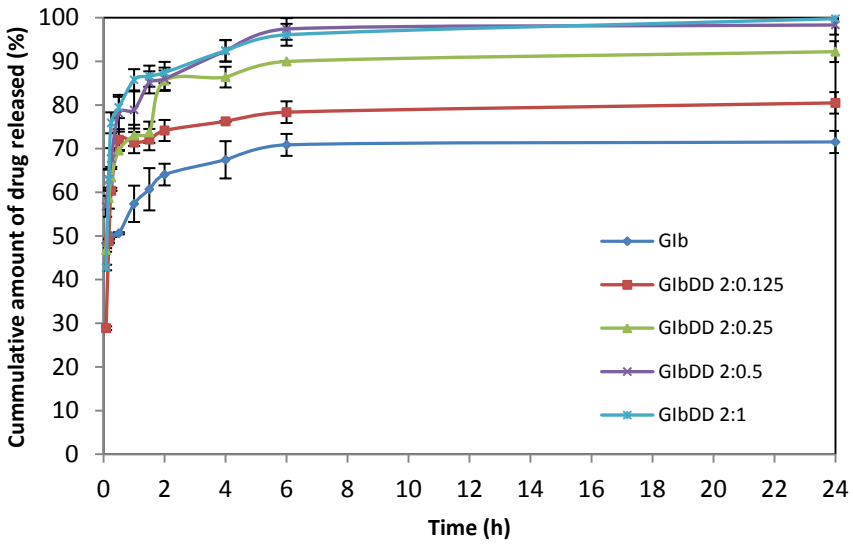

Figure 155 Release profile of ibuprofen from Gellan, Gellan-DEAE-Dextran composite films in PBS pH 7.4. Each data point represents mean ± SD (n = 4).

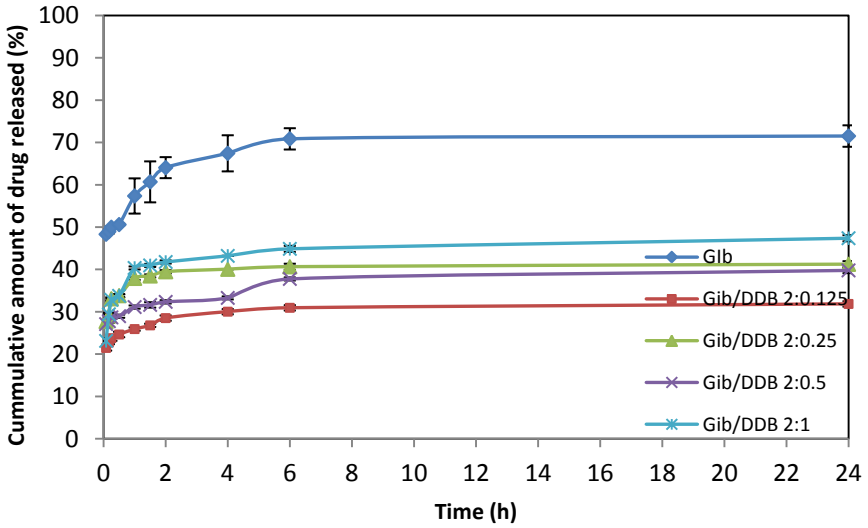

Figure 156 Release profile of ibuprofen from Gellan, Gellan-DEAE-Dextran complex bilayer films in PBS pH 7.4. Each data point represents mean ± SD (n = 4).

4.3.7. Drug release kinetics

To examine the drug release kinetics, the data were fitted to models representing zero order (Q v/s t), first order (Log Q_0 – Q) v/s t), Higuchi (Q v/s $t^{0.5}$) and Korsemeyer-Peppas (Log Q v/s Log t). The data was best fitted with the Korsemeyer-Peppas models for GIb, GIbDD and GIb/DDB films. The diffusional exponents (n) values obtained are shown in Table 98 and 99 for GIb, GIbDD and GIb/DDB films.

For GIb, GIbDD 2:0.25 composite and GIb/DDB bilayer films the release mechanisms exhibited were Fickian (n < 0.5); therefore the release rate was linear to $t^{0.5}$. While GIbDD 2:0.125, GIbDD 2:0.5 and GIbDD 2:1 composite films exhibited non-Fickian diffusion where diffusion exponent (n) is 0.5 < n < 1, therefore anomalous transport or polymer relaxation was the predominating mechanism [47]. Here, the diffusion rate of the solvent and the relaxation of the polymeric chains are of the same order of magnitude; and a deviation from the Fickian behaviour. Ozdemir and Floros also observed an anomalous diffusion mechanism for whey protein films with potassium sorbate [48]. This was also observed by Bierhalz *et al.* for alginate/pectin films with natamycin [33]

Table 98 Regression coefficient (r) values of different kinetic models and diffusion exponent (n) of Korsemeyer-Peppas models for the release of ibuprofen from Gellan, Gellan-DEAE-Dextran complex composite films in PBS pH 7.4.

Formulation	Zero order	First Order	Higuchi	Korsemeyer-Peppas	
	R^2	R^2	R^2	R^2	n
GIb	0.45	0.42	0.72	0.85	0.078
GIbDD 2:0.125	0.20	0.15	0.39	0.99	0.633
GIbDD 2:0.25	0.38	0.32	0.63	0.99	0.271
GIbDD 2:0.5	0.39	0.35	0.65	1.00	0.901
GIbDD 2:1	0.29	0.22	0.51	1.00	0.941

Table 99 Regression coefficient (r) values of different kinetic models and diffusion exponent (n) of Korsemeyer-Peppas models for the release of ibuprofen from Gellan, Gellan-DEAE-Dextran complex bilayer films in PBS pH 7.4.

Formulation	Zero order	First Order	Higuchi	Korsemeyer-Peppas	
	R^2	R^2	R^2	R^2	n
GIb	0.45	0.42	0.72	0.85	0.078
GIb/DDB 2:0.125	0.49	0.45	0.75	0.97	0.076
GIb/DDB 2:0.25	0.29	0.26	0.53	0.85	0.076
GIb/DDB 2:0.5	0.69	0.65	0.89	0.94	0.071
GIb/DDB 2:1	0.36	0.30	0.61	0.87	0.120

4.3.8. Similarity of drug release profiles (Similarity factor f_2)

Comparing the drug release profile of GIbDD (ternary) composite films with the GIb (binary) films based on model independent similarity factor, the f_2 values obtained were in the range of 52.32 to 76.11, decreasing with increase in concentration of DEAE-Dextran shown in Table 107. All the f_2 values were above the limit value of 50 suggesting that the drug release from the GIbDD composite films were similar to that of the GIb films. However, for the GIb/DDB bilayer films, the f_2 values of GIb/DDB 2:0.125 and GIb/DDB 2:0.5 films were lower than the limit value 50 (45.00 and 49.81 in Table 108) suggesting dissimilarity in the drug release profiles while GIb/DDB 2:0.25 and GIb/DDB 2:1 were above 50 suggesting similarity in the profiles.

4.4. Conclusion

A novel pharmaceutical nanoconjugate film was prepared by simple aqueous cast method to form composite films from electrostatic interaction between gellan and DEAE-Dextran. The bilayer films were formed by immersion of gellan films into DEAE-Dextran solutions. The inclusion of DEAE-Dextran produced weaker and less flexible films than the control gellan film. The DSC and TGA thermograms confirmed the formation of a single eutectic product which was evidenced by single endothermic peak. The swelling behavioural pattern showed a higher swelling ratio in the G/DDB complexes when compared with the GDD films. The gellan and PEC films loaded with ibuprofen showed layered spheres on the surface morphology suggesting inclusion of ibuprofen in the PEC nanoconjugates. This was confirmed by the FTIR findings which showed the disappearance of ibuprofen peaks in the spectra of the binary and ternary complexes suggesting electrostatic and hydrophobic interaction as well as hydrogen bonding between ibuprofen and the polymers. The GIbDD complexes showed higher swelling ratio compared with the GIb/DDB films indicating a possible mechanism of release of ibuprofen from the conjugate film. The maximum ibuprofen released from GIb, GIbDD and GIb/DDB films were 71.52%, 99.76% and 47.37% respectively. The most prominent release mechanisms were Fickian diffusion and anomalous mechanisms. Overall, the nanoconjugate composite films produced a near complete release (99.76%) compared with the control film within 48h. It was concluded that the nanoconjugate composite films demonstrated potential application in the delivery of poorly soluble drugs.

4.5. References

1. Ma, D.M., A. J., *The Interplay of Membrane Formation and Drug Release in Solution-Cast Films of Polylactide Polymers.* Int J Pharm, 2010. **388**: p. 1-12.
2. Patel, N.A., N.J. Patel, and R.P. Patel, *Design and Evaluation of Transdermal Drug Delivery System for Curcumin as an Anti-inflammatory Drug.* Drug Dev Ind Pharm, 2009. **35**(2): p. 234-242.
3. Jiang, B.B. and B.Y. Li, *Tunable Drug Loading and Release from Polypeptide Multilayer Nanofilms.* Int J Nanomedicine, 2009. **4**: p. 37-53.
4. Decher, G., *Fuzzy Nanoassemblies: Toward Layered Polymeric Multicomposites.* Science, 1997. **277**: p. 1232-1237.
5. Sato, K.Y., K. Takahashi, S. Anzai, J., *pH- and Sugar-Sensitive Layer-by-Layer Films and Microcapsules for Drug Delivery.* Adv Drug Deliv Rev, 2011. **63**(9): p. 809-821.

6. Kawashima, Y.H., T. Kasai, A. Takenaha, H. Lin, S. Y. Ando, Y., *Novel Method for the Preparation of Controlled-Release Theophylline Granules Coated with a Polyelectrolyte Complex of Sodium Polyphosphate-Chitosan.* J Pharm Sci, 1985. **74**: p. 264-268.
7. Pang, J.L., Y. Li, F. Cai, X. Du, J. Li, Z., *Ibuprofen-Loaded Poly(Lactic-co-Glycolic Acid) Films for Controlled Drug Release.* Int J Nanomedicine, 2011. **6**: p. 659-665.
8. Sanderson, G.R. and R.C. Clark, *Gellan Gum.* Food Technol, 1983. **37**: p. 63-70.
9. Pollock, T., *Gellan Related Polysaccharide and the genus Sphingomonas.* J Gen Microbiol, 1993. **139**: p. 1939-1945.
10. Lee, K.Y., J. Shim, and H.G. Lee, *Mechanical Properties of Gellan and Gelatin Composite Films.* Carboh Polym, 2004. **56**(2): p. 251-254.
11. Agnihotri, S.A., S.S. Jawalkar, and T.M. Aminabhavi, *Controlled Release of Cephalexin Through Gellan Gum Beads: Effects of Formulation Parameters on Entrapment Efficiency, Size and Drug Release,.* Eur J Pharm Biopharm, 2006. **63**: p. 249-261.
12. Miyazaki, S.K., N.Kubo, W.Endo, K.Attwood, D., *Comparison of In Situ Gelling Formulations for the Oral Delivery of Cimetidine.* Int J Pharm, 2001. **220**: p. 161-168.
13. Sanzgiri, Y.D.M., S.Crescenzi, V.Callegaro, L.Topp, E. M.Stella, V. J., *Gellan Based Systems for Opthalmic Sustained Delivery of Methylprednisolone.* J Control Rel, 1993. **1993**: p. 195-201.
14. Babu, R.J.S., S. Kumar, M.T. Pandit, J. K., *Formulation of Controlled Release Gellan Gum Macro Beads of Amoxicillin.* Curr Drug Deliv, 2010. **7**(1): p. 36-43.
15. Vipul, V. and B. Basu, *Formulation and Characterization of Novel Floating In-Situ Gelling System for Controlled Delivery of Ramipril.* Int J Drug Deliv, 2013. **5**(1): p. 834.
16. Yang, L. and A.T. Paulson, *Mechanical And Water Vapour Barrier Properties of Edible Gellan Films. .* Food Res Intl, 2000. **33**(7): p. 563-570.
17. Chang, S.J.K., S. M.Liu, W. T.Niu, G. C. C. Lee, M. W.Wu, C. S., *Gellan Gum Films for Effective Guided Bone Regeneration.* J Med Biol Eng, 2010. **30**(2): p. 99-103.
18. Rivera-Leyva, J.C.G.-F., M. Valladares-Mendez, A. Orozco-Castellanos, L. M. Martinez-Alfaro, M., *Comparative Studies on the Dissolution Profiles of Oral Ibuprofen Suspension and Commercial Tablets Using Biopharmaceutical Classification System Criteria.* Ind J Pharm Sci, 2012. **74**(4): p. 312-318.
19. Varani, J.F., S.E. Inman, D.R. Beals, T. F. Hillegas, W.J., *Modulation of Adhesive Properties of DEAE-dextran with Laminin.* J Biomed Mater Res, 1995. **29**(8): p. 993-997.
20. Aulton, M.E., *Aulton's Pharmaceutics: The Design and Manufacture of Medicines*. 3rd ed, ed. K. Taylor. 2007, London, UK: Elsevier.
21. ASTM, *Standard Test Methods for Tensile Properties of Thin Plastic Sheeting. Standard Designation: D882.*, in *Annual Book of American Standards Testing Methods Standard*, ASTM, Editor. 1985, ASTM: Philadelphia. p. 182-188.
22. Hadjiioannou, T.P., G.D. Cristian, M.A. Kouparris, and P.E. Macheras, *Quantitative Calculations in Pharmaceutical Practise and Research*. 1993, New York: VCH Publishers Inc.
23. Bourne, D.W.A., *Pharmacokinetics*, in *Modern Pharmaceutics*, G.S. Banker and C.T. Rhodes, Editors. 2002, Marcel Dekker Inc: New York. p. 94-144.
24. Higuchi, T., *Mechanism of Sustained-Action Medication. Theoretical Analysis of Rate of Release of Solid Drugs Dispersed in Solid Matrices.* J Pharm Sci, 1963. **52**(12): p. 1145-1149.
25. Korsemeyer, R.W., R. Gurny, E. Doelker, P. Buri, and N.A. Peppas, *Mechanism of Solute Release from Porous Hydrophilic Polymers.* Int J Pharm, 1983. **15**(1): p. 25-35.
26. Thakkar, V.T.S., P. A. Soni, T. G. Parmar, M. Y. Gohel M. C. Ghandi, T. R., *Goodness-of-fit Model-Dependent Approach for Release Kinetics of Levofloxacin Hemihydrates Floating Tablet.* Dissolution Technol, 2009. **1**: p. 35-39.
27. Moore, J.W., *Mathematical Comparison of Dissolution Profiles.* Drug Dev Ind Pharm, 1996. **12**: p. 969-992.
28. Pillay, J. and R. Fassihi, *Evaluation and Comparison of Dissolution Data Derived from Different Modified Release Dosage Forms: an Alternative Method.* J Control Release, 1998. **1998**: p. 45-55.
29. Zhu, Y., K.A. Mehta, and J.W. McGinity, *Influence of Plasticizer Level on the Drug Release from Sustained Release Film Coated and Hot-Melt Extruded Dosage Forms.* Pharm Dev Technol, 2006. **11**: p. 285-294.
30. Yang, L., A.T. Paulson, and M.T. Nickerson, *Mechanical and Physical Properties of Calcium-Treated Gellan Films.* Food Res Intl, 2010. **45**(5): p. 1439-1443.

31. Ashtaputre, A.A. and A.K. Shah, *Studies on the Exopolysaccharide from Sphingomonas paucimobilis-GS1:Nutritional Requirements and Precursor-Forming Enzymes.* Curr Microbiol, 1995. **31**(4): p. 234-238.
32. Ma, D. and A.J. McHugh, *The Interplay of Membrane Formation and Drug Release in Solution-Cast Films of Polylactide Polymers.* Int J Pharm, 2010. **388**(1-2): p. 1-12.
33. Bierhalz, A.C.K., M.A. da Silva, and T.G. Kieckbusch, *Natamycin Release from Alginate/Pectin Films for Food Packaging Applications.* J Food Eng, 2012. **110**: p. 18-25.
34. Winograd, N., *Ion Beams and Laser Postionization for Molecule-Specific Imaging.* Anal Chem, 1993. **65**: p. 622A.
35. Park, H.J.W., C. L.Vergano, P. J.Testin, R. F., *Permeability and Mechanical Properties of Cellulose-Based Edible Films.* J Food Sci, 1993. **58**: p. 1361-1364.
36. Xu, L.L., B.Kennedy, J. F.Xie, B. J.Huang, M., *Characterization of Konjac Glucomannam-Gellan Gum Blend Films and their Sutaibility for Release of Nisin Incorporated Therein.* Carboh Polym, 2007. **70**: p. 192-197.
37. Sudhamani, S.R., M.S. Prasad, and K. Udaya Sankar, *DSC and FTIR studies on Gellan and Polyvinyl Alcohol (PVA) blend Films.* Food Hydrocoll, 2003. **17**: p. 245-250.
38. Matkovic, S.R., G.M. Valle, and L.E. Briand, *Quantitative Analysis of Ibuprofen in Pharmaceutical formulations through FTIR Spectroscopy.* Lat Am Appl Res, 2005. **35**(3): p. 189-195.
39. Nokhodchi, A.A., O. Jelvehgari, M., *Physico-Mechanical and Dissolution Behaviours of Ibuprofen Crystals Crystallized in the Presence of Various Additives.* DARU, 2010. **18**(2): p. 74-83.
40. Socrates, G., *Infrared Characteristic Group Frequencies, Tables and Charts*. 2nd ed. 1994, New York: John Wiley & Sons. 249.
41. Commission, B.P., *British Pharmacopoeia 2012*. Vol. 1. 2011, Norwich, Great Britain: Stationery Office Books.
42. Kumar, D.P.S., D. C. Subrata, C. Soumen, R, *Formulation and Evaluation of Solid Lipid Nanoparticles of A Poorly Water Soluble Model Drug, Ibuprofen.* Int Res J Pharm, 2012. **3**(12): p. 132-137.
43. Barreiro-Iglesias, R.B., L. Temchenko, M. Hatton, T. A. Concheiro, A. Alvarez-Lorenzo, C., *Solubilization and Stabilization of Camptothecin in Micellar Solutions of Pluronic-g-poly(acrylic acid) Copolymers.* J Cont Rel, 2004. **97**(3): p. 537-549.
44. Yoon, J.-S.L., W. -S. Kim, K. -S. Chin, I. -J. Kim, M. -N. Kim, C., *Effect of Poly(ethylene glycol)-block-poly(L-lactide) on the Poly[(R)-3-hydroxy butyrate]/poly(L-lactide) blends.* Eur Polym J, 2000. **36**: p. 435-442.
45. Bajpai, J.B., A. K. Mishra, S., *Dynamics of Controlled Release of Potassium Nitrate from a Highly Swelling Binary Biopolymeric Blend of Alginate and Pectin.* J Macromol Sci, 2006. **43A**(1): p. 165-186.
46. Yan, W.H., V. K. S. Zheng, Y. B. Shariff, Y. M. Gao, T. Huang, T. Y., *Towards Nanoporous Polymer Thin Film-Based Drug Delivery Systems.* Thin Solid Films, 2009. **517**(5): p. 1794-1798.
47. Siepmann, J. and N.A. Peppas, *Modelling of Drug Release from Delivery Systems Based on Hydroxypropyl Methylcellulose (HPMC).* Adv Drug Del Rev, 2001. **48**(2-3): p. 39-157.
48. Ozdemir, M. and J.D. Floros, *Analysis and Modelling of Potassium Sorbate Diffusion through Edible Whey Protein Films.* J Food Eng, 2001. **47**(2): p. 149-155.

CHAPTER FIVE

5.0. Recommended future works

- The stability studies of the nanoconjugates, hydrogels and films will be carried out to determine the stability and predict the shelf life of the products.
- The effects of different pHs on the swelling kinetics of the hydrogels and films will be studied.
- The effects of pH and ionic strength on the drug release profiles of the nanoconjugate products will be studied.
- The potential mucoadhesive performance of the bilayer films based on the presence of the DEAE-Dextran will be investigated using a texture analyzer.
- Scaling up of production batches.
- Finally, the efficacy studies of the hydrogels will be evaluated based on animal models/ invitro test to determine the mechanism of enhanced effect of their analgesic and anti-inflammatory properties.

6.0. Appendix I

Table 100 Particle size measurements from SEM images of IbDMelt, IbDNaOH, IbDTw80 and IbDNic nanoconjugates.

Concentration code	Particle size measurements from SEM (nm)			
	IbDMelt	IbDNaOH	IbDTw80	IbDNic
1	170.67±34.15	364.90±6.34	111.6±6.56	77.52±8.55
2	295.87±73.54	108.40±1.32	101.88±16.16	108.73±3.56
3	315.33±63.09	249.73±34.21	62.72±3.88	150.93±5.00
4	807.10±89.41	89.93±6.44	51.03±10.31	161.90±18.23
5	122.73±14.00	60.36±6.77	38.76±4.73	162.73±5.34

Table 101 Particle size measurements from SEM images of IbDMelt, IbDNaOH, IbDTw80 and IbDNic nanoconjugates.

Concentration code	Particle size measurements from SEM (nm)			
	IbChMelt	IbChNaOH	IbChTw80	IbChNic
1	261.27±22.15	6320.00±170.00	166.20±42.88	114.83±9.60
2	303.13±37.50	2300.00±920.00	221.93±58.91	191.00±22.10
3	405.07±48.26	8050.00±2430.00	379.43±21.81	197.07±26.27
4	433.63±13.78	9290.00±1280.00	395.37±17.81	385.83±30.02
5	602.37±119.86	9840.00±700.00	498.87 ±160.20	2.60±0.40

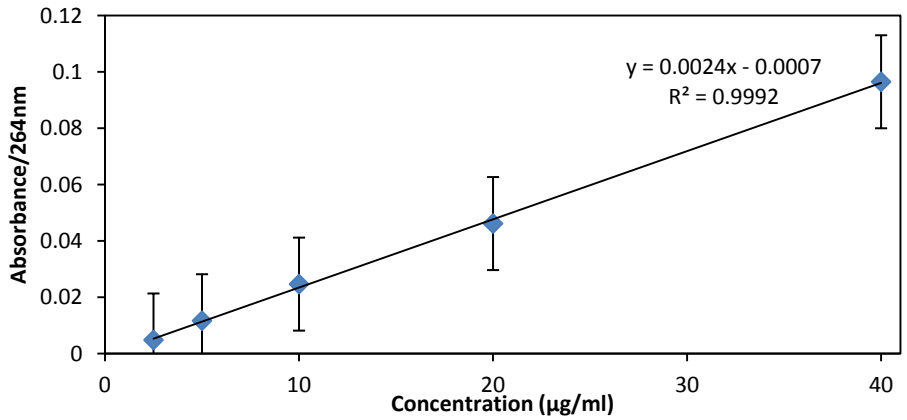

Figure 157 Calibration curve for ibuprofen at 264 nm. Each data point represents mean ± SD (n = 10).

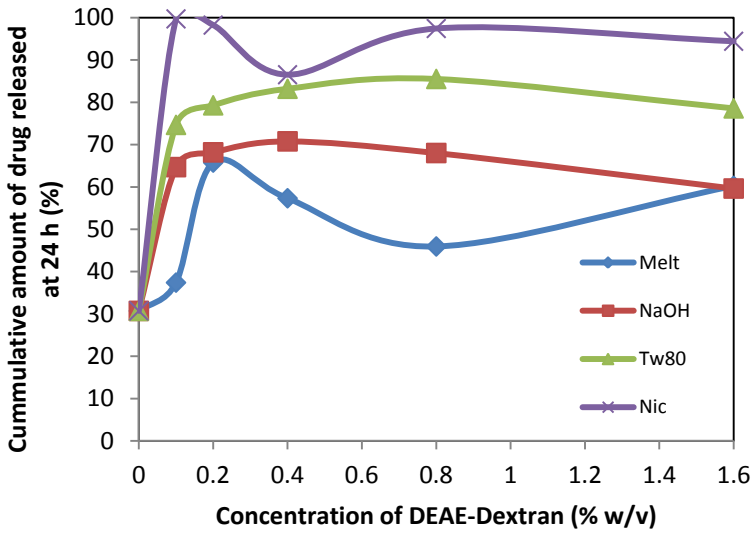

Figure 158 Effect of DEAEDextran on the release of ibuprofen from the conjugates at 24 h.

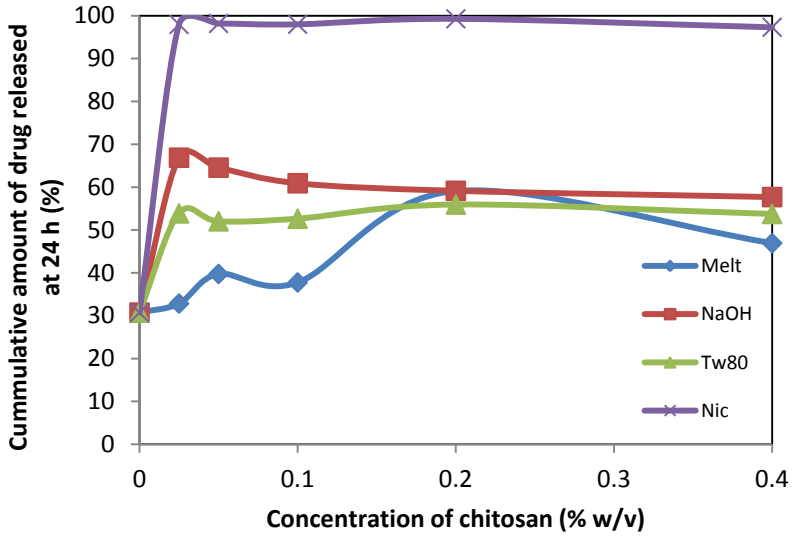

Figure 159 Effect of chitosan on the release of ibuprofen from the conjugates at 24 h.

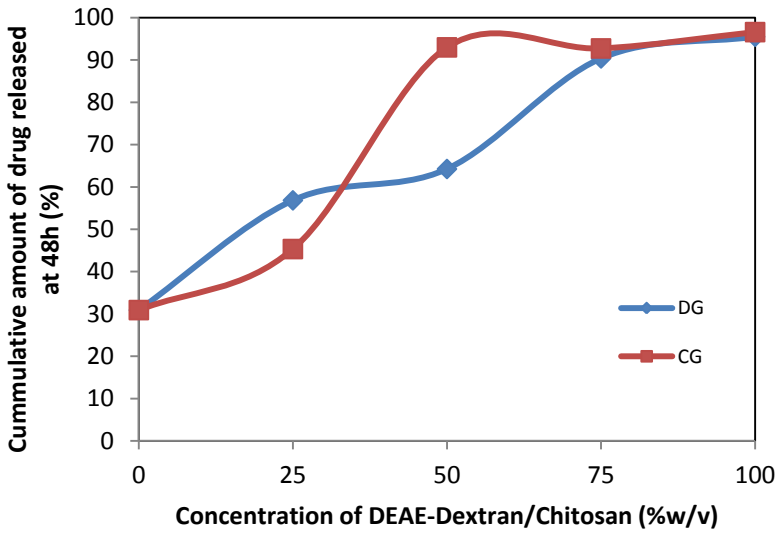

Figure 160 Effect of polymer concentrations on ibuprofen release from the ternary conjugates.

Table 102 Similarity factor f_2 for ibuprofen control versus ibuprofen – DEAE-Dextran conjugates.

Concentration code	f_2 – Similarity factor			
	IbDMelt	IbDNaOH	IbDTw80	IbDNic
1	79.53	45.94	40.38	30.61
2	45.27	43.83	38.22	31.08
3	51.19	42.38	36.54	35.21
4	63.08	43.92	35.60	31.34
5	48.95	49.41	38.54	32.34

Table 103 Similarity factor f_2 for ibuprofen control versus ibuprofen – chitosan conjugates.

Concentration code	f_2 – Similarity factor			
	IbChMelt	IbChNaOH	IbChTw80	IbChNic
1	95.17	44.60	54.18	31.17
2	73.78	46.03	55.96	31.10
3	78.58	48.49	55.35	31.16
4	49.81	49.79	52.35	30.75
5	61.76	50.92	54.30	31.38

Table 104 Similarity factor f_2 for ibuprofen control versus ibuprofen loaded DEAE-Dextran-gellan (DG) or chitosan/gellan (CG) conjugates.

Mixing ratio	f_2 – Similarity factor	
	DG	CG
0:100	33.38	34.73
25:75	53.02	65.46
50:50	47.62	34.18
75:25	35.11	34.27
100:0	33.32	32.96

Table 105 The pH of polymeric complex hydrogels. Each value represents mean ± SD (n = 4).

Formulation	pH
G	6.27±0.12
GDD 2:0.125	6.12±0.28
GDD 2:0.25	6.20±0.07
GDD 2:0.5	6.04±0.08
GDD 2:1	6.17±0.14
GIb	5.99±0.14
GIbDD 2:0.125	5.92±0.04
GIbDD 2:0.25	5.93±0.06
GIbDD 2:0.5	5.90±0.08
GIbDD 2:1	5.95±0.04

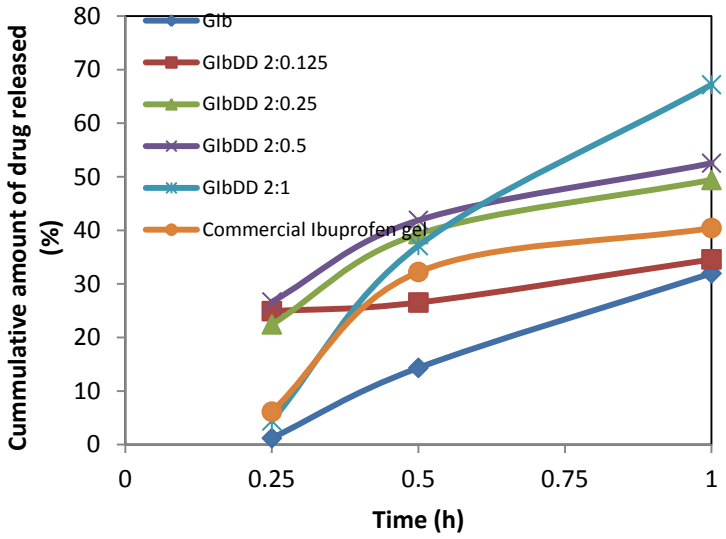

Figure 161 Release profile of ibuprofen from GIb and GIbDD complex hydrogels within the first hour.

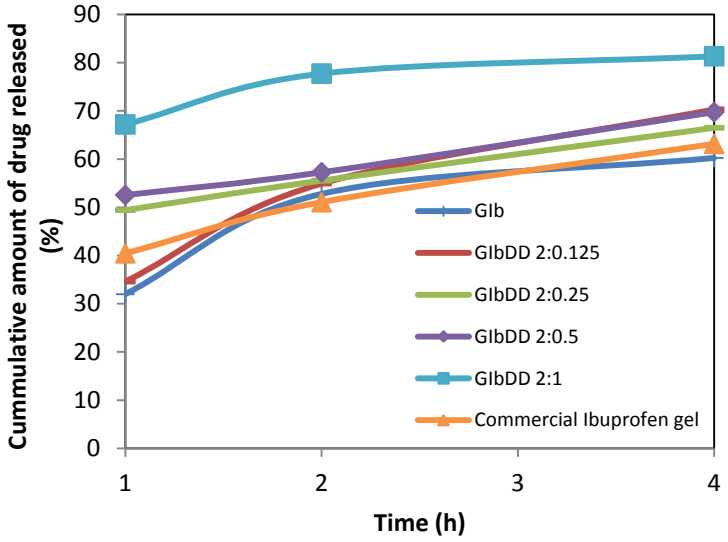

Figure 162 Release profile of ibuprofen from GIb and GIbDD complex hydrogels between 1 and 4 h.

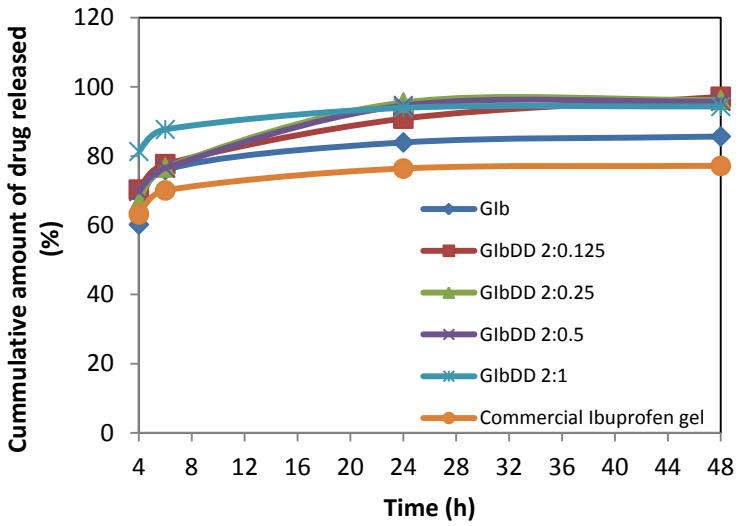

Figure 163 Release profile of ibuprofen from GIb and GIbDD complex hydrogels between 4 and 48 h.

Table 106 Similarity factor f_2 for GIb versus GIbDD complex hydrogels.

Formulation	f_2 – Similarity factor
GIbDD 2:0.125	68.97
GIbDD 2:0.25	70.64
GIbDD 2:0.5	71.48
GIbDD 2:1	74.60

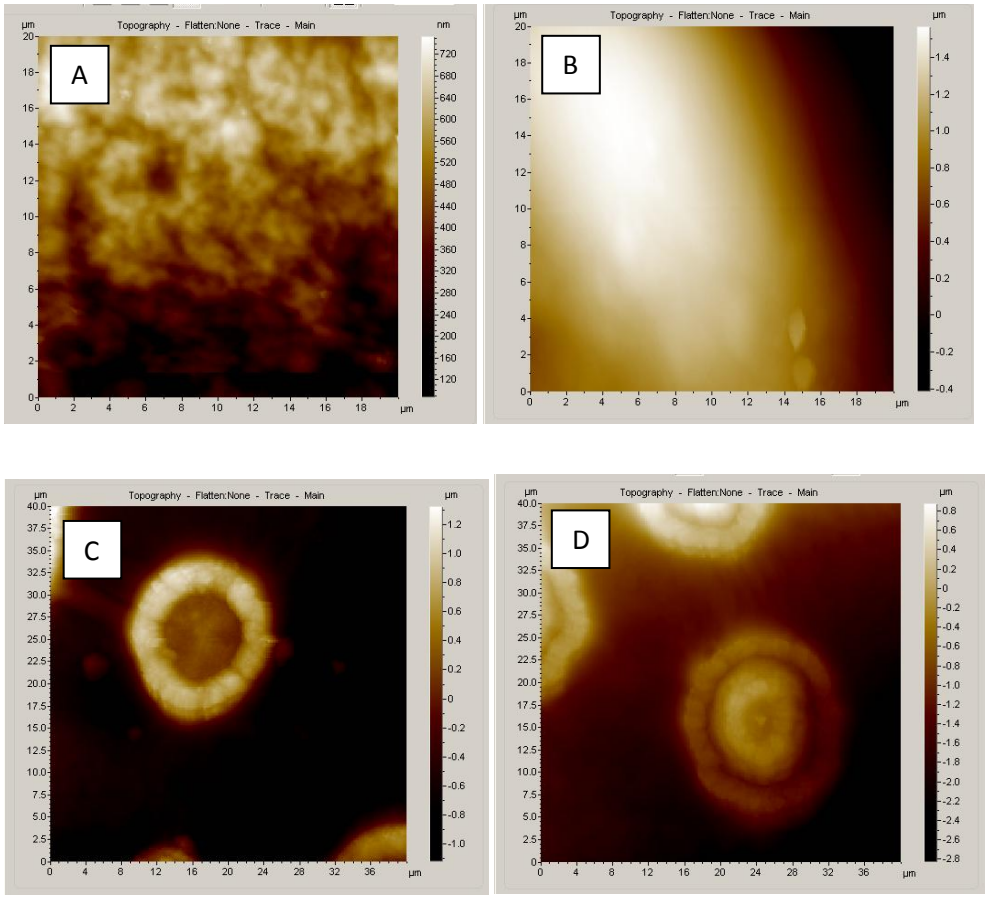

Figure 164 Topography trace images for (A) plain gellan G (B) composite GDD (C) ibuprofen loaded gellan GIb and (D) ibuprofen loaded composite GIbDD films.

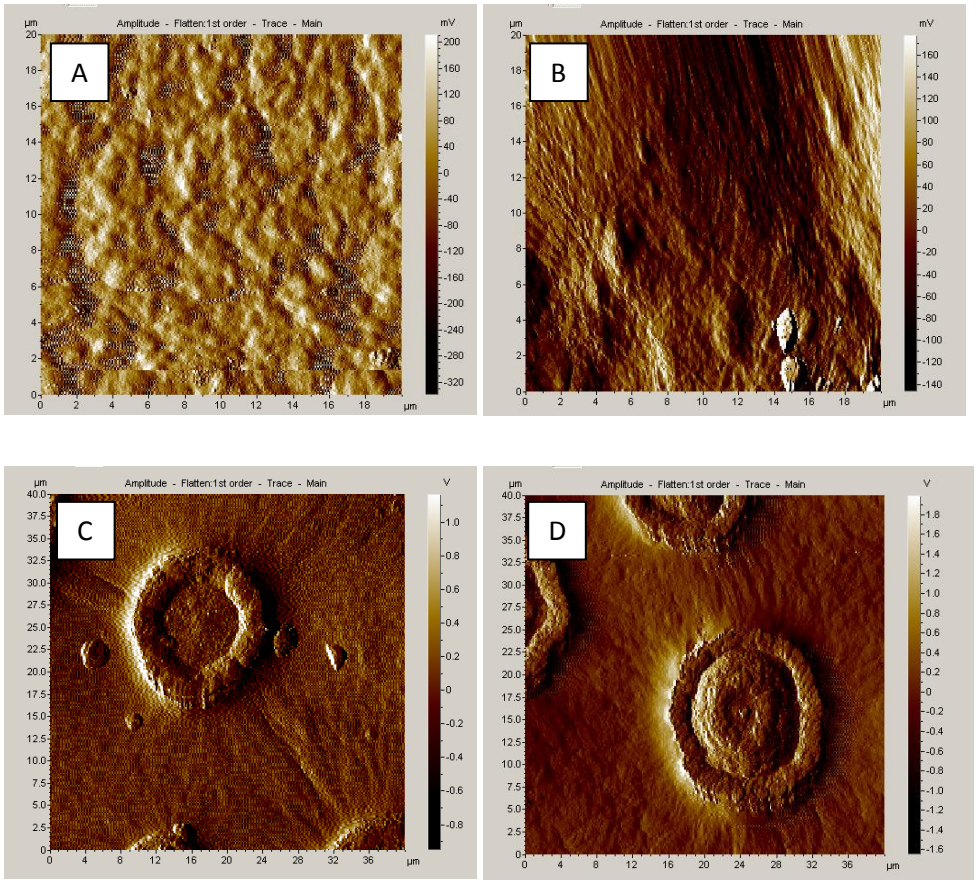

Figure 165 Amplitude trace images for (A) plain gellan G (B) composite GDD (C) ibuprofen loaded gellan GIb and (D) ibuprofen loaded composite GIbDD films.

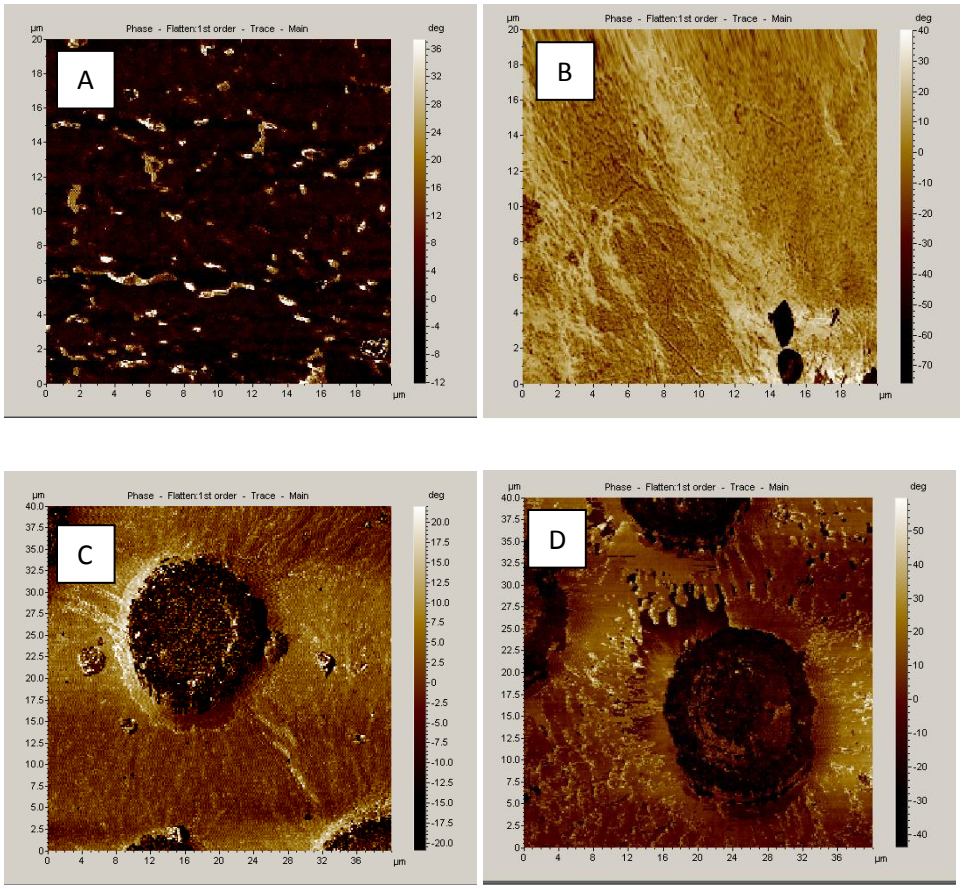

Figure 166 Phase trace images for (A) plain gellan G (B) composite GDD (C) ibuprofen loaded gellan GIb and (D) ibuprofen loaded composite GIbDD films.

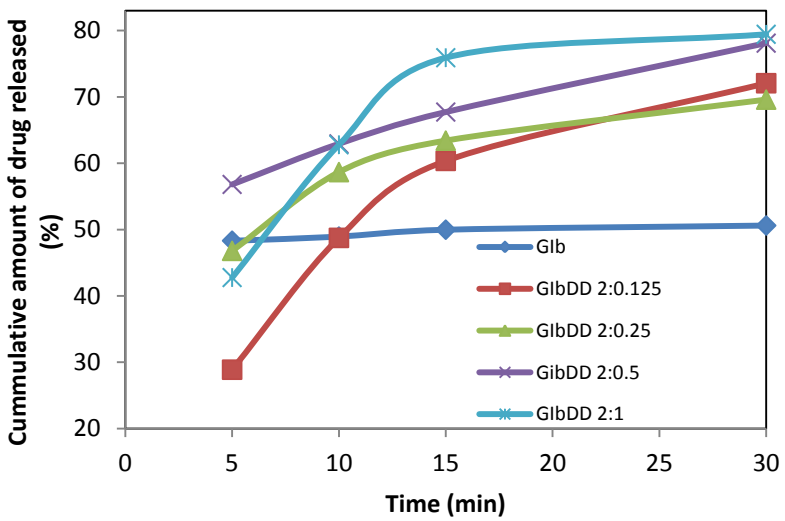

Figure 167 Release profile of ibuprofen from GIb and GIbDD complex composite films within the first 30 min.

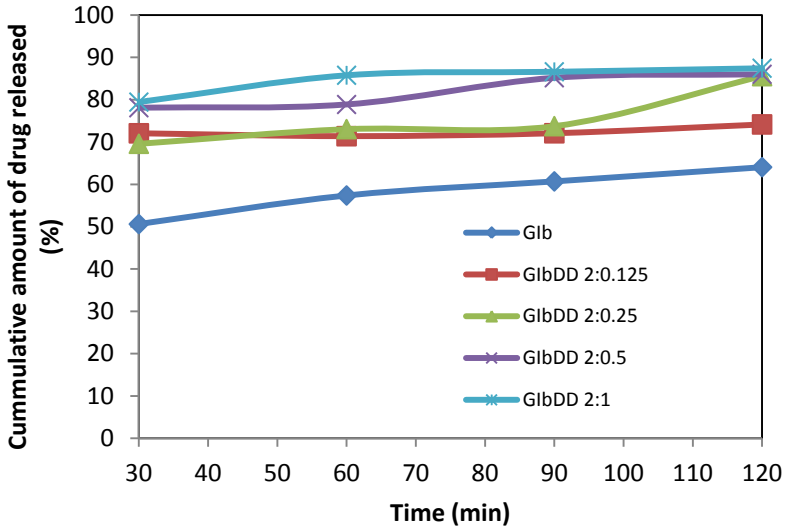

Figure 168 Release profile of ibuprofen from GIb and GIbDD complex composite films from 30 to 120 min.

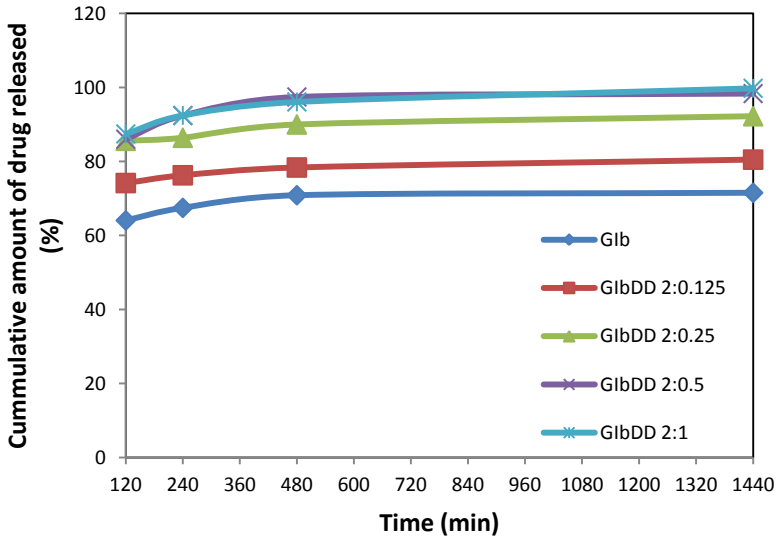

Figure 169 Release profile of ibuprofen from GIb and GIbDD complex composite films from 120 to 1440 min.

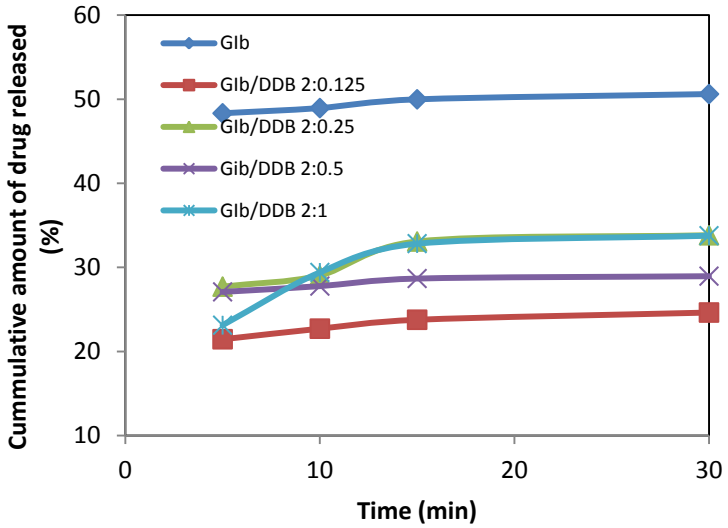

Figure 170 Release profile of ibuprofen from GIb and GIbDD complex bilayer films within the first 30 min.

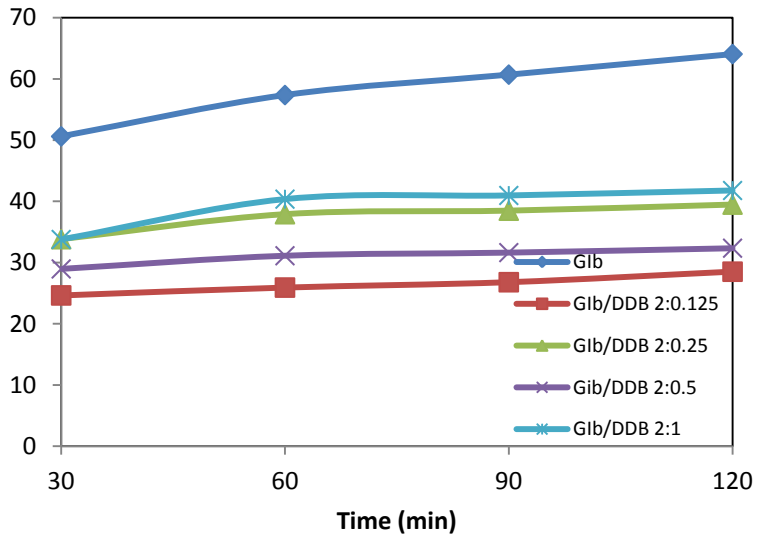

Figure 171 Release profile of ibuprofen from Glb and GlbDD complex bilayer films from 30 to 120 min.

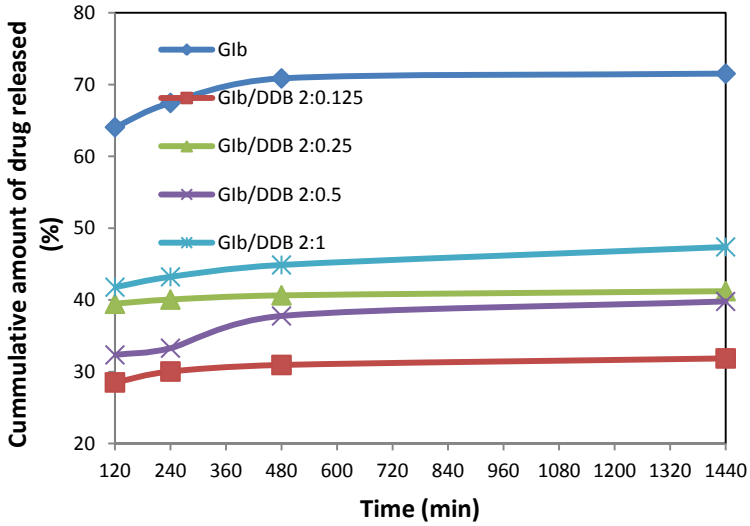

Figure 172 Release profile of ibuprofen from Glb and GlbDD complex bilayer films from 120 to 1440 min.

Table 107 Similarity factor f_2 for Glb versus GlbDD composite films.

Formulation	f_2 – Similarity factor
GlbDD 2:0.125	76.11
GlbDD 2:0.25	58.95
GlbDD 2:0.5	53.43
GlbDD 2:1	52.32

Table 108 Similarity factor f_2 for Glb versus Glb/DDB bilayer films.

Formulation	f_2 – Similarity factor
Glb/DDB 2:0.125	45.00
Glb/DDB 2:0.25	50.81
Glb/DDB 2:0.5	49.81
Glb/DDB 2:1	55.67

6.1. Appendix II APS poster presentation at the University of Nottingham UK (September 2012)

Release kinetics of Ibuprofen microparticles in carbopol gel formulations.

Adeola Kola-Mustapha[1], Amos Abioye[1] and Walkiria Schlindwein[1]

[1]Leicester School of Pharmacy, De Montfort University, LE1 9BH, UK.

Abstract – The drug release kinetics of ibuprofen microparticles dispersed in 1% carbopol gel was investigated. Ibuprofen-chitosan based microparticles were prepared by the solvent change method and incorporated into 1% carbopol gel. The *in vitro* drug release of 5% w/w ibuprofen microparticles in carbopol gel was compared to 5% w/w pure ibuprofen in carbopol gel. Formulation containing 1:5 drug: polymer ratio showed the highest drug release (21.79%) compared with pure ibuprofen (8.69%) at the end of 24h. Non-Fickian diffusion mechanism was exhibited by the ibuprofen microparticles.

INTRODUCTION

Ibuprofen is a non steroidal anti-inflammatory drug with analgesic and antipyretic properties. It is considered the safest of the NSAIDs in the treatment of pain due to inflammatory responses and feverish conditions. The high dose requirement and poor solubility of ibuprofen have limited its application in transdermal drug delivery and all efforts in this regard have not been successful. Although Ibuprofen is available as bulk topical gels, the incorporation efficiency has been limited by its poor solubility and the dosage is highly variable. Presently it is difficult to quantify the effective dose for pain relief in the existing Ibuprofen topical gels and other drug patches due to inadequate skin penetration profiles. Formulation strategies will be designed in the present studies to enhance dissolution and release profiles of Ibuprofen.

MATERIALS AND METHODS

Six formulations containing Ibuprofen (Fagron) – chitosan (Sigma Aldrich) based microparticles in different drug: polymer ratios 1:0.25, 1:0.5, 1:1, 1:2, 1:5 and 1:0 labelled as A1-A6 respectively were prepared by solvent change method [1]. Ibuprofen microparticles (5% w/w) were mixed into 1% w/w carbopol 934 (BF Goodrich) gel. Dissolution tests were conducted using Franz cell (Permegear USA) of 11.28mm diameter and 1.00cm^2 surface area. All UV readings were taken at 264nm. Drug release data were fitted to different kinetic models: zero order, first order, Higuchi plot and Korsemeyer-Peppas (first 60% release)[2].

RESULTS AND DISCUSSION

The drug release profiles showed formulation A5 had the highest release of 21.79mg/cm^2 or 21.79% compared with pure ibuprofen (8.69mg/cm^2 or 8.69%) in carbopol gel up to 24h (Figure 1). Drug release kinetics showed that the data was best fitted with the zero order models. The n values obtained (Table 1) indicated that for the ibuprofen microparticles, the release mechanism was anomalous (non-Fickian) diffusion while for pure ibuprofen, a Super Case II transport mechanism occurred.

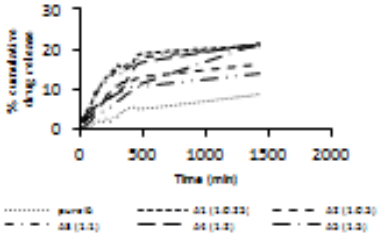

Figure 1 Percentage cumulative drug release over 24h for carbopol gel + pure ibuprofen and carbopol gel + 6 formulations of ibuprofen microparticles.

Table 1 Regression coefficient (r^2) values of different models and diffusion exponent (n) of Korsemeyer-Peppas models for pure ibuprofen and for ibuprofen microparticles in carbopol gel.

Formulation (Drug: Polymer)	Zero order	First Order	Higuchi	Korsemeyer-Peppas	
	r^2	r^2	r^2	r^2	n
Ibuprofen	0.9399	0.8299	0.9245	0.9257	1.0587
A1 (1:0.25)	0.9188	0.7798	0.9803	0.9887	0.6229
A2 (1:0.5)	0.9836	0.8488	0.9903	0.9917	0.6362
A3 (1:1)	0.9275	0.8135	0.9246	0.9679	0.6048
A4 (1:2)	0.9921	0.9200	0.9618	0.9504	0.6519
A5 (1:5)	0.9604	0.8527	0.9949	0.9852	0.4764
A6 (1:0)	0.9927	0.8578	0.9762	0.9864	0.7830

CONCLUSIONS

All the treated batches exhibited higher release profile than pure Ibuprofen. Non-Fickian diffusion release mechanism with zero order was indicated.

REFERENCE

1. S. Mutalik, et al, "Enhancement of dissolution rate and bioavailability of aceclofenac: A chitosan-based solvent change approach" *Int. J. Pharm.*, 350 (2008) 279-290.
2. R. W. Korsemeyer, et al, "Mechanisms of solute release from porous hydrophilic polymers" *Int. J. Pharm.* 15 (1983) 25-35.

AAPS Abstract poster presentation at San Anthonio Texas (November 2013)